PB81-106254

Technical Support of Standards for High-Level Radioactive Waste Management. Volume D Release Mechanisms

Arthur D. Little, Inc.
Cambridge, MA

Prepared for

Office of Radiation Programs
Washington, DC

Mar 80

U.S. Department of Commerce
National Technical Information Service
NTIS

TECHNICAL REPORT DATA

(Please read Instructions on the reverse before completing)

1. REPORT NO. EPA 520/4-79-007D	2.	3. RECIPIENT'S ACCESSION NO. PB81 106254
4. TITLE AND SUBTITLE Technical Support of Standards for High-Level Radioactive Waste Management Volume D - Release Mechanisms		5. REPORT DATE March 1980
		6. PERFORMING ORGANIZATION CODE
7. AUTHOR(S)		8. PERFORMING ORGANIZATION REPORT NO.
9. PERFORMING ORGANIZATION NAME AND ADDRESS Arthur D. Little, Inc. Cambridge, Massachusetts 02140		10. PROGRAM ELEMENT NO.
		11. CONTRACT/GRANT NO. 68-01-4470
12. SPONSORING AGENCY NAME AND ADDRESS Office of Radiation Programs U.S. Environmental Protection Agency Washington, D.C. 20460		13. TYPE OF REPORT AND PERIOD COVERED
		14. SPONSORING AGENCY CODE ANR-460

15. SUPPLEMENTARY NOTES

16. ABSTRACT

This volume is the result of work performed under the fourth part (Task D) of a four-part contract to gather technical information to evaluate environmental acceptability of various options for disposal of high-level wastes. The other tasks under the contract are: A-Source Term Characterization, B-Effectiveness of Engineering Controls; and C-Migration Pathways.

Task D analyzes the potential for the release of radionuclides from a deep-mined repository (generic in nature) for radioactive wastes. Repositories in five different geologic media were considered-bedded salt, dome salt, granite, basalt and shale. Various containment failure mechanisms are considered and compared to determine their relative importance. Ten failure mechanisms were selected for detailed modeling.

The results of Task D can be combined with radionuclide transport and dose calculations to assess the potential effects of a repository on human health.

17. KEY WORDS AND DOCUMENT ANALYSIS

a. DESCRIPTORS	b. IDENTIFIERS/OPEN ENDED TERMS	c. COSATI Field/Group
radioactive wastes high-level radioactive wastes deep-mined repositories		

18. DISTRIBUTION STATEMENT	19. SECURITY CLASS *(This Report)*	21. NO. OF PAGES
	20. SECURITY CLASS *(This page)*	22. PRICE

EPA Form 2220-1 (Rev. 4-77) PREVIOUS EDITION IS OBSOLETE

United States
Environmental Protection
Agency

Office of
Radiation Programs
Washington DC 20460

EPA 520/4-79-007D
March 1980

PB81-106254

Radiation

EPA

Technical Support of Standards for High-Level Radioactive Waste Management

Volume D

Release Mechanisms

REPRODUCED BY
NATIONAL TECHNICAL
INFORMATION SERVICE
U. S. DEPARTMENT OF COMMERCE
SPRINGFIELD, VA. 22161

TECHNICAL SUPPORT OF STANDARDS FOR HIGH-LEVEL RADIOACTIVE WASTE MANAGEMENT

TASK D REPORT

ASSESSMENT OF RELEASE MECHANISMS

EPA Contract No. 68-01-4470

Prepared by

Arthur D. Little, Inc.
Cambridge, Massachusetts 02140
March 1980

DISCLAIMER

This report was prepared as an account of work sponsored by the Environmental Protection Agency of the United States Government under Contract No. 68-01-4470. Neither the United States nor the United States Environmental Protection Agency makes any warranty, express or implied, or assumes any legal liability or responsibility for the accuracy, completeness, or usefulness of any information, apparatus, product, or process disclosed, or represents that its use would not infringe privately owned rights.

ACKNOWLEDGMENTS

Many individuals contributed to the work done under the direction of Arthur D. Little, Inc., for the U.S. Environmental Protection Agency under Contract No. 68-01-4470. John L. Russell and Daniel Egan of the Office of Radiation Programs at EPA served as constant guides in the process of our work. Dr. Bruce S. Old, James I. Stevens, and David I. Hellstrom of Arthur D. Little, Inc., were Program Director, Program Manager, and Assistant Program Manager, respectively, of the overall project. Key individuals involved in each of the reports prepared under the four tasks were:

TASK A
Donald Korn
Arthur D. Little, Inc.
Task Director

Robert McWhorter,
Michael Raudenbush,
and Lester Goldstein
S.M. Stoller Corp.

TASK B
Edwin L. Field
Arthur D. Little,Inc.
Task Director

Robert McWhorter and
Michael Raudenbush
S.M. Stoller Corp.

TASK C
Dr. P.J. O'Brien
Arthur D. Little,Inc.
Task Director

Dr. Ronald B. Lantz
Intera Environmental
Consultants, Inc.

Dr. John Gormley
D'Appolonia Consulting
Engineers, Inc.

TASK D
Dr. Charles R. Hadlock
Arthur D. Little,Inc.
Task Director

Peter D. Mattison and
Dr. Ajit Bhattacharyya
Arthur D. Little, Inc.

FOREWORD

A major Federal effort is underway to develop methods for disposal of high-level radioactive waste in deep geologic repositories. An important element of this program is the development and promulgation by the U.S. Environmental Protection Agency (EPA) of environmental standards for the management of these wastes.

In anticipation of its efforts to develop these standards, EPA recognized that it would be necessary to estimate the expected and potential environmental impacts from potential geologic repositories using modeling techniques based upon as thorough an understanding as possible of the uncertainties involved in the quantities and characteristics of the wastes to be managed, the effectiveness of engineering controls, and the potential migration and accidental pathways that might result in radioactive materials entering the biosphere. Consequently, in March 1977, the EPA contracted with Arthur D. Little, Inc., for a study to provide technical support for its development of environmental regulations for high-level radioactive wastes. This study was divided into the following four tasks:

Task A - Source Term Characterization/Definition

Task B - Effectiveness of Engineering Controls

Task C - Assessment of Migration Pathways

Task D - Assessment of Release Mechanisms

There are many national and international programs underway to develop additional data, especially in the fields of waste forms, knowledge of geology and geohydrology, and risk assessment. The information presented in these reports has been developed on conceptual bases and is not intended to be specific to particular conditions at geologic repositories.

TABLE OF CONTENTS

		Page
Acknowledgements		iii
Foreword		iv
List of Tables		ix
List of Figures		xvi
D-1.0	INTRODUCTION AND SUMMARY	1
1.1	BACKGROUND	1
1.2	OBJECTIVES AND SCOPE	1
1.3	SUMMARY OF RESULTS	2
1.4	GUIDE TO THIS REPORT	2
D-2.0	GUIDELINES AND METHOD OF APPROACH	21
2.1	GENERAL APPROACH	21
2.2	SPECIFIC GUIDELINES	23
2.3	SELECTION AND CHARACTERIZATION OF GENERIC GEOLOGIES	25
2.3.1	Bedded Salt	26
2.3.2	Granite	27
2.3.3	Basalt	30
2.3.4	Shale	34
2.3.5	Dome Salt	37
2.4	REPOSITORY ASSUMPTIONS	37
2.5	IDENTIFICATION OF FAILURE MECHANISMS	40
2.6	CONCEPTUAL FRAMEWORK FOR QUANTITATIVE ANALYSIS	40
2.6.1	Probabilities	42
2.6.2	Consequences	42
2.6.3	Uncertainty and Variability	44
D-3.0	TECHNOLOGICAL FAILURE ELEMENTS	47
3.1	FLOW THROUGH BULK ROCK	47
3.1.1	Summary	47
3.1.2	Background	49
3.1.3	Flow Through Bulk Rock Failure Model	51
3.1.4	Flow Through Bulk Rock Release Model	55
3.1.5	Literature Discussion	68

TABLE OF CONTENTS (cont.)

Page

3.2 SHAFT SEAL FAILURE 68
  3.2.1 Summary 68
  3.2.2 Background 70
  3.2.3 Shaft Seal Failure Model 80
  3.2.4 Shaft Seal Release Model 87
  3.2.5 Literature Discussion 116
D-3.3 BOREHOLE SEAL FAILURE 116
  3.3.1 Summary 116
  3.3.2 Background 118
  3.3.3 Borehole Seal Failure Model 126
  3.3.4 Borehole Seal Release Model 129
  3.3.5 Literature Discussion 154
D-3.4 UNDETECTED BOREHOLES 158
  3.4.1 Summary 158
  3.4.2 Background 158
  3.4.3 Undetected Borehole Failure Model 169
  3.4.4 Undetected Borehole Release Model 178
  3.4.5 Literature Discussion 191
D-3.5 OTHER TECHNOLOGICAL EVENTS AND PROCESSES 192
  3.5.1 Introduction 192
  3.5.2 Waste-Rock Interactions 193
  3.5.3 Brine Migration 194
  3.5.4 Canister Migration 196
  3.5.5 Criticality 197
D-4.0 HUMAN INTRUSION 199
D-4.1 FUTURE DRILLING ACTIVITIES 199
  4.1.1 Summary 199
  4.1.2 Background 202
  4.1.3 Future Drilling Failure Model 208
  4.1.4 Future Drilling Release Model 216

TABLE OF CONTENTS (cont.)

		Page
D-4.2	OTHER HUMAN INTRUSION EVENTS AND PROCESSES	224
4.2.1	Introduction	224
4.2.2	Solution Mining	224
4.2.3	Interference with Hydrologic Conditions	225
4.2.4	Waste Recovery	228
4.2.5	Sabotage	228
4.2.6	Acts of War	229
4.2.7	Innocent Extraordinary Penetration	229
D-5.0	NATURAL EVENT FAILURE ELEMENTS	231
5.1	FAULT MOVEMENT	231
5.1.1	Summary	231
5.1.2	Background	233
5.1.3	Fault Movement Failure Model	250
5.1.4	Fault Movement Release Model	259
5.1.5	Literature Discussion	270
D-5.2	VOLCANOES	277
5.2.1	Summary	277
5.2.2	Background	278
5.2.3	Volcano Failure Model	284
5.2.4	Volcano Release Model	287
5.2.5	Literature Discussion	288
D-5.3	IGNEOUS INTRUSIVES	289
5.3.1	Summary	289
5.3.2	Background	289
5.3.3	Igneous Intrusive Failure Model	293
5.3.4	Igneous Intrusive Release Model	294
5.3.5	Literature Discussion	294
D-5.4	METEORITE IMPACT	295
5.4.1	Summary	295
5.4.2	Background	295
5.4.3	Meteorite Impact Failure Model	302
5.4.4	Meteorite Impact Release Model	304
5.4.5	Literature Discussion	307

TABLE OF CONTENTS (cont.)

		Page
D-5.5	BRECCIA PIPES	308
5.5.1	Summary	308
5.5.2	Background	308
5.5.3	Breccia Pipe Failure Model	315
5.5.4	Breccia Pipe Release Model	317
5.5.5	Literature Discussion	319
D-5.6	OTHER NATURAL EVENTS AND PROCESSES	319
5.6.1	Introduction	319
5.6.2	Erosion	322
5.6.3	Sedimentation	327
5.6.4	Tectonism	327
5.6.5	Uplift and Downwarping	331
5.6.6	Sea Level Fluctuations	332
5.6.7	Climate	334
5.6.8	Salt Diapirism	337
5.6.9	Salt Dissolution	338
LIST OF REFERENCES		341

APPENDICES

Appendix D-I	Glossary	I-1
Appendix D-II	Repository Resaturation Times	II-1
Appendix D-III	Methodology for Dissolution Calculations	III-1
Appendix D-IV	Methodology for Diffusion Calculations	IV-1
Appendix D-V	Methodology for U-Tube Calculations	V-1
Appendix D-VI	Effect of Thermally Induced Buoyancy on Vertical Flow	VI-1
Appendix D-VII	Salt Creep	VII-1
Appendix D-VIII	Canister Capabilities for Long-Term Isolation	VIII-1
Appendix D-IX	Thermal Stress Cracking in Salt	IX-1

LIST OF TABLES

Table No.		Page
D-1	Summary of Flow Through Bulk Rock Failure Element	3
D-2	Summary of Shaft Seal Failure Element	4
D-3	Summary of Borehole Seal Failure Element	6
D-4	Summary of Undetected Borehole Failure Element	8
D-5	Summary of Future Drilling Failure Element	10
D-6	Summary of Fault Movement Failure Element	12
D-7	Summary of Volcano Failure Element	13
D-8	Summary of Igneous Intrusive Failure Element	15
D-9	Summary of Meteorite Impact Failure Element	16
D-10	Summary of Breccia Pipe Failure Element	18
D-11	Explanation of Symbols and Terms in Tables D-1 Through D-10	19
D-12	Nominal Repository Parameters Used for Model Calculations	39
D-13	Failure Element Chosen for Detailed Modeling	41
D-14	Summary of Flow Through Bulk Rock Failure Element	48
D-15	Model Permeabilities for Hard Rock Before and After Thermal Cycle	54
D-16	Effective Vertical Hydraulic Gradient in Surrounding Geologic Media from Thermally Induced Convection (Granite Repository)	56
D-17	Volumetric Flow Rates Through Bulk Rock (Granite Repository)	57
D-18	Fluid Velocities Through Bulk Rock (Granite Repository)	58
D-19	Fluid Transit Time from Repository to Aquifer through Bulk Rock (Granite Repository)	59
D-20	Effective Vertical Hydraulic Gradient in Surrounding Geologic Media from Thermally Induced Convection and Aquifer Interconnection (Basalt Repository)	61

LIST OF TABLES (cont.)

Table No.		Page
D-21	Volumetric Flcw Rates through Bulk Rock (Basalt Repository)	62
D-22	Fluid Velocities through Bulk Rock (Basalt Repository)	63
D-23	Fluid Transit Times through Bulk Rock (Basalt Repository)	64
D-24	Volumetric Flow Rates through Bulk Rock (Shale Repository)	65
D-25	Fluid Velocities through Bulk Rock (Shale Repository)	66
D-26	Fluid Transit Times through Bulk Rock (Shale Repository)	67
D-27	Summary of Shaft Seal Failure Element	71
D-28	Seal Material Characteristics	77
D-29	Properties of Possible Seal Materials	86
D-30	Permeability as a Function of Time for Shaft Seal Degradation Model	88
D-31	Repository Resaturation Times (Bedded Salt Repository)	90
D-32	Approximate Fluid Velocities and Transit Times to Aquifer Along Permeable Shafts During Period A (Bedded Salt Repository)	94
D-33	Effective Vertical Hydraulic Gradient in Permeable Shafts from U-Tube Effect During Period B (Bedded Salt Repository)	95
D-34	Volumetric Flow Rates through Permeable Shafts During Period B (Bedded Salt Repository)	96
D-35	Fluid Velocities through Permeable Shafts During Period B (Bedded Salt Repository)	97
D-36	Effective Vertical Hydraulic Gradient in Permeable Shafts from Thermally Induced Convection and U-Tube Effect (Granite Repository)	99
D-37	Volumetric Flow Rates through Permeable Shafts (Granite Repository)	101

LIST OF TABLES (cont.)

Table No.		Page
D-38	Fluid Velocities through Permeable Shafts (Granite Repository)	102
D-39	Effective Vertical Hydraulic Gradient in Permeable Shafts From Thermally Induced Convection and U-Tube Effect (Basalt Repository)	104
D-40	Volumetric Flow Rate Through Permeable Shafts (Basalt Repository)	105
D-41	Fluid Velocities Through Permeable Shafts (Basalt Repository)	106
D-42	Volumetric Flow Rates Through Permeable Shafts (Shale Repository)	108
D-43	Fluid Velocities Through Permeable Shafts (Shale Repository)	109
D-44	Repository Resaturation Times (Dome Salt Repository)	111
D-45	Approximate Fluid Velocities and Transit Times to Aquifer Along Permeable Shafts During Period A (Dome Salt Repository)	112
D-46	Effective Vertical Hydraulic Gradient in Permeable Shafts From U-Tube Effect During Period B (Dome Salt Repository)	113
D-47	Volumetric Flow Rate in Permeable Shafts During Period B (Dome Salt Repository)	114
D-48	Fluid Velocities Through Permeable Shafts During Period B (Dome Salt Repository)	115
D-49	Baseline Parameter Used by TASC in Fouled Shaft Seal Calculations	117
D-50	Summary of Borehole Seal Failure Element	119
D-51	Permeability as a Function of Time for a Borehole Seal Degradation Model	128
D-52	Approximate Fluid Velocities and Transit Times to Aquifer Along Permeable Boreholes During Period A (Bedded Salt Repository)	134

LIST OF TABLES (cont.)

Table No.		Page
D-53	Effective Vertical Hydraulic Gradient in Permeable Boreholes From Thermally Induced Convection and Aquifer Interconnection (Bedded Salt Repository)	135
D-54	Volumetric Flow Rates and Fluid Velocities in Deep Permeable Boreholes During Period B as Calculated Without Considering Dissolution Effects (Bedded Salt Repository)	136
D-55	Volumetric Flow Rates in Deep Permeable Boreholes During Period B Including Effects of Dissolution on Flow Rates (Bedded Salt Repository)	137
D-56	Effective Vertical Hydraulic Gradient in Permeable Boreholes from Thermally Induced Convection and the U-Tube Effect (Granite Repository)	139
D-57	Volumetric Flow Rates Through Permeable Boreholes (Granite Repository)	141
D-58	Fluid Velocities Through Permeable Boreholes (Granite Repository)	142
D-59	Effective Vertical Hydraulic Gradient in Permeable Boreholes From Thermally Induced Convection U-Tube Effect and Aquifer Interconnection (Basalt Repository)	143
D-60	Effective Vertical Hydraulic Gradients in Permeable Boreholes Connecting the Repository and the Lower Aquifer (Basalt Repository)	146
D-61	Volumetric Flow Rates Through Permeable Boreholes (Basalt Repository)	147
D-62	Fluid Velocities Through Permeable Boreholes (Basalt Repository)	148
D-63	Volumetric Flow Rates Through Permeable Boreholes (Shale Repository)	150
D-64	Fluid Velocities Through Permeable Boreholes (Shale Repository)	151
D-65	Approximate Fluid Velocities and Transit Times to Aquifer Along Permeable Boreholes During Period A (Dome Salt Repository)	153

LIST OF TABLES (cont.)

Table No.		Page
D-66	Effective Vertical Hydraulic Gradient in Permeable Boreholes From U-Tube Effect During Period B (Dome Salt Repository)	155
D-67	Volumetric Flow Rates Through Permeable Boreholes During Period B (Dome Salt Repository)	156
D-68	Fluid Velocities Through Permeable Boreholes During Period B (Dome Salt Repository)	157
D-69	Summary of Undetected Borehole Failure Element	159
D-70	Probabilities of Undetected Boreholes in Buffer Zone Around Bedded Salt Repository (First Estimate)	171
D-71	Effective Resistances α_1 through α_5 (Bedded Salt Repository)	180
D-72	Selected Values of α_1 and α_2 (Bedded Salt Repository)	181
D-73	Volumetric Flow Rates Through Undetected Boreholes (Granite Repository)	184
D-74	Fluid Velocities Through Undetected Boreholes (Granite Repository)	185
D-75	Volumetric Flow Rates Through Undetected Boreholes (Basalt Repository)	187
D-76	Fluid Velocities Through Undetected Boreholes (Basalt Repository)	188
D-77	Volumetric Flow Rates Through Undetected Boreholes (Shale Repository)	189
D-78	Fluid Velocities Through Undetected Boreholes (Shale Repository)	190
D-79	Summary of Future Drilling Activities Failure Element	200
D-80	Areal Borehole Densities From Past Drilling Activities	203
D-81	Future Drilling Rate Estimates for Bedded Salt	210
D-82	Future Drilling Rate Estimates for Granite	211

LIST OF TABLES (cont.)

Table No.		Page
D-83	Future Drilling Rate Estimates for Basalt	212
D-84	Future Drilling Rate Estimates for Shale	213
D-85	Future Drilling Rate Estimates for Dome Salt	214
D-86	Volumetric Flow Rates Through a Single Sealed Borehole	223
D-87	Summary of Fault Movement Failure Element	232
D-88	Fault Densities for Selected Areas of the United States	254
D-89	Volumetric Flow Rates Through a Fault (Bedded Salt Repository)	261
D-90	Fluid Velocities Through a Fault (Bedded Salt Repository)	263
D-91	Volumetric Flow Rates Through a Fault (Granite Repository)	266
D-92	Fluid Velocities Through a Fault (Granite Repository)	267
D-93	Volumetric Flow Rates Through a Fault (Basalt Repository)	268
D-94	Fluid Velocities Through a Fault (Basalt Repository)	269
D-95	Volumetric Flow Rates Through a Fault (Shale Repository)	271
D-96	Fluid Velocities Through a Fault (Shale Repository)	272
D-97	Effective Vertical Hydraulic Gradient in a Fault From Thermally Induced Convection and Aquifer Interconnection (Salt Dome Repository)	273
D-98	Volumetric Flow Rates Through a Fault (Dome Salt Repository)	274
D-99	Fluid Velocities Through a Fault (Dome Salt Repository)	275
D-100	Summary of Volcano Failure Element	279
D-101	Volcanic Phenomena with Surface Manifestation	282
D-102	Summary of Igneous Intrusive Failure Element	290
D-103	Summary of Meteorite Impact Failure Element	296

LIST OF TABLES (cont.)

Table No.		Page
D-104	Proven or Probable Large Meteorite Impact Craters in the United States	300
D-105	Effective Hydraulic Gradient in Extended Vertical Pathways	305
D-106	Volumetric Flow Rates Through Meteorite Induced Permeable Zone	306
D-107	Summary of Breccia Pipe Failure Element	309
D-108	Effective Vertical Hydraulic Gradient in a Breccia Pipe from Thermal Buoyancy and Aquifer Interconnection (Bedded Salt Repository)	318
D-109	Volumetric Flow Rate Through a Breccia Pipe (Bedded Salt Repository)	320
D-110	Fluid Velocities Through a Breccia Pipe (Bedded Salt Repository)	321
D-111	Estimates of the Rate of Erosion Under Various Conditions of Climate and Relief	333

LIST OF FIGURES

Figure No.		Page
D-1	Rock Salt Deposits in the United States	28
D-2	Repository in Bedded Salt	29
D-3	Crystalline Formations in the United States	31
D-4	Repository in Granite	32
D-5	Repository in Basalt	33
D-6	Argillaceous Formations in the United States	35
D-7	Repository in Shale	36
D-8	Repository in Salt Dome	38
D-9	Bedded Salt Repository Showing Vertical Shafts	69
D-10	Examples of Shaft Linings	74
D-11	Grouting Program for Shaft Stabilization	75
D-12	Example of Section of Multi-Layered Shaft Seal	83
D-13	Hydraulic Conductivity of Natural Materials	85
D-14	Typical Plugged Borehole	123
D-15	Electric Analog for Borehole Pathway Analysis in Basalt	145
D-16	Commercial Saline Deposits in the United States	162
D-17	Commercially Exploitable Organic Fuel Deposits in the United States	163
D-18	Diagram of Salt Dome Showing Associated Oil Reservoirs, Wells, and Deep Holes	166
D-19	Pathways Associated with the Analysis of Undetected Boreholes	179
D-20	Migration of Brine Bubble in Thermal Gradient	195
D-21	Petroleum Wells Drilled in the Contiguous 48 States, 1976 and 1977	204
D-22	Region Within Which Canister and Drill Hole Overlap	217

LIST OF FIGURES (cont.)

Figure No.		Page
D-23	Fluid Injection for Enhanced Well Production	227
D-24	Subparallel Faulting in Tertiary and Quaternary Periods	234
D-25	Basic Fault Types	236
D-26	Features Associated with Faulting	238
D-27	Dating of Non-tectonic Fault by Bed Displacements	239
D-28	Faulting in the Vicinity of a Salt Dome (Conceptual Drawing)	241
D-29	Typical Paradox Basin Salt Anticline Structure Derived from Seismic and Other Data	242
D-30	Age of Faults in the Gulf Coastal Region	243
D-31	Detection of Features by Seismic Reflection	245
D-32	Detection of Fault by Attenuation of Refracted Signals Across Discontinuity	246
D-33	Processed Seismic Record of Section of Paradox Basin	247
D-34	Faulting Associated with Folding and Tilting	249
D-35	Waste Drift Before and After Faulting	264
D-36	Sketch of Plutonic and Volcanic Structures	281
D-37	Volcanic Hazards	283
D-38	Relative Crater Production Rate with Solar System Evolution	298
D-39	Distribution of Impact Craters	301
D-40	Simplified Crater Geometry	303
D-41	Conceptual Drawing of Breccia Pipe in Delaware Basin	311
D-42	Characteristics of Dissolution from Above and Below Salt Formation	313
D-43	Average Rate of Denudation of Major Drainage Areas in the U.S.	323

LIST OF FIGURES (cont.)

Figure No.		Page
D-44	Glaciated Areas of the Coterminous United States Affected During Pleistocene Glaciation	326
D-45	Crustal Plates and Regions of the World in Which Major Earthquakes and Volcanoes Occur	329
D-46	Isostasy	330
D-47	Fresh Water Overlying Dense Sea Water	335
D-48	Erosion Rates vs. Plant Cover	336

D-1.0 INTRODUCTION AND SUMMARY

D-1.1 BACKGROUND

The U.S. Environmental Protection Agency (EPA) is responsible for the development of environmental standards for the disposal of high-level radioactive wastes. As part of its development effort, EPA contracted with Arthur D. Little, Inc., for a program of technical support. This program consists of four principal tasks:

Task A -- Source Term Characterization/Definition
Task B -- Effectiveness of Engineering Controls
Task C -- Assessment of Migration Pathways
Task D -- Assessment of Release Mechanisms

This report represents the results of the work done under Task D.

D-1.2 OBJECTIVES AND SCOPE

The purpose of Task D is to analyze the potential for the release of radionuclides from a deep mined repository for radioactive wastes. The analysis is not intended to correspond to a particular site or repository design, but rather it is to be generic in nature, representing the synthesis of assumptions and data from many sources. The EPA wishes to consider the potential performance of repositories in its determination of appropriate standards.

Repositories in five different geologic media were considered in this study. These media include bedded salt, dome salt, granite, basalt, and shale. A wide range of potential containment failure mechanisms have been proposed in the literature. These failure mechanisms were evaluated and compared with each other to determine their relative importance. As a result of this process, ten failure mechanisms were selected for detailed modeling. They were chosen with a view toward including those that appeared to be the most important, as well as ones that would span a wide range of risk characteristics (e.g., high probability/low consequence, low probability/high consequence). The list includes the following:

- flow through bulk rock;
- shaft seal failure;
- borehole seal failure;
- undetected boreholes;
- future drilling;
- fault movement;
- volcanoes;
- igneous intrusives;
- meteorite impacts;
- breccia pipes.

A number of other failure mechanisms, or processes that might contribute to failure, are discussed in this report, although detailed models have not been developed.

The results of Task D can be combined with radionuclide transport and dose calculations in order to assess the potential effects of a repository on human health.

D-1.3 SUMMARY OF RESULTS

Each of the ten failure elements was modeled in terms of its likelihood of occurrence and its physical characteristics. In six cases, the likelihood of occurrence is estimated in terms of an annual probability (events/year). However, some failure modes are considered sufficiently likely that they are modeled as deterministic events. Summaries of the model assumptions and parameters for each of the failure elements are given in Tables D-1 through D-10. A key to the symbols that appear in these tables can be found in Table D-11. The remainder of this report can be regarded as an explanation of these tables.

D-1.4 GUIDE TO THIS REPORT

Chapter D-2.0 contains a summary of the methods and guidelines adopted for this study. Chapters D-3.0, D-4.0, and D-5.0 contain detailed analyses of the ten failure elements that were modeled, as well as discussions of other potential failure elements. The first appendix

TABLE D-1
SUMMARY OF FLOW THROUGH BULK ROCK FAILURE ELEMENT

MEDIUM	PROBABILISTIC (P) DETERMINISTIC (D)	NATURE OF MODEL	RELEASE MODE	DRIVING FORCE	SOURCE TERM	PARAMETERS		FLUID FLOW RATES FROM REPOSITORY TO UPPER AQUIFER				COMMENTS
						1st ESTIMATE	2nd ESTIMATE	1st ESTIMATE		2nd ESTIMATE		
								t (yrs)	$\dot{Q}(t)$ (m^3/yr)	t (yrs)	$\dot{Q}(t)$ (m^3/yr)	
Bedded Salt	P	Cumulative occurrence probability	Groundwater	Pressure from salt closure, thermally induced convection, and gradient from aquifer interconnection	Uniform concentration	$p = 0$	$p = 0$	No releases need to be calculated.		No releases need to be calculated.		The probability that the spatial variability in rock strength could lead to an extensive pathway from the repository that would fracture under the stresses experienced was found to be negligible.
Granite	D	Change in permeability after thermal peak	Groundwater	Thermally induced convection	Uniform concentration	$K = 10^{-10}$ cm/sec for $t < 100$ yrs $K = 10^{-8}$ cm/sec for $t > 100$ yrs $\eta = 10^{-4}$ $A = 8 \times 10^6\ m^2$	$K = 10^{-8}$ cm/sec for $t < 100$ yrs $K = 10^{-7}$ cm/sec for $t > 100$ yrs $\eta = 10^{-4}$ $A = 8 \times 10^6\ m^2$	100 1000 10,000	1.4×10^2 8.8×10^1 3.8×10^1	100 1000 10,000	1.4×10^4 8.8×10^3 3.8×10^3	Permeability change after thermal peak is due to several factors: movement of blocks during thermal cycle, incomplete rebound of material in cracks, alteration of minerals in cracks.
Basalt	D	Change in permeability after thermal peak	Groundwater	Thermally induced convection and gradient from aquifer interconnection	Uniform concentration	$K = 10^{-8}$ cm/sec for $t < 100$ yrs $K = 10^{-8}$ cm/sec for $t > 100$ yrs $\eta = 10^{-4}$ $A = 8 \times 10^6\ m^2$	$K = 10^{-7}$ cm/sec for $t < 100$ yrs $K = 10^{-6}$ cm/sec for $t > 100$ yrs $\eta = 10^{-4}$ $A = 8 \times 10^6\ m^2$	100 1000 10,000	1.8×10^4 1.5×10^4 6.3×10^3	100 1000 10,000	7.9×10^6 7.7×10^6 6.8×10^6	Permeability change after thermal peak is due to several factors: movement of blocks during thermal cycle, incomplete rebound of material in cracks, alteration of minerals in cracks.
Shale	D	Change in permeability after thermal peak	Groundwater	Thermally induced convection and gradient from aquifer interconnection	Uniform concentration	$K = 10^{-9}$ cm/sec for $t < 100$ yrs $K = 10^{-8}$ cm/sec for $t > 100$ yrs $\eta = 10^{-4}$ $A = 8 \times 10^6\ m^2$	$K = 10^{-7}$ cm/sec for $t < 100$ yrs $K = 10^{-6}$ cm/sec for $t > 100$ yrs $\eta = 10^{-4}$ $A = 8 \times 10^6\ m^2$	100 1000 10,000	1.8×10^4 1.5×10^4 6.3×10^3	100 1000 10,000	7.9×10^6 7.7×10^6 6.8×10^6	Permeability change after thermal peak is due to several factors: movement of blocks during thermal cycle, incomplete rebound of material in cracks, alteration of minerals in cracks.
Dome Salt	P	Cumulative occurrence probability	Groundwater	Pressure from salt closure, thermally induced convection, and gradient from lower aquifer at edge of salt dome	Uniform concentration	$p = 0$	$p = 0$	No releases need to be calculated.		No releases need to be calculated.		The probability that the spatial variability in rock strength could lead to an extensive pathway from the repository that would fracture under the stresses experienced was found to be negligible.

See Table D-11 for explanation of symbols and terms.

TABLE D-2
SUMMARY OF SHAFT SEAL FAILURE ELEMENT

MEDIUM	PROBABILISTIC (P) DETERMINISTIC (D)	NATURE OF MODEL	RELEASE MODE	DRIVING FORCE	SOURCE TERM	PARAMETERS		FLUID FLOW RATES FROM REPOSITORY TO UPPER AQUIFER				COMMENTS
						1st ESTIMATE	2nd ESTIMATE	1st ESTIMATE		2nd ESTIMATE		
								t (yrs)	$\dot{Q}$ (t) (m^3/yr)	t (yrs)	$\dot{Q}$ (t) (m^3/yr)	
Bedded Salt	D	Linearly increasing permeability	Groundwater	Initially pressure from salt creep. Afterwards, U-tube effect.	Uniform concentration	K_0 = 10^{-8} cm/sec at time of sealing K_1 = 10^{-6} cm/sec after 10,000 years K increases linearly from K_0 to K_1 over 10,000 years η = 0.1 A = 100 m^2, total cross-sectional area of shafts	K_0 = 10^{-8} cm/sec at time of sealing K_1 = 10^{-4} cm/sec after 10,000 years K increases linearly from K_0 to K_1 over 10,000 years η = 0.1 A = 100 m^2, total cross-sectional area of shafts	200 223^- 223^+ 1000 10,000	40 } Period of salt creep 40 0.08 0.17 0.32	720 1000^- 1000^+ 10,000	2000 } Period of salt creep 2000 3.15 3.15	It is conservative to assume closure by salt creep for this failure mechanism; otherwise resaturation time would be extremely long. Closure also implies strong driving force for release.
Granite	D	Linearly increasing permeability	Groundwater	Thermally induced convection and U-tube effect.	Uniform concentration	K_0 = 10^{-8} cm/sec at time of sealing K_1 = 10^{-6} cm/sec after 10,000 years K increases linearly from K_0 to K_1 over 10,000 years η = 0.1 A = 100 m^2, total cross-sectional area of shafts	K_0 = 10^{-8} cm/sec at time of sealing K_1 = 10^{-4} cm/sec after 10,000 years K increases linearly from K_0 to K_1 over 10,000 years η = 0.1 A = 100 m^2, total cross-sectional area of shafts.	100 1000 10,000	0.3 1.0 1.8	100 1000 10,000	15.8 94.6 238.3	Release only begin after repository resaturation.
Basalt	D	Linearly increasing permeability	Groundwater	Thermally induced convection and U-tube effect.	Uniform concentration	K_0 = 10^{-8} cm/sec at time of sealing K_1 = 10^{-6} cm/sec after 10,000 years K increases linearly from K_0 to K_1 over 10,000 years η = 0.1 A = 100 m^2, total cross-sectional area of shafts	K_0 = 10^{-8} cm/sec at time of sealing K_1 = 10^{-4} cm/sec after 10,000 years K increases linearly from K_0 to K_1 over 10,000 years η = 0.1 A = 100 m^2, total cross-sectional area of shafts	100 1000 10,000	0.4 1.7 3.2	100 1000 10,000	28.6 157.6 472.6	Release only begin after repository resaturation.

See Table D-11 for explanation of symbols and terms.

TABLE D-2
SUMMARY OF SHAFT SEAL FAILURE ELEMENT (CONTINUED)

MEDIUM	PROBABILISTIC (P) DETERMINISTIC (D)	NATURE OF MODEL	RELEASE MODE	DRIVING FORCE	SOURCE TERM	PARAMETERS		FLUID FLOW RATES FROM REPOSITORY TO UPPER AQUIFER				COMMENTS
						1st ESTIMATE	2nd ESTIMATE	1st ESTIMATE		2nd ESTIMATE		
Shale	D	Linearly increasing permeability	Groundwater	Thermally induced convection and U-tube effect.	Uniform concentration	K_0 = 10^{-8} cm/sec at time of sealing K_1 = 10^{-6} cm/sec after 10,000 years K increases linearly from K_0 to K_1 over 10,000 years η = 0.1 A = 100 m^2, total cross-sectional area of shafts	K_0 = 10^{-8} cm/sec at time of sealing K_1 = 10^{-4} cm/sec after 10,000 years K increases linearly from K_0 to K_1 over 10,000 years η = 0.1 A = 100 m^2, total cross-sectional area of shafts	t (yrs) 100 1000 10,000	$\dot{Q}$ (t) (m^3/yr) 0.4 1.7 3.2	t (yrs) 100 1000 10,000	$\dot{Q}$ (t) (m^3/yr) 28.8 157.6 472.8	Releases only begin after repository resaturation.
Dome Salt	D	Linearly increasing permeability	Groundwater	Initially pressure from salt creep. Afterwards, U-tube effect.	Uniform concentration	K_0 = 10^{-8} cm/sec at time of sealing K_1 = 10^{-6} cm/sec after 10,000 years K increases linearly from K_0 to K_1 over 10,000 years η = 0.1 A = 100 m^2, total cross-sectional area of shafts	K_0 = 10^{-8} cm/sec at time of sealing K_1 = 10^{-4} cm/sec after 10,000 years K increases linearly from K_0 to K_1 over 10,000 years η = 0.1 A = 100 m^2, total cross-sectional area of shafts	t (yrs) 200 280 280 1000 10,000	$\dot{Q}$ (t) (m^3/yr) 15 } Period of salt creep 15 } 0.04 0.10 0.24	t (yrs) 748 1000^- 1000^+ 10,000	$\dot{Q}$ (t) (m^3/yr) 2000 } Period of salt creep 2000 } 3.15 3.15	It is conservative to assume closure by salt creep for this failure mechanism; otherwise resaturation time would be extremely long. Closure also implies strong driving force for release.

See Table D-11 for explanation of symbols and terms.

TABLE D-3
SUMMARY OF BOREHOLE SEAL FAILURE ELEMENT

MEDIUM	PROBABILISTIC (P) DETERMINISTIC (D)	NATURE OF MODEL	RELEASE MODE	DRIVING FORCE	SOURCE TERM	PARAMETERS		FLUID FLOW RATES FROM REPOSITORY TO UPPER AQUIFER				COMMENTS
						1st ESTIMATE	2nd ESTIMATE	1st ESTIMATE		2nd ESTIMATE		
Bedded Salt	D	Linearly increasing permeability	Groundwater	Initially pressure from salt creep. Afterwards, thermally induced convection and gradient from aquifer interconnection for boreholes extending to lower aquifer.	Uniform concentration	K_0 = 10^{-8} cm/sec at time of sealing K_1 = 10^{-5} cm/sec after 10,000 years K increases linearly from K_0 to K_1 over 10,000 years η = 0.1 50 boreholes penetrate to repository, 10 of which continue to lower aquifer A = 0.1 m^2/borehole	K_0 = 10^{-8} cm/sec at time of sealing K_1 = 10^{-4} cm/sec after 10,000 years K increases linearly from K_0 to K_1 over 10,000 years η = 0.1 50 boreholes penetrate to repository, 10 of which continue to lower aquifer A = 0.1 m^2/borehole	t (yrs) 200 223^- 223^+ 1000 10,000	$\dot{Q}$ (t) (m^3/yr) 14 Period 14 of salt creep 0.05 0.18 0.63	t (yrs) 720 1000^- 1000^+ 10,000	$\dot{Q}$ (t) (m^3/yr) 100 Period 100 of salt creep 19 167	Releases only begin after repository resaturation. Dissolution in salt layer is included in second estimate calculations for period after extensive salt creep.
Granite	D	Linearly increasing permeability	Groundwater	Thermally induced convection	Uniform concentration	K_0 = 10^{-8} cm/sec at time of sealing K_1 = 10^{-6} cm/sec after 10,000 years K increases linearly from K_0 to K_1 over 10,000 years η = 0.1 50 boreholes penetrate to repository A = 0.1 m^2/borehole	K_0 = 10^{-8} cm/sec at time of sealing K_1 = 10^{-4} cm/sec after 10,000 years K increases linearly from K_0 to K_1 over 10,000 years η = 0.1 50 boreholes penetrate to repository A = 0.1 m^2/borehole	t (yrs) 100 1000 10,000	$\dot{Q}$(t) (m^3/yr) 0.1 0.6 2.4	t (yrs) 100 1000 10,000	$\dot{Q}$ (t) (m^3/yr) 0.9 5.5 31.5	Releases only begin after repository resaturation.
Basalt	D	Linearly increasing permeability	Groundwater	Thermally induced convection and gradient from aquifer interconnection for boreholes extending to lower aquifer.	Uniform concentration	K_0 = 10^{-8} cm/sec at time of sealing K_1 = 10^{-6} cm/sec after 10,000 years K increases linearly from K_0 to K_1 over 10,000 years η = 0.1 50 boreholes penetrate to repository, 10 of which continue to lower aquifer A = 0.1 m^2/borehole	K_0 = 10^{-8} cm/sec at time of sealing K_1 = 10^{-4} cm/sec after 10,000 years K increases linearly from K_0 to K_1 over 10,000 years η = 0.1 50 boreholes penetrate to repository, 10 of which continue to lower aquifer A = 0.1 m^2/borehole	t (yrs) 100 1000 10,000	$\dot{Q}$ (t) (m^3/yr) 0.05 0.4 1.6	t (yrs) 100 1000 10,000	$\dot{Q}$ (t) (m^3/yr) 2.0 19.2 170.1	Releases only begin after repository resaturation

See Table D-11 for explanation of symbols and terms.

TABLE D-3
SUMMARY OF BOREHOLE SEAL FAILURE ELEMENT (CONTINUED)

MEDIUM	PROBABILISTIC (P) DETERMINISTIC (D)	NATURE OF MODEL	RELEASE MODE	DRIVING FORCE	SOURCE TERM	PARAMETERS		FLUID FLOW RATES FROM REPOSITORY TO UPPER AQUIFER				COMMENTS
						1st ESTIMATE	2nd ESTIMATE	1st ESTIMATE		2nd ESTIMATE		
								t (yrs)	$\dot{Q}$ (t) (m^3/yr)	t (yrs)	$\dot{Q}$ (t) (m^3/yr)	
Shale	D	Linearly increasing permeability	Groundwater	Thermally induced convection and gradient from aquifer interconnection for boreholes extending to lower aquifer.	Uniform concentration	K_0 = 10^{-8} cm/sec at time of sealing K_1 = 10^{-6} cm/sec after 10,000 years K increases linearly from K_0 to K_1 over 10,000 years q = 0.1 50 boreholes penetrate to repository, 10 of which continue to lower aquifer A = 0.1 m^2/borehole	K_0 = 10^{-8} cm/sec at time of sealing K_1 = 10^{-4} cm/sec after 10,000 years K increases linearly from K_0 to K_1 over 10,000 years q = 0.1 50 boreholes penetrate to repository, 10 of which continue to lower aquifer A = 0.1 m^2/borehole	100 1000 10,000	0.05 0.4 1.6	100 1000 10,000	2.0 19.2 170.1	Releases only begin after repository resaturation.
Dome Salt	D	Linearly increasing permeability	Groundwater	Initially pressure from salt creep. Afterwards, the U-tube effect.	Uniform concentration	K_0 = 10^{-8} cm/sec at time of sealing K_1 = 10^{-6} cm/sec after 10,000 years K increases linearly from K_0 to K_1 over 10,000 years q = 0.1 50 boreholes penetrate to repository A = 0.1 m^2/borehole	K_0 = 10^{-8} cm/sec at time of sealing K_1 = 10^{-4} cm/sec after 10,000 years K increases linearly from K_0 to K_1 over 10,000 years q = 0.1 50 boreholes penetrate to repository A = 0.1 m^2/borehole	200 200^- 200^+ 1000 10,000	5 } Period of salt creep 5 } 0.01 0.03 0.16	746 1000^- 1000^+ 10,000	100 } Period of salt creep 100 } 1.6 2.8	Releases only begin after repository resaturation. In contrast to undersealed borehole failure element, holes in this case are near or through repository and so cannot intersect lower aquifer at edge of salt dome.

See Table D-11 for explanation of symbols and terms.

TABLE D-4
SUMMARY OF UNDETECTED BOREHOLE FAILURE ELEMENT

MEDIUM	PROBABILISTIC (P) DETERMINISTIC (D)	NATURE OF MODEL	RELEASE MODE	DRIVING FORCE	SOURCE TERM	PARAMETERS		FLUID FLOW RATES FROM REPOSITORY TO UPPER AQUIFER		COMMENTS
						1st ESTIMATE	2nd ESTIMATE	1st ESTIMATE	2nd ESTIMATE	
Bedded Salt	P	Past drilling density and detection reliability yield probability of one or more partially filled holes.	Groundwater	Second estimate Period B flows derive from aquifer interconnection gradient. Other flows negligible.	Uniform concentration	prob (1 hole on site) = 0.016 ("site" = 300 m buffer zone only) prob (failure to detect) = 0.001 prob (undet. hole) = 1.6×10^{-5} $K = 10^{-4}$ cm/sec $\eta = 0.2$ $A = 0.1\ m^2$ Distance from drift = 100 m Holes extend to lower aquifer.	exp. no. holes on site = 3 prob (failure to detect indiv. hole) = 0.001 prob (3 undet. holes) = 0.003 (assumes partial dependence) $K = 10^{-3}$ cm/sec $\eta = 0.2$ $A = 0.3\ m^2$ (total) Distance from drift = 100 m Holes extend to lower aquifer.	Negligible with respect to other failure elements	t (yrs) | $\dot{Q}(t)$ (m^3/yr) 1000 | 945 10,000 | 945	Distance from drift precludes significant connection with repository except in case of significant dissolution. Negligible flow in most cases deduced from consideration of relative resistance of alternative pathways for water to enter and leave repository. Repository resaturation necessary for release.
Granite	P	Past drilling density and detection reliability yield probability of one or more partially filled holes.	Groundwater	Thermally induced convection.	Uniform concentration	prob (1 hole on site) = 0.005 ("site" = repos. + 300 m buffer zone.) prob (failure to detect) = 0.01 prob (undet. hole) = 5×10^{-5} $K = 10^{-4}$ cm/sec $\eta = 0.2$ $A = 0.1\ m^2$ Distance from drift = 5 m but flows assume hole through repository.	prob (1 hole on site) = 0.05 prob (failure to detect) = 0.01 prob (undet. hole) = 5×10^{-4} $K = 10^{-3}$ cm/sec $\eta = 0.2$ $A = 0.1\ m^2$ Distance from drift = 5 m but flows assume hole through repository.	t (yrs) | $\dot{Q}$ (m^3/yr) 100 | 1.7 1000 | 1.1 10,000 | 0.5	t (yrs) | $\dot{Q}$ (m^3/yr) 100 | 17 1000 | 11 10,000 | 5	Repository resaturation necessary for release to begin.
Basalt	P	Past drilling density and detection reliability yield probability of one or more partially filled holes.	Groundwater	Thermally induced convection and gradient from aquifer interconnection.	Uniform concentration	prob (1 hole on site) = 0.075 ("site" = repos. + 300 m buffer zone) prob (failure to detect) = 0.001 prob (undet. hole) = 7.5×10^{-5} $K = 10^{-4}$ cm/sec $\eta = 0.2$ $A = 0.1\ m^2$ Distance from drift = 5 m but flows assume hole through repository. Holes extend to lower aquifer.	prob (1 hole on site) = 0.2 prob (failure to detect) = 0.01 prob (undet. hole) = 2×10^{-3} $K = 10^{-3}$ cm/sec $\eta = 0.2$ $A = 0.1\ m^2$ Distance from drift = 5 m but flows assume hole through repository. Holes extend to lower aquifer.	t (yrs) | $\dot{Q}$ (m^3/yr) 100 | 4.4 1000 | 3.8 10,000 | 1.6	t (yrs) | $\dot{Q}$ (m^3/yr) 100 | 198 1000 | 192 10,000 | 170	Repository resaturation necessary for release to begin.

See Table D-11 for explanation of symbols and terms.

TABLE D-4
SUMMARY OF UNDETECTED BOREHOLE FAILURE ELEMENT (CONTINUED)

MEDIUM	PROBABILISTIC (P) DETERMINISTIC (D)	NATURE OF MODEL	RELEASE MODE	DRIVING FORCE	SOURCE TERM	PARAMETERS		FLUID FLOW RATES FROM REPOSITORY TO UPPER AQUIFER		COMMENTS
						1st ESTIMATE	2nd ESTIMATE	1st ESTIMATE	2nd ESTIMATE	
Shale	P	Past drilling density and detection reliability yield probability of one or more partially filled holes.	Groundwater	Thermally induced convection and gradient from aquifer interconnection.	Uniform concentration	prob (1 hole on site) = 0.05 ("site" = repos. + 300 m buffer zone) prob (failure to detect) = .01 prob (undet. hole) = 5×10^{-4} K = 10^{-4} cm/sec η = 0.2 A = 0.1 m^2 Distance from drift = 5 m but flows assume hole through repository. Holes extend to lower aquifer.	exp. no holes on site = 9 prob (failure to detect) = 0.01 prob (3 undet. holes) = 0.08 (Assumes partial dependence) K = 10^{-3} cm/sec η = 0.2 A = 0.1 m^2 Distance from drift = 5 m but flows assume hole through repository. Holes extend to lower aquifer.	t (yrs) | $\dot{Q}$ (m^3/yr) 100 | 4.4 1000 | 3.8 10,000 | 1.6	t (yrs) | $\dot{Q}$ (m^3/yr) 100 | 684 1000 | 576 10,000 | 510	Repository restoration necessary for release to begin.
Dome Salt	P	Past drilling density and detection reliability yield probability of one or more partially filled holes.	Groundwater	Second estimate Period B flows derive from aquifer interconnection gradient. Other flows negligible.	Uniform concentration	exp. no. holes on site = 3 ("site" = 300 m buffer zone only) prob (failure to detect indiv. hole) = 0.001 prob (3 undet. holes) = 0.003 (Assumes partial dependence) K = 10^{-4} cm/sec η = 0.2 A = 0.1 m^2 Distance from drift = 100 m. Holes extend to lower aquifer.	exp. no holes on site = 30 prob (failure to detect indiv. hole) = 0.001 prob (5 undet. holes) = 0.03 (assumes partial dependence) K = 10^{-3} cm/sec η = 0.2 A = 0.3 m^2 (total) Distance from drift = 100 m. Holes extend to lower aquifer.	Negligible with respect to other failure elements.	t (yrs) | $\dot{Q}$ (m^3/yr) 1000 | 630 10,000 | 630	Distance from drift precludes significant connection with repository except in case of significant dissolution. Negligible flow in most cases deduced from consideration of relative resistance of alternative pathways for water to enter and leave repository. Repository restoration necessary for release.

See Table D-11 for explanation of symbols and terms.

TABLE D-5
SUMMARY OF FUTURE DRILLING FAILURE ELEMENT

MEDIUM	PROBABILISTIC (P) DETERMINISTIC (D)	NATURE OF MODEL	RELEASE MODE	DRIVING FORCE	SOURCE TERM	PARAMETERS		FLUID TRANSPORTED TO SURFACE		COMMENTS
						1st ESTIMATE	2nd ESTIMATE	1st ESTIMATE	2nd ESTIMATE	
Bedded Salt	P, D	Postulated deterministic drilling rate, probabilistic for hitting canister.	A. Land surface B. Groundwater	A. Materials raised with drilling mud. B. Thermally induced convection and gradient from aquifer interconnection.	A. Part of canister and fluid from waste drift. B. Uniform concentration.	No holes first century; 5 holes next century; 2 holes each subsequent century. All holes to lower aquifer. Holes sealed with permeability K = 10^{-4} cm/sec η = 0.2, and A = 0.1 m^2. Probability of hitting a canister = 10^{-3} per hole, with expected removal of 15% contents.	No holes first century; 50 holes next century; 5 holes each subsequent century. All holes to lower aquifer. Holes sealed with permeability K = 10^{-3} cm/sec, η = 0.2, and A = 0.1 m^2. Probability of hitting a canister = 10^{-3} per hole, with expected removal of 15% contents.	0.07 m^3/drill hole	1400 m^3/drill hole	Analysis assumes no knowledge of repository before, during, or after drilling. Groundwater releases from post-sealing leakage are calculated in the text but are, in general, less significant than releases to the surface.
Granite	P, D	Postulated deterministic drilling rate, probabilistic for hitting canister.	A. Land surface B. Groundwater	A. Materials raised with drilling mud. B. Thermally induced convection.	A. Part of canister and fluid from waste drift. B. Uniform concentration.	No holes first century; 1 hole next century; 1 hole every four subsequent centuries. Holes sealed with permeability K = 10^{-4} cm/sec, η = 0.2, and A = 0.1 m^2. Probability of hitting a canister = 10^{-3} per hole, with expected removal of 15% contents.	No holes first century; 10 holes next century; 2 holes every subsequent century. Holes sealed with permeability K = 10^{-3} cm/sec, η = 0.2, and A = 0.1 m^2. Probability of hitting a canister = 10^{-3} per hole, with expected removal of 15% contents.	200 m^3/drill hole	5000 m^3/drill hole	Analysis assumes no knowledge of repository before, during, or after drilling. Groundwater releases from post-sealing leakage are calculated in the text but are, in general, less significant than releases to the surface.
Basalt	P, D	Postulated deterministic drilling rate, probabilistic for hitting canister.	A. Land surface B. Groundwater	A. Materials raised with drilling mud. B. Thermally induced convection and gradient from aquifer interconnection	A. Part of canister and fluid from waste drift. B. Uniform concentration.	No holes first century; 3 holes next century; 1 hole each subsequent century. All holes to lower aquifer. Holes sealed with permeability K = 10^{-4} cm/sec, η = 0.2, and A = 0.1 m^2. Probability of hitting a canister = 10^{-3} per hole, with expected removal of 15% contents.	No holes first century; 20 holes next century; 5 holes each subsequent century. All holes to lower aquifer. Holes sealed with permeability K = 10^{-3} cm/sec, η = 0.2, and A = 0.1 m^2. Probability of hitting a canister = 10^{-3} per hole, with expected removal of 15% contents.	200 m^3/drill hole	5000 m^3/drill hole	Analysis assumes no knowledge of repository before, during, or after drilling. Groundwater releases from post-sealing leakage are calculated in the text but are, in general, less significant than releases to the surface.

See Table D-11 for explanation of symbols and terms.

TABLE D-5
SUMMARY OF FUTURE DRILLING FAILURE ELEMENT (CONTINUED)

MEDIUM	PROBABILISTIC (P) DETERMINISTIC (D)	NATURE OF MODEL	RELEASE MODE	DRIVING FORCE	SOURCE TERM	PARAMETERS		FLUID TRANSPORTED TO SURFACE		COMMENTS
						1st ESTIMATE	2nd ESTIMATE	1st ESTIMATE	2nd ESTIMATE	
Shale	P, D	Postulated deterministic drilling rate, probabilistic for hitting canister.	A. Land surface B. Groundwater	A. Materials raised with drilling mud. B. Thermally induced convection and gradient from aquifer interconnection.	A. Part of canister and fluid from waste drift. B. Uniform concentration.	No holes first century; 5 holes next century; 2 holes each subsequent century. All holes to lower aquifer. Holes sealed with permeability $K = 10^{-4}$ cm/sec, $\eta = 0.2$, and $A = 0.1\ m^2$. Probability of hitting a canister = 10^{-3} per hole, with expected removal of 15% contents.	No holes first century; 50 holes next century; 5 holes each subsequent century. All holes to lower aquifer. Holes sealed with permeability $K = 10^{-3}$ cm/sec, $\eta = 0.2$, and $A = 0.1\ m^2$. Probability of hitting a canister = 10^{-3} per hole, with expected removal of 15% contents.	200 m^3/drill hole	5000 m^3/drill hole	Analysis assumes no knowledge of repository before, during, or after drilling. Groundwater releases from post-sealing leakage are calculated in the text but are, in general, less significant than releases to the surface.
Dome Salt	P, D	Postulated deterministic drilling rate, probabilistic for hitting canister.	A. Land surface B. Groundwater	A. Materials raised with drilling mud. B. Thermally induced convection.	A. Part of canister and fluid from waste drift. B. Uniform concentration.	No holes first century; 5 holes next century; 2 holes every subsequent century. Holes sealed with permeability $K = 10^{-4}$ cm/sec, $\eta = 0.2$, and $A = 0.1\ m^2$. Probability of hitting a canister = 10^{-3} per hole, with expected removal of 15% contents.	No holes first century; 30 holes next century; 5 holes every subsequent century. Holes sealed with permeability $K = 10^{-3}$ cm/sec, $\eta = 0.2$, and $A = 0.1\ m^2$. Probability of hitting a canister = 10^{-3} per hole, with expected removal of 15% contents.	0.04 m^3/drill hole	1300 m^3/drill hole	Analysis assumes no knowledge of repository before, during, or after drilling. Groundwater releases from post-sealing leakage are calculated in the text but are, in general, less significant than releases to the surface.

See Table D-11 for explanation of symbols and terms.

TABLE D-6
SUMMARY OF FAULT MOVEMENT FAILURE ELEMENT

MEDIUM	PROBABILISTIC (P) DETERMINISTIC (D)	NATURE OF MODEL	RELEASE MODE	DRIVING FORCE	SOURCE TERM	PARAMETERS		FLUID FLOW RATES FROM REPOSITORY TO UPPER AQUIFER				COMMENTS
						1st ESTIMATE	2nd ESTIMATE	1st ESTIMATE		2nd ESTIMATE		
								t (yrs)	$\dot{Q}$ (t) (m^3/yr)	t (yrs)	$\dot{Q}$ (t) (m^3/yr)	
Bedded Salt	P	Annual probability of occurrence of new fault or movement along old fault.	Groundwater	Thermally induced convection effect added to gradient from aquifer interconnection.	Canisters in fault zone broken and subject to leaching. Accumulated dissolved radionuclides by time of faulting assumed released through fault from 100-m wide zone around fault.	$\lambda = 2 \times 10^{-8}$ events/yr Flow path 1 m wide 4000 m long $K = 10^{-4}$ cm/sec $\eta = 0.1$ 100 canisters in fault zone. 5% repository in affected surrounding zone.	$\lambda = 4 \times 10^{-7}$ events/yr Flow path 1 m wide 4000 m long $K = 10^{-4}$ cm/sec $\eta = 0.1$ 100 canisters in fault zone. 5% repository in affected surrounding zone.	100 1000 10,000	8.2×10^4 6.9×10^4 2.6×10^4	100 1000 10,000	3.9×10^5 3.6×10^5 3.3×10^5	Fault may seal if flow rate is sufficiently small. Flow may be restricted by availability of water.
Granite	P	Annual probability of occurrence of new fault or movement along old fault.	Groundwater	Thermally induced convection	Canisters in fault zone broken and subject to leaching. Accumulated dissolved radionuclides by time of faulting assumed released through fault from 100-m wide zone around fault.	$\lambda = 2 \times 10^{-8}$ events/yr Flow path 1 m wide 4000 m long $K = 10^{-2}$ cm/sec $\eta = 0.1$ 100 canisters in fault zone. 5% repository in affected surrounding zone.	$\lambda = 10^{-6}$ events/yr Flow path 1 m wide 4000 m long $K = 10^{-2}$ cm/sec $\eta = 0.1$ 100 canisters in fault zone. 5% repository in affected surrounding zone.	100 1000 10,000	6.9×10^6 4.4×10^6 1.9×10^6	100 1000 10,000	6.9×10^6 4.4×10^6 1.9×10^6	Flow may be restricted by availability of water.
Basalt	P	Annual probability of occurrence of new fault or movement along old fault.	Groundwater	Thermally induced convection effect added to gradient from aquifer interconnection.	Canisters in fault zone broken and subject to leaching. Accumulated dissolved radionuclides by time of faulting assumed released through fault from 100-m wide zone around fault.	$\lambda = 5 \times 10^{-7}$ events/yr Flow path 1 m wide 4000 m long $K = 10^{-2}$ cm/sec $\eta = 0.1$ 100 canisters in fault zone. 5% repository in affected surrounding zone.	$\lambda = 10^{-6}$ events/yr Flow path 1 m wide 4000 m long $K = 10^{-2}$ cm/sec $\eta = 0.1$ 100 canisters in fault zone. 5% repository in affected surrounding zone.	100 1000 10,000	8.8×10^6 7.6×10^6 3.2×10^6	100 1000 10,000	4.0×10^7 3.8×10^7 3.4×10^7	Flow may be restricted by availability of water.
Shale	P	Annual probability of occurrence of new fault or movement along old fault.	Groundwater	Thermally induced convection effect added to gradient from aquifer interconnection.	Canisters in fault zone broken and subject to leaching. Accumulated dissolved radionuclides by time of faulting assumed released through fault from 100-m wide zone around fault.	$\lambda = 2 \times 10^{-8}$ events/yr Flow path 1 m wide 4000 m long $K = 10^{-4}$ cm/sec $\eta = 0.1$ 100 canisters in fault zone. 5% repository in affected surrounding zone.	$\lambda = 4 \times 10^{-7}$ events/yr Flow path 1 m wide 4000 m long $K = 10^{-4}$ cm/sec $\eta = 0.1$ 100 canisters in fault zone. 5% repository in affected surrounding zone.	100 1000 10,000	8.8×10^4 7.6×10^4 3.2×10^4	100 1000 10,000	4.0×10^5 3.8×10^5 3.4×10^5	Flow may be restricted by availability of water.
Dome Salt	P	Annual probability of occurrence of new fault or movement along old fault.	Groundwater	Thermally induced convection effect added to gradient from aquifer interconnection.	Canisters in fault zone broken and subject to leaching. Accumulated dissolved radionuclides by time of faulting assumed released through fault from 100-m wide zone around fault.	$\lambda = 3 \times 10^{-7}$ events/yr Flow path 1 m wide 4000 m long $K = 10^{-4}$ cm/sec $\eta = 0.1$ 100 canisters in fault zone. 5% repository in affected surrounding zone.	$\lambda = 10^{-5}$ events/yr Flow path 1 m wide 4000 m long $K = 10^{-4}$ cm/sec $\eta = 0.1$ 100 canisters in fault zone. 5% repository in affected surrounding zone.	1100 1000 10,000	8.2×10^4 5.0×10^4 2.6×10^4	100 1000 10,000	2.0×10^5 1.7×10^5 1.6×10^5	Fault may seal if flow rate is sufficiently small. Flow may be restricted by availability of water.

See Table D-11 for explanation of symbols and terms.

TABLE D-7
SUMMARY OF VOLCANO FAILURE ELEMENT

MEDIUM	PROBABILISTIC (P) DETERMINISTIC (D)	NATURE OF MODEL	RELEASE MODE	DRIVING FORCE	SOURCE TERM	PARAMETERS		RELEASE MODELING STEPS		COMMENTS
						1st ESTIMATE	2nd ESTIMATE	1st ESTIMATE	2nd ESTIMATE	
Bedded Salt	P	Annual occurrence probability.	Air and land surface.	Direct transport by moving gases and molten rock.	Fraction of repository brought to surface.	$\lambda = 1 \times 10^{-10}/yr$ Fraction of repository brought to surface is 0.4%, of which 1% is in respirable form, 9% consists of fine particles which can be easily dispersed, and 90% is reburied near the surface.	$\lambda = 1 \times 10^{-8}/yr$ Fraction of repository brought to surface is 0.4%, of which 1% is in respirable form, 9% consists of fine particles which can be easily dispersed, and 90% is reburied near the surface.	Direct release	Direct release	First estimate based on national average. Lower rates could probably be derived from additional siting assumption, such as location in East or Midwest.
Granite	P	Annual occurrence probability.	Air and land surface.	Direct transport by moving gases and molten rock.	Fraction of repository brought to surface.	$\lambda = 1 \times 10^{-10}/yr$ Fraction of repository brought to surface is 0.4%, of which 1% is in respirable form, 9% consists of fine particles which can be easily dispersed, and 90% is reburied near the surface.	$\lambda = 1 \times 10^{-8}/yr$ Fraction of repository brought to surface is 0.4%, of which 1% is in respirable form, 9% consists of fine particles which can be easily dispersed, and 90% is reburied near the surface.	Direct release	Direct release	First estimate based on national average. Lower rates could probably be derived from additional siting assumption, such as location in East or Midwest.
Basalt	P	Annual occurrence probability.	Air and land surface.	Direct transport by moving gases and molten rock.	Fraction of repository brought to surface.	$\lambda = 6 \times 10^{-10}/yr$ Fraction of repository brought to surface is 0.4%, of which 1% is in respirable form, 9% consists of fine particles which can be easily dispersed, and 90% is reburied near the surface.	$\lambda = 1 \times 10^{-8}/yr$ Fraction of repository brought to surface is 0.4%, of which 1% is in respirable form, 9% consists of fine particles which can be easily dispersed, and 90% is reburied near the surface.	Direct release	Direct release	Based on Columbia Plateau basalts.

See Table D-11 for explanation of symbols and terms.

TABLE D-7
SUMMARY OF VOLCANO FAILURE ELEMENT (CONTINUED)

MEDIUM	PROBABILISTIC (P) DETERMINISTIC (D)	NATURE OF MODEL	RELEASE MODE	DRIVING FORCE	SOURCE TERM	PARAMETERS		RELEASE MODELING STEPS		COMMENTS
						1st ESTIMATE	2nd ESTIMATE	1st ESTIMATE	2nd ESTIMATE	
Shale	P	Annual occurrence probability.	Air and land surface.	Direct transport by moving gases and molten rock.	Fraction of repository brought to surface.	$\lambda = 1 \times 10^{-10}/yr$ Fraction of repository brought to surface is 0.4%, of which 1% is in respirable form, 9% consists of fine particles which can be easily dispersed, and 90% is reburied near the surface.	$\lambda = 1 \times 10^{-8}/yr$ Fraction of repository brought to surface is 0.4%, of which 1% is in respirable form, 9% consists of fine particles which can be easily dispersed, and 90% is reburied near the surface.	Direct release	Direct release	First estimate based on national average. Lower rates could probably be derived from additional siting assumption, such as location in East or Midwest.
Dome Salt	P	Annual occurrence probability.	Air and land surface.	Direct transport by moving gases and molten rock.	Fraction of repository brought to surface.	$\lambda = 1 \times 10^{-10}/yr$ Fraction of repository brought to surface is 0.4%, of which 1% is in respirable form, 9% consists of fine particles which can be easily dispersed, and 90% is reburied near the surface.	$\lambda = 1 \times 10^{-10}/yr$ Fraction of repository brought to surface is 0.4%, of which 1% is in respirable form, 9% consists of fine particles which can be easily dispersed, and 90% is reburied near the surface.	Direct release	Direct release	Estimates based on national average. Could be refined to a lower value for salt dome region. First and second estimates are the same since from the standpoint of volcanism, the Gulf region shows no variation.

See Table D-11 for explanation of symbols and terms.

TABLE D-8
SUMMARY OF IGNEOUS INTRUSIVE FAILURE ELEMENT

MEDIUM	PROBABILISTIC (P) DETERMINISTIC (D)	NATURE OF MODEL	RELEASE MODE	DRIVING FORCE	SOURCE TERM	PARAMETERS		RELEASE MODELING STEPS	COMMENTS
						1st ESTIMATE	2nd ESTIMATE		
Bedded Salt	P	Annual probability of occurrence.	Groundwater	Physical transport of wastes by magma to upper aquifer.	Waste material intersected by magma.	$\lambda = 2 \times 10^{-10}$ Dimensions of dike: 1 m x 4 km, intersecting 0.05% waste inventory.	$\lambda = 4 \times 10^{-8}$ Dimensions of dike: 1 m x 4 km, intersecting 0.05% waste inventory.	Material moved to aquifer and subject to leaching. Leach characteristics of waste form assumed unchanged, although canisters would be removed.	Probabilities determined as 1% of values for faulting.
Granite	P	Annual probability of occurrence.	Groundwater	Physical transport of wastes by magma to upper aquifer.	Waste material intersected by magma.	$\lambda = 2 \times 10^{-10}$ Dimensions of dike: 1 m x 4 km, intersecting 0.05% waste inventory.	$\lambda = 10^{-7}$ Dimensions of dike: 1 m x 4 km, intersecting 0.05% waste inventory.	Material moved to aquifer and subject to leaching. Leach characteristics of waste form assumed unchanged, although canisters would be removed.	Probabilities determined as 1% of values for faulting.
Basalt	P	Annual probability of occurrence.	Groundwater	Physical transport of wastes by magma to upper aquifer.	Waste material intersected by magma.	$\lambda = 5 \times 10^{-8}$ Dimensions of dike: 1 m x 4 km, intersecting 0.05% waste inventory.	$\lambda = 10^{-7}$ Dimensions of dike: 1 m x 4 km, intersecting 0.05% waste inventory.	Material moved to aquifer and subject to leaching. Leach characteristics of waste form assumed unchanged, although canisters would be removed.	Probabilities determined as 1% of values for faulting.
Shale	P	Annual probability of occurrence.	Groundwater	Physical transport of wastes by magma to upper aquifer.	Waste material intersected by magma.	$\lambda = 2 \times 10^{-10}$ Dimensions of dike: 1 m x 4 km, intersecting 0.05% waste inventory.	$\lambda = 4 \times 10^{-8}$ Dimensions of dike: 1 m x 4 km, intersecting 0.05% waste inventory.	Material moved to aquifer and subject to leaching. Leach characteristics of waste form assumed unchanged, although canisters would be removed.	Probabilities determined as 1% of values for faulting.
Dome Salt	P	Annual probability of occurrence.	Groundwater	Physical transport of wastes by magma to upper aquifer.	Waste material intersected by magma.	$\lambda = 3 \times 10^{-8}$ Dimensions of dike: 1 m x 4 km, intersecting 0.05% waste inventory.	$\lambda = 5 \times 10^{-7}$ Dimensions of dike: 1 m x 4 km, intersecting 0.05% waste inventory.	Material moved to aquifer and subject to leaching. Leach characteristics of waste form assumed unchanged, although canisters would be removed.	Probabilities determined as 1% of values for faulting.

See Table D-11 for explanation of symbols and terms.

TABLE D-9
SUMMARY OF METEORITE IMPACT FAILURE ELEMENT

MEDIUM	PROBABILISTIC (P) DETERMINISTIC (D)	NATURE OF MODEL	RELEASE MODE	DRIVING FORCE	SOURCE TERM	PARAMETERS		FLUID FLOW RATES FROM REPOSITORY TO UPPER AQUIFER				COMMENTS
						1st ESTIMATE	2nd ESTIMATE	1st ESTIMATE		2nd ESTIMATE		
								t (yrs)	$\dot{Q}$ (t) (m^3/yr)	t (yrs)	$\dot{Q}$ (t) (m^3/yr)	
Bedded Salt	P	Annual occurrence probability.	A. Land surface B. Groundwater	A. Impact B. Thermal convection added to aquifer interconnection gradient.	A. 0.1% repository inventory to surface. B. 20% cumulative leached nuclides released to groundwater. Continued leaching of broken canisters in fracture or breccia zone (10%) and surrounding canisters (10%).	$\lambda = 4 \times 10^{-11}$/yr $A = 0.8\ km^2$ $K = 10^{-4}$ cm/sec $\eta = 0.2$	$\lambda = 4 \times 10^{-11}$/yr $A = 0.8\ km^2$ $K = 10^{-4}$ cm/sec $\eta = 0.2$	100 1000 10,000	1.6×10^7 1.4×10^7 5.0×10^6	100 1000 10,000	7.8×10^7 7.6×10^7 6.7×10^7	Water availability may severely limit flows below levels calculated.
Granite	P	Annual occurrence probability.	A. Land surface B. Groundwater	A. Impact B. Thermal convection.	A. 0.1% repository inventory to surface. B. 20% cumulative leached nuclides released to groundwater. Continued leaching of broken canisters in fracture or breccia zone (10%) and surrounding canisters (10%).	$\lambda = 4 \times 10^{-11}$/yr $A = 0.8\ km^2$ $K = 10^{-4}$ cm/sec $\eta = 0.2$	$\lambda = 4 \times 10^{-11}$/yr $A = 0.8\ km^2$ $K = 10^{-4}$ cm/sec $\eta = 0.2$	100 1000 10,000	1.4×10^7 8.8×10^6 3.8×10^6	100 1000 10,000	1.4×10^7 8.8×10^6 3.8×10^6	Water availability may severely limit flows below levels calculated.
Basalt	P	Annual occurrence probability.	A. Land surface B. Groundwater	A. Impact B. Thermal convection added to aquifer interconnection gradient.	A. 0.1% repository inventory to surface. B. 20% cumulative leached nuclides released to groundwater. Continued leaching of broken canisters in fracture or breccia zone (10%) and surrounding canisters (10%).	$\lambda = 4 \times 10^{-11}$/yr $A = 0.8\ km^2$ $K = 10^{-4}$ cm/sec $\eta = 0.2$	$\lambda = 4 \times 10^{-11}$/yr $A = 0.8\ km^2$ $K = 10^{-4}$ cm/sec $\eta = 0.2$	100 1000 10,000	1.8×10^7 1.5×10^7 6.3×10^6	100 1000 10,000	7.9×10^7 7.7×10^7 6.6×10^7	Water availability may severely limit flows below levels calculated.

See Table D-11 for explanation of symbols and terms.

TABLE D-9
SUMMARY OF METEORITE IMPACT FAILURE ELEMENT (CONTINUED)

MEDIUM	PROBABILISTIC (P) DETERMINISTIC (D)	NATURE OF MODEL	RELEASE MODE	DRIVING FORCE	SOURCE TERM	PARAMETERS		FLUID FLOW RATES FROM REPOSITORY TO UPPER AQUIFER				COMMENTS
						1st ESTIMATE	2nd ESTIMATE	1st ESTIMATE		2nd ESTIMATE		
								t (yrs)	$\dot{Q}(t)$ (m^3/yr)	t (yrs)	$\dot{Q}(t)$ (m^3/yr)	
Shale	P	Annual occurrence probability.	A. Land surface B. Groundwater	A. Impact B. Thermal convection added to aquifer interconnection gradient.	A. 0.1% repository inventory to surface. B. 20% cumulative leached nuclide released to groundwater. Continued leaching of broken canisters in fracture or breccia zone (10%) and surrounding canisters (10%).	$\lambda = 4 \times 10^{-11}$/yr $A = 0.8$ km^2 $K = 10^{-4}$ cm/sec $\eta = 0.2$	$\lambda = 4 \times 10^{-11}$/yr $A = 0.8$ km^2 $K = 10^{-4}$ cm/sec $\eta = 0.2$	100 1000 10,000	1.8×10^7 1.5×10^7 6.3×10^6	100 1000 10,000	7.9×10^7 7.7×10^7 6.8×10^7	Water availability may severely limit flows below levels calculated.
Dome Salt	P	Annual occurrence probability.	A. Land surface B. Groundwater	A. Impact B. Thermal convection added to aquifer interconnection gradient.	A. 0.1% repository inventory to surface. B. 20% cumulative leached nuclide released to groundwater. Continued leaching of broken canisters in fracture or breccia zone (10%) and surrounding canisters (10%).	$\lambda = 4 \times 10^{-11}$/yr $A = 0.8$ km^2 $K = 10^{-4}$ cm/sec $\eta = 0.2$	$\lambda = 4 \times 10^{-11}$/yr $A = 0.8$ km^2 $K = 10^{-4}$ cm/sec $\eta = 0.2$	100 1000 10,000	1.8×10^7 1.0×10^7 5.0×10^6	100 1000 10,000	4.0×10^7 3.4×10^7 2.9×10^7	Water availability may severely limit flows below levels calculated. Aquifer interconnection established by fracture zone at edge of salt dome.

See Table D-11 for explanation of symbols and terms.

TABLE D-10
SUMMARY OF BRECCIA PIPE FAILURE ELEMENT

MEDIUM	PROBABILISTIC (P) DETERMINISTIC (D)	NATURE OF MODEL	RELEASE MODE	DRIVING FORCE	SOURCE TERM	PARAMETERS		FLUID FLOW RATES FROM REPOSITORY TO UPPER AQUIFER				COMMENTS
						1st ESTIMATE	2nd ESTIMATE	1st ESTIMATE		2nd ESTIMATE		
								t (yrs)	$\dot{Q}$ (m^3/yr)	t (yrs)	$\dot{Q}$ (m^3/yr)	
Bedded Salt	P	Annual occurrence probability.	Upper aquifer	Thermally induced convection and aquifer interconnection.	Canisters in breccia pipe assumed to be broken and subject to leaching.	λ = 0 for t < 500 yrs λ = 10^{-8}/yr for t ≥ 500 yrs K = 10^{-2} cm/sec ϕ = 0.2 A = 3×10^4 m^2	λ = 0 for t < 500 yrs λ = 10^{-8}/yr for t ≥ 500 yrs K = 10^{-2} cm/sec ϕ = 0.2 A = 3×10^4 m^2	500 1000 10,000	6×10^7 5×10^7 2×10^7	500 1000 10,000	3×10^8 3×10^8 3×10^8	Limited availability of water from lower aquifer expected to significantly restrict flows below levels calculated.
Granite		N.A.										
Basalt		N.A.										
Shale		N.A.										
Dome Salt		N.A.										

See Table D-11 for explanation of symbols and terms.

TABLE D-11

EXPLANATION OF SYMBOLS AND TERMS IN TABLES D-1 THROUGH D-10

K = hydraulic conductivity, also referred to throughout as the permeability

t = time from repository closure

η = effective porosity of flow pathway

A = cross-sectional area of flow pathway

p = cumulative probability of occurrence

λ = annual probability of occurrence

$\dot{Q}$ = volumetric flow rate

n^-, n^+, where n is a value of time, t, refers to a jump in the value of a dependent variable (such as $\dot{Q}$) at $t = n$. The value associated with n^- is the limiting value as t approaches n through smaller values ($t < n$); the value associated with n^+ is the limiting value as t approaches n through larger values ($t > n$).

Groundwater -- Aquifer overlying the repository formation.

Salt closure or creep -- Tendency of salt to flow plastically under pressure.

Thermally induced convection -- Water heated by wastes has lower density and is forced upward by buoyancy effect.

Aquifer interconnection -- A pathway connecting aquifer above and below repository can lead to hydraulic imbalance (gradient) and corresponding flow. This flow has been modeled upward.

U-tube effect -- When at least two points in upper aquifer, at different hydraulic potentials, are connected to repository and to each other through backfilled tunnels, flow can result. The new pathway acts as a high resistance in parallel to the pathway through the aquifer connecting the two points.

Uniform concentration -- Average concentration in water in backfilled repository as a result of gradual leaching from waste package. May be limited either by leach rates or by solubility limits.

First estimate -- A parameter estimate assuming that the site exhibits favorable characteristics with respect to the particular breach mechanism in question (i.e., tending to reduce the risk).

Second estimate -- A parameter estimate assuming that the site exhibits somewhat less favorable characteristics (than first estimate) with respect to the particular breach mechanism in question, although it may be highly favorable with respect to other factors.

is a glossary of terms that are used in the main text, not just specialized geologic or engineering terms, but also terms that are used in the introductory chapters before they can be discussed at length. The remaining appendices generally discuss processes that take place in or near the repository and that affect the quantity of radionuclides that might be released in the event of a breach of containment.

D-2.0 GUIDELINES AND METHOD OF APPROACH

D-2.1 GENERAL APPROACH

There is wide current interest in the problem of estimating how well deep geologic repositories would be able to contain radioactive wastes. Research on this problem is being carried out by and for various government agencies and other institutions in the United States and abroad. The principal government programs in the United States are the following:

1. Environmental Protection Agency. The Agency is responsible for setting environmental standards governing the disposal of radioactive wastes. In this connection, it wants to take into account, among other factors, the estimated performance capabilities of geologic repositories, considered conceptually rather than on a design- or site-specific basis.
2. Nuclear Regulatory Commission. The Commission is responsible for licensing a geologic repository for high-level radioactive wastes. Therefore, it is developing its own modeling capabilities in order both to determine appropriate regulatory guidelines and to evaluate license applications.
3. Department of Energy. The Department is responsible for siting, constructing, obtaining a license for, and operating a system for high-level radioactive waste disposal; and the disposal option of a deep geologic repository is being pursued as its favored approach.(1) Therefore, it is developing modeling capabilities to use both in decisions regarding design and siting and in making application for a license.

Because of these and other programs, there is an extensive literature base on the potential performance of geologic repositories for nuclear wastes. Much of this literature is cited throughout this report.

There are two important aspects to the performance evaluation:

1. The identification of scenarios or failure modes that would result in or contribute to a breach of the repository containment.

2. The modeling of identified scenarios and failure modes in order to assess their impact on the environment or on human health.

Various approaches to the first aspect have been vigorously pursued, examples of which include:

1. The development of fault trees and, from them, event chains. This approach has received impetus from the Reactor Safety Study(2) and from the wide application of similar techniques in other safety analyses.
2. The convening of panels of experts to list every failure element or scenario they could reasonably imagine, and then to refine and combine such lists.
3. The identification of scenarios that would be extreme and whose consequences would be expected to bound those of any other scenarios, the latter of which would then not need to be defined in detail.

The present study drew extensively on this earlier work in failure mode identification,(3-12) rather than developing sets of potential failure elements independently.

With respect to the modeling of failure modes, it was not possible to rely heavily on earlier work. There were two principal reasons for this:

1. Other modeling efforts have generally been carried out for different purposes than those of the present study. In particular, models have been developed with specific sites in mind, or at least with a view to eventual application to specific sites. Therefore, these models can require detailed site-specific data that may not even be available at present. This study had to be more general in perspective and less demanding in data requirements.
2. High priority was attached to developing models that would be as simple as possible. Not only would these be more informative and understandable to the users of this report, but they would enable the easier identification of important assumptions and uncertainties.

In spite of the limited applicability of the results of other modeling efforts to the requirements of Task D, it has been possible to incorporate some of the modeling parameters derived elsewhere into models developed in this study. Whenever possible, the results of the Task D analysis have been compared or contrasted with results obtained elsewhere.

It is important to emphasize at the outset that it is not the intent of this study to draw any conclusions about the safety of the disposal of radioactive wastes in geologic repositories. Such responsibilities fall to the regulatory agencies and, more generally, to the public through their elected government officials. The purpose of this study, and in particular Task D, is to provide modeling techniques and calculational results that have been requested as input for the regulatory decision-making process. It should be noted that uncertainties enter the analysis at every phase, from specific input data, to the validity of modeling techniques, to the overall question of whether something important might have been left out. It is not possible to prove rigorously the correctness or completeness of the results. However, it would be unusual to find any serious decision process founded on complete and totally certain information. Therefore, in this report the intention has been simply to explain the analytical methods by which the results were obtained, to provide the rationale for the choice of models and parameters, and to relate these, as far as possible, to similar work being carried out by other groups. It is largely through the peer review process that studies such as this receive valuable feedback that can enhance the accuracy and precision of the results. An early draft report on Task D received a wide review, which has been very valuable in the preparation of this report.

D-2.2 SPECIFIC GUIDELINES

In developing a modeling strategy for nuclear waste repositories, it is necessary to determine initially the time period for which the models should apply. Various time periods have occasionally been suggested, ranging from relatively short ones, such as 300 years, to rather long ones, such as 10 million years. Part of the determination of time frames depends on the nature of the wastes that would be placed in a repository. Active and predominant fission products, such as cesium-137 and strontium-90, have half-lives on the order of 30 years, so that after a few hundred years they will have decayed to relatively low levels. Transuranic elements, as well as some fission products, such as technetium-99, have much longer half-lives. If spent reactor fuel is placed in a repository, there would be a higher proportion of the long-lived elements. The Task A Report discusses in greater detail how these activity levels vary with time.

The regulatory philosophy in evidence in the United States today on the subject of hazardous waste disposal is in a state of flux, largely because of increased quantities of wastes and a greater awareness of the pitfalls of past practice. Nevertheless, even new regulations make no attempt to guarantee the complete integrity of the containment system in perpetuity. Time periods of 30 to 100 years are generally the longest under consideration even though many hazardous materials do not decay or degrade with time. In the case of nuclear waste repositories, it was decided jointly by Arthur D. Little, Inc., and EPA to develop performance models for a period of 10,000 years. This was thought to be a conservatively long time period for repository evaluation, in the sense that even a shorter period might be sufficient and consistent with regulatory philosophy utilized in other areas. The 10,000-year period allows for the modeling not only of direct releases to the biosphere, but also of releases through groundwater pathways, which can require very long times before harmful effects might occur. If the modeling effort were carried even further into the future, the significance of the results would decrease accordingly because so many factors (available technology, population characteristics, future medical capabilities, dominant health concerns, etc.) might be changed. In fact, the past 10,000 years span the development of all important human civilizations, and it does not seem necessary to carry future projections into longer periods than this.

A second guideline for this study was that the performance evaluation period should begin at the time the repository is sealed. During the operational stage of the repository, there may exist some risk of the release of radionuclides. For example, an accident could occur in transporting or emplacing a waste canister. Risks of this type would be addressed by other regulations governing fuel cycle facilities, but they are not addressed here.

A third guideline relates to the degree of future institutional control or human knowledge of the repository. Consistent with EPA direction, no control of the site after 100 years from repository sealing has been assumed. In this study, this has been taken to imply even the loss of knowledge that a repository exists on the site. Up until this 100-year period has elapsed, however, full institutional control of the site has been assumed to be capable of preventing intrusions that could breach the containment system.

The last specific guideline has been referred to earlier, namely, that this study is directed to the concept of geologic repositories rather than to repositories at specific sites or with specific designs. Thus it has been necessary to abstract from the literature a set of engineering and geologic assumptions that represent so-called "generic" repositories. Because the question of the estimation and importance of uncertainties inevitably enters modeling efforts such as this, it is important to note that in the case of generic repositories this question takes an unusual form. It is not meaningful to assess the degree of certainty one attaches to a parameter for a generic repository, since by definition a generic repository is hypothetical and is defined by whatever parameters have been specified. Rather, the uncertainty question is transformed into the question of the variability of real sites vis-a-vis the parameter values used in the generic model. In the case of expected significant variability among real sites, two estimates for parameters have been given in the generic description, one corresponding to rather favorable conditions (i.e., supportive of containment) and another that would not appear to be so favorable. These are referred to as the "first" and "second" estimates, respectively. They are discussed in Section D-2.6.3.

D-2.3 SELECTION AND CHARACTERIZATION OF GENERIC GEOLOGIES

Based on the site selection programs of the Department of Energy and the supporting research work reported in the literature, the following five geologic host media were chosen for detailed treatment in this study:

- bedded salt
- granite
- basalt
- shale
- dome salt

There are other rock types that have been or are being seriously considered for repositories, among which are welded volcanic tuff, desert alluvium, anhydrite, and seabed sediments.(13-16) Nevertheless, the media chosen span a wide range of geologic structure and rock properties, and an analysis based on them is believed to be representative of the performance capabilities of geologic repositories in general. The subsequent paragraphs contain discussions of the chosen rock types and descriptions of the associated geologies assumed in this study. Naturally, there can be wide variability in the geologic parameters associated with a given type of rock.

D-2.3.1 Bedded Salt

Bedded salt has been prominently mentioned as a possible nuclear waste repository host rock ever since a committee of the National Academy of Sciences proposed that waste be buried in deep, stable geologic media.(17) Perhaps more research has gone into determining the suitability of salt for this purpose than for any other lithology.(3,4,18,19,20) In Germany, some low-level radioactive waste has already been deposited in unused salt mines.(21) This interest in salt is the result of some of its unique properties, in addition to its common occurrence in stable formations at depths being considered for repositories (200 m to 1000 m).

Salt is very soluble. However, it behaves plastically under pressure, thereby tending to creep back into voids and cracks and seal itself against the movement of water. This accounts for the lack of water in most salt mines. Salt is also a relatively good thermal conductor and thus has the ability to dissipate the heat generated by the wastes. The sedimentary sequences containing salt beds generally contain aquifers both above and below the salt.

Salt itself is frequently mined, and there may be associated deposits of other minerals or oil and gas. However, because massive salt deposits are numerous, locations can probably be found with minimal economic value and with a range of other desirable characteristics.

A map of prominent salt deposits in the United States is shown in Figure D-1. The generic bedded salt stratigraphy adopted for modeling purposes is shown in Figure D-2. It is implicit that the salt formation is in a stable basin, and that the strata are relatively uniform and continuous beyond the repository. For hydrologic modeling, both aquifers are assumed to have identical horizontal gradients of 0.002 and 0.02 for first and second estimates, respectively. An average upward vertical gradient for any connection between aquifers is assumed to exist and to have the values 0.01 and 0.5 for first and second estimates, respectively. (Note that a downward gradient may exist and would, in general, represent a more favorable condition since any leakage would then be to strata at greater depths. However, for conservatism, an upward gradient has been assumed even in the first estimate case.) The salt itself is assumed to be essentially impermeable to the flow of water.(22,23,24)

D-2.3.2 Granite

Granite, or some similar monolithic crystalline rock, is another important host rock. Canadian and Swedish studies of granitic rock as a storage medium have provided some insight and details into the nature of this candidate material.(25,26) Excavations in granite have been used for storage and military purposes.

Granite is an assemblage of minerals forming a rigid and essentially insoluble rock. It is relatively strong and does not flow plastically; thus, cracks can remain open to migrating fluids although some become filled with clay or other materials. It does not conduct heat well, but it does have a high heat capacity. In addition, the water passing through granite is generally less corrosive than the brines and bitterns associated with salt. Because it is an intrusive, and therefore not

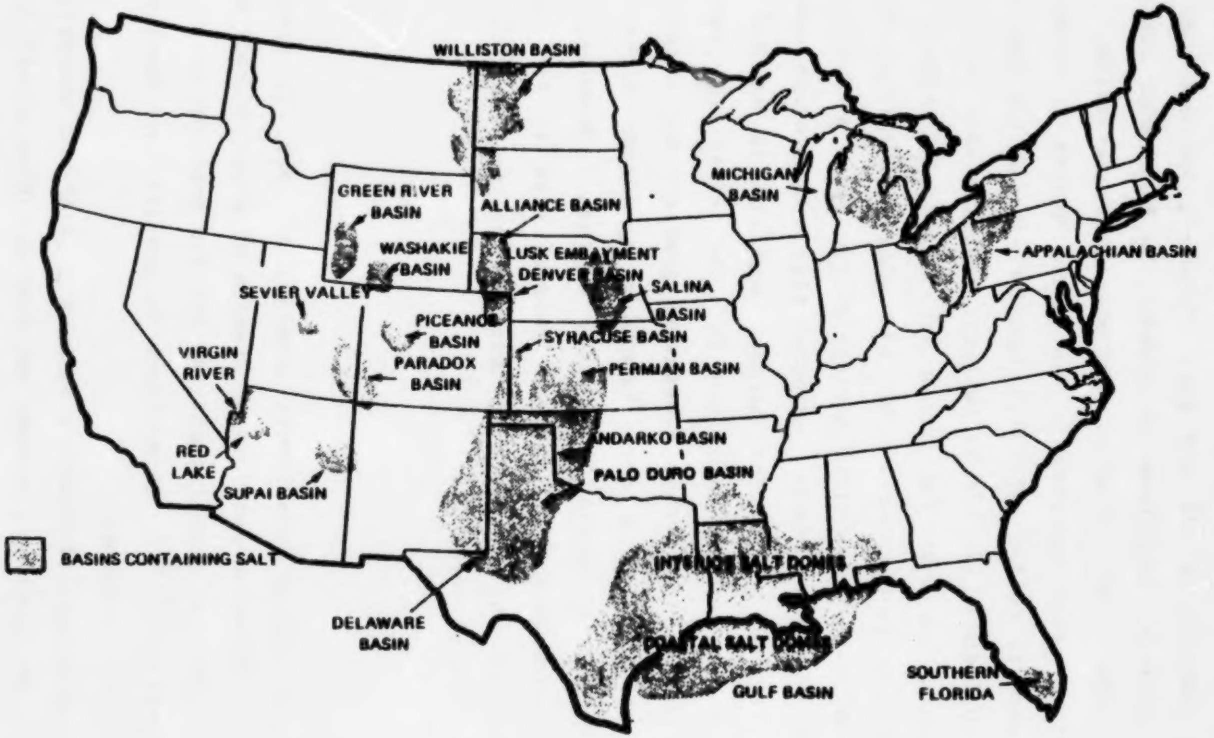

Source: Adapted from U.S. Department of Energy, *Draft Environmental Impact Statement: Management of Commercially Generated Radioactive Waste,* Volume I, April 1979.

FIGURE D–1 ROCK SALT DEPOSITS IN THE UNITED STATES

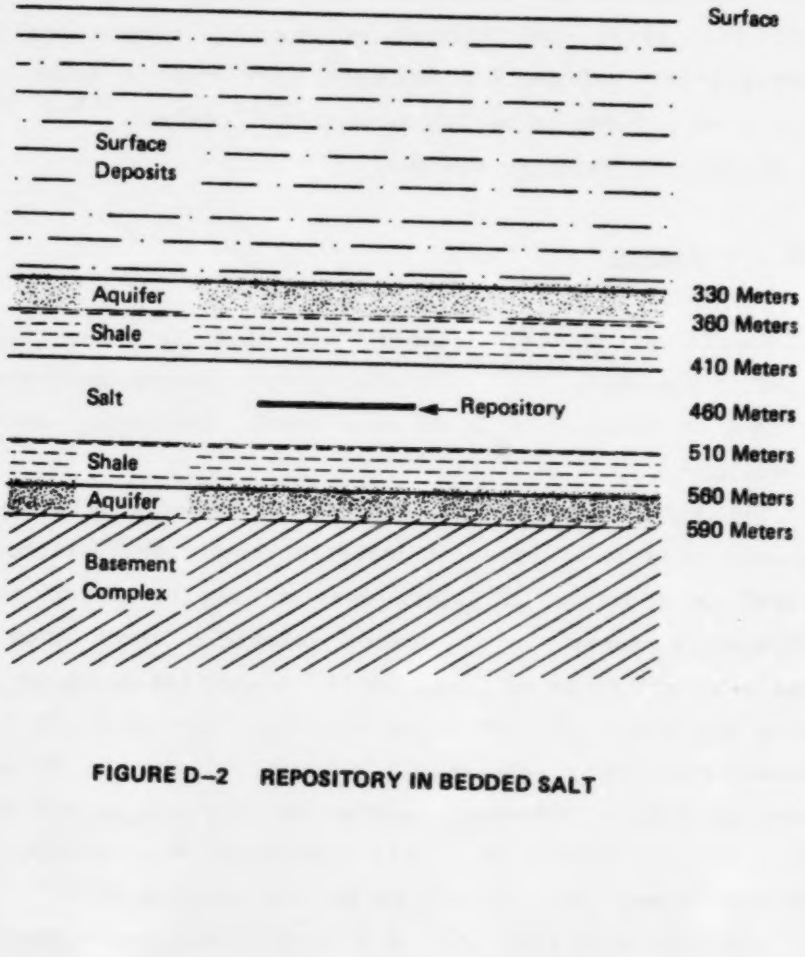

FIGURE D–2 REPOSITORY IN BEDDED SALT

stratified, granite is modeled without an underlying aquifer. This limits the mechanisms for water flow through the repository.

Many areas of the country have granite or similar rocks at suitable depths for a repository. Occasionally, vein minerals, pegmatites, or quarry stone make granite economically important, but the vast expanse of crystalline rocks suggests that many potential site locations remain.

A map of prominent granitic formations is shown in Figure D-3a. The generic granite geology adopted for modeling purposes is shown in Figure D-4. The aquifer is assumed to have horizontal gradients of 0.002 and 0.02 for first and second estimates, respectively. Reported permeability values for granite vary over a wide range of test conditions and may be as low as 4×10^{-12} cm/sec.(19,27-30) Fluid flow is governed by fracture systems.

D-2.3.3 Basalt

Basalt is another igneous rock that is being considered as a repository medium.(19,31) It shares with granite many properties common to igneous rocks. It is strong, rigid, insoluble, and has a complex mineralogy.

The extensive flow basalts being investigated are unlike other igneous rocks in a number of important ways. Because these basalts have formed as a series of layers over a long period of time, there are sedimentary interbeds and other permeable zones that can serve as aquifers, and these aquifers would be expected to exist both above and below any basalt flow in which the repository would be located. Basalt characteristically breaks into slender columns as it cools, producing vertical joints. However, weathering products of the rock often fill these cracks. Basalt is rarely associated with mineral resources, and its most common economic use is as fill material.

The principal flow basalts that are being investigated for possible repository siting are limited to the northwestern United States, in the states of Washington, Oregon, and Idaho. (See Figure D-3.) The generic basalt stratigraphy assumed in this study is shown in Figure D-5. The hydraulic gradients within and between aquifers are assumed to be the same as those specified earlier for bedded salt. Reported permeability

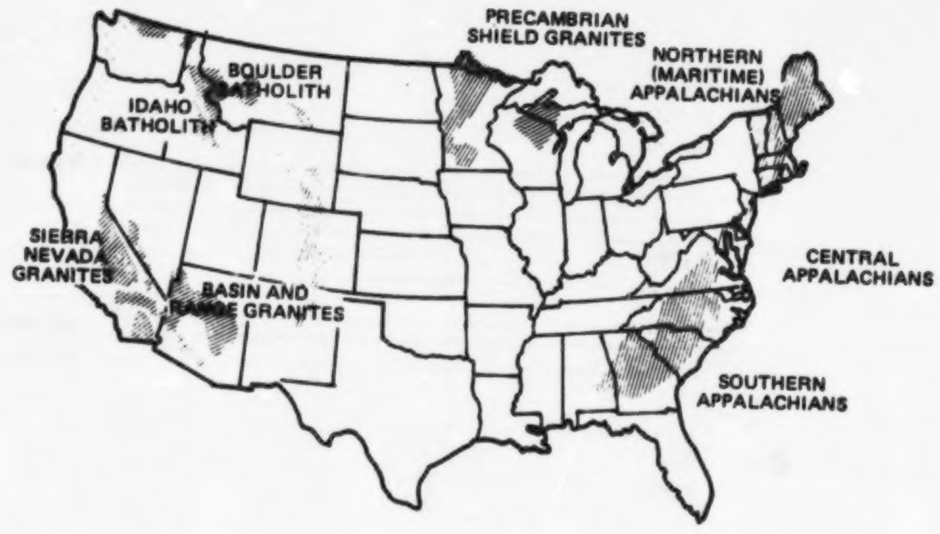

a. Granitic Rock

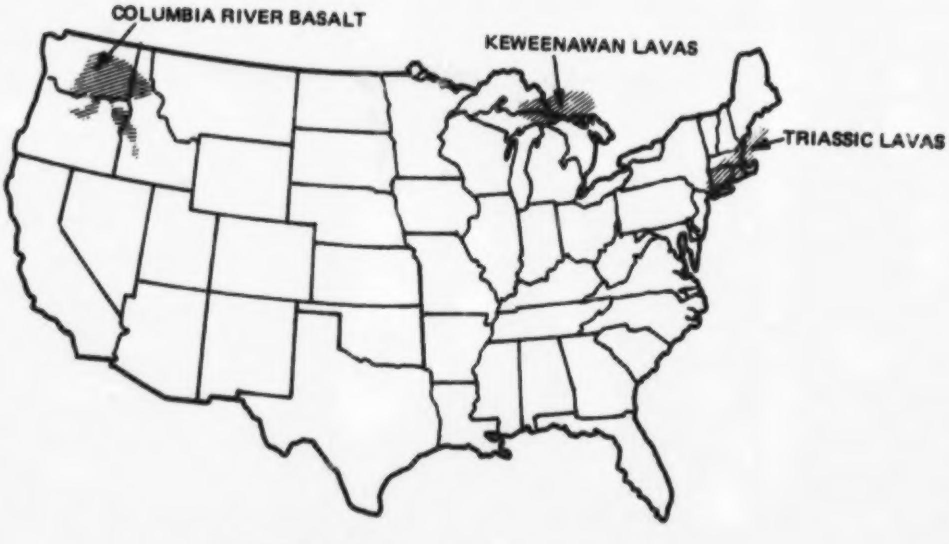

b. Potential Repository Basalts

Source: U.S. Department of Energy, *Draft Environmental Impact Statement: Management of Commercially Generated Radioactive Waste*, Volume 1, April 1979.

FIGURE D–3 CRYSTALLINE FORMATIONS IN THE UNITED STATES

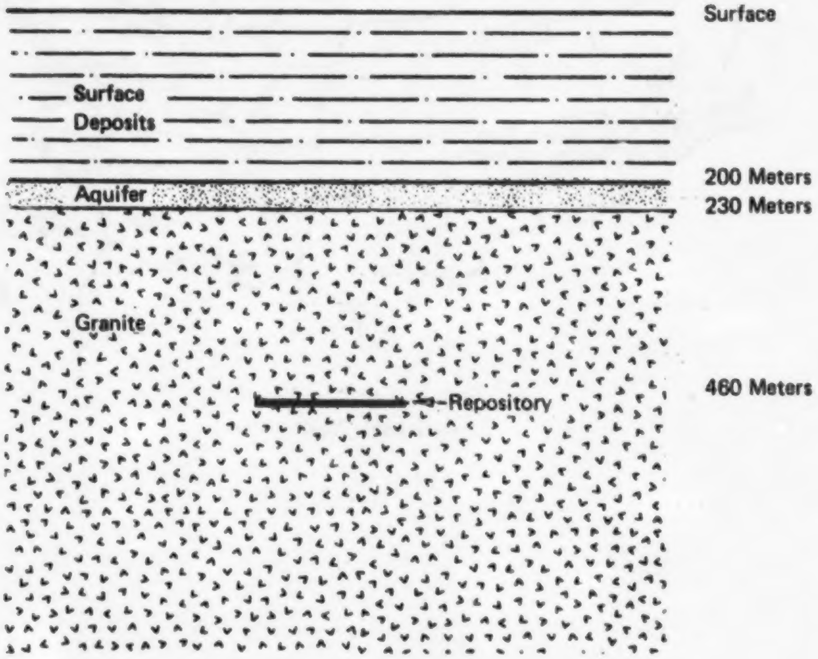

FIGURE D–4 REPOSITORY IN GRANITE

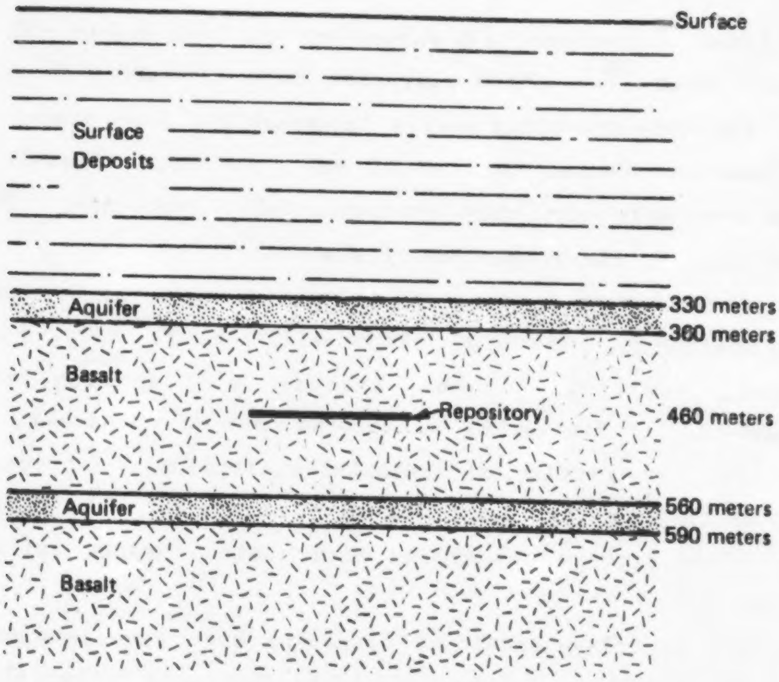

FIGURE D–5 REPOSITORY IN BASALT

values for basalt range as low as 10^{-13} cm/sec, but there is a wide range due to variable rock properties and test conditions.(19,31,32,33)

D-2.3.4 Shale

Argillites, siltstones, and shales are the most common and extensive sedimentary rocks.(34) These clay-rich rocks are often found in thick deposits, and they are often nearly impermeable. Some shales exhibit a plastic behavior similar to that of salt, but clay minerals have the advantage over salt that they are essentially insoluble. There is a very wide range in the properties of shales.

Clay minerals have a number of properties that may be important to waste containment. Several clays will absorb water into their structures, swelling in the process and sealing the water passageways.(35) Similarly, clays can adsorb chemicals, including radionuclides, restricting or essentially stopping their movement.(36) However, as they can hydrate, many clay minerals can be dehydrated by heating. This process may change both their chemical and mechanical properties.

Argillaceous (clay-containing) deposits have a variety of economic uses. Their abundance, however, suggests that many potential sites are available where economic and other social impacts would be minimal.

A map of shales and related argillaceous deposits in the United States is given in Figure D-6. The generic shale stratigraphy adopted for modeling purposes is shown in Figure D-7. It is assumed that the shale being modeled is highly indurated, which would aid the stability of a mine while perhaps increasing the potential for fluid flow through fractures. While some shales are nearly impermeable to the flow of water, the hard shale in the model is assumed to have hydrologic properties similar to those of basalt. Assumptions about the aquifer hydraulic potentials are taken to be the same as in the case of bedded salt and basalt. Reported shale permeabilities cover a very wide range.(12,19,22,29,37,38,39)

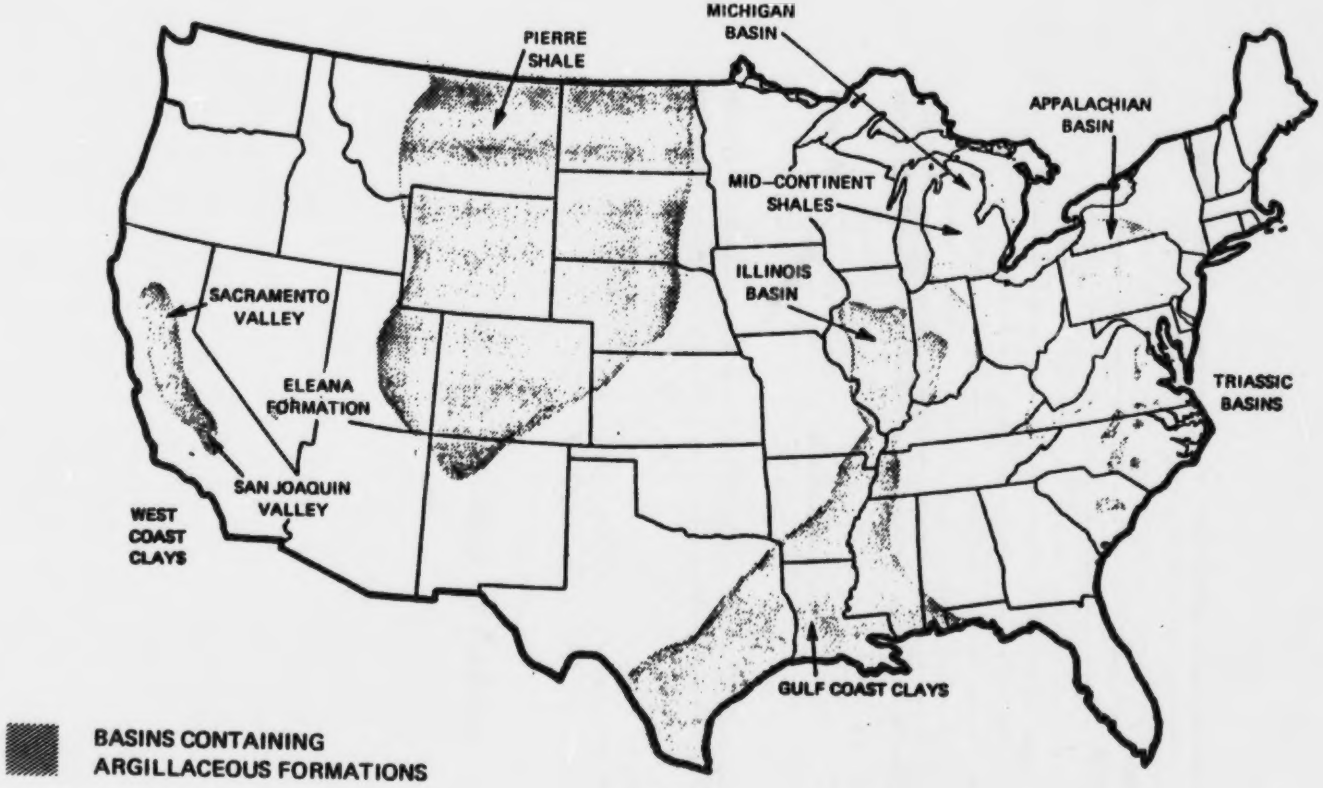

Source: U.S. Department of Energy, *Draft Environmental Impact Statement: Management of Commercially Generated Radioactive Waste*, Volume 1, April 1979.

FIGURE D–6 ARGILLACEOUS FORMATIONS IN THE UNITED STATES

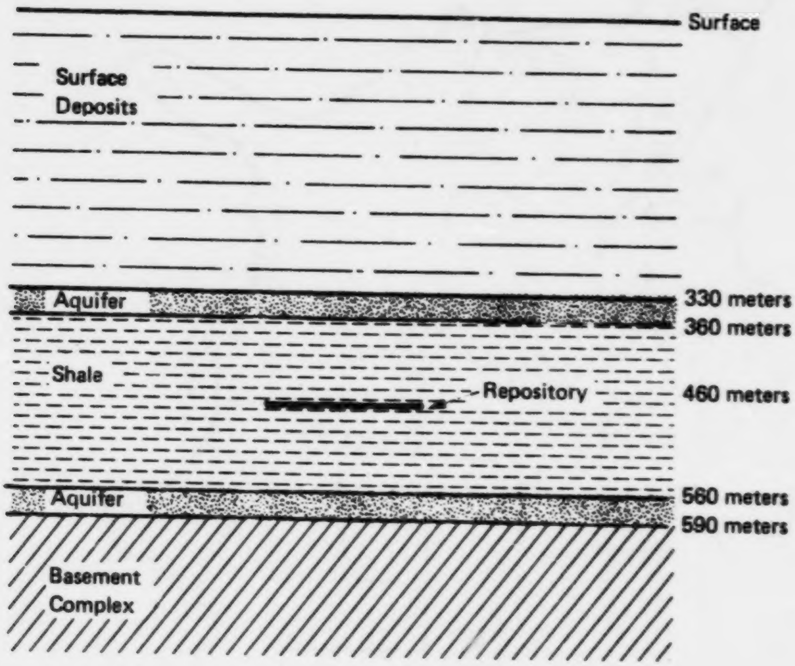

FIGURE D–7 REPOSITORY IN SHALE

D-2.3.5 Dome Salt

Many salt deposits are not bedded, but are formations that have been forced up through overlying rocks from original beds at considerable depths. These domes or stacks of salt are composed of fairly homogeneous halite and are generally devoid of interbeds or similar features found in bedded salt. Typically, a salt dome will be roughly a kilometer in diameter and capped with a blanket of less soluble evaporites.(40,41)

Because a dome is injected into the overlying rock, the latter is often shattered and disrupted with prevalent joints and fractures. The salt itself may come very near to, or even reach, the surface; but the source of the salt column may extend to depths near 10 kilometers.(42) The geometry of a dome implies that an aquifer directly below the repository will not exist. However, the fracturing of the adjacent rock indicates that the salt will be in contact with groundwater in adjacent aquifers. These and other differences between bedded and dome salt deposits indicate that each deserves a separate analysis. As with bedded salt deposits, domes are frequently associated with oil, gas, and various mineral resources.

Salt domes are found in several states in the South, as shown in Figure D-1. The generic dome salt stratigraphy adopted for modeling purposes is shown in Figure D-8. The hydraulic conditions in the upper aquifer are assumed to be the same as in all the other cases. For certain failure elements, the lower aquifer, while not directly below the repository, is relevant. The vertical hydraulic gradients upward between it and the upper aquifer have the values 0.01 and 0.2 for first and second estimates respectively. The salt itself is assumed to be essentially impermeable to the flow of water.(22,23,24)

D-2.4 REPOSITORY ASSUMPTIONS

Conceptual repository designs have been discussed in the Task A and B Reports and continue to be modified and refined in studies for the Department of Energy.(19,43) Based on this work, the parameters given in Table D-12 have been used in this report. It should be noted that

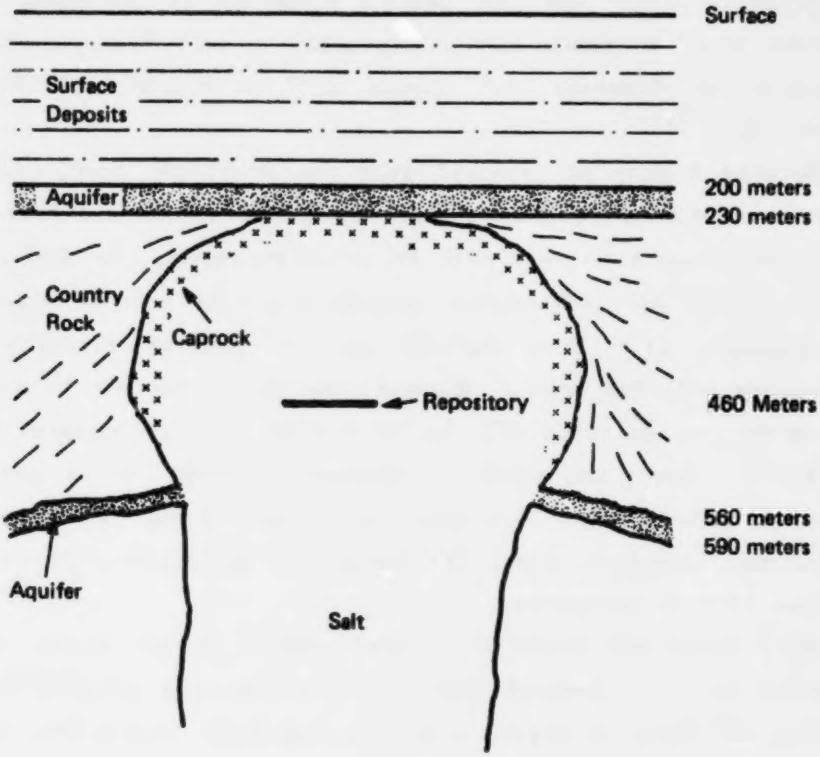

FIGURE D–8 REPOSITORY IN SALT DOME

TABLE D-12

NOMINAL REPOSITORY PARAMETERS USED FOR MODEL CALCULATIONS

Depth of repository	460 m
Areal dimensions	2 km x 4 km
Number of canisters	35,000
Number of waste drifts	350
Canisters per waste drift	100
Length of waste drift	500 m
Canister spacing	5 m
Total mined volume	10^7 m^3
Percent of total volume used for waste drifts	90%

actual designs might vary considerably from the values given. For example, a repository in an average-size salt dome could not occupy the horizontal area specified in the table. Such differences are not important for the purposes of the present performance model. Other parameters specific to individual model calculations will be introduced as necessary in later sections of this report.

D-2.5 IDENTIFICATION OF FAILURE MECHANISMS

The principal purpose of Task D is to identify potential breach-of-containment mechanisms for geologic repositories and to characterize them quantitatively. A review of the literature indicated a wide range of potential failure mechanisms that have been identified. These were evaluated and compared to determine their relative importance; and, as a result, ten were selected for detailed modeling. These are shown in Table D-13. It is believed that a repository performance assessment based on these mechanisms includes the dominant contributors to risk and covers the range from likely events with small consequences to very unlikely events with large consequences. A number of events and processes not chosen for detailed modeling are also discussed later in this report. Many of these are relatively slow geologic processes that would not be expected to have significant effects over the 10,000-year time frame chosen for this study.

D-2.6 CONCEPTUAL FRAMEWORK FOR QUANTITATIVE ANALYSIS

The quantitative evaluation of potential breach-of-containment mechanisms includes two principal aspects:

1. Estimates of the likelihood or probability of occurrence of various mechanisms.
2. Estimates of the consequences of such mechanisms.

Naturally, it is important to take into account interactions between various mechanisms when these appear to be capable of increasing either their likelihood or their consequences.

TABLE D-13

FAILURE ELEMENTS CHOSEN FOR DETAILED MODELING

TECHNOLOGICAL

- Flow through bulk rock with altered permeability
- Shaft seal failure
- Borehole seal failure
- Undetected boreholes

HUMAN INTRUSION

- Future drilling

NATURAL

- Fault movement
- Volcanoes
- Igneous intrusives
- Meteorites
- Breccia pipes

D-2.6.1 Probabilities

It is inevitable that probabilistic considerations enter into any performance assessment program for repositories, even if they do not enter explicitly. This is true even for the approach using so-called "worst case scenarios", since the judgment is made therein that cases worse than those treated have negligible probabilities of occurrence. Despite the ubiquitous necessity of at least qualitative judgments on likelihoods and probabilities, efforts to systematize and quantify such judgments are difficult to carry out and often lacking in precedent.

Probabilities may be interpreted in different senses, according to various schools of thought.(44) They may, for example, be used to refer to the long-term frequency of occurrence of certain events. On the other hand, they may be taken as subjective measures of belief that a certain event will occur. Statistical analyses usually derive probabilities from data on frequency of occurrence; decision analysis and strategic planning often deal more with probabilities as measures of belief. In these and other interpretations of probabilities, the same mathematical formulations apply, and in areas where the different interpretations overlap, the results will ordinarily be consistent. The approach of the present study was strictly pragmatic. It was desired to use the best information available to clarify and improve otherwise qualitative judgments, even though the result might fall somewhat short of a mathematically axiomatized probability theory. Thus the probabilities assigned to various breach-of-containment mechanisms had to be derived on an *ad hoc* basis. Some result from crude statistical analyses, some from simple models with statistical components, and some primarily from the judgment of the authors, based on personal experience and a review of the literature. In each case the derivation of the probabilities has been explained.

D-2.6.2 Consequences

The ultimate consequences of concern in evaluating repository performance capabilities are adverse effects on the health of present and future generations. The estimation of such consequences requires several steps:

1. The physical characterization of a breach of containment mechanism.
2. The characterization of a source term, i.e., the radionuclide inventory affected by the breach.
3. The identification and quantification of driving forces that would tend to move the radionuclides out of the repository.
4. The modeling of the actual leaching of radionuclides and their transport through groundwater systems or through surface pathways.
5. The calculation of doses to individuals and populations.
6. The estimation of the health effects of the calculated doses.

The scope of Task D only pertains to the first three of these steps. The last three are being modeled by the EPA, based on methods described in Task C and elsewhere.

The physical characterization of breach mechanisms generally involves considerations such as size, depth, location, permeability, and porosity of the resulting pathway. Not all of these apply to all cases since the mechanisms vary widely. The characterization of the source term generally refers to the extent of the repository subject to the effects of the breach. For example, one waste drift might be subject to leaching as the result of a borehole passing through it. The term "uniform concentration" is frequently used in the sequel to refer to the average concentration of radionuclides in the waste drifts as a result of canister degradation and leaching of the waste form. Parameters and models relating to corrosion and leaching have been discussed in the reports of Tasks B and C. (Appendix D-VIII of this report also discusses some aspects of canister performance.)

Driving forces that enter into various release calculations include direct physical transport and transport in groundwater. Groundwater flows can be driven by a number of factors that affect hydraulic potentials, such as artesian conditions in confined aquifers, buoyancy forces resulting from density differences, and others. Several of these are discussed in the appendices, the principal results being employed in the main text.

A prerequisite for a number of the release mechanisms is that the repository and the surrounding rock return to a saturated condition after the perturbation caused by the operational stage, during which any water in the surrounding rock would tend to flow into the cavity and then be pumped out. Resaturation times for all cases have been estimated in Appendix D-II. For all but the two repositories in salt, these times are not judged to be significant enough to warrant further consideration. However, since salt tends to flow plastically and close up void spaces, the time to establish resaturation is closely related to the total quantity of water present under that condition. For this reason, resaturation is considered in connection with a number of release mechanisms in the salt repositories.

D-2.6.3 Uncertainty and Variability

The subject of uncertainty analysis has been briefly referred to earlier (Section D-2.1), where it was pointed out that the basic question is one of variability, namely, to what extent might the properties of real sites vary from those used in the generic description. When significant variability is identified, it is incorporated into the analysis by the use of so-called "first" and "second" estimates, defined as follows:

First Estimate -	a parameter estimate assuming that the site exhibits favorable characteristics with respect to the particular breach mechanism in question (i.e., tending to reduce the risk).
Second Estimate -	a parameter estimate assuming that the site exhibits somewhat less favorable characteristics with respect to the particular breach mechanism in question, although it may be highly favorable with respect to other factors.

In both cases, models and approximations have been chosen to err on the conservative side, i.e., tending to overestimate the likelihood or the consequences of the events. It is believed that, for each first estimate, sites will be able to be identified where the corresponding property is at least as good as the estimate. Many more sites can probably be found where the property is better than the second estimate. The use of relatively simple models in the report, rather than complex computerized ones, facilitates the determination of the sensitivities of results to the various input parameters and assumptions.

It is important to emphasize that the primary emphasis in this study has been on rough order-of-magnitude estimates. Therefore specific details that could only slightly perturb the results are often ignored. At the same time, a number of the calculations are reported with greater precision than the input data or the goals justify. This has been done simply to aid readers who wish to retrace the calculations in order to test their understanding of the methods employed.

D-3.0 TECHNOLOGICAL FAILURE ELEMENTS

The failure elements considered in this chapter correspond either to the degradation or failure of engineered systems or to the effect of the repository on the host geologic formation. Those elements chosen for detailed modeling are all capable of providing pathways for the movement of radionuclides from the repository to the aquifer system. Failures in some individual components, such as waste forms, are briefly discussed in Section D-3.5.

D-3.1 FLOW THROUGH BULK ROCK

D-3.1.1 Summary

A major consideration in both the design and the performance assessment of a repository is the fact that high-level radioactive wastes generate considerable quantities of heat. This heat can affect both engineered barriers to waste migration, such as waste forms and canisters, and the surrounding rock. The present model deals with the latter aspect.

In particular, temperature changes cause stress changes in the rock, which can alter its hydraulic conductivity. Examples of mechanisms for this alteration include additional fracturing, movement along fractures, or changes in the dimensions of fractures or pores. For repositories in salt, either bedded or domed, probabilistic calculations were carried out, based on a statistical characterization of spatially varying materials properties, to determine the probability of a fracture pathway developing through the salt. For the non-salt repositories -- granite, basalt, and shale -- a simple deterministic model was used for the variation of the hydraulic conductivity as a function of time.

A summary of the analysis is given in Table D-14, and the details follow in subsequent sections.

Preceding page blank

TABLE D-14
SUMMARY OF FLOW THROUGH BULK ROCK FAILURE ELEMENT

MEDIUM	PROBABILISTIC (P) DETERMINISTIC (D)	NATURE OF MODEL	RELEASE MODE	DRIVING FORCE	SOURCE TERM	PARAMETERS		FLUID FLOW RATES FROM REPOSITORY TO UPPER AQUIFER				COMMENTS
						1st ESTIMATE	2nd ESTIMATE	1st ESTIMATE		2nd ESTIMATE		
								t (yrs)	$\dot{Q}(t)$ (m^3/yr)	t (yrs)	$\dot{Q}(t)$ (m^3/yr)	
Bedded Salt	P	Cumulative occurrence probability	Groundwater	Pressure from salt closure, thermally induced convection, and gradient from aquifer interconnection	Uniform concentration	$p = 0$	$p = 0$	No releases need to be calculated.		No releases need to be calculated.		The probability that the spatial variability in rock strength could lead to an extensive pathway from the repository that would fracture under the stresses experienced was found to be negligible.
Granite	D	Change in permeability after thermal peak	Groundwater	Thermally induced convection	Uniform concentration	$K = 10^{-10}$ cm/sec for $t < 100$ yrs $K = 10^{-9}$ cm/sec for $t > 100$ yrs $\eta = 10^{-4}$ $A = 8 \times 10^6\ m^2$	$K = 10^{-8}$ cm/sec for $t < 100$ yrs $K = 10^{-7}$ cm/sec for $t > 100$ yrs $\eta = 10^{-4}$ $A = 8 \times 10^6\ m^2$	100 1000 10,000	1.4×10^2 8.8×10^1 3.8×10^1	100 1000 10,000	1.4×10^4 8.8×10^3 3.8×10^3	Permeability change after thermal peak is due to several factors: movement of blocks during thermal cycle, incomplete rebound of material in cracks, alteration of minerals in cracks.
Basalt	D	Change in permeability after thermal peak	Groundwater	Thermally induced convection and gradient from aquifer interconnection	Uniform concentration	$K = 10^{-9}$ cm/sec for $t < 100$ yrs $K = 10^{-8}$ cm/sec for $t > 100$ yrs $\eta = 10^{-4}$ $A = 8 \times 10^6\ m^2$	$K = 10^{-7}$ cm/sec for $t < 100$ yrs $K = 10^{-6}$ cm/sec for $t > 100$ yrs $\eta = 10^{-4}$ $A = 8 \times 10^6\ m^2$	100 1000 10,000	1.8×10^4 1.5×10^4 6.3×10^3	100 1000 10,000	7.9×10^6 7.7×10^6 6.8×10^6	Permeability change after thermal peak is due to several factors: movement of blocks during thermal cycle, incomplete rebound of material in cracks, alteration of minerals in cracks.
Shale	D	Change in permeability after thermal peak	Groundwater	Thermally induced convection and gradient from aquifer interconnection	Uniform concentration	$K = 10^{-9}$ cm/sec for $t < 100$ yrs $K = 10^{-8}$ cm/sec for $t > 100$ yrs $\eta = 10^{-4}$ $A = 8 \times 10^6\ m^2$	$K = 10^{-7}$ cm/sec for $t < 100$ yrs $K = 10^{-6}$ cm/sec for $t > 100$ yrs $\eta = 10^{-4}$ $A = 8 \times 10^6\ m^2$	100 1000 10,000	1.8×10^4 1.5×10^4 6.3×10^3	100 1000 10,000	7.9×10^6 7.7×10^6 6.8×10^6	Permeability change after thermal peak is due to several factors: movement of blocks during thermal cycle, incomplete rebound of material in cracks, alteration of minerals in cracks.
Dome Salt	P	Cumulative occurrence probability	Groundwater	Pressure from salt closure, thermally induced convection, and gradient from lower aquifer at edge of salt dome	Uniform concentration	$p = 0$	$p = 0$	No releases need to be calculated.		No releases need to be calculated.		The probability that the spatial variability in rock strength could lead to an extensive pathway from the repository that would fracture under the stresses experienced was found to be negligible.

D-3.1.2 Background

Heat generation by high-level wastes. High-level radioactive wastes generate heat, on the order of up to several kW per canister according to present packaging concepts. Depending on the average planar heat density at which the wastes are placed in a repository (ranging from 60 to 200 kW/acre in conceptual designs) and on the proportions of short- and long-lived radionuclides in the wastes, the temperature of the rock surrounding the repository can rise considerably. In the immediate vicinity of the wastes, this rise might be as great as 100-200°C, depending on the age of the waste, the quantity per canister, and the spacing between canisters. Representative temperature profiles were calculated and reported in the Task B Report (Engineering Controls), and simplified approximations to these are discussed in Appendix D-VI of this report.

Effects of heat. Heat can affect both engineered and natural barriers to waste migration. The focus of this failure element is on changes in the rock characteristics that control the movement of fluids. In particular, heat can:

- modify basic rock properties, such as brittleness, ductility, and strength;
- alter mineralogical structure (e.g., by dehydrating clays), thereby also affecting rock properties;
- cause stress buildups and movement from thermal expansion. New stresses may cause fracturing.

These effects all contribute to modifications in the ability of rock to serve as a barrier to fluid migration.

In fact, there is not a simple heating effect, but rather a heating-cooling cycle, because the heat-generating wastes gradually decay to low levels. This factor will be considered further in Section D-3.1.3 on the failure model.

Fluid flow model. The Task C Report (Migration Pathways) contains a discussion of Darcy's law and its application to fluid flow calculations in both porous and fractured rock; further discussion may be found in Appendices D-V and D-VI of this report. A summary of the principal points follows.

The flow of groundwater in saturated porous rock can be described by Darcy's law, in the form of the equation:

$$\dot{Q} = KiAc(\mu)$$

where

$\dot{Q}$ = volumetric flow rate (volume/time);

K = hydraulic conductivity (length/time);

i = hydraulic gradient (dimensionless);

A = cross-sectional area of the flow path being considered;

$c(\mu)$ = viscosity correction factor (dimensionless) that accounts for increased flow at lower viscosities.

K is frequently given in cm/sec, which is also the basic unit used here. However, because of the magnitude of the flows that result in the present situation, for calculational purposes K will be transformed to units of m/yr and $\dot{Q}$ will be given in m^3/yr. Although Darcy's law is generally applied only to relatively homogeneous porous media, it has been found suitable for application to fractured media to describe the hydrologic system on a macro scale. Although the law may not be sufficiently accurate to model the yield of a single well, for example, which depends on the local distribution of fractures, it can be applied to describe gross water movement over large areas or regions.(28) In fact, the hydraulic conductivity, K, corresponding to fracture flow can be modeled analytically, using fracture parameters and the principles of fluid mechanics,(46,47) although research continues into improving these models.

The expression $Kic(\mu)$ has the units of velocity and is sometimes called the Darcy velocity. It is not a true fluid velocity at all, but rather a measure of the volumetric flow rate per unit of cross-sectional area of the flow path. By dividing by the effective porosity, η, of the rock, the actual average fluid movement rate is obtained. This velocity,

$$v = \frac{Kic(\mu)}{\eta},$$

is useful for estimating how long it would take for noninteracting solute to be carried along the flow pathway with the groundwater. Of course, it is only an average value and therefore an approximation to the actual rates in different fracture paths. For porous rock like sandstone, the value of η may be in the range of 0.1 to 0.5 . For fractured but tightly squeezed rock, as in deep granitic stocks, η may be in the vicinity of 10^{-4}. Such low values of η mean that transit times may be fast, even when the hydraulic conductivity and volumetric flow rates are low.

Ranges of parameter values have been given in the Task C Report (Migration Pathways) and in Chapter D-2.0 of this report. They will be cited as appropriate in the next section, where the present failure element is characterized in terms of changes in K. The parameter K is often loosely referred to as the permeability, especially when the fluid under consideration is known and fixed. In fluid mechanics, there is also an "intrinsic" permeability, k (in units of area), which permits the separation of fluid properties from those of the rock itself; but this latter permeability will not be used here. Therefore, in keeping with common practice, K will often be referred to as the permeability.

Permeability measurements. Specific permeability values are applied in subsequent sections to characterize rocks or other materials. It is not easy to measure values in the ranges given, especially by in-situ techniques, which would be expected to represent more accurately the fluid flow properties of the bulk rock mass. Thus, the actual verification that a specific rock mass has an approximate permeability in some of the ranges referred to may be quite difficult. However, because of this relatively new need for measuring very low permeabilities, techniques are being actively developed for this purpose.

D-3.1.3 Flow Through Bulk Rock Failure Model

The breach-of-containment mechanism under discussion here refers to fluid movement through the bulk rock itself, independent of the development of additional permeable pathways, such as faults, leaky shafts, and borehole seals. As long as two conditions hold, namely,

- the rock has a permeability greater than zero, and
- a hydraulic gradient is present,

there will be fluid flow through the rock. If the permeability is sufficiently small, then the flow volume can be considered negligible. Some of the calculations reported in the next section do lead to such negligible flows.

The purpose of this section is to characterize the permeability and porosity of the rock surrounding the repository for use in the flow calculations of Section D-3.1.4.

D-3.1.3.1 Bedded Salt and Dome Salt

Relatively pure salt at the depths considered in this study has a permeability that is so low that it is nearly impossible to measure.(22,23,24) For the purposes of this study, intact salt may be regarded as impermeable. The heat generated by the wastes is not expected to change the value, except perhaps to decrease it by compression of pores, unless sufficient stresses are generated to cause fracturing. Rock mechanics calculations based on uniform rock salt characteristics do not predict such fracturing because the stresses do not exceed the rock strength and, in addition, they can be relieved by salt deformation. Additional calculations were carried out with a stochastic model that accounts for local spatial variation of rock properties. The question was whether there might be a combination of weaker zones in the salt through which a long fracture pathway might develop. These probabilistic calculations, reported in detail in Appendix D-IX, show that this probability is negligible. Thus the permeability value of the salt is assumed not to increase with time. Because of this and because there is negligible flow with the baseline salt permeability value, no detailed flow calculations are necessary.

D-3.1.3.2 Granite, Basalt, and Shale

Granite and basalt are igneous rocks in which fluid flow is almost entirely within fracture systems. Shale is a sedimentary rock whose characteristics are extremely variable, ranging from relatively soft, plastic material to highly indurated rock similar in many properties to igneous rocks. The latter type of shale has been assumed for modeling purposes, so that fracture flow also dominates in this case.

The following processes will, in general, occur during the period of temperature rise:

- expansion of rock, thereby decreasing the size of openings such as pore spaces, fractures, and other discontinuities;
- compaction of fill material (such as clays) in fractures;
- slippage and movement along fractures; and
- alteration of mineral content, such as by dehydration of clays.

In addition, new fractures may develop, but this is not considered likely to occur to a significant degree from the temperature changes expected in the rock surrounding the repository. Some of the above processes can contribute to a decrease in bulk permeability during this period.(48,49) However, no attempt has been made in this report to model this effect quantitatively.

More important is the fact that after the temperatures peak and then begin to decrease, several effects can contribute to a new higher bulk rock permeability. For example, the surfaces of fractures may not return to their original position, and asperities may keep them apart. Clay fill that has been compacted may not rebound completely, leading to open channels. Clays that have been altered may crumble and fail to fill their original volume. Mechanistic models are not available to predict the net effect of these processes, either generically or in specific instances. Nevertheless, by considering the range of permeability values for the types of rock formations in question, modified permeabilities may be estimated. The values chosen for modeling purposes are summarized in Table D-15. For purposes of conservatism, the increase in permeability is modeled at the 100-year point after repository closure, even though the increase is expected to be gradual and may actually occur later. Note that it is difficult to estimate the level of assurance with which a given specific site can be determined to have the kind of low permeabilities assumed here. This problem must be addressed in the detailed characterization of specific sites.

TABLE D-15

MODEL PERMEABILITIES FOR HARD ROCK BEFORE AND AFTER THERMAL CYCLE

		Bulk Rock Permeability (K) (cm/sec)	
		First Estimate	Second Estimate*
Granite	$t < 100$ yrs**	10^{-10}	10^{-8}
	$t \geq 100$ yrs	10^{-9}	10^{-7}
Basalt	$t < 100$ yrs	10^{-9}	10^{-7}
	$t \geq 100$ yrs	10^{-8}	10^{-6}
Shale	$t < 100$ yrs	10^{-9}	10^{-7}
	$t \geq 100$ yrs	10^{-8}	10^{-6}

*Note: Permeabilities of these rocks can be much higher than the values given in this column. The second estimate corresponds in this case to suboptimal values, but ones that might reasonably still be in the range of consideration for repository siting.

**Years after repository closure.

D-3.1.4 Flow Through Bulk Rock Release Model

D-3.1.4.1 Bedded Salt

Because thermal effects do not alter the permeability of the surrounding salt and because salt is essentially an impermeable medium, all flows in the bulk rock are negligible in comparison with other release mechanisms. Consequently, no calculations are presented for this case.

D-3.1.4.2 Granite

Of the driving forces discussed in the appendices, only thermal convection is relevant for this release mechanism. This driving force depends on time because the temperature profile varies over time. The methodology for evaluating this driving force is presented in Appendix D-VI and the resulting effective gradients are shown in Table D-16. As pointed out in the appendix, these values represent upper bounds on the possible buoyancy forces.

The volumetric flow rate can be calculated from Darcy's law. The values of K have been given in Section D-3.1.3; A is 8 km^2; and $c(\mu)$ is 5, in accordance with Appendix D-VI. The results are presented in Table D-17.

As discussed in Appendix D-VI, the average vertical fluid velocity is obtained from the equation

$$v = \frac{Ki}{100\mu\eta} ,$$

The resulting velocities and transit times are presented in Tables D-18 and D-19. As discussed in Appendix VI, because water may be more readily available near the edge of the repository, the vertical velocity may be as much as ten times higher in some locations, leading to shorter transit times to the aquifer.

The source term for this failure element consists of the concentration of radionuclides that have leached into the water in the

TABLE D-16

EFFECTIVE VERTICAL HYDRAULIC GRADIENT IN SURROUNDING GEOLOGIC MEDIA FROM THERMALLY INDUCED CONVECTION (GRANITE REPOSITORY)

	Hydraulic Gradient (i)		
	100 years*	1000 years	10,000 years
First Estimate	0.011	0.007	0.003
Second Estimate	0.011	0.007	0.003

*Years after repository closure.

Source: Appendix D-VI, taking into account a ten-fold reduction because of the resistance of the recharge pathway, as discussed in the last section of that appendix.

TABLE D-17

VOLUMETRIC FLOW RATES THROUGH BULK ROCK (GRANITE REPOSITORY)

	Volumetric Flow ($\dot{Q}$) (m^3/yr)		
	100 years*	1000 years	10,000 years
First Estimate	1.4×10^2	8.8×10^1	3.8×10^1
Second Estimate	1.4×10^4	8.8×10^3	3.8×10^3

*Years after repository closure.

TABLE D-18

FLUID VELOCITIES THROUGH BULK ROCK
(GRANITE REPOSITORY)

	Velocity (v) (m/yr)		
	100 years*	1000 years	10,000 years
First Estimate	0.20	0.11	0.05
Second Estimate	18.0	11.0	4.7

*Years after repository closure.

TABLE D-19

FLUID TRANSIT TIME FROM REPOSITORY TO AQUIFER THROUGH BULK ROCK (GRANITE REPOSITORY)

	Time (yrs)		
	100 years*	1000 years	10,000 years
First Estimate	1150	2100	4600
Second Estimate	13	20	50

*Years after repository closure.

repository during the time frame of interest. This is the uniform concentration situation described earlier.

D-3.1.4.3 Basalt

The two possible driving forces for this case are thermally induced convection and an aquifer interconnection. Because the temperature profile varies with time, the magnitude of the combined effect also varies with time. The methodology used to evaluate thermally induced convection is developed in Appendix D-VI, and estimates for the effective vertical hydraulic gradient are presented in Table D-20. These values represent upper bounds on the possible gradients. Using these hydraulic gradients, the volumetric flows can be calculated from Darcy's law. Table D-21 presents the results of the calculation. As discussed earlier, the vertical fluid velocity is obtained by dividing the volumetric flow rates by n. This leads to the velocity and transit time estimates in Tables D-22 and D-23.

The source term for this failure element consists of the concentration of radionuclides that have leached into the water in the repository during the time frame of interest. This is the uniform concentration situation discussed earlier.

D-3.1.4.3 Shale

All modeling parameters relevant to this release mechanism are identical for the shale and basalt repositories. Therefore the discussion and calculations for the two repositories are identical. The results are summarized in Tables D-24, D-25 and D-26.

D-3.1.4.4 Dome Salt

As in the case of bedded salt, all flows in the bulk rock are negligible in comparison with the other release mechanisms. Consequently, no detailed calculations are required for this case.

TABLE D-20

EFFECTIVE VERTICAL HYDRAULIC GRADIENT IN SURROUNDING GEOLOGIC MEDIA FROM THERMALLY INDUCED CONVECTION AND AQUIFER INTERCONNECTION (BASALT REPOSITORY)

	Hydraulic Gradient (i)		
	100 years*	1000 years	10,000 years
Thermally Induced Convection**			
First Estimate	0.13	0.11	0.04
Second Estimate	0.13	0.11	0.04
Aquifer Interconnection***			
First Estimate	0.01	0.01	0.01
Second Estimate	0.5	0.5	0.5
Total			
First Estimate	0.14	0.12	0.05
Second Estimate	0.63	0.61	0.54

*Years after repository closure.

**These values are from Table D-VI-4, Appendix D-VI.

***These values are from Section D-2.3.3.

TABLE D-21

VOLUMETRIC FLOW RATES THROUGH BULK ROCK
(BASALT REPOSITORY)

	Volumetric Flow ($\dot{Q}$) (m^3/yr)		
	100 years*	1000 years	10,000 years
First Estimate	1.8×10^4	1.5×10^4	6.3×10^3
Second Estimate	7.9×10^6	7.7×10^6	6.8×10^6

---

*Years after repository closure.

TABLE D-22

FLUID VELOCITIES THROUGH BULK ROCK
(BASALT REPOSITORY)

	Velocity (v) (m/yr)		
	100 years[*]	1000 years	10,000 years
First Estimate	23	19	7.9
Second Estimate	9.9×10^3	9.6×10^3	8.5×10^3

[*] Years after repository closure.

TABLE D-23

FLUID TRANSIT TIMES THROUGH BULK ROCK (BASALT REPOSITORY)

		Time (yrs)	
	100 years*	1000 years	10,000 years
First Estimate	4.3	5.3	13
Second Estimate	0.01	0.01	0.01

---

*Years after repository closure.

TABLE D-24

VOLUMETRIC FLOW RATES THROUGH BULK ROCK
(SHALE REPOSITORY)

	Volumetric Flow ($\dot{Q}$) (m^3/yr)		
	100 years*	1000 years	10,000 years
First Estimate	1.8×10^4	1.5×10^4	6.3×10^3
Second Estimate	7.9×10^6	7.7×10^6	6.8×10^6

*Years after repository closure.

TABLE D-25

FLUID VELOCITIES THROUGH BULK ROCK
(SHALE REPOSITORY)

	Velocity (v) (m/yr) 100 years*	1000 years	10,000 years
First Estimate	23	19	7.9
Second Estimate	9.9×10^3	9.6×10^3	8.5×10^3

---

*Years after repository closure.

TABLE D-26

FLUID TRANSIT TIMES THROUGH BULK ROCK
(SHALE REPOSITORY)

	Time (yrs)		
	100 years*	1000 years	10,000 years
First Estimate	4.3	5.3	13
Second Estimate	0.01	0.01	0.01

*Years after repository closure.

D-3.1.5 Literature Discussion

Flow through bulk rock has been considered in a number of studies (11,29) as well as in the Task C Report for this project. In addition, some researchers have discussed waste-induced permeability changes.

The NRC/Sandia risk program(12) proposes a model for stress-induced fracturing in terms of "reference cracks." A reference crack is a vertical planar crack whose horizontal cross-section has dimensions 1 mm x 3 km. The effect of stress buildups on the rock is measured in terms of a number of new reference cracks. This number is obtained from the expression 5h, where h is the vertical displacement in centimeters. Since the vertical displacement is expected to be on the order of one or several meters, somewhat over 500 reference cracks might be expected. The authors do note large sources of error in this approximate model.

The BNWL/ONWI/DOE WISAP program(50) has also noted this failure element, although quantitative estimates of permeability changes have not been reported.

D-3.2 SHAFT SEAL FAILURE

D-3.2.1 Summary

During the operational stage of the repository, several vertical shafts will be required for ventilation and for the transport of personnel and materials between the underground workings and the surface. (See Figure D-9). Part of the process of sealing the repository for long-term isolation of the radioactive wastes requires that these shafts be filled with appropriate materials in order to prevent them from serving as pathways for fluid flow or radionuclide migration.

The sealing materials will need to be chosen with a specific environment in mind so that they may approach, as nearly as possible, chemical and mechanical equilibrium with the surrounding rock. The seal may consist of several layers of completely distinct types to provide a multi-barrier line of defense against expected or unexpected forces.

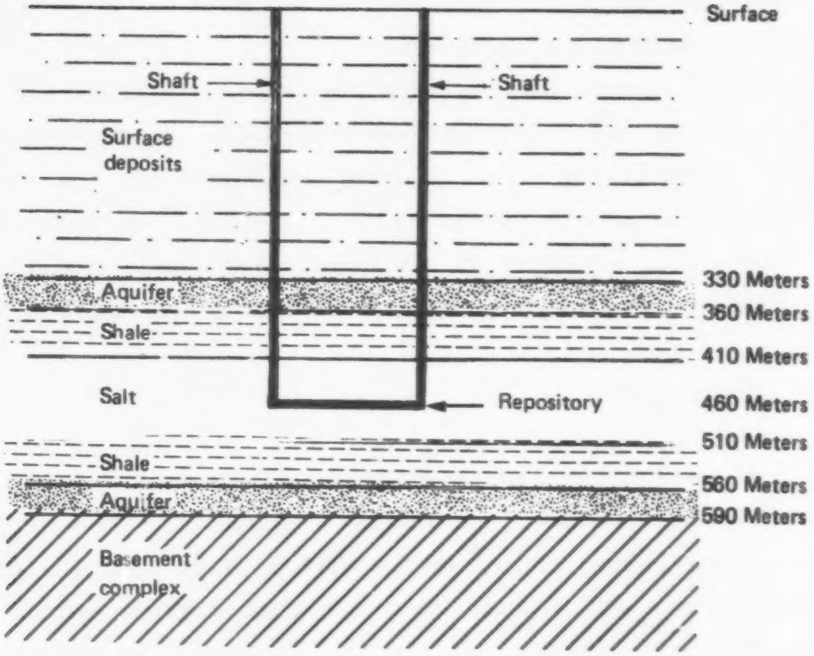

FIGURE D–9 BEDDED SALT REPOSITORY SHOWING VERTICAL SHAFTS

Nevertheless, it is reasonable to expect that over a long period of time, such as 10,000 years, the combination of processes such as settling, leaching, expansion and contraction due to fluctuations in water content or temperature, earth movements, weathering, and fatigue may lead to some degradation in the integrity of the seal.

The shaft seal performance model considered here is not derived from a particular design. It is intended to be generic in nature and conservative; that is, it is believed that the performance characteristics described here can be equalled or exceeded by actual designs for specific circumstances.

The generic model used in this report characterizes the shaft seal integrity by a spatially uniform hydraulic conductivity K. One hydraulic conductivity value (K_0) is estimated for the time of seal emplacement, and another value (K_1) is estimated for the time 10,000 years later. It is assumed that K increases linearly from K_0 to K_1 over this period. A summary of the analysis is given in Table D-27.

D-3.2.2 Background

The excavation and operation of an underground repository require the sinking of a number of shafts to provide access, ventilation, removal of rock, etc. These shafts will vary in size and construction depending upon their function and the rock through which they pass. Even in relatively simple geologic settings, such as those represented by the generic models in this report, a variety of construction and maintenance techniques may be required for the shafts to remain usable during the operational life of the repository. It is important to review these technologies in order to set the framework for discussion of the shaft sealing problem.

Much of the focus of mine shaft engineering is on the problems of hole stability and water inflow. These problems are often interrelated, and even when they are not, some of the same engineering techniques may be effective for both. For example, the portion of a shaft penetrating either incompetent or water-bearing rock, or occasionally an entire shaft, may be lined with a tubular structure, and the annular space between this liner and the rock then filled with a sealer or grout. The

TABLE D-27
SUMMARY OF SHAFT SEAL FAILURE ELEMENT

MEDIUM	PROBABILISTIC (P) DETERMINISTIC (D)	NATURE OF MODEL	RELEASE MODE	DRIVING FORCE	SOURCE TERM	PARAMETERS		FLUID FLOW RATES FROM REPOSITORY TO UPPER AQUIFER				COMMENTS
						1st ESTIMATE	2nd ESTIMATE	1st ESTIMATE		2nd ESTIMATE		
								t (yrs)	$\dot{Q}(t)$ (m^3/yr)	t (yrs)	$\dot{Q}(t)$ (m^3/yr)	
Bedded Salt	D	Linearly increasing permeability	Groundwater	Initially pressure from salt creep. Afterwards, U-tube effect.	Uniform concentration	$K_0 = 10^{-8}$ cm/sec at time of sealing $K_1 = 10^{-6}$ cm/sec after 10,000 years K increases linearly from K_0 to K_1 over 10,000 years $\eta = 0.1$ $A = 100\ m^2$, total cross-sectional area of shafts	$K_0 = 10^{-8}$ cm/sec at time of sealing $K_1 = 10^{-4}$ cm/sec after 10,000 years K increases linearly from K_0 to K_1 over 10,000 years $\eta = 0.1$ $A = 100\ m^2$, total cross-sectional area of shafts	200 223^- 223^+ 1000 10,000	40 } Period of salt creep 40 } 0.08 0.17 0.32	720 1000^- 1000^+ 10,000	2000 } Period of salt creep 2000 } 3.15 3.16	It is conservative to assume closure by salt creep for this failure mechanism; otherwise resaturation time would be extremely long. Closure also implies strong driving force for release.
Granite	D	Linearly increasing permeability	Groundwater	Thermally induced convection and U-tube effect.	Uniform concentration	$K_0 = 10^{-8}$ cm/sec at time of sealing $K_1 = 10^{-6}$ cm/sec after 10,000 years K increases linearly from K_0 to K_1 over 10,000 years $\eta = 0.1$ $A = 100\ m^2$, total cross-sectional area of shafts	$K_0 = 10^{-8}$ cm/sec at time of sealing $K_1 = 10^{-4}$ cm/sec after 10,000 years K increases linearly from K_0 to K_1 over 10,000 years $\eta = 0.1$ $A = 100\ m^2$, total cross-sectional area of shafts	100 1000 10,000	0.3 1.0 1.6	100 1000 10,000	15.9 94.6 236.3	Releases only begin after repository resaturation.
Basalt	D	Linearly increasing permeability	Groundwater	Thermally induced convection and U-tube effect.	Uniform concentration	$K_0 = 10^{-8}$ cm/sec at time of sealing $K_1 = 10^{-6}$ cm/sec after 10,000 years K increases linearly from K_0 to K_1 over 10,000 years $\eta = 0.1$ $A = 100\ m^2$, total cross-sectional area of shafts	$K_0 = 10^{-8}$ cm/sec at time of sealing $K_1 = 10^{-4}$ cm/sec after 10,000 years K increases linearly from K_0 to K_1 over 10,000 years $\eta = 0.1$ $A = 100\ m^2$, total cross-sectional area of shafts	100 1000 10,000	0.4 1.7 3.2	100 1000 10,000	28.6 157.6 472.6	Releases only begin after repository resaturation.

TABLE D-27
SUMMARY OF SHAFT SEAL FAILURE ELEMENT (CONTINUED)

MEDIUM	PROBABILISTIC (P) DETERMINISTIC (D)	NATURE OF MODEL	RELEASE MODE	DRIVING FORCE	SOURCE TERM	PARAMETERS		FLUID FLOW RATES FROM REPOSITORY TO UPPER AQUIFER				COMMENTS
						1st ESTIMATE	2nd ESTIMATE	1st ESTIMATE		2nd ESTIMATE		
								t (yrs)	$\dot{Q}$ (t) (m^3/yr)	t (yrs)	$\dot{Q}$ (t) (m^3/yr)	
Shale	D	Linearly increasing permeability	Groundwater	Thermally induced convection and U-tube effect.	Uniform concentration	K_0 = 10^{-8} cm/sec at time of sealing K_1 = 10^{-6} cm/sec after 10,000 years K increases linearly from K_0 to K_1 over 10,000 years η = 0.1 A = 100 m^2, total cross-sectional area of shafts	K_0 = 10^{-8} cm/sec at time of sealing K_1 = 10^{-4} cm/sec after 10,000 years K increases linearly from K_0 to K_1 over 10,000 years η = 0.1 A = 100 m^2, total cross-sectional area of shafts	100	0.4	100	28.6	Releases only begin after repository resaturation.
								1000	1.7	1000	157.6	
								10,000	3.2	10,000	472.6	
Dome Salt	D	Line[illegible]creasing permeability	Groundwater	Initially pressure from salt creep. Afterwards, U-tube effect.	Uniform concentration	K_0 = 10^{-8} cm/sec at time of sealing K_1 = 10^{-6} cm/sec after 10,000 years K increases linearly from K_0 to K_1 over 10,000 years η = 0.1 A = 100 m^2, total cross-sectional area of shafts	K_0 = 10^{-8} cm/sec at time of sealing K_1 = 10^{-4} cm/sec after 10,000 years K increases linearly from K_0 to K_1 over 10,000 years η = 0.1 A = 100 m^2, total cross-sectional area of shafts	200	15 } Period of salt creep	748	2000 } Period of salt creep	It is conservative to assume closure by salt creep for this failure mechanism; otherwise resaturation time would be extremely long. Closure also implies strong driving force for release.
								280	15	1000^-	2000	
								280	0.04	1000^+	3.15	
								1000	0.10	10,000	3.15	
								10,000	0.24			

liner may consist of a single layer, such as steel, cast iron, or reinforced concrete, or a multi-layered system. Examples are shown in Figure D-10. Other methods of stabilization, discussed below, include freezing the ground around the shaft or filling the rock column with grout before excavation.

Freezing requires the installation of refrigerant tubes in the section requiring stabilization. These may be placed from the surface, through an array of drilled holes, from within the shaft as a ring against the shaft walls, or in holes drilled from the shaft. Refrigerant is then forced through the tubes, cooling the ground and freezing the interstitial water. Since it is the water in the rock that freezes, this method of stabilization is suitable only for saturated or nearly saturated rock. Furthermore, if the rock is kept frozen during the operational life of the repository, the distance or depth of freezing can continue to expand. The permanent effects on the rock would depend, in part, on the extent of freezing, and hence on the time span of the operation.

Grouting to stabilize soil and rock involves drilling a series of closely spaced holes and injecting grout under pressure. The injection pressure must be carefully controlled to ensure that grout is forced a sufficient distance into the rock without causing additional fracturing. The grout is designed to fill voids in the rock before it sets and forms a rigid bonding agent. The spacing of the holes must be close enough to permit grout from one hole to spread to the next and coalesce. When grout has been injected into all the holes, a continuous curtain or column of rock and soil, cemented by the grout, remains in the ground. Excavation of the shaft can then proceed within the curtain wall or along the column. Figure D-11 shows a typical grouting program. Neat cement (cement without aggregate) or cement with fine fillers are the most common grout materials. Chemicals, such as sodium silicate gel and epoxy and polyester resins, are used in some instances; the limited availability of these specialized products and their expense have restricted their general use.

Methods used to sink shafts are affected by the stability and water content of the ground, and they affect stability and water content in return. In the fairly competent rock expected near a repository, rotary

(a) Schematic of drop shaft

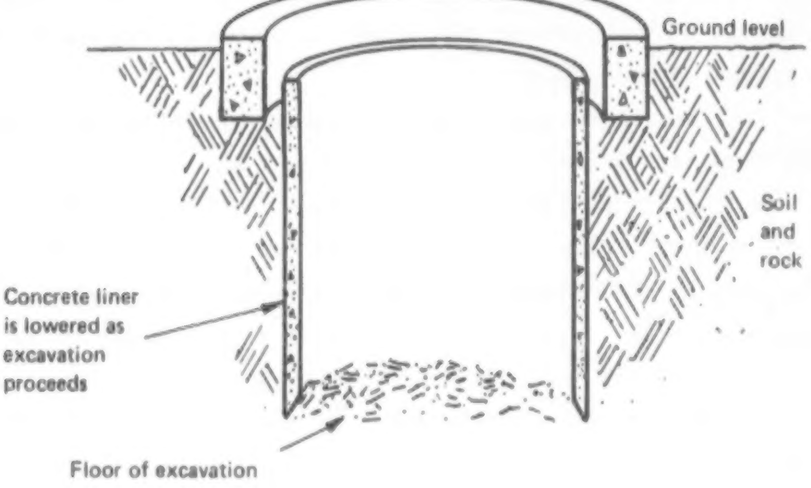

Source: Arthur D. Little,Inc.

(b) Shaft lining used in Asse Salt Mine Repository, Federal Republic of West Germany.

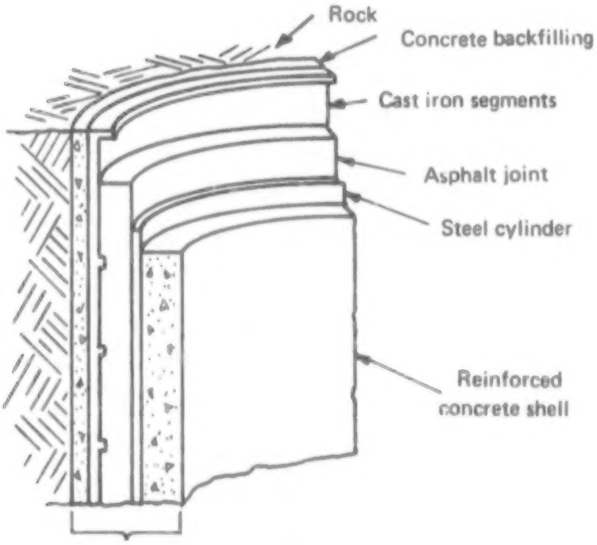

Source: On the Safety of Disposing of Radioactive Wastes in the Asse Salt Mine,Gesellschaft für Strahlen und Umweltforschung mbH, Munich, Germany, undated.

FIGURE D–10 EXAMPLES OF SHAFT LININGS

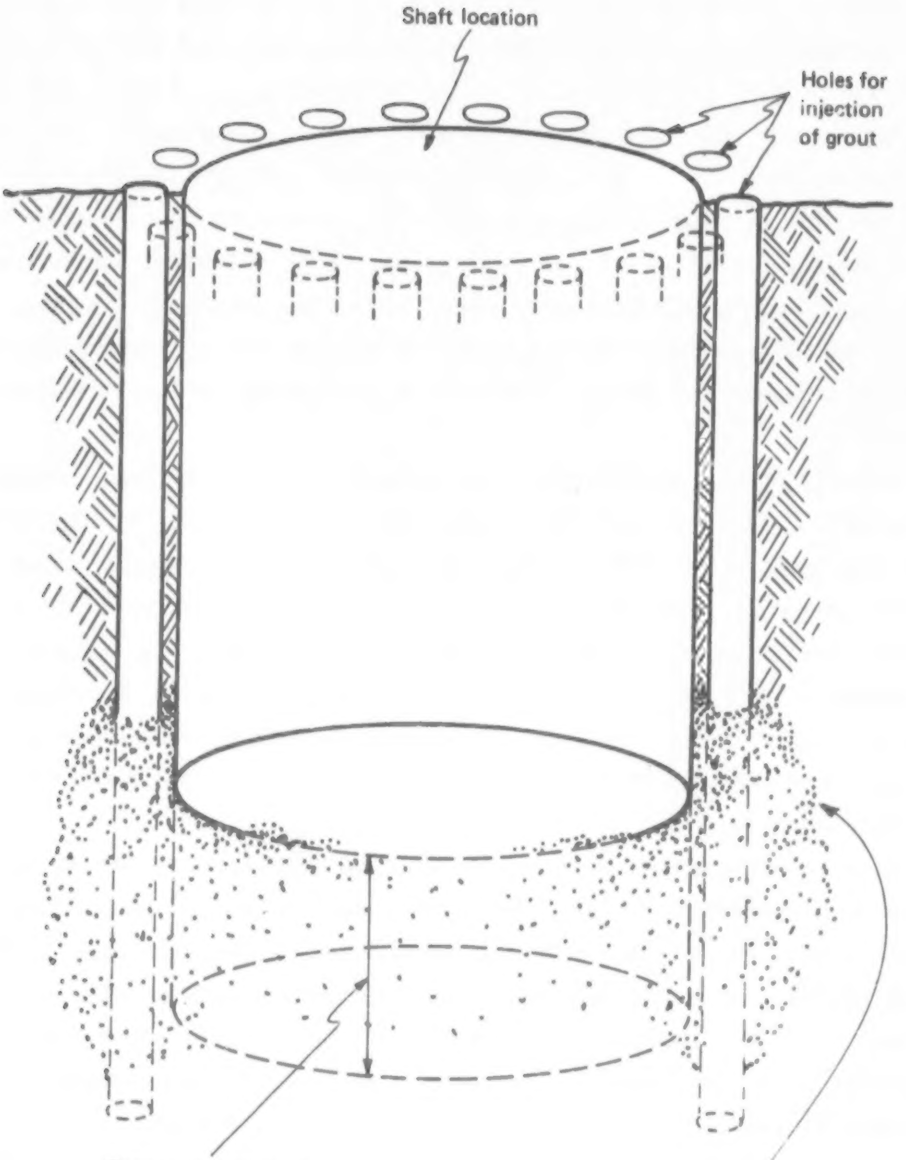
Shaft location
Holes for injection of grout
Zone to be stabilized before excavation
Grout is injected in holes around shaft location. Sufficient grout is injected to form continuous curtain around shaft.

Source: Arthur D. Little, Inc.

FIGURE D–11 GROUTING PROGRAM FOR SHAFT STABILIZATION boring or percussion drilling and explosives may be most practical. Each technique differs somewhat in its effect on the rock surrounding the shaft. Typically, some fracturing of the wall rock is expected as the stress field changes when rock is removed from the shaft. Explosives and percussion drilling shatter rock around the shaft opening, with the degree of shattering depending upon the forces generated, rock type, and in-situ stresses. Rotary boring, in which rock is more or less continuously removed, generally has less effect on wall rock. For each rock formation, the relative advantages of different excavation techniques must be weighed against the stabilization problems introduced by excavation in order to estimate the most economical and safest combination for sinking and stabilizing a shaft.

Upon closing a repository, the several shafts from the surface must be sealed to prevent or retard the vertical movement of fluids to or from the repository level. Sealing abandoned or inactive mines is a common practice, but the seals are usually intended more to prevent humans and livestock from falling into a shaft, to permit later reopening of a mine, or, to a lesser extent, to reduce flooding of or outflow from a mine. The special requirement of long-term isolation of a repository demands that shaft seals be placed with exceptional care and thoroughness.

Careful preparation for sealing will be important to ensure that the shaft seal performs to its full potential. These preparations will entail removal from the shafts of operational equipment, pipes, cables, guide tracks, and other hardware. Contaminants, such as oils and loose earth, must be removed from the walls if these substances might interfere with the bonding properties of the sealing agents. Also, liners will probably have to be stripped from the shafts.

Sealing the shaft, including the possibly altered or fractured rock immediately surrounding it, is likely to require a combination of materials and techniques if the desired impermeability and longevity are to be achieved. A number of studies have examined individual aspects of repository shaft or borehole sealing.(11,50-55) Some have suggested the use of specific materials, equipment, and procedures, as summarized in Table D-28.

TABLE D-28

SEAL MATERIAL CHARACTERISTICS

Material	Emplacement Requirements and Practices	Comments
Concrete (Cement with aggregate added)	Pumped or placed continuously or in batches. Equipment and techniques are in common use.	Forms rigid mass. Sulfate-resistant cements available. Additives are possible for specific problems or rock/cement interaction. Cannot fill fine cracks or pores. Strength and permeability worsen at high temperature. Good longevity expected. Some ability to "heal" if fractured.
Chemical Grouts (Both organics: epoxy, etc., and inorganics: sulfur, silica gel)	Pumped or injected as liquid. May require catalyst or subsequent treatment, e.g., heating. Use is limited to specific problem areas.	Forms rigid or semi-rigid seal. May be sensitive to rock/water chemistry. Bond to wet rock may be weak. Range of viscosities permit filling of fine cracks, etc. Long-term stability uncertain. Temperature sensitivities range from very low to extreme. Plastic materials can generally deform without fracture.
Bitumens (Tar, asphalt)	Pumped or injected. Often heated to facilitate emplacement. Technology existent but seldom applied.	Forms plastic or viscous seal. Insensitive to rock/water chemistry. Sensitive to hydrocarbons in rock formations.

TABLE D-28 (continued)

Material	Emplacement Requirements and Practice	Comments
Bitumens (continued)		Adhesion to rock often greater than cohesion of bitumen. Viscosity is temperature sensitive. Contraction during cooling may cause cracks or separation from rock. Long stability expected. Can deform viscously or "heal" fractures.
Compacted Formation Rock	Batch or continuous feed down shaft. Continuous or intermittent compaction by machinery. Equipment and procedures require development. Crushing of rock may be necessary for handling.	Forms rigid plug. Insensitive to rock chemistry; may be water sensitive. Poor bond in to rock. Difficulty in filling fine cracks, etc. Sensitive to feed rate, compaction process, particle size, moisture content. Temperature sensitivity is similar to *in-situ* rock. Unless supported or mixed with binder, strength is low. Compaction may improve with time and overburden.
Compacted Earthen Materials (Clays, sands, etc. Mixed with or distinct from formation rock)	(Same as above)	Forms rigid plug. Reaction with rock/water expected to be slight. Poor bond to *in-situ* rock. Sensitivity to water somewhat controllable. Difficulty in filling fine cracks. Sensitive to feed rate, compaction, etc.

TABLE D-28 (continued)

Material	Emplacement Requirements and Practice	Comments
Compacted Earthen Materials (continued)		Temperature sensitivity may differ from *in-situ* rock. Low unsupported strength. Long stability expected. Some plastic deformation possible without fracturing. Compaction may improve with time.
Melted Rock	Rock delivered to work face either molten or solid, melted in place, and sprayed or pooled. Feed, melting, and applying equipment and techniques are experimental.	Forms solid mass. Chemistry similar to *in-situ* rock. Most suitable material is low-melting-point rock with few and single-phase minerals (e.g., salt). Cracking and separation expected on cooling. May fuse or fill small fissures in *in-situ* rock. If properly emplaced, good stability expected.
Rock Mineral Solution (Calcite, silica)	Same as above except that the rock is dissolved in solution, not molten. Application and equipment are experimental.	Forms solid mass. Insensitive to *in-situ* rock chemistry. May be sensitive to water chemistry. Implies a single mineral phase. Good adhesion expected. Low sensitivity to temperature. Solubility of solid seal in question. Good stability expected. Does not heal.

Sources: References 52, 54, 55, 62.

In general, the sealing operation will probably attempt to fill the shaft in such a way that it has mechanical, hydraulic, and chemical properties as near as possible to those of the virgin rock. Some concepts may approach this ideal in specific rocks; for example, the melting and fusing of salts has been suggested as a possibility for shafts through evaporites.(52) Other methods are applicable to a wider range of rock types, e.g., using compacted earth as a seal, or filling the shaft with concrete and using the excavated rock for aggregate. An important factor in sealing a shaft is the fact that the rock surrounding a shaft is likely to differ in certain characteristics from the virgin rock. This is true not only for the very short distance (say one or two meters) from the shaft, where grouting is possible to seal excavation-induced fractures, but also for distances on the order of up to tens of meters. The following are examples of changes in characteristics that must be considered in designing and emplacing seals:

- Moisture content may change because of drainage into the shaft.
- Hydraulic conductivity may change because of leaching, fracturing, and stress changes.
- Rock chemistry may change because of exposure to atmospheric conditions, leaching, and interaction with grouts and lining materials.
- Volume changes may result from pore water pressure changes, temperature changes, and freezing.

After the shaft is sealed, the entire system will move toward chemical, mechanical, and hydrologic equilibrium, and how the system will adjust must be carefully considered in the design. The effects of various processes on shaft seal integrity are discussed in the next section.

D-3.2.3 Shaft Seal Failure Model

Scope of Model. For this analysis, the performance of a shaft seal is characterized by the seal's ability to restrict fluid movement along the shaft. The principal parameter affecting such movement is the hydraulic conductivity of the filled shaft, including the immediately surrounding rock. While the fill material may vary from one point to another, for simplicity and in the absence of a definitive proposed design, an effective uniform hydraulic conductivity has been assumed to characterize the sealed shaft or any portions thereof. Auxiliary parameters, such as cross-sectional area and porosity, are also necessary to determine fluid flow rates.

The model's emphasis on fluid flow is not meant to imply that there may not be other potentially important purposes for the shaft seal. Naturally, one of the prime purposes of the seal is to prevent or discourage accidental entry into an abandoned shaft; however, this is rather easy to accomplish and does not affect design. In addition, it is possible that a seal may be sought with favorable radionuclide-retention properties, in which case its chemical and mineralogical composition would be important. This factor is not included in the present model.

The present model hypothesizes a linear increase in shaft seal permeability over a period of 10,000 years. Specific parameters are presented after the following discussion of degradation mechanisms.

Mechanisms for Shaft Seal Degradation. Degradation of the shaft seal over a long period of time, such as 10,000 years, is the likely result of a combination of processes, examples of which are discussed in the following paragraphs.

Leaching, which involves the removal of material by dissolution in groundwater, has occasionally caused rapid deterioration of sealants. Examples have recently been collected and documented in which cemented borehole plugs have disintegrated and disappeared because of leaching of the cementitious material, usually by sulfate-rich or acidic water (see Section D-3.3). In response, a number of cements that are resistant to sulfate attack have been developed.(51,56,57) With the proper characterization of the local groundwater, carefully chosen rock and seal materials would be expected to have very low solubilities; nevertheless, increases in temperature and changes in water pH or chemical composition may increase the rate of leaching.

Pressure and volume changes in the seal material can cause the development of fractures and void spaces. For example, thermal expansion will result from the heat generated by the wastes, but this heating effect will eventually decrease because of radioactive decay, giving the effect of a thermal cycle. The corresponding stress changes can result in fractures or voids. Changes in moisture content can also lead to similar effects; certain clays exhibit considerable swelling as water is absorbed, then crack upon drying. Some synthetic grouts and sealers are formed in place by polymerization of their components. Corresponding volume changes often involve shrinkage, so that if the polymerization is not complete at the time shaft filling is resumed, or if the stresses in the material are excessive, cracks or voids may develop.

Degradation from tectonic stresses and earth movements is a most difficult engineering problem. Because it is highly unlikely that a site will be free of differential stresses, gradual ground deformation over time may be expected even if no ground movement is felt. For example, pipes in oil fields have been known to be distorted, crushed, closed, and inclined from the vertical by such forces.(58) Although some of these movements occur along faults, they may also occur independently.(58-60) While such deformation is expected to be relatively slow in the stable areas being considered for repositories, the 10,000-year time frame is sufficiently long that the cumulative effect could be substantial.

Other forces and processes that may have an impact on the integrity of the shaft seal include settling within the fill material, changes in overburden pressure from natural processes (e.g., erosion, glaciation), chemical interaction between fill material and surrounding rock, changes in physical properties caused by variations in water content, and chemical changes within the fill material itself (such as reactions between aggregate and cement in a concrete).

Specific Model Assumptions. The previous discussion suggests a picture of a shaft seal with somewhat different appearance and properties after 10,000 years than immediately after emplacement. This concept is sketched in Figure D-12. The development of the corresponding model is described in the paragraphs below. It is important to keep in mind that the intention here is to present a generic characterization of shaft seal performance and that this has been done by selecting performance characteristics that are believed to be achievable without technological breakthroughs. With specific

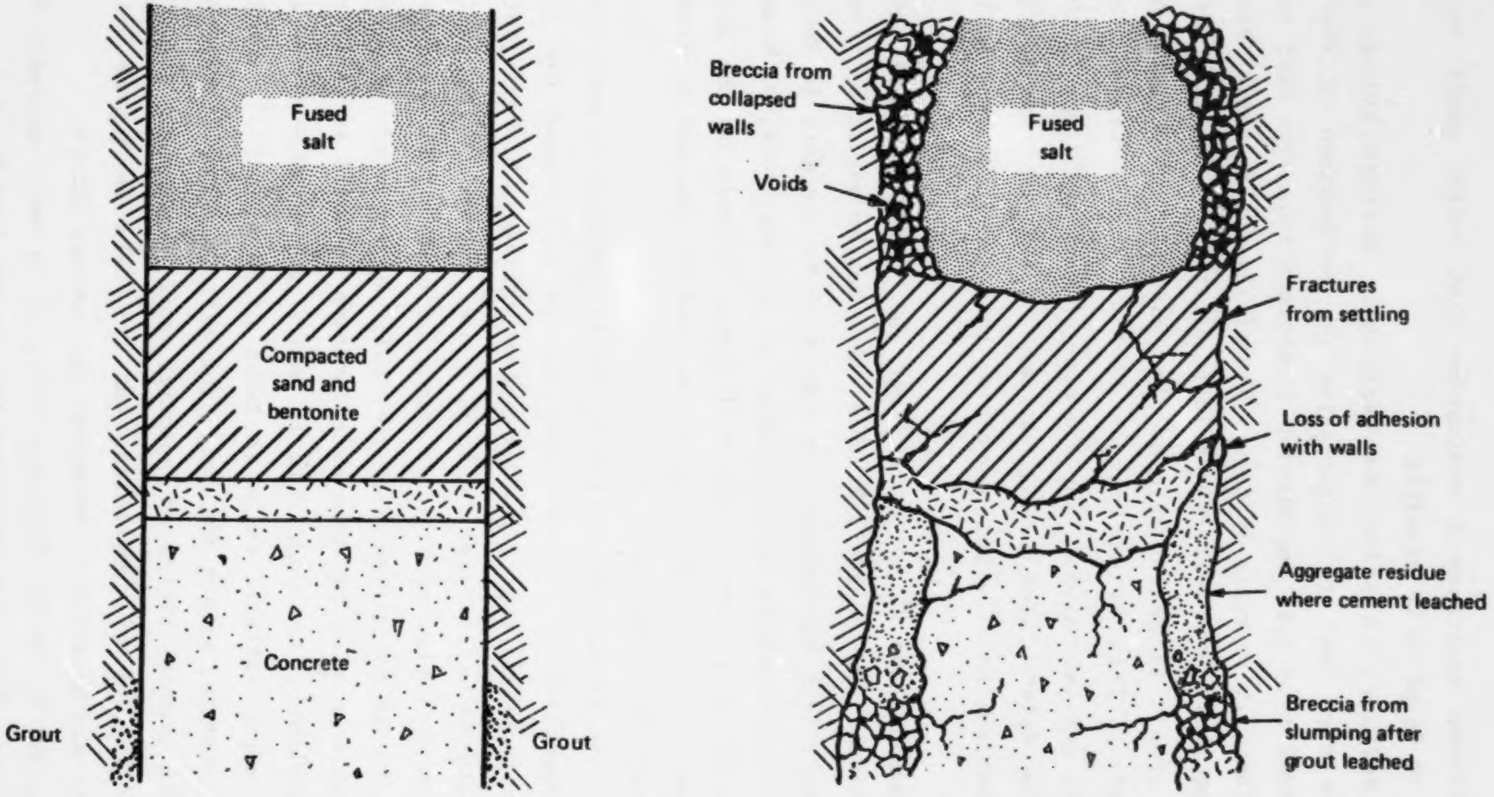

(a) At Time of Emplacement

(b) After 10,000 Years
(Degradation may be exaggerated)

Source: Arthur D. Little, Inc.

FIGURE D–12 EXAMPLE OF SECTION OF MULTI-LAYERED SHAFT SEAL designs and thorough experimental evaluation even better shaft seal performance may be found to be possible.

As stated earlier, an effective, spatially uniform hydraulic conductivity has been used to characterize the performance of shaft seals. Consideration of seal degradation mechanisms indicates that the conductivity value will increase in time. Therefore, the essential step in characterizing shaft seal performance is to determine a function K(t) which for each time t is an estimate of the hydraulic conductivity of the filled shaft. This determination involves three steps: the estimation of the initial value K_0 for the time of seal emplacement, the estimation of the deteriorated (i.e., larger) value K_1 at time 10,000 years, and the estimation of a rule governing the transition from K_0 to K_1.

Initial permeabilities K_0 for both first and second estimates are taken as 10^{-8} cm/sec. It appears that this value can be met or bettered by a number of materials and designs, as suggested by the data in Table D-29. The performance measure is independent of the host rock, although the specific design to achieve it may well depend closely on the host rock. (For example, various additives may be used in concrete in order to aid bonding with the surrounding rock.)

Estimates of the final permeability K_1 can be expected to vary from site to site, depending on the harshness of the environment for the seal, so it is appropriate that first and second estimates be different. The first estimate value is taken to be $K_1 = 10^{-6}$ cm/sec, which is in the range of permeabilities expected of sandy or silty clays or clayey sands. That is, it is envisioned that the design of the shaft seal can be so chosen that even with moderate deterioration it would be expected to behave equivalently to such natural soils after 10,000 years. Similarly, the second estimate value is taken to be $K_1 = 10^{-4}$ cm/sec, which lies, for example, within the range for silty sand or silty sand and gravel. The permeabilities of specific soil types vary greatly depending on conditions of compaction, but the data in Figure D-13 provide a context within which to interpret the numbers chosen.

Values of K_0 and K_1 having been specified, it is next necessary to estimate the function K(t) that describes the changes from K_0 to K_1. In the absence of detailed seal designs and models for degradation

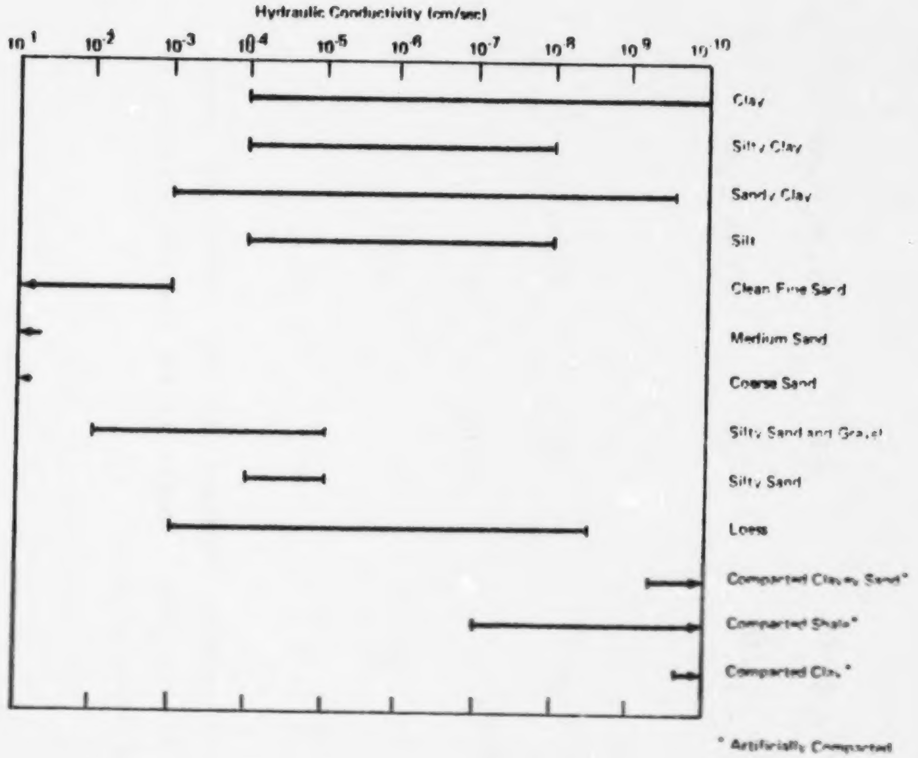

Sources: Stockton, S.L. and A.H. Balch. The Utility of Petroleum Seismic Exploration Data in Delineating Structural Features within Salt Anticlines. USGS Open File Report 78–591. 1978.

Karol, R.H. Soils and Engineering. Prentice-Hall, Inc., Englewood Cliffs, N.J. 1960.

Lambe, T.W. and R.V. Whitman. Soil Mechanics, John Wiley & Sons, Inc., New York.1969.

Terzaghi, K. and R.P. Peck. Soil Mechanics in Engineering Practice, 2nd Edition. John Wiley & Sons, Inc., New York.1969.

Charles Stark Draper Labs., Inc. (McGowan, C. et al.). Borehole Plugging by Compaction Process, Final Report. For Office of Waste Isolation. Y–OWI–Sub 7087–1. August 1976.

FIGURE D–13 HYDRAULIC CONDUCTIVITY OF NATURAL MATERIALS

TABLE D-29

PROPERTIES OF POSSIBLE SEAL MATERIALS

Seal Material	Permeability* (cm/sec)	Porosity (%)	References
Concrete	$10^{-6} - 10^{-12}$	1-5	51,56,61,62
Compacted Earth	$10^{-6} - 10^{-10}$	1-15	51,54,63,64
Sand/ Montmorrillonite Bentonite	$10^{-8} - 10^{-10}$	1-15	30,51,64
Fused Salt	10^{-10}	0-0.5	52
Chemical Grout	$10^{-8} - 10^{-10}$	0	51,65
Bitumens	10^{-10}	0	51,62

*These values cover the ranges reported in the references cited. Testing procedures are not uniform. Larger variations are possible as materials and conditions are varied.

mechanisms, the simplest model, namely a linear increase from K_0 to K_1, has been adopted. This results in the equation

$$K = K_0 + \frac{K_1 - K_0}{10^4} t$$

A summary of the corresponding numerical formulas in two sets of units is given in Table D-30.

A constant porosity value,

$$\eta = 0.1,$$

is assumed in conjunction with the above permeability values in order to calculate actual fluid velocities. This parameter is also subject to variation depending on the design of the shaft seal.

D-3.2.4 Shaft Seal Release Model

A permeable shaft seal represents a possible pathway for fluid migration from the repository level to the groundwater system and to the surface. If radionuclides have been leached from the waste package as well, they may be transported to the geosphere or biosphere along with the fluid. Releases to the groundwater system would be expected to dominate over those to the surface for several reasons. For example, the hydrologic assumptions for the generic repositories admit the possibility of fluid flow from the repository to the upper aquifer, whereas there is no mechanism or sufficient driving potential to force water all the way to the surface. Transport of radionuclides to the surface could only be by diffusion in any water that might be seeping downward to the water table; diffusion calculations (see Appendix D-IV) show that mass transport by this process is exceedingly small. Furthermore, radionuclides migrating as far up as the aquifer would be largely washed into it by the groundwater flow. Therefore, only releases to groundwater, and in particular to the upper aquifer, have been modeled. Because certain parameter values and the dominant driving

TABLE D-30

PERMEABILITY AS A FUNCTION OF TIME FOR SHAFT SEAL DEGRADATION MODEL

	Permeability (K)	
	(cm/sec)	(m/yr)
First Estimate	$10^{-8} + 9.9 \times 10^{-11}\ t$	$3.15 \times 10^{-3} + 3.12 \times 10^{-5}\ t$
Second Estimate	$10^{-8} + 9.9 \times 10^{-9}\ t$	$3.15 \times 10^{-3} + 3.15 \times 10^{-3}\ t$

forces vary from one host rock to another, the release models are discussed here for each of the five geologic settings separately.

D-3.2.4.1 Bedded Salt

Repository resaturation times for a bedded salt repository are shown in Table D-31 based on calculations presented in Appendix D-II. Since the pore volume tends to decrease because of salt creep at the same time that water seeps into the repository, these resaturation times represent a balance point at which the remaining pore volume is exactly equal to the volume of water that has seeped in. Naturally there will be some non-uniformities in water distribution as well as in salt closure, but these factors are not included in the model.

Since the shafts extend down only to the repository level, they do not provide a connection between the upper and lower aquifers. It is possible that they may be coupled with other pathways from the repository to the lower aquifer, but this possibility will be discussed in connection with these other pathways (e.g., deep degrading boreholes). The hydraulic gradients generated in the cases of thermally induced convection or the U-tube effect are at most on the order $i = 0.1$ or 0.2 . Furthermore, mass transport by diffusion is much less. The effective hydraulic gradient generated by salt creep may be estimated as follows. The pressure exerted by the salt on the pore water is roughly equal to (and certainly bounded by) lithostatic pressure, which can be approximated by twice the hydrostatic pressure of a column of water extending to the surface. For a repository whose depth is 460 meters (recall Figure D-9), this corresponds to a pressure head of 920 meters of water. The permeable shafts cover a distance of 100 meters from the repository to the bottom of the aquifer, at which point the hydrostatic pressure is roughly 30 meters of water. Therefore, a net pressure head of $920-100-30 = 790$ meters of water acts over a path length of 100 meters, corresponding to a hydraulic gradient $i = 7.9$. This number is slightly conservative in the sense of overestimating the driving force, and hence appropriate to the approach of the present report, because as long as there is a permeable pathway from the repository, full lithostatic pressure on the pore water will never quite be achieved.

TABLE D-31

REPOSITORY RESATURATION TIMES
(BEDDED SALT REPOSITORY)

	Time to Resaturation (yrs)	Fluid Volume at Resaturation (m^3)
First Estimate	200	1.2×10^3
Second Estimate	720	5.6×10^5

Source: Appendix D-II.

It is clear from this calculation that salt creep provides the dominant driving force until the salt reaches a state of approximate mechanical equilibrium. The period between resaturation and arrival at this equilibrated state will be called Period A.

The effective hydraulic gradient just calculated can be used in Darcy's law to calculate volumetric fluid flow and fluid velocity. In particular

$$\dot{Q} = KiAc(\mu),$$

where

$\dot{Q}$ = volumetric fluid flow rate through permeable shafts;

K = hydraulic conductivity;

i = hydraulic gradient;

A = total cross-sectional area of the shafts;

$c(\mu)$ = viscosity correction factor, given by $.01/\mu$, where μ is the viscosity in poise. (Note that 0.01 represents the viscosity of water at 20°C, so that $c(\mu)$ is dimensionless.)

Values of the function $K(t)$ have been given in Section D-3.2.3 and are summarized there in Table D-30. The total cross-sectional shaft area was also specified in that section as $A = 100\ m^2$. While the viscosity μ varies with temperature and hence with depth, the value $\mu = 0.002$ poise, which corresponds to a temperature of 125°C, will be used throughout, so that $c(\mu) = 5$. (For further details on temperature and viscosity distributions, see Appendix D-VI.)

It is important to keep in mind that releases via this pathway continue to occur for a limited time only, determined by the time necessary for essentially all the water that has seeped into the repository to be squeezed back out. Using the first estimate parameter values, the cumulative outflow by time T is given by

$$Q(T) = \int_{200}^{T} \dot{Q} dt$$

$$= \int_{200}^{T} 3950(3.15 \times 10^{-3} + 3.12 \times 10^{-5}\ t)dt$$

$$= 0.062\ T^{2} + 12.4\ T - 4953$$

Complete depletion of the volume V of water in the repository would be achieved by this single pathway at the time T when Q(T) = V; that is

$$Q(T) = V$$

$$0.062\ T^{2} + 12.4\ T - 4953 = 1.2 \times 10^{3}$$

$$T = 231 \text{ years.}$$

However, permeable boreholes are additional pathways. Since these account for some of the outflow, the water will be depleted slightly sooner. Calculations in Section D-3.3.4 show that this time is the period from 200 to 223 years; thus the volumetric flow rate $\dot{Q}$ through the shafts is almost 40 m^3/yr. Note that this is only an approximate release period, not only because of variability and uncertainty in parameter values but also because the fluid volume will change somewhat because of the dissolution of some of the salt. Corresponding calculations for second estimate parameter values require some modification in the method. These calculations yield a total water release by a time that is earlier than the hypothesized time of complete repository closure, given as 1000 years. This implies that the rate of closure is the controlling factor in this case, the permeability of the shafts being sufficiently high so that the water moves out relatively easily. The release rate will therefore be modeled simply as the constant rate of void space volume change assumed in the closure model of Appendix D-VII, namely 2×10^6 $m^3/10^3$ years or 2×10^3 m^3/year.

Vertical fluid velocities may be obtained by dividing the "Darcy velocity,"

$$Kic(\mu),$$

by the effective porosity n, which was given in Section D-3.2.3 as $n = 0.1$. Therefore, the velocity v is given by the formula:

$$\begin{aligned} v &= \frac{Kic(\mu)}{n} \\ &= \frac{\dot{Q}}{nA} \\ &= \frac{\dot{Q}}{10} \end{aligned}$$

where the units are m/yr. It follows that the approximate average fluid velocities and the corresponding transit times from repository to aquifer are as given in Table D-32.

All the calculations performed so far in this section have been for Period A, which represents the period of non-negligible salt creep. During this period, the dominant driving mechanism is the pressure produced by this process. By the end of this period, the salt has reached a state of approximate mechanical equilibrium. The water that seeped in during the resaturation period has been forced back out, and the repository is still saturated but the fluid volume is relatively small. The tunnel backfill has been compacted, probably to near equilibrium, but it still has some permeability to fluid flow.

During the ensuing period of time, called Period B, the U-tube effect is the dominant driving force. The effective gradients have been calculated in Appendix D-V and are summarized in Table D-33. These gradients may be applied with Darcy's law to calculate the volumetric flow rates shown in Table D-34. (The cross-sectional area is $A = 50$ m^2.) Corresponding fluid velocities are given in Table D-35. The source term for this failure element consists of the concentration of

TABLE D-32

APPROXIMATE FLUID VELOCITIES AND TRANSIT TIMES TO AQUIFER ALONG PERMEABLE SHAFTS DURING PERIOD A (BEDDED SALT REPOSITORY)

	Fluid Velocity (m/yr)	Transit Times (yr)
First Estimate	4	25
Second Estimate	200	0.5

TABLE D-33

EFFECTIVE VERTICAL HYDRAULIC GRADIENT IN PERMEABLE SHAFTS FROM U-TUBE EFFECT DURING PERIOD B (BEDDED SALT REPOSITORY)

	Hydraulic Gradient (i)		
	223 years*	1000 years	10,000 years
First Estimate	0.03	0.02	0.004
Second Estimate	Not applicable**	0.004	0.0004

---

*Years after repository closure.

**Period B only begins at 1000 years after repository closure in the case of second estimates.

TABLE D-34

VOLUMETRIC FLOW RATES THROUGH PERMEABLE SHAFTS
DURING PERIOD B
(BEDDED SALT REPOSITORY)

	Volumetric Flow ($\dot{Q}$) (m^3/yr)		
	223 years*	1000 years	10,000 years
First Estimate	0.08	0.17	0.32
Second Estimate	Not applicable	3.15	3.15

---

*Years after repository closure.

TABLE D-35

FLUID VELOCITIES THROUGH PERMEABLE SHAFTS DURING PERIOD B (BEDDED SALT REPOSITORY)

	Velocity (v) (m/yr)		
	223 years*	1000 years	10,000 years
First Estimate	0.02	0.03	0.06
Second Estimate	Not applicable	0.63	0.63

---

*Years after repository closure.

radionuclides that have leached into the water in the repository during the time frame of interest.

Dissolution along the flow pathway is expected to be minimal because of the limited volume of fluid that would come into contact with the actual boundary of the shaft. In addition, half of the shaft length between repository and aquifer is through a shale layer. Even if the entire portion of the shaft through the salt were to be "short circuited" by dissolution pathways along the edges, the resulting flow would increase at most by a factor of two (since the driving potential would be dissipated over half the length, thereby doubling the gradient). The coupling of this pathway with others, such as degrading deep boreholes, is possible during the period before salt creep closes the repository, but the corresponding hydraulic potential would be sufficiently small that this effect would neither persist nor be significant compared with the release model presented above.

D-3.2.4.2 Granite

Assuming that repository resaturation has taken place, two driving forces need to be evaluated for their potential contribution to fluid flow from the repository to the aquifer. These forces are thermally induced convection and the U-tube effect. (Note that molecular diffusion is always negligible compared with mechanisms that move radionuclides by fluid flow, and that there is no lower aquifer in the generic granite repository.) Both of these forces are functions of time. Thermally induced convection depends on time because the temperature profile changes with time. The U-tube effect depends on time because of the gradual change in the hydraulic conductivity of the shaft seals. The values of the corresponding gradients, if calculated independently, are shown in Table D-36. These values are based on Appendices D-V and D-VI. These effects interact, tending to move water in opposite directions in those shafts where the U-tube effect would lead to a downward flow. For the present calculations, flow rates are based on the larger of the two effects. Since the flow pathway for the U-tube effect is half that for thermally induced convection, the

TABLE D-36

EFFECTIVE VERTICAL HYDRAULIC GRADIENT IN PERMEABLE SHAFTS FROM THERMALLY INDUCED CONVECTION AND U-TUBE EFFECT (GRANITE REPOSITORY)

	Hydraulic Gradient (i)		
	100 years*	1000 years	10,000 years
Thermally Induced Convection			
First Estimate	0.10	0.06	0.01
Second Estimate	0.10	0.06	0.01
U-Tube Effect			
First Estimate	0.02	0.02	0.02
Second Estimate	0.17	0.12	0.03

*Years after repository closure.

Source: Appendices D-V and D-VI.

effective gradients for the former need to be more than twice as large for that effect to dominate.

The volumetric flow rate is calculated from the equation:

$$\dot{Q} = KiAc(\mu)$$

where

$$K = K_0 + \frac{K_1 - K_0}{10^4} t$$

$$A = 50 \text{ or } 100$$

$$c(\mu) = 5$$

and i is given as a function of time in Table D-36. The value of permeability K as a function of time has been given previously in Table D-30. Note that $A = 50\ m^2$ in the U-tube cases because only half the total cross-sectional shaft area is used for transport upwards. The results of the calculation are given in Table D-37. By a modification of these results one obtains the fluid velocity from the formula

$$v = Kic(\mu)/n$$

$$= \dot{Q}/nA$$

in m/yr, where the porosity $n = 0.1$, given earlier, has been employed. The corresponding velocities are given in Table D-38.

The source term for this failure element consists of the concentration of radionuclides that have leached into the water in the repository during the time frame of interest.

No significant coupling is expected between this failure element and others. In addition, the flows evaluated here are much smaller than those through the bulk rock, and therefore this failure element is not very significant for the granite repository.

TABLE D-37

VOLUMETRIC FLOW RATES THROUGH PERMEABLE SHAFTS (GRANITE REPOSITORY)

	Volumetric Flow ($\dot{Q}$) (m^3/yr)		
	100 years*	1000 years	10,000 years
First Estimate	0.3	1.0	1.6
Second Estimate	15.9	94.6	236.3

*Years after repository closure.

TABLE D-38

FLUID VELOCITIES THROUGH PERMEABLE SHAFTS
(GRANITE REPOSITORY)

	Velocity (v) (m/yr)		
	100 years[*]	1000 years	10,000 years
First Estimate	0.03	0.1	0.3
Second Estimate	3.2	18.9	47.3

[*] Years after repository closure.

D-3.2.4.3 Basalt

Assuming that repository resaturation has taken place, two driving forces need to be evaluated for their potential contribution to fluid flow from the repository to the aquifer. These forces are thermally induced convection and the U-tube effect. With respect to other potential driving forces, note first that molecular diffusion is always negligible compared with mechanisms that move radionuclides by fluid flow. Second, the other potential driving mechanism--the hydraulic gradient resulting from the connection between the lower and upper aquifer--cannot result from shaft seal degradation alone because this does not provide a pathway to the lower aquifer. It is possible that the shaft seal failure may interact with other pathways to the aquifer, such as degrading deep boreholes, and this possibility will be evaluated later in this section. Both thermally induced convection and the U-tube effect are functions of time, and the analysis for basalt closely parallels that presented in the previous section for granite. Therefore, this section will concentrate on a summary of the corresponding results for the basalt repository.

The values of the effective hydraulic gradients corresponding to thermally induced convection and the U-tube effect, if calculated independently, are shown in Table D-39. As discussed earlier, it follows that for the purposes of calculating the joint effect the maximum of the individual effects may be utilized. The volumetric flow rate calculations are summarized in Table D-40, and the actual fluid velocities are shown in Table D-41. As in the case of granite it turns out that these quantities are negligible with respect to those calculated earlier for flow through the bulk rock, and therefore they are relatively unimportant. The source term for this failure element consists of the concentration of radionuclides that have leached into the water in the repository during the time frame of interest.

A certain degree of coupling between this failure element, and others, such as permeable boreholes, is possible. In the case of first-estimate calculations, the assumed hydraulic potential between the upper and lower aquifers (see Chapter D-2.0) is sufficiently small so that even if this factor were added to the gradient operative from the

TABLE D-39

EFFECTIVE VERTICAL HYDRAULIC GRADIENT IN PERMEABLE SHAFTS FROM THERMALLY INDUCED CONVECTION AND U-TUBE EFFECT (BASALT REPOSITORY)

	Hydraulic Gradient (i)		
	100 years*	1000 years	10,000 years
Thermally Induced Convection			
First Estimate	0.12	0.10	0.03
Second Estimate	0.12	0.10	0.03
U-Tube Effect			
First Estimate	0.04	0.04	0.04
Second Estimate	0.36	0.20	0.04

*Years after repository closure.

Source: Appendices D-V and D-VI.

TABLE D-40

VOLUMETRIC FLOW RATES THROUGH PERMEABLE SHAFTS
(BASALT REPOSITORY)

	Volumetric Flow ($\dot{Q}$) (m^3/yr)		
	100 years*	1000 years	10,000 years
First Estimate	0.4	1.7	3.2
Second Estimate	28.6	157.6	472.6

*Years after repository closure.

TABLE D-41

FLUID VELOCITIES THROUGH PERMEABLE SHAFTS
(BASALT REPOSITORY)

	Velocity (v) (m/yr)		
	100 years*	1000 years	10,000 years
First Estimate	0.04	0.2	0.6**
Second Estimate	5.7	31.5	63**

*Years after repository closure.

**Although the maximum volumetric flow rate in this case would result from thermally induced convection, the maximum velocity corresponds to the U-tube effect.

U-tube or thermal convection cases the result would not be significantly modified. The value of the second estimate for the average hydraulic gradient for the upper and lower aquifers is considerably larger, however, namely, 0.5. This corresponds to a hydraulic potential equivalent to 100 meters of water acting over the 200-meter distance between the upper and lower aquifers. The corresponding flow would be in the upward direction. If a significant portion of this driving force is dissipated over the upper half of the flow pathway, namely, from the repository to the upper aquifer, then it is possible that the corresponding gradient over this pathway is greater than that from either thermally induced convection or the U-tube effect. Calculations (see Section D-3.3) show that this is not the case, however. In the case of second estimates, the permeability function describing the performance of the shaft seals is identical to the permeability function describing the performance of the boreholes. Therefore the drop in hydraulic potential over the shaft seal pathway from the repository to the upper aquifer compares with that over the 10 boreholes from the repository to the lower aquifer in inverse proportion to the corresponding cross-sectional areas. Since these cross-sectional areas have been assumed to be in the ratio 100 to 1, it is clear that the overwhelming fraction of the hydraulic potential drop is dissipated over the lower half of the pathway and the contribution to flow in permeable shafts is negligible. Therefore this interactive effect does not need to be considered further. Even beyond considerations such as this, however, is the fact that the flows through the shafts are themselves small in terms of both volumetric rates and fluid velocities with respect to those through the bulk rock.

D-3.2.4.4 Shale

With respect to all the modeling parameters relevant to the present release mechanisms, the basalt and shale repositories appear identical. Therefore the discussion and the numerical computations for basalt carry over the shale. Tables D-42 and D-43 summarize these results for shale.

TABLE D-42

VOLUMETRIC FLOW RATES THROUGH PERMEABLE SHAFTS (SHALE REPOSITORY)

		Volumetric Flow ($\dot{Q}$) (m^3/yr)	
	100 years*	1000 years	10,000 years
First Estimate	0.4	1.7	3.2
Second Estimate	28.6	157.6	472.6

*Years after repository closure.

TABLE D-43

FLUID VELOCITIES THROUGH PERMEABLE SHAFTS (SHALE REPOSITORY)

	Velocity (v) (m/yr)		
	100 years[*]	1000 years	10,000 years
First Estimate	0.04	0.2	0.6[**]
Second Estimate	5.7	31.5	63.0[**]

[*] Years after repository closure.

[**] Although the maximum volumetric flow rate in this case would result from thermally induced convection, the maximum velocity corresponds to the U-tube effect.

D-3.2.4.5 Dome Salt

Repository resaturation times for a repository in a salt dome are shown in Table D-44, based on calculations presented in Appendix D-II. Since the pore volume tends to decrease because of salt creep at the same time that water seeps into the repository, these resaturation times represent a balance point at which the remaining pore volume is exactly equal to the volume of water that has seeped in. Naturally there will be some non-uniformities both in water distribution and in salt closure, but these factors are not included in the model.

The analysis of the dominant driving forces to cause water to move from a salt dome repository to the groundwater is analogous to that for bedded salt. Therefore this section will simply summarize differences in the parameter values and in the numerical results.

First, for the period of extensive salt creep (Period A), the effective hydraulic gradient tending to force water along permeable shafts needs to be recalculated because the distance from the repository to the upper aquifer is different in this case. In particular there is a net pressure head of 920-230-30 = 660 meters of water acting over a path length of 230 meters (cf. earlier calculations for bedded salt). This yields an effective hydraulic gradient of $i = 2.9$. Calculations proceed analogously to the case of bedded salt. For the first estimate case, Period A extends from 200 to about 260 years after repository closure, with an average volumetric flow rate Q equal to about 15 m^3/yr. For the second estimate case, Period A extends from 748 to 1000 years after repository closure, with an average volumetric flow rate Q equal to about 2×10^3 m^3/yr. The corresponding fluid velocities and transit times are shown in Table D-45. Fluid flows during Period B result from the U-tube effect. Effective gradients are given in Table D-46, volumetric flow rates in Table D-47, and fluid velocities in Table D-48. The source term for this failure element consists of the concentration of radionuclides which have leached into the water in the repository during the time frame of interest.

Dissolution along the flow pathway is expected to be minimal because of the limited volume of fluid which would come into contact with the actual boundary of the shaft. In addition, half of the shaft length

TABLE D-44

REPOSITORY RESATURATION TIMES
(DOME SALT REPOSITORY)

	Time to Resaturation (yrs)	Fluid Volume at Resaturation (m^3)
First Estimate	200	865
Second Estimate	748	5×10^5

Source: Appendix D-II.

TABLE D-45

APPROXIMATE FLUID VELOCITIES AND TRANSIT TIMES TO AQUIFER ALONG PERMEABLE SHAFTS DURING PERIOD A (DOME SALT REPOSITORY)

	Fluid Velocity (m/yr)	Transit Times (yr)
First Estimate	1.5	150
Second Estimate	200	1

TABLE D-46

EFFECTIVE VERTICAL HYDRAULIC GRADIENT IN PERMEABLE SHAFTS FROM U-TUBE EFFECT DURING PERIOD B (DOME SALT REPOSITORY)

	Hydraulic Gradient (i)		
	260 years*	1000 years	10,000 years
First Estimate	0.014	0.012	0.003
Second Estimate	Not applicable	0.004	0.0004

*Years after repository closure.

TABLE D-47

VOLUMETRIC FLOW RATES IN PERMEABLE SHAFTS DURING PERIOD B (DOME SALT REPOSITORY)

	Volumetric Flow ($\dot{Q}$) (m^3/yr)		
	260 years*	1000 years	10,000 years
First Estimate	0.04	0.10	0.24
Second Estimate	Not applicable	3.15	3.15

*Years after repository closure.

TABLE D-48

FLUID VELOCITIES THROUGH PERMEABLE SHAFTS DURING PERIOD B (DOME SALT REPOSITORY)

	Velocity (v) (m/yr) 260 years*	 1000 years	 10,000 years
First Estimate	0.01	0.02	0.05
Second Estimate	Not applicable	0.63	0.63

*Years after repository closure.

between repository and aquifer is through a shale layer. Even if the entire portion of the shaft through the salt were to be "short-circuited" by dissolution pathways along the edges, the resulting flow would increase at most by a factor of two (since the driving potential would be dissipated over half the length, thereby doubling the gradient).

D-3.2.5 Literature Discussion

The shaft seal failure model has also been discussed by TASC.(51,53) While recognizing that the condition of a sealed shaft is both temporally and spatially dependent, they do not try to quantify this dependence. Instead they perform a number of flow calculations based on the assumption of a shaft with "failed backfill." The parameters used for the analyses are summarized in Table D-49. For purposes of sensitivity analysis, permeabilities were varied by up to three orders of magnitude, and porosities by one order of magnitude. These parameters were not based on specific designs or site characteristics.

D-3.3 BOREHOLE SEAL FAILURE

D-3.3.1 Summary

During both the preliminary and the detailed site evaluation for a repository, a number of boreholes will be drilled to various depths at the site. These will be used for geologic and hydrologic characterization of the site as well as to determine the potential for mineral and energy resources that may be sought on the site by future generations. In addition to these boreholes, which will be drilled specifically for repository site investigations, there may be old boreholes on the site representing previous water, mineral, or energy resource exploration or exploitation. In some cases, it may be difficult or impossible to find these older boreholes; the risks associated with those that remain undetected are discussed as a separate failure event in Section D-3.4. All old boreholes that are found,

TABLE D-49

BASELINE PARAMETERS USED BY TASC IN FAILED SHAFT SEAL CALCULATIONS

	Permeability (cm/sec)	Porosity (%)	Area (m^2)
Fracture zone around shaft through shale	10^{-4}	10^{-3}	10
Fracture zone around shaft through salt	10^{-6}	10^{-3}	60
Shaft with failed backfill	10^{-4}	10^{-2}	64

Sources: The Analytic Sciences Corporation (Berman, L.E., et al.). Analysis of Some Nuclear Waste Management Options. For Lawrence Livermore Laboratory. UCRL/13917; TR-1100-1-1. October 10,1978.

The Analytic Sciences Corporation (Koplik, C.M. et al.). Information Base for Waste Repository Design. Vol. I. Borehole and Shaft Sealing. For U.S. Nuclear Regulatory Commission. NUREG/CR-0495, TR - 1210-1. March 1979.

however, are expected to be redrilled and replugged according to the same specifications as the new boreholes drilled during the repository site evaluation. The purpose of this section is to present a model of the performance of borehole plugs emplaced as part of the repository sealing process. Both the general considerations and the specific model approach parallel to a considerable extent the discussion on shaft seal failure presented in the previous section, to which reference will frequently be made.

The borehole sealing materials will need to be chosen with a specific environment in mind, so that they may approach, as nearly as possible, chemical and mechanical equilibrium with the surrounding rock. The seal may consist of several layers of completely distinct types that provide a multi-barrier line of defense against expected or unexpected forces. Nevertheless, it is reasonable to expect that over a long period of time, say, 10,000 years, the combination of processes such as settling, leaching, expansion or contraction from fluctuations in water content or temperature, earth movements, weathering, and fatigue may lead to some degradation in the integrity of the seal.

The borehole seal performance model in this report is not based upon a particular design. It is intended to be "generic" in nature and conservative; that is, it is believed that the performance characteristics described here can be equalled or exceeded by actual designs for specific circumstances.

The specific model in this report characterizes the borehole seal integrity in terms of a spatially uniform hydraulic conductivity K. One hydraulic conductivity value (K_0) is estimated for the time of seal emplacement, and another value (K_1) is estimated for the time 10,000 years later. It is assumed that K increases linearly from K_0 to K_1 over this period. The specific values of the parameters used as well as a summary of the corresponding release models are given in Table D-50.

D-3.3.2 Background

Site exploration and repository monitoring will involve the drilling of a number of small diameter (less than 0.5 meter) boreholes into the host rock and surrounding formations. These borings will provide

TABLE D-50
SUMMARY OF BOREHOLE SEAL FAILURE ELEMENT

MEDIUM	PROBABILISTIC (P) DETERMINISTIC (D)	NATURE OF MODEL	RELEASE MODE	DRIVING FORCE	SOURCE TERM	PARAMETERS		FLUID FLOW RATES FROM REPOSITORY TO UPPER AQUIFER				COMMENTS
						1st ESTIMATE	2nd ESTIMATE	1st ESTIMATE		2nd ESTIMATE		
								t (yrs)	$\dot{Q}$ (t) (m^3/yr)	t (yrs)	$\dot{Q}$ (t) (m^3/yr)	
Bedded Salt	D	Linearly increasing permeability	Groundwater	Initially pressure from salt creep. Afterwards, thermally induced convection and gradient from aquifer interconnection for boreholes extending to lower aquifer.	Uniform concentration	$K_0 = 10^{-8}$ cm/sec at time of sealing $K_1 = 10^{-6}$ cm/sec after 10,000 years K increases linearly from K_0 to K_1 over 10,000 years $\eta = 0.1$ 50 boreholes penetrate to repository, 10 of which continue to lower aquifer A = 0.1 m^2/borehole	$K_0 = 10^{-8}$ cm/sec at time of sealing $K_1 = 10^{-4}$ cm/sec after 10,000 years K increases linearly from K_0 to K_1 over 10,000 years $\eta = 0.1$ 50 boreholes penetrate to repository, 10 of which continue to lower aquifer A = 0.1 m^2/borehole	200 223^- 223^+ 1000 10,000	14 } Period of salt creep 14 } 0.05 0.18 0.63	720 1000^- 1000^+ 10,000	100 } Period of salt creep 100 } 19 167	Release only begin after repository resaturation. Dissolution in salt layer is included in second estimate calculations for period after extensive salt creep.
Granite	D	Linearly increasing permeability	Groundwater	Thermally induced convection	Uniform concentration	$K_0 = 10^{-8}$ cm/sec at time of sealing $K_1 = 10^{-6}$ cm/sec after 10,000 years K increases linearly from K_0 to K_1 over 10,000 years $\eta = 0.1$ 50 boreholes penetrate to repository A = 0.1 m^2/borehole	$K_0 = 10^{-8}$ cm/sec at time of sealing $K_1 = 10^{-4}$ cm/sec after 10,000 years K increases linearly from K_0 to K_1 over 10,000 years $\eta = 0.1$ 50 boreholes penetrate to repository A = 0.1 m^2/borehole	100 1000 10,000	0.1 0.8 2.4	100 1000 10,000	0.9 8.5 31.5	Release only begin after repository resaturation.
Basalt	D	Linearly increasing permeability	Groundwater	Thermally induced convection and gradient from aquifer interconnection for boreholes extending to lower aquifer.	Uniform concentration	$K_0 = 10^{-8}$ cm/sec at time of sealing $K_1 = 10^{-6}$ cm/sec after 10,000 years K increases linearly from K_0 to K_1 over 10,000 years $\eta = 0.1$ 50 boreholes penetrate to repository, 10 of which continue to lower aquifer A = 0.1 m^2/borehole	$K_0 = 10^{-8}$ cm/sec at time of sealing $K_1 = 10^{-4}$ cm/sec after 10,000 years K increases linearly from K_0 to K_1 over 10,000 years $\eta = 0.1$ 50 boreholes penetrate to repository, 10 of which continue to lower aquifer A = 0.1 m^2/borehole	100 1000 10,000	0.05 0.4 1.6	100 1000 10,000	2.0 19.2 170.1	Release only begin after repository resaturation

TABLE D-50
SUMMARY OF BOREHOLE SEAL FAILURE ELEMENT (CONTINUED)

MEDIUM	PROBABILISTIC (P) DETERMINISTIC (D)	NATURE OF MODEL	RELEASE MODE	DRIVING FORCE	SOURCE TERM	PARAMETERS		FLUID FLOW RATES FROM REPOSITORY TO UPPER AQUIFER				COMMENTS
						1st ESTIMATE	2nd ESTIMATE	1st ESTIMATE		2nd ESTIMATE		
								t (yrs)	$\dot{Q}(t)$ (m^3/yr)	t (yrs)	$\dot{Q}(t)$ (m^3/yr)	
Shale	D	Linearly increasing permeability	Groundwater	Thermally induced convection and gradient from aquifer interconnection for boreholes extending to lower aquifer.	Uniform concentration	K_0 = 10^{-8} cm/sec at time of sealing K_1 = 10^{-6} cm/sec after 10,000 years K increases linearly from K_0 to K_1 over 10,000 years η = 0.1 50 boreholes penetrate to repository, 10 of which continue to lower aquifer A = 0.1 m^2/borehole	K_0 = 10^{-8} cm/sec at time of sealing K_1 = 10^{-4} cm/sec after 10,000 years K increases linearly from K_0 to K_1 over 10,000 years η = 0.1 50 boreholes penetrate to repository, 10 of which continue to lower aquifer A = 0.1 m^2/borehole	100	0.06	100	2.0	Release only begin after repository resaturation.
								1000	0.4	1000	19.2	
								10,000	1.6	10,000	170.1	
Dome Salt	D	Linearly increasing permeability	Groundwater	Initially pressure from salt creep. Afterwards, the U-tube effect.	Uniform concentration	K_0 = 10^{-8} cm/sec at time of sealing K_1 = 10^{-5} cm/sec after 10,000 years K increases linearly from K_0 to K_1 over 10,000 years η = 0.1 50 boreholes penetrate to repository A = 0.1 m^2/borehole	K_0 = 10^{-8} cm/sec at time of sealing K_1 = 10^{-4} cm/sec after 10,000 years K increases linearly from K_0 to K_1 over 10,000 years η = 0.1 50 boreholes penetrate to repository A = 0.1 m^2/borehole	200	5 } Period of salt creep	748	100 } Period of salt creep	Release only begin after repository resaturation. In contrast to undetected borehole failure element, holes in this case are near or through repository and so cannot intersect lower aquifer at edge of salt dome.
								260^-	5 }	1000^-	100 }	
								260^+	0.01	1000^+	1.6	
								1000	0.03	10,000	2.8	
								10,000	0.16			

information on the depth, thickness, lithology, geohydrology, and structure of the geologic formations at the site. Core samples taken from the drill holes can be used for laboratory studies of mineralogy, chemistry, porosity, permeability, strength, etc., and the collective data can be used in the evaluation of the site's suitability for a repository. Major factors of interest include the effectiveness of the geology in providing a barrier to radionuclide escape and the possible presence of natural resources that might be sought by future generations.

In addition to holes that are related to the repository, a number of boreholes may have been drilled previously for unrelated purposes, for example, to explore or to exploit water, mineral, and energy resources at the site. Drilling records from such holes might also serve to enhance the information obtained from the repository-related borings, particularly in assessing the economic potential of a site and the effects of its loss to future generations. Of course, it is possible that one or more pre-existing holes may fail to be identified. The problem of undiscovered boreholes is discussed in Section D-3.4; this section is concerned only with those that are identified.

The technology for plugging boreholes for abandonment has been well developed, especially in response to legal requirements by the petroleum producing states. These requirements are primarily intended to prevent the contamination of water supplies or the escape of fluids to the surface. Plugging or replugging has also been carried out in order to seal off depleted gas fields so that they might be used for storage of injected gas. In addition to sealing for abandonment, plugging techniques have been developed for a number of other purposes, such as separating productive horizons, diverting drill strings from a blocked hole, and preventing blowouts.(51,56,62,66,67)

The most common sealing materials for abandoned boreholes are cement and heavy mud. They are usually used in combination, with the cement being placed against permeable or soluble formations and the dense mud providing support for the cement. The cement is formulated to withstand chemical attack and to provide adhesion with the rock. For example, salt is typically added to the cement if the plug is placed in a salt formation, in circulating brines, or in water sensitive shales.

Sulfate-resistant cements are used near evaporites or where groundwater contains sulfate ions, and other formulations are available for different adverse conditions. Typical muds consist of starches and clays suspended in water and brine, and barite or other dense minerals may be added to adjust the mud's density. (51) A cement-mud plug is shown schematically in Figure D-14.

Studies examining the suitability of concrete plugs for boreholes into a nuclear repository have noted some of the problems that can arise in connection with plug emplacement and long-term stability.(53) Furthermore, because a cement slurry has a high viscosity compared with water, it is questionable whether cement could successfully seal the fine fissures or permeable zones in the rock immediately surrounding the borehole.(68)

If injection pressure were to be high enough to force the cement deeply enough into the rock to seal fine fissures, the fissures might be extended by induced fracturing.

The problems involved in designing cement seals and in emplacing them properly are emphasized by some failures that have been noted in the past. For example, in one study, the quality of plugs in abandoned holes was checked about 40 years after emplacement.(62) Twenty holes were rebored and the findings compared with plugging records. Forty-nine plugs had been set in these twenty wells. The findings were:

- 11 plugs (22%) were missing,
- 6 plugs (12%) were soft,
- 5 wells (25%) had all plugs soft or missing,
- 10 wells (50%) had soft or missing bottom plugs, and
- 2 wells (10%) had no top plugs.

Naturally, one expects significant improvements after the many intervening years of development of materials and engineering practices. But it is also true that the degradation referred to took place over 40 years, and the repository model is concerned with a period of 10,000 years. In any case, uncertainties remain about the long-term performance capabilities of cement plugs.

Along with continuing investigations into cement's behavior as a borehole plug material, work has also been conducted on the properties of other sealants and fillers, and on other plugging methods. Among the

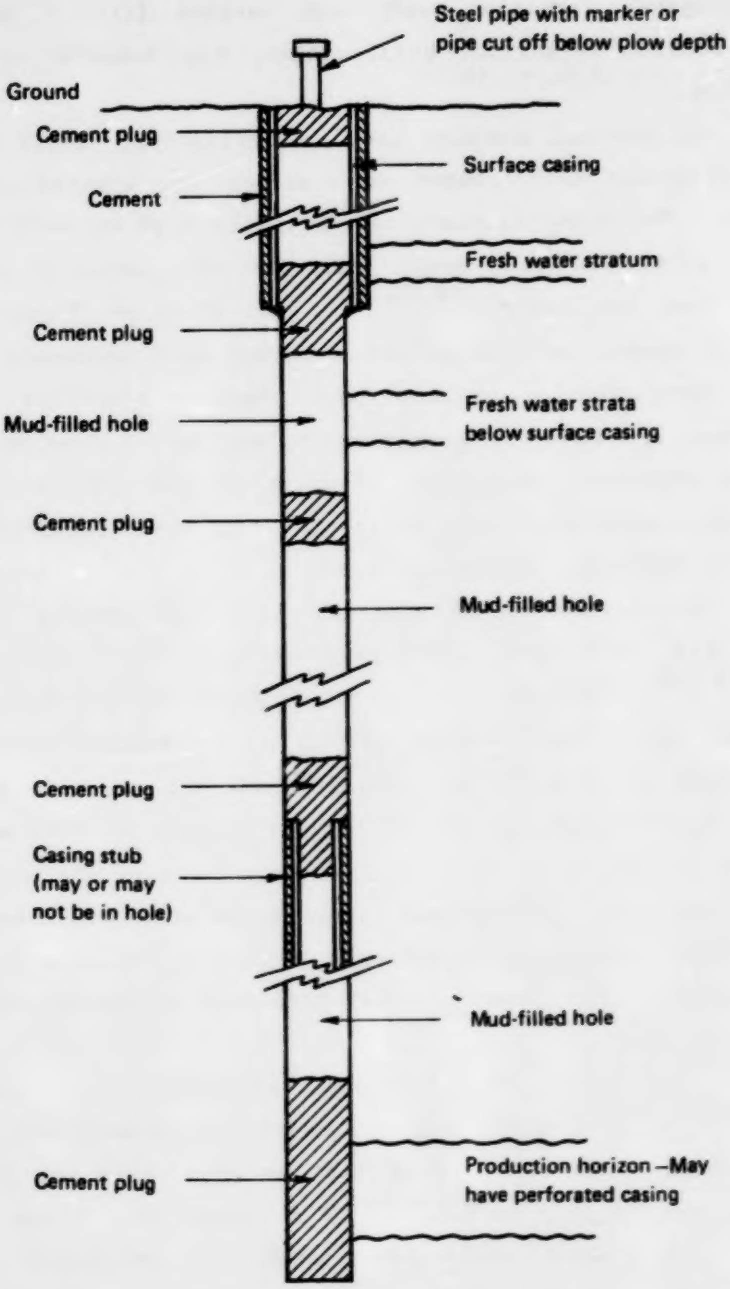
Steel pipe with marker or pipe cut off below plow depth
Ground
Cement plug
Surface casing
Cement
Fresh water stratum
Cement plug
Mud-filled hole
Fresh water strata below surface casing
Cement plug
Mud-filled hole
Cement plug
Casing stub (may or may not be in hole)
Mud-filled hole
Cement plug
Production horizon – May have perforated casing

Source: Adapted from Herndon, J. and D.K. Smith. Plugging Wells for Abandonment: A State of the Art Study. For Office of Waste Isolation. Y/OWI/Sub–76/99068, 1976.

FIGURE D–14 TYPICAL PLUGGED BOREHOLE

other materials examined are a variety of chemical sealants, natural sealants, original formation rock, and earthen fills. Emplacement techniques include injection, catalyzation, high-temperature melting, and compaction.(47,52,54,55,58)

Some of the chemical sealants have properties that enable them to be used in conjunction with cement to overcome the limitations of the latter alone. For example, plasticizing resins with viscosities as low as that of water can fill small fractures and permeable zones more effectively than can cement.(58,68,69) They also are frequently more flexible than cement and can adjust to minor rock movements. On the other hand, many chemical sealants have unproven stability over long periods. Some are moisture sensitive or may have differing physical properties in different rock types. Also, since most synthetic sealants contain organic compounds, there arise questions about possible chemical breakdown from bacterial action.

Natural sealants, such as asphalt, tar, and similar bituminous materials, may have long life expectancies under a variety of conditions.(47,58) However, emplacement of these materials may require heating, which could result in contraction of the sealant upon cooling. The contraction could pull the sealant from the borehole walls and negate its effectiveness. Alternatively, a plastic or viscous sealant may seep out of the borehole into fractures or into the rock pores. This volume loss could initiate additional movement in other sections of the seal column. The organic components of natural sealants may also be subject to some of the same bacterial breakdown mechanisms as are the synthetic compounds.

The use of rock or earthen materials has also been suggested.(26,52,54) Plugging with molten rock represents one approach, the intent being to provide a plug that is chemically and physically identical to the in-situ rock.(52) To do this, rock taken from the formation to be plugged would be crushed and introduced into the borehole. There, heaters would melt the crushed rock and either spray it on the walls or allow it to pool at the bottom of the open hole. Alternatively, the rock could first be melted at the surface. Although a promising concept, this method has not yet been successfully demonstrated in practice, and it has potential problems. Cracking of the plug and wall rock during cooling is likely. Also, the method is essentially limited to rocks with low melting points and temperature-insensitive mineralogies, such as rock salt. The compaction of earthen materials represents another approach to create a plug with a long probable life. In this case, clays, clay-sand mixes, or excavated formation rock would be introduced into a borehole and compacted at the bottom of the hole. A number of methods of compaction are possible. Impact compaction could be accomplished by dropping a cable tool manipulated from the surface or by pneumatic or electric hammers within the hole. Static compaction might require hydraulic or pneumatic rams affixed to the sides of the hole. Kneading of the fill could be carried out using rotary drill equipment at the surface to operate a roller compactor at the end of a drill string.(54) Since the compacted earth would consist of materials with chemical and physical properties similar to those of the formation rock, interaction with the rock may be very minor. However, as with the molten rock concept, other problems can arise. For example, compacted-earth plugging requires the development of new equipment. Adhesion between the plug and the native rock may be poorer than for other seal materials, and initial permeabilities may be higher than expected and difficult to control.(51,54)

Both the initial quality of a plug and its longevity are affected by the care with which the borehole is prepared and the plug emplaced. Several stages of preparation are involved regardless of the plugging material or emplacement methods. In general, anything that might interfere with the plug, the rock, or the bond between the plug and the rock must be remedied. All foreign matter should be removed. This entails stripping from the hole any remaining casing, equipment, or debris. If such materials cannot be extracted, it is sometimes necessary to overbore the hole or to cut windows in the casings or obstructions so that sealants may be forced past. Residual drilling fluid, mud, oil, or other contaminants must be removed. Both mechanical scrubbers and specialized solvents are available, but their use requires care and judgment in order to avoid substituting one contamination problem for another. Next, the walls of the borehole should be logged so that the position and characteristics of the rock along its length are well known. This step is essential in order to match sealants with the rock, to determine quantities of plugging material to be used, and to select the best emplacement method.

At present, no plugging method appears assured of providing both low initial hydraulic conductivity and long-term stability. The purpose of the previous paragraphs has been to highlight possible techniques and indicate potential problem areas.

D-3.3.3 Borehole Seal Failure Model

For this analysis, the performance of a borehole plug is defined by its ability to restrict fluid movement along the borehole. The hydraulic conductivity of the plug is the principal parameter controlling fluid movement. Although the fill material and its properties may vary from point to point, for the purpose of this model it is sufficient to assume an effective uniform hydraulic conductivity for the entire length of the filled hole. Auxiliary parameters, such as number and size of boreholes and the porosity of the fill, must also be specified in order to compute total volumetric fluid flows and fluid velocities.

Many of the same degradation mechanisms that we discussed in the section on shaft seals also apply to borehole seals, and so a gradual increase in hydraulic conductivity is expected over time. Therefore, modeling plug performance requires the determination of a function K(t) that expresses the hydraulic conductivity of the plug as a function of time. Determination of this function involves the specification of three items: the initial value K_0 for the time of plug emplacement, the deteriorated (greater) value K_1 for 10,000 years, and a rule governing the transition from K_0 to K_1.

Initial permeabilities, K_0, for both first and second estimates are taken as 10^{-8} cm/sec. It appears that this value can be met or bettered by a number of materials and designs, as suggested by the data in Table D-29. (See Section D-3.2) This performance measure is independent of the host rock, although the specific design to achieve it may well depend on the host rock. It is further assumed that all known boreholes are sealed to this degree of impermeability. Previously plugged holes must be reamed out, all junk, old casings, and loose materials must be stripped from them, and mud, oil, or other contaminants must be cleaned from the walls.

Estimates of final permeabilities, K_1, follow the rationale set forth for shaft seal performance. For borehole plugs, however, the first estimate permeabilities are taken to be 10^{-5} cm/sec rather than 10^{-6} cm/sec, as was assumed for the shaft seals. This difference reflects perceived difficulties in placing and testing a borehole plug. Unlike a shaft seal, a borehole plug must be inspected or tested remotely. The quality of plugs is therefore more suspect, and a more rapid degradation is assumed.

The second estimate for the final permeability, K_1, is taken to be 10^{-4} cm/sec, as it was for the shaft seal. This condition also corresponds to a borehole filled with silty sand, or silty sand and gravel. The permeabilities of specific soil types vary greatly depending on conditions of compaction, but the data given earlier in Figure D-13 (see Section D-3.2) provide a context within which to interpret these numbers.

Values of K_0 and K_1 having been specified, it is next necessary to estimate a function K(t) that describes the change from K_0 to K_1. In the absence of detailed plug designs and models for degradation mechanisms, the simplest model, namely a linear increase from K_0 to K_1, has been adopted. This results in the equation

$$K = K_0 + \frac{K_1 - K_0}{10^4} t .$$

A summary of the corresponding numerical formulas in two sets of units is given in Table D-51.

Flow volume along a filled borehole is proportional to its cross-sectional area, other factors being fixed. Therefore, in order to calculate quantities of water moving through a borehole, a value for its cross-sectional area is required. For the present model, each hole has been assigned a conservatively large cross section of 0.1 m^2. For this analysis, 50 holes have been assumed to reach the repository. Where the generic medium is modeled with a lower aquifer, 10 of these 50 holes have been assumed to reach the lower aquifer. A constant porosity value, $n = 0.1$, is used in conjunction with the other parameter values

TABLE D-51

PERMEABILITY AS A FUNCTION OF TIME FOR BOREHOLE SEAL DEGRADATION MODEL

	Permeability (K) (cm/sec)	Permeability (K) (m/yr)
First Estimate	$10^{-8} + 9.9 \times 10^{-10}\ t$	$3.15 \times 10^{-3} + 3.15 \times 10^{-4}\ t$
Second Estimate	$10^{-8} + 9.9 \times 10^{-9}\ t$	$3.15 \times 10^{-3} + 3.15 \times 10^{-3}\ t$

in order to calculate actual fluid velocities. This parameter is also subject to variation, depending on the design of the borehole plug.

It is likely that a repository will be planned so that the rock surrounding the boreholes will not be excavated. The intention would be to contain the boreholes in such pillars as an additional barrier to fluid flow. Nevertheless, at a depth of 500 meters there is likely to be some uncertainty over the exact location of a borehole, and so it is possible that the excavation may actually intersect it. Furthermore, previously undetected boreholes may be discovered by the excavation process itself. Because of these uncertainties, it has been conservatively assumed for this analysis that all the boreholes actually intersect mine drifts.

D-3.3.4 Borehole Seal Release Model

A permeable borehole seal represents a possible pathway for fluid migration from the repository level to the groundwater system and to the surface. If radionuclides have been leached from the waste package as well, they may be transported to the geosphere or biosphere with the fluid. Releases to the groundwater system would be expected to dominate over those to the surface for the same reasons discussed earlier for shaft seals. Therefore, only releases to groundwater, and in particular to the upper aquifer, have been modeled. Because both the parameter values and the dominant driving forces vary from one rock to another, the release models are discussed here for each of the five geological settings separately.

D-3.3.4.1 Bedded Salt

Repository resaturation times for a bedded salt repository have been given in Table D-31 (see Section D-3.2) based on calculations presented in Appendix D-II. Since the pore volume tends to decrease because of salt creep at the same time that water seeps into the repository, these resaturation times represent a balance point at which the remaining pore volume is exactly equal to the volume of water that has seeped in. Naturally, there will be some non-uniformities in water distribution as well as in salt closure, but these factors have not been included in the model.

All of the driving forces discussed in Chapter D-3.0 are present to a certain extent in the case of borehole seal degradation, and different ones dominate at different points in time. The period of possible fluid migration may be divided into two basic parts:

Period A--From resaturation time until effective closure of cavities and void spaces by extensive salt creep; and

Period B--Following Period A.

During Period A, the hydraulic pressure generated by salt creep can result in substantial gradients along permeable boreholes. The analysis for the corresponding situation with permeable shafts (Section D-3.2.4) also applies here, yielding a gradient on the order $i = 7.9$ in the portion of a borehole connecting the repository and the upper aquifer. According to the model assumptions discussed in Section D-3.3.3, there are 50 borehole pathways to the upper aquifer, 10 of which also connect to the lower aquifer. The 10 boreholes that penetrate to the lower aquifer also provide a small flow pathway downward, but the lower section of these boreholes has not been included in the calculations. The effect of omitting them from consideration for Period A releases is conservative in the sense of assuming that the fixed amount of fluid in the repository will all be forced into the upper aquifer, where the consequences of radionuclide concentrations would be expected to be more significant (albeit at the expense of a slight increase in the duration of the release).

Period A fluid flows were first calculated without consideration of the interactive effect with the permeable shafts (Section D-3.2). That is, all the water that entered the repository during the resaturation period was assumed to be forced out through the boreholes. The result of this calculation is therefore an upper bound on flow through the boreholes; in addition it enables a comparison between the effects of shafts and boreholes.

The calculations for first estimate parameter values proceed as follows. The volumetric fluid flow rate $\dot{Q}$ is given by

$$\dot{Q} = KiAc(\mu)$$

where

K = hydraulic conductivity, or permeability;

i = hydraulic gradient;

A = total cross section of all boreholes;

$c(\mu)$ = viscosity correction factor, given by $0.01/\mu$, where μ is the viscosity in poise. (Note that 0.01 represents the viscosity of water at 20°C, so that $c(\mu)$ is dimensionless.)

The values of these parameters are

$K = 3.15 \times 10^{-3} + 3.15 \times 10^{-4}\ t$ m/yr (from Table D-51)

$i = 7.9$

$A = 50 \times 0.1 = 5\ m^2$ (from Section D-3.2.3)

$c(\mu) = 5$ (from Section D-3.2.4)

It follows that the cumulative outflow from resaturation time (200 years) to an arbitrary time T is given by

$$
\begin{aligned}
Q(T) &= \int_{200}^{T} T\dot{Q}dt \\
&= \int_{200}^{T} 197.5(3.15 \times 10^{-3} + 3.15 \times 10^{-4}t)dt \\
&= (0.62t + 0.031t^2)\Big|_{200}^{T} \\
&= 0.031\ T^2 + 0.62\ T - 1364.
\end{aligned}
$$

If this flow pathway were to account for the complete depletion of the water in the repository at resaturation time, namely a volume

$V = 1.2 \times 10^3,\ m^3$ (from Table D-31)

then the flow would continue at the increasing rate $\dot{Q}$ until $Q(T) = V$. This would enable the determination of T as follows:

$$
\begin{aligned}
0.031\ T^2 + 0.62\ T - 1364 &= 1.2 \times 10^3 \\
T &= 278 \text{ years.}
\end{aligned}
$$

However, it is more accurate to take into account the fact that the outflow pathway consists of both shafts and boreholes, so that the volumetric flow rate is actually the sum of the individual functions Q(T) obtained here and in Section D-3.2.4. This approach yields the function:

$$Q(T) = 0.093\ T^2 + 13\ T - 6317.$$

The water available will then be depleted when Q(T) = V, which implies: that

$$0.093\ T^2 + 13\ T - 6317 = 1.2 \times 10^3$$
$$T = 223 \text{ years}.$$

The flow through the boreholes during this period (220-223 years) is approximately 14 m^3/yr.

As in the case of shaft seals, the analysis with second estimate parameters is somewhat different. Since the shaft seal analysis showed that in this case the limiting factor is the rate of salt creep rather than the conductivity of the flow path, the consideration of borehole pathways ought not affect the flow rates. In addition, the permeability functions for both shaft and borehole seals are identical, so that their relative importance is in the same proportion as their total cross-sectional areas, namely, 100:5. Therefore, the borehole pathway is quite insignificant by comparison. The volumetric flow rate is about 100 m^3/yr through this pathway.

Vertical fluid velocities within the boreholes may be obtained by dividing the Darcy velocity, Kic(μ), by the effective porosity η, which was given in Section D-3.2.3 as $\eta = 0.1$. Therefore, the velocity v is given by the formula:

$$\begin{aligned} v &= Kic(\mu)/\eta \\ &= \dot{Q}/\eta A \\ &= 2\dot{Q}, \end{aligned}$$

where the units are m/yr. It follows that the approximate average fluid velocities and the corresponding transit times from the repository to the aquifer within each borehole are as given in Table D-52.

All the calculations performed so far in this section have been for Period A, which represents the period of non-negligible salt creep. During this period, the dominant driving mechanism is the pressure produced by this process. At the end of this period the salt has reached a state of approximate mechanical equilibrium. The water that seeped in during the resaturation period has been forced back out; and the repository is still saturated, but the fluid volume is relatively small. The tunnel backfill has been compacted, probably to near equilibrium, but it still has some permeability to fluid flow.

The boreholes that descend only to the repository horizon cease to be important at this point compared with those that extend through to the lower aquifer and that can still serve as release pathways. In this case, the driving force consists of the combination of the difference in hydraulic potentials of the two aquifers and the thermally induced convection effect. These effects are essentially additive, so the effective hydraulic gradient in these boreholes may be obtained as given in Table D-53. By means of Darcy's law, these gradients yield the volumetric flow rates (for the 10 boreholes) and fluid velocities shown in Table D-54. The first estimate value for T = 223 years (the approximate starting point for Period B) has been obtained by interpolation. The values shown in Table D-54 do not account for possible dissolution around the borehole, which could lead to development of a wider channel and hence to greater flows. Detailed calculations in Appendix D-III indicate that the flow rates corresponding to first estimate parameter values are sufficiently small that salt creep is capable of preventing the development of an open channel. For the case of second estimate parameter values, however, dissolution does have the capability to develop an open channel through the salt. As a result, only that portion of the borehole through the upper and lower shale levels should be assumed to act as a partial barrier to fluid flow. Since this comprises one-half of the total length of the borehole between the aquifers, the flow rates are roughly doubled. Table D-55 incorporates these dissolution considerations into the calculation of flow rates.

TABLE D-52

APPROXIMATE FLUID VELOCITIES AND TRANSIT TIMES TO AQUIFER ALONG PERMEABLE BOREHOLES DURING PERIOD A (BEDDED SALT REPOSITORY)

	Fluid Velocities (v) (m/yr)	Transit Time (yrs)
First Estimate	29	4
Second Estimate	200	0.5

TABLE D-53

EFFECTIVE VERTICAL HYDRAULIC GRADIENT IN PERMEABLE BOREHOLES FROM THERMALLY INDUCED CONVECTION AND AQUIFER INTERCONNECTON (BEDDED SALT REPOSITORY)

	Hydraulic Gradient (i)		
	100 years*	1000 years	10,000 years
Thermally Induced Convection			
First Estimate	0.12	0.10	0.03
Second Estimate	0.12	0.10	0.03
Aquifer Interconnection			
First Estimate	0.01	0.01	0.01
Second Estimate	0.50	0.50	0.50
Effective Total Gradient			
First Estimate	0.13	0.11	0.04
Second Estimate	0.62	0.60	0.53

*Years after repository closure.

Source: First column from Appendix D-VI; second column from Chapter D-2.0.

TABLE D-54

VOLUMETRIC FLOW RATES AND FLUID VELOCITIES IN DEEP PERMEABLE BOREHOLES DURING PERIOD B AS CALCULATED WITHOUT CONSIDERING DISSOLUTION EFFECTS

(BEDDED SALT REPOSITORY)

		Volumetric Flow (m^3/yr)	Fluid Velocity (m/yr)
T = 223 years	First Estimate	0.05	0.5
	Second Estimate	Not applicable*	Not applicable*
T = 1000 years	First Estimate	0.18	1.8
	Second Estimate	9.5	95
T = 10,000 years	First Estimate	0.63	6.3
	Second Estimate	83.5	835

*Note: T = 223 is not included in Period B for second estimate assumptions, since Period A extends to T = 1000.

TABLE D-55

VOLUMETRIC FLOW RATES IN DEEP PERMEABLE BOREHOLES DURING PERIOD B INCLUDING EFFECTS OF DISSOLUTION ON FLOW RATES (BEDDED SALT REPOSITORY)

		Volumetric Flow ($\dot{Q}$) (m^3/yr)
T = 223 years	First Estimate	0.05
	Second Estimate	Not applicable*
T = 1000 years	First Estimate	0.18
	Second Estimate	19.0
T = 10,000 years	First Estimate	0.63
	Second Estimate	167.0

*Note: T = 223 is not included in Period B for second estimate assumptions, since Period A extends to T = 1000.

The source term for this failure element consists of the concentration of radionuclides that have leached into the water in the repository during the time frame of interest. Wastes would not be expected to be placed in or near the path of a borehole, and so none would be expected to be directly in the path of the flows calculated above.

D-3.3.4.2 Granite

Once repository resaturation has taken place, two driving forces need to be evaluated for their potential contribution to fluid flow from the repository to the aquifer. These forces are thermally induced convection and the U-tube effect. (Note that molecular diffusion is always negligible compared with mechanisms that move radionuclides by fluid flow, and there is no lower aquifer in the generic granite repository.) Both of these forces are functions of time. Thermally induced convection depends on time because the temperture profile changes with time. The U-tube effect depends on time because of the gradual change in the hydraulic conductivity of the borehole plug. The values of the corresponding gradients, if calculated independently, are shown in Table D-56. These values are based on Appendices D-V and D-VI. In particular, in the calculation of the gradients resulting from thermally induced convection, the minimal average density of a water column from the upper aquifer to an unspecified point below the repository has been used, rather than that of a water column simply from the upper aquifer to the repository itself. It is pointed out in Appendix D-VI that the corresponding numerical values represent upper bounds on the buoyancy force. It is believed that this approach is both conservative and particularly appropriate here because at least some of the boreholes may extend below the repository. By the reasoning presented earlier, it follows that, for the purpose of calculating the joint effect, the maximum of the individual effects may be utilized. Therefore, the gradient resulting from the thermally induced buoyancy effect dominates in most cases.

TABLE D-56

EFFECTIVE VERTICAL HYDRAULIC GRADIENT IN PERMEABLE BOREHOLES FROM THERMALLY INDUCED CONVECTION AND THE U-TUBE EFFECT (GRANITE REPOSITORY)

	Hydraulic Gradient (i)		
	100 years*	1000 years	10,000 years
Thermally Induced Convection			
First Estimate	0.11	0.07	0.03
Second Estimate	0.11	0.07	0.03
U-Tube Effect			
First Estimate	0.01	0.01	0.01
Second Estimate	0.09	0.09	0.08

*Years after repository closure

Source: Appendices D-V and D-VI

The volumetric flow rate can be calculated from the equation

$$\dot{Q} = KiAc(\mu)$$

where

K is given in Table D-51,

i is obtained from Table D-56,

A equals 50 x 0.1 = 5, or 2.5 for the U-tube case, and

$c(\mu)$ equals 5.

The results of this calculation are given in Table D-57. The corresponding fluid velocities are given in Table D-58.

The source term for this failure element consists of the concentration of radionuclides that have leached into the water in the repository during the time frame of interest. This is the uniform concentration situation referred to earlier. Because a number of flow pathways may exist through the bulk rock in the neighborhood of the repository, there is expected to be sufficient convective movement so that transport to the borehole is not limited by very slow diffusion rates.

D-3.3.4.3 Basalt

Once repository resaturation has taken place, there are three driving forces that need to be evaluated for their potential contribution to fluid flow from the repository to the aquifer. These forces are thermally induced convection, the U-tube effect, and the gradient from an aquifer interconnection. The gradients from these three forces, if calculated independently, are shown in Table D-59. The gradient values shown for the thermally induced convection effect correspond to Table D-VI-4 in Appendix D-VI. They represent bounds on this effect for boreholes that penetrate only to the repository layer as well as for those that penetrate all the way to the lower aquifer. In the case of first-estimate parameter values, the U-tube effect is always dominated by thermally induced convection, and so the former will not be considered in the flow calculations. In the case of second estimates for boreholes extending all the way to the lower aquifer, the aquifer

TABLE D-57

VOLUMETRIC FLOW RATES THROUGH PERMEABLE BOREHOLES (GRANITE REPOSITORY)

	Volumetric Flow ($\dot{Q}$) (m^3/yr)		
	100 years*	1000 years	10,000 years
First Estimate	0.1	0.6	2.4
Second Estimate	0.9	5.5	31.5

*Years after repository closure.

TABLE D-58

FLUID VELOCITIES THROUGH PERMEABLE BOREHOLES (GRANITE REPOSITORY)

	Velocity (v) (m/yr)		
	100 years*	1000 years	10,000 years
First Estimate	0.2	1.2	4.8
Second Estimate	1.8	11.0	125.9

*Years after repository closure.

TABLE D-59

EFFECTIVE VERTICAL HYDRAULIC GRADIENT IN PERMEABLE BOREHOLES FROM THERMALLY INDUCED CONVECTION, U-TUBE EFFECT, AND AQUIFER INTERCONNECTION

(BASALT REPOSITORY)

	Hydraulic Gradient (i)		
	100 years*	1000 years	10,000 years
Thermally Induced Convection			
First Estimate	0.13	0.11	0.04
Second Estimate	0.13	0.11	0.04
U-Tube Effect			
First Estimate	0.02	0.02	0.02
Second Estimate	0.20	0.19	0.16
Aquifer Interconnection**			
First Estimate	0.01	0.01	0.01
Second Estimate	0.50	0.50	0.50

*Years after repository closure.

**Only applies to the 10 of the 50 boreholes that are assumed to penetrate to the lower aquifer.

Source: Appendices D-V and D-VI.

interconnection gradient dominates the U-tube effect. In the case of second estimates for the boreholes that do not extend to the lower aquifer, it is possible that some U-tube flows might occur. Nevertheless, these would not be significant compared to the other flows calculated.

In calculating fluid flow rate through the boreholes, it is necessary to consider the interconnection between the deep boreholes (those extending to the lower aquifer) and the others, since this interconnection can have the effect of increasing the flow rates. In particular, the system may be analyzed with the aid of its electrical analog, shown in Figure D-15. (The use of electrical analogs is discussed in Appendix D-V.) Since the relatively large permeability and cross-sectional area of the repository tunnels imply a relatively low resistance, compared with boreholes, the system shown in Figure D-15 has been adopted as the basis for the analysis. All the resistances have the same value. The driving potential between points A and B is not dissipated uniformly in the vertical direction, but in inverse proportion to the resistance of each of the two parts of the pathway. Therefore, the lower part experiences five-sixths of the potential drop. If more resistances were added in parallel to the upper part (for example, by considering additional pathways, such as degrading shaft seals), then the fraction of the potential drop over the lower half would be even larger. Therefore it is both conservative and yet not a significant overestimate to assume for the purpose of calculation that the entire potential drop is experienced over the lower half. The resulting flow in this half also represents the flow in the upper half because the two halves are connected in series. To effect these assumptions in the actual calculations, the gradients for thermally induced convection and aquifer interconnection, as given in Table D-59, should be doubled and then added to represent the combined effect. The resulting values are given in Table D-60. Using these gradients in Darcy's law yields the flow rates shown in Table D-61. Assuming that these flows all move from the repository to the upper aquifer within boreholes (rather than through shafts or other breach pathways), the actual fluid velocities can be estimated as shown in Table D-62.

(a) Basic System

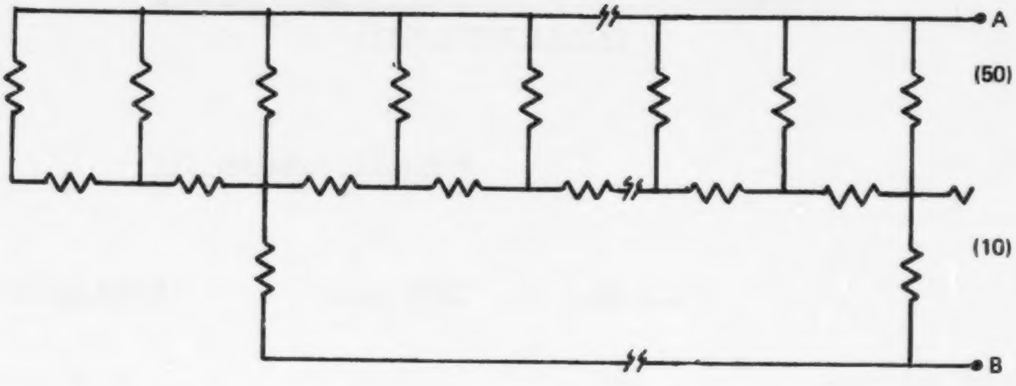

(b) Simplified System Ignoring Resistance of Tunnel Backfill

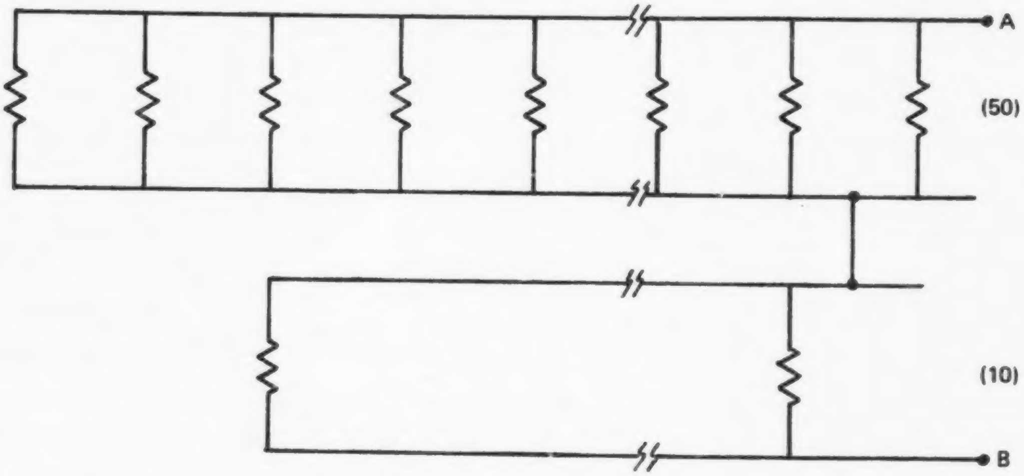

Note: Vertical resistances represent boreholes. Horizontal resistances represent segments of backfilled tunnels.

FIGURE D–15 ELECTRICAL ANALOG FOR BOREHOLE PATHWAY ANALYSIS IN BASALT

TABLE D-60

EFFECTIVE VERTICAL HYDRAULIC GRADIENT IN PERMEABLE BOREHOLES CONNECTING THE REPOSITORY AND THE LOWER AQUIFER (BASALT REPOSITORY)

	Hydraulic Gradient (i)		
	100 years*	1000 years	10,000 years
First Estimate	0.28	0.24	0.10
Second Estimate	1.26	1.22	1.08

*Years from repository closure.

TABLE D-61

VOLUMETRIC FLOW RATES THROUGH PERMEABLE BOREHOLES (BASALT REPOSITORY)

	Volumetric Flow ($\dot{Q}$) (m^3/yr)		
	100 years*	1000 years	10,000 years
First Estimate	0.05	0.4	1.6
Second Estimate	2.0	19.2	170.1

*Years after repository closure.

TABLE D-62

FLUID VELOCITIES THROUGH PERMEABLE BOREHOLES
(BASALT REPOSITORY)

	Velocity (v) (m/yr)		
	100 years*	1000 years	10,000 years
First Estimate	0.1	0.8	3.2
Second Estimate	4.0	38.4	340.2

*Years after repository closure.

Consideration of additional flow pathways for the same flow rates would decrease the fluid velocities calculated.

The source term for this failure element consists of the concentration of radionuclides that have leached into the water in the repository during the time frame of interest. This is the uniform concentration situation described earlier.

D-3.3.4.4 Shale

For all the modeling parameters relevant to the present release mechanism, the basalt and shale repositories appear identical. Therefore the discusion and the numerical computations for basalt are identical for shale. The results for shale are shown in Tables D-63 and D-64.

D-3.3.4.5 Dome Salt

Repository resaturation times for a dome salt repository are calculated in Appendix D-II. As indicated there, these resaturation times represent a balance point at which the remaining pore volume is exactly equal to the volume of seepage water. Non-uniformities in water distribution and in salt creep rates are not included in the model.

The analysis of releases from a salt dome repository through leaky boreholes during the initial period of extensive salt creep parallels very closely that for a bedded salt repository. Reference will also be made to the analysis of releases through permeable shafts in the case of a salt dome repository, which were discussed in Section D-3.2.4. The period of possible fluid migration may be divided into two basic parts:

Period A--From resaturation time until effective closure of cavities and void spaces by extensive salt creep.

Period B--Following Period A.

During Period A the hydraulic pressure generated by salt creep can result in substantial gradients along plugged but permeable boreholes. The analysis for the corresponding situation with shafts (Section D-3.2.4) also applies here, yielding a gradient on the order of 1 - 2 in the portion of the borehole connecting the repository and the upper

TABLE D-63

VOLUMETRIC FLOW RATES THROUGH PERMEABLE BOREHOLES (SHALE REPOSITORY)

	Volumetric Flow (Q) (m^3/yr)		
	100 years*	1000 years	10,000 years
First Estimate	0.05	0.4	1.6
Second Estimate	2.0	19.2	170.1

*Years after repository closure.

TABLE D-64

FLUID VELOCITIES THROUGH PERMEABLE BOREHOLES (SHALE REPOSITORY)

	Velocity (v) (m/yr)		
	100 years*	1000 years	10,000 years
First Estimate	0.1	0.8	3.2
Second Estimate	4.0	38.4	340.2

*Years after repository closure.

aquifer. According to the model assumptions specified in Section D-3.3.3, there are 50 borehole pathways to the upper aquifer. The hydraulic gradient resulting from salt creep tends to force water from the repository through these boreholes to the upper aquifer. At the same time, this gradient is also forcing water out through the filled shafts. The combined outflow along these two pathways continues until the total amount of water that has entered the repository during the resaturation period has been forced out. (This is an approximation; there will always be some residual water that is not squeezed out.) The corresponding flow rates and time periods can be calculated in the same way as they were for bedded salt.

For the first estimate case, the volumetric flow rate during Period A (200-260 years) is approximately 5 m^3/yr. In the second estimate case, the flow rate during Period A (748-1000 years) is approximately 100 m^3/yr. It follows from these results that the approximate average fluid velocities and the corresponding transit times from repository to aquifer within each borehole are as given in Table D-65. All these calculations are for Period A, which represents the period of extensive salt creep when the dominant driving mechanism is the pressure produced by this process. By the end of this period the salt has reached a state of approximate mechanical equilibrium. The water that seeped in during the resaturation period has been forced back out and the repository is still saturated, but the fluid volume is relatively small. The tunnel backfill has been compacted, probably to near equilibrium, but it still has some permeability to fluid flow.

The period following Period A has been called Period B. In the case of bedded salt, 10 of the boreholes were assumed to penetrate to the lower aquifer and during Period B movement of fluid along these boreholes could lead to releases to the upper aquifer. In the case of the salt dome repository, however, there is no lower aquifer in the generic model. As a result there is no gradient present in these boreholes from an aquifer interconnection and there is no recharge pathway available for the thermally induced convection effect. The only driving force expected to be present, therefore, is the U-tube effect. This is the driving force used to calculate releases during Period B.

TABLE D-65

APPROXIMATE FLUID VELOCITIES AND TRANSIT TIMES TO AQUIFER ALONG PERMEABLE BOREHOLES DURING PERIOD A (DOME SALT REPOSITORY)

	Fluid Velocity (v) (m/yr)	Transit Time (yr)
First Estimate	11	21
Second Estimate	200	1.1

The gradients in the boreholes which represent the vertical parts of the U-tube, have been calculated by methods outlined in Appendix D-V and are shown in Table D-66. Although the gradients decrease with time, because of a decrease in the resistance of the borehole segments relative to that of the tunnel, the flow rates will increase because the total U-tube resistance is still decreasing as the borehole plugs degrade. Utilizing these gradients in Darcy's law, the volumetric flow rates and fluid velocities may be calculated as shown in Tables D-67 and D-68, respectively.

The source term for this failure element consists of the concentration of radionuclides that have leached into the water in the repository during the time frame of interest.

D-3.3.5 Literature Discussion

Borehole plug failure has also been discussed by Claiborne and Gera(3) and by TASC.(11,53)

Claiborne and Gera were concerned with a specific area in southeastern New Mexico. On the basis of their analyses of site hydrologic data, they concluded that if a connection were to be established between upper and lower aquifer by failure of a borehole plug, then flow would be in a downward direction and very slow. In the case of a borehole which extended only to the repository level, they argue that water in it would simply stagnate and not exhibit a flow that could carry radionuclides.

TASC addressed borehole failure in the framework of a threshold definition. In particular, a failed borehole was defined as one with a permeability of 10^{-4} cm/sec. They postulated that 10% were in this failed condition initially, 30% after 500 years, and 50% after 5000 years. They also assumed that each failed borehole plug had a porosity value of 0.01 and that 0.5% of the repository was affected by each failed plug.

TABLE D-66

EFFECTIVE VERTICAL HYDRAULIC GRADIENT IN PERMEABLE BOREHOLES FROM U-TUBE EFFECT DURING PERIOD B
(DOME SALT REPOSITORY)

	Hydraulic Gradient (i)		
	260 years*	1000 years	10,000 years
First Estimate	0.009	0.008	0.004
Second Estimate	Not applicable	0.04	0.007

*Years after repository closure.

TABLE D-67

VOLUMETRIC FLOW RATES THROUGH PERMEABLE BOREHOLES DURING PERIOD B (DOME SALT REPOSITORY)

	Volumetric Flow ($\dot{Q}$) (m^3/yr)		
	260 years*	1000 years	10,000 years
First Estimate	0.01	0.03	0.16
Second Estimate	Not applicable	1.6	2.8

*Years after repository closure.

TABLE D-68

FLUID VELOCITIES THROUGH PERMEABLE BOREHOLES
DURING PERIOD B
(DOME SALT REPOSITORY)

	Velocity (v) (m/yr)		
	260 years*	1000 years	10,000 years
First Estimate	0.04	0.12	0.64
Second Estimate	Not applicable	6.4	11.2

*Years after repository closure.

Source: Appendices D-V and D-VI.

D-3.4 UNDETECTED BOREHOLES

D-3.4.1 Introduction

The repository site selection process is expected to favor sites on which there has been little or no known deep drilling activity in the past.(20,70) Nevertheless, past drilling is frequently not well documented and therefore it is possible that a given site may contain old boreholes about which the site selection group is unaware. Because of this possibility, thorough searches for old boreholes can be expected before and during repository construction. Boreholes that are found on the site are expected to be replugged according to the best available technology; the effect of these on repository integrity has been discussed in Section D-3.2. Nevertheless, even after thorough searches, one or more undetected boreholes may remain.

This section analyzes the effect of undetected boreholes on repository integrity by considering the following aspects:

- the probability of boreholes on a hypothetical site;
- the probability of detection of a borehole, given that it is present; and
- the physical characteristics of a borehole that might elude a comprehensive detection program.

A summary of this analysis is shown in Table D-69. A detailed explanation of the model parameters is found in Sections D-3.4.3 and D-3.4.4. Section D-3.4.2 provides background information on drilling and detection activities.

D-3.4.2 Background

A potential repository site may contain old boreholes that were drilled for any of several purposes, such as

- oil and gas exploration or recovery,
- water exploration or recovery,
- geothermal resource evaluation,
- brine injection or disposal of other wastes,
- mineral exploration,

TABLE D-69
SUMMARY OF UNDETECTED BOREHOLE FAILURE ELEMENT

MEDIUM	PROBABILISTIC (P) DETERMINISTIC (D)	NATURE OF MODEL	RELEASE MODE	DRIVING FORCE	SOURCE TERM	PARAMETERS		FLUID FLOW RATES FROM REPOSITORY TO UPPER AQUIFER		COMMENTS
						1st ESTIMATE	2nd ESTIMATE	1st ESTIMATE	2nd ESTIMATE	
Bedded Salt	P	Past drilling density and detection reliability yield probability of one or more partially filled holes.	Groundwater	Second estimate Period B flows derive from aquifer interconnection gradient. Other flows negligible.	Uniform concentration	prob (1 hole on site) = 0.016 ("site" = 300 m buffer zone only) prob (failure to detect) = 0.001 prob (undet. hole) = 1.6×10^{-5} K = 10^{-4} cm/sec η = 0.2 A = 0.1 m^2 Distance from drift = 100 m Holes extend to lower aquifer.	exp. no. holes on site = 3 prob (failure to detect indiv. hole) = 0.001 prob (3 undet. holes) = 0.003 (assumes partial dependence) K = 10^{-3} cm/sec η = 0.2 A = 0.3 m^2 (total) Distance from drift = 100 m Holes extend to lower aquifer.	Negligible with respect to other failure elements	t (yrs) | $\dot{Q}(t)$ (m^3/yr) 1000 | 945 10,000 | 945	Distance from drift precludes significant connection with repository except in case of significant dissolution. Negligible flow in most cases deduced from consideration of relative resistance of alternative pathways for water to enter and leave repository. Repository resaturation necessary for release.
Granite	P	Past drilling density and detection reliability yield probability of one or more partially filled holes.	Groundwater	Thermally induced convection.	Uniform concentration	prob (1 hole on site) = 0.005 ("site" = repos. + 300 m buffer zone.) prob (failure to detect) = 0.01 prob (undet. hole) = 5×10^{-5} K = 10^{-4} cm/sec η = 0.2 A = 0.1 m^2 Distance from drift = 5 m but flows assume hole through repository.	prob (1 hole on site) = 0.06 prob (failure to detect) = 0.01 prob (undet. hole) = 5×10^{-4} K = 10^{-3} cm/sec η = 0.2 A = 0.1 m^2 Distance from drift = 5 m but flows assume hole through repository.	t (yrs) | $\dot{Q}$ (m^3/yr) 100 | 1.7 1000 | 1.1 10,000 | 0.5	t (yrs) | $\dot{Q}$ (m^3/yr) 100 | 17 1000 | 11 10,000 | 5	Repository resaturation necessary for release to begin.
Basalt	P	Past drilling density and detection reliability yield probability of one or more partially filled holes.	Groundwater	Thermally induced convection and gradient from aquifer interconnection.	Uniform concentration	prob (1 hole on site) = 0.075 ("site" = repos. + 300 m buffer zone) prob (failure to detect) = 0.001 prob (undet. hole) = 7.5×10^{-5} K = 10^{-4} cm/sec η = 0.2 A = 0.1 m^2 Distance from drift = 5 m but flows assume hole through repository. Holes extend to lower aquifer.	prob (1 hole on site) = 0.2 prob (failure to detect) = 0.01 prob (undet. hole) = 2×10^{-3} K = 10^{-3} cm/sec η = 0.2 A = 0.1 m^2 Distance from drift = 5 m but flows assume hole through repository. Holes extend to lower aquifer.	t (yrs) | $\dot{Q}$ (m^3/yr) 100 | 4.4 1000 | 3.8 10,000 | 1.6	t (yrs) | $\dot{Q}$ (m^3/yr) 100 | 198 1000 | 192 10,000 | 170	Repository resaturation necessary for release to begin.

TABLE D-69
SUMMARY OF UNDETECTED BOREHOLE FAILURE ELEMENT (CONTINUED)

MEDIUM	PROBABILISTIC (P) DETERMINISTIC (D)	NATURE OF MODEL	RELEASE MODE	DRIVING FORCE	SOURCE TERM	PARAMETERS		FLUID FLOW RATES FROM REPOSITORY TO UPPER AQUIFER		COMMENTS
						1st ESTIMATE	2nd ESTIMATE	1st ESTIMATE	2nd ESTIMATE	
Shale	P	Past drilling density and detection reliability yield probability of one or more partially filled holes.	Groundwater	Thermally induced convection and gradient from aquifer interconnection.	Uniform concentration	prob (1 hole on site) = 0.05 ("site" = repos. + 300 m buffer zone) prob (failure to detect) = .01 prob (undet. hole) = 5×10^{-4} K = 10^{-4} cm/sec η = 0.2 A = 0.1 m^2 Distance from drift = 5 m but flows assume hole through repository. Holes extend to lower aquifer.	exp. no holes on site = 9 prob (failure to detect) = 0.01 prob (3 undet. holes) = 0.05 (Assumes partial dependence) K = 10^{-3} cm/sec η = 0.2 A = 0.1 m^2 Distance from drift = 5 m but flows assume hole through repository. Holes extend to lower aquifer.	t (yrs) $\dot{Q}$ (m^3/yr) 100 4.4 1000 3.5 10,000 1.6	t (yrs) $\dot{Q}$ (m^3/yr) 100 594 1000 575 10,000 510	Repository resaturation necessary for release to begin.
Dome Salt	P	Past drilling density and detection reliability yield probability of one or more partially filled holes.	Groundwater	Second estimate Period II flows derive from aquifer interconnection gradient. Other flows negligible.	Uniform concentration	exp. no. holes on site = 3 ("site" = 300 m buffer zone only) prob (failure to detect indiv. hole) = 0.001 prob (3 undet. holes) = 0.003 (Assumes partial dependence) K = 10^{-4} cm/sec η = 0.2 A = 0.1 m^2 Distance from drift = 100 m. Holes extend to lower aquifer.	exp. no holes on site = 30 prob (failure to detect indiv. hole) = 0.001 prob (5 undet. holes) = 0.03 (assumes partial dependence) K = 10^{-3} cm/sec η = 0.2 A = 0.3 m^2 (total) Distance from drift = 100 m. Holes extend to lower aquifer.	Negligible with respect to other failure elements.	t (yrs) $\dot{Q}$ (m^3/yr) 1000 620 10,000 630	Distance from drift precludes significant connection with repository except in case of significant dissolution. Negligible flow in most cases deduced from consideration of relative resistance of alternative pathways for water to enter and leave repository. Repository resaturation necessary for release.

- scientific investigation, or
- fluid storage.

Holes may have also been drilled for other purposes, but these have been excluded from the above list either because they are too shallow (e.g., soil borings for planning foundations of structures) or too localized (e.g., borings related to nuclear testing). Although the current site selection process would generally attempt to avoid locations with previous deep drilling (i.e., to the formation that would contain the repository), documentation of such drilling may be incomplete, records may be lost or undiscovered, and physical evidence may be difficult to find.(71)

This section treats the following topics:

- nature of past drilling activities in the five generic geologic settings,
- methods of detection, and
- experience in applying these detection methods in the past.

Subsequent sections will provide actual data from which to estimate the parameters that characterize this failure element.

D-3.4.2.1 Nature of Past Drilling Activities

Bedded Salt. Bedded salt formations are particularly attractive for a variety of drilling activities. Salt is a valuable commodity itself, and it is also frequently associated with other mineral resources such as gypsum, anhydrite, and potassium salts. The range of commercial deposits of these minerals is indicated in Figure D-16. The sedimentary sequences containing salt beds frequently contain deposits of oil and gas, the ranges of which are shown approximately in Figure D-17. While salt deposits are generally shunned in the development of water resources, permeable strata close to salt layers may be penetrated by injection wells for brine disposal. Such wells are usually abandoned petroleum production wells and, therefore, do not represent additional drilling. Nevertheless, possible dissolution and fracturing around them require that they be considered. Storage of oil or compressed gas in abandoned excavations in salt is a relatively recent development. Access to the excavation horizon is usually obtained through old

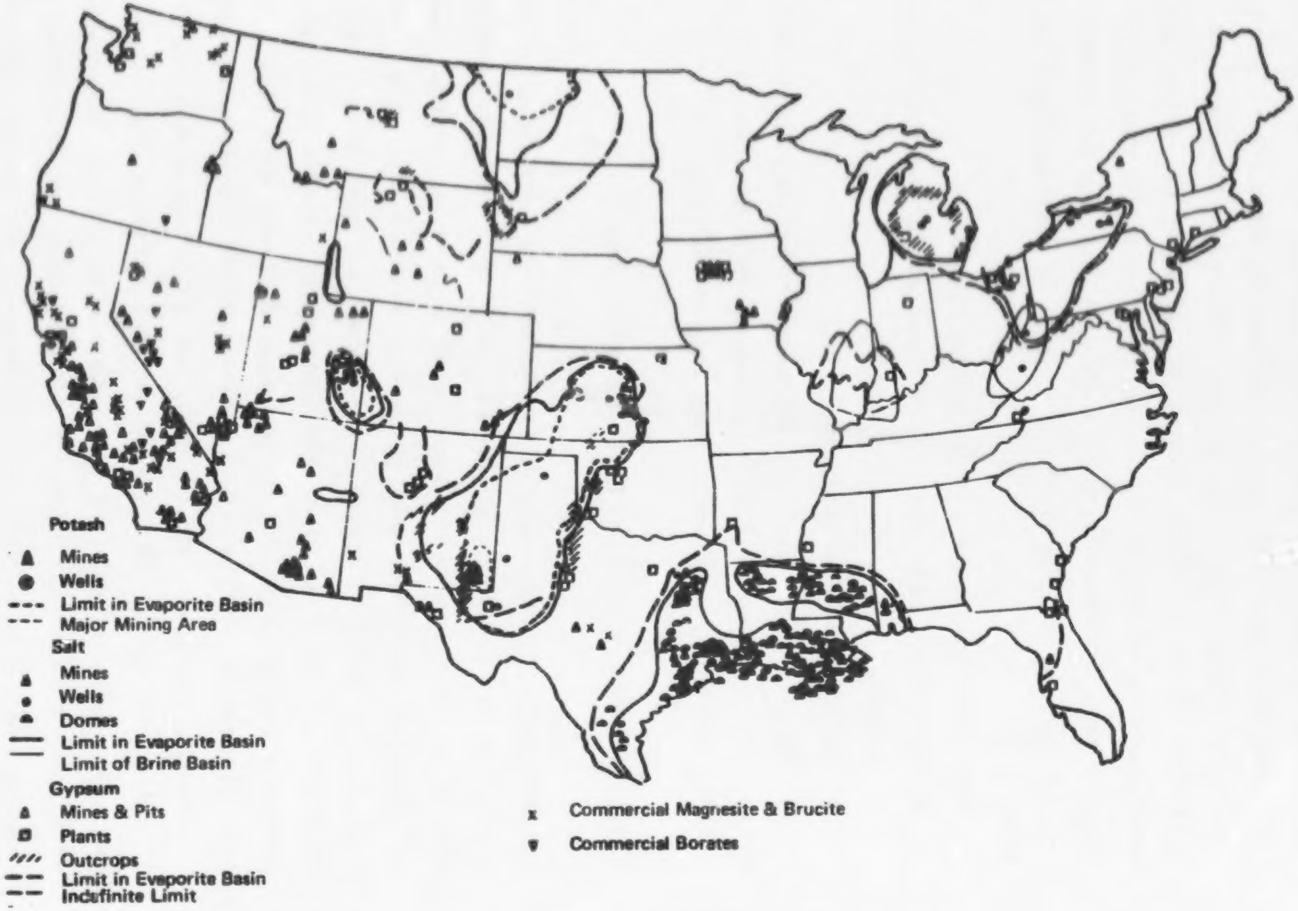

Source: The National Atlas of the United States of America, U.S. Geological Survey, 1970.

FIGURE D–16 COMMERCIAL SALINE DEPOSITS IN THE UNITED STATES

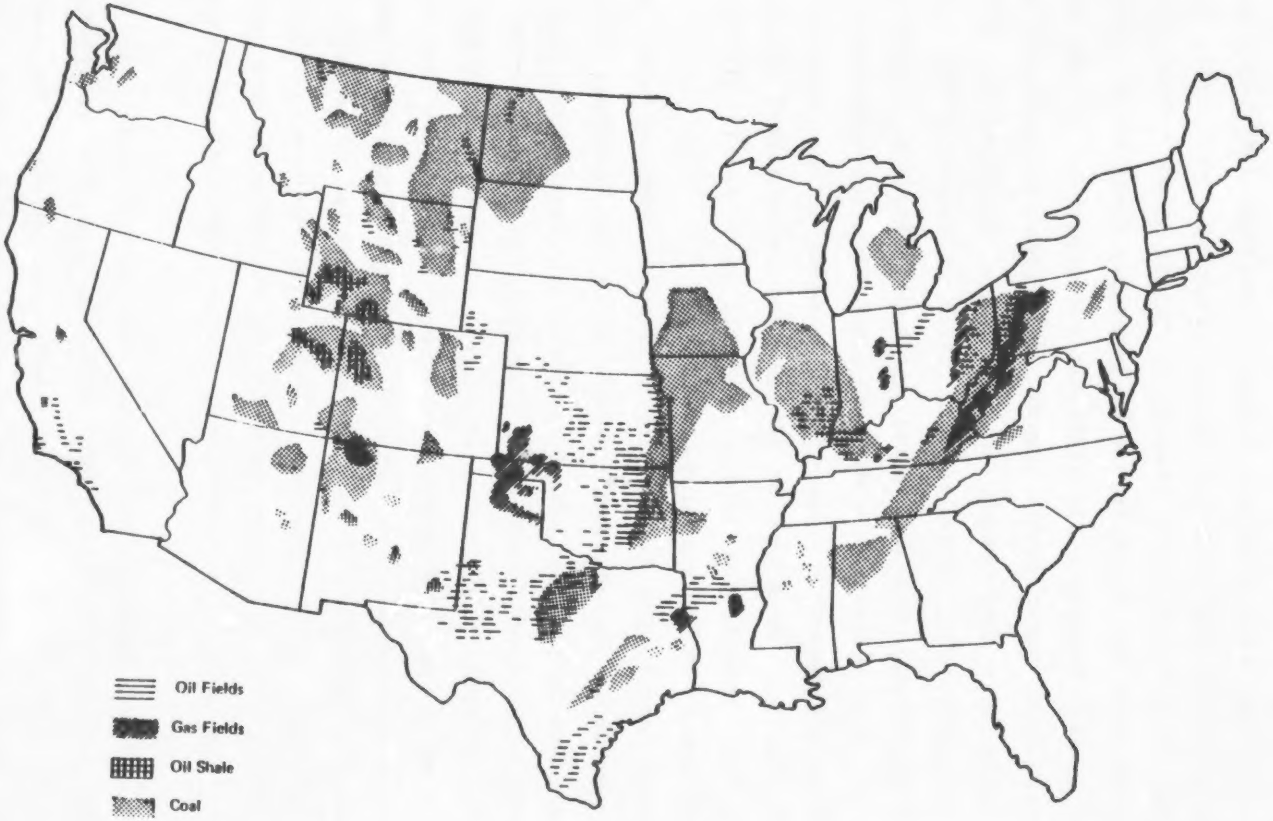

Source: The National Atlas of the United States of America, U.S. Geological Survey, 1970.

FIGURE D–17 COMMERCIALLY EXPLOITABLE ORGANIC FUEL DEPOSITS IN THE UNITED STATES boreholes and, therefore, this process does not require the drilling of new holes.

Granite. Mineral and water exploration are the principal reasons for past drilling into granitic rocks. Precious and heavy metals, including gold, silver, tin, copper, tungsten, and lead, may be concentrated in enriched zones (veins) in felsic rocks. Mica, lithium minerals, and other ore minerals may be generally distributed throughout a granitic stock. Because it is difficult and expensive to mine in such rock, especially at considerable depths, only granitic ores with a high economic value have been sought in the past. Searches for gold and copper, in particular, have been carried to considerable depths. However, this has occurred only after surface exploration suggested the existence of deep deposits. Many of the minerals associated with igneous rocks are found in veins at the contacts between igneous rocks and the surrounding formations or in zones of hydrothermal alteration. Therefore, deep penetration into a granitic mass devoid of signs of minerals is likely to be fruitless.

Important crystalline rock aquifers exist in various parts of the country, especially in the Appalachians of North Carolina, Virginia, Vermont, and New Hampshire. These aquifers are highly fractured zones and, if present at depths near those considered for repositories, would tend to discourage interest in an area as a potential repository site. There are a small number of cases where granitic rocks have been drilled for petroleum exploration and extraction, when the petroleum has been trapped against the flank of the intrusive or in its fractures. There has also been more recent interest in geothermal resource evaluation in granitic intrusions, but this interest is sufficiently new and well documented that undetected boreholes in this connection are extremely unlikely.

Basalt. Flood basalts, assumed for the generic basalt geology in this report, often contain alluvial or other permeable interbeds, and these may be drilled as important sources of water. In addition, sedimentary deposits underlying basalt flows may also contain oil and gas. Nevertheless, because basalt is difficult and costly to drill through and because geophysical techniques for identifying petroleum reservoirs are difficult to assess in basalt, petroleum exploration and exploitation have been limited. Valuable metals such as platinum, nickel, chromium, and iron ore are occasionally found in basalt, though less frequently in flood basalts, and some enrichment can be noted where leaching and rock alteration have taken place. However, because of the general lack of ore-forming fluids in these rocks, concentrated deposits are unlikely.(72) (Copper associated with basalt in Michigan may be an exception.) Geothermal exploration is sufficiently recent not to be of concern for undetected boreholes; furthermore, source areas rather than the basalt flows themselves would be the principal source of heat.

Shale. Shales are the most common sedimentary rocks and may be associated with almost any assemblage of other sedimentary rocks. They generally have little or no economic value in themselves, except for oil shales and building stone, but they may be extensively drilled during the exploration or recovery of associated resources. Oil and gas wells may penetrate shale formations, since the relatively low permeability of the shale often causes the accumulation of exploitable reservoirs underneath these formations. Coal may also be associated with shales, and previous coal exploration could be the source of old boreholes. Uranium, vanadium, and phosphates are among the mineral resources commonly found in shale or its associated rocks. Exploration for uranium has intensified over the last 30 years. Shales can also act as aquicludes, leading to artesian heads in underlying aquifers. One of the most outstanding examples of this geology involves the Dakota sandstone aquifer, which is overlaid by thick sections of Cretaceous shales. Since this aquifer is one of the principal sources of water in the Great Plains, the shales there have frequently been penetrated in the development of water resources.

Salt Domes. Salt domes, including the rock surrounding them, have been of considerable interest for drilling. The salt itself can be of commercial value, as can the associated minerals, which are similar to those found with bedded salt. Concentrated mineral deposits, such as sulfur, may be found above or on the flanks of a salt dome, since discontinuities and upturned strata, which tend to collect oil and gas, often result from the intrusion of the dome through the overlying sediments. (See Figure D-18.) Deep borings directly through the salt are uncommon, although borings through overhanging portions that may

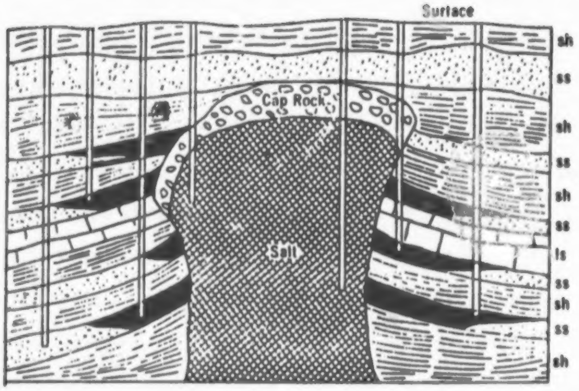

Source: Adapted from Bateman, M. The Formation of Mineral Deposits, John Wiley & Sons, New York, 1951.

FIGURE D–18 DIAGRAM OF SALT DOME SHOWING ASSOCIATED OIL RESERVOIRS, WELLS, AND DEEP HOLES

serve to trap petroleum below are frequently carried out. While geothermal resources may be associated with salt domes, there has not been sufficient investigation to add to the risk of undetected boreholes.

D-3.4.2.2 Methods for Detection of Old Boreholes

The first step in a program of identifying old boreholes is to review mineral claims, drilling permits, and leases recorded by various government agencies for information on locations, depths, and plugs.(71) These records may also indicate unusual situations, such as multiple shafts from a single surface hole, offshoot holes, obstructions, etc. Unfortunately, regulations governing such documentation are relatively recent, so that while records may be an aid in locating old holes, they are not completely reliable. Documentation of unsuccessful water or mineral exploration holes, particularly in states where regulations have not been motivated by extensive petroleum or mineral industries, is often lacking.

Documentation may be supplemented by aerial photographs and interviews with local residents. Aerial photographs often reveal access roads, ground damage from drill machinery, pits for drill mud, and other scars. Interviews are particularly useful where obvious traces are obliterated by vegetation or construction, or where records are incomplete or in error.(71)

After the general location of a borehole has been determined. the hole itself must be found. Sometimes the uppermost pipe extends above the ground or some other marker has been left. Metal detectors can be used to find casings and debris close to the surface.(71) Hydrocarbon detectors can be used to locate gas escaping from leaking holes as well as traces of oil or gas that may have permeated the ground during drilling or pumping operations. Even the location of scars or traces from guy cables from the drill derrick may be useful in finding the approximate location of an old borehole. Once a possible boresite has been located, it may be necessary to remove the top layers of earth in order to find the actual hole.

Underground methods, such as sonar and radar, are also used to detect boreholes from other boreholes or from excavations. In these cases, interpretation of reflected signals by skilled personnel may indicate underground structures. Radar uses electromagnetic signals to detect fractures with anomalous electrical properties, such as empty or brine-filled holes, cracks or voids, or metals (such as casings). However, the cracks and voids of fractured rock scatter radar signals, and wet rock, with high electrical conductivity, can severely attenuate the signal and thereby limit the range. In salt or other dry rock it is possible to detect an open, caved, or brine-filled borehole at a distance of many meters.(73-75)

Sonar, which uses sound waves, is not affected by moisture in the rock to the same degree as radar. Sonar's range through dry, fractured rock may be limited, however, since energy is lost at each rock/air interface. Also, a filled borehole may have acoustic properties very similar to those of the surrounding rock.

Radar and sonar use short wavelength signals; the shorter the wavelength, the more limited the range but the better the resolution. Experience suggests that in fractured or wet rock it may be possible to detect a borehole at distances of 10 to 100 meters away. In salt, the detection capability is over 100 meters. Because of the water bound-up in shale minerals, even uniform and apparently dry shales limit the detection capabilities to about the same level as for crystalline rocks.(74)

D-3.4.2.3 Experience in Borehole Detection

The petroleum and mining industries have devoted considerable effort to the technology of detecting (and replugging) abandoned boreholes. The motivation for this includes legal requirements (concerning gas leakage from old fields), the desire to limit oil and gas loss into barren strata, protection of miners against flooding or dangerous gas accumulations, and the use of depleted gas fields as gas storage reservoirs. Several examples of this last case have recently been documented(62) and are summarized below.

The Webb storage field in Oklahoma had 25 old wells, which were found primarily through a search of records. The Lyons, Kansas field, however, contained many wells that could not be found from records. Aerial photographs proved useful in locating drilling sites, and then metal detectors and excavating equipment were used to locate the wellbores. The Jackson, Mississippi storage field proved even more difficult. About 80 boreholes had to be located and replugged, but the few existing records were often inaccurate. Houses and other buildings had even been built over some of the old wells. Eventually, however, the abandoned wells were found and the field was successfully put into service.

D-3.4.3 Undetected Borehole Failure Model

The quantitative characterization of the undetected borehole failure element consists of three elements:

- the probability of a borehole or the expected number of boreholes present on the repository site;
- the probability of failure to detect any such boreholes; and
- physical parameters to describe the nature of an undetected borehole so that consequence calculations may be carried out.

The first two factors vary considerably from one geologic medium to another, but the third has been modeled independently of the medium, except for the location and length of the borehole.

D-3.4.3.1 Bedded Salt

Number of boreholes. First estimate values are based on the assumption of a site where the major productive oil and gas horizons, if any, lie above the formation containing the repository; mineral resource recovery has also been generally limited to considerably shallower depths; and sufficient water is available near or at the surface so that deep water wells would not have been necessary. Much of the Salina and Appalachian basins, for example, meet these criteria. In the case of the Salina basin, it has been estimated that holes extending into the deep Silurian salt deposits that might be considered for a repository occur with a spatial density of about one hole per 100 square miles (256 km^2).(76) Because of the capabilities of radar and other detection techniques in salt deposits, boreholes within the actual repository boundary have been assumed to have a negligible probability of failing to be detected. (Because of the network of drifts and tunnels, any such borehole would be within a few meters of the mine opening).

The calculations here concentrate on a 300-meter-wide buffer zone around the repository; the area of this zone is about 4 km^2. Boreholes beyond 300 meters are assumed to be too far away to contribute significantly to any risk. Thus, the boreholes referred to in this subsection on bedded salt are assumed to be in this zone. The probability of such a borehole existing is thus 4 x (1/256) = 0.016 if the site is randomly chosen. In particular, the Poisson distribution describes the probabilities of various numbers of holes on the site, the probability of N holes being given by $e^{-0.016} (0.016)^N/N!$. The values of this function for small values of N are given in Table D-70.

Multiple holes are seen to have negligible probabilities compared with a single hole, and thus the event of a single hole is the one that has been modeled in the first estimate case. Since site selection is expected to favor sites with lower than average past drilling rates, it is conservative to use the average rates as the basis for the probabilities.

Second estimate values correspond to regions with extensive mineral and energy resource recovery activities. Typical of such regions is the Carlsbad, New Mexico mining district, where approximately 125 holes to a candidate repository formation are known in an area of 166 km^2.(20) (Approximately 60% of these are potash exploration holes, which generally terminate above the actual strata that have been proposed for the Waste Isolation Pilot Plant. However, the total number has been used as an estimate for the generic calculations in this report.) For an area of 4 km^2, this leads to an expected number of about three holes per repository.

Failure to detect boreholes. Statistical analyses of the effectiveness of borehole detection techniques are not available, and the estimates adopted here are based on very limited data. Conventional

TABLE D-70

PROBABILITIES OF UNDETECTED BOREHOLES IN BUFFER ZONE AROUND BEDDED SALT REPOSITORY (FIRST ESTIMATE)

N(number of holes)	Probability $(e^{-0.016})(0.016)^N/N!$
0	0.9841
1	0.0157
2	1.26×10^{-4}
3	6.72×10^{-7}
4	2.69×10^{-9}

surface methods have been totally effective in several cases, but failures are sometimes unknown and often not documented. One significant failure involved the interception of an unknown abandoned borehole by an advancing mine excavation.(75) In that case, the unknown hole represented one out of about 100 boreholes in the area, yielding a detection failure rate of 1%.

When conventional surface techniques are augmented by techniques such as radar, the detection probability can be expected to improve. For example, with skilled operators working in dry, homogeneous salt, it may be possible to find all boreholes out to a distance of 100 meters or more. However, since operators can make errors and geologic conditions vary, finding all abandoned holes is not an absolute certainty. Instead, it has been assumed for the case of both first and second estimates that radar can reduce the failure rate to 0.1% per hole. This detection failure probability has been combined with the expected number of boreholes as follows.

For the first estimate case, the event being modeled is the existence of one undetected borehole, whose probability is the product of the probabilities that a hole is present (0.016) and the probability of detection failure (0.001). The resulting probability is 1.6×10^{-5}. For the second estimate case, where more than one borehole is expected on the site, the probability of at least one undetected borehole out of three is $1 - (0.999)^3 = 0.003$. Note: 0.999 is the probability of detecting each individual hole, so $(0.999)^3$ is the probability of detecting all three, assuming independence. While the case of exactly one undetected borehole is the largest contributor to this probability, to allow for some dependence among detection failures, the event corresponding to this probability has been modified to be the existence of three undetected boreholes on the site. (It is appropriate to make some allowance for dependence because the causes for detection failures, such as faulty equipment operation, inadequate coverage of the area, or interfering geologic features, may encourage multiple detection failures.) This is a rough approximation to a more detailed analysis based on hypotheses of dependencies in borehole detection; however, it is believed to be adequate for the purposes of this study.

Nature of undetected boreholes. It is reasonable to assume that boreholes that escape detection do so because, in terms of density and water content, they are not very different from the surrounding rock. Thus they can be assumed to be filled or plugged. Their hydraulic conductivity has been modeled to be uniform over time and spatial extent, and to have the values of 10^{-4} cm/sec as a first estimate and 10^{-3} cm/sec as a second estimate. These values are in the range corresponding to silty sand and gravel, as well as other materials, as shown previously in Figure D-13 (see Section D-3.2). They represent relatively permeable fill material such as might be expected from material falling from the sides of the hole in loose upper levels or from a poor concrete-drill mud plug. Their cross-sectional area has been taken as 0.1 m^2, their porosity as 0.2, and their distance from the nearest point of the repository as 100 m. For conservatism, all such holes have been assumed to penetrate to the lower aquifer.

D-3.4.3.2 Granite

Number of boreholes. Deep drilling in granite is much less common than in bedded salt. Granite rarely contains reserves such as gas or oil that can be exploited through boreholes. In general, it is penetrated only when some surface indications suggest that deep mining may be profitable,(77) or when fractures in the rock are extensive enough that the granite can be tapped for water. Indeed, there may be locations where it can be assumed that no drilling has taken place, such as a National Park. However, such locations are also likely to be unavailable or undesirable for a repository.

The first estimate assumes a location that shows no surface indications of ore minerals deep in the granite, and where water is either readily available at the surface or else past land use suggests that deep water exploration has not been carried out. Detailed drilling data for such regions are often lacking. For example, local statutes may not require reporting of drilling, or the mineral companies performing the drilling may be reluctant to release their information. In the absence of adequate data, it has been conservatively assumed that granite is penetrated to the depth of a potential repository one tenth as often as in the first estimate bedded salt situation. This results in a deep borehole density of one hole per thousand square miles (2560 km^2). Since the area of the repository plus a 300-meter-wide parameter is about 12 km^2, this implies a probability of about 0.005 that there is a borehole at the site. The second estimate for granite is based on a drilling rate ten times as high as in the first estimate, resulting in a probability of 0.05 that there is a borehole on the site.

Failure to detect boreholes. Conventional borehole-locating techniques are expected to be as reliable for granite as for bedded salt, although specific data to prove this assumption are not available. The use of radar for detection of features in granite has not been demonstrated, and it is not assumed to contribute to the probability of finding abandoned holes. For both first and second estimates, the detection failure rate has been assumed to be 1%, equivalent to that for bedded salt without the advantage of radar. This failure rate is combined with the expected number of boreholes as follows. For both cases, the event being modeled is the existence of one undetected borehole, for which the probability is the product of the probability that a hole is present and the probability of detection failure. For the first estimate the resulting probability is 5×10^{-5} that an undetected borehole is present. For the second estimate, the probability is 5×10^{-4} for an undetected borehole.

Nature of undetected boreholes. As in the case of bedded salt, it has been assumed that a borehole escaping detection does so because, in terms of density and water content, it is not too different from the surrounding rock. Thus, it has been assumed to be filled or plugged. The hydraulic conductivity has been modeled to be uniform over time and spatial extent, and to have the values 10^{-4} cm/sec as a first estimate and 10^{-3} cm/sec as a second estimate. Its cross-sectional area has been taken as 0.1 m^2, its porosity as 0.2, and its distance from the nearest point of the repository as five meters. (Five meters is intended to be a conservative estimate. Boreholes closer than five meters are highly likely to be found during excavation, either by leakage or through detection techniques.)

D-3.4.3.3 Basalt

Number of boreholes. Borehole densities in the basalt regions of the Pacific Northwest have been used in estimating the probability of a borehole at the repository site. In that region deep drilling has been dominated by water wells, and reported numbers of wells are used to derive borehole density estimates. The first estimate is based on a study of wells in the Pasco Basin,(78) where 34 wells were reported reaching or exceeding depths of 1000 feet (300 m). The area covered in that study included approximately 5400 km^2, and so for a repository and perimeter of 12 km^2, there is a probability of approximately 0.075 that an old borehole exists on a randomly chosen site. The second estimate is based on well populations for a larger area (30,000 km^2) of southeastern Washington state, where an estimated 500 wells may reach depths of 1500 feet (400 m).(79) For a randomly chosen site with an area of 12 km^2, this implies a probability of about 0.2 that an old borehole will be present. (Multiple occurrences have sufficiently small probabilities that they need not be considered.)

Failure to detect boreholes. Much of the Pasco Basin area has been under close government control, and most of the deep drilling has been supervised by the Federal government. The location of these holes is well known and well documented. Although special techniques, such as radar, are not expected to be adaptable to borehole detection in basalt, the exceptional quality of records kept for this particular area should improve the chances of finding holes to the degree that the probability of detection failure is reduced to the level achievable in bedded salt, i.e., 0.001. Combining this probability with the probability that a borehole is present (0.075) results in a first estimate probability of an undetected borehole of 7.5×10^{-5}.

The second estimate probability of detection failure is taken to be the same as for other areas where surface detection techniques alone are relied upon (0.01) since much of the area defined above for the second estimate is not under tight control and the location of wells may not be accurately known. The probability of an undetected borehole is again the probability of a hole (0.2) multiplied by the probability of failing to detect it (0.01), with a resulting probability of 2.0×10^{-3}.

Nature of undetected boreholes. Boreholes in basalt are assumed to have the same characteristics as those in granite. For conservatism, it is further assumed that all holes penetrate to the lower aquifer.

D-3.4.3.4 Shale

Number of boreholes. First-estimate values are based on assumptions of a site where productive gas, oil, coal, and water lie above the shale. Such a site is analogous to that assumed for bedded salt and so the same borehole density applies. However, because of poorer detection capabilities in shale, the entire area of site and buffer zone (12 km^2) has been used. Therefore, the probability of a borehole on the site is 0.05. Second estimate values are also based on the case of bedded salt, leading to nine expected boreholes on a 12-km^2 site.

Failure to detect boreholes. For shale areas, conventional detection techniques cannot be augmented by radar since the fractures and moisture in shale severely limit the range of radar and similar techniques. Therefore, the first and second estimates for the probability of failure to detect boreholes are the same as for conventional detection methods (0.01). As before, the probability of an undetected borehole is calculated as the product of the probability that a borehole is present and the probability of failing to detect it. For a first estimate, the resulting probability is 5×10^{-4}. For the second estimate, the probability of failure to detect at least one borehole in the expected nine is about 0.09. To allow for dependence among failures, the event with which this probability has been associated is that of three undetected boreholes, as in the case of bedded salt.

Nature of undetected boreholes. The boreholes that escape detection are assumed to be similar to the surrounding rock. Their hydraulic conductivity has been modeled as uniform over time and space, and to have the values of 10^{-4} cm/sec as a first estimate and 10^{-3} cm/sec as a second estimate. Their cross-sectional area has been taken as 0.1 m^2, their porosity as 0.2, and their distance to the nearest point of the repository as 5 m. For conservatism, all holes are assumed to penetrate to the lower aquifer.

D-3.4.3.5 Dome Salt

Number of Boreholes. The cross-sectional area of a salt dome is generally of the same order of magnitude as the area required for a repository. As explained in the section on bedded salt, boreholes located within the actual repository boundary are most unlikely to go undetected because of the effectiveness of detection techniques in salt. Therefore, the area that has been modeled for undetected boreholes is that of a 300 meter wide buffer zone around the repository. Since this zone is expected to be close to the flanks of the salt dome, where drilling activities are concentrated, the total number of holes reported as penetrating the dome will be used as the number of holes penetrating the buffer zone. Surveys of records for a number of interior domes in Texas, Louisiana, and Mississippi place this number in the range 0 to 30. For the first-estimate value, three boreholes have been assumed; for the second estimate, 30 have been assumed.

Failure to detect boreholes. As in the case of bedded salt, failure to detect a given borehole has been assumed to have a probability of 0.001 for both first and second estimates. Thus, in the first estimate case, the probability of failure to detect at least one borehole, assuming independence, is $1 - (0.999)^3 = 0.003$. A simple and conservative way to allow for the possibility of dependence among detection failures is to use this probability for the event of failing to detect three boreholes, which has been done here. A similar approach has been taken for the second estimate. Assuming independence, the probability of failure to detect at least one of 30 boreholes is $1 - (0.999)^{30} = 0.03$. Some dependence is roughly introduced by using this same probability to correspond to a different event, namely the failure to detect five boreholes.

Nature of undetected boreholes. It is reasonable to assume that boreholes that escape detection do so because, in terms of density and water content, they are not too different from the surrounding rock. Thus, they have been assumed to be filled or plugged. Their hydraulic conductivity has been modeled as uniform over time and spatial extent, and to have the values of 10^{-4} cm/sec as a first estimate and 10^{-3} cm/sec as a second estimate. Their cross-sectional area has been taken as 0.1 m^2, their porosity as 0.2, and their distance from the nearest point of the repository as 100 m. For conservatism, all such holes have been assumed to penetrate to a lower aquifer or pressurized brine reservoir along the flank of the dome.

D-3.4.4 Undetected Borehole Release Model

The purpose of this section is to analyze how undetected boreholes may constitute or contribute to a breach of the repository. As discussed in the previous section, undetected boreholes do not intersect repository drifts. Furthermore, because of the assumed reliability of detection techniques carried out from the repository itself, conservative estimates of minimum distances between repository drifts and such undetected boreholes were given in the previous section as 100 meters for salt and 5 meters for the other rock types. Consequently, for such boreholes to serve as pathways for the release of radionuclides, communication must exist between them and the backfilled repository drifts. An electrical resistance analog is useful in representing this situation and in identifying cases in which significant levels of flow may take place. The general situation is represented in Figure D-19a. The quantitative analysis for each of the two salt formation repositories will be presented in the following sections in terms of the diagram in Figure D-19b. Effective resistance will be calculated as in earlier sections and as explained in Appendix D-III, according to the formula $\alpha = L/KA$, where L is the pathway length, K is its permeability, and A is its cross-sectional area. (The unlabeled resistances along the aquifers are relatively low and do not enter into the calculations.)

D-3.4.4.1 Bedded Salt

The values of the effective resistances α_1 through α_5, based on parameter values presented earlier, are shown in Table D-71. Since α_1 and α_2 are functions of time, selected values are tabulated in Table D-72. The values of α_3 and α_4 ignore the possibility of dissolution

(a) Physical Pathways

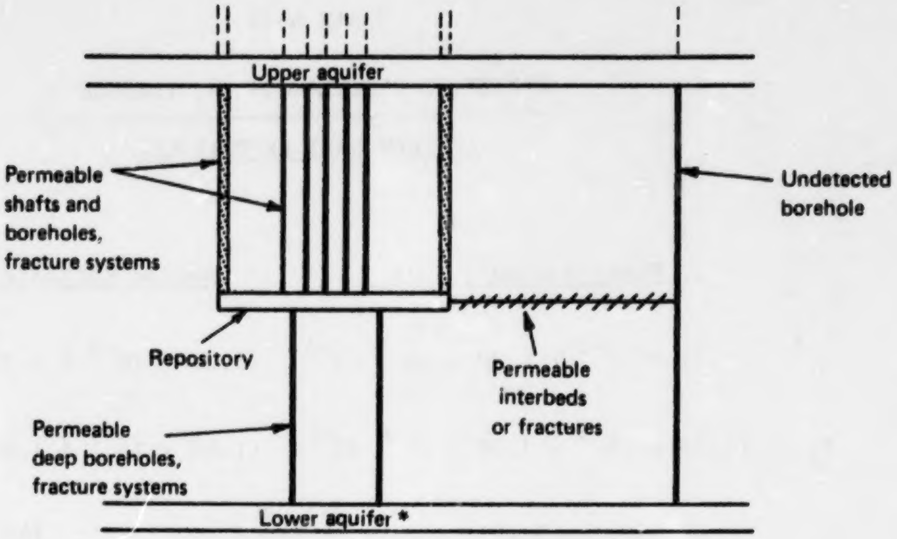
Upper aquifer
Permeable shafts and boreholes, fracture systems
Undetected borehole
Repository
Permeable interbeds or fractures
Permeable deep boreholes, fracture systems
Lower aquifer *

(b) Electrical Analog

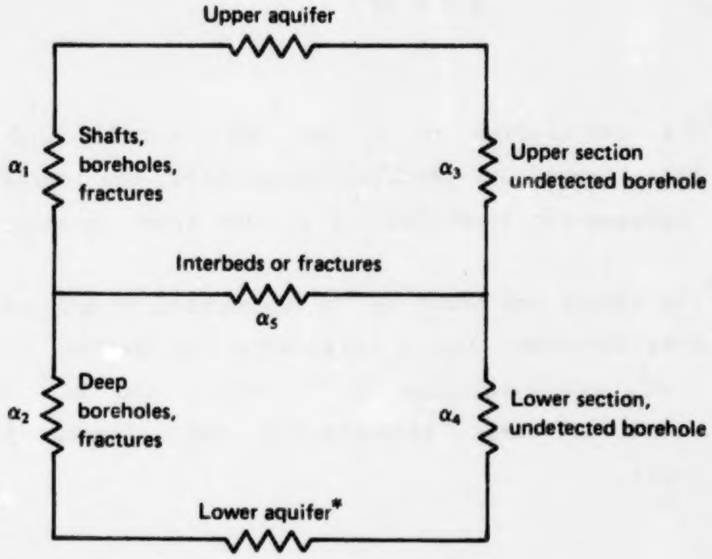
Upper aquifer
α_1
Shafts, boreholes, fractures
α_3
Upper section undetected borehole
Interbeds or fractures
α_5
α_2
Deep boreholes, fractures
α_4
Lower section, undetected borehole
Lower aquifer*

* Lower aquifer not present for certain rock types.

FIGURE D–19 PATHWAYS ASSOCIATED WITH THE ANALYSIS OF UNDETECTED BOREHOLES

TABLE D-71

EFFECTIVE RESISTANCES α_1 THROUGH α_5

(BEDDED SALT REPOSITORY)

	First Estimate (y/m^2)	Second Estimate (y/m^2)
α_1*	$(3.31 \times 10^{-3} + 4.70 \times 10^{-3}\ t)^{-1}$	$(3.31 \times 10^{-3} + 3.31 \times 10^{-3}\ t)^{-1}$
α_2	$(1.58 \times 10^{-5} + 1.58 \times 10^{-6}\ t)^{-1}$	$(1.58 \times 10^{-5} + 1.58 \times 10^{-5}\ t)^{-1}$
α_3	31.75	105.8
α_4	31.75	105.8
α_5**	3.2×10^6	317.5

*The calculation of α_1 has been carried out by considering the situation of two parallel resistances, one representing shafts and one representing boreholes. t is time from repository closure.

**The values are based on the assumption of communication through one or more interbeds with a total effective pathway cross-sectional area of 1 m^2, permeabilities 10^{-10} cm/sec, and 10^{-6} cm/sec for first and second estimates, respectively, and a length of 100 m. (Cf. Figure D-13).

TABLE D-72

SELECTED VALUES OF α_1 AND α_2
(BEDDED SALT REPOSITORY)

	Resistance (y/m^2)	
	α_1	α_2
First Estimate		
10*	1.99×10^{1}	3.16×10^{4}
100	2.11×10^{0}	5.75×10^{3}
500	4.25×10^{-1}	1.24×10^{3}
1000	2.13×10^{-1}	6.27×10^{2}
5000	4.25×10^{-2}	1.26×10^{2}
10,000	2.13×10^{-2}	6.32×10^{1}
Second Estimate		
10	3.02×10^{1}	5.75×10^{3}
100	3.02×10^{0}	6.27×10^{2}
500	6.04×10^{-1}	1.26×10^{2}
1000	3.02×10^{-1}	6.32×10^{1}
5000	6.04×10^{-2}	1.27×10^{1}
10,000	3.02×10^{-2}	6.33×10^{0}

*Years after repository closure.

along the portion of the borehole with the salt strata; the case of dissolutioning will be discussed later.

Without performing detailed network calculations, it is possible to dismiss the importance of the undetected borehole pathway, in most cases, by the following reasoning. Because α_5 is much greater than α_1, flows out of the repository via the undetected borehole-interbed pathway would be expected to be insignificant compared with flows through shafts and boreholes to the upper aquifer. Because α_5 is much greater than α_2, at least for $t > 1000$ years in the case of second estimates, flows into the repository through the interbed are small compared with those through the degrading deep borehole seals. (For $t < 1000$ years, releases are dominated by salt creep, and other driving forces are not important.) In either case, consideration of this pathway would lead to flows that are insignificant compared with those calculated in the previous two sections.

The one additional possibility that needs to be considered is that of dissolution around an undetected borehole and the resulting consequences, if any, for repository integrity. Dissolution calculations in Appendix D-III show that in the case of second estimates, where borehole permeability is high ($K = 10^{-3}$ cm/sec) and there is a significant aquifer interconnection gradient ($i = 0.5$), the potential for dissolution is great. After the period of extensive salt creep (Period A), releases through an undetected borehole connected to the repository as a result of dissolution can be estimated simply by assuming that the flow passes through the repository and encounters resistance only in the part of the borehole extending from the lower aquifer to the bottom of the salt stratum (since a dissolution pathway extends through the salt and the part above may crumble and fall into that void). Darcy's equation,

$$\dot{Q} = KiAc(\mu),$$

with parameters given earlier, leads to the volumetric flow rate

$$\dot{Q} = 945 \text{ m}^3/\text{yr}$$

during Period B. (See Section D-3.2.4 for the definition of Period B.)

The source term for this failure element consists of the concentration of radionuclides that have leached into the water in the repository during the time frame of interest. This is the uniform concentration situation described earlier.

D-3.4.4.2 Granite

An undetected borehole has been modeled at a distance of five meters from a repository drift in the case of granite. Over this short distance the flow between the repository and the borehole cannot be adequately modeled by Darcy's law for flow through porous media, since this law can only be applied to fracture flow on a larger scale. Direct communication through a single open fracture could eliminate any significant resistance along this part of the pathway. Therefore, the borehole has been modeled as passing directly through the repository, and volumetric flow rates have been calculated as they were in Section D-3.3.4. Using the driving forces summarized in that section in combination with the pathway parameters given in Section D-3.4.3, the volumetric flow rates and fluid velocities shown in Tables D-73 and D-74 result.

The source term for this failure element consists of the concentration of radionuclides that have leached into the water in the repository during the time frame of interest. This is the usual uniform concentration situation.

D-3.4.4.3 Basalt

As in the case of granite, flows through an undetected borehole in the generic basalt repository have been calculated as though the borehole passed through the repository itself. The flow calculations in Section D-3.3.4 indicated that, because of multiple pathways from the

TABLE D-73

VOLUMETRIC FLOW RATES THROUGH UNDETECTED BOREHOLES (GRANITE REPOSITORY)

	Volumetric Flow ($\dot{Q}$) (m^3/yr)		
	100 years*	1000 years	10,000 years
First Estimate	1.7	1.1	0.5
Second Estimate	17	11	5

*Years after repository closure.

TABLE D-74

FLUID VELOCITIES THROUGH UNDETECTED BOREHOLES (GRANITE REPOSITORY)

	Velocity (v) (m/yr)		
	100 years*	1000 years	10,000 years
First Estimate	85	55	25
Second Estimate	850	550	250

*Years after repository closure.

repository to the upper aquifer (e.g., permeable shafts and boreholes), the limiting factor in flows through deep boreholes is the resistance over their lower sections (from lower aquifer to repository). It follows that the driving hydraulic potential is almost entirely dissipated over this part of the pathway. This reasoning was used in the earlier section to derive the hydraulic gradients given there in Table D-60. By using these gradients in Darcy's law, the marginal increase in fluid flows caused by an undetected borehole through the repository can be calculated; these are given in Table D-75. Corresponding fluid velocities, assuming that the flow continues to the upper aquifer through the same borehole (a conservative assumption in that it tends to overestimate the velocity) are given in Table D-76.

The source term for this failure element consists of the concentration of radionuclides that have leached into the water in the repository during the time frame of interest.

D-3.4.4.4 Shale

Although the probability of an undetected borehole differs in the case of shale from that calculated for basalt, the flow calculations for each such borehole are identical. Therefore, Tables D-75 and D-76 carry over to this case, except that on the second estimate for shale three boreholes are used. The results for shale are given in Tables D-77 and D-78. The source term is also the same as in the case of basalt.

D-3.4.4.5 Dome Salt

The analysis for a salt dome repository closely parallels that for bedded salt. Since an undetected borehole will be close to the periphery of the dome, there is a significant possibility that it will pass through an overhanging flank and make contact with an aquifer (or pressurized brine reservoir) below. This has been assumed in the model for all undetected boreholes in dome salt. As in the case of bedded salt, the only significant flows can occur during Period B and under second estimate model assumptions. In this case, there are five such boreholes and the original hydraulic gradient of 0.2 (from the aquifer

TABLE D-75

VOLUMETRIC FLOW RATES THROUGH UNDETECTED BOREHOLES (BASALT REPOSITORY)

	Volumetric Flow ($\dot{Q}$) (m^3/yr) 100 years*	1000 years	10,000 years
First Estimate	4.4	3.8	1.6
Second Estimate	198	192	170

*Years after repository closure.

TABLE D-76

FLUID VELOCITIES THROUGH UNDETECTED BOREHOLES (BASALT REPOSITORY)

	Velocity (v) (m/yr)		
	100 years*	1000 years	10,000 years
First Estimate	220	190	80
Second Estimate	9900	9600	8500

*Years after repository closure.

TABLE D-77

VOLUMETRIC FLOW RATES THROUGH UNDETECTED BOREHOLES (SHALE REPOSITORY)

	Volumetric Flow ($\dot{Q}$) (m^3/yr)		
	100 years*	1000 years	10,000 years
First Estimate	4.4	3.8	1.6
Second Estimate	594	576	510

*Years after repository closure.

TABLE D-78

FLUID VELOCITIES THROUGH UNDETECTED BOREHOLES (SHALE REPOSITORY)

	Velocity (v) (m/yr)		
	100 years*	1000 years	10,000 years
First Estimate	220	190	80
Second Estimate	9900	9600	8500

*Years after repository closure.

interconnection) leads to a concentration of the driving force over the undissolved and unbrecciated section of the borehole between the lower aquifer and the point where it enters the salt. If this distance is one quarter the distance between the aquifers, the effective gradient is four times the original value of 0.2. The corresponding volumetric flow rate is given by

$$\dot{Q} = KiAc(\mu)$$

$$= (10^{-3}\ \mathrm{cm/sec})(3.15 \times 10^{5}\ \mathrm{cm/sec/m/yr})(.8)(.5\ \mathrm{m}^{2})(5)$$

$$= 630\ \mathrm{m}^{3}/\mathrm{yr}$$

which applies to Period B.

The source term for this failure element consists of the concentration of radionuclides that have leached into the water in the repository during the time frame of interest.

D-3.4.5 Literature Discussion

Undetected boreholes have also been discussed by an NRC-Sandia group(13) and by Battelle Pacific Northwest Laboratory (BNWL)(50) under the WISAP Program.

In the NRC Sandia report, a general methodology is proposed for modeling this phenomenon. Input requirements are the following:

β = mean areal density of undetected boreholes

f = fraction of the undetected holes that are unsealed

S = a random variable representing the shortest distance from an undetected borehole to a waste drift, whose distribution would be calculated from the repository geometry

$\sigma(s)$ = a function describing the time required for solutioning along a borehole to extend the radius to value s

$\psi(t)$ = a function representing the failure rate for initially sealed holes, i.e., the probability per unit time that a plug has closed to block the flow of water

$\dot{V}$ = rate of salt removal from a cavity formed by flow through an unsealed borehole

$\dot{W}$ = rate of salt removal from a cavity formed by the failure of a sealed borehole.

The report suggests values $\dot{V} = 1.5\ m^3/yr$, $\dot{W} = 0.15\ m^3/yr$, and the range 27 to 113 meters for the distances between an undetected borehole and a waste drift. (These parameters apply to the generic bedded salt reference repository defined in detail in the same report.)

In the BNWL project, it has been asserted that for the Columbia Plateau (basalt) the identification of all old boreholes to the repository depth should be a relatively simple task. In addition, it is argued that two additional factors would need to be present in order for such a borehole to lead to a breach of the repository containment: a connection with the repository and a hydraulic driving force.

D-3.5 OTHER TECHNOLOGICAL EVENTS AND PROCESSES

D-3.5.1 Introduction

Mechanisms and processes that fall into the "technological" category are those related to the presence of the wastes or the repository, or those related to the site exploration process. In other projects on disposal of high-level radioactive wastes, the term "near field" effects has been used to include most of these processes.(80) The analysis of such effects is difficult with a generic repository because detailed engineering assumptions are necessary for a complete analysis, and the repository systems treated here are not defined to such a level of detail. For example, questions have been raised concerning the stability of borosilicate glass as a waste form when placed in a salt environment.(81) Since stability is related to both waste form and temperature, it would be necessary to specify a waste form and a level of thermal loading for the repository, calculate estimated temperature profiles, and then determine what laboratory data and thermodynamic/kinetic analysis could contribute to a quantitative assessment of the magnitude of the potential problem. A different approach has been adopted here, one more suitable for a generic study. Potential problem areas have been reviewed and, except in the case of those identified as particular failure elements in previous sections, it has been assumed that they represent engineering problems amenable to analysis and solution.

D-3.5.2 Waste-Rock Interactions

Interaction between the radioactive wastes and the surrounding rock can affect both the waste package and the rock. Examples of particular effects are discussed in the following paragraphs.

Waste form degradation. The waste forms under consideration in this study range from spent fuel to special solid matrices (e.g., cement, glass, synthetic minerals) for processing or reprocessing wastes. In each case and in each geologic environment, the effects of the host rock and groundwater on the waste forms must be addressed. A particular case that has received considerable recent attention is the effect of hot brines on borosilicate glass. A straightforward engineering solution to such a problem might be to decrease the level of waste loading so that the temperature remains at a level where such a reaction would occur at a negligible rate, if at all. Other questions would be whether the altered waste form is significantly more leachable than the original, whether the canister (i.e., the package) might be able to insulate the waste form from the environment until the critical thermal period has passed, whether brines or otherwise active groundwater can ever reach the waste form, etc. Current research on waste forms should provide the information necessary to deal with these questions effectively.

Canister degradation. Canister research and development work in the United States and abroad reflects several different philosophies about this component of the waste containment system. These range from the view that the canister is important only through the handling and emplacement stage, to the view that the canister can be one of the most important barriers to radionuclide release, perhaps for periods up to hundreds of thousands or millions of years. More details on canister capabilities may be found in Appendix D-VIII of this report and in the

Task B Report. In any case, the geochemical, thermal, and mechanical parameters of the emplacement environment can certainly affect the integrity of the canisters, and therefore these factors must be considered carefully in the engineering design of the system.

Rock alteration. Rock in the immediate vicinity of the waste canisters will be subjected to heat and radiation, which can affect it in a variety of ways. For example, heat can lead to spalling, cracking, or decrepitation through differential expansion or high vapor pressure of fluids in the rock. Such fracturing would be expected to increase the hydraulic conductivity, but probably only within a few meters of the wastes. (This increase is different from the bulk rock failure element discussed in Chapter 3.0, wherein large scale movement along existing joints was considered.) In the special case of shales and some other rocks composed of certain hydrous clay minerals and metastable minerals, more extensive changes are possible. Some clays, such as montmorillonite, contain loosely bonded water in the crystal structure, and this can be liberated at temperatures in the range of 100-200° C. As a result of dehydration, the clay contracts, cracks, and loses strength; in addition, water is provided to the repository. Other modes of alteration are also possible but are not discussed here since it is believed that they are likely to be less significant.

D-3.5.3 Brine Migration

Salt deposits frequently contain fluid inclusions, which are (generally very small) bubbles or pockets of fluid within the salt matrix. These inclusions occasionally have both a liquid and a vapor phase. Some of these inclusions may represent connate water contained in the salt since its deposition, although other mechanisms may also account for such inclusions. Geochemical studies now under way may provide a greater understanding of this phenomenon.(82)

Fluid inclusions can migrate in a thermal gradient as a result of several possible mechanisms,(83) one of which is sketched in Figure D-20. In the situation represented, salt dissolves on the left side of the bubble and reprecipitates on the right side because of the variation

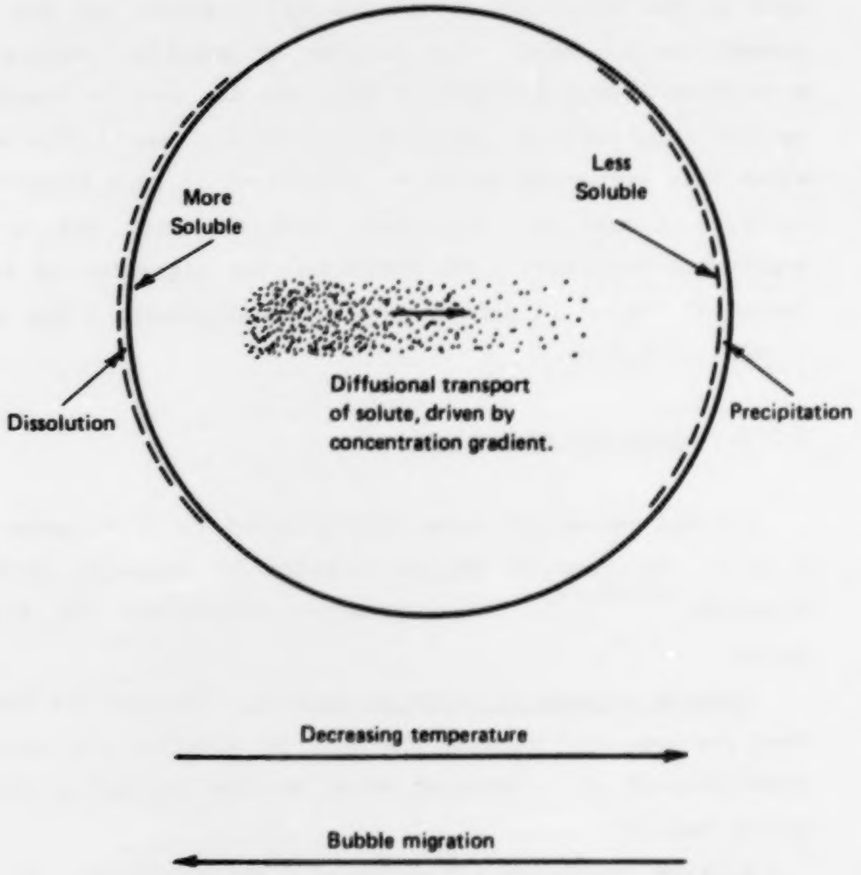

FIGURE D–20 MIGRATION OF BRINE BUBBLE IN THERMAL GRADIENT of solubility with temperature. This has the effect of moving the fluid inclusion to the left, toward the heat source.

The rate of brine migration and the total amount that might accumulate near the hot waste canisters depends on a number of factors, such as the magnitude of the thermal gradient and the amount of water present in the salt. The results of modeling efforts and laboratory experimental programs now in progress may provide further illumination on the relationships among the parameters and indicate the extent to which this mechanism should be considered in site selection (e.g., fluid content of salt may vary from site to site) and in the choice of engineered barriers. The potential for migration of brine will be an important factor in determining the requirements a the waste package in a salt repository.

D-3.5.4 Canister Migration

Various mechanisms have been proposed by which canisters emplaced in a salt environment might physically migrate either upward or downward.(40,84-92) Representative mechanisms are briefly described below.

Sinking because of canister density. Because the canister is denser than the salt and because the salt is plastic, the canister might sink right through it. (Movement might be slow because of the high viscosity of the salt.)

Sinking because of formation of a brine bubble. If the canister is enveloped by fluid (through brine migration, discussed in the previous section), it would sink to the bottom of the surrounding bubble. The higher temperatures at the bottom, where the canister would rest on the salt, could lead to preferential dissolution there, and thus continue the sinking process.

Rising caused by thermal buoyancy (induced salt diapirism). The salt surrounding one or more waste canisters or the entire repository would be expected to expand upon heating. The resulting decreased density might cause this entire mass to rise, carrying the canisters with it.

A number of scientists at different laboratories using different analytical and experimental tools have investigated possible waste migration in salt.(53,87-92) A substantial effort to characterize behavior of the salt of the Delaware Basin has been carried out and is continuing at Sandia Laboratories. This effort includes laboratory measurements of salt creep, constitutive modeling of salt response, and the application of numerical stress analysis procedures for predicting canister movement.

Analysis of the steady-state and transient response of a single 3-m long, 30-cm diameter canister were performed using lower bound (worst case) viscosity estimates.(87) The predicted velocities are in the order of 1 cm/1000 years. The long-term total movement predicted from convective cell movement is 5-10 meters per 10^5 years. The Sandia effort has also examined various canister and repository configurations and emplacement schemes with a view toward determining the effects of those factors on both individual canister motion and repository motion. The studies indicate that movement of the salt mass would not cause a salt dome to form.

In the present study of generic repository designs and geologic formations, canister or repository movement is not modeled as a failure element since most recent investigations agree that such motions are not a serious concern. The mechanisms described are amenable to engineering analysis, based on the parameters appropriate to a specific situation (salt viscosity, temperature profiles, etc.). If such movement is predicted to be a problem in a particular case, the design (e.g., shape or thermal loading of canisters), can be modified or a repository considered elsewhere.

D-3.5.5 Criticality

Concentration of certain radioactive material can result in self-sustaining nuclear reactions. This condition of high concentration is referred to as criticality. To avoid the possibility of reaching critical levels, waste forms, concentrations of fissionable material, and canister spacing can be planned with this factor in mind. Criticality calculations are straightforward and well understood.

Naturally, allowance must be made for the movement of canisters and for the introduction of water, as discussed in the previous sections. The concentration of fissionable material by chemical means (i.e., by dissolving out of the waste form matrix and reconcentrating elsewhere) is also a theoretical possibility, but no reasonable mechanism has been postulated by which this might occur in a repository.

D-4.0 HUMAN INTRUSION

One failure element, future drilling, is modeled in detail in this chapter, and several additional possible failure mechanisms are discussed. Some repository risk assessments have avoided quantitative models for future human intrusion events, but it appears that this approach is unrealistic. There are large uncertainties associated with the prediction of future natural events or technological failures as well, and to neglect one important class of events may cause too much emphasis or importance to be placed on others. While the estimates given here must obviously be speculative, they would appear to be useful not only for rough estimates of repository performance, but also to clarify the importance of key assumptions in the assessment process.

D-4.1 FUTURE DRILLING ACTIVITIES

D-4.1.1 Summary

Future deep drilling on the repository site could lead to the direct transport of radioactive material to the surface or to the establishment of an additional groundwater pathway. Estimates of the possible extent of such drilling depend on assumptions made about future knowledge and control of the repository site. EPA guidelines for this study require the assumption that after a period of 100 years from repository closure, control of the site is lost and it reverts to prevailing land use patterns of the area in which it is located. Based on this assumption, estimates were made of the frequency of future deep drilling. Three modes of release were modeled: transport of pieces of canister to the surface with the drilling fluid in the case of a direct hit; transport of fluids, from the repository to the surface during drilling; and the establishment of a groundwater pathway from the repository to the upper aquifer by means of an imperfectly plugged hole. A summary of assumptions, parameters, and calculational results is given in Table D-79.

TABLE D-79
SUMMARY OF FUTURE DRILLING FAILURE ELEMENT

MEDIUM	PROBABILISTIC (P) DETERMINISTIC (D)	NATURE OF MODEL	RELEASE MODE	DRIVING FORCE	SOURCE TERM	PARAMETERS		FLUID TRANSPORTED TO SURFACE		COMMENTS
						1st ESTIMATE	2nd ESTIMATE	1st ESTIMATE	2nd ESTIMATE	
Bedded Salt	P, D	Postulated deterministic drilling rate, probabilistic for hitting canister.	A. Land surface B. Groundwater	A. Materials raised with drilling mud. B. Thermally induced convection and gradient from aquifer interconnection.	A. Part of canister and fluid from waste drift. B. Uniform concentration.	No holes first century; 5 holes next century; 2 holes each subsequent century. All holes to lower aquifer. Holes sealed with permeability $K = 10^{-4}$ cm/sec $\eta = 0.2$, and $A = 0.1\ m^2$. Probability of hitting a canister = 10^{-3} per hole, with expected removal of 15% contents.	No holes first century; 50 holes next century; 5 holes each subsequent century. All holes to lower aquifer. Holes sealed with permeability $K = 10^{-3}$ cm/sec, $\eta = 0.2$, and $A = 0.1\ m^2$. Probability of hitting a canister = 10^{-3} per hole, with expected removal of 15% contents.	0.07 m^3/drill hole	1400 m^3/drill hole	Analysis assumes no knowledge of repository before, during, or after drilling. Ground-water releases from post-sealing leakage are calculated in the text but are, in general, less significant than releases to the surface.
Granite	P, D	Postulated deterministic drilling rate, probabilistic for hitting canister.	A. Land surface B. Groundwater	A. Materials raised with drilling mud. B. Thermally induced convection.	A. Part of canister and fluid from waste drift. B. Uniform concentration.	No holes first century; 1 hole next century; 1 hole every four subsequent centuries. Holes sealed with permeability $K = 10^{-4}$ cm/sec, $\eta = 0.2$, and $A = 0.1\ m^2$. Probability of hitting a canister = 10^{-3} per hole, with expected removal of 15% contents.	No holes first century; 10 holes next century; 2 holes every subsequent century. Holes sealed with permeability $K = 10^{-3}$ cm/sec, $\eta = 0.2$, and $A = 0.1\ m^2$. Probability of hitting a canister = 10^{-3} per hole, with expected removal of 15% contents.	200 m^3/drill hole	5000 m^3/drill hole	Analysis assumes no knowledge of repository before, during, or after drilling. Ground-water releases from post-sealing leakage are calculated in the text but are, in general, less significant than releases to the surface.
Basalt	P, D	Postulated deterministic drilling rate, probabilistic for hitting canister.	A. Land surface B. Groundwater	A. Materials raised with drilling mud. B. Thermally induced convection and gradient from aquifer interconnection	A. Part of canister and fluid from waste drift. B. Uniform concentration.	No holes first century; 3 holes next century; 1 hole each subsequent century. All holes to lower aquifer. Holes sealed with permeability $K = 10^{-4}$ cm/sec, $\eta = 0.2$, and $A = 0.1\ m^2$. Probability of hitting a canister = 10^{-3} per hole, with expected removal of 15% contents.	No holes first century; 20 holes next century; 5 holes each subsequent century. All holes to lower aquifer. Holes sealed with permeability $K = 10^{-3}$ cm/sec, $\eta = 0.2$, and $A = 0.1\ m^2$. Probability of hitting a canister = 10^{-3} per hole, with expected removal of 15% contents.	200 m^3/drill hole	5000 m^3/drill hole	Analysis assumes no knowledge of repository before, during, or after drilling. Groun-water releases from post-sealing leakage are calculated in the text but are, in general, less significant than releases to the surface.

TABLE D-79
SUMMARY OF FUTURE DRILLING FAILURE ELEMENT (CONTINUED)

MEDIUM	PROBABILISTIC (P) DETERMINISTIC (D)	NATURE OF MODEL	RELEASE MODE	DRIVING FORCE	SOURCE TERM	PARAMETERS		FLUID TRANSPORTED TO SURFACE		COMMENTS
						1st ESTIMATE	2nd ESTIMATE	1st ESTIMATE	2nd ESTIMATE	
Shale	P, D	Postulated deterministic drilling rate, probabilistic for hitting canister.	A. Land surface B. Groundwater	A. Materials raised with drilling mud. B. Thermally induced convection and gradient from aquifer interconnection.	A. Part of canister and fluid from waste drift. B. Uniform concentration.	No holes first century; 5 holes next century; 2 holes each subsequent century. All holes to lower aquifer. Holes sealed with permeability K = 10^{-4} cm/sec, η = 0.2, and A = 0.1 m^2. Probability of hitting a canister = 10^{-3} per hole, with expected removal of 15% contents.	No holes first century; 50 holes next century; 5 holes each subsequent century. All holes to lower aquifer. Holes sealed with permeability K = 10^{-3} cm/sec, η = 0.2, and A = 0.1 m^2. Probability of hitting a canister = 10^{-3} per hole, with expected removal of 15% contents.	200 m^3/drill hole	5000 m^3/drill hole	Analysis assumes no knowledge of repository before, during, or after drilling. Groundwater releases from post-sealing leakage are calculated in the text but are, in general, less significant than releases to the surface.
Dome Salt	P, D	Postulated deterministic drilling rate, probabilistic for hitting canister.	A. Land surface B. Groundwater	A. Materials raised with drilling mud. B. Thermally induced convection.	A. Part of canister and fluid from waste drift. B. Uniform concentration.	No holes first century; 5 holes next century; 2 holes every subsequent century. Holes sealed with permeability K = 10^{-4} cm/sec, η = 0.2, and A = 0.1 m^2. Probability of hitting a canister = 10^{-3} per hole, with expected removal of 15% contents.	No holes first century; 30 holes next century; 5 holes every subsequent century. Holes sealed with permeability K = 10^{-3} cm/sec, η = 0.2, and A = 0.1 m^2. Probability of hitting a canister = 10^{-3} per hole, with expected removal of 15% contents.	0.04 m^3/drill hole	1300 m^3/drill hole	Analysis assumes no knowledge of repository before, during, or after drilling. Groundwater releases from post-sealing leakage are calculated in the text but are, in general, less significant than releases to the surface.

D-4.1.2 Background

Estimates of the likelihood of future penetration of a repository by drilling activities must be made in the context of past and present drilling rates as well as the extent to which the rates, purposes, and characteristics of drilling activity vary with time. These topics are discussed in this section. In addition, there are subsections on various activities associated with drilling, since these activities may affect whether an unknown repository is detected before or during drilling. They may also affect the consequences of drilling into a repository.

Past drilling activity. The reasons for and extent of past drilling into potential repository formations are relevant to estimating the potential for future drilling. Data on historical drilling activity were presented in Section D-3.4 and will only be summarized here. The scope of drilling activities discussed in that section includes:

- oil and gas exploration and recovery,
- water exploration and recovery,
- geothermal resources evaluation,
- brine injection or disposal of other wastes,
- mineral exploration,
- scientific investigation,
- fluid storage, and
- other special and localized drilling.

The areal densities that were estimated for old boreholes are summarized in Table D-80. They were determined on the basis of the expected dominant types of activity in the past: oil and gas, water, and mineral exploration and/or recovery.

Present drilling rates. The present drilling rate appears to be well documented only for the petroleum industry. Figure D-21 shows numbers of oil and gas holes drilled by state (or groups of states) in 1976 and 1977. Of these, about 37,000 holes drilled in 1977 exceeded 1250 feet (385 m).(93) This represents an average rate of 0.04 hole per year per repository area, using 8 km^2 for the area of the repository and 7.8×10^6 km^2 for the area of the 48 contiguous states. Since this drilling was generally confined to potential oil- and gas-bearing

TABLE D-80

AREAL BOREHOLE DENSITIES FROM PAST DRILLING ACTIVITIES

	Holes per Repository Area*	
	First Estimate	Second Estimate
Bedded Salt	0.08	6.0
Granite	0.003	0.03
Basalt	0.05	0.13
Shale	0.03	6.0
Dome Salt**	2.0	20.0

*These estimates are based on Section D-3.4 of this report and refer to holes at least 300-500 m deep. Depending on the rock type, the areal densities were given earlier for either the buffer zone around the repository (4 km^2) or the repository plus buffer zone (12 km^2). The numbers in this table have all been normalized to the repository area (8 km^2).

**The holes in salt domes tend to be concentrated near the flanks of the dome. Since the repository would be in the interior of the dome, the average density of holes is a bound on the expected number penetrating the repository area itself. Thus, it is a conservative estimate.

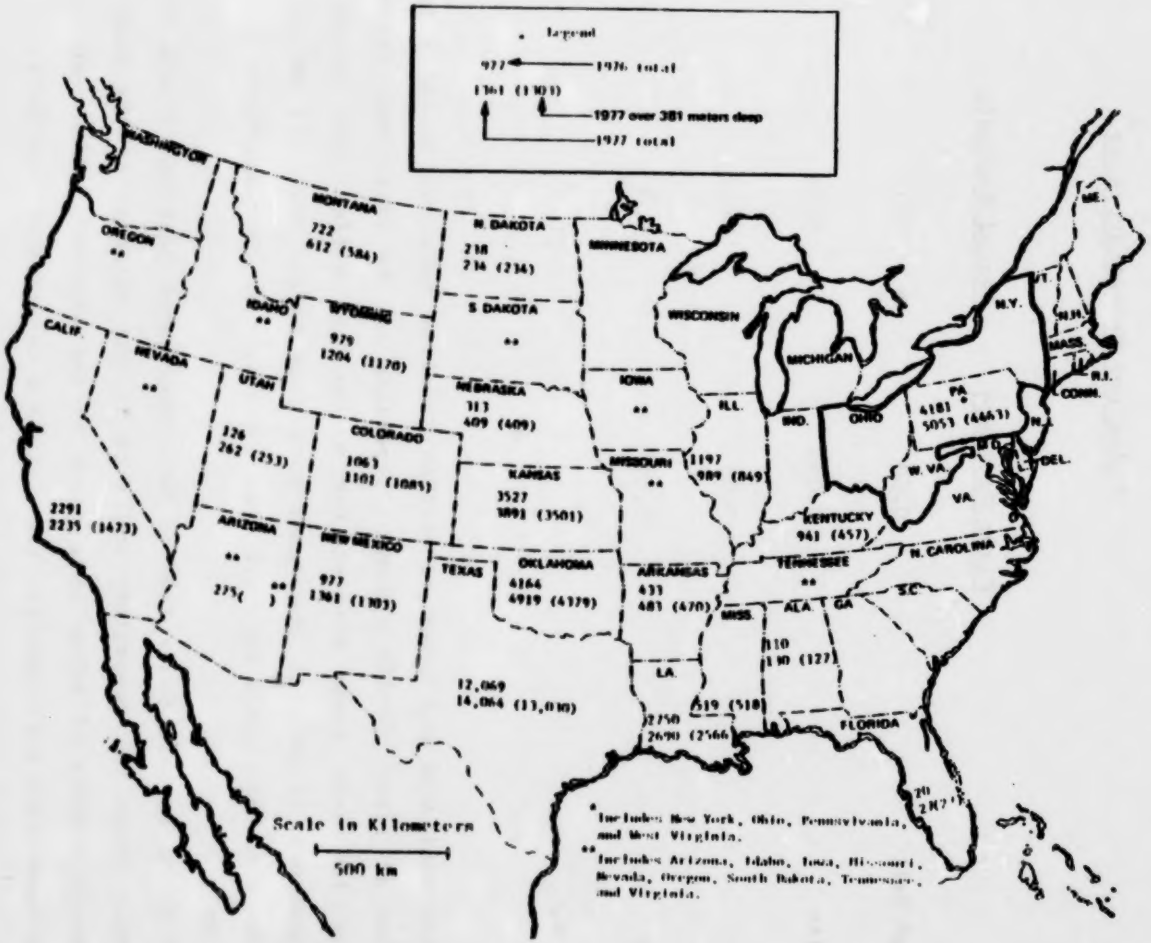

Sources: 1977 Joint Association Survey on Drilling Costs, sponsored by: American Petroleum Institute, Independent Petroleum Association of America, and Mid-Continent Oil and Gas Association, February 1979.

1976 Joint Association Survey on Drilling Costs, The American Petroleum Institute , Dec., 1977 Edition.

FIGURE D–21 PETROLEUM WELLS DRILLED IN THE CONTIGUOUS 48 STATES, 1976 AND 1977 sedimentary basins, the areal density is far from uniform and, in fact, is much higher for such basins.

Non-uniformity of drilling rates with time. It is important to note that extreme changes in drilling rates may occur with time. Reasons for this include the following:

- Scarcity of oil, gas, water, or certain minerals may encourage more extensive exploration.
- New recovery methods may make deposits attractive that were previously partially depleted or not worth exploiting at all.
- New drilling techniques may make it feasible to exploit additional formations.
- New resource recognition may initiate entirely distinct drilling programs.
- Demographic changes may encourage extensive drilling for water or other resources in new areas.
- Other purposes for drilling may assume prominence.

Examples of these factors can be seen in the evolution of the petroleum industry. A little over 100 years ago there was no such industry, and the drilling of more than two million petroleum holes in the United States over the period of a century(94) was presumably not foreseen. Several thousand holes are drilled annually in search for uranium, and the recognition of this resource is only about forty years old. Geothermal energy is in its commercial infancy, and it is impossible to predict to what extent this industry will grow. Population movement to the southwest has encouraged deep drilling for water in recent years, and with the gradual depletion of water stored in certain formations, additional resources will have to be sought in the future. Furthermore, the development of extensive drilling programs for new purposes, such as monitoring or control of tectonic events, waste disposal, or scientific research, may well occur.

Activities prior to drilling. In assessing the possibility of future drilling through a nuclear waste repository, it is relevant to consider whether the repository might be detected prior to drilling. The extent of such exploration depends on the nature of the resource being sought. In the case of petroleum, which is generally found in specific structural traps, extensive geologic and geophysical exploration usually precedes the drilling. In the case of water wells, drilling may start with little or no geophysical work, although the types of geologic formations being drilled would be known on a regional basis. Geothermal drilling may be preceded by detailed area heat flow analyses, although it is not yet clear what practices will be followed when and if this resource becomes heavily exploited in the future.

Activities during drilling. The ways in which the presence of a repository might be recognized during drilling are relevant to the consequences that could follow from such a breach. As above, this depends on the purpose for which the hole is being drilled. Activities associated with petroleum well drilling are reviewed in the following paragraphs.

Drilling boreholes involves a continuous process of investigation and examination of the drill progress and the geology of the rocks being penetrated. Typically, drilling to any considerable depth into consolidated rock involves the use of rotary equipment cooled and lubricated with any of a number of fluids (muds). In the process, chips of rock are broken at the bottom of the hole and carried to the surface with the fluid. A regular inspection of the rock chips is made to determine their nature and composition, as a guide for estimating the formation being drilled. Thus, the drill crew is constantly aware of the nature of the rock being penetrated. A written log of rock type, as determined from the cuttings, is retained, at least within the depth range of interest to the exploration program.

Other factors and conditions noted during drilling with common rotary equipment are fluid used, gases and other contaminants, drilling rate, and depth of drill string. From this information, a drill crew can interpret the down-hole conditions and rock formation with occasional reference to the material brought up by the drill and by correlation with other holes in the vicinity.

Periodically, particularly when some unusual formation is reached, when the drill stem has been pulled for some reason, or when it is suspected that a productive horizon is being penetrated, the hole is logged. This procedure involves a number of processes and different equipments. Logging may simply measure the diameter and depth of the hole, or it may entail use of more sophisticated and sensitive equipment to measure certain rock properties. Specialized logging devices include electric resistance sondes, gamma radiation logs, sonic logs, neutron logs, and magnetic and temperature sensors. These assist in determining the rock type at depth, its physical properties, and its economic potential. In some cases, the drill mud and cuttings are continuously monitored by automatic equipment to indicate to the drill crew when petroleum, radioactive minerals, or rock with specific properties (such as high density) have been reached.

When circumstances permit and dictate (when drilling into competent rock with important properties or characteristics such as distinctive structure or minerals) a core of the rock may be taken. This procedure requires a special drill bit, typically diamond faced. The core sample is then examined and the results recorded. Important information obtained from cores includes not only rock type, but porosity, strength, permeability, structure, and mineral composition. Some of this information is found through laboratory tests performed on the recovered cores.

Much of the continuous investigation during drilling depends upon the experience and expectations of the drill crew. In locations where other boreholes have penetrated a considerable depth of unproductive rock in reaching a readily identified horizon, logging and mud checking may not be as conscientiously applied as in situations where the sub-surface geology is less well known. This on-site subjectivity is augmented by thorough preliminary geologic and geophysical surveys of the area. Seldom, if ever, is a borehole started without a substantial commitment of time and energy to determine the suitability of the drill site. The occasional exception is when limited finances encourage a private landowner to accept the risk of a blindly drilled hole for water or mineral exploration. However, in such situations, the drill crew can usually supplement the lack of knowledge with their own experience in drilling other holes within the same geologic domain.

D-4.1.3 Future Drilling Failure Model

In accordance with EPA guidelines on assumptions about future institutional control of a radioactive waste repository site, the following have been assumed for purposes of this study:

- Institutional control of the site can prevent drilling for 100 years after repository closure.
- After the 100-year period of institutional control, the site returns to the ordinary land use patterns of the area in which it is located.

It should be emphasized that these are model assumptions, not assertions about future events. Indeed, one can easily imagine conditions under which one or both of these would be violated. For example, the increasing scarcity of energy and perhaps other resources over the first 100-year period could result in strong pressures on the government to permit exploration for and recovery of such resources on the site. These resources might today be completely unrecognized or undiscovered, or be regarded as commercially worthless. The government might yield to such pressures and permit drilling under controlled conditions. Because such a decision would be made in full knowledge of the presence of the repository, however, responsibility for any adverse consequences would seem to rest with those future decision-makers. If such drilling were undertaken, it is likely that assurances of its safety would also be required. Therefore, conditions under which the first assumption is violated have not been pursued here.

The second assumption may also not accurately represent the true situation. It is highly probable that knowledge of the repository will be preserved beyond 100 years and that this will influence activities on the site even if the level of institutional control decreases or disappears. In the absence of institutional control, however, knowledge of the existence of the repository may still not be sufficient to preclude activities that threaten the repository's integrity.

Obviously, one cannot predict the future or extrapolate scientifically from past data to estimate future drilling rates at a repository site. Nevertheless, it is believed that the probability is sufficiently high of future deep drilling at the site that the question is not "whether" but "how often." That is, a rate of future drilling should be a model parameter and various values should be used for sensitivity analyses. The purpose of this section of the report is to provide nominal values for this and associated parameters under first and second estimate assumptions for each of the five geologic host media being evaluated.

Estimated future drilling rates are presented in Tables D-81 through D-85. The drilling rates given in the tables are not the result of scientific or statistical observation. They are rough estimates by members of the Arthur D. Little, Inc. staff who have experience in resource exploration and recovery. In the case of exploration, they are generally based on the time interval over which factors may change sufficiently to justify another exploratory drill hole.

The drilling rates are given in terms of holes per century. For exploratory holes they might be spread out rather evenly in time, and for holes for petroleum production they might be closely grouped in time. The choice of a single more heavily drilled century was the result of a two-step process. First, it appears likely that a valuable resource on the site will be exploited over a limited period of time. This period of time could fall during any century within the 10,000 years over which the repository is being evaluated. Thus, one century is hypothesized to have a higher drilling rate. The choice of the first century after the end of institutional control as this period of heavier drilling was based on several factors:

1. Having been withdrawn from use for an entire century or more, the site is more attractive for exploration since less is known about it.
2. The commercial viability of mineral or energy resources will have changed over that first 100 years, so that the new availability of this site may open the door to new commercial recovery operations.
3. The thermal anomaly represented by the repository itself may encourage drilling.

Furthermore, it is in keeping with the conservative approach of this modeling effort to assume drilling at the earliest possible moment, since the radioactivity levels are highest then. A counterbalancing

TABLE D-81

FUTURE DRILLING RATE ESTIMATES FOR BEDDED SALT

	First Estimate	Second Estimate
Characteristics of Resources at Site		
Hydrocarbons	Essentially none in the entire sedimentary sequence.	Present but not of current commercial interest, or "depleted" formations, or unexplored horizons with hydrocarbon potential (possibly very deep).
Water	Abundant water at or near surface.	Limited water available at or near surface. Deep aquifer(s) below repository formations even if not potable.
Minerals	No minerals at or below repository formation ever expected to become commercially valuable.	No commercially attractive reserves in present terms.
Geothermal	No thermal anomaly.	No thermal anomaly.
Deep Holes Drilled per Century		
First century after institutional control ends.	5	50
Subsequent centuries.	2	5
Bases for Rate Estimates	Unsuccessful petroleum or mineral exploration.	One period of commercial resource exploitation, followed by occasional exploration or water wells.

TABLE D-82

FUTURE DRILLING RATE ESTIMATES FOR GRANITE

	First Estimate	Second Estimate
Characteristics of Resources at Site		
Hydrocarbons	None in or on flanks of pluton.	None in or on flanks of pluton.
Water	Abundant water at or near surface. No large fracture system aquifers expected at depth. Fractures generally closed at depth.	Water supplies generally from fracture systems. None known at depth. Limited surface water.
Minerals	No expectation of significantly valuable mineral deposits, based on detailed understanding of regional geology.	Mineral potential uncertain.
Geothermal	No thermal anomaly.	Higher than average regional heat flux.
Deep Holes Drilled per Century		
First century after institutional control ends.	1	10
Subsequent centuries.	0.25 (i.e., one hole every four centuries).	2
Bases for Rate Estimates	Undetermined purpose, perhaps geothermal exploration.	Water, geothermal, and mineral exploration. Possible geothermal wells.

TABLE D-83

FUTURE DRILLING RATE ESTIMATES FOR BASALT

	First Estimate	Second Estimate
Characteristics of Resources at Site		
Hydrocarbons	Essentially no petroleum in any sedimentary strata below basalt flow.	Unexplored horizons with hydrocarbon potential, even if not presently commercially attractive.
Water	Abundant water at or near surface.	Limited water at or near surface. Deep aquifer(s) below repository formation even if not potable.
Minerals	No expectation of significantly valuable mineral deposits, based on detailed understanding of regional geology.	Mineral potential uncertain.
Geothermal	No thermal anomaly.	Higher than average regional heat flux.
Deep Holes Drilled per Century		
First century after institutional control ends.	3	20
Subsequent Centuries	1	5
Basis for Rate Estimates	Petroleum or mineral exploration.	Commercial exploitation of petroleum resources, with hole economy due to difficulty in drilling basalt. Followed by occasional exploration and water wells.

TABLE D-84

FUTURE DRILLING RATE ESTIMATES FOR SHALE

	First Estimate	Second Estimate
Characteristics of Resources at Site		
Hydrocarbons	Essentially none in the entire sedimentary sequence.	Present but not of current commercial interest, or "depleted" formation, or unexplored horizons with hydrocarbon potential (possibly very deep).
Water	Abundant water at or near surface.	Limited water avalable at or near surface. Deep aquifer(s) below repository formations even if not potable.
Minerals	No minerals at or below repository formation ever expected to become commercially valuable. No good indications of valuable minerals.	No commercially attractive reserves in present terms.
Geothermal	No thermal anomaly.	No thermal anomaly.
Deep Holes Drilled per Century		
First century after institutional control ends.	5	50
Subsequent centuries	2	5
Basis for Rate Estimates	Unsuccessful petroleum or mineral exploration.	One period of commercial resource exploitation, followed by occasional exploration or water wells.

TABLE D-85

FUTURE DRILLING RATE ESTIMATES FOR DOME SALT

	First Estimate	Second Estimate
Characteristics of Resources at Site		
Hydrocarbons	No oil- or gas-bearing formations in contact with dome at any depth. No oil or gas of promise in sedimentary strata below deep underlying salt beds.	Present but not of current commercial interest, or "depleted" formations or reserves along flanks of dome. Unexplored horizons below deep underlying salt beds.
Water	Abundant water at or near surface.	Limited water at or near surface. Deep aquifers with significant potential, even if not potable.
Minerals	No minerals associated with dome ever expected to be of commercial interest.	Limited dome exploration, or minerals present but not valuable in current commercial terms.
Geothermal	No resource potential, even very deep.	Undetermined potential.
Deep Holes Drilled per Century		
First century after institutional control ends.	5	30
Subsequent centuries.	2	5
Basis for Rate Estimates	Petroleum or mineral exploration.	Petroleum, water, and mineral exploration and/or recovery.

possibility, that during the first few hundred years the canisters remain intact and thus the wastes are not leached into the surrounding repository, should be omitted from the consequence analysis of this failure element as long as the simplifying assumption of early maximum drilling is retained.

In drawing the distinction between first and second estimates on the subject of water resources, a paradoxical situation occurs. From the point of view of future drilling, it is indeed preferable for abundant water to be available at the surface or in aquifers overlying the repository, since this eliminates or decreases the need to drill deep for future water supplies. This distinction between first and second estimates does not mean that from the total perspective of repository evaluation it is better to have a productive aquifer above the repository. The answer to this latter question depends on a number of considerations, centering on the nature of all the pathways that could allow radionuclides to enter the aquifer system. The literature of nuclear waste management frequently exhibits the assumption that productive aquifers should not overlie the repository,(95,96) but the present authors are unaware of conclusive evidence that this is, in general, a necessary or desirable criterion. With respect to water potability, prospects for efficient desalination appear to make potability an unreliable factor in evaluating the usefulness of aquifer systems to future generations.

Consistent with previous sections of this report, the boreholes here are assumed to have a cross-sectional area of 0.1 m^2 at the time they are sealed, and they are assumed to penetrate at least as far down as to the lower aquifer. After use they are assumed to be sealed to the same standards as assumed for the case of presently undetected boreholes. This assumption entails hydraulic conductivities of 10^{-4} cm/sec and 10^{-3} cm/sec for first and second estimates, respectively, and a porosity of 0.2. The holes are randomly distributed over the repository site.

Assuming that a future drill hole passes through the repository, there is some probability that it will actually directly hit a waste canister. This probability depends on the cross-sectional area of the canister as well as on that of the drill bit and hole. The assumed dimensions are as follows:

	Radius	Area
Drill hole	0.1 m	$0.03\ m^2$
Canister	0.15 m	$0.07\ m^2$

Note that the cross-sectional area of the borehole, when considered as a fluid pathway, is somewhat larger (i.e., $0.1\ m^2$) than the area of the drill bit and initial hole. This is because some enlargement may take place over the period during which the hole is used and cleaned for sealing. Moreover, the rock immediately surrounding the hole may also be fractured and therefore augment the fluid flow. The dark ring in Figure D-22 indicates a region where, if the center of the drill hole lies within it, the drill will intersect part of the waste canister. The area of this region is

$$\begin{aligned} A &= (0.10 + 0.15)^2 \\ &= 0.2\ m^2. \end{aligned}$$

Since the area of the repository is $8\ km^2$, the probability that a drill will actually hit one of the 35,000 canisters is given by

$$\begin{aligned} p &= \frac{35000 \times 0.2}{8 \times 10^6} \\ &= 0.0009 \\ &\cong 0.001. \end{aligned}$$

The value $p = 0.001$ has been adopted in this model.

D-4.1.4 Future Drilling Release Model

Drilling into the repository may lead to the release of radionuclides by several mechanisms, the principal ones being:

1. Direct transport of parts of the waste package to the surface in the case of a direct hit.
2. Transport of radionuclide-contaminated water from the repository to the surface. In the case of repositories in salt formations, this water may be encountered under pressure.

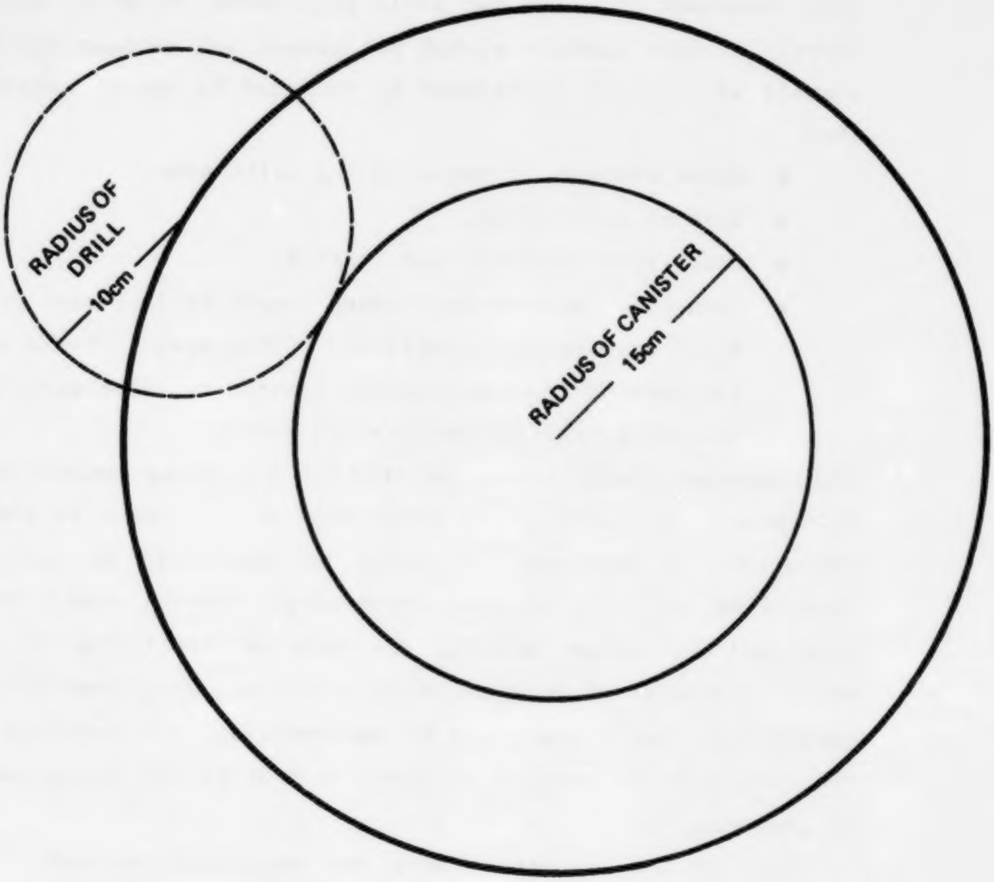

Note: Drill hole intersects canister if and only if its center is within outer circle, which has radius of 25 cm.

FIGURE D–22 REGION WITHIN WHICH CANISTER AND DRILL HOLE OVERLAP

3. Transport with groundwater to the upper aquifer through the filled but permeable borehole pathway.

The extent of releases via any of these mechanisms depends on the degree to which the drillers recognize the repository and its associated hazards when they intercept it. If the drill bit passes directly into a waste drift backfilled with densely packed yet porous and unconsolidated material, an anomaly will in all likelihood be detected by any of several signs, among them:

- rapid downward movement of the drill stem,
- loss of drill fluid,
- drill stem wandering and chatter,
- down-hole temperature changes caused by increased cooling of the drill by water in repository. (This would only be detected in the case of constant thermal monitoring, as presently practiced in some geothermal exploration work.)

The unconsolidated zone identified by these anomalies might be interpreted as an extensive shear zone or, if there is some idea of a repository in the area, it might be identified as such. If it is identified as part of the repository, caution would presumably be exercised in either sealing the hole or continuing to drill. For example, samples of rock and water could be taken, down-hole logging and geophysical techniques could be employed, and the repository section of the hole could be grouted or cased to seal it off during subsequent use of the hole.

Even if the repository were not recognized as such, it is likely that the hole would be cased through the backfilled level at least during the active life of the well. In case the drill passes through a rock pillar rather than a mined opening, recognition of the repository is much less likely. Pre-existing fractures or fractures induced by drilling could establish sufficient interconnection with a nearby drift to lead to fluid changes or loss of drill mud.

Despite the foregoing discussion, model calculations have not assumed recognition of the repository by future drillers, although alternative assumptions could be used to modify parameters in a sensitivity analysis. This approach is based on three considerations:

1. Although the mined portion of the repository occupies only 25% of the total cross-sectional area, inclusion of portions of the pillars in close proximity to the drifts significantly increases this fraction.
2. The earlier assumption about loss of control and knowledge of the repository site makes it likely that the repository would simply be interpreted as a zone of incompetent rock.
3. Ignoring considerations about recognition leads to a simple and conservative model.

Specific parameter values to model fluid or radionuclide releases are given in the following paragraphs.

D-4.1.4.1 Direct Hit

In case a drill bit hits a waste canister, some fraction of the canister's contents will be transported to the surface. Based on the geometry presented in Figure D-22, the expected fraction of the canister intersected by a drill hole whose center is randomly located within the dark ring is approximately 0.15, which can be derived by a lengthy but elementary geometric analysis. It is possible that the drillers will notice that they have hit a strange object, either by examination of chips at the surface, deflection of the drill stem, or clogging of the cutters on lead or other materials that may form part of the waste package. However, this observation by the drillers is not assured, and so it has not been assumed in the model. Consequently, the drill has been assumed to pass right through the portion of the canister it intersects, which implies that the fraction 0.15 also corresponds to the expected volumetric fraction of the canister that is raised to the surface.

D-4.1.4.2 No Direct Hit -- Fluid Released During Drilling

The analysis of this situation depends on the nature of the repository host rock.

Bedded Salt. As discussed in Appendix D-II, water is expected to seep gradually into the backfilled repository through slightly permeable shaft and borehole seals. (There may also be seepage along some natural pathways, such as interbeds.) In addition, fluid inclusions in the seemingly intact rock may migrate because of thermal gradients, thereby increasing the water content of the backfill close to the canisters. Therefore, whenever the repository is penetrated by a drill hole, the accumulated fluid may leak out, taking with it any radionuclides that may have leached out of the waste package. The amount of fluid present at any moment is a function of time. There is an increase in this amount during resaturation and then a decrease as salt creep tends to squeeze some of it back out. For simplicity of calculations, the maximum amount, which is the amount present just as the resaturation condition is reached, has been assumed to be present whenever a drill hole intersects the repository. This simplifying assumption tends to overestimate the level of release. These volumes are calculated in Appendix D-II and are as follows:

First estimate: 1.2×10^3 m^3

Second estimate: 5.6×10^5 m^3.

By means of the parameters given in Table D-12 (Chapter D-2.0), the fluid volume per canister and per waste drift can be calculated. While such volumes only represent averages and do not account for inhomogeneities in fluid distribution, they are believed to be adequate for modeling purposes.

The first estimate for fluid volume released during drilling is 0.07 m^3 per drill hole. This is based on the low porosity and fluid availability in the first estimate case, because of rapid salt creep, and the assumption that at most the fluid associated with the two nearest canisters would leak out. For simplicity, this value is also applied to the case where a drill hole does not pass through a waste drift, but rather through another backfilled room (other than a waste drift) or a pillar. Possible fracturing or dissolution during drilling do not permit adequate assurance that a drill hole through a pillar will not communicate with a waste drift. The second estimate for fluid volume released during drilling is 1400 m^3 per drill hole, based on the total fluid volume of one waste drift.

Granite. The fluid volumes per canister and per waste drift remain constant after repository resaturation, with the approximate values

50 m^3 and 5000 m^3 respectively. The first estimate for fluid volume released during drilling is based on the assumption of backfill material that is cohesive and will not easily wash into the drill hole. In this case, the integrity of the backfill is expected to prevent more than 200 m^3 from flowing into the drill hole. (This is, for example, the quantity of water contained in a 20-m long section of the waste drift, centered at the drill hole.) The second estimate value is based on less cohesive backfill, the possibility that the hole is being drilled for water, and the possibility that the drilling crew pump the repository horizon to test it as a source of water. It would not prove to be a desirable water supply, but the test might well empty most of the contents of one waste drift, or 5000 m^3.

Basalt. The assumptions for basalt are identical to those for granite, resulting in fluid flows to the surface of 200 m^3 and 5000 m^3 as the first and second estimates, respectively.

Shale. The assumptions for shale are identical to those for granite and basalt, resulting in fluid flows to the surface of 200 m^3 and 5000 m^3 as the first and second estimates, respectively.

Dome Salt. The analysis for the case of dome salt is analogous to that for bedded salt, except that the available fluid volumes are slightly different. Total fluid volumes for the resaturated repository are calculated in Appendix D-II to be:

First estimate: 8.7×10^2 m^3
Second estimate: 5×10^5 m^3

The first estimate for the fluid released per drill hole is 0.04 m^3, based on the fluid associated with two canisters. The second estimate is 1300 m^3, based on the fluid in one waste drift.

D-4.1.4.3 Fluid Flows After Plugging of Borehole

If the hole drilled is an unsuccessful exploratory hole, then it would be expected to be plugged soon after being drilled. If it is suitable for some resource recovery operation, it will probably be cased where it passes the repository (interpreted as a horizon of incompetent or soluble rock). The casing will prevent leakage during the production stage. After this stage, sealing will take place. In either case (initial plugging or plugging after production), there may be subsequent fluid migration along the sealed borehole up to the overlying aquifer. This pathway is analogous to borehole pathways discussed in Sections D-3.3 and D-3.4. First and second estimates of hydraulic conductivities have been taken to be the same as for present undetected boreholes (Section D-3.4), i.e., 10^{-4} cm/sec and 10^{-3} cm/sec, respectively. By adopting the methods and results of Sections D-3.3 and D-3.4, the volumetric flow rates shown in Table D-86 have been obtained. The radionuclide source term for risk calculations based on these flows is the average concentration in the fluid in the backfilled repository.

D-4.1.5 Literature Discussion

Quantitative estimates of the likelihood and consequences of future drilling activity do not seem to appear in other repository risk assessments, although there is the realization that this may be an important failure element.

The NRC/Sandia risk assessment(12) does not treat this problem quantitatively, although it does argue that the associated hazards are small. The reason given is that the first exploratory hole would probably lead to recognition of the repository and reestablishment of administrative control. Local contamination by material brought to the surface would be recognized and decontamination would be carried out.

Claiborne and Gera(3) argue that even if a future drilling crew were too unsophisticated to detect radioactive material brought to the surface, the resulting contamination would only be local and limited in consequence.

The Swedish KBS study(26) argues that their proposed repository is in one of their most common types of rock (granite) and "does not contain any valuable minerals which could conceivably be considered for profitable extraction." The depth and low water content also make water exploration unlikely. They also argue that future drilling would probably be preceded by exploration work that would detect the repository.

TABLE D-86

VOLUMETRIC FLOW RATES THROUGH A SINGLE SEALED BOREHOLE

Rock Type	Time (yrs)	Volumetric Flow (Q) (m³/yr) First Estimate	Volumetric Flow (Q) (m³/yr) Second Estimate
Bedded Salt(1)	250	2.0	Not applicable(6)
	1000	1.7	189
	10,000	.6	167
Granite(2)	100	1.7	17
	1000	1.1	11
	10,000	0.5	5
Basalt(3)	100	4.4	198
	1000	3.8	192
	10,000	1.6	170
Shale(4)	100	4.4	198
	1000	3.8	192
	10,000	1.6	170
Dome Salt(5)		Negligible at all times	

(1) Based on gradients in Table D-53, Section D-3.3., and corresponding discussion of dissolution.

(2) Based on Table D-73, Section D-3.4.

(3) Based on Table D-75, Section D-3.4.

(4) Based on Table D-77, Section D-3.4, dividing by 3 since only one hole is modeled here.

(5) Cf. Table D-67, Section D-3.3, and corresponding discussion.

(6) For this case, Period B only begins at 1000 years after closure. See Appendix D-II.

D-4.2 OTHER HUMAN INTRUSION EVENTS AND PROCESSES

D-4.2.1 Introduction

The most common and widespread human activity that could affect a deep geologic repository is drilling for oil, water, and other resources. This has already been examined as a specific failure element. It is natural to consider whether future human endeavors other than drilling programs may add substantially to the risk of releases from a repository. Since future incentives, technologies, and opportunities to intrude into a repository can be only imagined now, the discussion must be speculative. It is believed that detailed modeling of these other phenomena would not contribute significantly to the assessments made in this generic study.

D-4.2.2 Solution Mining

Because of its high solubility, salt is often extracted from underground formations by solution mining. In this process, water, usually heated, is forced through wells into the salt. The water dissolves the salt and the solution is pumped to the surface, where the salt is removed and the water reinjected. This technique can also be used for certain other minerals, such as sulfur. Solution mining is applicable to both dome and bedded salt deposits. Some abandoned solution cavities are used for the storage of hydrocarbons, and other cavities have been developed exclusively for this purpose. It is possible that in the future solution cavities will be developed and used for additional purposes, such as the disposal of chemical wastes or energy storage in the form of compressed air.

The potential hazard associated with solution mining is apparent. An extraction well passing near or through a repository would circulate large volumes of water that could accelerate leaching and transport of the stored waste. The brine, with any waste material dissolved in it, would be brought directly to the surface and distributed to any of a number of users, such as the food and chemical industries. Although quality controls and purity requirements of the consumers may detect the unusual radioactive constituents before they are dispersed, it is questionable whether such measures can be relied upon. Furthermore, when solutioning is carried out for the primary purpose of creating a cavity, as for example for hydrocarbon storage, little or no attention is paid to the composition of the waste brines.

The cavity developed in solution mining operations is typically "carrot" shaped if a single well is used for water injection and extraction. The usual dimensions of a single well cavity are about 15 meters (diameter) and 76 meters (height), although diameters twice this size have been reported.(97) Paired well mining, where water is introduced through one well and brine is extracted from another nearby, produces tunnels or lateral cavities. Wells are spaced from 100 to 400 meters apart and are connected by hydrofracturing the rock between. Tunnel dimensions range from a few to perhaps 100 meters in cross section.(97) Crude oil storage cavities constructed in salt domes have diameters of more than 70 meters and heights of more than 200 meters. If future solution mining were carried out at a repository site, canisters located in the dissolution zone could collect near the bottom of the cavity, possibly generating more concentrated heat and radiation. These effects would depend largely upon canister size, spacing, original source term, and age.

Solution mining has not been analyzed as a separate failure element because the exploratory drilling and testing usually performed before mining facilities are installed are likely to detect a repository. Furthermore, since salt is such a common mineral, the likelihood of this activity at a repository site appears to be extremely low.

D-4.2.3 Interference with Hydrologic Conditions

Recovery or injection of fluids in the rocks bounding the repository can alter hydraulic conditions, possibly changing flow characteristics and apparent rock strength. The risk to a repository from interference with groundwater is distinct from direct drilling risks.

Active control of hydraulic conditions is practiced in both water and petroleum production. This technique is used to increase secondary recovery of oil, for example, where water or brine is injected into a production zone through a nonproductive well. The water, under pressure, displaces the petroleum and forces it toward production wells, as illustrated by Figure D-23. In a similar manner, recharge wells in arid regions provide conduits for surface water to replenish depleted aquifers.

Changes in the hydraulic regime in aquifers bounding a repository are not, strictly speaking, failure elements, but they do affect modeling parameters. The degree to which changes could occur depends upon several indeterminate factors such as amount and pressure of fluid injected or discharged and the duration of interference. In general, pumping of aquifers adjacent to a repository would have only a local effect, perhaps to a range of hundreds of meters. The effect would be to change flow rates and direction for a brief period compared with the total life of the repository. Since wells affecting a repository would have to be very near or directly over the site, their probability of occurrence has already been considered in Section D-4.1, and the additional risk from changes in flow rates is insignificant.

Variations in rock strength due to water content are difficult to quantify. To produce meaningful estimates, such factors as pore water pressure and contact area between rock particles must be known. A repository would be essentially unaffected, however, by strength variations in the rock of the overlying aquifer. Lowering the strength of the aquifer would, at worst, increase fracturing in this rock. Fractures would increase the permeability of the aquifer somewhat, but would not lead directly to water flow to or from the repository. Changing rock strength and volume in the underlying aquifer by pumping would be preceded by drilling through the repository level, a failure which has already been examined. Nevertheless, the potential for inducing fractures between the repository and the underlying aquifer may exist for a given site and should be considered in the site selection process.

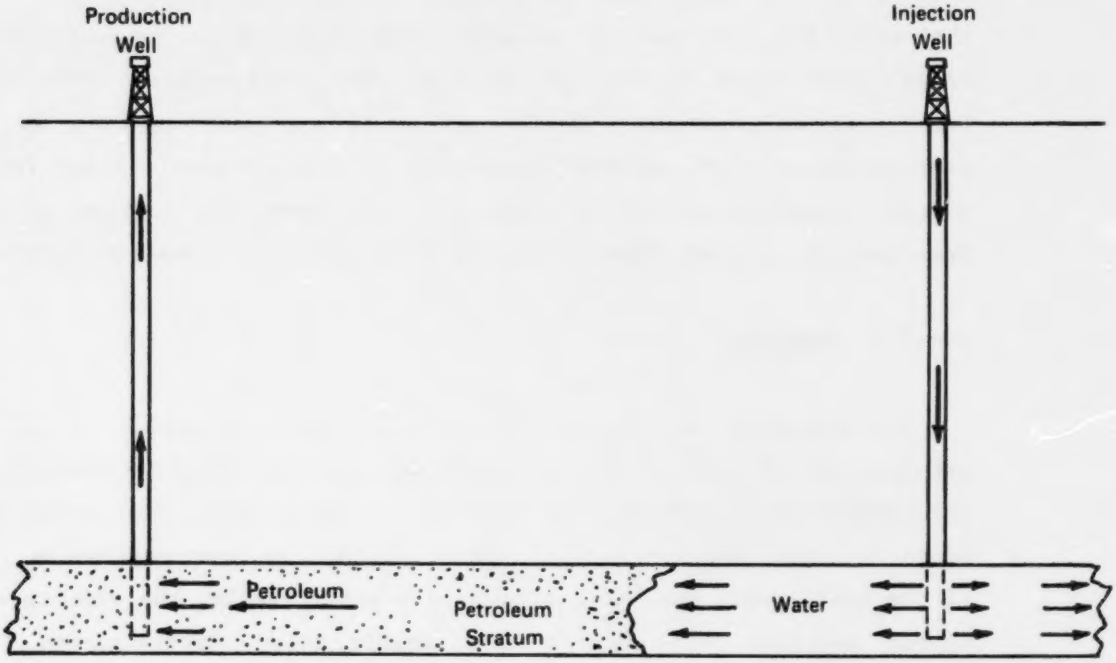

FIGURE D-23 FLUID INJECTION FOR ENHANCED WELL PRODUCTION

D-4.2.4 Waste Recovery

It is possible that radioactive waste may be considered a valuable resource sometime in the future, especially if the waste includes unreprocessed spent reactor fuel. Therefore, the possibility that the waste may be sought for some useful purpose in the future deserves consideration.

Since authorized reentry of the repository for recovery implies both consent of the responsible government and substantial understanding of the situation, it can be assumed that appropriate precautions and technologies would be employed in this case. This suggests that future sanctioned entry would provide safeguards at least as good as, and perhaps better than, existing ones. In any case, responsibility for any adverse consequences would seem to rest with the future society. Unauthorized recovery operations are discussed in the next paragraph.

D-4.2.5 Sabotage

The potential for buried waste to be used as toxins or for the construction of nuclear explosives raises the question of a repository's susceptibility to sabotage or unauthorized intrusion. The waste forms would preclude any convenient conversion into nuclear explosives, and if the wastes were used to contaminate a water supply, the effects would become apparent only after a considerable delay. Nevertheless, it is possible that the waste might be perceived as a resource by terrorists. However, reaching a repository would require unusual resources and expertise. Sinking a mine shaft would involve many people, much specialized equipment, supplies, energy, planning, engineering and operating skills, and uninterrupted access to the site for periods of months. If the repository were finally breached, removing, processing, and using the stolen waste would involve planning and engineering on a similar scale. Also, unless the people involved possessed exceptional skills, they would be placing themselves at great personal risk from the waste they would be attempting to recover. Therefore, unauthorized recovery of waste material does not appear to be a credible scenario.

If the intent were simply to pollute a water supply with the waste, the saboteurs would still need substantial drilling equipment, specialized workers, free access to the site, and a great deal of patience, since the effects of their act would not be apparent for years, if at all. Sabotage of visible and accessible objectives, such as a chemical plant or a surface nuclear facility, would be more likely. Less time, material, skill, and organization, with far less risk to the saboteurs, would be required to obtain substances with the equivalent potential for terrorism.

D-4.2.6 Acts of War

Similar to the question of sabotage is the question of damage to the repository through some act of war. The only credible act that could even fracture the rock down to about 500 meters would be the detonation of at least a ten-megaton or larger nuclear device.(98) During a war, it is hardly likely that bombs would be aimed at a repository. Cities and strategic installations are far more attractive targets. In addition, the effects on the biosphere from a damaged repository would be insignificant compared with the other damage inflicted in such a conflict.

D-4.2.7 Innocent Extraordinary Penetration

No buried repository of the sort considered in this study has (to present society's knowledge) ever existed. However, a similarity can be drawn between a repository and other hidden artifacts. The possibility remains that curiosity or other motivation could encourage future penetration or exploration of a repository.

For example, archeologists have excavated under pyramids and other traces of human activity; tunnels for transportation are common in mountainous terrain, and subway tunnels underlie many cities. The possibility of treasure is also a strong motivation. The classic example is the recurring effort to discover whatever may be at the bottom of a shaft originally dug two or more centuries ago on Oak Island, Nova Scotia.(99) While nothing of great value has ever been recovered, persistent attempts during the last century to reopen the mysterious shaft have reached depths of 100 meters or more.

While a repository is not the equivalent of a treasure trove, future generations may have no knowledge of its function and may be intrigued by signs of mining and the unusual care with which the openings are sealed. There is no firm basis for determining if a repository will become an attractive site for explorers in the future. However, if it were to be entered by an astute investigator, its function and the nature of the canisters should become apparent. It is more than likely that steps would then be taken to return the repository to its original integrity.

D-5.0 NATURAL EVENT FAILURE ELEMENTS

A number of natural events and processes are modeled in this chapter, with additional ones being discussed in lesser detail. Most of these are geologic phenomena, although some are not, such as changes in climate or the impact of large meteorites. In all cases the models are simple and only intended to enable very approximate quantitative judgments. For the evaluation of repositories at specific sites, it is possible that quite different models, based on extensive data gathering, might be appropriate. Nevertheless, for the evaluation of the performance of generic repositories, it is believed that the models developed here are adequate.

D-5.1 FAULT MOVEMENT

D-5.1.1 Summary

The repository site selection process is expected to favor sites that are relatively stable geologically and where renewed or new faulting is unlikely.(70) Nevertheless, old faults are common geologic structures in almost any location and may be expected at or near any repository site. They may only intersect strata above or below the repository formation, and some may even go undetected through the entire site evaluation process. This analysis assumes the presence of a certain number of faults on the site and, on the basis of their age and density, estimates:

- the probability of renewed movement along the old faults,
- the probability of the occurrence of new faults.

The model consists of a constant annual rate based on the age of the most recent fault activity. In addition, physical parameters that characterize the groundwater flow pathway along the fault are estimated. Releases from the repository are assumed to be by groundwater flow to the upper aquifer. Sufficient displacement to move the entire repository into contact with the aquifer or to the surface is not considered possible in the time frame considered in this report (10,000 years). A summary of the analysis is given in Table D-87. Section

TABLE D-87
SUMMARY OF FAULT MOVEMENT FAILURE ELEMENT

MEDIUM	PROBABILISTIC (P) DETERMINISTIC (D)	NATURE OF MODEL	RELEASE MODE	DRIVING FORCE	SOURCE TERM	PARAMETERS		FLUID FLOW RATES FROM REPOSITORY TO UPPER AQUIFER				COMMENTS
						1st ESTIMATE	2nd ESTIMATE	1st ESTIMATE		2nd ESTIMATE		
								t (yrs)	$\dot{Q}$ (t) (m^3/yr)	t (yrs)	$\dot{Q}$ (t) (m^3/yr)	
Bedded Salt	P	Annual probability of occurrence of new fault or movement along old fault.	Groundwater	Thermally induced convection effect added to gradient from aquifer interconnection.	Canisters in fault zone broken and subject to leaching. Accumulated dissolved radionuclides by time of faulting assumed released through fault from 100-m wide zone around fault.	$\lambda = 2 \times 10^{-8}$ events/yr Flow path 1 m wide 4000 m long $K = 10^{-4}$ cm/sec $\eta = 0.1$ 100 canisters in fault zone. 5% repository in affected surrounding zone.	$\lambda = 4 \times 10^{-7}$ events/yr Flow path 1 m wide 4000 m long $K = 10^{-4}$ cm/sec $\eta = 0.1$ 100 canisters in fault zone. 5% repository in affected surrounding zone.	100 1000 10,000	8.2×10^4 6.9×10^4 2.5×10^4	100 1000 10,000	3.9×10^5 3.8×10^5 3.3×10^5	Fault may seal if flow rate is sufficiently small. Flow may be restricted by availability of water.
Granite	P	Annual probability of occurrence of new fault or movement along old fault.	Groundwater	Thermally induced convection.	Canisters in fault zone broken and subject to leaching. Accumulated dissolved radionuclides by time of faulting assumed released through fault from 100-m wide zone around fault.	$\lambda = 2 \times 10^{-8}$ events/yr Flow path 1 m wide 4000 m long $K = 10^{-2}$ cm/sec $\eta = 0.1$ 100 canisters in fault zone. 5% repository in affected surrounding zone.	$\lambda = 10^{-5}$ events/yr Flow path 1 m wide 4000 m long $K = 10^{-2}$ cm/sec $\eta = 0.1$ 100 canisters in fault zone. 5% repository in affected surrounding zone.	100 1000 10,000	6.9×10^6 4.4×10^6 1.9×10^6	100 1000 10,000	6.9×10^6 4.4×10^6 1.9×10^6	Flow may be restricted by availability of water.
Basalt	P	Annual probability of occurrence of new fault or movement along old fault.	Groundwater	Thermally induced convection effect added to gradient from aquifer interconnection.	Canisters in fault zone broken and subject to leaching. Accumulated dissolved radionuclides by time of faulting assumed released through fault from 100-m wide zone around fault.	$\lambda = 5 \times 10^{-7}$ events/yr Flow path 1 m wide 4000 m long $K = 10^{-2}$ cm/sec $\eta = 0.1$ 100 canisters in fault zone. 5% repository in affected surrounding zone.	$\lambda = 10^{-5}$ events/yr Flow path 1 m wide 4000 m long $K = 10^{-2}$ cm/sec $\eta = 0.1$ 100 canisters in fault zone. 5% repository in affected surrounding zone.	100 1000 10,000	8.8×10^6 7.6×10^6 3.2×10^6	100 1000 10,000	4.0×10^7 3.8×10^7 3.4×10^7	Flow may be restricted by availability of water.
Shale	P	Annual probability of occurrence of new fault or movement along old fault.	Groundwater	Thermally induced convection effect added to gradient from aquifer interconnection.	Canisters in fault zone broken and subject to leaching. Accumulated dissolved radionuclides by time of faulting assumed released through fault from 100-m wide zone around fault.	$\lambda = 2 \times 10^{-8}$ events/yr Flow path 1 m wide 4000 m long $K = 10^{-4}$ cm/sec $\eta = 0.1$ 100 canisters in fault zone. 5% repository in affected surrounding zone.	$\lambda = 4 \times 10^{-7}$ events/yr Flow path 1 m wide 4000 m long $K = 10^{-4}$ cm/sec $\eta = 0.1$ 100 canisters in fault zone. 5% repository in affected surrounding zone.	100 1000 10,000	8.8×10^4 7.6×10^4 3.2×10^4	100 1000 10,000	4.0×10^5 3.8×10^5 3.4×10^5	Flow may be restricted by availability of water.
Dome Salt	P	Annual probability of occurrence of new fault or movement along old fault.	Groundwater	Thermally induced convection effect added to gradient from aquifer interconnection.	Canisters in fault zone broken and subject to leaching. Accumulated dissolved radionuclides by time of faulting assumed released through fault from 100-m wide zone around fault.	$\lambda = 3 \times 10^{-7}$ events/yr Flow path 1 m wide 4000 m long $K = 10^{-4}$ cm/sec $\eta = 0.1$ 100 canisters in fault zone. 5% repository in affected surrounding zone.	$\lambda = 10^{-6}$ events/yr Flow path 1 m wide 4000 m long $K = 10^{-4}$ cm/sec $\eta = 0.1$ 100 canisters in fault zone. 5% repository in affected surrounding zone.	1100 1000 10,000	8.2×10^4 6.0×10^4 2.5×10^4	100 1000 10,000	2.0×10^5 1.7×10^5 1.5×10^5	Fault may seal if flow rate is sufficiently small. Flow may be restricted by availability of water.

D-5.1.2 provides a brief review of background material on the occurrence and detection of faults. Detailed explanations of the model parameters are given in Sections D-5.1.3 and D-5.1.4.

D-5.1.2 Background

Definition and examples. A fault is a fracture within the rocks of the earth's crust along which relative movement of the two sides has taken place. Faults can range in length from less than a centimeter to hundreds of kilometers.(60) Very small faults, on the order of tens of meters or less in length, are not important for the present analysis. In depth, faults may intersect only a single geologic formation or part thereof, or they may extend all the way from the surface to deep in the basement rocks. Cumulative displacement along faults, whether in the horizontal or vertical direction, can range up to tens of kilometers or more, representing the sum of relatively small individual movements over an extended period. Notable examples of large faults in the United States include the San Andreas fault, whose length exceeds 600 km, and the Lewis overthrust fault, representing the east side of the Rocky Mountains in Montana, with a cumulative vertical displacement of more than 12 km.(58,60) Often, a large fault is associated with a multitude of smaller fractures, and both large and small faults may occur as a series of subparallel features reflecting a distinct trend.(100) (See Figure D-24.) Faults are very common features in most geologic settings and it is unlikely that any repository site can be found that will be completely free from past faulting activity. For example, a detailed geologic study of the area surrounding the proposed Charlestown nuclear power plant in Rhode Island led to the identification of one major fault and over 2600 minor faults and joints within five miles.(101) Additional faults are generally expected to be encountered on plant sites once the overburden is removed.(22,102,103) The important issue is whether additional movement along faults on (or under) the site can be expected and whether new faults might also develop.

Nature and types of faults. Faults are the result of differential compressive stresses in the crust that exceed the strength of the rock formation. The geometry of faults can be categorized into three types,

(A) Nevada (Basin and Range Province)

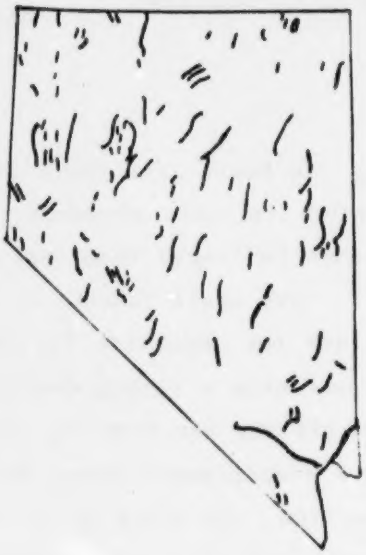

(B) Gulf Coast Region

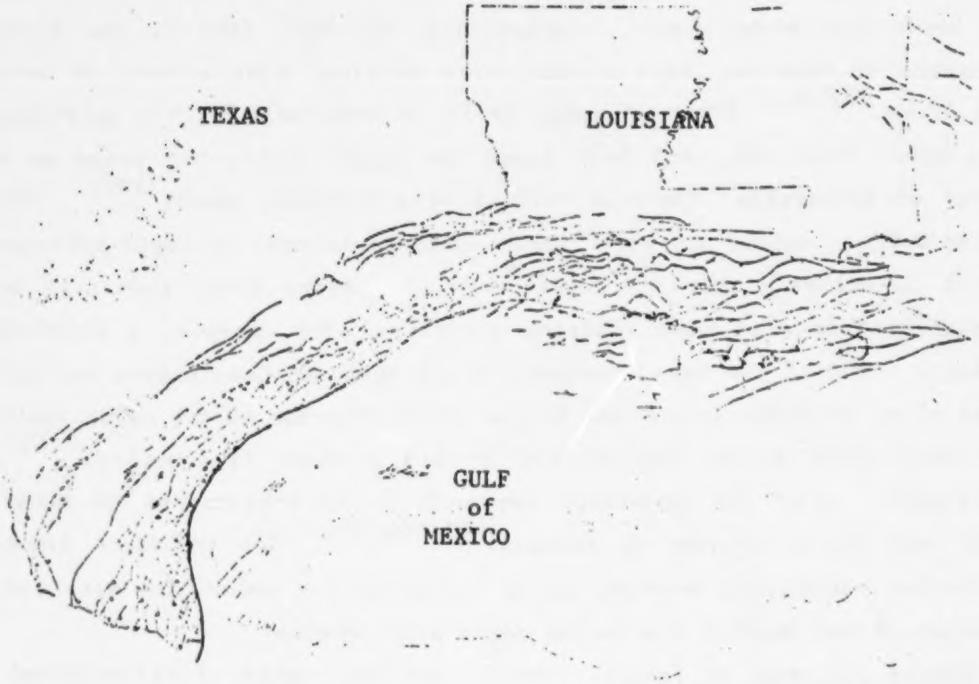

Source: Adapted from USGS Map M.F. 916.

FIGURE D–24 SUBPARALLEL FAULTING IN TERTIARY AND QUATERNARY PERIODS reflecting the stress system giving rise to the fracturing. (See Figure D-25). Normal faults occur when the maximum compressive stress, σ_1, is vertical and the minimum compressive stress, σ_3, is horizontal. Reverse and thrust faults (the former steeper than 45°, from the horizontal, the latter flatter than 45° occur when the maximum compressive stress is horizontal and the minimum vertical. Strike-slip faults occur when the maximum and minimum compressive stresses are both horizontal. Oblique faults represent a combination of vertical and horizontal movement.

Evolution of regional stress systems. Many geologic processes can contribute to the development of stress systems that may cause faulting. Examples of these processes, some of which are related, are the following:

- Plate tectonics, involving the movement of crustal sections, called plates, toward or away from each other.
- Slowing of the earth's rotation, with corresponding changes in centrifugal forces.
- Earth tides, resulting from gravitational interaction with the sun and moon.
- Changes in heat flow and temperature in the earth's crust.
- Increases in overburden stress, caused by sediment deposition, lava flows, glaciers, rises in sea level, etc.
- Decreases in overburden stress, caused by erosion, glacial melting, retreat of seas, etc.
- Volcanic activity, involving movement of magma through the crust.
- Diapirism, involving the penetration of plastically flowing rock (such as salt or shale) through overlying rock.
- Dissolution, leading to settling or collapse into the resulting voids.
- Folding and downwarping associated with the movement of the crust toward mechanical equilibrium after some of the processes mentioned above may have caused differential stresses.

The above list is only intended to give some representation of the range of processes with which faulting may be associated. Two important conclusions can be drawn. First, because at a given location many of the processes listed occur only during specific periods in geologic history, if at all, many (probably most) faults have exhibited movement

(a) Normal (Gravity) Fault

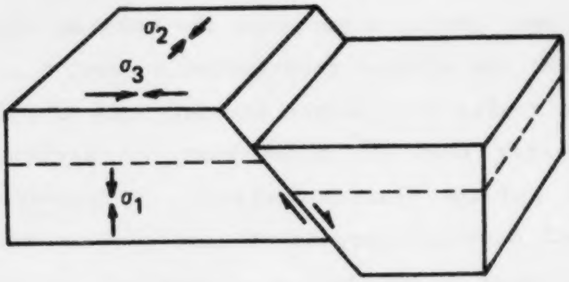

(b) Reverse or Thrust Fault

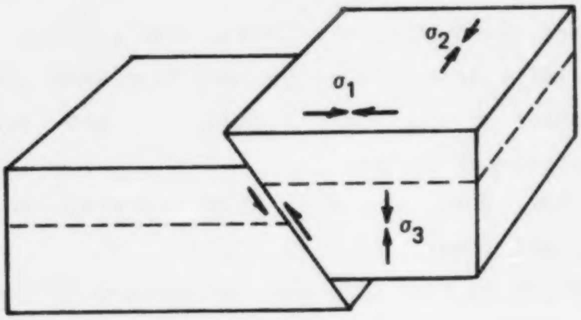

(c) Strike-Slip Fault

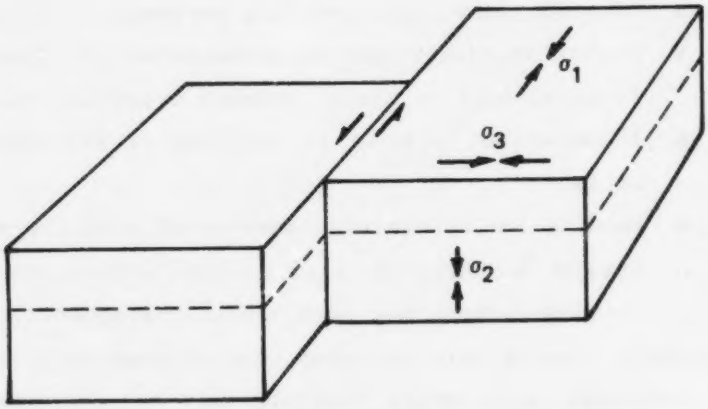

Note: (σ_1 = maximum stress, σ_2 = intermediate stress, σ_3 = minimum stress)

FIGURE D–25 BASIC FAULT TYPES

only during particular periods and have not been reactivated during later periods with different stress regimes.(60) Second, an analysis of the geologic evolution of a region and the corresponding regional stress patterns is important in predicting future faulting or fault movement. It should be pointed out, nevertheless, that faults do represent a zone of weakness, and therefore reactivation is occasionally experienced and even reverse movement has been noted.(104)

Movement along faults. Movement along existing faults depends on a number of factors besides the relative levels of stress. Among these are the lithology, the fluid pressures within the fault, and the nature and quantity of material, such as rock dust, that may fill the fault. Movement may take the form of a continual slippage (creep) or recurring abrupt jerks (stick-slip).(60,104) Creep may pass unnoticed unless detected by measuring cumulative displacement, whereas stick-slip movements are often accompanied by sensible seismicity. Depending upon types of faults, lithology, confining pressure, temperature, rate of movement, and other factors, the rock bounding a fault may be fractured, polished (slickensides), folded (drag folds), or essentially unchanged. These features are represented in Figure D-26. The rate of displacement over time can vary considerably. The San Andreas fault has shown occasional displacement of up to five centimeters per year although maximum rates of one or two centimeters per year are probably more common.

Ages of faults. Two ages that are important in studying a fault are the time when the fault began and the time of its most recent movement. In many cases, these may be estimated on the basis of stratigraphy, as sketched in Figure D-27. Since the fault shown there does not intersect bed C, it must have begun sometime since the deposition of that bed. On the other hand, since it does not intersect bed A, it is highly unlikely that it has moved more recently than the period when A was deposited. (In rare circumstances it could have moved below A without actually moving A, although generally some manifestation of such movement, e.g., deformation, would be found in A.) Faults may also be dated by associating them with a specific geologic process whose age is otherwise well determined. For example, the salt domes of the Gulf region caused extensive faulting and fracturing as they pushed through the overlying

(a) Drag Folds

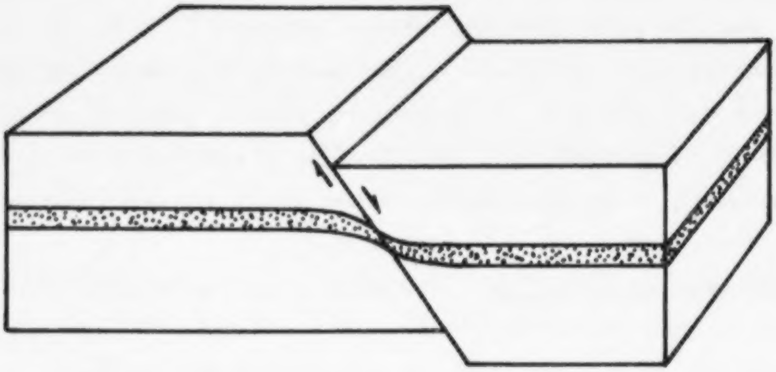

(b) Gouge, Breccia, Slickensides, and Subsidary Faults

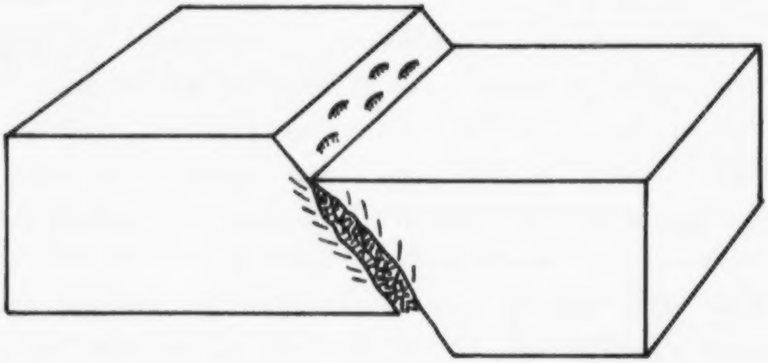

(c) Parallel Shear Zone

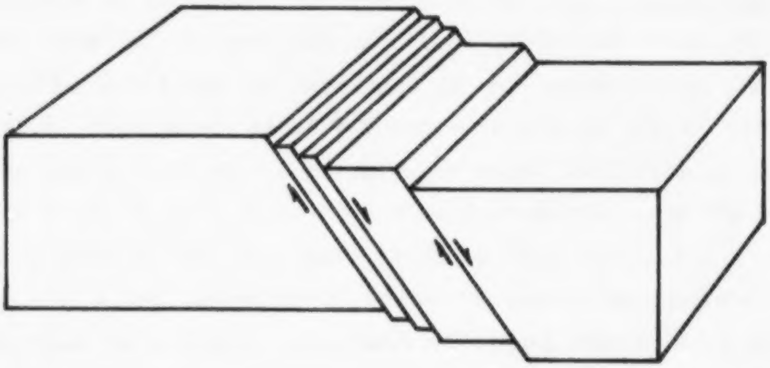

FIGURE D–26 FEATURES ASSOCIATED WITH FAULTING

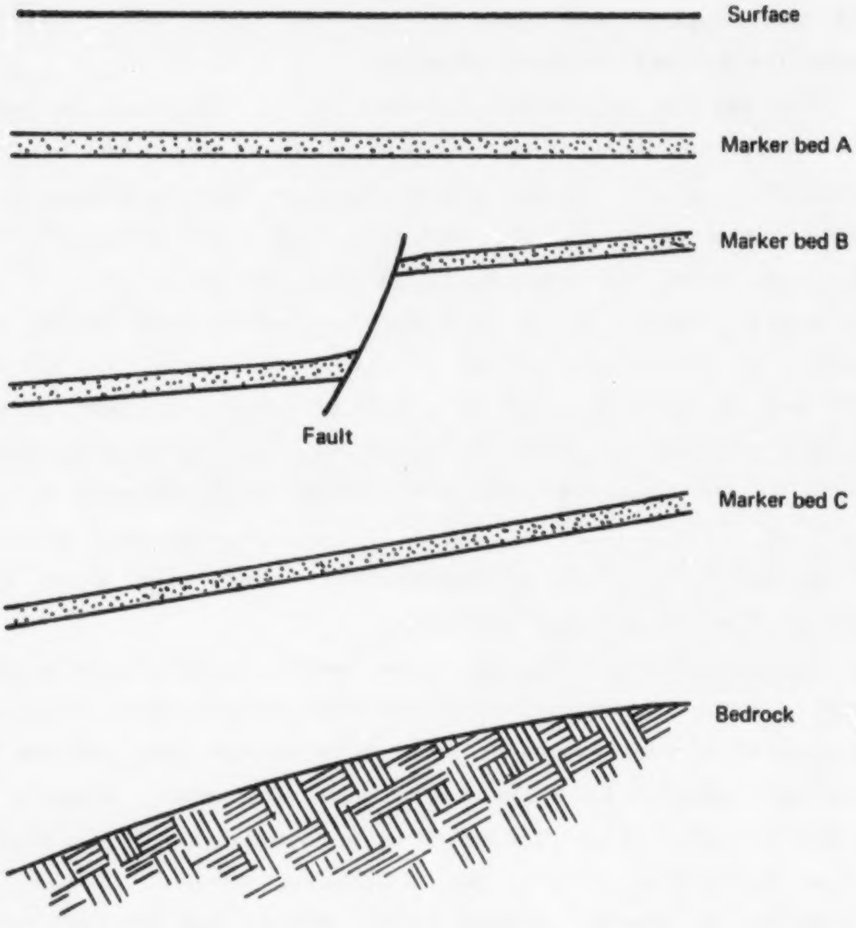

FIGURE D–27 DATING OF NON-TECTONIC FAULT BY BED DISPLACEMENTS rock. (See Figure D-28.) Similarly, both the development and the upper surface dissolution of the salt anticlines in the Paradox Basin have caused most of the faulting that has been observed there. (See Figure D-29.) Other faults in the Gulf region were caused by slippage and settling of new sediments as the shoreline migrated southward. Thus, these faults parallel the shoreline and decrease in age as one moves southward. (See Figure D-30.) There are also radiochemical, magnetic, and mineralogical techniques for studying faults with a view to learning about the history of their movement.

The age and nature of the most recent movement are generally the most important data in determining whether additional movement can be expected. Active faults are those that have experienced relatively recent movement by geologic standards (with the period of 10,000 years often chosen as the criterion) and that may be expected to show future movements. Young faults include those whose most recent movement is within the Quaternary Period (extending back about 1.8 million years). The dating of faults and the determination of their capability for further movement are difficult problems with significant uncertainties. There is no universal agreement among earth scientists on criteria defining a fault that is capable of further movement; moreover, paucity of geologic data leaves considerable uncertainty about the age and extent of previous fault movement.

Identification of faults. Some faults, particularly young ones, are easy to recognize by surface observation because their displacements are manifested in escarpments or other offsets that have neither been eroded away nor covered by later sedimentary deposits. Because faults may either be particularly permeable or act as a barrier to groundwater flow along permeable strata (by offsetting them), changes in surface vegetation in linear patterns often indicate the possible presence of a fault. These and other linear features (lineaments) visible on aerial photographs are frequently used to detect faults. Surface geodetic surveys may indicate changes over time that imply ground movement, possibly along faults. The angles and depths of marker beds as observed at outcrops or in a series of boreholes may also indicate whether some offset has taken place. Trenches can be dug across areas of interest

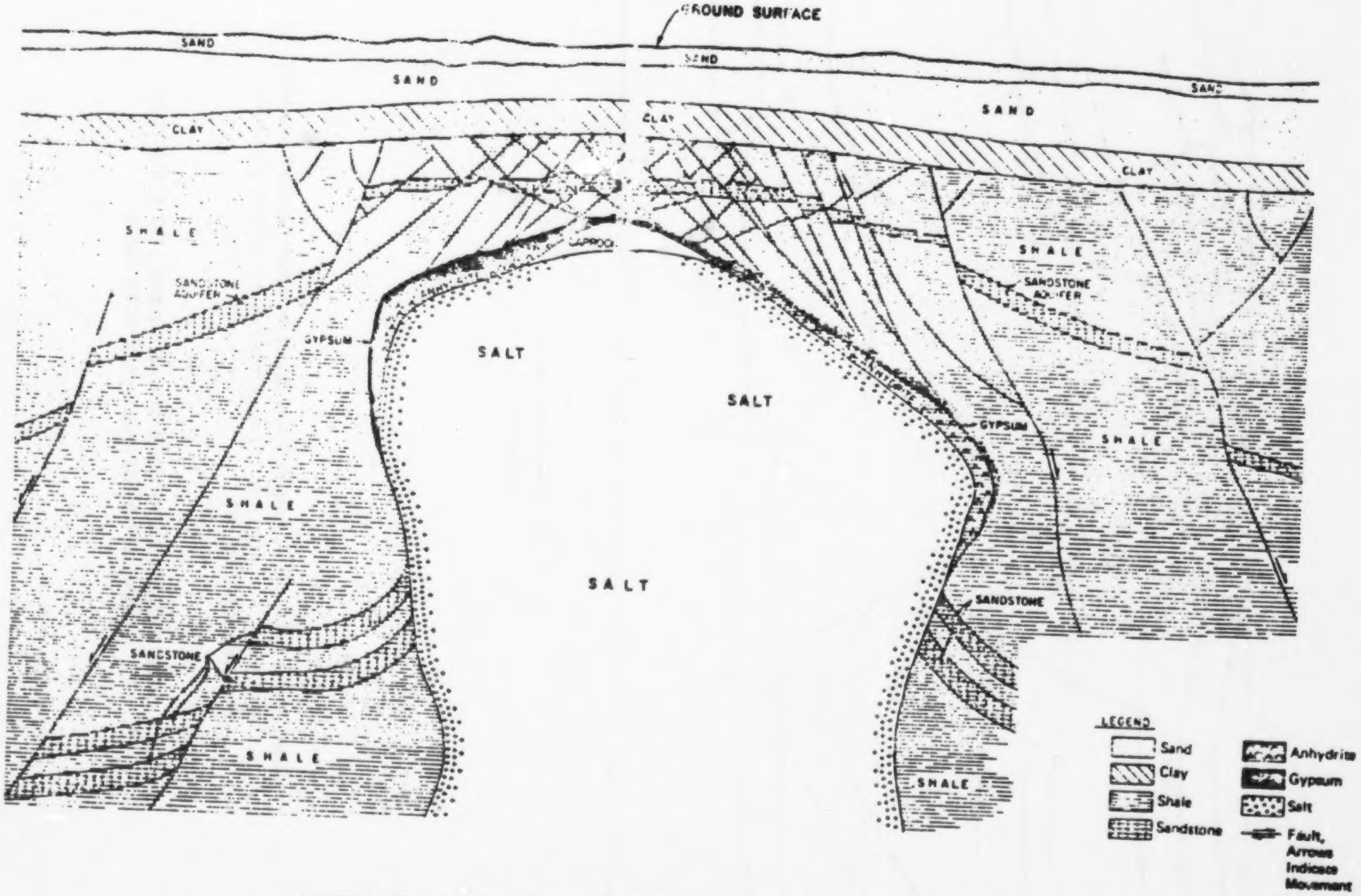

FIGURE D–28 FAULTING IN THE VICINITY OF A SALT DOME (Conceptual Drawing)

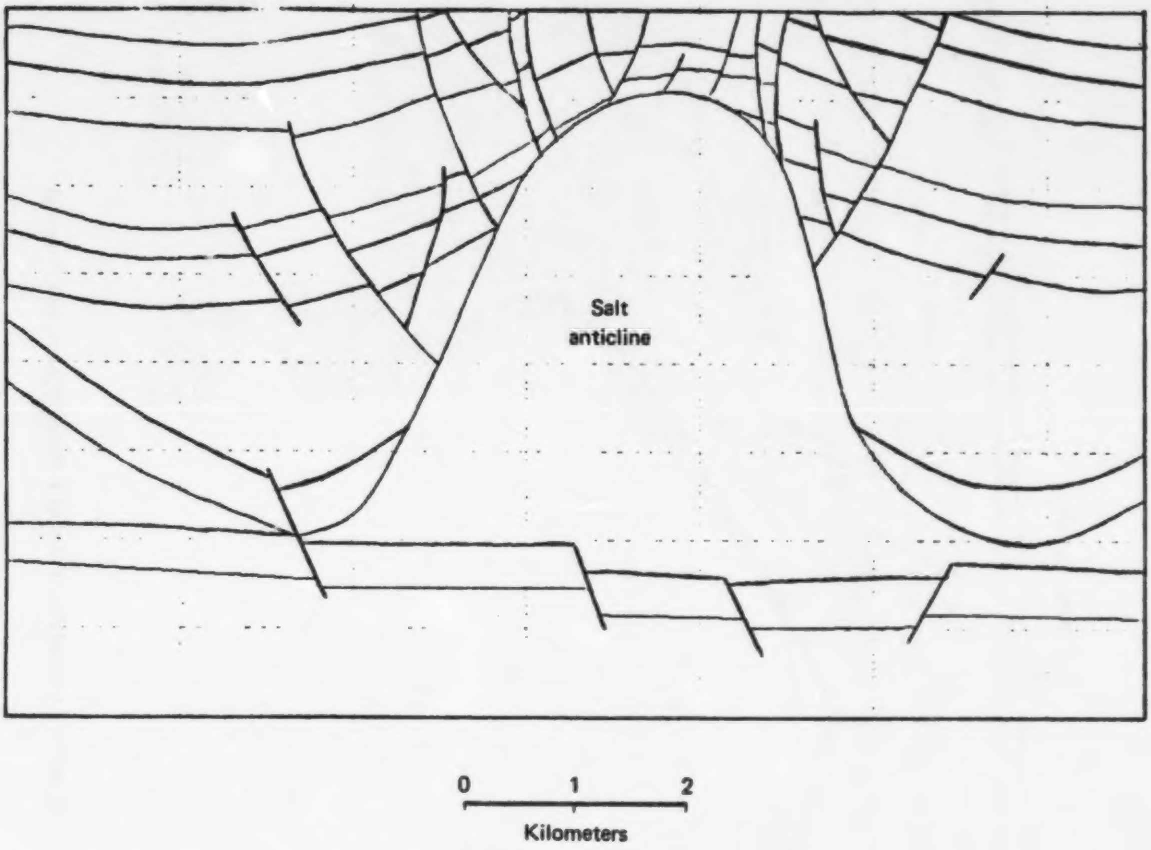

Source: Stockton,S.L. and A.H. Balch. The Utility of Petroleum Seismic Exploration Data in Delineating Structural Features Within Salt Anticlines. USGS Open File Report 78–591, 1978.

FIGURE D–29 TYPICAL PARADOX BASIN SALT ANTICLINE STRUCTURE DERIVED FROM SEISMIC AND OTHER DATA

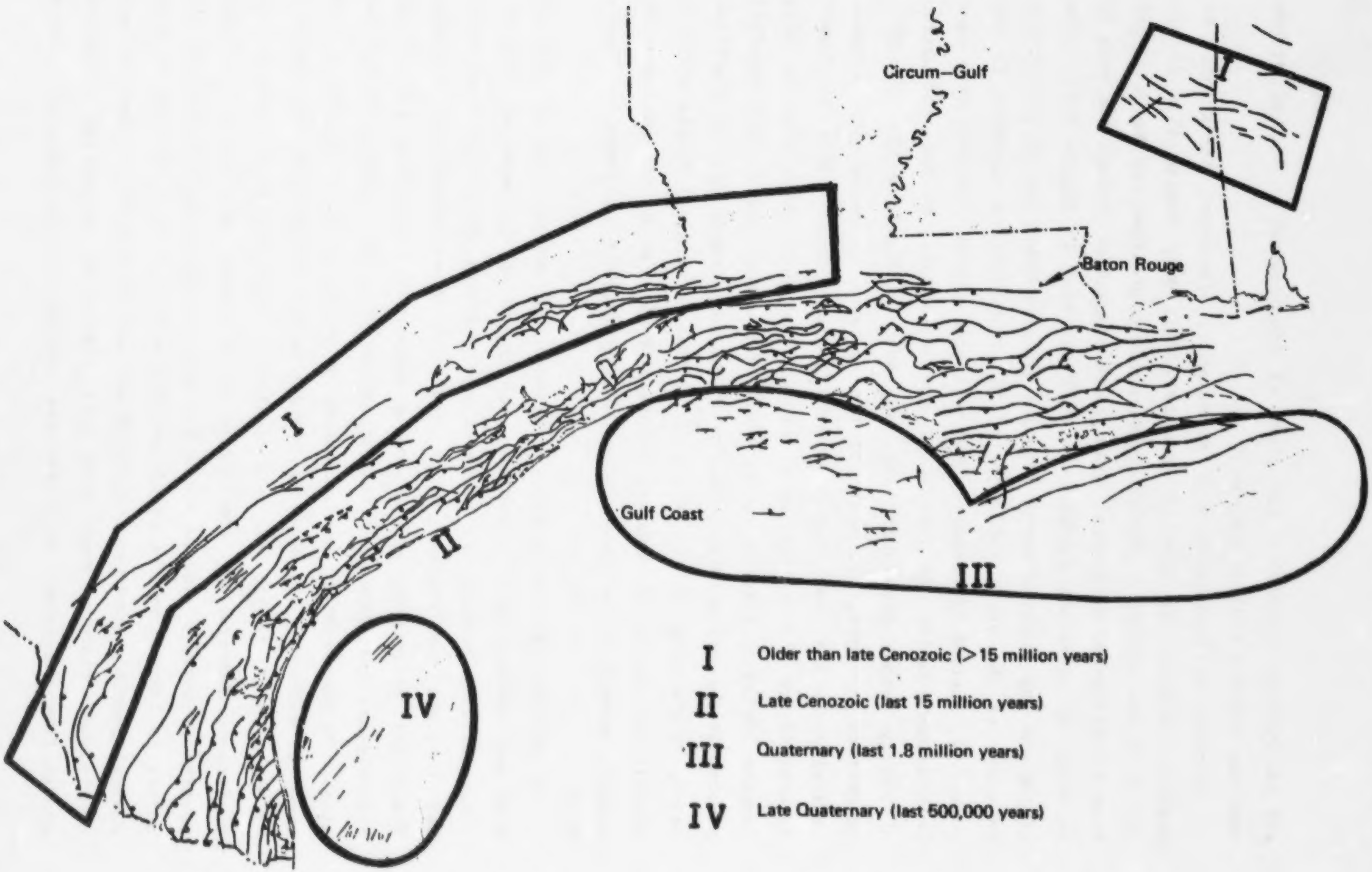
Circum–Gulf
I
Baton Rouge
I
II
Gulf Coast
III
IV
I Older than late Cenozoic (>15 million years)
II Late Cenozoic (last 15 million years)
III Quaternary (last 1.8 million years)
IV Late Quaternary (last 500,000 years)

Source: Adapted from USGS Map M.F. 916.

FIGURE D–30 AGE OF FAULTS IN THE GULF COASTAL REGION and be examined carefully for signs of displacement. Natural stream cuts may serve a similar purpose.

Geophysical techniques such as seismic, electrical resistance, or magnetic surveys can also be used to detect deep faults that do not appear at the surface. For example, seismic profiles can be developed from recordings of mechanical shock waves propagated through the rock to an array of receivers (geophones) as diagrammed in Figure D-31. The timing and amplitude of waves reaching the geophones can be interpreted in terms of the depth and orientation of reflective surfaces in the rock. If, instead of measuring the reflected signal, the refracted wave is examined, faults may also be identified, usually by the attenuation of energy across the fault face, as shown in Figure D-32. Whatever techniques are used, the scale of the features to be detected depends basically on the wave length of the seismic wave. This is itself determined by the energy loss through the rock, with shorter wave lengths having a greater energy loss than longer ones. The possible resolution is approximately one-half the wavelength or, in practical terms, in the range of ten meters.(22) Thus, a vertical displacement of roughly ten meters is required before a fault can be distinguished by seismic surveys. An interpreted seismic profile is shown in Figure D-33.

Electrical resistance surveys measure the conductivity of rock or soil and compare the measurements with models of the expected results. Irregularities between the measured and expected electrical resistance may indicate the presence of a fault or other structural feature. Electrical resistance mapping of a potential repository site would probably use measurements taken through an array of boreholes across the site. By determining the resistance of representative strata or rock types at differing orientations, detecting and determining the position of structural faults is made easier. Unfortunately, electrical resistance surveys are complicated by a number of factors. Since resistance surveys measure deviation from a model, the accuracy of the survey is limited by the precision of the model. Results tend to have several possible interpretations and are usually simplifications of real conditions. Features must also have electrical properties different enough from the intact rock that the contrast can be measured. Large

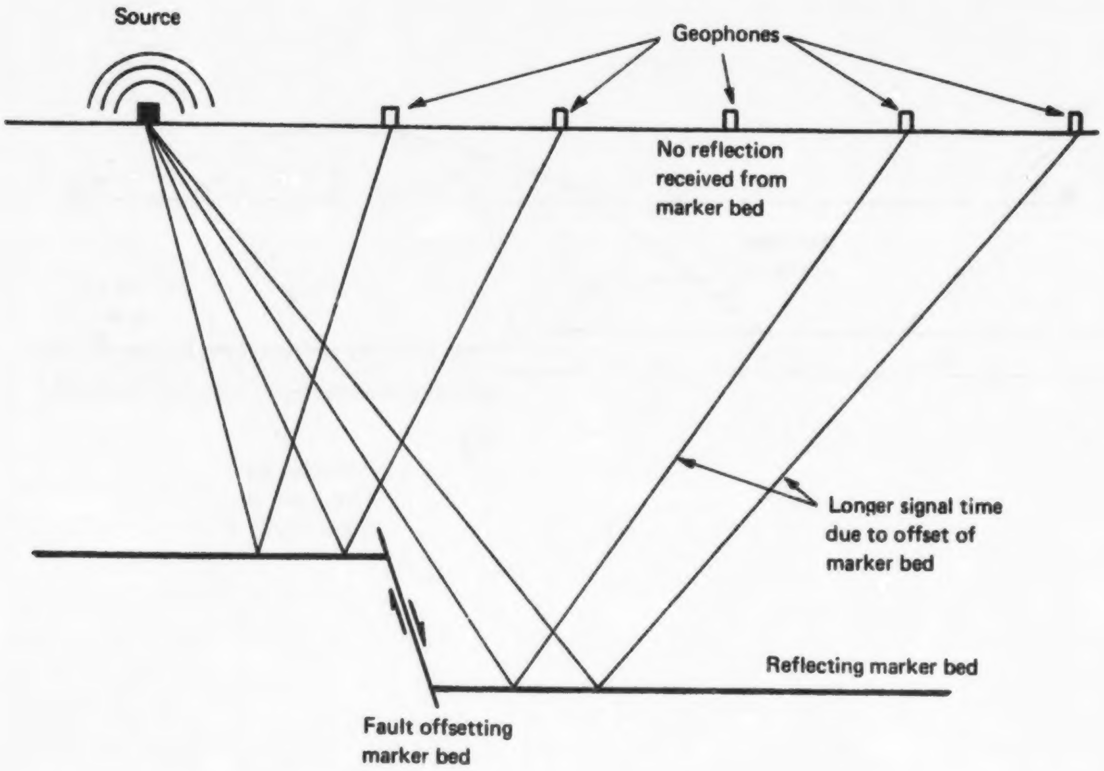
Source
Geophones
No reflection received from marker bed
Longer signal time due to offset of marker bed
Reflecting marker bed
Fault offsetting marker bed

FIGURE D–31 DETECTION OF FEATURES BY SEISMIC REFLECTION

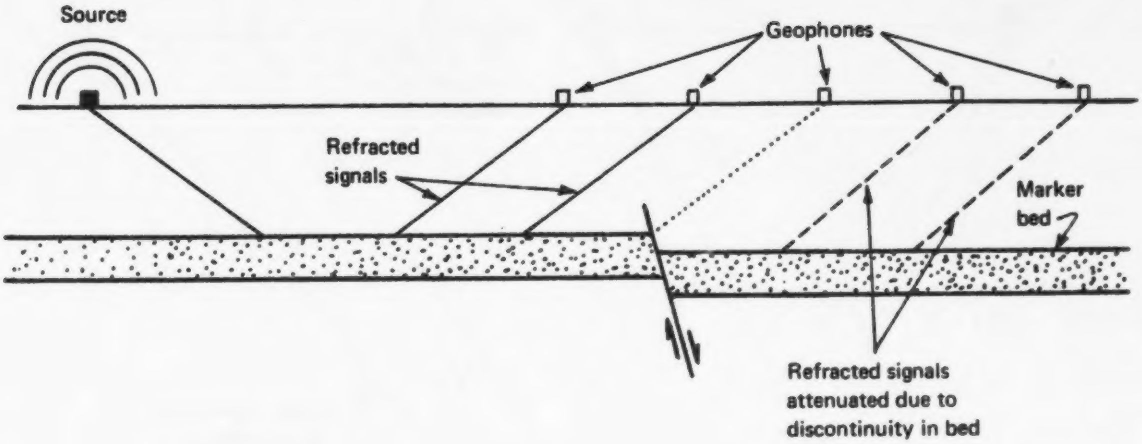

FIGURE D–32 DETECTION OF FAULT BY ATTENUATION OF REFRACTED SIGNALS ACROSS DISCONTINUITY

(a) **Uninterpreted**

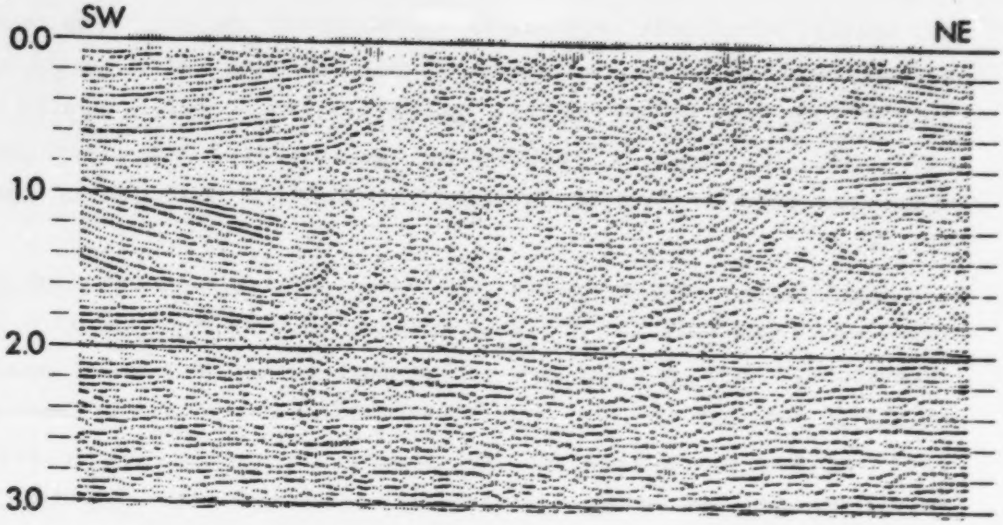

(b) **Interpreted to Show Structure**

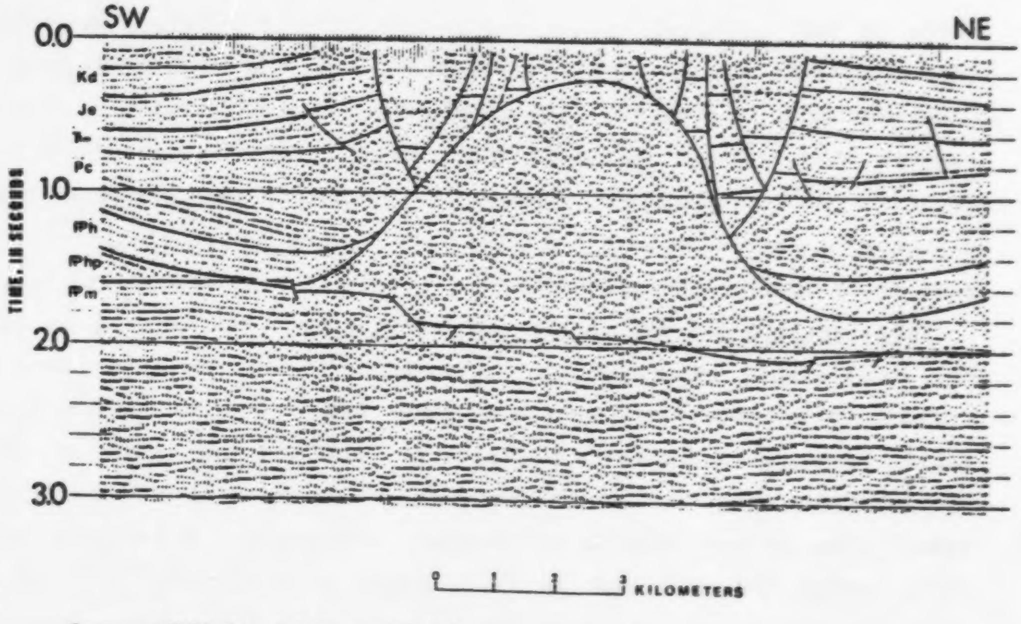

Source: USGS Open File Report 78-591.

FIGURE D–33 PROCESSED SEISMIC RECORD OF SECTION OF PARADOX BASIN shallow features generally show more contrast than small or deep features, and normal variation in the rock's electrical resistance may obscure the electrical vibration caused by a fault.(22)

Lastly, since most earthquakes are generally thought to be caused by movements along faults, a record of the seismicity of a region can be helpful in understanding the potential for active faults. In particular, the foci of earthquakes tend to lie along linear trends, which can then be studied further for the identification of specific faults.

New faults. While faults are among the most common structural features in geology, few (if any) new faults have been reported in the literature. Most apparent new faults have turned out to be extensions of old or unmapped faults. Nonetheless, locations with a propensity for faulting may be suggested by identifying other characteristics indicative of the stress differential necessary for faulting. For example, in-situ stress measurements can be made to determine the direction and intensity of lithic stress at a particular location. If the stresses approach the fracture strength of rock, or if stresses increase in time, faulting is possible.(105) Alternatively, folding, which is indicative of stress change (see Figure D-34), also suggests that faulting, particularly parallel to the fold axis, is possible. Other geologic indicators, such as block tilting or warping of a basin, suggest that stress intensification may be occurring. Conversely, locations showing little tectonism in the recent geologic past may be expected to have a reduced likelihood of future faulting because of the time delay involved before sufficient stress for faulting could build.

Availability and reliability of information. The mapping of faults has considerable importance. For example, faults may form traps that contain petroleum, or they may pose safety risks to industrial facilities such as nuclear power plants. The U.S. Geological Survey has published geologic maps of all portions of the country and continues to update them as new information becomes available. A national map of young faults was published in 1978, based on 1975 data.(100) As this reference points out, the availability of data is very uneven across the country. For example, far fewer recent searches for young faults have been made in the mid-continent than in California. Even where extensive

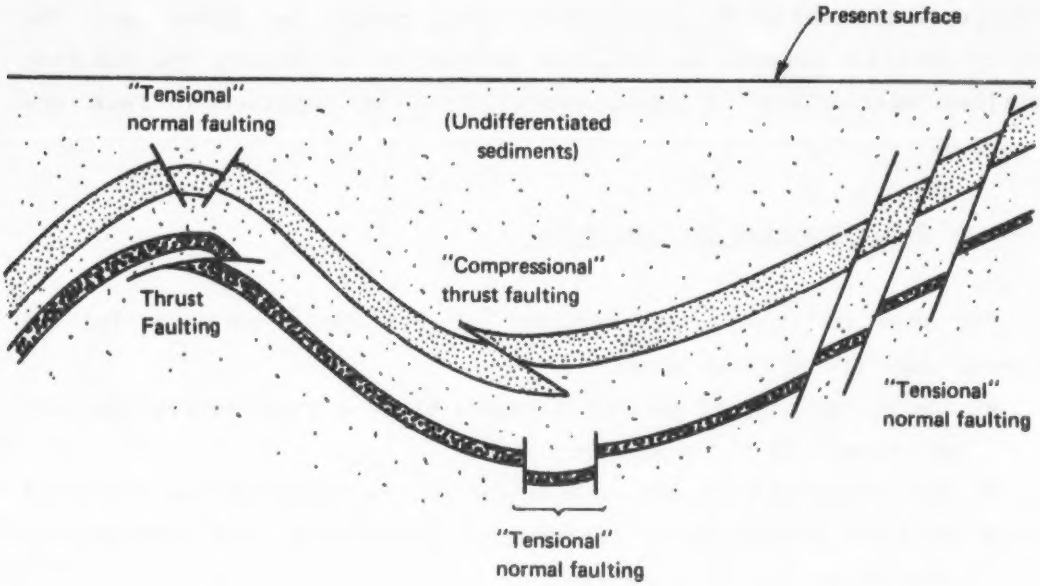
Present surface
"Tensional" normal faulting
(Undifferentiated sediments)
Thrust Faulting
"Compressional" thrust faulting
"Tensional" normal faulting
"Tensional" normal faulting

FIGURE D–34 FAULTING ASSOCIATED WITH FOLDING AND TILTING surveys have been made, considerable uncertainty often remains. Much of the variability depends both on the intensity of exploration and on the field workers' interpretations of what constitutes a "mappable fault." Usually, only faults that can be discerned at the surface are mapped, and these only if they show significant displacement. Furthermore, as most faults caused by a particular stress regime are roughly parallel, they are occasionally identified as a single large fault, rather than many individual ones. Therefore, the actual number of faults may be significantly higher than the number mapped. As a supplement to the geologic maps published by the USGS, this report has drawn upon the safety analysis reports for proposed nuclear power plants, wherein more detailed evaluations of fault capabilities in particular areas are reported.

D-5.1.3 Fault Movement Failure Model

The quantitative characterization of the fault movement failure element consists of three parts:

- the probability of renewed movement along any old faults that may be present at the repository site;
- the probability of the development of new faults at the site; and
- physical parameters to describe the groundwater flow pathway resulting from fault movement.

The general method used for estimating the probabilities is the same for all geologic settings and is described in the next paragraph. Its application to specific settings will then be discussed in subsequent paragraphs.

Renewed movement along old faults. Suppose an old fault is present at the site and that its most recent movement has been reliably dated at about N years before the present. The model uses the reciprocal 1/N as an estimate of the annual probability of renewed movement along that fault. The rationale for this approach is as follows. Movement along faults may be regarded as a stochastic process, with the intervals between movements analogous to the time between failures of mechanical components in classical reliability theory.(106) The simplest model for such a stochastic process is based upon a constant annual failure rate λ, approximately representing the probability of failure between times t and t + 1 given that the component has not failed (fault has not moved) by time t. According to this model, λ is the reciprocal of the mean time to failure. That is, if a type of component is known to fail after an average duration of n, then $\lambda = 1/n$ is the value of the parameter λ consistent with this observation.

Applying this analogy to the fault case, suppose it is known that over the history of the fault, times of n_1, n_2. . . ., n_k elapsed between movements. One should also add to this list the period N since the last movement. Since fault movement has not yet recurred, N underestimates the true value of the time to the next movement, which may even be infinite (i.e., no new movement ever occurs). If the process were truly stationary in time (i.e., having failure probabilities dependent only on the time elapsed since the last event rather than depending also on historical time) then a reasonable estimate of the mean time to failure would be the average of the numbers n_1, n_2, . . ., n_k, N. (It would be biased on the low side because of the bias involved in using N, as mentioned above. This would be consistent with the conservative approach adopted in this study.) The corresponding failure rate would then be the reciprocal of this average. However, as mentioned in the previous section, movement along a fault is strongly affected by the long-term evolution of regional stress patterns associated with slow geologic processes. Because of these changes with time, in estimating the mean time to failure one might wish to use a weighted average of n_1, n_2, . . ., n_k, N, weighting the more recent observations more heavily. In the cases to be considered below, N, the time since the most recent movement, is generally sufficiently great in geological terms (tens or hundreds of millions of years) that in itself it covers the entire period of site history relevant to whether additional fault movement will occur. Thus, the appropriate weighted average of n_1, n_2,...n_K, N assigns all the weight to N, implying a failure rate $\lambda = 1/N$. This implies that N is the only observed value needed to estimate the failure rate from renewed fault movement.

It is not uncommon for geologists to assign, implicitly or explicitly, a zero probability for renewed movement in the near future to certain old faults that are well dated and understood.(110) Thus, the estimation of a small positive probability by the above algorithm is believed to be consistent with present practice and somewhat conservative. It should be noted that this discussion further assumes that the geology of a site is well understood and that new evolving processes that could lead to renewed fault movement will not be significant over the 10,000-year period of repository evaluation. (On the other hand, it is also possible that in specific cases, regional site investigations may lead to higher fault movement estimates, based on a detailed understanding of the geologic processes at work.)

New faults. A region containing a potential repository site may have had several episodes of faulting in its geologic history. For example, there might be contemporaneous faulting during a period of sedimentation, followed by tilting and block faulting associated with tectonic forces. In attempting to estimate the probability of new faulting in the region, it is reasonable to consider only the most recent episode of faulting, because previous processes are even less related to the present state of the region. If this most recent episode of faulting and fault movement spanned the period from M to N years before the present and if a fault density of f faults per repository area (or some other measure of density) is observed, then the average rate of new faulting over the last M years is given by f/M faults per year per repository area. In a location with a long history of stability since the last faulting episode, and where no new geologic processes offer countervailing evidence, this average rate can be interpreted as a conservative estimate of the rate governing the more recent past and the near future. In fact, M is often more difficult to determine than N, the latter being of greater concern in any case; and since N is less than M, the larger rate, f/N, has been adopted for modeling purposes. As was mentioned for the case of renewed movement along old faults, in site-specific circumstances there may be reason to estimate a different rate.

Combined estimate for reactivated and new faults. Suppose it is observed that as a result of the most recent episode of faulting in a given region (excluding minor surficial faulting), faults occur with a density of about f per repository area. Assume further that the most recent movement is dated at about N years before the present. Then the previous two subsections each lead to occurrence rates of f/N, in the first case for old fault movement and in the second for new faults. (The second calculation is probably more conservative than the first.) Then the combined rate of occurrence of either type of fault movement is given by:

$$\lambda = \frac{2f}{N} .$$

With respect to the estimation of the parameter f, there are insufficient reliable data on which to base a statistical analysis. Some evidence for appropriate values of f can be obtained from the following:

- Examination of fault densities from surface surveys at various locations. Examples are shown in Table D-88.
- Fault maps prepared in connection with a number of power plant applications.
- Seismic surveys for parts of the Delaware Basin.
- Reported spacings of faults along anticlines in the Columbia Plateau.

On the basis of these data, it appears that for most locations it is very unlikely to find faults spaced less than about one to two kilometers (10 to 15 kilometers is more common). Hence the first estimate f = 2 faults per repository and the second estimate f = 5 faults per repository have been adopted for all geologic settings. Therefore, the sections on the specific geologies simply associate dates with these periods of faulting so as to calculate values of λ, the faulting failure rate.

Flow pathway. The reference repository has dimensions 2 km x 4 km. It is assumed for the sake of conservatism that a fault intersecting the repository cuts through parallel to the long side, so that the length of the intersection is 4000 m. The width of the fault zone is assumed to be one meter. The widths of fractured zones associated with faults vary widely. Many are very small (a few centimeters) although some extend 100 meters or more.(107) In light of the assumption of relative

TABLE D-88

FAULT DENSITIES FOR SELECTED AREAS OF THE UNITED STATES

	Density (per km^2)
Montana	0.0236
San Juan, Utah	0.2807
Central Oregon	0.154
Nevada Test Site	0.058
Karnes, Texas	0.0567
Sweetwater, Wyoming	0.0998
Coconino, Arizona	0.1737
North Michigan	0.1993
Western Massachusetts	0.0871
Eastern Kentucky	0.0031
Bonneville, Idaho	0.820
Eastern Pennsylvania	0.370

Source: Geotechnical Engineers, Inc.

geologic stability and careful selection of a repository site, for both first and second estimates a width of one meter is believed to be adequate to model all fault movements that could reasonably occur over the next 10,000 years. Larger zones are in fact generally associated with growth during extended periods of activity. The porosity of the fault zone has been assumed to be 0.1. This parameter is used only for velocity calculations and even with this relatively high value (tending to underestimate velocities), transit times to the aquifer system are quite short. The only rock-specific parameter in the model is the permeability of the fault. This depends on the strength of the rock and will be discussed below for the various cases.

D-5.1.3.1 Bedded Salt

The first estimate for bedded salt assumes most recent faulting to be of Permian age, and hence at least 230 million years old. This is generally a valid assumption for the Delaware Basin, for example,(20) and there is evidence that in much of the Salina Basin the most recent faulting is even of Pennsylvanian age (280 million years old).(108,109) The assumption $N = 2.3 \times 10^8$ years yields the value

$$\lambda = \frac{2f}{N} = \frac{4}{2.3 \times 10^8} = 2 \times 10^{-8} \text{ events/year.}$$

The second estimate is based on mid-Tertiary faulting in the Paradox Basin, corresponding to $N = 2.5 \times 10^7$ years. The corresponding failure rate is

$$\lambda = 4 \times 10^{-7} \text{ events/year.}$$

There has been more recent faulting in some evaporite basins. For example, faulting associated with salt dissolution in the Paradox Basin may be of Quaternary age (1 million years old); however, the faults do not appear to cut through the salt beds.(110,111,112) There is probably significant Cretaceous faulting (63 million years old) in parts of the Salina Basin, and there is an active fault suspected to have moved within 100,000 years in western New York.(108) Therefore, the second estimate used for the calculation of λ is not a "worst case," but is intended to represent a general type of area being seriously considered for repository siting.

The permeability of the fractured zone associated with a fault in a salt repository could vary widely. In fact, it is highly possible for the salt simply to deform to relieve the stresses that would induce fracturing in adjoining strata, rather than for the salt to fracture at all. Since salt is rather weak, any fracturing would be expected to lead to fairly well crushed salt. The permeability of compacted crushed salt has been estimated at about 10^{-4} cm/sec,(113) which is the value adopted here for both first and second estimates. Crushed shale actually may have a lower permeability (depending upon the degree of crushing), but for conservatism the entire fault pathway, even through the overlying and underlying shale beds, has been assumed to have the same permeability as the pathway through the salt.

D-5.1.3.2 Granite

The first estimate for granite is based on the assumption of an ancient, stable batholith or other pluton. Some faulting would generally be expected since emplacement or metamorphosis. In western Massachusetts, Triassic faulting was the most recent faulting identified in the geologic exploration associated with the Montague Power Plant application.(102) Adopting this age, 180 million years, the corresponding failure rate is:

$$\lambda = 2 \times 10^{-8} \text{ events/year.}$$

The second estimate is based on a more active site in the basin and range province. Assuming that site selection avoids areas with Quaternary faulting ("young faults"), the age would be at least one million years, giving

$$\lambda = 10^{-5} \text{ events/year.}$$

Less stringent site selection or inaccurate site characterization could lead to a still higher rate.

The permeability of the fractured zone is based on the assumption that the granite is brecciated and fractured more than pulverized, due in part to its high strength. It is believed that 10^{-2} cm/sec is a reasonable estimate for this permeability, although a large range is possible. This value of permeability corresponds to the high range for silty sand and gravel (Figure D-13; see Section D-3.2) and to the parallel plate model of ten parallel smooth fractures per meter, each of aperture 0.5 mm.(47,50)

D-5.1.3.3 Basalt

The first estimate for basalt is based upon relatively stable areas of the Columbia Plateau, where at least the uppermost basalt layers (dated at eight million years) show large areas free of faults. It is possible that the most recent faulting is still older than this, but because of active tectonic forces in the general region it is believed that eight million years is a reasonable age to assume. This age yields the value:

$$\lambda = 5 \times 10^{-7} \text{ events/year.}$$

There are certainly areas of more recent faulting within this area.(100) For example, a scarp in the Horse Haven uplift indicates Quaternary movement.(31) The second estimate is based on a site in an area where the most recent faulting is at least earlier than Quaternary age (one million years), yielding the value

$$\lambda = 10^{-5} \text{ events/year.}$$

For the same reasons as in the case of granite, the permeability is assumed to be 10^{-2} cm/sec through the fault zone.

D-5.1.3.4 Shale

The first and second estimates for shale are based upon the same geologic assumptions as for bedded salt, and therefore the failure rates are

$$\lambda = 2 \times 10^{-8} \text{ events/year (first estimate)}$$
$$\lambda = 4 \times 10^{-7} \text{ events/year (second estimate).}$$

A permeability of 10^{-4} cm/sec has been assumed, based on the high range of the permeability of compacted crushed shale evaluated for backfill.(112)

D-5.1.3.5 Dome Salt

The first estimate for dome salt is based on contemporaneous faulting in the Gulf Interior region, where faulting continued even after the domes stablized.(114) The youngest faults identified in one detailed site evaluation(115) were dated at 13 million years. This age yields the value

$$\lambda = 3 \times 10^{-7} \text{ events/year.}$$

As one moves down to the Gulf Coast, more recent sedimentation has led to contemporaneous faulting even in the Quaternary period. Assuming that the site selection rules out areas with Quaternary faulting, the minimum age of one million years to the last movement implies the value

$$\lambda = 10^{-5} \text{ events/year,}$$

which is taken as the second estimate value.

The permeability of a fault through a salt dome repository has been taken as 10^{-4} cm/sec, as in the case of bedded salt.

D-5.1.4 Fault Movement Release Model

The purpose of this section is to calculate fluid flows through an assumed ruptured fault. Parameters to characterize the physical pathway have been estimated in the previous section. A number of conservative assumptions (i.e., tending to overestimate flow rates) have been made in the analysis so that the net effect may be to overestimate flows by one or more orders of magnitude. For example, the capability of the associated aquifers to produce or receive the estimated fluid flows may be highly restricted. Faults may heal either by the plastic deformation of the surrounding rock or by the accumulation of fill material in the fractures. For the sake of simplicity in the present model, these factors have not been included. If it is determined that the risk (accounting for both probability and consequences) indicated by the bounding calculations carried out here warrants more detailed analysis, then it would be necessary to conduct a wider survey of specific fault characteristics in order to improve the precision of the estimates. The present level of detail is believed to be sufficient for this generic analysis. For further simplification, repository resaturation is assumed to have taken place in all cases by the time the fault movement occurs.

In addition to transport of radionuclides by groundwater flow through the faulted rock, there is the possibility that continued movement of the fault may lead to physical transport of a portion of the repository to the surface. Rate estimates show that this process would be extremely slow, however. Further discussion is provided in Section D-5.6.

D-5.1.4.1 Bedded Salt

It is unlikely that fault movement would occur during the period of extensive salt creep and repository resaturation since the mechanical stability of the site would be expected to be most certain in the time period closest to the present. (This period has been referred to as Period A in previous sections). Furthermore, the pressures resulting from salt creep are sufficient to cause the relatively rapid "squeezing out" of fluid through degrading shaft and borehole seals during this period as well, and so the addition of another pathway, such as a ruptured fault, would not significantly alter this process. The fault does have the capability, however, to lead to additional releases through groundwater movements, and these are the movements that have been modeled for faulting at any point in the 10,000 year period of evaluation. The dominant driving forces are thermally induced convection and the gradient from interconnecting the upper and lower aquifers.

The values of the combined effective gradients tending to move fluid through a fault are the same as those given earlier in Table D-53 (see Section D-3.3). When these gradients are used in Darcy's law, along with the other parameters given in Section D-5.1.3, the volumetric flow rates shown in Table D-89 are obtained. Since these flows are not nearly so small as those calculated for a number of other failure elements, it is natural to ask whether the conservative viscosity correction factor

$$c(\mu) = 5,$$

corresponding to pressurized water at about 125°C, should be re-estimated as a function of time here so as to give more realistic flow rates, especially at later periods, when radioactive decay will have reduced the heat output from the wastes. From Table D-VI-2 in Appendix D-VI, it is seen that even reducing the fluid temperature to 60° (50° is the average temperature at 10,000 years), the viscosity correction factor would be reduced by only a factor of about two. Therefore the original value of $c(\mu)$ is retained for the sake of simplicity.

Another area of concern that arises is whether the calculated fluid flows might lead to considerable dissolution along the pathway. The implications of this might include:

- a decrease in the distance between the flow pathway and waste canisters, either by widening of the pathway or gradual plastic flow of the salt and repository toward the fault in order to replace salt that had been carried away; and

TABLE 89

VOLUMETRIC FLOW RATES THROUGH A FAULT
(BEDDED SALT REPOSITORY)

	Volumetric Flow ($\dot{Q}$) (m^3/yr)		
	100 years*	1000 years	10,000 years
First Estimate	8.2×10^4	6.9×10^4	2.5×10^4
Second Estimate	3.9×10^5	3.8×10^5	3.3×10^5

*Years after repository closure.

- an increase in fluid flow rate from the widening of the flow channels.

This is indeed a possibility. However, another factor offsets these problems, namely, the tendency of fractures in salt to heal themselves by plastic flow and recrystallization. While it is beyond the scope of this report to attempt to prove, by an analytical model or otherwise, that the healing effect more than offsets the dissolution, the present model may be interpreted as being based on this assumption. Other reports have also noted the healing potential for breaches in a salt repository.(11,18)

The volumetric fluid flow rates in Table D-89 lead to the interstitial velocities given in Table D-90, based on a porosity of 0.1 in the fault zone.

Estimation of the source term for this failure element requires consideration of several processes. First, because of the possible leaching of radionuclides prior to the fault event, the water saturating the backfilled repository will contain an approximately uniform concentration of each species (see Figure D-35a). The value of the concentration may vary from one radionuclide to another depending on leach characteristics and possible solubility limits. When the fault pathway is established (Figure D-35b), some of the fluid will mix with the fluid moving up from below so that some of the radionuclides in solution will be released. This effect decreases with distance from the fault. It is assumed for modeling purposes that the zone of influence is a band extending 50 meters from each side of the fault. Such a zone is expected to contain 5% of the repository area and inventory. For conservatism, it is assumed that the initial fluid flows through the fault from the repository to the upper aquifer contain all these dissolved radionuclides at their initial uniform concentration. (That is, this inventory is assumed to be depleted somewhat more rapidly than would actually be the case.)

Second, any canisters in the actual path of the fault may be damaged, and so the waste form is assumed to be subject to direct leaching. (Other canisters might be given credit for container integrity.) The material expected to be leached from canisters in the direct flow pathway should be added to that calculated according to the

TABLE D-90

FLUID VELOCITIES THROUGH A FAULT
(BEDDED SALT REPOSITORY)

		Velocity (v) (m/yr)	
	100 years*	1000 years	10,000 years
First Estimate	205	173	63
Second Estimate	975	950	825

*Years after repository closure.

(a) Backfilled Waste Before Fault Event

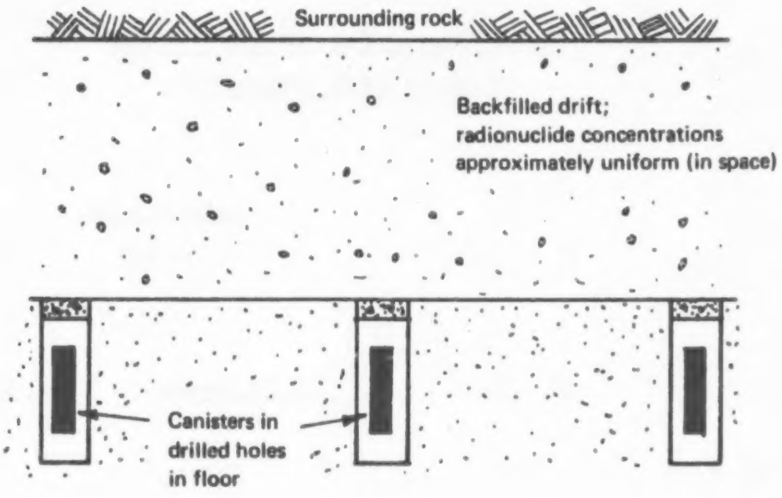

(b) Backfilled Waste Drift Intercepted by Fault

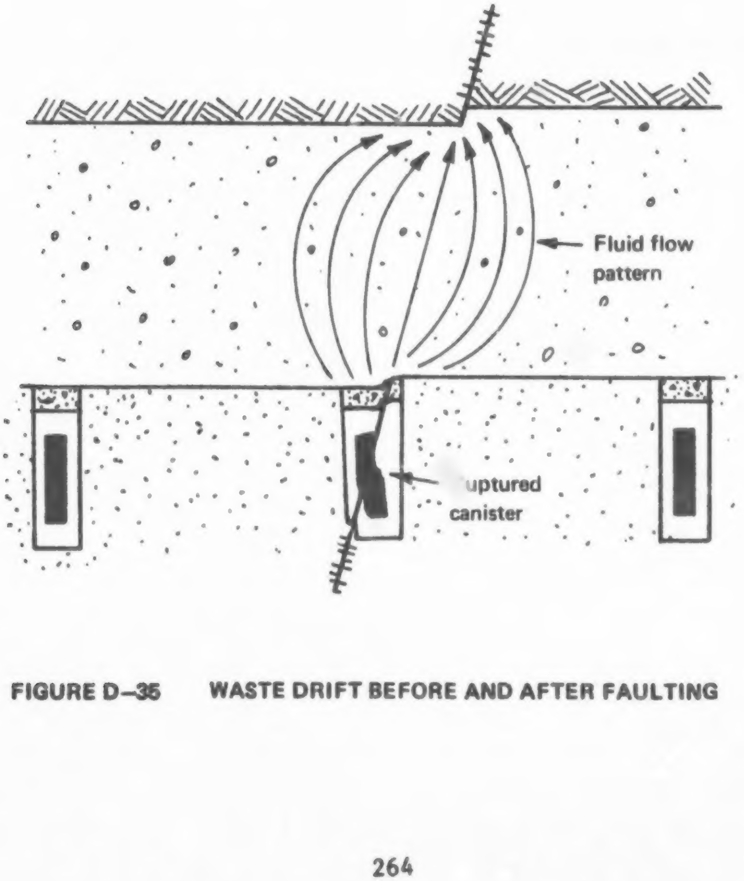

FIGURE D–35 WASTE DRIFT BEFORE AND AFTER FAULTING previous paragraph. It is assumed that 100 canisters fall into this category.

Third, continued leaching from other canisters is also expected to occur, with movement of the radionuclides by diffusion and fluid mixing. This contribution to the releases is expected to be much smaller than in the previous two cases, so it is not included in the model.

D-5.1.4.2 Granite

Thermally induced convection is the dominant driving force for fault pathways through a granite repository. The effective gradients have been calculated as 0.11 at 100 years, 0.07 at 1000 years, and 0.03 at 10,000 years. (See Appendix D-VI). Using these gradients in conjunction with the parameters given in the previous section, the volumetric flow rates shown in Table D-91 may be calculated by Darcy's law. Corresponding fluid velocities are given in Table D-92. The source term in this case may be treated according to the same procedure as that given for bedded salt.

D-5.1.4.3 Basalt

The effective hydraulic gradient in the case of basalt is the combined result of thermally induced convection and an aquifer interconnection. The values have been given in Table D-59 in Section D-3.3. Using these gradients in conjunction with the parameters given in the previous section, the volumetric flow rates shown in Table D-93 may be calculated by Darcy's law. Corresponding fluid velocities are given in Table D-94. The source term in this case may be calculated according to the same procedure as that given for bedded salt.

D-5.1.4.4 Shale

The effective hydraulic gradient in the case of shale is the combined result of thermally induced convection and an aquifer interconnection. Their values are the same as for basalt. Using these gradients in conjunction with the parameters given in the previous

TABLE D-91

VOLUMETRIC FLOW RATES THROUGH A FAULT (GRANITE REPOSITORY)

	Volumetric Flow ($\dot{Q}$) (m^3/yr)		
	100 years*	1000 years	10,000 years
First Estimate	6.9×10^6	4.4×10^6	1.9×10^6
Second Estimate	6.9×10^6	4.4×10^6	1.9×10^6

*Years after repository closure.

TABLE D-92

FLUID VELOCITIES THROUGH A FAULT
(GRANITE REPOSITORY)

	Velocity (v) (m/yr)		
	100 years*	1000 years	10,000 years
First Estimate	1.7×10^4	1.1×10^4	4.8×10^3
Second Estimate	1.7×10^4	1.1×10^4	4.8×10^3

*Years after repository closure.

TABLE D-93

VOLUMETRIC FLOW RATES THROUGH A FAULT (BASALT REPOSITORY)

	Volumetric Flow ($\dot{Q}$) (m^3/yr)		
	100 years*	1000 years	10,000 years
First Estimate	8.8×10^6	7.6×10^6	3.2×10^6
Second Estimate	4.0×10^7	3.8×10^7	3.4×10^7

*Years afer repository closure.

TABLE D-94

FLUID VELOCITIES THROUGH A FAULT
(BASALT REPOSITORY)

	Velocity (v) (m/yr)		
	100 years*	1000 years	10,000 years
First Estimate	2.2×10^4	1.9×10^4	7.9×10^3
Second Estimate	9.9×10^4	9.6×10^4	8.5×10^4

*Years after repository closure.

section, the volumetric flow rates shown in Table D-95 may be calculated by Darcy's law. Corresponding fluid velocities are given in Table D-96. The source term in this case may be calculated according to the same procedure as that given for bedded salt.

D-5.1.4.5 Dome Salt

It can reasonably be assumed that a fault intersecting a salt dome will extend beyond the flank of the dome on one or both sides. Consequently, a connection will be established between the upper aquifer and the lower aquifer (or pressurized brine reservoir) extending to the side of the dome. This interconnection provides for two driving forces whose effect is additive. First, an aquifer interconnection gradient tending to move fluid upward has been assumed in the generic repository setting in dome salt (see Chapter D-2.0). Second, adequate recharge is available to permit the establishment of a thermally induced convection cell. The values of the effective gradients are given in Table D-97. Using these gradients in conjuncion wih the parameters given in the previous section, the volumetric flow rates shown in Table D-98 may be calculated by Darcy's law. Corresponding fluid velocities are given in Table D-99. The discussion of healing and dissolution that was presented in the case of bedded salt also applies to this case. The source term in this case may be calculated according to the same procedure as that given for bedded salt.

D-5.1.5 Literature Discussion

Faulting models and parameters have been reported in a number of other studies, several of which are summarized below.

Battelle Pacific Northwest Laboratory, working under the ONWI/WISAP program, has developed general models for faulting at a hypothetical site in Columbia Plateau Basalts.(50) Components of the model include:

- probability of significant changes in regional tectonic forces over the next million years;
- probability of changes in local strain ratios over the next million years;

TABLE D-95

VOLUMETRIC FLOW RATES THROUGH A FAULT (SHALE REPOSITORY)

	Volumetric Flow ($\dot{Q}$) (m^3/yr)		
	100 years*	1000 years	10,000 years
First Estimate	8.8×10^4	7.6×10^4	3.2×10^4
Second Estimate	4.0×10^5	3.8×10^5	3.4×10^5

*Years after repository closure.

TABLE D-96

FLUID VELOCITIES THROUGH A FAULT
(SHALE REPOSITORY)

		Velocity (v) (m/yr)	
	100 years*	1000 years	10,000 years
First Estimate	2.2×10^{2}	1.9×10^{2}	8.0×10^{1}
Second Estimate	1.0×10^{3}	9.5×10^{2}	$8.5 \times LO^{2}$

*Years after repository closure.

TABLE D-97

EFFECTIVE VERTICAL HYDRAULIC GRADIENT IN A FAULT FROM THERMALLY INDUCED CONNECTION AND AQUIFER INTERCONNECTION (SALT DOME REPOSITORY)

	100 years*	1000 years	10,000 years
Thermally Induced Convection**			
First Estimate	0.12	0.07	0.03
Second Estimate	0.12	0.07	0.03
Aquifer Interconnection***			
First Estimate	0.01	0.01	0.01
Second Estimate	0.2	0.2	0.2
Total			
First Estimate	0.13	0.08	0.04
Second Estimate	0.32	0.27	0.23

*Years after repository closure.
**From Table D-VI-4, Appendix D-VI.
***From Chapter D-2.0.

TABLE D-98

VOLUMETRIC FLOW RATES THROUGH A FAULT
(DOME SALT REPOSITORY)

	Volumetric Flow ($\dot{Q}$) (m^3/yr)		
	100 years*	1000 years	10,000 years
First Estimate	8.2×10^4	5.0×10^4	2.5×10^4
Second Estimate	2.0×10^5	1.7×10^5	1.5×10^5

*Years after repository closure.

TABLE D-99

FLUID VELOCITIES THROUGH A FAULT (DOME SALT REPOSITORY)

	Velocity (v) (m/yr)		
	100 years*	1000 years	10,000 years
First Estimate	2.0×10^2	1.3×10^2	6.3×10^1
Second Estimate	5.0×10^2	4.3×10^2	3.6×10^2

*Years after repository closure.

- probability of an undetected fold as a function of both distance from the site and degree of site investigation;
- probability of a fault associated with an undetected anticline;
- probability of shear deformation along pre-existing joints, the cause being movement in an undetected anticline; and
- probability of rupture of a fault in the basement strata.

The last probability in this list is estimated at

$$\lambda = 10^{-6} \text{ events/year.}$$

The determination of various probabilities is associated with seismicity data.

TASC, in work for Lawrence Livermore Laboratory,(11) modeled movement along old faults in a shale repository as having an annual rate of

$$\lambda = 5 \times 10^{-7} \text{ events/year.}$$

They argued that for bedded salt the probability would be less. Consequence modeling parameters included permeabilities of 10^{-5} cm/sec and 10^{-4} cm/sec through the repository and barrier layers, respectively, with partial healing after 70 years reducing these values by two orders of magnitude. Fault zone porosity was estimated at 10^{-3}.

Claiborne and Gera evaluated faulting probabilities for a site in southeastern New Mexico.(3) They estimated a faulting rate of

$$\lambda = 4 \times 10^{-11} \text{ events/year,}$$

based on the regional tectonic data and geometrical analysis. They further argued that containment failure by faulting is even less likely, involving a reduction of about two more orders of magnitude in the failure rate.

The KBS study(26) in Sweden estimated a fault movement rate of

$$\lambda = 10^{-9} \text{ events/year}$$

for a 1-km^2 repository in that country.

A University of New Mexico study(10) for the EPA considered the possibility of faulting in shale and salt repositories in the Delaware Basin. The following occurrence rates were given

$$\lambda = 2.2 \times 10^{-7} \text{ events/year} \quad \text{(shale)}$$
$$\lambda = 1.4 \times 10^{-7} \text{ events/year} \quad \text{(bedded salt).}$$

The model was based on 13 years of earthquake data and a relation between earthquake magnitude and faulting parameters, in order to estimate an annual average fault surface area over which movement has been experienced. This value was used to estimate the net faulting rate as a product of three probabilities

$$p_1 \times p_2 \times p_3$$

where:

$$p_1 = \frac{\text{average fault surface moving per year}}{\text{total surface of Permian-Penn. faults}}$$

p_2 = probability of an old fault beneath repository

p_3 = probability of a rupture in old fault extending as far up as repository.

For bedded salt the respective values are 0.012 km^2/10^4 km^2, 0.6, and 0.2, leading to the λ value given above.

D-5.2 VOLCANOES

D-5.2.1 Summary

The repository site selection process is expected to avoid sites where future volcanic activity is at all likely. Nevertheless, volcanic trends can cover large distances over a period of time, and occasionally completely new volcanic centers erupt, even within stable crustal plates. This section of the report is concerned with the intersection of a repository by a volcanic structure that vents to the surface. The case of subsurface intrusive structures is treated in Section D-5.3. The model adopted here consists of a constant annual rate for penetration of the repository and transport of material to the air and land surface. Rates are estimated by counting the number of vents in various areas, dividing by their age to obtain vent formation rates, and multiplying by the probability that such a vent would intersect a randomly cited repository in the region of interest. A summary of the analysis is given in Table D-100.

D-5.2.2 Background

A volcano is generally defined as a hill or mountain resulting from accumulations of congealed lava or other ejecta that have been spewed from a vent by deep geologic pressure and heat. From the point of view of a repository, the physical form is less important than the probability of recurrence, the nature of the eruption, and the range of influence. Figure D-36 illustrates a number of volcanic or igneous features. Several important surface phenomena are described in Table D-101.

Volcanism is usually related to areas of crustal plate collision, where magma from a subduction zone can be freed up through the overlying crust, or to areas under tensional stress, where rift zones can develop. These conditions generally are found along continental margins and mid-oceanic rises,(116-118) although intracontinental rifts are also found. (See Figure D-45 in Section 5.6.) Most such activity therefore follows linear or arched trends.

During the last ten million years, the only volcanism in the coterminous 48 states has been in the West. Most of this activity has paralleled the Pacific Coast, but some has followed the graben of the Rio Grande, arched southward from Albuquerque toward Las Vegas, or extended westward from Yellowstone Park. These trends are shown in Figure D-37. There have been only three eruptions in the 48 states

TABLE D-100
SUMMARY OF VOLCANO FAILURE ELEMENT

MEDIUM	PROBABILISTIC (P) DETERMINISTIC (D)	NATURE OF MODEL	RELEASE MODE	DRIVING FORCE	SOURCE TERM	PARAMETERS		RELEASE MODELING STEPS		COMMENTS
						1st ESTIMATE	2nd ESTIMATE	1st ESTIMATE	2nd ESTIMATE	
Bedded Salt	P	Annual occurrence probability.	Air and land surface.	Direct transport by moving gases and molten rock.	Fraction of repository brought to surface.	$\lambda = 1 \times 10^{-10}$/yr Fraction of repository brought to surface is 0.4%, of which 1% is in respirable form, 9% consists of fine particles which can be easily dispersed, and 90% is reburied near the surface.	$\lambda = 1 \times 10^{-8}$/yr Fraction of repository brought to surface is 0.4%, of which 1% is in respirable form, 9% consists of fine particles which can be easily dispersed, and 90% is reburied near the surface.	Direct release	Direct release	First estimate based on national average. Lower rates could probably be derived from additional siting assumption, such as location in East or Midwest.
Granite	P	Annual occurrence probability.	Air and land surface.	Direct transport by moving gases and molten rock.	Fraction of repository brought to surface.	$\lambda = 1 \times 10^{-10}$/yr Fraction of repository brought to surface is 0.4%, of which 1% is in respirable form, 9% consists of fine particles which can be easily dispersed, and 90% is reburied near the surface.	$\lambda = 1 \times 10^{-8}$/yr Fraction of repository brought to surface is 0.4%, of which 1% is in respirable form, 9% consists of fine particles which can be easily dispersed, and 90% is reburied near the surface.	Direct release	Direct release	First estimate based on national average. Lower rates could probably be derived from additional siting assumption, such as location in East or Midwest.
Basalt	P	Annual occurrence probability.	Air and land surface.	Direct transport by moving gases and molten rock.	Fraction of repository brought to surface.	$\lambda = 6 \times 10^{-10}$/yr Fraction of repository brought to surface is 0.4%, of which 1% is in respirable form, 9% consists of fine particles which can be easily dispersed, and 90% is reburied near the surface.	$\lambda = 1 \times 10^{-8}$/yr Fraction of repository brought to surface is 0.4%, of which 1% is in respirable form, 9% consists of fine particles which can be easily dispersed, and 90% is reburied near the surface.	Direct release	Direct release	Based on Columbia Plateau basalts.

TABLE D-100
SUMMARY OF VOLCANO FAILURE ELEMENT (CONTINUED)

MEDIUM	PROBABILISTIC (P) DETERMINISTIC (D)	NATURE OF MODEL	RELEASE MODE	DRIVING FORCE	SOURCE TERM	PARAMETERS		RELEASE MODELING STEPS		COMMENTS
						1st ESTIMATE	2nd ESTIMATE	1st ESTIMATE	2nd ESTIMATE	
Shale	P	Annual occurrence probability.	Air and land surface.	Direct transport by moving gases and molten rock.	Fraction of repository brought to surface.	$\lambda = 1 \times 10^{-10}$/yr Fraction of repository brought to surface is 0.4%, of which 1% is in respirable form, 9% consists of fine particles which can be easily dispersed, and 90% is reburied near the surface.	$\lambda = 1 \times 10^{-8}$/yr Fraction of repository brought to surface is 0.4%, of which 1% is in respirable form, 9% consists of fine particles which can be easily dispersed, and 90% is reburied near the surface.	Direct release	Direct release	First estimate based on national average. Lowe rates could probably be derived from additional siting assumption, such as location in East or Midwest.
Dome Salt	P	Annual occurrence probability.	Air and land surface.	Direct transport by moving gases and molten rock.	Fraction of repository brought to surface.	$\lambda = 1 \times 10^{-10}$/yr Fraction of repository brought to surface is 0.4%, of which 1% is in respirable form, 9% consists of fine particles which can be easily dispersed, and 90% is reburied near the surface.	$\lambda = 1 \times 10^{-10}$/yr Fraction of repository brought to surface is 0.4%, of which 1% is in respirable form, 9% consists of fine particles which can be easily dispersed, and 90% is reburied near the surface.	Direct release	Direct release	Estimates based on national average. Could be refined to a lower value for salt dome region. First and second estimates are the same since from the standpoint of volcanism, the Gulf region shows no variation.

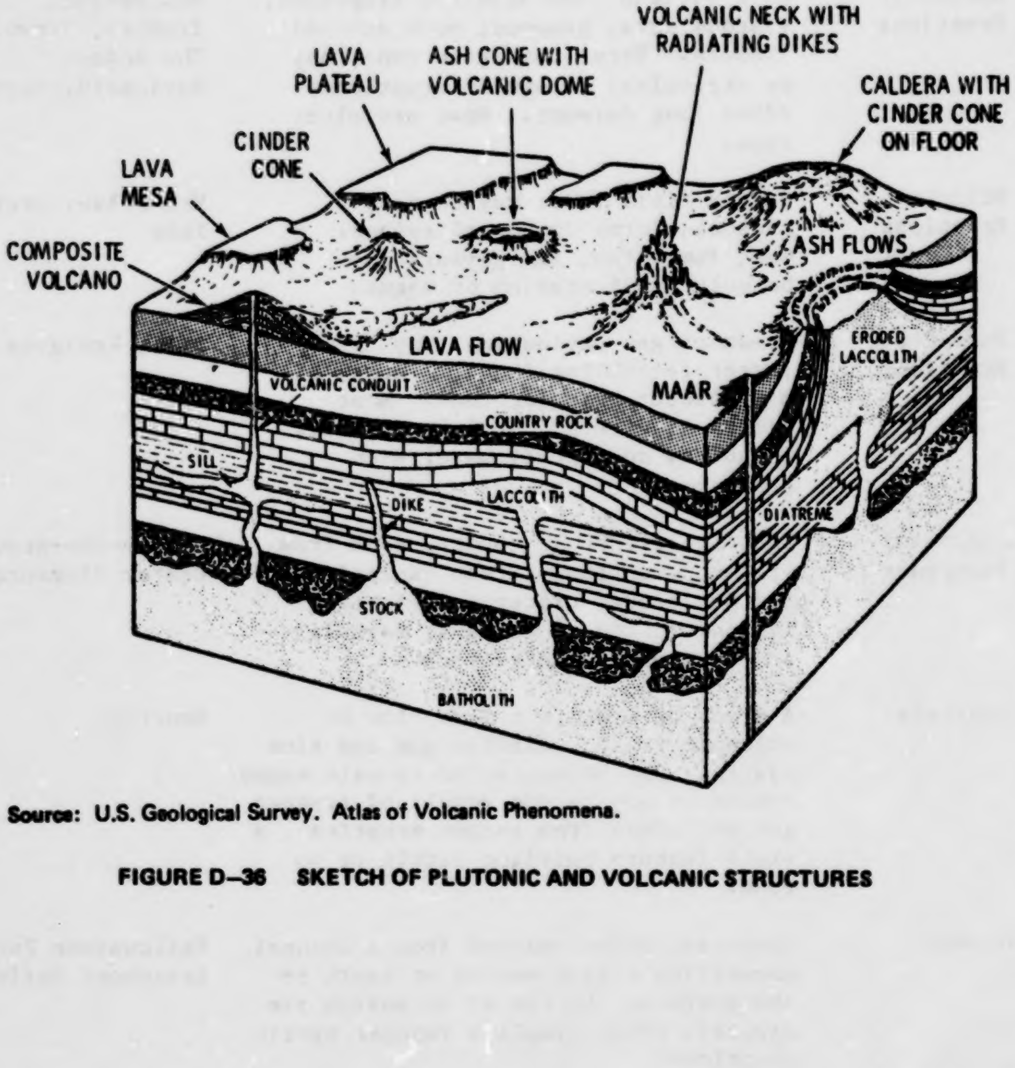

Source: U.S. Geological Survey. Atlas of Volcanic Phenomena.

FIGURE D–36 SKETCH OF PLUTONIC AND VOLCANIC STRUCTURES

TABLE D-101

VOLCANIC PHENOMENA WITH SURFACE MANIFESTATION

Type	Characteristics	Examples
Basaltic Eruptions	Mild eruptions; fluid lava; small gaseous component; silica deficient; regular or continuous eruptions.	Hawaii, Columbia Plateau, Stromboli
Andesitic Eruptions	More violent than basaltic eruptions; viscous lava; gaseous; much ash and cinders. Forms composite cone; may be explosive; irregular eruptions; often long dormant. Most prevalent type.	Mt. Ranier, Tamboro, Vesuvius, The Andes, Paricutin, Katmai
Silicic Eruptions	Nearly rigid lava; may be very gaseous; forms domes and spines. Gas, fumaroles, and geysers may be only manifestation of magma.	Mt. Pelee, Crater Lake
Phreatic Eruptions	Steam or gas explosion. May create crater resembling impact crater, or may shatter existing cone. Most ejecta fragmented, or dust and gas. Caused by contact of water with hot magma.	Taal, Krakatoa
Maars and Diatremes	Eruption crater in country rock from violent eruption. Steam explosion and jet erodes crater and ejects limited volume of volcanic material and shattered country rock.	Hole-in-the-ground, Crater Elegante.
Fumarole	A crack or vent in a lava flow or volcanic region emitting gas and fine ejecta. May be connected to main magma source or may be the result of trapped gas and steam from recent eruption. A small feature building little or no cone.	Numerous
Geyser	Steam and water emitted from a channel connecting a heat source at depth to the surface. Little or no solids are ejected; often displays regular cyclic eruptions.	Yellowstone Park, Steamboat Springs.

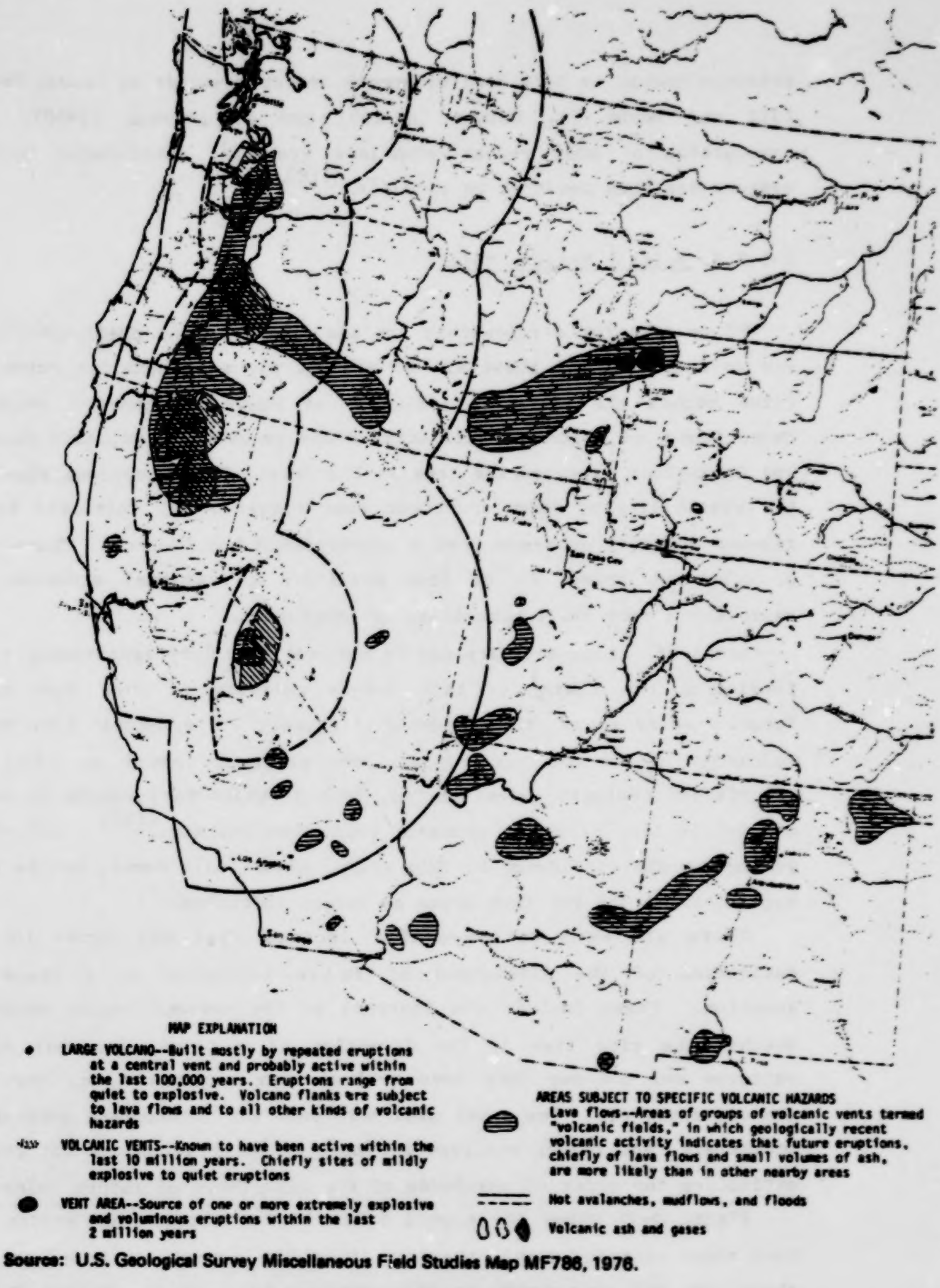
MAP EXPLANATION
● LARGE VOLCANO--Built mostly by repeated eruptions at a central vent and probably active within the last 100,000 years. Eruptions range from quiet to explosive. Volcano flanks are subject to lava flows and to all other kinds of volcanic hazards
VOLCANIC VENTS--Known to have been active within the last 10 million years. Chiefly sites of mildly explosive to quiet eruptions
● VENT AREA--Source of one or more extremely explosive and voluminous eruptions within the last 2 million years
AREAS SUBJECT TO SPECIFIC VOLCANIC HAZARDS
▨ Lava flows--Areas of groups of volcanic vents termed "volcanic fields," in which geologically recent volcanic activity indicates that future eruptions, chiefly of lava flows and small volumes of ash, are more likely than in other nearby areas
Hot avalanches, mudflows, and floods
Volcanic ash and gases
Los Angeles
San Diego
Albuquerque

Source: U.S. Geological Survey Miscellaneous Field Studies Map MF786, 1976.

FIGURE D–37 VOLCANIC HAZARDS

recently enough to have been witnessed and documented: at Lassen Peak in 1915 and Mount St. Helens in 1857 and at present (1980). The composition of most recent eruptions from the continental volcanic systems has been andesite or rhyolite.(119)

D-5.2.3 Volcano Failure Model

Of concern for a repository are the frequency and predictability of new volcanism, since there are no present plans to consider repository sites within the range of influence of known volcanoes. With few exceptions, new volcanism will occur close to existing volcanic features and in regions experiencing tensional stress. The exceptions stem from the possibility of maar eruptions (see Figure D-36) initiated by the release of gases or steam from a subterranean heat source. These types of eruptions appear to be less sensitive to regional stresses, but represent a very small percentage of eruptions.

Areas of future activity can be defined only very approximately, and predicting the timing of this future activity is even less exact. Future estimates of the expected frequency of eruptive activity at volcanoes or in volcanic regions are generally based on historical records and geologic investigation, both of which vary widely in detail and reliability from one volcanic region to another.(120) All of the geologic media considered in this study, except salt domes, can be found both close to and far from areas of recent volcanism.

There are many site-specific factors that can enter into an estimation of the likelihood of future volcanism at a repository location. These include the distance to the nearest recent activity, whether the site lies in the direction of a trend, regional stress patterns and the way they have evolved over geologic time, heat flow measurements, etc. The model used here does not incorporate geophysical parameters, but rather utilizes a simple counting technique for roughly estimating the order of magnitude of the likelihood of future volcanism.

Figure D-37 shows all mapped vents in the coterminous states that have shown activity within the last 10 million years. As noted earlier, these are all restricted to the western third of the United States. These vents actually formed over a longer period than 10 million years.

However, in estimating the rate of formation, it is conservative to use this lower, more readily available figure. The map shows approximately 1300 vents over this western area of 3×10^6 km^2. Thus, a gross regional average rate of vent formation is

$$\lambda = 1300 \text{ vents per } 3 \times 10^6 \text{ km}^2 \text{ per } 10^7 \text{ years}$$

$$= 4 \times 10^{-11} \text{ vents/km}^2\text{/year.}$$

For a repository of area 8 km^2, the corresponding rate of intersection would be 8 times the above, or

$$\lambda = 3 \times 10^{-10} \text{ intersections/year.}$$

This number does not represent either a first or second estimate for model purposes, but is used as an example calculation to represent the model equation

$$\lambda = 8V/AT \text{ intersections/year,}$$

where V is the number of vents formed in the area A over a period at least as long as T. This equation will be used for various regions to estimate appropriate values of λ. The 10-million-year cutoff for data on vents was chosen to be consistent with the USGS use of this time frame for their volcanic hazards maps.

A simple first estimate value of λ for all media except basalt can be derived from the assumption that, with careful site selection, it should be possible to locate a repository so that the probability of future volcanism is less than the national average. This is because bedded salt, granite, shale, and salt domes are either widely distributed or concentrated in areas of negligible volcanic activity. The national average is thus a conservative estimate of λ. This value is obtained exactly as above, except that the entire area of the coterminous states is used, so that

$$\lambda = \frac{(8)(1300)}{(7.83 \times 10^6)(10^7)}$$

$$= 1 \times 10^{-10} \text{ intersections/year.}$$

Basalt is not covered by this reasoning because the only basalt deposits being seriously considered for a repository are located in a single region, namely, the Pacific Northwest. By their mere presence, these basalts are indicative of significant volcanic activity in the past. Most of the Columbia Plateau flood basalts were apparently deposited about 14 to 17 million years ago, but some volcanic activity continues in locations such as Mount Lassen farther to the west. Regional stress studies suggest that there may be locations in this region where the probability of future volcanism is low. First estimate calculations consider the states of Washington, Oregon, and Idaho, exclusive of the north-south volcanic trend represented by the Cascade and Klamath Mountains. (This latter zone is probably associated with an existing subduction zone and hence a different tectonic zone from the region of greater interest.) From the map in Figure D-37, the following parameters have been estimated:

$$A = 4 \times 10^5 \text{ km}^2$$
$$V = 300 \text{ vents}$$
$$T = 10^7 \text{ years}$$

The resulting value of λ from the model equation is

$$\lambda = 6 \times 10^{-10} \text{ intersections/year.}$$

This number is the first estimate for basalt.

Second estimate values correspond to repository sites in locations of modest volcanic activity over the past 10 million years. A number of volcanic fields shown on Figure D-37 were considered, with values of A, V, and T being estimated for each. For example, for the Flagstaff, Arizona area, 85 vents are estimated to exist in a region 6400 km^2 in area, and the time over which these developed is thought to be at least 10^7 years. These parameters yield the value

$$\lambda = 1 \times 10^{-8}.$$

It is important to note that such values should not be applied to the specific volcanic fields from whose parameters they have been calculated. They represent only averages, and detailed site investigations could introduce other factors that might significantly alter the estimate for an individual site. They are, however, believed to be reasonable for generic calculations.

Many of the other calculations yielded similar values, and so this value, $\lambda = 1 \times 10^{-8}$, has been adopted as the second estimate for all media except salt domes. In the case of salt domes, which are not found in any of the volcanic regions, the second estimate value is identical to the first, i.e., 1×10^{-10}.

It should be noted that in the calculation of the volcanic vent formation rate, λ, the choice of regions to be considered has a great effect on the resulting numerical value. For example, application of the above procedure to the eastern United States would yield essentially zero rates. Since the values calculated by this procedure are generally very low, it did not seem desirable to refine them by making further site selection assumptions. Simple modifications, such as eliminating from consideration the vents along the Pacific coastal volcanic mountain zone, would indeed lower the rate for the rest of the country. However, since this modification only changes the result by about a factor of 2, it is not deemed important in these order-of-magnitude calculations. Another modification would be to consider only intra-plate silicic eruptions. While the consequences of these would be more severe, they would also involve lower probabilities than the already low ones calculated, as well as the possibility of detecting developing magma chambers that could lead to silicic eruptions over the next 10,000 years.

D-5.2.4 Volcano Release Model

The dominant release mode for the interception of a repository by a volcanic vent is the transport of radioactive material directly to the surface. Since the size of the vent and the nature of the eruption can vary considerably, this analysis simply estimates parameters that would characterize an "average" new vent.

The area of the vent is taken to be 3×10^4 m^2, corresponding to the area of a circle with radius 100 m. This cross-sectional area also characterizes the portion of the repository that would be affected, or 0.4% of the repository inventory. Of the affected contents, it is assumed that 1% is widely dispersed as fine particulates or gases, 9% is included with unconsolidated ash or cinder on the surface, and 90% is incorporated into solidified lava or welded ash. Most recent eruptions in America have involved andesitic ejecta with fragmented, molten, and gaseous components. The fractions assigned to each component are thought to be reasonable for such a typical eruption. Explosive and calamitous events, such as the obliteration of Krakatoa and Mt. Mazama (Crater Lake), are not only exceptional, but they are apparently more likely with large, established volcanic systems than with newer eruptions. Similarly, maars require abundant water, a condition not expected at most candidate repository sites. If it were desired to model the "worst possible" case in terms of consequences, then the probabilities would need to be revised downward accordingly.

D-5.2.5 Literature Discussion

Volcanism has been discussed in a number of repository studies. However, models and quantitative analyses are usually not included, and ones that are included are difficult to compare with those derived here.

The University of New Mexico/EPA study(10) characterized volcanic events with annual probabilities ranging from 2.4×10^{-12} to 8.1×10^{-12} for disruption of a repository. These probabilities are based on an estimate of renewed volcanism in the Delaware Basin with an annual rate of 5×10^{-9}, in combination with a geometric argument on repository intersection.

Claiborne and Gera,(3) also in an analysis of the Delaware Basin, simply state that volcanism in such a stable area is much less likely than formation of a "great fault." In addition, they argue that the consequences would be less than for a giant meteorite impact.

Recent probability calculations carried out for a potential repository site at Yucca Mountain on the Nevada Test Site yield an annual rate of 10^{-9} for repository disruption by volcanism.(121)

Some of the calculations carried out in other studies appear to count volcanic craters rather than individual vents, which may explain why some of these other rates are lower than those calculated here.

D-5.3 IGNEOUS INTRUSIVES

D-5.3.1 Summary

The previous section on volcanoes discussed extrusive igneous activity (movement of magma out through vents to the surface or the atmosphere). The repository might also be disrupted by intrusive igneous bodies (magma that moves through the earth's crust but never reaches the surface). The important difference between extrusive and intrusive activity is that while extrusive activity, volcanism, can transport waste directly to the biosphere, intrusive activity requires groundwater as a secondary transport mechanism.

The model in this section assumes that a planar intrusive body intersecting the repository will transport a fraction of the intersected waste to the overlying aquifer. Waste within the aquifer will then be leached and moved by the natural flow of groundwater. The model requires two parameters: the probability of an intrusive intersecting the repository, and the dimensions of the intrusive. Intrusives are common structures, particularly in volcanic and crystalline rocks; but, by their very nature, their emplacement has not been directly observed and there is little information from which probabilities for intrusions may be estimated. In the present model, the probability of an intrusive intersecting a repository is modeled as a fraction of the probability of faulting. Dimensions of intrusives used in the model are consistent with those reported in the literature. It is assumed that the waste is not sealed into the resolidified igneous rock, which may be heavily fractured especially in zones where it encounters groundwater. Detailed explanations of the model are given in Sections D-5.3.3 and D-5.3.4. A summary of the analysis is given in Table D-102.

D-5.3.2 Background

Definitions and examples. Intrusive igneous rock masses are created when magma or molten rock is injected into crustal rock below the surface, as opposed to extrusives, which erupt at the surface. Some intrusive bodies may be the result of extreme metamorphism and partial

TABLE D-102
SUMMARY OF IGNEOUS INTRUSIVE FAILURE ELEMENT

MEDIUM	PROBABILISTIC (P) DETERMINISTIC (D)	NATURE OF MODEL	RELEASE MODE	DRIVING FORCE	SOURCE TERM	PARAMETERS		RELEASE MODELING STEPS	COMMENTS
						1st ESTIMATE	2nd ESTIMATE		
Bedded Salt	P	Annual probability of occurrence.	Groundwater	Physical transport of wastes by magma to upper aquifer.	Waste material intersected by magma.	$\lambda = 2 \times 10^{-10}$ Dimensions of dike: 1 m x 4 km, intersecting 0.05% waste inventory.	$\lambda = 4 \times 10^{-8}$ Dimensions of dike: 1 m x 4 km, intersecting 0.05% waste inventory.	Material moved to aquifer and subject to leaching. Leach characteristics of waste form assumed unchanged, although canisters would be removed.	Probabilities determined as 1% of values for faulting.
Granite	P	Annual probability of occurrence.	Groundwater	Physical transport of wastes by magma to upper aquifer.	Waste material intersected by magma.	$\lambda = 2 \times 10^{-10}$ Dimensions of dike: 1 m x 4 km, intersecting 0.05% waste inventory.	$\lambda = 10^{-7}$ Dimensions of dike: 1 m x 4 km, intersecting 0.05% waste inventory.	Material moved to aquifer and subject to leaching. Leach characteristics of waste form assumed unchanged, although canisters would be removed.	Probabilities determined as 1% of values for faulting.
Basalt	P	Annual probability of occurrence.	Groundwater	Physical transport of wastes by magma to upper aquifer.	Waste material intersected by magma.	$\lambda = 6 \times 10^{-8}$ Dimensions of dike: 1 m x 4 km, intersecting 0.05% waste inventory.	$\lambda = 10^{-7}$ Dimensions of dike: 1 m x 4 km, intersecting 0.05% waste inventory.	Material moved to aquifer and subject to leaching. Leach characteristics of waste form assumed unchanged, although canisters would be removed.	Probabilities determined as 1% of values for faulting.
Shale	P	Annual probability of occurrence.	Groundwater	Physical transport of wastes by magma to upper aquifer.	Waste material intersected by magma.	$\lambda = 2 \times 10^{-10}$ Dimensions of dike: 1 m x 4 km, intersecting 0.05% waste inventory.	$\lambda = 4 \times 10^{-9}$ Dimensions of dike: 1 m x 4 km, intersecting 0.05% waste inventory.	Material moved to aquifer and subject to leaching. Leach characteristics of waste form assumed unchanged, although canisters would be removed.	Probabilities determined as 1% of values for faulting.
Dome Salt	P	Annual probability of occurrence.	Groundwater	Physical transport of wastes by magma to upper aquifer.	Waste material intersected by magma.	$\lambda = 3 \times 10^{-8}$ Dimensions of dike: 1 m x 4 km, intersecting 0.05% waste inventory.	$\lambda = 5 \times 10^{-7}$ Dimensions of dike: 1 m x 4 km, intersecting 0.05% waste inventory.	Material moved to aquifer and subject to leaching. Leach characteristics of waste form assumed unchanged, although canisters would be removed.	Probabilities determined as 1% of values for faulting.

melting of older rock, and therefore are not truly igneous. However, this distinction is not important for the purpose of generic modeling, and so, for the sake of simplicity, all intrusives will be regarded as igneous throughout the discussion.

Intrusives may be classified according to a number of features, including size, orientation, and petrography. The most important classifications are discussed here and illustrated in Figure D-36 (Section D-5.2). The generic term, pluton, refers to any intrusive igneous rock body, independent of structure or mode of emplacement. Sills are planar and parallel to rock strata or contacts. Dikes are also roughly planar, but they cut across strata. Laccoliths can be described as very thick sills that cause doming of the overlying rock. Stocks are vertical masses, roughly round in cross section, that pierce the country rock. Batholiths are very large stocks, apparently formed at considerable depths.

Plutons may intrude any rock: sedimentary, igneous, or metamorphic; and they may have any igneous petrography. Examples are found of both acid and basic rocks forming all types of intrusive structures. Usually, however, magmas of low viscosity tend to form dikes and sills while those of higher viscosity form the thicker laccoliths and stocks. Batholiths are most often granitic in composition, apparently the result of melting of older continental rocks. Local stresses at the time of emplacement may also affect the morphology of intrusives; high vertical stresses favor the formation of dikes and other discordant bodies, and low vertical stresses favor the formation of sills.

Effects on country rock. The viscosity, temperature, and chemistry of the magma influence the range of effects accompanying intrusion. Forcible injection tends to break free pieces of the surrounding rock, incorporating these rock fragments in the intrusive mass as xenoliths. Intrusion often produces secondary fracturing of the country rock. These fractures are typically, but not always, filled by the fluid magma. The temperature differential between the hot magma and the cool invaded rock may produce a zone of chilling in the intrusive and heating in the country rock, creating local areas of metastable minerals as the rocks pass rapidly through the stable temperatures for such minerals. Chemical alteration (metasomatism) of both magmatic and country rock occurs where water and other volatiles in one or both rocks react in the vicinity of the intrusive contact. The term "contact metamorphism" is used to describe the change in the mineralogy or fabric of the original rock as a result of the intrusion. The area of contact metamorphism may be extensive and contain a variety of economic minerals, depending, of course, on the composition of the intrusive and the accompanying fluids.

The sizes and extent of intrusives can vary widely. Some sills and dikes have dimensions reported in centimeters, while others extend for many kilometers and are many meters thick.(58,122,123) Classic examples of the latter are the Palisades sill along the Hudson River, the dikes near Shiprock, Arizona, and the dike swarms across Scotland and England.(123,124,125) Batholiths, such as the Idaho batholith, have areas on the order of 100 km^2 or larger, while stocks are smaller.(58,126)

Intrusives are frequently associated with volcanism, as evidenced by the numerous sills and dikes radiating from or concentric to volcanic vents. However, not all intrusives show this relationship, although the relationship can also be obliterated by subsequent erosion.(60)

Depth of igneous emplacement also varies over a wide range. Some plutons, particularly those associated with volcanism, may have been emplaced very near the surface. Others cooled slowly and at depths of several kilometers, as indicated by their minerals and their crystal size.(122) As the distance from the magma source increases, plutonic intrusion clearly becomes less likely.

Detection of intrusives. Intrusives are most generally identified through field surveys by stratigraphic and petrographic comparison with surrounding rock. These basic techniques may be supplemented by drilling and geophysical investigations of magnetic and gravitational anomalies. Intrusives often differ markedly in magnetic properties and density from many sedimentary rocks and may be readily detected in some situations. The geologic history of plutons near a repository site gives some indication of the potential for future activity. Furthermore, current magmatic activity near a repository site may be detected through geothermal heat flow measurements. In general, heat gradients across the United States indicate that, except for a very few locations, rock melting is not likely within several kilometers of the surface.(119)

Measurement of surface rise or ground tilt may also be used to interpret magmatic movements at depth.(127) However, to maintain a conservative approach and because rates of magmatic movement are too poorly understood, the potential advantage of geothermal or geophysical surveys is not considered in the present model.

D-5.3.3 Igneous Intrusive Failure Model

The model developed for igneous intrusions is analogous to that used for faulting in that it requires:

- the probability of new intrusions intersecting a repository; and
- the physical parameters to describe transport of waste by an intrusive.

The actual formation of intrusives has seldom, if ever, been witnessed, although some have been inferred near volcanic centers. Only a few investigators have reported the number, size, and spacing of plutons in different regions.(122,127) Therefore, an approach using areal densities and ages of plutons to establish the probability of their occurrence is difficult to apply. Many plutons apparently form at considerable depths, suggesting that the number reaching a relatively shallow repository would be far fewer than indicated by a count of plutons visible at the surface after extensive uplift and erosion. For example, in one study of a granitic region, dikes were reported at the rate of three per linear mile, or approximately 10 per square kilometer.(122) However, as they had been emplaced roughly 6.5 kilometers below the surface, it is clear that extrapolation to establish representative probabilities for intrusions into a shallow formation would be of questionable validity.

Alternatively, the argument has been made that the rate of intrusion is a fraction of the rate of faulting, since most intrusives apparently fill faults or joints, while many faults or joints have no associated intrusives.(12) Conditions are envisioned similar to those for normal faulting, where vertical stress is greater than horizontal stress. Vertical faults could form, intersecting the repository and admitting magma in the form of dikes. The magma could then carry the waste to the upper aquifer. Horizontal flows of magma through a repository are considered less important since they would not carry waste to the aquifers or nearer to the surface.

Very limited data permit only a rough estimate of the ratio of dikes to faults. Further analysis based on geophysical considerations may be possible for a particular region. However, to be consistent with estimates proposed in similar studies,(12) the present model assumes that dikes are one percent as frequent as faults. The probability of an igneous intrusion disrupting the repository is thus estimated to be 10^{-2} times the rate of faulting for the geologic medium, as determined in Section D-5.1.

D-5.3.4 Igneous Intrusive Release Model

The dimensions of an intersecting dike are used to determine the fraction of stored waste transported to the aquifer by the molten rock. For the sake of conservatism, it is assumed that a dike would cut the repository across its longest dimension. For a repository of 8 km^2 with sides of 2 km and 4 km, the dike would be 4 km long. The thickness of the dike is assumed to be 1 meter.(122) The dike would then intersect 0.05% of the repository. Also for conservatism, it is assumed that this entire fraction is carried to the overlying aquifer and is not sealed into the matrix of the dike. Because this transport mechanism assumes immediate introduction of the waste into the aquifer, the contribution of groundwater flow along the contact is insignificant by comparison and may be neglected. Furthermore, it is likely that this boundary will be resealed by melting of the country rock.

This model is independent of the host rock. Accordingly, the same parameters apply for all media discussed in this study.

D-5.3.5 Literature Discussion

Igneous intrusives have been modeled as possible failure mechanisms in several other studies, which are mentioned below. Most of these studies have not identified igneous intrusion as a separate failure mechanism, but as a variation of volcanism.(3,10,50,128) Two sources distinguish between extrusive and intrusive magmatic activity, citing the additional requirement of groundwater to transport waste after magmatic intrusion as the main distinction.(12,128) These studies also discuss qualitatively the effects of concentrated geothermal heat on the natural groundwater regime and possible local perturbations in flow. Only one study develops a failure rate for intrusives,(12) and this is the basis for the approach used here.

D.5.4 METEORITE IMPACT

D-5.4.1 Summary

The impact of a large meteorite could cause a breach of the repository either by directly releasing material to the air or land surface or by fracturing the surrounding rock, thereby permitting greater groundwater access. Meteorites large enough to create such breaches are very uncommon. Furthermore, the potential hazard associated with repository releases would appear to be negligible compared with the possible effects on surface installations, the environment, and the surrounding population. Therefore, the following discussion is more abbreviated than that for most other failure elements. A summary of the parameters used to characterize this failure element is given in Table D-103.

D-5.4.2 Background

In the history and evolution of the solar system, meteorites have been very common, representing a process that has had measurable effects on the planets and their satellites. Indeed, it has been theorized that some meteorites over 1000 km in diameter may be responsible for variations in the thickness of the crust on the earth and the moon.(129) From observations of cratering history on the inner planets and their satellites and by correlation with the ages of portions of their surfaces (e.g., by lunar rock samples), estimates have been made of meteorite fluxes since the formation of the solar system. Figure D-38 shows how this rate has slowed since the early period of the solar

TABLE D-103
SUMMARY OF METEORITE IMPACT FAILURE ELEMENT

MEDIUM	PROBABILISTIC (P) DETERMINISTIC (D)	NATURE OF MODEL	RELEASE MODE	DRIVING FORCE	SOURCE TERM	PARAMETERS		FLUID FLOW RATES FROM REPOSITORY TO UPPER AQUIFER				COMMENTS
						1st ESTIMATE	2nd ESTIMATE	1st ESTIMATE		2nd ESTIMATE		
								t (yrs)	$\dot{Q}$ (t) (m^3/yr)	t (yrs)	$\dot{Q}$ (t) (m^3/yr)	
Bedded Salt	P	Annual occurrence probability.	A. Land surface B. Groundwater	A. Impact B. Thermal convection added to aquifer interconnection gradient.	A. 0.1% repository inventory to surface. B. 20% cumulative leached nuclides released to groundwater. Continued leaching of broken canisters in fracture or breccia zone (10%) and surrounding canisters (10%).	λ = 4 x 10^{-11}/yr A = 0.8 km^2 K = 10^{-4} cm/sec η = 0.2	λ = 4 x 10^{-11}/yr A = 0.8 km^2 K = 10^{-4} cm/sec η = 0.2	100 1000 10,000	1.6 x 10^7 1.4 x 10^7 9.0 x 10^6	100 1000 10,000	7.8 x 10^7 7.8 x 10^7 6.7 x 10^7	Water availability may severely limit flows below levels calculated.
Granite	P	Annual occurrence probability.	A. Land surface B. Groundwater	A. Impact B. Thermal convection.	A. 0.1% repository inventory to surface. B. 20% cumulative leached nuclides released to groundwater. Continued leaching of broken canisters in fracture or breccia zone (10%) and surrounding canisters (10%).	λ = 4 x 10^{-11}/yr A = 0.8 km^2 K = 10^{-4} cm/sec η = 0.2	λ = 4 x 10^{-11}/yr A = 0.8 km^2 K = 10^{-4} cm/sec η = 0.2	100 1000 10,000	1.4 x 10^7 8.8 x 10^6 3.8 x 10^6	100 1000 10,000	1.4 x 10^7 8.8 x 10^6 3.8 x 10^6	Water availability may severely limit flows below levels calculated.
Basalt	P	Annual occurrence probability.	A. Land surface B. Groundwater	A. Impact B. Thermal convection added to aquifer interconnection gradient.	A. 0.1% repository inventory to surface. B. 20% cumulative leached nuclides released to groundwater. Continued leaching of broken canisters in fracture or breccia zone (10%) and surrounding canisters (10%).	λ = 4 x 10^{-11}/yr A = 0.8 km^2 K = 10^{-4} cm/sec η = 0.2	λ = 4 x 10^{-11}/yr A = 0.8 km^2 K = 10^{-4} cm/sec η = 0.2	100 1000 10,000	1.8 x 10^7 1.5 x 10^7 8.3 x 10^6	100 1000 10,000	7.9 x 10^7 7.7 x 10^7 6.8 x 10^7	Water availability may severely limit flows below levels calculated.

TABLE D-103
SUMMARY OF METEORITE IMPACT FAILURE ELEMENT (CONTINUED)

MEDIUM	PROBABILISTIC (P) DETERMINISTIC (D)	NATURE OF MODEL	RELEASE MODE	DRIVING FORCE	SOURCE TERM	PARAMETERS		FLUID FLOW RATES FROM REPOSITORY TO UPPER AQUIFER				COMMENTS
						1st ESTIMATE	2nd ESTIMATE	1st ESTIMATE		2nd ESTIMATE		
								t (yrs)	$\dot{Q}$ (t) (m^3/yr)	t (yrs)	$\dot{Q}$ (t) (m^3/yr)	
Shale	P	Annual occurrence probability.	A. Land surface B. Groundwater	A. Impact B. Thermal convection added to aquifer interconnection gradient.	A. 0.1% repository inventory to surface. B. 20% cumulative leached nuclides released to groundwater. Continued leaching of broken canisters in fracture or breccia zone (10%) and surrounding canisters (10%).	$\lambda = 4 \times 10^{-11}$/yr $A = 0.8$ km^2 $K = 10^{-4}$ cm/sec $n = 0.2$	$\lambda = 4 \times 10^{-11}$/yr $A = 0.8$ km^2 $K = 10^{-4}$ cm/sec $q = 0.2$	100 1000 10,000	1.8×10^7 1.5×10^7 6.3×10^6	100 1000 10,000	7.9×10^7 7.7×10^7 6.8×10^7	Water availability may severely limit flows below levels calculated.
Dome Salt	P	Annual occurrence probability.	A. Land surface B. Groundwater	A. Impact B. Thermal convection added to aquifer interconnection gradient.	A. 0.1% repository inventory to surface. B. 20% cumulative leached nuclides released to groundwater. Continued leaching of broken canisters in fracture or breccia zone (10%) and surrounding canisters (10%).	$\lambda = 4 \times 10^{-11}$/yr $A = 0.8$ km^2 $K = 10^{-4}$ cm/sec $n = 0.2$	$\lambda = 4 \times 10^{-11}$/yr $A = 0.8$ km^2 $K = 10^{-4}$ cm/sec $q = 0.2$	100 1000 10,000	1.8×10^7 1.0×10^7 5.0×10^6	100 1000 10,000	4.0×10^7 3.4×10^7 2.8×10^7	Water availability may severely limit flows below levels calculated. Aquifer interconnection established by fracture zone at edge of salt dome.

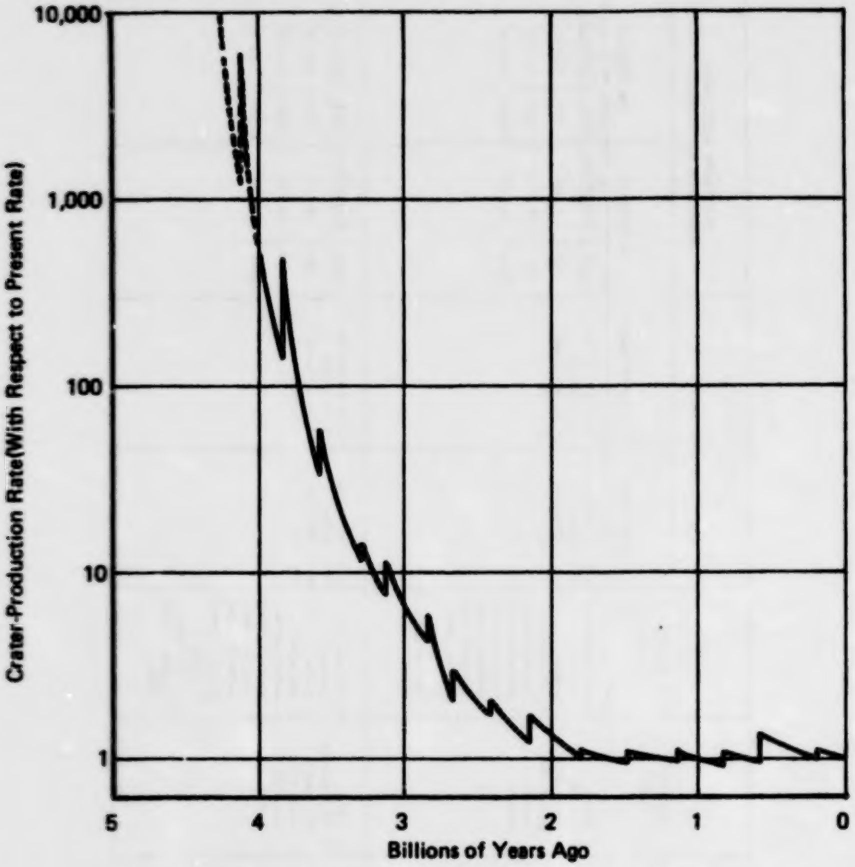

Note: Graph is for lunar cratering but it is representative for inner planets.

Source: Hartmann, W.K., Cratering in the Solar System. Scientific American 236:84, January 1972.

FIGURE D–38 RELATIVE CRATER PRODUCTION RATE WITH SOLAR SYSTEM EVOLUTION system, when interplanetary debris was rapidly being removed by the gravitational attraction of the planets. The rate appears to have been roughly constant for the last two billion years.

Meteorite impacts have been much more common on earth than may generally be realized. The surface geology of the earth is so active that even very large craters are eroded or buried with time. Table D-104 lists all proven or probable impact craters in the United States with diameters of at least one kilometer. Proven structures involve meteorite remnants, and probable structures are determined from evidence of shock metamorphism. Many other possible impact craters have also been identified.(130) The list of impact craters worldwide includes a number over 100 km in diameter. Figure D-39 is a map of proven and probable impact craters. The highly non-uniform spatial distribution can be attributed to the varying geologic stability of different regions as well as to differences in the degree to which areas have been investigated for craters.

The rate of cratering, by size, has been studied rather carefully because comparison of this rate with actual counts of detectable features yields information on the history and evolution of a planet and its surface. For craters at least 1 km in diameter, the frequency of occurrence appears to be roughly inversely proportional to the square of the diameter. This rule has both an empirical and a theoretical justification.(130,131) Calibrating with data from well studied stable regions of the earth, a cratering production rate, ϕ, has been determined to be given by the equation(131)

$$\log_{10} \phi = -11.85 - 2 \log_{10} D.$$

Here D is crater diameter in km and ϕ is the number of craters per square kilometer per year at least as large as D. In particular, for $D = 1$ km, $\phi = 1.4 \times 10^{-12}$. This means that for a land surface of 7.8×10^6 km^2, the area of the 48 coterminous states, there should be about 1.1×10^{-5} falls per year of meteorites capable of creating craters at least 1 km in diameter. The mean time between such occurrences is the reciprocal of this rate, or about 90,000 years. It should be noted that $D=1$ is near the lower limit of applicability of the given formula, but

TABLE D-104

PROVEN OR PROBABLE LARGE METEORITE IMPACT CRATERS IN THE UNITED STATES

Location	**Diameter** (km)	**Age** (millions of years)
Barringer, Arizona	1.2	0.025
Crooked Creek, Missouri	5.6	320 ± 80
Decaturville, Missouri	6	300
Flynn Creek, Tennessee	3.8	360 ± 20
Kentland, Indiana	13	300
Manson, Iowa	32	70
Middlesboro, Kentucky	6	300
Redwing Ck., N. Dakota	9	200
Serpent Mound, Ohio	6.4	300
Sierra Madera, Texas	13	100
Wells Ck., Tennessee	14	200 + 100

Source: Grieve, R.A.F. and P.B. Robertson. The Terrestrial Cratering Record. Icarus 38:212, 1979.

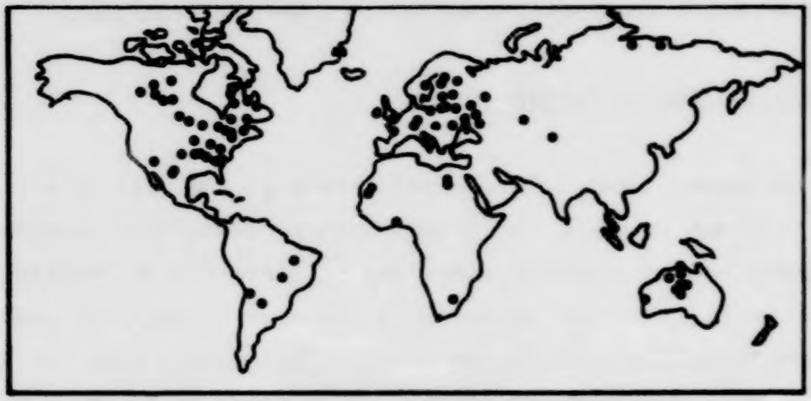

Source: Hughes, D.W. Earth's Cratering Rate. Nature 281:11, September 6, 1979. Based on: Grieve, R.A.F. and P.B. Robertson. The Terrestrial Cratering Record. Icarus 38:212, 1979.

FIGURE D–39 DISTRIBUTION OF IMPACT CRATERS

for present purposes, where the emphasis is on orders of magnitude, the formula suffices.

The geometry of craters is relevant in determining their effect on a nuclear waste repository. There are simple bowl-like craters, as well as ones with complex structures, including ringed ridges and peaks in the interior and depressed sections along the boundaries. Craters up to about 4 km in diameter in crystalline rock and 2-3 km in sedimentary strata are usually simple, while larger ones have complex structures. A schematic representation of a simple crater, shown in Figure D-40, forms the basis for the analysis in this section. For a repository about 500 m deep, as in the generic models, a crater diameter of at least 1 km is a reasonable cutoff for defining meteorite events of interest.

D-5.4.3 Meteorite Impact Failure Model

The failure model concentrates on meteorites giving rise to craters of diameter 1-2 km because the frequency of meteorite cratering decreases rapidly with increasing size, and the larger size impacts are even more likely to cause widespread environmental effects of greater importance than breaching a waste repository. The target area has been taken to be 24 km^2, corresponding to the repository area (2 km x 4 km) and a one-kilometer wide buffer zone around it. The failure element consists of the center of the crater lying within this area. Using the production rate of $\phi = 1.4 \times 10^{-12}$ per km^2 per yr for craters of diameters at least 1 km, the annual failure rate is given by

$$\lambda = 1.4 \times 10^{-12} \times 24$$

$$= 3 \times 10^{-11} \text{ events per year.}$$

This rate is assumed to be independent of the host rock formation, since variations in geophysical properties are not significant for the purposes of these rough calculations. Moreover, there are no distinct first and second estimates in this case, since this is a statistically derived estimate and is independent of location.

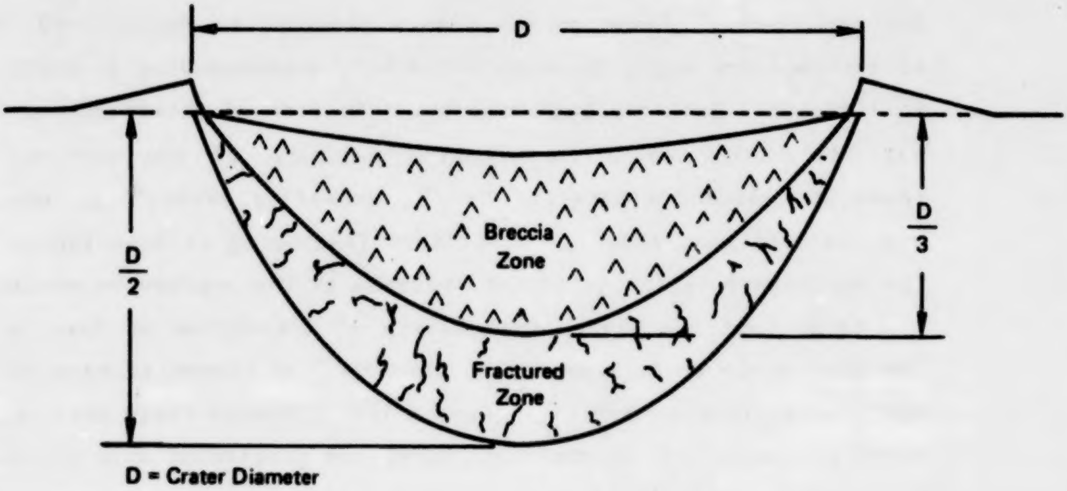

Source: Adapted from Innes, M.J.S. The Use of Gravity Methods to Study the Underground Structure and Impact Energy of Meteorite Craters. J. Geophysical Research, 66 (7), July 1971.

FIGURE D–40 SIMPLIFIED CRATER GEOMETRY

D-5.4.4 Meteorite Impact Release Model

A meteorite impact crater formed on the repository site would be expected to be smaller than the repository, since crater sizes are biased toward the lower end of the range under consideration. A crater of 1-km diameter would have a cross-sectional area at the surface of 0.8 km^2.

The breccia zone would not even reach 500 m in depth, and the fracture zone at that depth would be very small. (See Figure D-40.) For a crater with a diameter of 2 km, the breccia zone would intersect the repository. Based on the simple geometry in Figure D-40, the area of intersection would be roughly 0.8 km^2, corresponding to a circle 1 km in diameter. For modeling purposes, this area of intersection, 0.8 km^2, has been taken as a conservative estimate of the portion of the repository directly affected by the meteorite event. It has further been assumed that there is sufficient fracturing or brecciation down to the repository depth for direct releases to the surface to occur.

Because of the higher probability of meteorites at the low end of the size scale being considered, the expected direct release to the air and land surface is probably very small. Although there does not appear to be an analytical or empirical model for predicting this event, it has been assumed that 1% of the wastes in the affected zone (i.e., 0.1% of the repository inventory) would be released to the land surface. The remaining wastes are subject to enhanced leaching by groundwater because of permeability increases in the surrounding rock. The hydrologic parameters assumed for this pathway are:

$$K = 10^{-4} \text{ cm/sec}$$

$$n = 0.2$$

and the cross-sectional area is again $A = 0.8$ km^2. Flows through this zone can be calculated analogously to Section D-5.1.4 on fault pathways, and in other sections. In particular, Darcy's Law is applied with the hydraulic gradients given in Table D-105. The corresponding fluid flow rates are given in Table D-106. These would very likely be restricted well below the calculated values because of limitations on the amount of water present.

TABLE D-105

EFFECTIVE HYDRAULIC GRADIENT IN EXTENDED VERTICAL PATHWAYS

	100 years*	1000 years	10,000 years
Bedded Salt			
First Estimate	0.13	0.11	0.04
Second Estimate	0.62	0.60	0.53
Granite			
First Estimate	0.11	0.07	0.03
Second Estimate	0.11	0.07	0.03
Basalt			
First Estimate	0.14	0.12	0.05
Second Estimate	0.63	0.61	0.54
Shale			
First Estimate	0.14	0.12	0.05
Second Estimate	0.63	0.61	0.54
Dome Salt			
First Estimate	0.13	0.08	0.04
Second Estimate	0.32	0.27	0.23

*Years after repository closure.

TABLE D-106

VOLUMETRIC FLOW RATES THROUGH METEORITE INDUCED PERMEABLE ZONE

	Volumetric Flow $\dot{Q}$ (m^3/yr)		
	100 years*	1000 years	10,000 years
Bedded Salt			
First Estimate	1.6×10^7	1.4×10^7	5.0×10^6
Second Estimate	7.8×10^7	7.6×10^7	6.7×10^7
Granite			
First Estimate	1.4×10^7	8.8×10^6	3.8×10^6
Second Estimate	1.4×10^7	8.8×10^6	3.8×10^6
Basalt			
First Estimate	1.8×10^7	1.5×10^7	6.3×10^6
Second Estimate	7.9×10^7	7.7×10^7	6.8×10^7
Shale			
First Estimate	1.8×10^7	1.5×10^7	6.3×10^6
Second Estimate	7.9×10^7	7.7×10^7	6.8×10^7
Dome Salt			
First Estimate	1.6×10^7	1.0×10^7	5.0×10^6
Second Estimate	4.0×10^7	3.4×10^7	2.9×10^7

*Years after repository closure.

The source term for the groundwater release has several components. First, radionuclides that may have leached out into any water in the repository before the meteorite event would be able to move with that water up through the permeable pathway. Second, canisters in the affected zone of the repository would probably be broken up and subject to direct leaching after the event. Third, canisters in other portions of the repository could also continue to contribute leached radionuclides to the water in the repository. These radionuclides could gradually migrate through the backfilled tunnels and drifts to the actual release pathway. The third effect is expected to be the least important by far, and so it has not been modeled. To account in a conservative and simple way for the other source terms, it can be assumed that the cumulative leached radionuclides from 20% of the repository are released into the pathway at the time of the breach, and that thereafter 20% of the repository is subject to continuous leaching in the groundwater flows calculated.

D-5.4.5 Literature Discussion

Various estimates for the likelihood of a meteorite breaching the repository are found in the literature. The Swedish KBS study(26) cites a rate

$$\lambda = 10^{-13} \text{ per km}^2 \text{ per year}$$

for craters at least 100 meters deep, and on this basis dismisses this failure element. The NRC/Sandia study(12) uses the rate

$$\lambda = 2 \times 10^{-13} \text{ per repository per year}$$

for impacts on an area of 8 km^2, a value attributed to Claiborne and Gera. These latter authors assume a reference crater at least 2 kilometers in diameter.(3) The University of New Mexico study(10) for the EPA suggested a rate

$$\lambda = 1 \times 10^{-13} \text{ per repository per year}$$

for a 10-km^2 repository. A source term for consequence calculations was given in this last study as 5% of the repository inventory to the air and 5% to the land surface.

D-5.5 BRECCIA PIPES

D-5.5.1 Summary

Deep dissolution processes in bedded salt deposits can lead to the development of brine-filled cavities on the lower sides of the formations. These cavities, after reaching a certain critical size, can cause the collapse of the overlying rock and the propagation of a chimney of broken rock up to or toward the surface.(22,132,133) Such a chimney structure is called a breccia pipe. It provides a permeable pathway through which groundwater can flow and leach radionuclides from the waste canisters. The model described here assumes that breccia pipes develop at a constant annual rate, except that none can breach the repository for the first 500 years after sealing because their incipient development would be detected during site investigations. Fluid flows are assumed to be upward, with release of radionuclides to the upper aquifer. Significant dissolution of the salt formation around the breccia pipe is assumed not to occur, based on qualitative considerations of water availability and degree of salt saturation, but healing of the column by cementation and recrystallization is also not assumed. A summary of the analysis is given in Table D-107.

D-5.5.2 Background

Salt is a very soluble mineral, and every salt deposit shows geologic or topographic features associated with various dissolution phenomena. The Delaware Basin in New Mexico contains massive salt beds, for example, but it has been estimated that this represents only about half of the salt originally deposited there.(133) In fact, essentially all the salt in the Rustler Formation in that basin has been leached out. Saline groundwater, springs, or streams associated with most salt basins are further indications of continuing dissolution.

TABLE D-107
SUMMARY OF BRECCIA PIPE FAILURE ELEMENT

MEDIUM	PROBABILISTIC (P) DETERMINISTIC (D)	NATURE OF MODEL	RELEASE MODE	DRIVING FORCE	SOURCE TERM	PARAMETERS		FLUID FLOW RATES FROM REPOSITORY TO UPPER AQUIFER				COMMENTS
						1st ESTIMATE	2nd ESTIMATE	1st ESTIMATE		2nd ESTIMATE		
								t (yrs)	$\dot{Q}$ (m^3/yr)	t (yrs)	$\dot{Q}$ (m^3/yr)	
Bedded Salt	P	Annual occurrence probability.	Upper aquifer	Thermally induced convection and aquifer interconnection.	Canisters in breccia pipe assumed to be broken and subject to leaching.	λ = 0 for $t < 500$ yrs λ = 10^{-6}/yr for $t \geq 500$ yrs K = 10^{-2} cm/sec η = 0.2 A = 3×10^4 m^2	λ = 0 for $t < 500$ yrs λ = 10^{-6}/yr for $t \geq 500$ yrs K = 10^{-2} cm/sec η = 0.2 A = 3×10^4 m^2	500 1000 10,000	6×10^7 5×10^7 2×10^7	500 1000 10,000	3×10^8 3×10^8 3×10^8	Limited availability of water from lower aquifer expected to significantly restrict flows below levels calculated.
Granite		N.A.										
Basalt		N.A.										
Shale		N.A.										
Dome Salt		N.A.										

Because salt deposits can be massive (tens to hundreds of meters thick, with some interbeds) and nearby groundwater flows may be relatively low, dissolution may be an extremely slow process. In fact, because salt is practically impermeable to the movement of water, dissolution generally takes place only at the boundaries of the deposits. Slow average rates of dissolution would not lead to breaches of the repository for tens or hundreds of millions of years.(134) However, there are certain localized dissolution features that result from much higher than average rates of salt removal. These features are generally caused by the collapse of the overlying rocks into cavities or voids in the soluble rocks below. Depending on the size and other characteristics of these collapse structures, they are known by a variety of names: kettles, sinks, swales, collapse chimneys, and breccia pipes. The last two terms are used to denote structures that originate near the bottom of soluble strata and extend toward the surface, being somewhat taller than they are wide and filled with rubble (breccia) from the overlying rock. Although the term "breccia pipe" is also used to describe a distinct geologic structure of volcanic origin, some early investigators of the dissolution phenomenon have used the term to indicate collapse features with considerable vertical extent, and this meaning is adopted here.

Physical Characteristics. Breccia pipes are roughly circular features from a few tens of meters to more than 0.5 kilometer in diameter, with an average depth three times the diameter.(132) The upper portions are filled with broken rock ranging from small granulars to blocks a meter or more across. (See Figure D-41.) These features have usually been recognized only when they have reached the surface, and limited tests have suggested that the pipes bottom near the lower margin of the salt strata.(133) Only a few not reaching the surface are reported in the literature, although it is possible that many remain undiscovered.

Sometimes, breccia pipes are seen as domes or topographic highs, contrary to the general expectation for a collapse feature. One hypothesis suggested to account for this structure is that dissolution of the surrounding salt has lowered the elevation of the area below the more resistant brecciated column. This process is enhanced by anhydrite

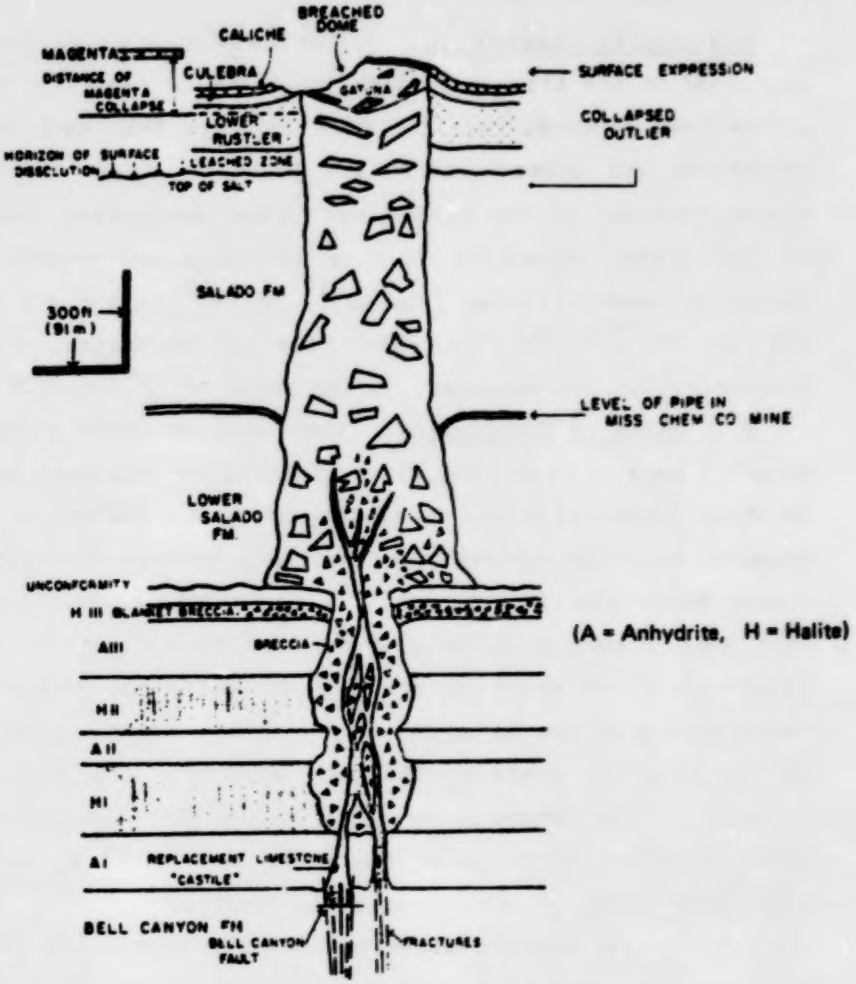

Source: Adapted from Anderson, R.Y. Report to Sandia Laboratories on Deep Dissolution of Salt, Northern Delaware Basin, New Mexico, April 1978.

FIGURE D–41 CONCEPTUAL DRAWING OF BRECCIA PIPE IN DELAWARE BASIN

in the breccia reacting with available water and catalyzed by bacterial or organic processes to form calcite, which may be more resistant to dissolution.(133,135)

Hydrologic properties. Relatively few measurements have been performed on the breccia filling the pipes to ascertain their hydrologic properties. However, existing data indicate that very broad spectra of porosities and permeabilities are possible. Pipes within the Carlsbad mining district in New Mexico have shown properties ranging from those of the intact evaporite section to those of typical gravels, with hydraulic conductivities from 10^{-10} to 10^{-3} cm/sec and porosities from 20% to 1%.(104,133) At the time of formation, higher hydraulic conductivities are expected, in the range of 10^{-3} to 1.0 cm/sec.(132)

Mechanisms of dissolution. When salt or other soluble material is attacked by a solvent, the shape of the dissolved void and the direction in which dissolution progresses depend upon a number of conditions. For example, water in contact with the upper surface of a salt mass tends to spread laterally. In the case of water reaching the lower boundary of a salt mass, dissolution is upward, forming a vertical cavity, provided relatively fresh water is supplied and brine is removed at the bottom. These phenomena can be explained in terms of brine density. (See Figure D-42.) Water in contact with salt dissolves the salt until it nears saturation. The saturated brine is denser than undersaturated water and tends to sink. If it is at the upper salt surface, the brine forms a stratified layer at the interface, inhibiting further dissolution. On the other hand, water dissolving the salt from below becomes saturated with salt and sinks away, to be replaced with fresher water, promoting further dissolution. This latter situation sets a convection cell into motion (driven by density differences), and the rate of convection can be expected to increase as the water density differences are more pronounced. Initially, the cavity thus formed at the bottom of the salt is not large and is able to support itself. However, if dissolution continues, the cavity may reach a critical size, become unable to support the overburden, and collapse.

Implicit in this explanation for a dissolution mechanism developing a vertical cavity is the need for sufficient hydraulic head to raise the underlying water to the salt layer. Furthermore, fresh water must be

(a) **Dissolution from above. Denser brine accumulates and spreads out along top of salt formation. Saturation limits further dissolution.**

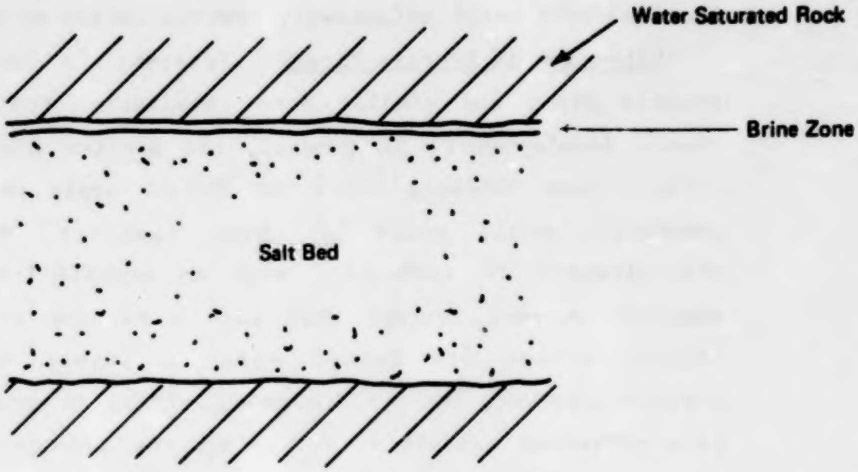

(b) **Dissolution from below. Density difference between brine and fresh water leads to convection cell and transport of salt away by lower aquifer.**

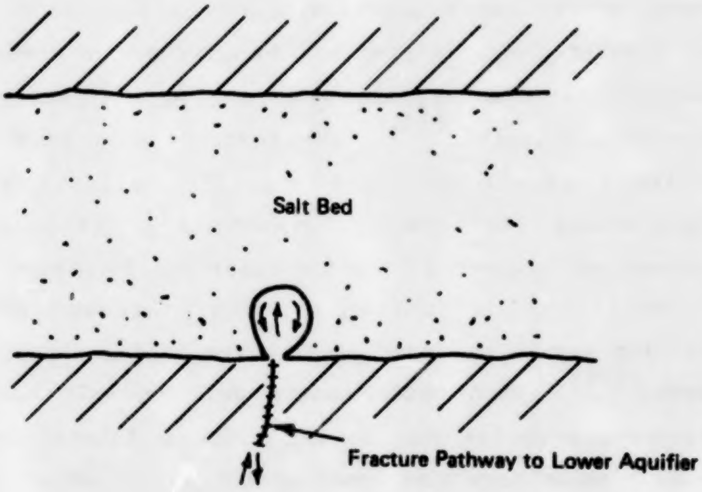

FIGURE D–42 CHARACTERISTICS OF DISSOLUTION FROM ABOVE AND BELOW SALT FORMATION supplied and saturated brine removed if dissolution is to continue at any appreciable rate. Thus, an impermeable barrier separating the water from the salt could effectively prevent cavity growth or propagation.

Detection of Breccia Pipes. Interest in detecting and surveying breccia pipes and similar deep dissolution features is a relatively recent development. In general, the earlier discussions of detection methods (see Sections D-5.2 and D-5.1) apply to breccia pipes. The generally small scale of these features, however, limits the effectiveness of techniques such as gravitational, resistivity, and magnetic surveys, except when such a feature is suspected. Seismic investigations are better able to detect collapse structures, particularly when the breccia or other filling material is characterized by a different seismic velocity than the surrounding rock, or when the collapse has disrupted a distinctive marker bed. The difficulties presented by seismic work are typically related to the area that can be investigated within an actual exploration program, and to resolution loss with depth, which may limit interpretation of seismic records. This is particularly true when attempting to detect breccia pipes in the early stages of formation.(22)

Finding breccia pipes within a large area may most easily be accomplished through the use of aerial or Landsat photographs.(135) Domes, sinks, and other topographic relief can be located and selected for further investigation on the ground. A number of pipes have been detected in this way, and sites for more intensive seismic exploration have been selected.(104) The features seen on photographs are not all collapse structures, and not all collapse structures are deep dissolution features. Nevertheless, many apparent dissolution depressions suggest a location deserving further study.

Of all the detection methods discussed previously, radar and drilling may be the most precise for confirming the presence of breccia pipes.(132) Since radar works well in salt and could be used from exploratory shafts and tunnels, it is likely that scanning the rock below a repository site could detect any dissolution cavity in its early stages. The reported effective range of radar is in excess of the salt thickness in the generic repository model. Proponents of radar have suggested that targets as small as a drill pipe can be detected at hundreds of meters; therefore, it is likely that natural brine-filled cavities of a similar size could be discovered at a lesser range.

Drilling, while not an efficient method for detecting collapse structures, may sometimes be necessary to confirm the indications of radar or other detection methods. Drilling into a selected target would confirm the existence of a breccia pipe and could be used to test the structural and hydrologic conditions of the feature.

D-5.5.3 Breccia Pipe Failure Model

The failure model for a breccia pipe consists of estimates of hydrologic properties and probabilities of occurrence. As noted earlier, bedded salt is the only medium to which this failure element applies.

Probability of occurrence. The probability of occurrence of a breccia pipe on the repository site is specified in terms of a constant annual rate, λ, after an initial period of 500 years during which the probability is 0. An initial period of zero probability results from the fact that it takes some time for a critical cavity to develop, and if one were already at a significant stage of growth at the time the repository was sealed, then it would have been detected by geophysical techniques, such as radar, operating from the mine. The time required for critical cavity growth is probably much larger than 500 years,(132) but this conservative value has been adopted to account for the probability of waste (heat) induced acceleration of dissolutioning. The values adopted are as follows:

First Estimate: $\lambda = 10^{-8}$ events/year/repository
for $t \geq 500$ years

Second Estimate: $\lambda = 10^{-6}$ events/year/repository
for $t \geq 500$ years

The second estimate will be discussed first because the first estimate was derived from it. It comes from previous studies(11,132) and has been normalized here to account for a different repository area. The method used to derive this estimate can be briefly summarized as follows. Information on areal densities of possible breccia pipes in several evaporite basins was collected from the literature and from the study of aerial photographs. The volumetric rate of salt removal via deep dissolution was then estimated, based on the time period during which this dissolution has been occuring. By comparing this rate with estimates of critical cavity size necessary for chimney initiation and propagation at least to an upper aquifer, estimates of the rate of formation were calculated. These numbers are comparable to estimates developed in other more empirical surveys, based simply on the number of features, basin area, and time period of dissolution processes.(132,133,135) Field investigation to determine whether the features were deep seated was generally not carried out. While some shallow features are surely included in the counts, there are probably also deep features for which surficial indication was either not present or not recognized. In spite of these limitations and sources of error, the resulting rate still appears to be a reasonable "best estimate" based on available data. This number was adopted as the second estimate because it is assumed that the avoidance of features that could lead to deep dissolution will have high priority in the repository site selection process, and therefore a chosen site should be at least as good as a randomly chosen one. (This would be the case, for example, if the potential for deep dissolution is difficult to estimate for a particular site.) The first estimate assumes that the structures underlying a potential repository formation are simple and well mapped, and that any underlying aquifers are heavily saturated with salt, slow moving, at relatively low piezometric head, and well isolated from the host salt formation in the vicinity of the repository. It is believed that these conditions can be verified with sufficient certainty to reduce the occurrence rate by two orders of magnitude, which leads to the first estimate cited above.

Hydrologic processes. The following parameters have been chosen as representative of conditions in a newly formed breccia pipe

$K = 10^{-2}$ cm/sec (hydraulic conductivity)
$\eta = 0.2$ (effective porosity)
$A = 3 \times 10^{4}$ m^2 (cross-sectional area)

The hydraulic conductivity is the value recommended in Reference 11 and is in the range given in Reference 132. In fact, breccia pipes have a tendency to heal over time, due to recrystallization of salt and cementation of the broken pieces of rock. Since dissolution is also possible, depending on the available groundwater, healing has not been assumed for the present model. The values of porosity and cross-sectional area are also consistent with those in the literature.

D-5.5.4 Breccia Pipe Release Model

If a breccia pipe were to develop from underneath the repository, eventually part of the repository would either slump or fall into the chimney-like structure. Physical damage to the waste package would be expected in this process, since the rock itself is generally rather thoroughly broken. At this point the canisters would be subject to leaching by groundwater circulating from and back to an aquifer below the repository. The present model does not treat separately releases to the lower aquifer. Rather, since chimney growth propagates rapidly, it is assumed that a connection is established between upper and lower aquifers, and that water flows upward, driven by both an aquifer interconnection gradient and thermal buoyancy. The counterbalancing effect of increased density from salt dissolution is difficult to quantify; in the interest of bounding the flows, it has not been included. Significant additional dissolution could in fact lead to the leaching of a significant portion of the salt formation, and it is probable that some sections of salt deposits that are known to have been removed did so by this process. Nevertheless, field observation of recrystallized and cemented breccia pipes through salt formations suggests that in a carefully chosen site, this would be most unlikely. As has been mentioned in the previous section, no healing of the breccia pipe is assumed in the model.

Upward flows are calculated by Darcy's law using the parameters given in the previous section and the hydraulic gradients given in Table D-108. As in other sections, the version of Darcy's law here includes a factor of 5 to account for the lower viscosity of water at elevated temperatures. As was discussed in Section D-5.1.4, even as the temperatures in the repository decrease after the thermal peak, this factor does not appear to introduce excessive conservatism. Estimated volumetric flow rates and fluid velocities are summarized in Tables

TABLE D-108

EFFECTIVE VERTICAL HYDRAULIC GRADIENT IN A BRECCIA PIPE FROM THERMAL BUOYANCY AND AQUIFER INTERCONNECTION (BEDDED SALT REPOSITORY)

	Hydraulic Gradient (i)		
	500 years*	1000 years	10,000 years
Thermal Buoyancy			
First Estimate	0.11	0.10	0.03
Second Estimate	0.11	0.10	0.03
Aquifer Interconnection			
First Estimate	0.01	0.01	0.01
Second Estimate	0.50	0.50	0.50
Total			
First Estimate	0.12	0.11	0.04
Second Estimate	0.61	0.60	0.53

*Years after repository closure.

Source: First effect is from Appendix D-VI, interpolated to give values at 500 years. Second effect is from Chapter D-2.0 of this Report.

D-109 and D-110, respectively. It is important to note that, as in the case of faults, water limitations from the lower aquifer may significantly reduce these flows. Therefore, in a real site, aquifer capability may be the limiting factor, although it is not simply the lower aquifer closest to the repository that needs to be considered.

The canisters in the breccia pipe include about 0.4% of the repository inventory, based on the cross-sectional area given earlier, and these are subject to direct leaching. Furthermore, any radionuclides that had previously leached out of the waste packages would also be washed out with the groundwater flowing through the brecciated zone. It is assumed that an area with twice the diameter of the pipe itself is affected by this process, so that the cumulative leached inventory for 1.6% of the canisters should be assumed to be released to groundwater upon the occurrence of the failure element.

D-5.5.5 Literature Discussion

One model used in the literature has already been referred to in Section D-5.5.3. While there has been considerable recent geologic interest in learning more about the breccia pipe phenomenon, it does not appear that other models for their occurrence or consequences have yet been published.

D-5.6 OTHER NATURAL EVENTS AND PROCESSES

D-5.6.1 Introduction

In addition to the natural events and processes modeled earlier as specific failure elements, other processes could have some impact on the repository in a time frame much longer than the 10,000 year period used as the principal focus for this study. No location on earth is expected to be completely stable over very long periods (hundreds of millions of years or more). Parts of the Appalachian Mountains were once low-lying swamps, not unlike the Florida Everglades, and the Rocky Mountains also arose from what must have been warm shallow seas. Not only have

TABLE D-109

VOLUMETRIC FLOW RATES THROUGH A BRECCIA PIPE
(BEDDED SALT REPOSITORY)

	Volumetric Flow ($\dot{Q}$) (m^3/yr)		
	500 years*	1000 years	10,000 years
First Estiamte	6×10^7	5×10^7	2×10^7
Second Estimate	3×10^8	3×10^8	3×10^8

*Years after repository closure.

TABLE D-110

FLUID VELOCITIES THROUGH A BRECCIA PIPE
(BEDDED SALT REPOSITORY)

	Velocity (v) (m/yr)		
	500 years*	1000 years	10,000 years
First Estimate	1×10^4	9×10^3	3×10^3
Second Estimate	5×10^4	5×10^4	5×10^4

*Years after repository closure.

tectonic forces raised such mountains, but other forces have worn them down. The ancient Appalachians once had peaks reaching 4000 meters, roughly twice as high as at present. Some natural processes occur more rapidly than the growth and decay of mountains; for example, glaciers can come and go in a cycle of tens of thousands of years. The purpose of this section is to survey a range of natural events and processes that have not been modeled in detail in this study and to give some indication of the rates at which they occur.

D-5.6.2 Erosion

The most prevalent natural process on land is erosion. Gravity is the driving force, and wind, water, and ice provide the vehicles for rapid movement of rock and soil.

Fluvial erosion (erosion by water) is the most important process at work. No part of the United States is completely devoid of rainfall. Rain striking bare earth dislodges soil fragments and suspends them momentarily, moving them downhill with the general flow of water. When water is confined to a stream or river channel, its greater volume and velocity can move more and larger fragments greater distances. One of the most dramatic examples of fluvial erosion is the Grand Canyon of the Colorado River, which is roughly 20 kilometers wide and 1.6 kilometers deep. It was incised during the last two to ten million years, with an average rate of downcutting of 8×10^{-4} to 1.6×10^{-4} meters per year.(58,60) Although higher rates of erosion have been reported for brief periods for unconsolidated sediments, this erosion rate of the Colorado River is the highest for any major river system in the country, as indicated in Figure D-43. At its sustained rate, the Colorado River would require more than 500,000 years to strip away the overburden from a repository located directly below the canyon. Since long-term drainage patterns are fairly predictable, having remained largely unchanged for millions of years, it is unlikely that river erosion would be a serious concern for a repository even over a time span longer than that considered in this report.

Glaciers, which are moving masses of ice, can remove great quantities of rock and soil in a relatively short time. A glacier can

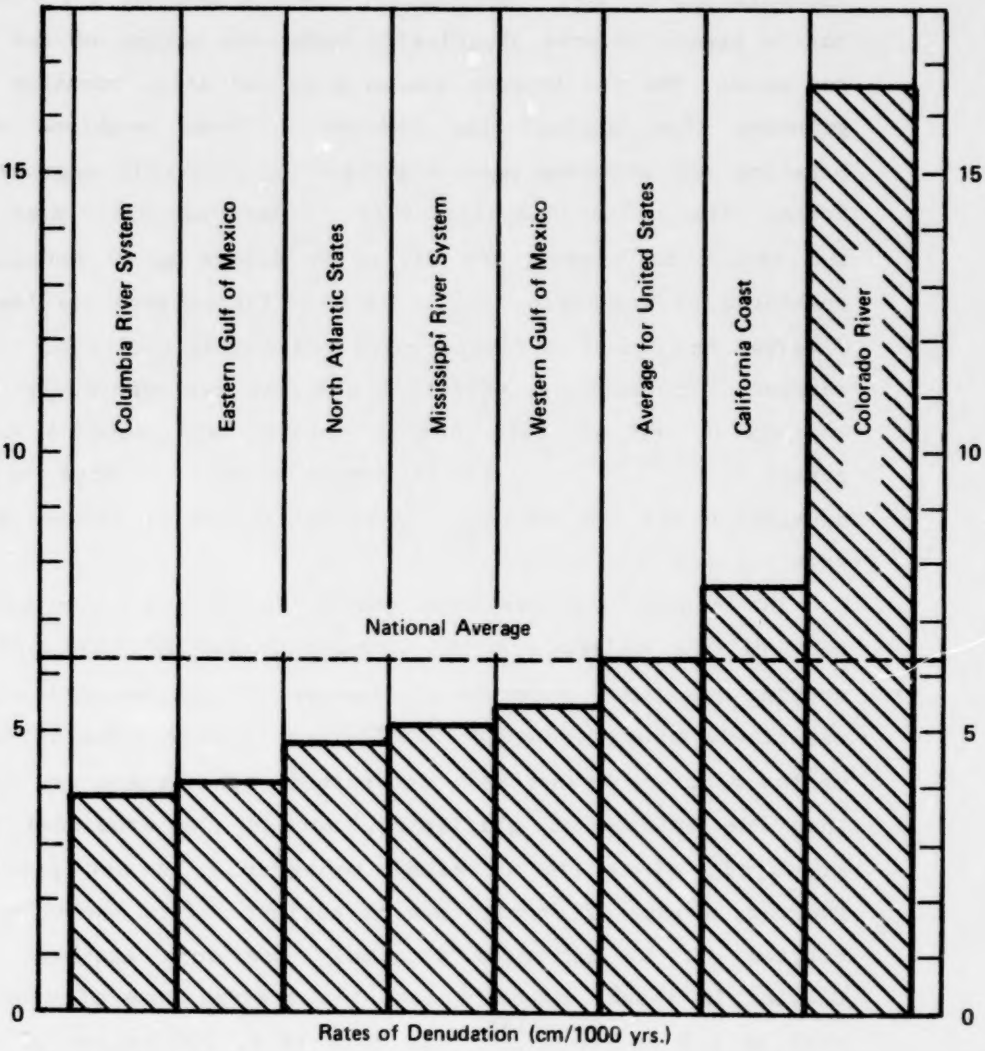

Source: Gilluly, J., A.C. Waters, and A.O. Woodford. Principles of Geology. 3rd edition. W.H. Freeman and Co., San Francisco, 1968.

FIGURE D–43 AVERAGE RATE OF DENUDATION OF MAJOR DRAINAGE AREAS IN THE U.S.

usually be classified as alpine or continental, depending on whether it is confined to a mountain valley or covers a broader region. Glaciers form when snowfall exceeds melting and evaporation, causing an accumulation of ice. Eventually, the ice becomes thick enough for the bottom layers to move plastically under the weight of the overlying ice and snow. The ice freezes around rock and soil, breaking them free and grinding them against the bedrock. These combined mechanisms of breaking and grinding make a glacier an extremely aggressive erosional force. Also, because a glacier is a relatively solid mass, it can alter the course of streams and rivers by diverting or damming them. The scablands of Washington and Idaho were formed when continental glaciers diverted the Columbia River many times during cycles of ice advance and retreat. The enormous weight of glaciers has apparently depressed some regions up to several hundred meters, and rebound has also been detected.(58,136,137) It is possible that crustal adjustments for depression and rebound could cause fracturing or renewed movement along existing faults.

The alpine glaciers that carved California's Yosemite Valley and many of the valleys in the Cascade Range and the Northern Rockies, gouging the land to depths of hundreds of meters, did so during their relatively short (roughly 10,000-year) lives. The duration of these valley glaciers is not well determined, since there was apparently more than one episode of glaciation, nor is the erosional depth exactly measured, since the original topography is not precisely known. However, a rate of erosion can be estimated from the volume of material carried off by meltwater streams. One such estimate for the Muir Glacier in Alaska suggests that the average rate of erosion may be as high as 1.9 cm/year.(138) At this rate, 500 meters of rock could be removed in 25,000 years. A study of two Icelandic glaciers determined that their average erosional rates were 0.06 and 0.6 cm/yr.(137,139) Between 6 and 60 meters of cover could be removed by such glaciers during a 10,000-year ice age. Thus, a repository buried directly under a valley prone to glaciation could be seriously jeopardized within tens of thousands of years after the onset of moving ice. While such times are not much more than the time frame chosen for this study, the hazard can be eliminated by ensuring that a site is selected where there is no expectation of alpine glaciation.

Continental glaciers, such as those that covered the northern portions of the United States several times during the Pleistocene age, account for more widespread erosion than do valley glaciers, but erosion depths are harder to estimate. It is likely that their movement is slower than valley glaciers' since the driving force would depend upon differences in ice thickness between the glacier center and edge, rather than the gradient of a valley floor. Rates of ice advance are more difficult to establish than ice retreat since advancing ice often obliterates evidence from which dates can be determined. Erosion by continental glaciers is non-uniform and varies widely, but rates are in general much less than for valley glaciers.

In addition to its erosional power, a glacier is expected to have effects reaching far beyond the limits of the ice itself. For example, the increased precipitation often associated with periods of glaciation and the runoff of glacial meltwater can increase fluvial erosion in advance of the ice. Furthermore, the presence of ice and accompanying water will affect both surface and groundwater hydrology in a variety of ways: diverting rivers, recharging aquifers, and forming lakes.

The timing of the next glacial epoch is speculative, at best. However, the frequency of major glacial advances in the last several million years suggests that another continental glacier is a real possibility in less than 100,000 years, the average cycle time of ice ages during the last 850,000 years.(50) Thus, effects of a glacier upon a repository could appear in a geologically short time. Nevertheless, locating a repository some distance from the boundaries of Pleistocene and recent glaciation, shown in Figure D-44, could provide adequate long-term control against disruption of a repository from glacial processes, if necessary.

The wind can transport fine sands and silts long distances and against the general trend of fluvial erosion. However, the depth to which the wind can erode is limited, especially compared with the erosional power of water or ice. From the standpoint of a repository, aeolian (wind) erosion is of little consequence, as it is essentially unable to remove the overburden. The two more likely effects of the

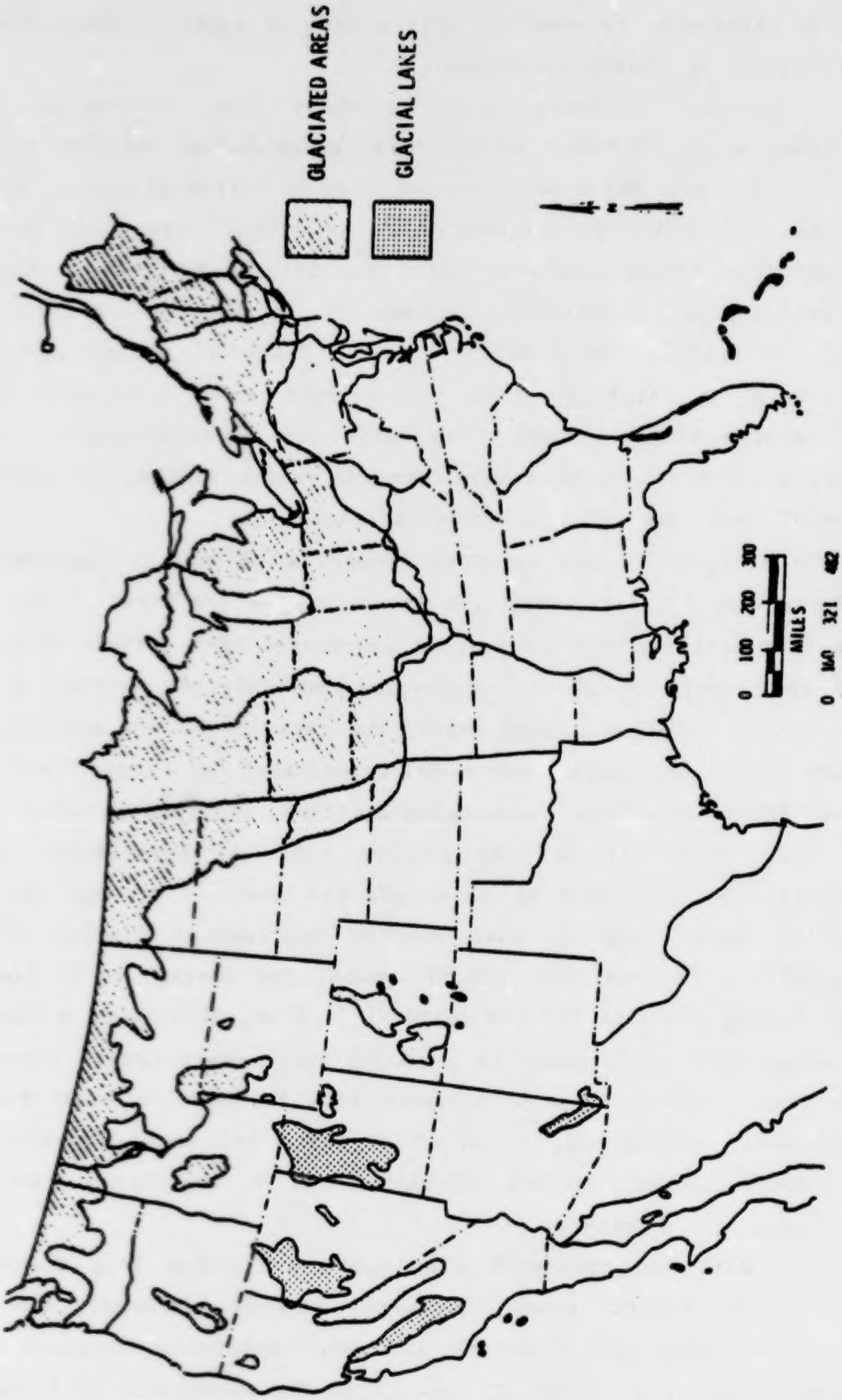

FIGURE D—44 GLACIATED AREAS OF THE COTERMINOUS UNITED STATES AFFECTED DURING PLEISTOCENE GLACIATION wind are stripping of vegetation at the site, which would increase its susceptability to fluvial erosion, and obliteration of site markers and survey points, which would increase the chances of the repository's existence and location being forgotten.

D-5.6.3 Sedimentation

Sedimentation is the complement of erosion. Material removed from one place is deposited in another. Final deposition is typically in the ocean, but there may be many intermediate depositional stages, such as stream beds, terraces, and sand dunes.

The effect of sedimentation on a repository is likely to be positive. That is, any process that thickens the overburden and further increases the distance from the repository to the biosphere is likely to aid the isolation of the wastes. However, some detrimental effects are possible. Not only can extensive deposition obliterate site markers, but the added weight of thick sediments can, by increasing the stress on the buried rocks, induce fracturing or, in the case of less brittle rocks, plastic deformation. Since it is expected that the repository will be backfilled, the damage that could result from an extreme increase in vertical stress is expected to be slight, and a general compaction of the repository and its contents is most likely. Possible displacement of the repository through differential sedimentation is discussed in Section D-5.6.8.

D-5.6.4 Tectonism

Mountain building and the formation of continents, which involve many related processes under the general description of tectonism, may alter overburden thickness, ground and surface water patterns, erosion rates, and permeabilities. Examples of tectonic phenomena include faulting, folding, tilting, uplift, and subsidence. These structural changes in the earth's crust are explained, for the most part, by two compatible theories: continental drift and isostasy. Continental drift, or plate tectonic theory, explains the forces necessary to cause structural changes on the basis of collision between thin plates of crustal rock. While the relative velocities of the colliding plates are very low, their huge masses produce extraordinary forces, sufficient to rupture the crust. Since the deformation is primarily along the plate margins, which are relatively specific locations, future folding, faulting, volcanism, and the like are expected to be confined to these limited margins, shown in Figure D-45.

The theory of isostasy views the continents as bodies of relatively low density material floating on a dense mantle. If some portion of the crust is higher than the rest, there must be a proportionally deep mass of crustal rock below the rise to provide the necessary buoyancy, as depicted in Figure D-46. If some process, such as erosion, alters the land contour and hence the buoyant equilibrium, the crust will rebound. A rebound in brittle rock may result in faulting, whereas rebounding softer rocks can deform by folding.

Both theories suggest that deformation, by folding or faulting, will be more likely in regions of previous tectonism and high relief since these regions represent local areas of high stress in a state of disequilibrium: either plate margins under compression or thick zones of the crust. The importance of tectonic forces upon a repository depends upon the rate at which structural processes may occur. Faulting and folding may occur in the same settings and at the same rates. However, faulting is perceived to be more consequential than folding since folds may leave the overburden at its original thickness, requiring considerable erosion to expose a deeply buried repository, while a fault transecting a repository may raise it to the surface. Therefore, the following discussion will focus on the possible results of severe tectonic faulting. The possibility of a fault permitting water that may have contacted the buried wastes to enter the biosphere has been consided as a failure element.

It is also possible that repeated vertical displacement along a fault could bring part of the repository itself to the surface. Using an extreme rate of fault movement yields a conservative estimate of the time required to exhume the repository. An example of a fault with a rapid vertical displacement is the fault forming the east boundary of Colorado's Front Range. This fault is approximately 20 million years old and has moved roughly 1000 meters over that period. At that rate, a

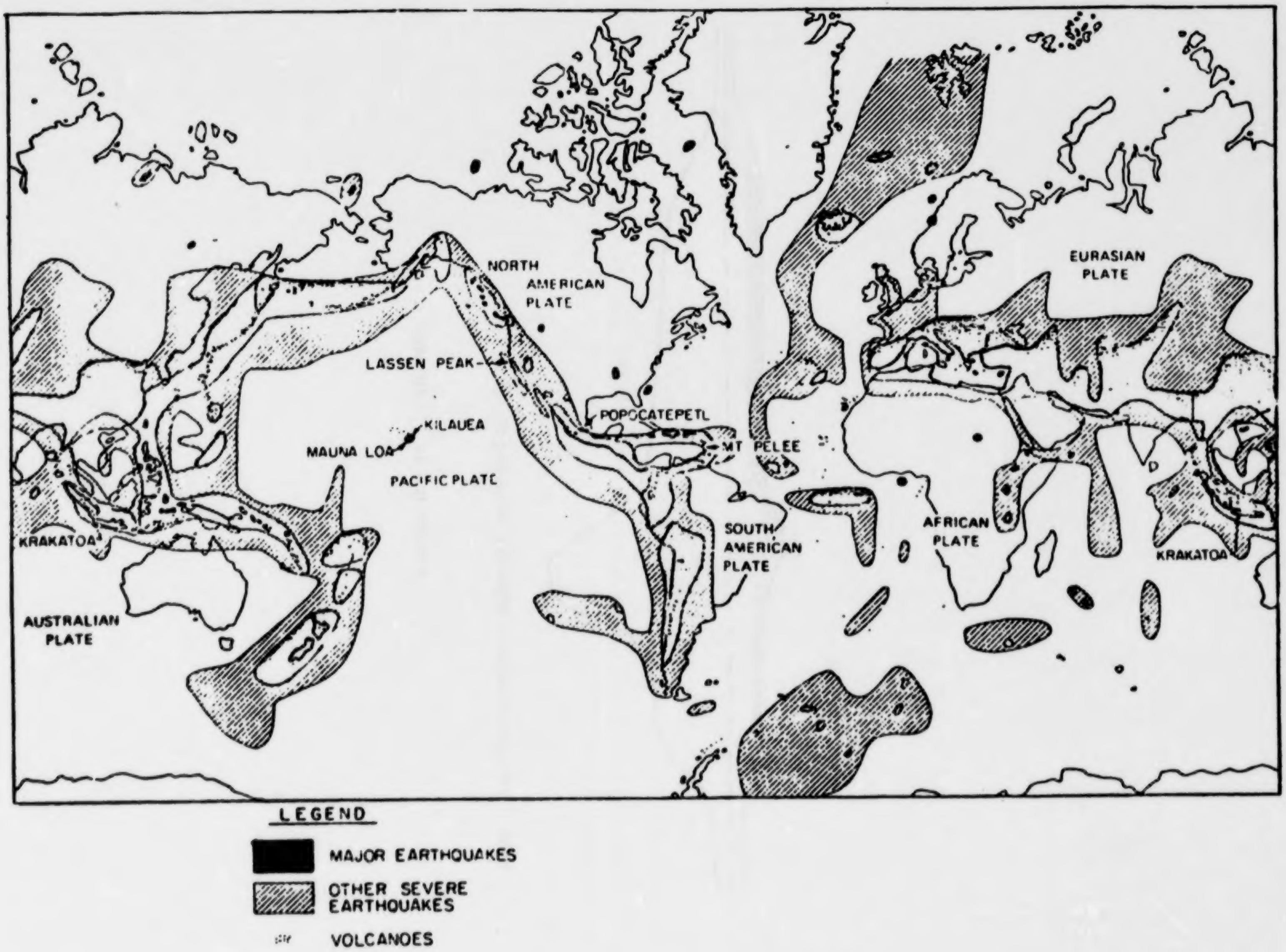

Sources: Dewey, J.F., Scientific American, May 1972. Williams, H., Scientific American, November 1955.

FIGURE D—45 CRUSTAL PLATES AND REGIONS OF THE WORLD IN WHICH MAJOR EARTHQUAKES AND VOLCANOES OCCUR

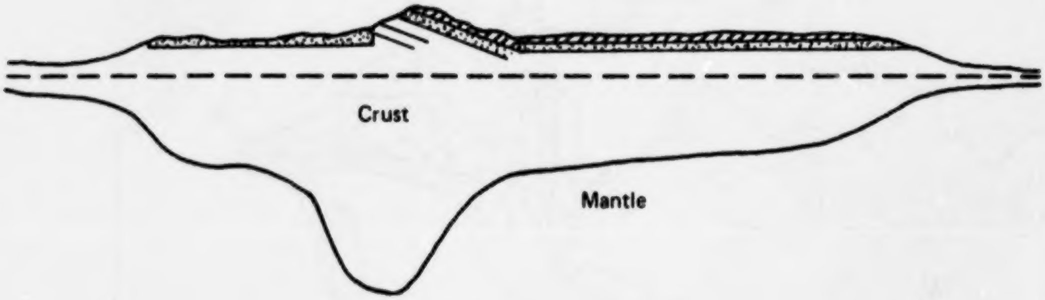

Note: Elevation of surface is reflected in deepening of crust.

FIGURE D – 46 ISOSTASY

fault through the repository would require about 10 million years to raise part of the repository to the surface.

It is possible that a fault could divert a stream or river course and make the stream follow the trend of the fault, as the Snake River follows the fault forming the face of the Teton Range in Wyoming. In such a case, the combined river erosion and fault movement would reduce the time before the repository might be exposed. However, this more rapid mechanism would commence only after the creation of the transecting fault. Given the very low probability of a new fault occurring and the long time before the repository could be exposed, this mechanism appears to be much less significant than the faulting failure element discussed in Section D-5.1.

Earthquakes generally are the manifestation of movement along a fault but, unlike a fault, their effects are felt over a wide area. In examining the possibility of damage to a repository from quaking it was found that damage is typically limited to surface structures and features, and that damage to underground workings is slight, if present at all.(140) For open underground workings, damage from very strong earthquakes was seen only in the portals and shallow tunnels. Deep excavations showed no damage at all. A backfilled repository could be expected to endure severe shaking with essentially no adverse effects.

D-5.6.5 Uplift and Downwarping

Relative movement of large regions, such as orogeny, or mountain building, may contribute to a general degradation of the repository. This degradation might occur through fracturing and faulting and changes in the hydraulic regime surrounding the repository, in addition to the tectonic mechanisms already discussed. The geologic record shows that in the United States, present mountain ranges have arisen from the remains of ancient mountains, and these areas would be most susceptible to future uplifts. The time for such pronounced events as the emergence of a mountain range or high plateau are moderately long, even in geologic terms. For example, the Laramide orogeny, which created parts of the Rocky Mountains, started in the Cretaceous period and has continued into the Quaternary, spanning more than 50 million years. If such a long period is deemed appropriate in evaluating the performance of a repository, the model of geologic failure elements previously developed would require substantial changes to accomodate the structural changes possible over such spans of time.

More immediate effects of changes in ground level would be shifts in stream and river direction and the rate of stream erosion. However, as has already been indicated, the presence of a stream near or over a repository would not immediately affect the repository. The rate of land tilt and stream shift would be so gradual as to be insignificant.

A region experiencing downwarping or subsidence is likely to be eroded more slowly than higher ground and may become a region of deposition. In general, subsidence or deposition at or on a repository is not a disadvantage and may increase the isolation of the contained waste. A problem may arise, however, if subsidence and accompanying sedimentation occur near a repository in salt. This is discussed in Section D-5.6.8.

D-5.6.6 Sea Level Fluctuations

The relative elevations of a repository and sea level can alter conditions of erosion, sedimentation, and hydrology. Usually the "base level" of erosion is sea level. Erosion does not generally occur below that base level; instead, sedimentation takes place. The slope of land toward the sea affects the rate of erosion, higher slopes having a higher rate of erosion, as shown in Table D-111. If the sea level were to rise, a repository sited in a high plateau area may see a reduction in the average slope (over the long run) and a corresponding decrease in erosion. Conversely, lowering the sea level would lower the base level of erosion and increase the gradient, increasing the rate of erosion. However, for an inland repository site, the effects of changes in base level would be slight, if apparent at all.

The most recent and best recorded sea level fluctuations have been attributed to changes in the water volume of global ice caps. During the last ice ages, sufficient water was withheld from the oceans to produce an approximate 100-meter decline in sea level. Since then, a general warming trend has prevailed. If this trend continues, the sea

TABLE D-111

ESTIMATES OF THE RATE OF EROSION UNDER VARIOUS CONDITIONS OF CLIMATE AND RELIEF

Physiographic setting	Estimated Rate of Erosion (cm/1000 yrs)
Lowlands--Gradient = 0.001 or less	
Hot moist climate with dry season	3.2
Climate with cold winter	2.9
Intermediate maritime climate	2.7
Equatorial climate (dense rain forest)	2.2
Hot dry climate (Mediterranean, New Mexico)	1.2
Mountains--Gradient = 0.01 or more	
Hot moist climate (Guatemala-Mexico border)	92
Extremely snowy climate (Southeastern Alaska)	80
Semi-humid, near-glacial climate	60
High Mediterranean mountains	45
Hot dry climate (Southwestern United States, Tunisia)	18

Source: Press, F. and R. Siever. Earth.
W.H. Freeman & Co.. San Francisco. 1974.

level could rise as much as 50 meters.(137) A repository less than 50 meters above present sea level would be inundated, but one higher than 50 meters would be relatively unaffected.

What may be most important to an inundated site is the effect on groundwater with an advance of the ocean. Eventually, a layer of salt water would spread over the repository and separate it from fresher water floating on top, as shown in Figure D-47. Before equilibrium is reached, however, the encroaching seawater may cause a reversal of the previous groundwater flow on the site. However, the changes in gradient and groundwater velocity would be expected to be slow and their effects minor.

D-5.6.7 Climate

Of all natural processes influencing a repository, weather and climate are the most variable and rapid. Climate affects virtually all surface processes and, indirectly, many subsurface processes. The most important characteristic of climate is precipitation, and its effect on hydrology and on erosion and sedimentation.

Precipitation affects both surface and groundwater flows. Changes in rates of infiltration and in the level of surface bodies of water can modify the water table and the hydraulic potential throughout confined and unconfined aquifers. Changes in hydraulic potential can alter rates and directions of flows.

A more subtle influence of climate includes the types and density of vegetation. Vegetation exerts some control on erosion and sedimentation. As shown in Figure D-48, the amount of material stripped from the surface actually decreases with increased rainfall. This is because a protective cover of plant growth prevents raindrops from striking bare soil and dislodging dirt. Also, plant roots and detritus slow running water, entrapping soil being carried with the runoff.

More important for a repository, however, are the more dramatic effects of climatic change. Glaciers, for example, are the result of a shift in climate, and their disruptive effects have already been noted in Section D-5.6.2. During the last ice age, glacial advances were accompanied by an abundance of precipitation and a reduction in

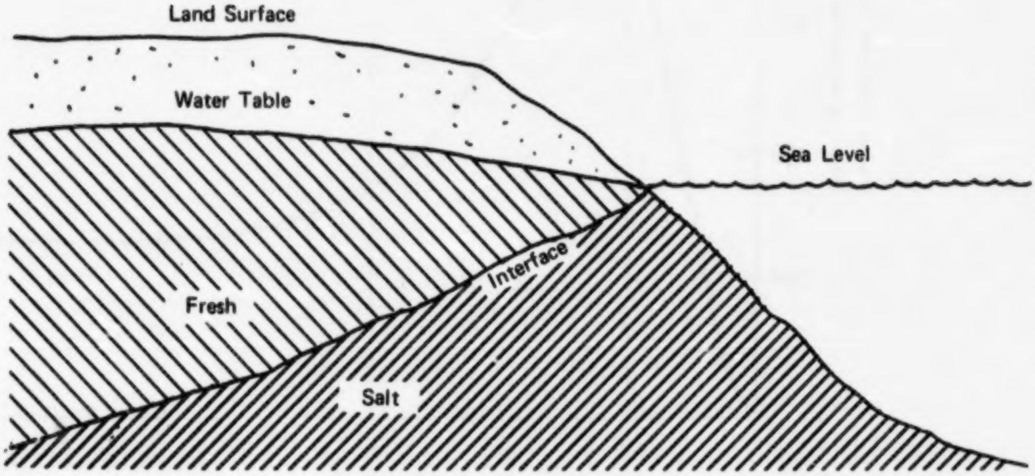

FIGURE D–47 FRESH WATER OVERLYING DENSE SEA WATER

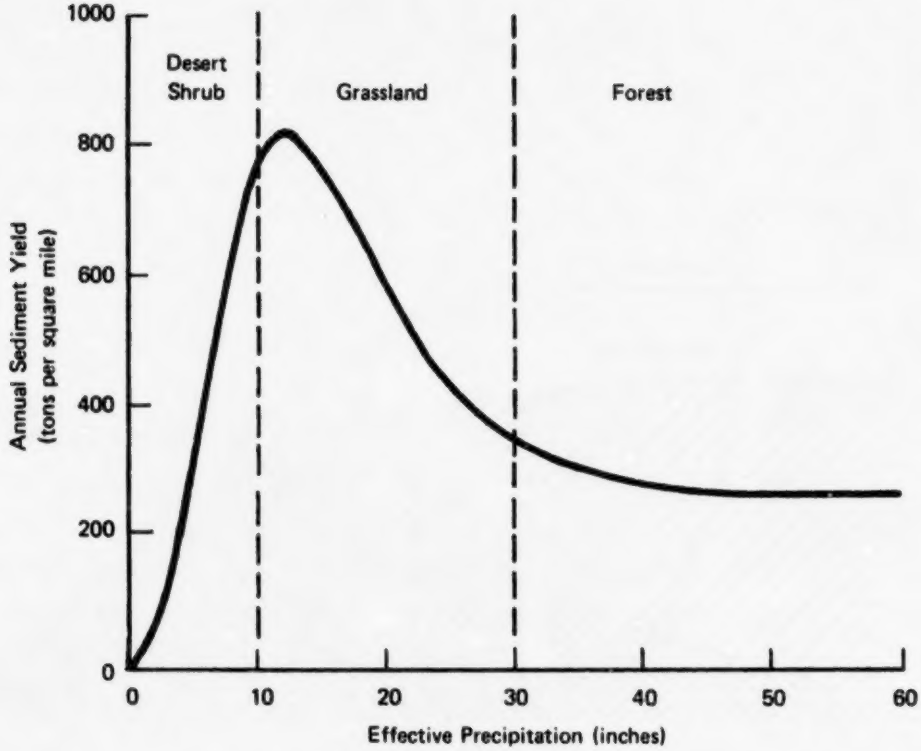

Source: Gilluly, J., A.C. Waters, and A.O. Woodford. Principles of Geology, 2nd edition. W.H. Freeman & Company, San Francisco. 1958.

FIGURE D – 48 EROSION RATES VS. PLANT COVER evaporation, giving rise to many lakes and ponds that have now dried altogether or have shrunk to relative insignificance. Great Salt Lake is the dessicated remnant of Lake Bonneville, which was deeper by 300 meters and covered roughly eight times the area of the present lake. Another lake, Lake Missoula, was formed by an ice dam preventing normal flow into the Columbia and Snake Rivers. Several times, when the dam broke, the rush of water rapidly carved channels and formed giant ripples in the lake bottom. A new glacial age could also bring about the return of lakes such as Bonneville and Missoula. If these lakes were to develop over a repository or over the recharge area of aquifers passing through the site, decided changes in groundwater hydraulic gradients could occur.

By selecting a site without indications of previous lacustrine environment or where no geographic barriers form an enclosed basin, any problems associated with future lake expansion can be minimized. However, the importance of this site selection factor has not been investigated quantitatively in this study.

D-5.6.8 Salt Diapirism

Because salt deforms plastically, it can be displaced, carrying a repository with it. If the displacement is vertical, the repository waste could actually be carried to the surface. The presence of salt domes and anticlines in various parts of the country is evidence of the fluid behavior of this rock.

Studies in salt tectonism have concluded that certain conditions are essential before salt flow can proceed.(40,141,142) Among these conditions are an overburden of sufficient thickness to provide the necessary stress differential for flow to start, and a salt bed thick enough to react to the stress. While there is no clear minimum thickness or depth, diapirism apparently needs a salt thickness of 300-400 meters and a burial depth of at least 2000 meters. The salt thickness cannot increase after the salt deposit is formed, but the depth of burial may increase with subsidence and sedimentation. For a bedded salt formation under about 500 meters of cover, additional deposits 1500 meters thick would have to accumulate before the onset of diapirism. If deposition and downwarping of a region proceed at the same rate, it may be possible to determine the minimum delay between siting a repository in salt and the first salt flowage. The section of the United States with the most rapid downwarping bounds the Gulf of Mexico and has a average rate of approximately 5-10 mm/year.(142) With sedimentation keeping pace with this downward movement 150 thousand years would elapse before the overburden would increase by the extra 1500 meters necessary even to start salt flowage.

Where salt diapirs have already formed, less or no added overburden may be necessary to restart upward movement. Stabilized domes may be either in static equilibrium or may have exhausted the supply of underlying salt. In the latter case, no further movement is possible, but in the former case, movement may be expected to keep pace with the rate of sedimentation. For many of the salt domes of the Gulf Coast, diapir growth appears to have occurred at about the same rate as sedimentation.(40) For these domes, the subsidence has increased the distance between the top and bottom of the dome while maintaining the top in nearly the same relation to sea level.

D-5.6.9 Salt Dissolution

High solubility is a distinctive property of salt. If water were to have free access to salt containing a repository, eventually the isolating rock would be dissolved away and water could attack the waste directly. Both the bedded and dome salt deposits typically have caprock deposits or dissolution surfaces indicating that part of the salt has dissolved. Sometimes the salt has been lost from the entire formation; other times the salt is lost along a horizontally moving front or dissolution wedge. For some specific locations, the rate of salt loss has been estimated. For example, approximately half of the salt originally present in the Delaware Basin may have dissolved and a dissolution wedge has moved eastward in one formation at a rate between 5 and 20 miles per million years.(133) Similarly, the Palo Duro Basin has active dissolution fronts moving horizontally on the order of centimeters per year and vertically at the rate of a few millimeters per year.(135) Very large volumes of caprock mantle some salt domes. These thick caprock deposits can indicate that as much as 6000 vertical meters of salt dissolved from a single dome, although lesser amounts of salt loss are more common. In some locations within the Salina Basin and the Michigan Basin, salt beds have disappeared entirely, with remnant gypsum indicating their previous presence.(143) Since the rate of salt loss is controlled by local conditions and is a continuous process, the time that would be necessary for the dissolution of a significant quantity of salt can and should be determined from site-specific data rather than by repository model parameters.

LIST OF REFERENCES

1. U.S. Department of Energy. Draft Environmental Impact Statement. Management of Commercially Generated Radioactive Waste. DOE/EIS-0046-D. April 1979.

2. U.S. Nuclear Regulatory Commission. Reactor Safety Study. WASH-1400; NUREG-75/014. October 1975.

3. Oak Ridge National Laboratory (Claiborne, H. C., and F. Gera). Potential Containment Failure Mechanisms and Their Consequences at a Radioactive Waste Repository in Bedded Salt in New Mexico. ORNL-TM-4639. October 1974.

4. U.S. Department of Energy. Draft Environmental Impact Statement. Waste Isolation Pilot Plant. DOE/EIS-0026-D. April 1979.

5. Girardi, F., G. Bertozzi, and M. D'Allessandro. Long-Term Risk Assessment of Radioactive Waste Disposal in Geological Formations. Transactions of the American Nuclear Society 26: 1-610, 1977.

6. Battelle Pacific Northwest Laboratories (Schneider, K. J., and A. M. Platt). High-Level Radioactive Waste Management Alternatives. BNWL-1900. May 1974.

7. Energy Research and Development Administration. Alternatives for Long-Term Management of Defense High Level Radioactive Waste, Savannah River Plant, Aiken, S.C. ERDA 77-42/1. May 1977.

8. Proske, R. Contributions to the Risk Analysis of a Repository for High Level Radioactive Waste in Geologic Salt Formations. Transactions of the American Nuclear Society 26: 1-610, 277. 1977.

Preceding page blank

9. deMarsily, G., et al. Nuclear Waste Disposal: Can the Geologist Guarantee Isolation? Science 197: 519-527. 1977.

10. University of New Mexico (Logan, S. E. and M. C. Berbano). Development and Application of a Risk Assessment Method for Radioactive Waste Management. For U.S. Environmental Protection Agency. EPA 520/6-78-005. July 1978.

11. The Analytic Sciences Corporation (Berman, L. E., et al.). Analysis of Some Nuclear Waste Management Options. For Lawrence Livermore Laboratory. UCRL/13917; TR-1100-1-1. October 10, 1978.

12. Sandia Laboratories (Campbell, J. E., et al.). Risk Methodology for Geologic Disposal of Radioactive Waste: Interim Report. For U.S. Nuclear Regulatory Commission NUREG/CR-0458;SAND 78-0029 RW. October 1978.

13. Nevada Operations Office, U.S. Dept. of Energy. Annual Report on Nevada Waste Isolation Program. 1978.

14. Clynne, M. A., and R. W. Potter II. P-T-X Relations of Anhydrite and Brine and their Implications for the Suitability of Anhydrite as a Nuclear Waste Repository Medium. In: Scientific Basis for Nuclear Waste Management. G. J. McCarthy, ed. Plenum Publishing Corporation, New York. 1979.

15. Storage and Disposal of Radioactive Waste. Hearing before the Joint Committee on Atomic Energy, Congress of the United States, Ninety-Fourth Congress. November 19, 1975.

16. Sandia Laboratories. Seabed Disposal Program. Annual Report - Part 1, January-December 1976. SAND 77-1270. October 1977.

17. National Academy of Sciences/National Research Council. The Disposal of Radioactive Waste on Land. Publication 519. NTIS-PB130035/AS. September 1957.

18. National Academy of Sciences/National Research Council. Disposal of Solid Radioactive Wastes in Bedded Salt Deposits. NTIS-PB 265 197, November 1970.

19. U.S. Department of Energy. Technology for Radioactive Waste Management. Vol. 4. DOE/ET-0028. May 1979.

20. Sandia Laboratories (Powers, W., et al.). Geologic Characterization Report, Waste Isolation Pilot Plant (WIPP) Site, Southeastern New Mexico, Vols. I and II. SAND-78-1596. December 1978.

21. On the Safety of Disposing of Radioactive Wastes in the Asse Salt Mine, Gesellschaft für Strahlen und Umweltforschung mbH, Munich, Germany, Undated.

22. Geotechnical Engineers Inc. Uncertainties in the Detection, Measurement, and Analysis of Selected Features Pertinent to Deep Geologic Repositories. For Lawrence Livermore Laboratories. September 13, 1978.

23. Gloyna, E. F., and T. D. Reynolds. Permeability Measurements of Rock Salt. J. Geophysical Research 66:3913. 1961.

24. Dames & Moore. Technical Support for GEIS: Radioactive Waste Isolation in Geologic Formations. Vol. 4: Baseline Rock Properties - Salt. For Office of Waste Isolation, Union Carbide Corporation. Y/OWI/TM-36/4. April 1978.

25. Tomlinson, M., et al. Paper presented at IAEA International Conference on Nuclear Power and Its Fuel Cycle, Salzburg, Austria, May 2-13, 1977. Atomic Energy of Canada, Ltd. AECL-57CG. 1977.

26. Kärnbränslesäkerhet (KBS). Handling of Spent Nuclear Fuel and Final Storage of Vitrified High Level Reprocessing Waste. Stockholm, Sweden, December 12, 1978.

27. Dames & Moore. Technical Support for GEIS: Radioactive Waste Isolation in Geologic Formations. Vol. 5: Baseline Rock Properties - Granite. For Office of Waste Isolation, Union Carbide Corporation. Y/OWI/TM-36/5. April 1978.

28. Brace, W. F., J. B. Walsh, and W. T. Frangos. Permeability of Granite under High Pressure. J. Geophysical Research 73:2225. March 15, 1968.

29. Dames & Moore. Technical Support for GEIS: Radioactive Waste Isolation in Geologic Formations. Vol. 21: Groundwater Movement and Nuclide Transport. For Office of Waste Isolation, Union Carbide Corporation. Y/OWI/TM-36/21. April 1978.

30. Kärnbränslesäkerhet (KBS). Handling and Final Storage of Unreprocessed Spent Nuclear Fuel. Stockholm, Sweden. 1978.

31. Rockwell Hanford Operations. Basalt Waste Isolation Program Annual Report-FY 1978. RHO-OWI-78-100. October 1978.

32. Rockwell Hanford Operations. Basalt Waste Isolation Program Annual Report-FY 1977. RHO-ST-9. September 30, 1977.

33. Dames & Moore. Technical Support for GEIS: Radioactive Waste Isolation in Geologic Formations. Vol. 7: Baseline Rock Properties - Basalt. For Office of Waste Isolation, Union Carbide Corporation. Y/OWI/TM-36/7. April 1978.

34. Pettijohn, F. J. Sedimentary Rocks. Harper & Row Publishers, Inc., New York. 1975.

35. Grim, R. E. Clay Mineralogy. McGraw-Hill Book Company, New York. 1953.

36. Erdal, B. R., et al. Sorption and Migration of Radionuclides in Geologic Media. In: Scientific Basis for Nuclear Waste Management. G. J. McCarthy, ed. Plenum Publishing Corporation, New York. 1979.

37. Dames & Moore. Technical Support for GEIS: Radioactive Waste Isolation in Geologic Formations. Vol 6: Baseline Rock Properties - Shale. For Office of Waste Isolation, Union Carbide Corporation. Y/OWI/TM-36/6. April 1978.

38. MIT Research Report 75-28 (Martin, R.T.). Feasibility of Sealing Boreholes with Compacted Natural Earthen Material. For Office of Waste Isolation, Union Carbide Corporation. June 1975.

39. Sandia Laboratories (McVey, D. F., et al.). Test Results and Supporting Analysis of a Near Surface Heater Experiment in the Eleana Argillite.

40. Gera, F. Review of Salt Tectonics in Relation to the Disposal of Radioactive Waste in Salt Formations. Geological Society of America Bulletin 83:3551. December 1972.

41. Bateman, A. M. The Formation of Mineral Deposits. John Wiley & Sons, Inc., New York. 1964.

42. Atwater, G.I. Gulf Coast Salt Dome Field Area in Saline Deposits. Geological Society of America. Spec. Paper 88:29. 1968.

43. Stearns-Roger Engineering Company. National Waste Terminal Storage Repository for Storing Reprocessing Wastes in a Dome Salt Formation. Conceptual Design Report. For U.S. Dept. of Energy, Oak Ridge, Tennessee. November 9, 1978.

44. Kenney, J. F., and E. S. Keeping. Mathematics of Statistics, Part Two. D. Van Nostrand Company, Princeton, New Jersey. 1963.

45. Freeze, R. A., and J. A. Cherry. Groundwater. Prentice - Hall, Inc., Englewood Cliffs, N. J. 1979

46. Sharp, J. C., and Y. N. T. Maini. Fundamental Considerations on the Hydraulic Characteristics of Joints in Rock. In: Proc. Symposium on Percolation Through Fissured Rock. Stuttgart, Germany. 1972.

47. Snow, D. T. Rock Fracture Spacings, Openings, and Porosities. J. of the Soil Mechanics and Foundations Division, Proc. of American Society of Civil Engineers. 99(SM1):73. January 1968.

48. Kärnbränslesäkerhet (KBS). (Lundstrom, L. and H. Stille.) Large Scale Permeability Test of the Granite in the Stripa Mine and Thermal Conductivity Test. Technical Project Report No. 2. For Swedish Nuclear Fuel Supply Co. and Lawrence Berkeley Laboratory. LBL-7052; SAC-02, TID-4500-R66. July 1978.

49. Lawrence Berkeley Laboratory (Carlsson, H.). A Pilot Heater Test in the Stripa Granite, Technical Project Report No. 6. For Swedish Nuclear Fuel Supply Company and Lawrence Berkeley Laboratory. LBL-7086; SAC-06. August 1978.

50. Battelle Pacific Northwest Laboratory (Stottlemyre, J. A., et al.). Waste Isolation Safety Assessment Program - A Conceptual Simulation Model for Release Scenario Analysis of a Hypothetical Site in Columbia Plateau Basalts. Oral presentation and working paper presented at WISAP Review Meeting, Seattle. August 1979.

51. Dowell Division of Dow Chemical Co. (Eilers, L. H.). Borehole Sealing, Final Report. For Office of Waste Isolation, Union Carbide Corporation. ORNL/Sub/15966-73/1. October 31, 1973.

52. Westinghouse Astronuclear Laboratory (Black, D. L. et al.). Study of Borehole Plugging in Bedded Salt by Earth Melting Technology. For Oak Ridge National Laboratory. ORNL/Sub-75/76230. June 1975.

53. The Analytic Sciences Corporation (Koplik, C. M., et al.). Information Base for Waste Repository Design. For U.S. Nuclear Regulatory Commission. NUREG/CR-0495; TR-1210-1. March 1979.

54. The Charles Stark Draper Laboratory, Inc. (Fernandez, R., et al.). Borehole Plugging by Compaction Process, Final Report. For Office of Waste Isolation, Union Carbide Corporation. Y-OWI-Sub 7087-1. August 1976.

55. The Pennsylvania State University (Roy, D. M., and W. B. White). Borehole Plugging by Hydrothermal Transport. For Office of Waste Isolation, Union Carbide Corporation. ORNL/Sub-4091/3. May 1975.

56. American Petroleum Institute. Oil Well Cementing Practices in the United States. 1959.

57. Significance of Tests and Properties of Concrete and Concrete Making Materials. American Society for Testing and Materials. ASTM Special Technical Publication, No. 169-A. 1966.

58. Gilluly, J., A. C. Waters, and A. O. Woodford. Principles of Geology, 3rd edition, W.H. Freeman & Company, San Francisco. 1968.

59. Flint, R. F., and B. F. Skinner. Physical Geology. John Wiley & Sons, Inc., New York. 1966.

60. Billings, M.P. Structural Geology. 2nd Edition. Prentice-Hall, Inc., Englewood Cliffs, N.J. 1954.

61. Standard Handbook for Civil Engineers. F.S. Merritt, ed. McGraw-Hill Book Company, New York. 1976.

62. Herndon, J. and D. K. Smith. Plugging Wells for Abandonment: A State of the Art Study. For Office of Waste Isolation, Union Carbide Corporation. Y/OWI/Sub-76/99068. 1976.

63. Lambe, T. W., and R. V. Whitman. Soil Mechanics. John Wiley & Sons, Inc., New York. 1968.

64. Terzaghi, K., and R. P. Peck. Soil Mechanics in Engineering Practice. 2nd Edition. John Wiley & Sons, Inc., New York. 1968.

65. Karol, R. H. Soils and Engineering. Prentice-Hall, Inc., Englewood Cliffs, N.J. 1960.

66. Modern Petroleum Technology. I. Hobson and G. Douglas, eds. Institute of Petroleum, London. Halsted Press. 1973.

67. Pasini, J., et al. Plugging Abandoned Gas and Oil Wells. Mining Congress Journal. December 1972.

68. Personal Communication, Herbert Einstein, MIT, 1978.

69. Erickson, H. Chemical Grouting at NORAD. In: Proc. 6th Symposium on Rock Mechanics, U. of Missouri, Rolla, Mo. 1964.

70. Environmental Evaluation Group, State of New Mexico (Goad, D.). A Compilation of Site Selection Criteria, Considerations and Concerns Appearing in the Literature on the Deep Disposal of Radioactive Wastes. EEG-1. June 1979.

71. Bureau of Mines (Johnson, K., et al.). How to Find Abandoned Wells: A Manual. BU Mines IC 8578. March 1973.

72. Barnes, H. L., ed. Geochemistry of Hydrothermal Ore Deposits. Holt, Rinehart, and Winston, Inc., New York. 1967.

73. Stewart, R. D., and R. R. Unterberger. Seeing through Rock Salt with Radar. Geophysics 41:123. 1976.

74. Unterberger, R. R. Looking through Rocks with Radar. Mining Congress J. 63:38. 1977

75. Cook, J. C. How to Locate Water Hazards in Salt Mines. In: Proc. 4th Symposium on Salt, Cleveland. Proc. Northern Ohio Geological Society 2:27. 1974.

76. Netherland, Sewell & Assoc., Inc. Preliminary Regional Study of the Present and Possible Future Oil and Gas Development in the Areas of Thick Rock Salt and Shale Deposits of Michigan, Ohio, Pennsylvania, and Western New York. For Office of Waste Isolation, Union Carbide Corporation. ORNL/SUB-4091/3. February 28, 1976.

77. Personal Communication. William Mallio, Resource Engineers, Inc. November 1979.

78. W. K. Summers & Associates, Inc. (Summers, W.K., and P.A. Webber). Description of Wells Penetrating the Wanapum Basalt Formation in the Pasco Basin Area, Washington. For Rockwell-Hanford Operations. RHO-BWI-C-22. April 1978.

79. Personal Communication. John Swerta, Washington Department of Ecology. June 1979.

80. Office of Nuclear Waste Isolation (Burkholder, H.C.). Waste Isolation Performance Assessment - A Status Report. ONWI-60. November 1979.

81. McCarthy, G. J., et al. Interactions Between Nuclear Waste and Surrounding Rock. Nature 273:216. May 18, 1978.

82. Roedder, E., and H. E. Belkin. Application of Studies of Fluid Inclusions in Permian Salado Salt, New Mexico, to Problems of Siting the Waste Isolation Pilot Plant. In: Scientific Basis for Nuclear Waste Management. G. J. McCarthy, ed. Plenum Publishing Corporation, New York. 1979.

83. Battelle Laboratories (Olander, D. R., and A. J. Machiels). Thermal Gradient Brine Inclusions: Migration in Salt Study: Gas-Liquid Inclusions - Preliminary Model. For Office of Nuclear Waste Isolation. ONWI - 85. October 1979.

84. U.S. Geological Survey (Bredehoeft, J. D., et al.). Geologic Disposal of High-Level Radioactive Waste - Earth Science Perspectives. USGS Circular 779. 1978.

85. Hyder, C. On Diapirs and Diapirism. Southwest Research and Information Center, Albuquerque, N.M. Paper presented at Hearings before the United States Senate, Subcommittee on Science, Technology, and Space of the Committee on Commerce, Science and Transportation, Albuquerque, N.M., March 31, 1978. Serial No. 95-92.

86. Stewart, D. B., and W. R. Potter, II. Application of Physical Chemistry of Fluids in Rock Salt at Elevated Temperatures and Pressures to Repositories for Radioactive Waste. In: Scientific Basis for Nuclear Waste Management. G.J. McCarthy, ed. Plenum Publishing Corporation, New York. 1979.

87. Sandia Laboratories (Wawersik, W. R.). Interim Summary of Sandia Creep Experiments on Rocksalt for the WIPP Study Area, SE N.M. SAND 79-0115. February 1979.

88. Sandia Laboratories (Dawson, P. R.). Constructive Models Applied in the Analysis of Creep of Rock Salt. SAND-79-0137. June 1978.

89. Sandia Laboratories (Dawson, P.R., and P.R. Chavez). COUPLEFLO - A Computer Code for Coupled Creeping Viscous Flow and Conductive-Convective Heat Transfer, Part I, Theoretical Background. SAND-78-1406. November 1978.

90. Sandia Laboratories (Dawson, P. R., and J. R. Tillerson). Nuclear Waste Thermally Induced Motion. SAND 78-0566. June 1978.

91. Dawson, P. R., and J. R. Tillerson. Salt Motion Following Nuclear Waste Disposal. In: Proc. International Conference on the Evaluation and Prediction of Subsidence, Pensacola, Fla. January 15-20, 1978.

92. Sandia Laboratories (Dawson, P. R., and J. R. Tillerson). Comparative Evaluations of the Thermomechanical Responses for Three High Level Canister Emplacement Alternative. SAND 77-0388. December 1978.

93. American Petroleum Institute. 1977 Joint Association Survey on Drilling Costs. February 1979.

94. Halbouty, M. T. The U.S. Is Not Drilled Out. The Wall Street Journal. December 27, 1979.

95. U.S. Geological Survey (Ekren, E. B. et al.). Geologic and Hydrologic Considerations for Various Concepts of High Level Radioactive Waste Disposal in the Conterminous U.S. USGS Open File Report 74-158. 1974.

96. U.S. Nuclear Regulatory Commission. Disposal of High-Level Radioactive Wastes in Geologic Repositories. Draft 10 of Planned Addition to 10 CFR 60. January 9, 1980.

97. Solution Mining Research Institute (Walters, R. F.). Land Subsidence in Central Kansas Associated with Rock Salt Dissolution. Flossmoor, Illinois. June 1976.

98. Brode, H. L. Rock Mechanics Considerations in the Design of Underground Protective Structures. In: Proc. International Conference on State of Stress in the Earth's Crust. Santa Monica, California. June 13-14, 1963.

99. Snow, E. R. Ghosts, Gales and Gold. Dodd, Mead & Company, New York. 1972.

100. U. S. Geological Survey. Preliminary Map of Young Faults in the United States as a Guide to Possible Fault Activity. USGS Map MF-916. 1977.

101. New England Nuclear Power Co. Preliminary Safety Analysis Report. Charlestown Station, Units 1 and 2. February 1979.

102. Northeast Nuclear Energy Co. License Application and Preliminary Safety Analysis Report, Vol. 2, Montague Nuclear Power Station, Units 1 and 2. July 12, 1974.

103. Baecher, G. B. Site Exploration, A Probabilistic Approach. Ph. D. Dissertation, Department of Civil Engineering, Massachusetts Institute of Technology. 1972.

104. Byerlee, J. D., and W. F. Brance. Stick Slip, Stable Sliding, and Earthquakes. J. Geophysical Research 78:6031. 1968.

105. Sbar, M. L., and L. R. Sykes. Contemporaneous Compression Stress and Seismicity in Eastern North America: An Example of Intra-Plate Tectonics. Geological Society of America Bulletin 84:1861. June 1973.

106. Hillier, F. S., and G. J. Lieberman. Introduction to Operations Research. Holden-Day, San Francisco. 1967.

107. Davies, J. V.,,The Astoria Tunnel Under the East River in New York City. Trans. American Society of Civil Engineers 80:594-674. 1916.

108. Personal Communication, Stanley E. Norris, U. S. Geological Survey. December 1979.

109. U. S. Geological Survey (Norris, S. E.). Hydrologic Environment of the Silurian Salt Deposits in Parts of Michigan, Ohio, and New York. USGS Open-File Report 78-684. June 1978.

110. Personal Communication, Robert J. Hite, U. S. Geological Survey. November 1979.

111. U. S. Geological Survey (Stockton, S. L., and A. H. Balch). The Utility of Petroleum Seismic Exploration Data in Delineating Structural Features Within Salt Anticlines. USGS Open-File Report 78-591. 1978.

112. Bechtel National, Inc. Regional Characterization Report for the Paradox Bedded Salt Region and Surrounding Territory. For Office of Nuclear Waste Isolation, Battelle Memorial Institute, Columbus, Ohio. ONWI/SUB-78/42507/1. May 1978..

113. The Analytical Sciences Corp. (Giuffre, M. S. et al.). Information Base for Waste Repository Design, Vol. 5: Decommissioning of Underground Facilities. For U. S. Nuclear Regulatory Commission. NUREG/CR-0495; TR-1210-1. March 1979.

114. Bechtel National, Inc. Regional Environmental Characterization Report for the Gulf Interior Region and Surrounding Territory. For Office of Nuclear Waste Isolation, Battelle Memorial Institute, Columbus, Ohio. ONWI/SUB-78/512-01600-1. November 1978.

115. Louisiana Power and Light Co. Preliminary Safety Analysis Report, Waterford Steam Electric Station, Units 3 and 4. Docket 50382-2. January 1971.

116. Macdonald, G. A. Volcanoes. Prentice Hall, Inc., Englewood Cliffs, N. J. 1972.

117. Civetta, L. et al., eds. Physical Volcanology. Elsevier Scientific Publishing Co., New York. 1974.

118. Catalogue of Active Volcanoes of the World. International Volcanological Association, Naples, Italy. 1955.

119. U. S. Geological Survey (White, D. E., and D. L. Williams, eds.). Assessment of Geothermal Resources of the United States. USGS Circular 726. 1976.

120. U. S. Geological Survey (Millineaux, D. R.). Preliminary Overview Map of Volcanic Hazards in the United States. USGS Miscellaneous Field Studies Map, MF 786. 1976.

121. Nevada Operations Office, U. S. Department of Energy. Nevada Nuclear Waste Storage Investigations, July through September 1979. NVO-196-12. December 1979.

122. Fowler-Billings, K., and M. P. Billings. Geology of the Gorham Quadrangle, New Hampshire - Maine. N. H. Department of Resources and Economic Development Bull. 6. 1975.

123. Geology Society of Great Britain. Geological Map of Great Britain, Second Edition. 1957.

124. Bowen, N. L. Evolution of Igneous Rocks. Princeton University Press, Princeton, N. J. 1928.

125. Shelton, J. S. Geology Illustrated. W. H. Freeman & Company, San Francisco. 1966.

126. U. S. Geological Survey (Maldonado, F.). Summary of the Geology and Physical Properties of the Climax Stock, Nevada Test Site. USGS Open-File Report 77-356. 1977.

127. Eaton, J. P., and K. J. Murata. How Volcanoes Grow. Science 132:925. October 7, 1960.

128. Battelle Pacific Northwest Laboratory (Scott, B. L. et al.). A Summary of FY-1978 Consultant Input for Scenario Methodology Development. For Office of Nuclear Waste Isolation PNL-2851. November 1979.

129. Hartmann, W. K. Cratering in the Solar System. Scientific American 236:84. January 1977.

130. Grieve, R. A. F., and P. B. Robertson. The Terrestrial Cratering Record. Icarus 38:212. 1979.

131. Hughes, D. W. Earth's Cratering Rate. Nature 281:11. September 6, 1979.

132. Geotechnical Engineers, Inc. Geological Studies Pertinent to Site Suitability Criteria for High-Level Waste Repositories. For Lawrence Livermore Laboratory, UCRL 13741. May 25, 1977.

133. Anderson, R. Y. Report to Sandia Laboratories on Deep Dissolution of Salt, Northern Delaware Basin, New Mexico. April 1978.

134. Swenson, E. A. Rates of Salt Dissolution in the Permian Basin. USGS J. of Research 2:253. 1974.

135. Personal Communication, Thomas Gustavson, University of Texas. December 1979.

136. Brochie, J. F., and R. Sylvester. On Crustal Flexures. J. Geophysical Research 74: 5240. 1969.

137. Flint, R. F. Glacial and Quaternary Geology. John Wiley & Sons, New York. 1971.

138. Reid, H. F. Studies of Muir Glacier, Alaska. National Geographic Magazine 4:19. 1892.

139. Okko, V. Glacial Drift in Iceland, Its Origin and Morphology. Comm. Geol. de Finlande Bull. 170:133. 1955.

140. Rozen, A. Response of Tunnels to Earthquake Shaking. S.M. Thesis, Massachusetts Institute of Technology. 1976.

141. Ewing, M., and J. Ewing. Rate of Salt Dome Growth. American Association of Petroleum Geologists Bull. 46:708

142. Press, F., and R. Siever. Earth. W. H. Freeman & Company, San Francisco. 1974.

143. Landes, K. K., et al. Geology of the Mackinac Straits Region. Michigan Geological Society, Publ. 44. 1945.

APPENDIX D-I

GLOSSARY

Andesitic	Andesitic refers to volcanoes and related features with composition part way between basalt and silicic rock, suggestive of the mixture of wet basalt and continental rocks at a plate subduction zone.
Anticline	A geologic structure having rock folded into an arch. The opposite is a syncline which has the rock folded downward into a trough.
Aquiclude	A relatively impermeable geologic formation which effectively prevents the passage of water. Contrasts with an aquifer.
Aquifer	A rock formation or stratum of relatively high permeability that may readily yield or transmit water.
Anisotrophy	Having properties which are not the same in all directions.
Argillaceous	Clay bearing. Here argillaceous is used to describe any of a range of sedimentary rocks with clay as a major constituent, including shale, mudstone, argillite, and siltstone.
Barite	Barium sulfate, $BaSO_4$. A dense mineral and chief source of barium, barite is used in the deep drilling industry as an additive to drill mud to increase its density. This helps to buoy the weight of a long drill string and to increase the pressure at the bottom of the hole which assists in preventing blow-outs.
Basalt	A dense, dark, hard, fine-grained igneous rock containing iron and magnesium rich minerals and lacking free silica. In this study, basalt is taken to be a family of fine-grained igneous rocks without specifying a particular mineral assemblage.
Batholith	A body of intrusive igneous rock larger in area than 100 km^2.
Breccia	Broken rock with fragments larger than sand.

Breccia Pipe	A geologic structure steep sided and roughly circular in plan composed of breccia. In the context of this report, a breccia pipe is a feature in salt formed by the collapse of overlying rock into a cavity formed by dissolution.
Catalysis	The modification of the rate of a chemical process through the use of an agent which is not consumed in the process.
Cement with Fine Fillers	Portland cement or similar material mixed with clay and silt-sized inert particles instead of coarser aggregates.
Connate Water	Water entrapped in a rock at the time of its formation. Contrasted with meteoric water.
Creep	Slow plastic or viscous fluid deformation of rock under stress.
Critical Cavity	The maximum void or cavity in rock salt able to support itself. Cavities larger than the critical cavity will experience the fall of rock blocks or breccia into the cavity.
Criticality	The conditions necessary for a self sustaining nuclear chain reaction to start or continue. Criticality is reached when a necessary quanitity of nuclear material is brought and held in close proximity.
Crust	The exposed rocks of the earth. The relatively rigid outer layer of the earth exhibiting relatively slow seismic velocities. The crust varies in thickness from about 60 km under certain mountainous parts of the continents to about 5 km under the oceans.
Crystalline Rock	Referring to igneous or highly metamorphic rocks composed of minerals with crystals large enough to be distinguished by the unaided eye.
Darcy's Law	A mathematical description of laminar fluid flow through a permeable medium, to the effect that flow is proportional to the hydraulic gradient. In particular, $\dot{Q} = KiA$, where $\dot{Q}$ is the volumetric flow rate through a surface of area A, orthogonal to the flow, under a gradient i. A factor $c(\mu)$ must also be included when viscosity can vary significantly.

Diapir	A geologic structure formed by the forceful intrusion of one geologic material into overlying material, especially the non-igneous intrusion of a relatively plastic or fluid material, such as salt.
Differential Stress	Stress differences in different directions.
Dike Swarm	A cluster of dikes oriented roughly parallel or radiating from a common point. Parallel dike swarms are noted in the British Isles and the Pacific Northwest. Radial swarms are common near volcanic centers.
Drilling Mud	Fluid used to cool and lubricate the bit of a rock drill and to float the cuttings to the surface. Muds may be water or organic fluid based with a number of possible additives including clays, starches, and density modifying materials.
Drill String	A length of steel pipe segments joined together and used to operate a drill bit suspended below the surface.
Evaporite	A rock or mineral deposited when the waters in which it was dissolved evaporated. Common evaporites include salt, gypsum, sulfates, and potash salts.
Fault	A fracture showing displacement of the material on either side along the plane of the break. Faults are distinguished from joints, the latter showing no relative displacement.
Felsic Rocks	Igneous rocks composed primarily of feldspars and free silica (quartz), such as granite.
First Estimate	In this study, the conditions or event probabilities appropriate to a repository site selected for its particular advantages regarding a specific criterion. For example, a first estimate with regard to abandoned boreholes would assume a site with no history of deep well development and conditions unfavorable for gas or oil reserves.
Graben	A block of rock bounded by parallel gravity faults which has moved downward in relation to the blocks on either side.
Gravity Fault	A synonym for a normal fault. A sloped geologic fracture along which the overlying (hanging wall) rocks have apparently moved downward with respect to the underlying (foot wall) rocks.

Head	Hydraulic pressure represented by a column of water of a given height.
Horst	The counterpart of a graben. A fault-bounded structure which has moved upward in relation to the rocks on either side.
Hydraulic Conductivity	The coefficient of proportionality, K, in Darcy's Law. In this report, it is used synonymously with permeability.
Hydraulic Gradient	The rate of change in hydraulic head with respect to distance.
Igneous rock	A rock formed by the cooling of melted rock.
Incompetent Rock	Rock unable to support itself or an applied force. In engineering, incompetent rock requires additional support.
Indurated	Solidified into a massive rock. Usually used to describe sediments which have hardened into rock, e.g. indurated clay is shale or mudstone.
Intrusion	A rock body forcibly injected into pre-existing rock or soils. Generally intrusion denotes an igneous rock which invaded surrounding rock but never reached the land surface.
Joints	Fractures or separations in a rock having no apparent displacement parallel to the plane of the fracture.
Lithology	The character of rocks and rock formations, particularly their gross features such as structure, color, mode of emplacement, fossil content, and stratigraphy. Also, the study of rocks.
Lithostatic Pressure	Pressure applied by the weight of the overlying rock. Lithostatic pressure at a given depth can be estimated by multiplying the weight density of rock by the depth below the surface.
Magma	Melted rock beneath the earth's surface.

Mantle	The layer of the earth between the core and the crust, starting about 3400 km from the center. The mantle has higher seismic velocities than the crust and is apparently composed of dense iron and magnesium rich rocks.
Metastable	Temporarily stable. Metastable is used to describe minerals or other phenomena which are not in equilibrium with their surroundings but which require a finite disturbance to initiate a change toward equilibrium. A typical example is a supercooled liquid which remains liquid until made to solidify upon the addition of a grain of the solid phase. Metastable is not synonomous with unstable which denotes a shift toward equilibrium without the addition of energy or a disturbance.
Mine Drift	A tunnel or horizontal mine opening. Particularly a blind tunnel not connecting to others at one end.
Montmorillonite	A clay mineral (hydrous aluminum silicate), generally the weathering product of lava, with the capacity to readily absorb water between crystal layers causing marked expansion.
Near Field	Within the vicinity of the waste or the repository tunnels. Near field effects are those caused by the presence of the waste or the repository and are contrasted with far field effects which are essentially unrelated to the repository or its contents.
Neat Cement	Portland cement mixed without fillers or aggregate and generally used as a grout or sealing agent.
Normal Fault	Synonym for gravity fault. An inclined fracture along which the rocks above have apparently moved downward with respect to the rocks below.
Permeability	A measure of the ease with which a fluid can pass through the continuous voids of a material. (See hydraulic conductivity.)
Petrography	Description of a rock including mineral composition, grain size and shape, fabric, and evolution.
Piezometric Head	The height to which water in an aquifer rises or could rise if penetrated by a well. The hydraulic head.

Planar	Forming a plane or flat surface. Used here, planar describes features or structures which are wide, long, and roughly uniform in thickness.
Plastic	Capable of being permanently deformed without rupture.
Pluton	A body of intrusive igneous rock.
Poise Units	A measure of fluid dynamic viscosity. 1 poise = 1 gm/cm-sec.
Polymerization	Formation of long chain molecules from short molecules. Through polymerization, certain light volatile molecules combine to form more rigid dense ones.
Productive Horizon	A stratum from which mineral wealth is recovered; especially a stratum from which petroleum or gas is taken.
Resaturation	The filling of a repository with water. If a repository is partially back-filled with rock materials, resaturation denotes the filling of the void spaces within the backfill.
Second Estimate	In this study, conditions appropriate for a repository sited in circumstances unfavorable in regard to a specific criterion. For example, a second estimate for undetected abandoned boreholes would assume a site within a long abandoned gas or oil field.
Shale	Sedimentary rock formed from clay and silt and that is laminated and fissile. In this study, shale is intended to denote all fine-grained clay rich clastic sedimentary rocks including argillites, mudstones, siltstone, graywacke, and so forth.
Shear Stress	A stress or force acting to cause slippage of two adjacent parts of a body past one another.
Silicic	High in silica. Silicic refers to silica rich magmas which are typically viscous, and confined to regions of continental crust, suggesting that they are the result of remelting of crustal rocks. Typical rocks from silicic magmas are granites, granodiorides, and their fine-grained equivalents.

Sonde	A device to obtain and transmit remote measurements. A borehole sonde may be used to determine the properties of rock penetrated by the hole.
Source Term	The quantity and composition of radioactive waste contained in a repository or subject to release by a particular breach mechanism.
Spall	To fracture concentrically, to form "onion skin" joints where movement is largely perpendicular to the plane of the fracture.
Stochastic process	A process or model whose evolution over time is governed by probabilistic factors.
Stock	An igneous intrusive which is smaller than a batholith, steep sided, and assumed to be cylindrical or widening with depth.
Stratum (Pl. Strata)	A layer of rock, especially a layer of uniform characteristics distinguishable from overlying and underlying strata.
Stress	A force acting to deform, usually measured as force per unit area; may vary with direction.
Subcircular	Not circular in the mathematical sense but describing a figure which is closed and convex, approximately circular, as the cross section of a tree trunk is subcircular.
Subduction	The forcing down toward the mantle of the earth of crustal rocks at the junction of two colliding crustal plates.
Subparallel	Not parallel in the mathematical sense but near enough to parallel that linear features do not actually intersect.
Tectonic	Pertaining to the earth's broad structural features.
Thermally Induced Buoyancy	Upward forces brought on by expansion of material when heated resulting in a lower density than that of the surrounding material. The low density material will tend to rise through the denser material.
Uniform Concentration	Average concentration of radionuclides in backfilled repository as a result of gradual leaching from waste packages. May be limited either by leach rates or by solubility limits.

U-Tube Effect	A term to describe water movement through a repository involving water entering from an overlying·aquifer at the upstream side of the repository and returning to the aquifer at the downstream side.
Virgin Rock	Rock which is unaffected by drilling or mining.
Waste Drift	A mine tunnel or drift containing waste.

APPENDIX D-II

REPOSITORY RESATURATION TIMES

A. INTRODUCTION

Many of the mechanisms that permit the transport of radionuclides from the repository to the upper aquifer require that the hydrologic system be in a saturated condition. Before repository construction, essentially all the rock below the water table (defined in the generic repositories by the level of the upper aquifer) is saturated with water at pressure at least equal to hydrostatic pressure. (See Figure D-II-1).

The excavation of the repository disturbs this saturation because water flows from the surrounding rock into the resultant cavity, as shown in Figure D-II-2. During the operational phase of the repository, this water, if significant, will be pumped out, as is commonly done during mining operations. After the backfilling and closing of the repository, water flowing down the filled shafts and/or in through the rock walls will gradually fill the pores of the backfill until saturation is again established. The purpose of this discussion is to estimate the time required for such "repository resaturation" to take place.

B. SIMPLIFICATIONS

The repository will be modeled as a rectangular solid with base area A_R, height h, mined fraction M, and backfill porosity η. Thus, the volume of pore space needing to be resaturated is:

$$V = A_R h M \eta .$$

For the present calculations, the following values will be used:

$$A_R = 8\ \mathrm{km}^2 = 8 \times 10^6\ \mathrm{m}^2$$

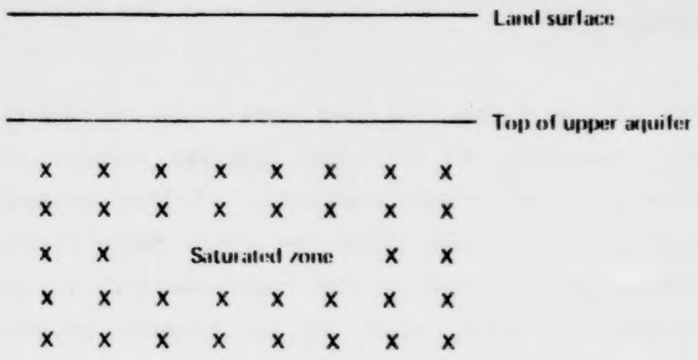

FIGURE D-II-1 PRE–REPOSITORY HYDROLOGY

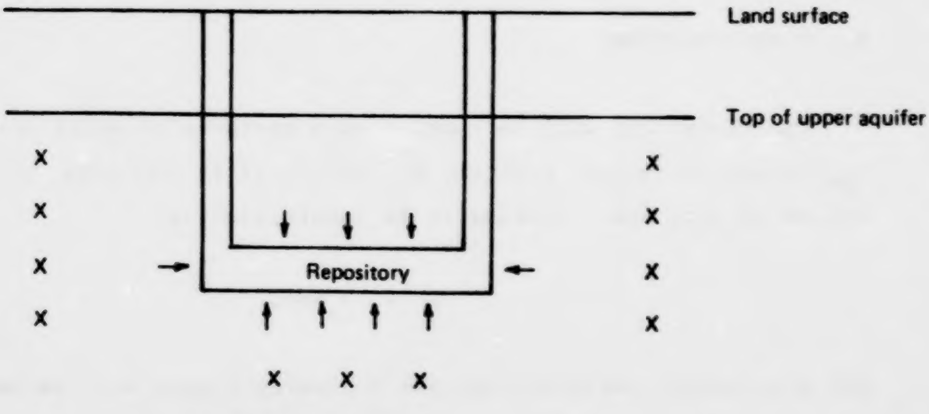

FIGURE D-II-2 FLOW INTO REPOSITORY EXCAVATION

$h = 5$ m

$M = 0.25$

$n = 0.2$.

These values lead to a pore volume $V = 2 \times 10^6$ m^3. Resaturation also requires filling of the pores in the unsaturated zone of rock surrounding the repository and in the backfilled (or sealed) shafts and boreholes. These latter volumes are negligible in relation to the pore volume of the repository cavity and so will be omitted from the analysis. The resulting calculation is conservative, in that it will predict recharge slightly earlier than in the real case.

The flow into the mined repository is driven by a pressure gradient. The repository is initially at atmospheric pressure while the water in the surrounding rock exceeds this by its corresponding hydrostatic pressure. This hydrostatic pressure will be modeled as that from a column of water extending to the top of the upper aquifer. The pressure in the repository would gradually rise during recharge, thereby decreasing the effective gradient. However, for the sake of these simple conservative calculations, this effect will be ignored. For flows through the rock itself (as opposed to flows through permeable shafts or boreholes), it will be assumed that recharge also occurs through the bottom of the repository and that this is equal to recharge through the top. With respect to the latter, it will be assumed to occur through the column of rock immediately above the repository. Edge effects are assumed to be insignificant and, in any case, more than balanced by the conservative assumption of equal flow up through the floor.

C. OUTLINE OF COMPUTATIONS

The outline of the steps in the calculation of recharge times is shown in Figure D-II-3. To illustrate the steps, several preliminary calculations will be carried out below.

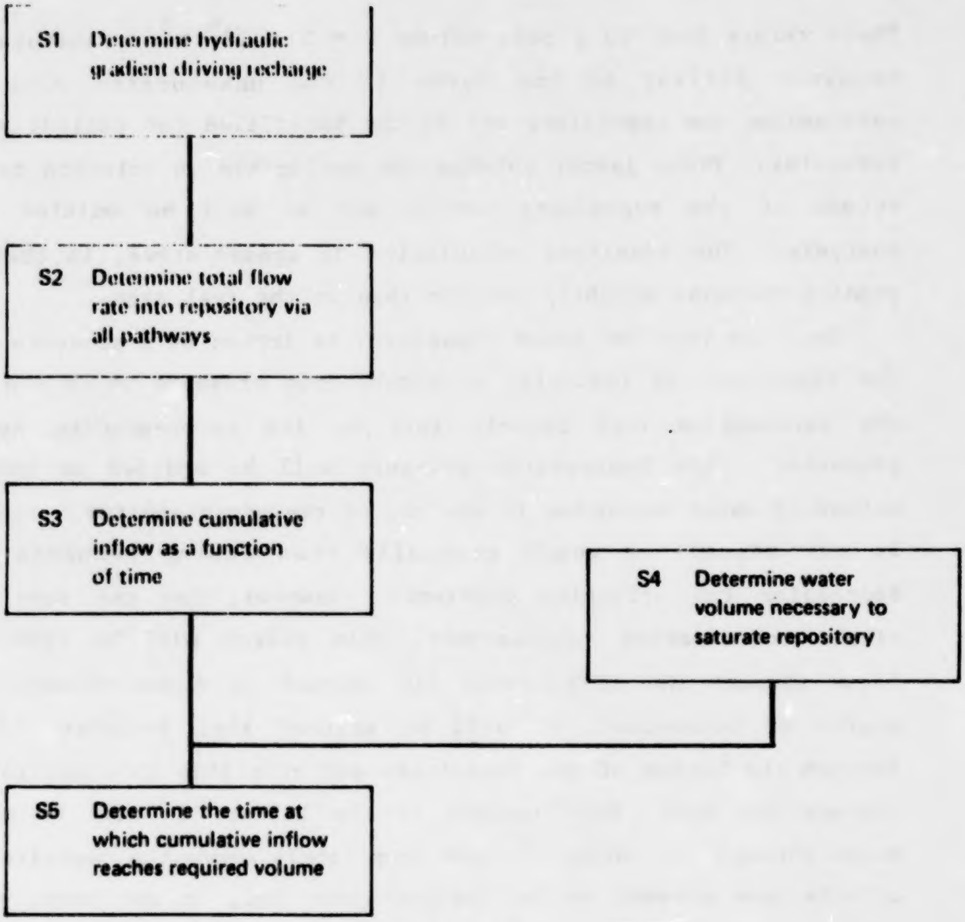
S1 Determine hydraulic gradient driving recharge
S2 Determine total flow rate into repository via all pathways
S3 Determine cumulative inflow as a function of time
S4 Determine water volume necessary to saturate repository
S5 Determine the time at which cumulative inflow reaches required volume

FIGURE D-II-3 COMPUTATIONAL SEQUENCE FOR RECHARGE TIMES

1. Two repository-aquifer distances are represented among the generic repositories. For bedded salt, shale, and basalt, the top of the upper aquifer is 130 meters above the repository. This determines the driving hydrostatic head. The head is essentially dissipated entirely over the 100-meter barrier layer, so that the effective gradient is:

$$i = \frac{130}{100} = 1.3.$$

In the case of granite and dome salt, the gradient is:

$$i = \frac{260}{230} = 1.1.$$

2. Total flow rate into the repository is assumed to be the sum over all possible recharge pathways. Each pathway is characterized by a permeability (which may vary with time) and a cross-sectional area.

In the case of shaft recharge, the permeabilities are based on Section D-3.2. For the first estimate, K degrades linearly from 10^{-8} cm/sec to 10^{-6} cm/sec over 10^4 years. The permeabilities are more convenient to deal with in units of meters per year, to which the conversion is accomplished by multiplying by 3.15×10^5. The linear degradation from 3.15×10^{-3} m/yr to 3.15×10^{-1} m/yr corresponds to the equation:

$$K(t) = 3.15 \times 10^{-3} + \frac{3.15(0.099)}{10^4} t$$

$$= 3.15 \times 10^{-3} + 3.12 \times 10^{-5} \ t \ \text{(m/yr)}$$

For the second estimate, K degrades linearly from 10^{-8} cm/sec to 10^{-4} cm/sec over 10^4 years. In this case, one obtains:

$$K(t) = 3.15 \times 10^{-3} + \frac{31.5 - 3.15 \times 10^{-3}}{10^4} t$$

$$= 3.15 \times 10^{-3} + 3.15 \times 10^{-3} t \text{ (m/yr)}$$

The total cross-sectional area of the shafts will be taken as 100 m^2 (e.g., four shafts, each of which is 5 m x 5 m).

In the case of borehole recharge, the first estimate calls for degradation from 10^{-8} cm/sec to 10^{-5} cm/sec over 10^4 years, which is represented by the equation:

$$K(t) = 3.15 \times 10^{-3} + 3.15 \times 10^{-4} t \text{ (m/yr)}.$$

For the second estimate, degradation from 10^{-8} cm/sec to 10^{-4} cm/sec over 10^4 years, is given by:

$$K(t) = 3.15 \times 10^{-3} + 3.15 \times 10^{-3} t \text{ (m/yr)}.$$

Each borehole has a cross-sectional area of 0.1 m^2.

3. The output of Step 2 is a function $\dot{Q}(t)$ representing the rate of flow into the repository at time t. This rate is calculated by Darcy's law:

$$\dot{Q} = \frac{KiA}{100\mu}$$

where μ is the water viscosity at the ambient temperature in the rock. For these calculations, μ will be conservatively taken as 0.002 poise so that $\dot{Q}$ has the form:

$$\dot{Q} = 5 KiA$$

for each pathway. The integral of this function from 0 to t gives the cumulative inflow by time t.

4. The required water volume has already been calculated to be

$$V = A_R h M n$$

which has the numerical value

$$V = 2.0 \times 10^6 \text{ m}^3$$

for the parameter values that have been adopted. This represents the initial pore space at the time of repository sealing. In the case of salt, which is a plastic medium that tends to flow under applied stress, the pore space will decrease as a function of time due to the overburden pressure. The modeling of creep behavior is discussed in greater detail in Appendix D-VII, where representative numerical results are estimated. For the present calculations, the pore space has been assumed to decrease linearly to 0 (an approximation) over a certain period following sealing of the repository. For first estimate calculations, this period has been taken to be 200 years. For second estimate calculations, this period has been taken to be 1000 years. The slower rate of creep represents a less desirable situation with respect to this mechanism because more water can enter the repository before the salt has effectively sealed itself tight.

5. The equation:

$$Q(t) = V$$

is solved for t in order to determine the recharge time.

D. BEDDED SALT RESATURATION TIMES

For a repository in bedded salt, resaturation would generally be restricted to two sets of pathways: permeable shaft and borehole seals.

The bulk rock permeability is too low to contribute significantly to the inflow.

First estimate. Using parameters given earlier, the inflow due to shafts is given by:

$$\dot{Q}_1 = 5\ KiA$$

$$= 2.048 + 0.02048\ t$$

so that the cumulative amount of water present is:

$$Q_1 = 2.048t + 0.01024\ t^2 .$$

Similarly, assuming 60 borehole pathways (50 to upper aquifer, 10 to lower), they contribute an amount of inflow given by:

$$\dot{Q}_2 = 0.123 + 0.0123\ t$$

so that the cumulative amount of water present is:

$$Q_2 = 0.123t + 0.00614\ t^2 .$$

Since the pore space in the first estimate case is given by:

$$Q = (2 \times 10^6)(200 - t)/200$$

for t between 0 and 200 years, resaturation is achieved at the time t which satisfies the equation:

$$Q = Q_1 + Q_2 .$$

This value of t is approximately 200 years (199.883) and the corresponding water volume is 1.2×10^3 m^3 (1171).

Second estimate. Second estimate parameters lead to the formulas:

$$\dot{Q}_1 = 2.048 + 2.048t$$

$$Q_1 = 2.048t + 1.024\ t^2$$

$$\dot{Q}_2 = 0.123 + 0.123t$$

$$Q_2 = 0.123t + 0.061\ t^2$$

$$Q = (2 \times 10^6)(1000 - t)/1000 .$$

The resaturation time in this case is approximately 720 years, with a corresponding water volume of 5.6×10^5 m^3.

E. GRANITE RESATURATION TIMES

For a repository in granite, there are three sources of inflow: permeable shaft seals, permeable borehole seals, and flow through the bulk rock. Because the cross-sectional area for flow through the bulk rock is so much larger than for shafts and boreholes (almost five orders of magnitude), and because this difference is not balanced by a correspondingly lower permeability, the flow through the bulk rock dominates.

The permeability values given in Section D-3.1 for the first estimate case lead to the formulas:

$$\dot{Q} = 5\ KiA$$

$$= 2.8 \times 10^3\ m^3/yr \quad \text{for } t < 100\ yr$$

$$= 2.8 \times 10^4\ m^3/yr \quad \text{for } t \geq 100\ yr$$

The value of A used here is 1.6×10^7 m^3, twice the area of the repository, to account for recharge from both above and below the repository. The cumulative inflow by 100 years after repository closure is thus:

$$Q(100) = 2.8 \times 10^3 \times 10^2$$

$$= 2.8 \times 10^5 \text{ m}^3$$

In order for resaturation to be complete, an additional inflow equal to 1.72×10^6 m^3 is necessary, in order to give the required total of 2×10^6 m^3. At the rate of 2.8×10^4 m^3/yr, this would take an additional 61 years, so that the resaturation time would be approximately 161 years.

For the second estimate case, the inflow over the first 100 years is

$$\dot{Q} = 2.8 \times 10^5 \text{ m}^3/\text{yr}$$

so that resaturation takes place almost immediately, i.e., about 7 years after closure. Since the calculated value is so small, it does not extend into the peak thermal period. Therefore, the conservative viscosity assumption (0.002 poise) is overly conservative. This observation also applies to subsequent calculations, but since the times would be rather short in any case, there is no need for a more refined calculation.

F. BASALT RESATURATION TIMES

As in the case of granite, the dominant inflow for resaturation is through the bulk rock.

The parameter values given in Section D-3.1 for the first estimate case lead to the inflow rate:

$$\dot{Q} = 3.3 \times 10^4 \text{ m}^3/\text{yr}$$

over the first 100 years, which implies resaturation at about 61 years after repository closure. In the second estimate case, the permeability is two orders of magnitude higher, so that resaturation takes place in less than one year (0.6 year).

G. SHALE RESATURATION TIMES

The parameters that govern resaturation times are identical to those for basalt. Therefore, the first and second estimates of resaturation times for a repository in shale are 61 years and 0.6 years, respectively.

H. DOME SALT RESATURATION TIMES

The analysis of resaturation of a repository in a salt dome is similar to the case of bedded salt. There are two parameter changes to be accounted for. First, since there is no lower aquifer immediately below the repository, only 50 borehole pathways should be included. Second the vertical gradient in shafts and boreholes is 1.1 instead of 1.3. Using the same notation as earlier, the first estimate calculations yield the functions:

$$Q_1 = 1.73t + 0.0086\, t^2$$

$$Q_2 = 0.086t + 0.004\, t^2 .$$

Since the pore space is

$$Q = (2 \times 10^6)(200 - t)/200$$

for t between 0 and 200 years after repository closure, resaturation is again achieved at the time t which solves the equation

$$Q = Q_1 + Q_2 .$$

This value of t is approximately 200 years (199.91) and the corresponding water volume is 865 m^3.

Similarly, for the second estimate, the following functions apply:

$$Q_1 = 1.73t + 0.86\ t^2$$

$$Q_2 = .086t + 0.04\ t^2$$

$$Q = (2 \times 10^6)(1000-t)/1000\ .$$

The result is a resaturation time of 748 years with a corresponding water volume of $5.0 \times 10^5\ m^3$.

I. SUMMARY OF CALCULATIONS

Resaturation times calculated earlier are summarized in Table D-II-1.

J. QUALIFICATIONS

The numerical results of this section have been derived under a set of specific assumptions and parameter values. Depending on the manner in which the repository is designed, the resaturation times calculated here may or may not be reasonable estimates of the time before which certain release mechanisms can become operative. A particularly complicating factor is the fact that engineering choices which may add to repository integrity with respect to one breach mechanism may detract from its integrity with respect to another. Examples of this are discussed below.

Porosity of backfill. Since the rate of inflow to the repository is fixed by the pathway parameters, the recharge time will be increased if the volume V of water required to saturate the repository is increased. The limiting case of no backfill yields a volume $V = 10^7\ m^3$ and hence recharge times five times as long as those calculated above. Nevertheless, the use of highly porous (and hence permeable) backfill would aid the movement of radionuclides through the repository should some breach pathways be established.

TABLE D-II-1

CALCULATED RESATURATION TIMES

Medium	First Estimate (yrs)	Second Estimate (yrs)
Bedded Salt	200	720
Granite	161	7
Basalt	61	0.6
Shale	61	0.6
Dome Salt	200	748

Bulkheads. It is possible that the repository designs will include sealing off waste drifts and segmenting tunnels with carefully constructed bulkheads. These measures will reduce the potential for water and radionuclide transport through the repository. At the same time, if these barriers are essentially impermeable, they also seal off portions of the repository from certain inflow sources, such as permeable shafts and boreholes. The result will be that the segments of the repository which include (or are close to) the water sources may become resaturated rather soon. In this case, mechanisms for hydrologic transport of radionuclides may become operative sooner than envisioned from the times calculated earlier. For repositories in which resaturation through the bulk rock dominates, this factor is not important.

K. CONCLUSIONS

While resaturation mechanisms may delay the initiation of potential radionuclide transport from the repository, for the reasons cited in the previous section it is recommended that considerable care be exercised in applying credit for this delay in assessing repository performance. It is a matter that should be investigated when specific repository plans are being evaluated, at which time the uncertainties may be sufficiently resolvable to allow greater credit for this factor in the repository performance assessment.

APPENDIX D-III

METHODOLOGY FOR DISSOLUTION CALCULATIONS

A. INTRODUCTION

The dissolution mechanisms discussed here apply exclusively to repositories in salt. Similar problems do not arise with the other host rocks under consideration.

Breach mechanisms that permit water to flow from a repository in salt to an aquifer may develop either by gradual processes (e.g., shaft seal degradation) or abrupt events (e.g., faulting). In either case, the water may dissolve and carry off some of the salt, thereby perhaps worsening the breach. The harmful effects could consist of the formation of a less resistive pathway for the water and hence greater water flow, the accessibility of more canisters to leaching, or structural changes in the surrounding rock.

The purpose of this appendix is to estimate the rate at which such dissolution could take place, consistent with other assumptions in the report. Throughout, the following constant value for salt (NaCl) solubility in water is used:

$$0.37 \text{ gm/cc water} = 0.168\text{cc salt/cc water.}$$

This is the solubility of salt at about 100°C. The concern here is for boreholes and shafts that have been filled and sealed according to the specifications given elsewhere in the report. Dissolution during the operational phase of new wells drilled in the future is assumed to be a problem that the drillers will have to meet in engineering their systems. For the sake of conservative calculations (i.e., tending to overestimate the dissolution), it will be assumed that water leaving the salt layer through the breach pathway is saturated with salt.

B. BOREHOLES

In Section D-3.3, the degradation of a sealed borehole has been modeled as a deterministic process. The parameters assumed were:

$$\text{Area, } A = 0.1 \text{ m}^2$$

$$\text{Porosity, } n = 0.1$$

$$\text{Permeability, } K = 10^{-8} + \frac{10^{-5} - 10^{-8}}{10^4}\, t$$

(for the first estimate,
t in years, K in cm/sec)

$$K = 10^{-8} + \frac{10^{-4} - 10^{-8}}{10^4}\, t$$

(for the second estimate,
t in years, K in cm/sec)

These parameters enable the calculation of flow as a function of hydraulic gradient. For conservatism, the viscosity will be taken as 0.0022 poise, which has been used elsewhere for flow calculations. (See Appendix D-VI for the dependence of viscosity on temperature.) Dissolution is expected to be greatest at the point where unsaturated water enters the salt layer. As a consequence, it is conservative to assume uniform dissolution in estimating dissolution at the repository level. Calculations here are consistent with the generic stratigraphies and repository assumptions given earlier in the report.

A water flow rate $\dot{Q}$ through the filled borehole corresponds to a salt dissolution rate equal to 0.168 $\dot{Q}$. If the borehole has radius r and length L_s through the salt, then the rate of change of the radius is given by:

$$\frac{dr}{dt} = \frac{0.168\,\dot{Q}}{2\pi r L_s}$$

For bedded salt, $L_s = 100$ m for a borehole extending to the lower aquifer. For dome salt, $L_s = 230$ for a borehole extending to the repository. Recall that $\dot{Q}$ is given by:

$$\dot{Q} = \frac{KiA}{100\mu}$$

for a hydraulic gradient i. The computational procedure is to proceed as follows:

1. Compute $\dot{Q}(t) = \frac{KiA}{100\mu}$
2. Compute Q(t) by integrating $\dot{Q}(t)$ and using the initial condition $Q(0) = 0$.
3. $q(t) = 0.168\,Q(t)$ is the cumulative volume of salt removed.
4. Compute r(t) from the formula

   $$r(t) = \sqrt{r_o^2 + \frac{q(t)}{\pi L_s}}$$

   where r_o is the initial radius. This formula simply derives from volumetric considerations.
5. Compute $\frac{dr}{dt}$, if it is of interest, from the earlier formula

   $$\frac{dr}{dt} = \frac{q(t)}{2\pi r(t) L_s}$$

For ease of computation, the integration of $\dot{Q}(t)$ is worked out below, where K is assumed to degrade linearly from K_0 to K_1 over 10^4 years:

$$K(t) = [K_0 + \frac{K_1 - K_0}{10^4} t][10^{-2}][3.15 \times 10^7]$$

where K_0 and K_1 are in cm/sec and K is in m/yr. The factor 10^{-2} converts centimeters to meters and the factor 3.15×10^7 converts seconds to years. As long as the other parameters remain constant,

$$Q(t) - Q(0) = \int_0^t [K_0 + \frac{K_1 - K_0}{10^4} t][10^{-2}][3.15 \times 10^7][\frac{1A}{100\mu}]dt$$

$$Q(t) = [K_0 t + \frac{K_1 - K_0}{2 \times 10^4} t^2][3.15 \times 10^5][\frac{1A}{100\mu}]$$

Note for future reference that the expression inside the integral sign is $\dot{Q}(t)$. Note also that dissolution may change the value of A for the section of the borehole within the salt, but as long as the changes are very small, corrections for this change need not be introduced. For significant dissolution over a large extent of the borehole, Darcy's law would no longer apply since there would essentially be a conduit for water flow.

Using the scheme just outlined, the numerical results shown in Table D-III-1 are obtained. These calculations suggest that, at least within the parameter range under consideration, the change in r is relatively slow. Therefore, the derivative dr/dt may be approximated by the formula:

$$\frac{dr}{dt} = \frac{0.168 \dot{Q}}{2\pi r_o L_s}$$

TABLE D-III-1

CHANGES IN BOREHOLE RADIUS AS A RESULT OF DISSOLUTION

(Using a gradient $i = 0.01$, $r_o = 0.18$))

	Time (years)	First Estimate r(meters)	Second Estimate r(meters)
Bedded Salt	100	0.1800	0.1800
	500	0.1800	0.1800
	1000	0.1800	0.1801
	5000	0.1803	0.1826
	10,000	0.1811	0.1903
Dome Salt	100	0.1800	0.1800
	500	0.1800	0.1800
	1000	0.1800	0.1800
	5000	0.1801	0.1812
	10,000	0.1805	0.1846

instead of by the original formula:

$$\frac{dr}{dt} = \frac{0.168\dot{Q}}{2\pi r L_s} .$$

The difference is in using r_o, the original radius, instead of r, which always results in a conservative calculation (i.e., tending to overestimate dr/dt) because r is greater than or equal to r_o. For the case of bedded salt, using $L_s = 100$ m and $r_o = 0.18$ m, this yields the formula:

$$\frac{dr}{dt} = 1.485 \times 10^{-3} \dot{Q} .$$

Similarly, for dome salt, using $L_s = 230$ m and $r_o = 0.18$ m, one obtains

$$\frac{dr}{dt} = 6.458 \times 10^{-4} \dot{Q} .$$

As an example of the application of these formulas, consider the value $\dot{Q} = 0.875$ m^3/yr, which is the value calculated in Section D-3.4 for first estimate fluid flows at 1000 years after repository closure. In the case of bedded salt, the resulting value of dr/dt is 1.3×10^{-3} m/yr. This slow rate of increase is or would probably be compensated for by salt creep, which would tend to close any channels created by dissolution. For example, rough calculations suggest that dr/dt for an open borehole at repository depth would be about -3×10^{-3} m/yr, which would more than balance the dissolution. Further discussion of salt creep may be found in Appendix D-VII.

Dissolution around other breach pathways can be analyzed in a manner exactly analogous to the examples worked out above for boreholes. The values in Table D-III-1 roughly scale with the gradient, so that the effects of the larger second estimate gradients in certain cases are apparent.

APPENDIX D-IV

METHODOLOGY FOR DIFFUSION CALCULATIONS

A. INTRODUCTION

In the case of a breach of a nuclear waste repository, either by a gradual process (e.g., borehole plug degradation) or a distinct event (e.g., faulting), there are basically two processes for movement of radionuclides from the canisters to the release pathway. These processes are convection and diffusion. Convection, the carrying of radionuclides by moving water, may be driven by several mechanisms, which are discussed elsewhere in this report. Molecular diffusion, driven by a concentration gradient, is the principal subject of this appendix.

A simplified plan view of a portion of a repository is shown in Figure D-IV-1. The canisters of wastes are emplaced in holes in the floor of the waste drifts. For purposes of this appendix it has been assumed that the waste drifts are 5 m x 5 m in cross section, although most of the formulas will first be worked out in terms of a parametric cross-sectional area A. The waste drifts may be quite long, say 500 meters, and the canisters may be placed at intervals on the order of 5 to 10 meters.

Potential breach mechanisms, such as faults and boreholes, may intersect the waste drifts, the main tunnels, or simply the rock pillars. (The pillars are expected to cover 50-90% of the total repository area.) The drifts and tunnels will be backfilled with porous material. The pillars may also be porous, due either to basic rock porosity or to fracture systems. In any case, diffusion is through porous media, not simply through bulk fluid.

B. BASIC PRINCIPLES AND HYPOTHESES

The basic goal here is to calculate the rate of mass transport from a "source" to a "sink". The source is one or more canisters of nuclear waste, and its strength is determined by the concentration of material

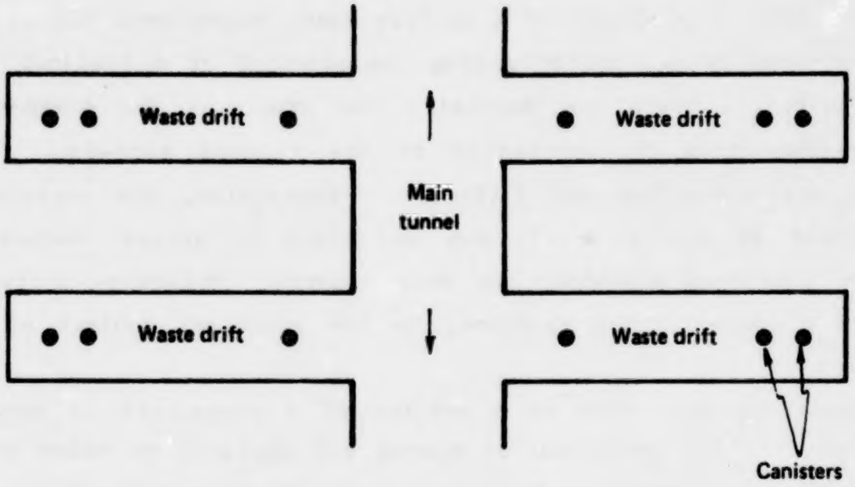

FIGURE D-IV-1 PLAN VIEW OF PORTION OF REPOSITORY (NOT TO SCALE) at its boundary. In general, this concentration will vary from one radionuclide to another. The concentration will be bounded by the solubility limit of the relevant species, which in many cases is very small, and it may be further limited by the rate at which the species can be leached from the canister/waste-form package. The sink consists of a release pathway, such as the portion of a borehole passing through the repository. (Transport along the release pathway is generally dominated by convective forces, which are discussed elsewhere in this report.)

Molecular diffusion is driven by a concentration gradient in the same way that heat conduction is driven by a temperature gradient or fluid flow by a pressure gradient. The basic mathematical model is thus a partial differential equation, which for steady-state problems is simply the Poisson equation (reducing to the Laplace equation away from sources and sinks). The purpose here is not to derive or assume this body of mathematical theory, but rather to present simple, self-contained models that are sufficiently accurate to predict diffusional mass transfer in the present case. Geometric simplifications, always intended to err on the conservative side, will be employed freely. The purpose is generally to reduce problems to a single dimension.

The fundamental principle that the diffusion rate is proportional to the concentration gradient takes the form:

$$J = D \frac{dC}{dx}$$

in one dimension, where

J = flux rate (mass per cross-sectional area per time). The direction of movement is understood to be from regions of higher concentrations to lower ones. With this convention, no minus sign is needed in the equation.

D = diffusion constant. This depends on the fluid, the porous medium, the diffusing solute, and the conditions present.

$C(x)$ = concentration of the solute at distance x from the sink.

This equation, called Fick's law, is exactly analogous to Darcy's law for fluid flow in a porous medium. J will be a function of x. The total mass transport rate $\dot{q}$ through any cross-sectional area A will be obtained as the product JA. The two sections that immediately follow use Fick's law to calculate diffusion rates in certain fundamental cases.

C. DIFFUSION THROUGH A TUBE OR TUNNEL (MODEL A)

Consider the situation sketched in Figure D-IV-2a. Suppose the concentration at the left end is kept fixed at C_2 and that at the right end at C_1, where $C_2 > C_1$. The corresponding concentration gradient and flow is strictly one dimensional, and may be modeled as in Figure D-IV-2b. As long as the porous medium is uniform (an assumption used throughout), the concentration will change uniformly, so that:

$$C(x) = \frac{x}{L}(C_2 - C_1)$$

Thus the diffusive flux is:

$$J = \frac{D(C_2 - C_1)}{L} ,$$

and the mass transport rate $\dot{q}$ is:

$$\dot{q} = JA = \frac{D(C_2 - C_1)}{L} A$$

where A is the cross-sectional area.

While it would be desirable to have measurements of the diffusion coefficient D for the given solute in the given medium, such data are not generally available for the materials of interest in this study. Indeed, the diffusion rates in water are not well known and must often be approximated from other known values. Given the diffusion rate in water, the rate in the water-saturated porous medium may be approximated. We shall do this by multiplying the tunnel cross-sectional area A by the porosity η of the backfill material, since ηA better represents the effective cross section through which the diffusive flux acts. The effective pathway through a real medium is

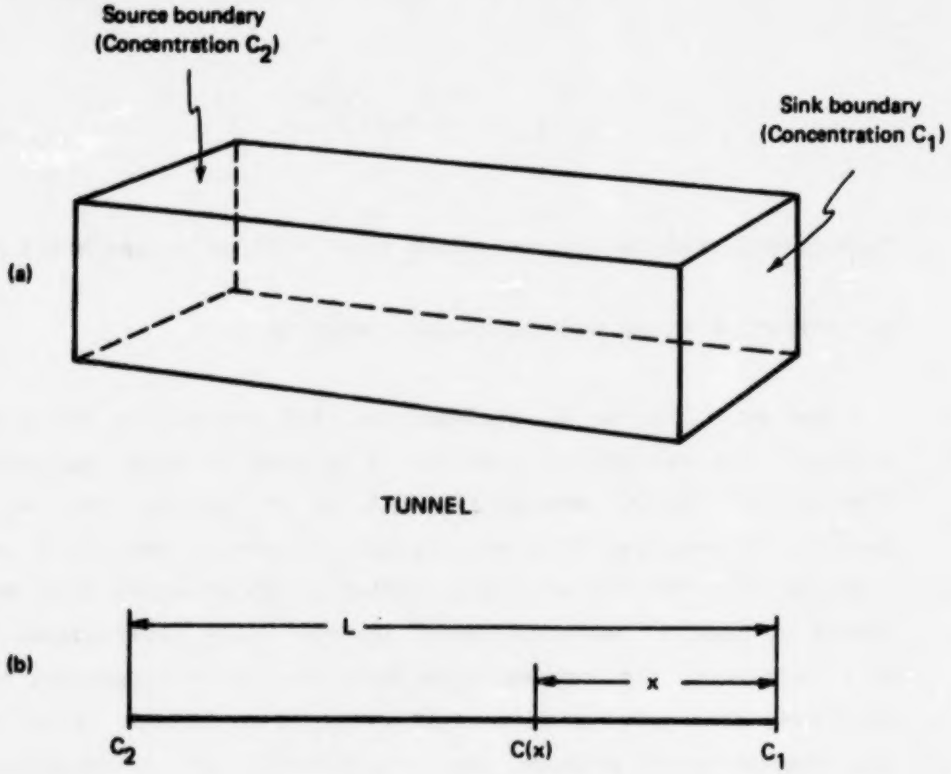

FIGURE D-IV-2 DIFFUSION ALONG A TUNNEL

also not expected to be the straight line suggested in Figure D-IV-2b, but this distance multiplied by a "tortuosity" factor. Since for many porous media this factor is still less than 2, it is not incorporated in the present analysis. Therefore, accounting for porosity but ignoring tortuosity, the mass transport may be calculated approximately by:

$$\dot{q} = \frac{D(C_2 - C_1)A\eta}{L}$$

This formula and the corresponding model will be called Model A.

D. DIFFUSION IN AN ANNULAR REGION (MODEL B)

The situation to be analyzed in this section is shown in Figure D-IV-3a. The cylindrical source will be used to bound the contributions from several point sources located on or outside such a cylinder. Because of symmetry, flow is strictly horizontal and radial and may be analyzed with the aid of Figure D-IV-3b. Steady-state flow requires an identical rate of mass transport through every intermediate boundary. As x increases, the boundary area increases proportionately, so for the same mass transport rate, a smaller flux rate holds. Since flux rate and concentration gradient are proportional, the concentration varies non-uniformly in this case.

The reasoning just described actually enables the calculation of mass transport. Whatever the steady-state overall mass transport rate may be, it must hold that $\dot{q}$ is the rate of material movement through any intermediate cylindrical boundary; that is, for all x,

$$\begin{aligned} \dot{q} &= JA \\ &= (D \frac{dC}{dx})(2\pi xL) \end{aligned}$$

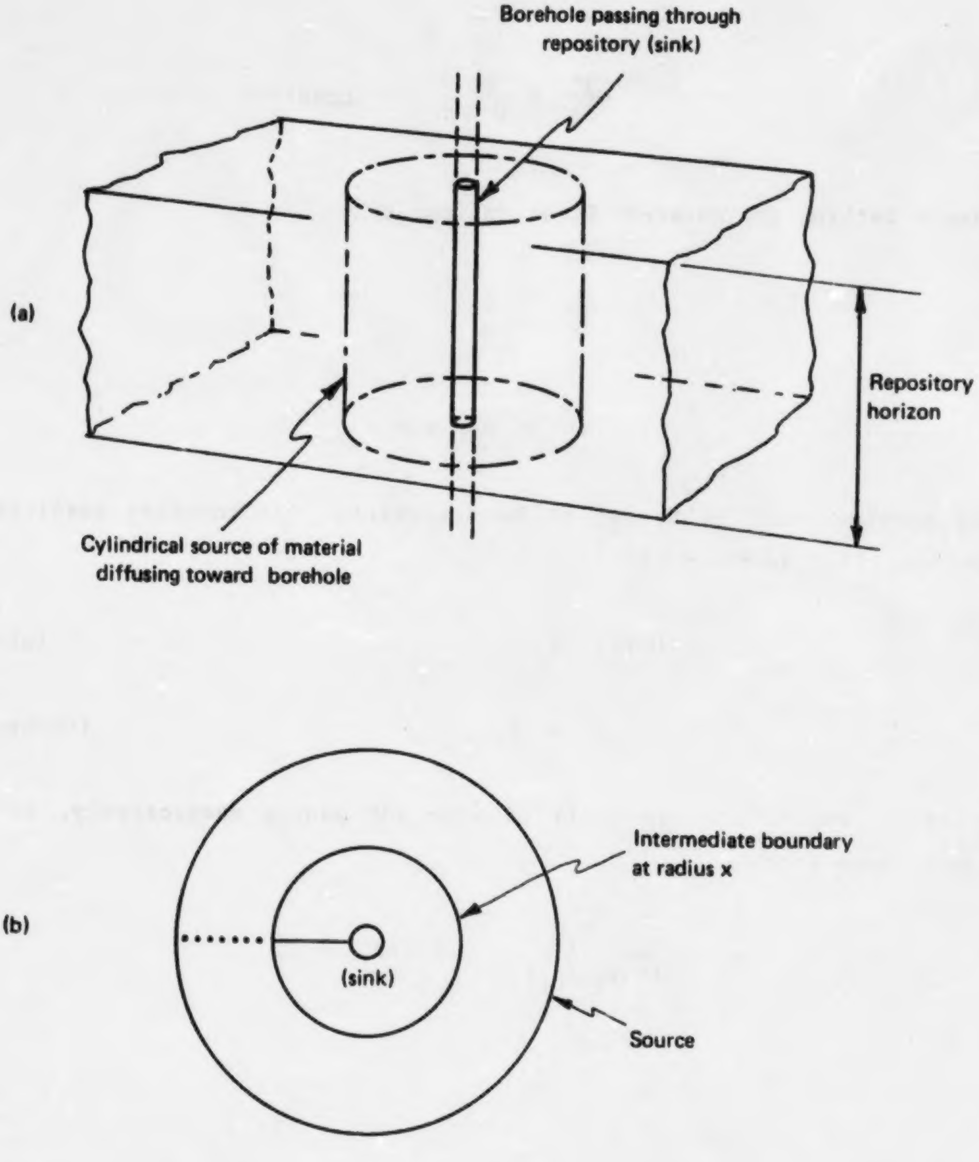
Borehole passing through repository (sink)
(a)
Repository horizon
Cylindrical source of material diffusing toward borehole
(b)
Intermediate boundary at radius x
(sink)
Source

FIGURE D-IV-3 CYLINDRICAL SOURCE AND SINK LEADING TO DIFFUSION IN AN ANNULAR REGION where h is the height of the cylinders. Therefore:

$$x\frac{dC}{dx} = \frac{\dot{q}}{D\cdot 2\pi h} = \text{constant}$$

Simply calling the constant B, it follows that:

$$\frac{dC}{dx} = \frac{B}{x}$$

$$C(x) = B\ln x + E$$

for another constant E, yet to be determined. If boundary conditions are specified in the form:

$$C(r_1) = C_1 \qquad \text{(sink)}$$

$$C(r_2) = C_2 \qquad \text{(source)}$$

where r_1 and r_2 are the radii of sink and source respectively, it is easily seen that:

$$C = \frac{C_2 - C_1}{\ln(r_2/r_1)} \cdot \ln(x/r_1) + C_1$$

The corresponding mass transport rate is thus:

$$\dot{q} = \dot{q}(r_1)$$

$$= D \cdot \frac{dC}{dx}(r_1) \cdot 2\pi r_1 h$$

$$= D \cdot \frac{C_2 - C_1}{r_1 \ln(r_2/r_1)} \cdot 2\pi r_1 h$$

Cancelling the r_1's and now inserting the porosity factor, we obtain:

$$\dot{q} = \frac{2\pi D h \eta (C_2 - C_1)}{\ln(r_2/r_1)}$$

This formula and the corresponding model will be called Model B. Note that for conservative calculations one wants to err on the side of underestimating r_2 and overestimating r_1.

E. EXAMPLE: DIFFUSION INTO MAIN TUNNEL

Consider the situation previously shown in Figure D-IV-1. If flow through the main tunnel is initiated by some mechanism, such as degrading shaft seals at either end, the release of material along waste drifts to the tunnel may be primarily from diffusion. We shall model this situation as shown in Figure D-IV-4 for radionuclides whose concentration is limited by a relatively low solubility limit C_2. It is conservative to replace the first canister by a planar source at concentration C_2, and fill the entire waste drift cross section. Furthermore, the remaining canisters in the drift cannot contribute to the mass transport, since the hypothetical source has maximal concentration. (There could not be a net concentration gradient driving

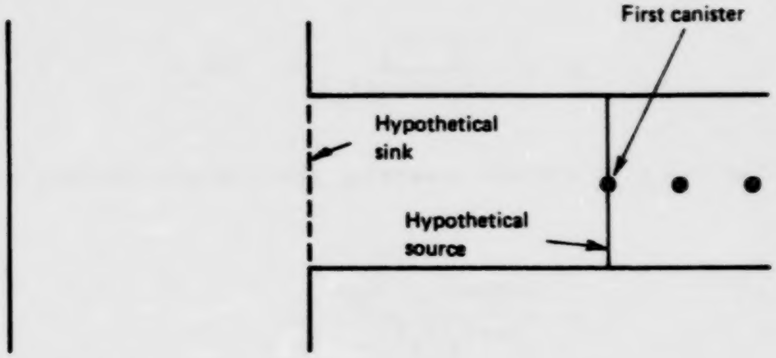

FIGURE D–IV–4 GEOMETRY FOR DIFFUSION INTO MAIN TUNNEL material toward it from the right). We take as the sink the entrance from the main tunnel to the waste drift. This is the situation in Model A. Nominal parameters will be taken as follows:

$A = 25\ m^2$
$n = 0.2$
$D = 10^{-6}\ cm^2/sec$
$C_2 = 10^{-5}\ Ci/m^3$ (Ci = curies)
$C_1 = 0$
$L = 20\ m.$

The corresponding mass transport is found to be:

$$\dot{q} = 8 \times 10^{-9}\ Ci/yr.$$

This represents the maximum contribution of one waste drift to the main tunnel by diffusion, according to the parameter values given above.

It is important to compare this mass transport with that possibly driven by other forces. In particular, consider the following question: What hydraulic gradient acting along a waste drift would result in the same transport rate? A permeability of $K = 10^{-4}$ cm/sec and a viscosity of $\mu = 0.005$ will be used in answering this. The unknown gradient i causes fluid flow at the rate

$$\frac{KiA}{100\mu} = 1.6 \times 10^3 i\ \ m^3/yr$$

Assuming that this water is saturated with the solute in question, i may be found to be:

$$8 \times 10^{-9} = 1.6 \times 10^3 \times i \times 10^{-5}$$

$$i = 5 \times 10^{-7}.$$

This is an extremely low gradient and suggests that much care should be exercised before diffusion is regarded as the dominant transport mechanism.

F. EXAMPLE: BOREHOLE THROUGH A PILLAR

The repository pillars may be considered as long rectangles of constant width w; a borehole drilled randomly through such a pillar will have its expected distance from a wall approximately equal to w/4. For the present calculations we shall take w = 16 m, so that the expected shortest distance from borehole to drift will be 4 m. In fact, the borehole may receive material from the nearby drift as well as from the one on the opposite side of the pillar. An upper bound on diffusional transport may be obtained by using Model B, with nominal parameters as follows:

$r_1 = 0.2$ m
$C_1 = 0$
$h = 5$ m
$r_2 = 4$ m
$C_2 = 10^{-5}$ Ci/m^3
$\eta = 10^{-4}$
$D = 10^{-6}$ cm^2/sec.

The corresponding mass transport is found to be:

$$\dot{Q} = 3.3 \times 10^{-11} \text{ Ci/yr}$$

As earlier, it is important to compare this with the potential transport by a convective process. By the analogous structure of Darcy's and Fick's laws, the equation corresponding to Model B for fluid flow rate $\dot{Q}$ may be written:

$$\dot{Q} = \frac{2\pi K h \Delta p}{100 \mu \ln(r_2/r_1)}$$

where Δp is the head difference and μ is the viscosity. Taking $\mu = 0.005$ and $K = 10^{-9}$ cm/sec, this yields:

$$\dot{Q} = 7 \times 10^{-3} \times \Delta p \ \mathrm{m^3/yr}.$$

If this fluid is saturated at 10^{-5} Ci/m^3, say, then Δp may be found from:

$$3.3 \times 10^{-11} = 7 \times 10^{-8} \times \Delta p$$

$$5 \times 10^{-4} \ \mathrm{m} = \Delta p$$

Along a distance of 5 m of the borehole, the pressure drop corresponding to a gradient of 0.001, say, will be 5×10^{-3} m. Therefore, no matter what the pressure in the waste drift, it will differ from that in part of the borehole by at least 2.5×10^{-3}, which is five times the difference needed to approximate diffusional transport. This suggests that diffusion will not dominate this process.

G. TRANSIENT BEHAVIOR

If the repository is breached some time after the canisters have corroded and radionuclides have diffused through the repository, then initially the mass transport out through the release pathway will be greater than its steady-state value. This is because the maximum concentration C_2 determined by solubility limits may be experienced very close to the breach, leading to a high concentration gradient and hence a high diffusion flow. The initial flow is best approximated by assuming it is at concentration C_2 or whatever other initial values may be estimated for that point in time.

Exit flows at concentration C_2 should continue to be used in the models until steady flow has been obtained. A conservative approach for dealing with this factor may be developed as follows:

1. Determine the radionuclide flow rate (in Ci/yr, say) out the release path.

2. Determine the initial stored radionuclide content in the diffusional pathway being modeled. (Concentration limits x water volume).
3. Determine how long it would take for the quantity calculated in Step 2 to be removed by the rate from Step 1.
4. The time calculated in Step 3 may be used to shift to a steady-state diffusion model. In fact, for the Model A situation, one half of this time suffices.

This calculation is not intended to determine the time at which steady-state behavior is achieved, but it shifts the mass transport rate in time so that the cumulative amount released by any point in time is greater than or equal to the actual value. In this sense it is a conservative approach.

APPENDIX D-V

METHODOLOGY FOR U-TUBE CALCULATIONS

A. INTRODUCTION

The purpose of this section is to analyze the flow through the repository for the conditions outlined in Figure D-V-1, where the degrading shaft seals and the permeable tunnel backfill lead to an alternative path from point A to B. While this additional path may tend to decrease slightly the driving potential (head) between points A and B, it is conservative to ignore this effect. Since the overall resistivity of the alternative path is in general still considerably higher than that of the aquifer, this assumption is probably not overly conservative.

B. MATHEMATICAL FORMULATION

Darcy's formula will form the basis for the present analysis. In its simplest form, it appears as follows:

$$\dot{Q} = KiA$$

where

$\dot{Q}$ = flow rate through pathway cross section

K = hydraulic conductivity, also referred to loosely as the permeability

i = hydraulic gradient

A = cross-sectional area

The hydraulic conductivity, in units of length per time, depends not only on the medium through which water is flowing, but also on the water's viscosity, which varies with temperature. The numbers reported in the literature are ordinarily for water at relatively low temperatures ($\approx 20^\circ C$) at which the viscosity is approximately 0.01 poise. Since the hydraulic conductivity is inversely proportional to the viscosity, the reported K values must be divided by the ratio $\mu/0.01$

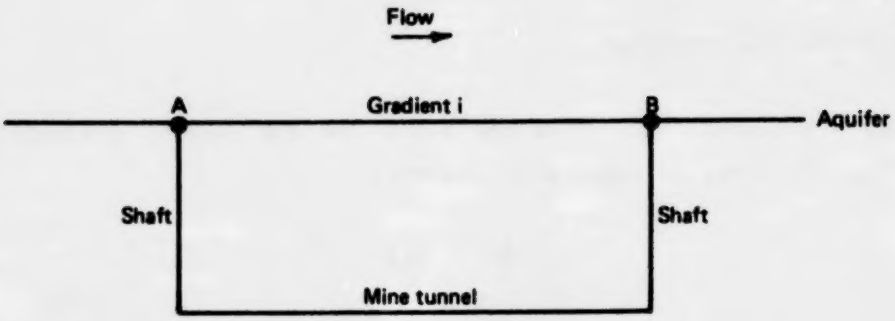

FIGURE D-V-1 TYPICAL U–TUBE SITUATION

when the viscosity μ is expected to deviate significantly from 0.01 poise. This might be the case, for example, with water flowing through the repository during its period of high thermal output. A table of viscosity values is given as Table D-V-1. Dependence on pressure is not sufficiently important to require consideration for present purposes.

Consideration of viscosity, as outlined above, leads to the following revised form of Darcy's law:

$$\dot{Q} = \frac{KiA}{100\mu}$$

where the dimensions are as follows:

K	length/time
i	dimensionless
A	length squared
100μ	dimensionless (actually, poise/0.01 poise)
$\dot{Q}$	length cubed/time

The factor

$$\frac{Ki}{100\mu}$$

is sometimes called the Darcy velocity. It has the units of length/time but should be interpreted as a flux: volume per cross-sectional area per unit time. When the Darcy velocity is divided by the porosity η, an approximation to the average fluid velocity is obtained.

Darcy's law may be considered from the point of view of its electrical analog, Ohm's law:

$$I = \frac{E}{R},$$

where

R = resistance,

E = the voltage over the resistance, and

I = the current.

In the present case, the porous medium is the resistance, the head drop is the voltage, and the flow rate is the current. If the gradient i

TABLE D-V-1

VISCOSITY OF LIQUID WATER AT ATMOSPHERIC PRESSURE

Temperature (°C)	Viscosity (poise)
20	0.0100
40	0.0065
60	0.0047
75	0.0038
100	0.0029
125	0.0022
150	0.0018

Source: American Institute of Physics Handbook, 1972.
Data compiled from other sources.

originally derives from a head drop Δ over a length L, that is,

$$i = \frac{\Delta}{L},$$

then the basic equation is

$$\dot{Q} = \frac{KA\Delta}{100\mu L}$$

from which the parameter correspondence is seen to be:

resistance	⟷	$\frac{100\mu L}{KA}$
voltage	⟷	Δ
current	⟷	$\dot{Q}$

This correspondence is useful in analyzing series and parallel flow paths, as in the present problem.

C. ANALYSIS IN PARAMETRIC FORM

The following symbols will be used for the parameters characterizing the situation shown in Figure D-V-1:

Δ	head drop from A to B
D_1	distance from A to B which also equals length of mine tunnel
K_1	permeability of filled mine tunnel
A_1	cross-sectional area of mine tunnel
n_1	porosity of filled mine tunnel
D_2	length of each shaft
K_2	permeability of filled shafts
A_2	cross-sectional area of each shaft
n_2	porosity of filled shafts

As mentioned earlier, the slight change of head difference between points A and B, due to the development of an additional pathway between

them will be omitted from the analysis. Thus, the problem amounts to three resistances in series, as sketched in Figure D-V-2.
The flow rate is thus:

$$\dot{Q} = \frac{\Delta}{\alpha_1 + 2\alpha_2}.$$

Interstitial velocities in each segment are given by:

$$v_1 = \frac{\dot{Q}}{A_1 n_1}$$

$$v_2 = \frac{\dot{Q}}{A_2 n_2}.$$

Head drops over individual segments are proportional to the resistances, so that:

$$\Delta_1 = \frac{\alpha_1}{\alpha_1 + 2\alpha_2} \Delta$$

$$\Delta_2 = \frac{\alpha_2}{\alpha_1 + 2\alpha_2} \Delta$$

where the subscripts 1 and 2 correspond to tunnel and shaft, respectively.

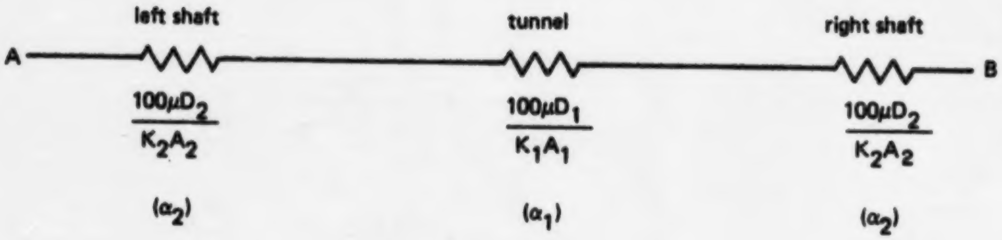
A
left shaft
$\frac{100\mu D_2}{K_2 A_2}$
(α_2)
tunnel
$\frac{100\mu D_1}{K_1 A_1}$
(α_1)
right shaft
$\frac{100\mu D_2}{K_2 A_2}$
(α_2)
B

FIGURE D–V–2 SERIES RESISTANCE MODEL FOR U–TUBE CALCULATIONS

D. NUMERICAL RESULTS

Of particular importance in this report is the upward vertical gradient i_2 in the so-called right shaft. On the basis of the previous discussion, this can be calculated from the equations:

$$i_2 = \frac{\Delta_2}{L_2}$$

$$= \frac{\alpha_2}{\alpha_1 + 2\alpha_2} \cdot \frac{\Delta}{L_2}$$

$$= \frac{\alpha_2}{\alpha_1 + 2\alpha_2} \cdot \frac{iD_1}{L_2}$$

where i is the gradient in the upper aquifer. For calculational purposes, the variable inputs will generally be i, K_1, and K_2. The gradient i will vary between first and second estimates, taking the value 0.002 and 0.02, respectively. K_1 has the value 10^{-6} cm/sec for salt and 10^{-4} cm/sec for granite, basalt, and shale. K_2 is a function of time due to the assumed gradual degradation of the shaft seals. The first estimate is:

$$K_2 = 3.15 \times 10^{-3} + 3.12 \times 10^{-5}\ t$$

and the second estimate is:

$$K_2 = 3.15 \times 10^{-3} + 3.15 \times 10^{-3}\ t,$$

both based on Section D-3.2.3. The other parameters have been given previously in this appendix. Corresponding values of i_2 are summarized in Table D-V-2. Note that while the gradients decrease with time, the flow rates would actually increase since the total resistance of the series pathway is decreasing.

A similar U-tube effect occurs with sealed boreholes. Assume that 50 boreholes penetrate to the repository and that they are located randomly. Then the resulting flow would be downward in roughly 25 holes

TABLE D-V-2

HYDRAULIC GRADIENTS IN VERTICAL SHAFTS DUE TO U-TUBE EFFECT

		Hydraulic Gradient (i)	
Medium	Years*	First Estimate	Second Estimate
Bedded Salt	100	0.033	0.036
	250	0.030	0.015
	1,000	0.019	0.004
	10,000	0.004	0.0004
Granite	100	0.017	0.167
	1,000	0.017	0.121
	10,000	0.017	0.033
Basalt	100	0.040	0.363
	1,000	0.040	0.200
	10,000	0.036	0.036
Shale	100	0.040	0.363
	1,000	0.040	0.200
	10,000	0.036	0.036
Dome Salt	100	0.016	0.032
	250	0.015	0.015
	1,000	0.012	0.004
	10,000	0.003	0.0004

*Years after repository closure.

and upward in the other 25, and the mean distance (projected to a plane parallel to the direction of aquifer flow) between the boreholes in these two sets would be 2000 m, half the length of the repository. Using area and permeability parameters given in Section D-3.3.3, the vertical gradients shown in Table D-V-3 may be calculated.

APPENDIX D-VI

EFFECT OF THERMALLY-INDUCED BUOYANCY ON VERTICAL FLOW

A. INTRODUCTION

The heat generated by radioactive wastes in a repository will decrease the density of any water present. The reduced density will result in an upward force (due to buoyancy) for any water column extending from the repository to the upper aquifer. The water column of interest may include all the water contained in rock pores or fractures above the repository, or may be the water present in a specific breach of containment pathway such as a slightly permeable borehole. The situation is illustrated in Figure D-VI-1. Note that the emphasis is on the water above the repository, not on the rock itself, and therefore reference is to the (generally moving) column of water. This phenomenon has been discussed elsewhere(1.2.3), although various conclusions have been drawn concerning its significance. These previous discussions have been based on numerical solutions to two-dimensional fluid-flow equations and on other fluid-mechanical techniques. The purpose of this appendix is to discuss the question in terms of basic physical principles, without numerical simulations or advanced analytical techniques. This approach should serve to clarify the important factors and lead to useful numerical approximations of the forces created by this buoyancy effect.

B. SIMPLIFICATIONS

Any vertical movement of the water in the rock surrounding a repository will be superimposed on the prevailing, largely horizontal flow pattern. However, the water velocities through the surrounding rock are sufficiently small that these horizontal forces and motions can be omitted from the analysis without significantly affecting the results. In fact, it is also conservative to ignore such motions because they tend to decrease the density gradient and hence the buoyancy effect. In the absence of horizontal flows induced by regional

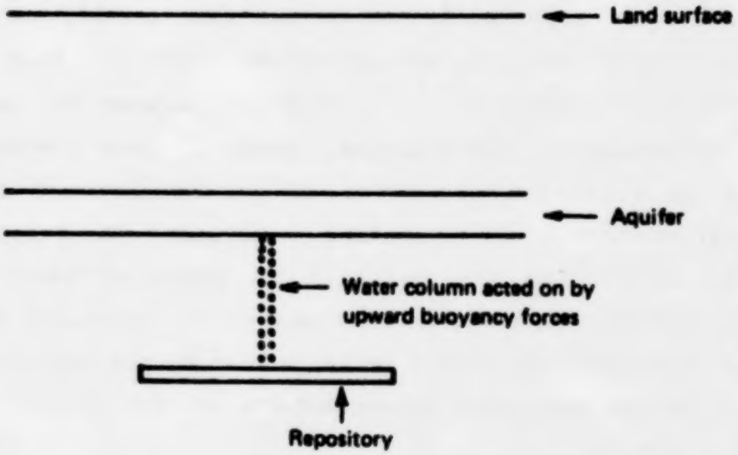

FIGURE D-VI-1 CONCEPTUAL FRAMEWORK FOR BUOYANCY ANALYSIS

groundwater movement, there will still be horizontal flows induced by the differential vertical forces that result from density differences in the water column under consideration. The resulting flow pattern has the general shape shown in Figure D-VI-2. However, these horizontal components may also be ignored for the present approximate analysis, as becomes especially clear by redrawing the previous figure with identical horizontal and vertical scales. See Figure D-VI-3.

C. OUTLINE OF APPROACH

The structure of this analysis is illustrated by the sequence of drawings in Figure D-VI-4. Figure D-VI-4a shows two vertical columns of water connected by a tube at the bottom. Heating of the left column results in a lower density, so there is a tendency for water to move through the connecting tube from right to left. The driving force for this motion can be maintained approximately constant by inlet and outlet pipes to maintain constant water levels, as shown in Figure D-VI-4b. The same driving force and flow rate can be obtained by considering an equivalent difference in water levels, rather than water densities. This difference is shown in Figure D-VI-4c. In order for the flow to achieve a steady state, the driving force must be balanced by an equal and opposite resisting force. In the present case, the dominant resisting force comes from the low permeability of the medium through which the water flows. While it may be argued that the corresponding repository situation implies that this resistance should be present in both columns of water, at the outset of the analysis the conservative assumption of resistance only in the rising column will be used. This is shown in Figure D-VI-4d. The driving force can be represented by the effective hydraulic gradient over this vertical column, calculated by dividing the excess height of the right column over that of the left column (= head) by the length of the left column. (The effect of resistance in the right column is discussed later in this appendix.)

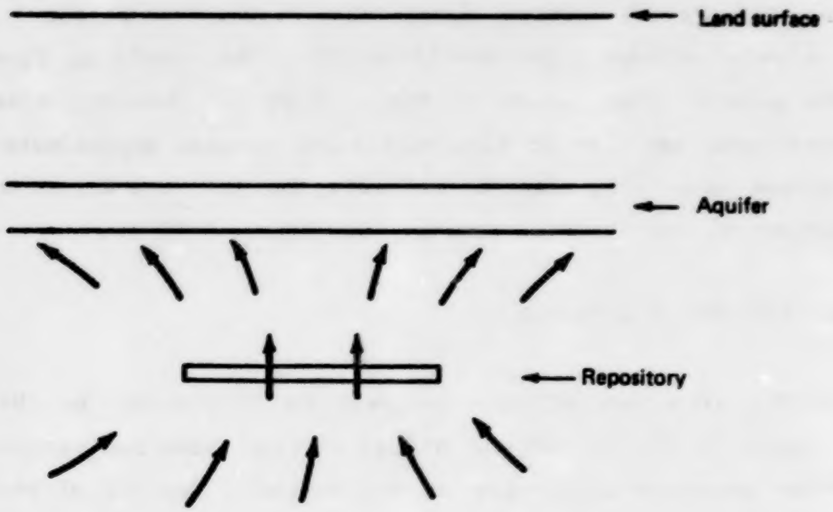

FIGURE D-VI-2 CONVECTIVE FLOW PATTERN

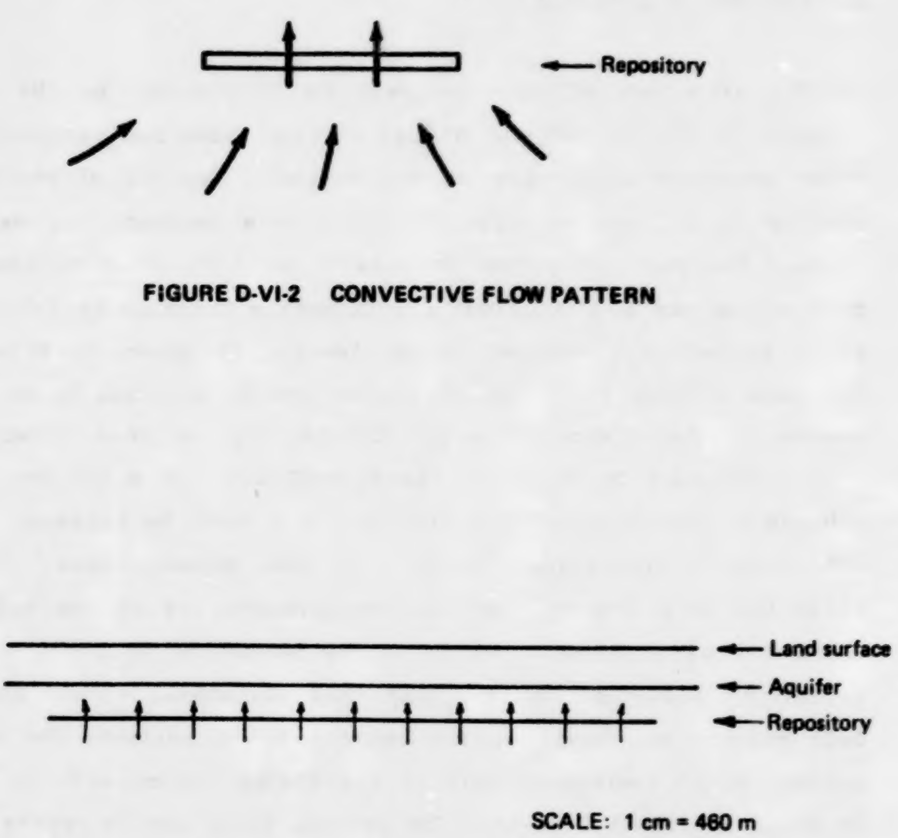

FIGURE D-VI-3 SCALE DRAWING OF REPOSITORY

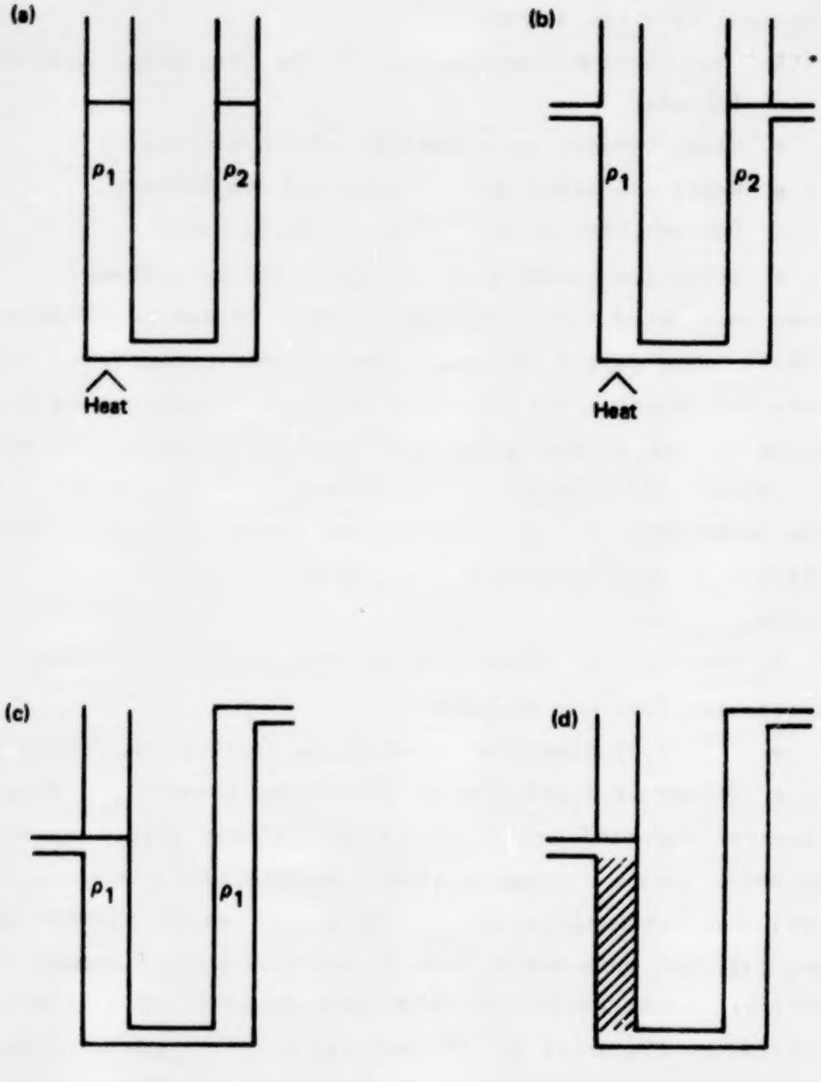

FIGURE D-VI-4 CONCEPTUAL DEVELOPMENT OF BUOYANCY MODEL

D. OUTLINE OF COMPUTATIONAL APPROACH

In order to apply the conceptual model described earlier, the following data are needed:

- Temperature distribution in the overlying rock at the time of interest.
- Water density as a function of temperature.
- Water viscosity as a function of temperature.
- Permeability of the water column pathway.
- Effective porosity of the water column pathway.

These data enter into the computational framework illustrated in Figure D-VI-5. The output of such computations consists of volumetric flow rates and travel times for water from the repository to the aquifer when driven by the thermally induced buoyancy effect. For the purposes of this study, this output may be interpreted as a lower bound on travel time and hence a conservative estimate. The equivalent hydraulic gradient is also important for comparing this driving force with other driving forces.

In addition to model limitations previously noted, the following factors are also not included:

- Effect of dissolved material on density and viscosity.
- Effect of fluid flow on underlying temperature distribution.

Dissolved material could have a significant effect on density in case the water passes through a highly soluble medium such as salt. In this case, the vertical column moving upward would contain more dissolved material, and this would tend to counteract the buoyancy effect. It is therefore conservative to omit this factor. The effect of dissolved material on viscosity is too small to warrant consideration. It is also conservative to omit the effect of fluid flow on the temperature distribution, since this effect is to decrease thermal, and hence, density gradients. Furthermore, the amount of heat transfer that can be accomplished by the fluid flow appears to be rather small (<10%) compared with the total heat transfer.(1)

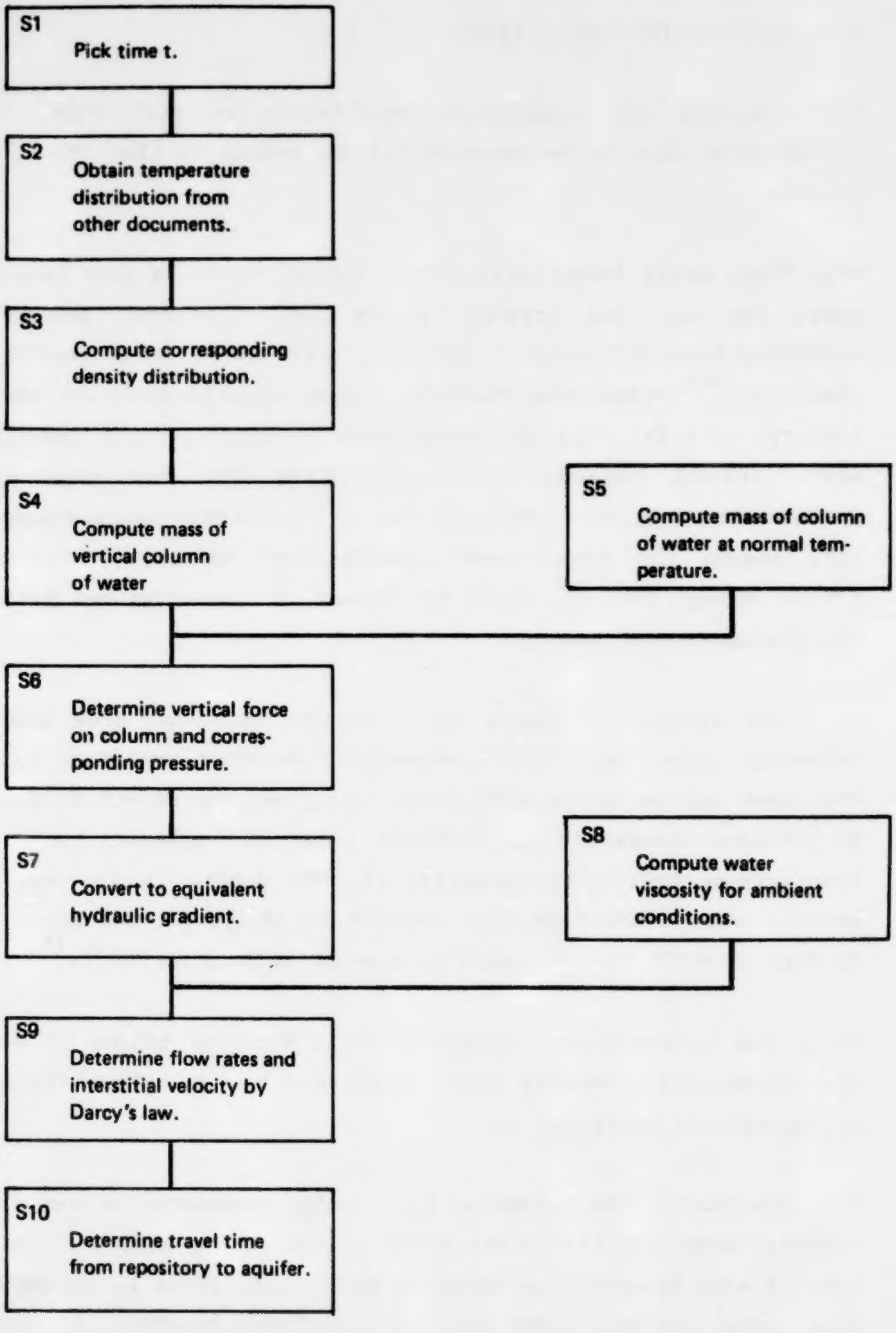
S1
Pick time t.
S2
Obtain temperature distribution from other documents.
S3
Compute corresponding density distribution.
S4
Compute mass of vertical column of water
S5
Compute mass of column of water at normal temperature.
S6
Determine vertical force on column and corresponding pressure.
S7
Convert to equivalent hydraulic gradient.
S8
Compute water viscosity for ambient conditions.
S9
Determine flow rates and interstitial velocity by Darcy's law.
S10
Determine travel time from repository to aquifer.

FIGURE D-VI-5 INFORMATION FLOW CHART FOR BUOYANCY COMPUTATIONS

E. DISCUSSION OF INDIVIDUAL STEPS

S1: Because the temperature profile varies with time, these calculations need to be repeated for the points in time that are of interest.

S2: Temperature distributions for various points in time have been given for salt and granite in the Task B Report. Temperature distributions for basalt, granite, and shale have been given elsewhere.(4) These distributions depend significantly on several factors, such as: age and composition of wastes, areal density of waste, thermal conductivity of surrounding rock, heat capacity of surrounding rock, etc. For purposes of the present calculations, we will assume the temperature distributions indicated in Figures D-VI-6 through D-VI-10, which are "generic" approximations based on the aforementioned sources.

S3: The density of liquid water may be estimated from standard reference data. Table D-VI-1 summarizes selected numerical values. Pressures are not given with these data, but the effect on density of pressure changes in the range of 1 bar (atmospheric) to 50 bars (approximate hydrostatic pressure at 500m depth) is too small to warrant consideration in this approximate analysis. One notes that 50 bars is sufficient pressure to prevent boiling at 250°C.(5)

Given the temperature distribution in a vertical column of water, the corresponding density distribution is then calculated by means of the data in Table D-VI-1.

S4: Previously, the column of water under consideration has always extended from the repository level to the upper aquifer. In the case of many breach-of-containment mechanisms, there is no question about this choice. For some calculations, however, it may be preferable to consider a column of water extending from the upper aquifer down to some point below the repository.

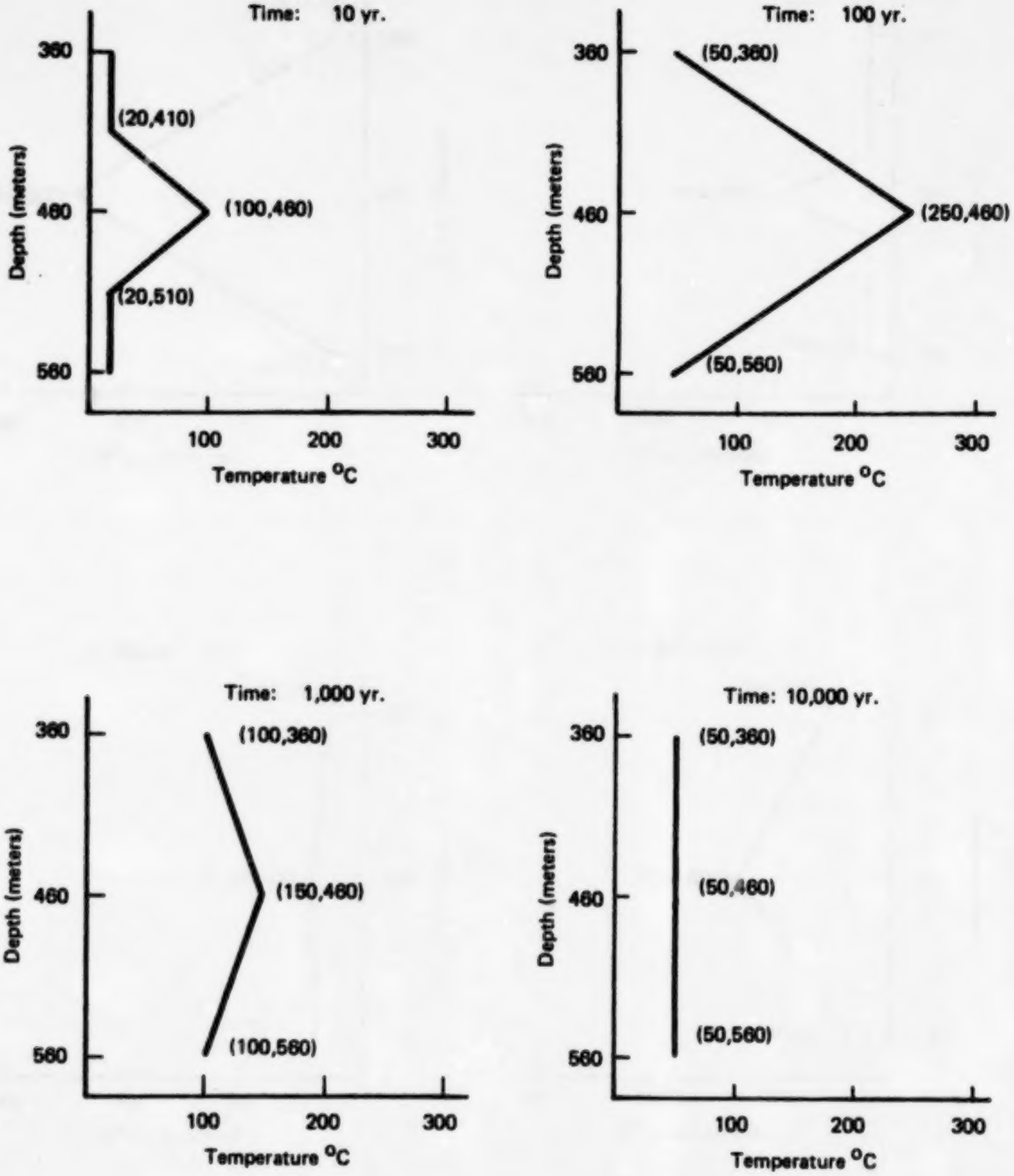

FIGURE D–VI–6 TEMPERATURE DISTRIBUTION FOR BEDDED SALT REPOSITORY

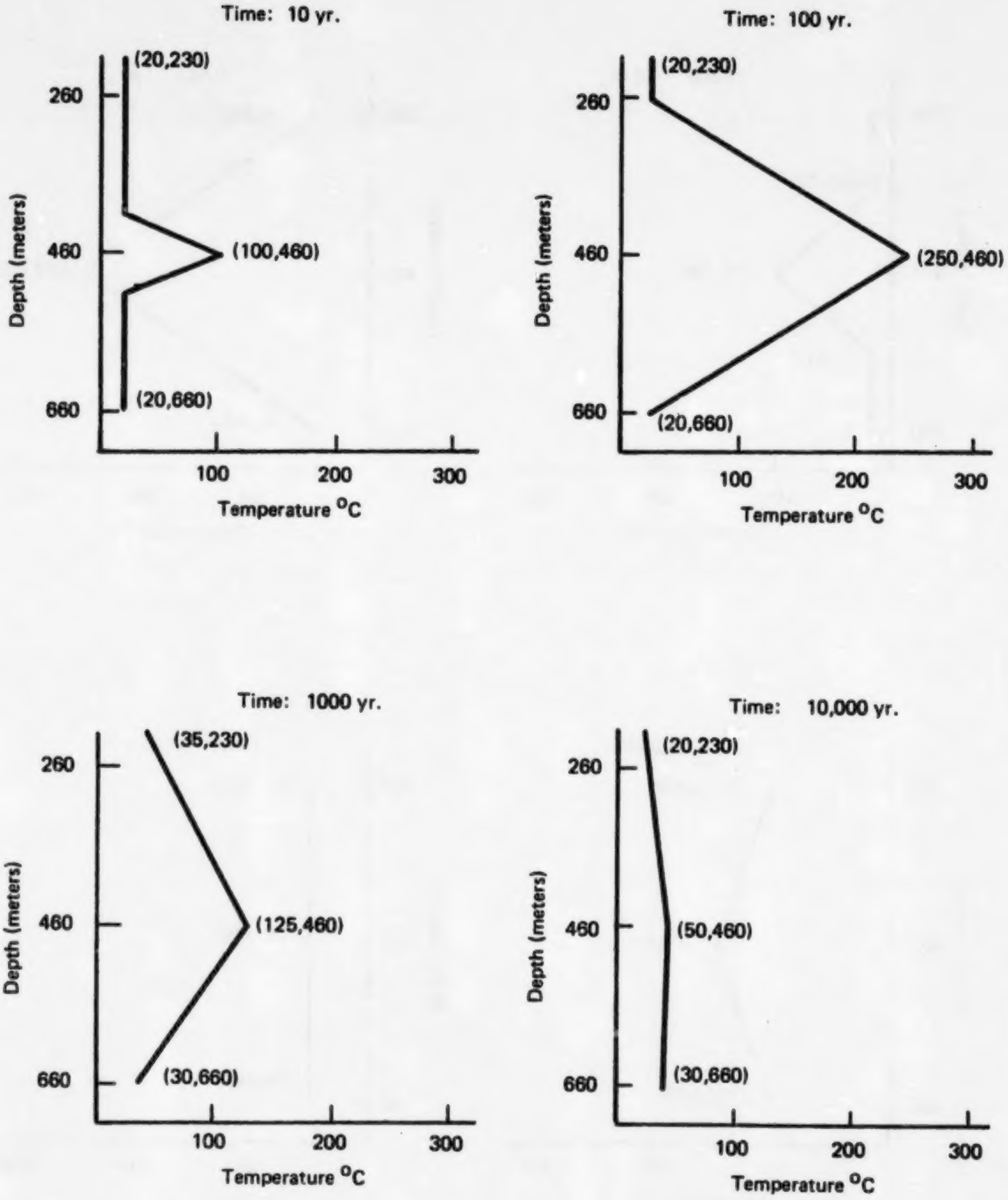

FIGURE D–VI–7 TEMPERATURE DISTRIBUTIONS FOR GRANITE REPOSITORY

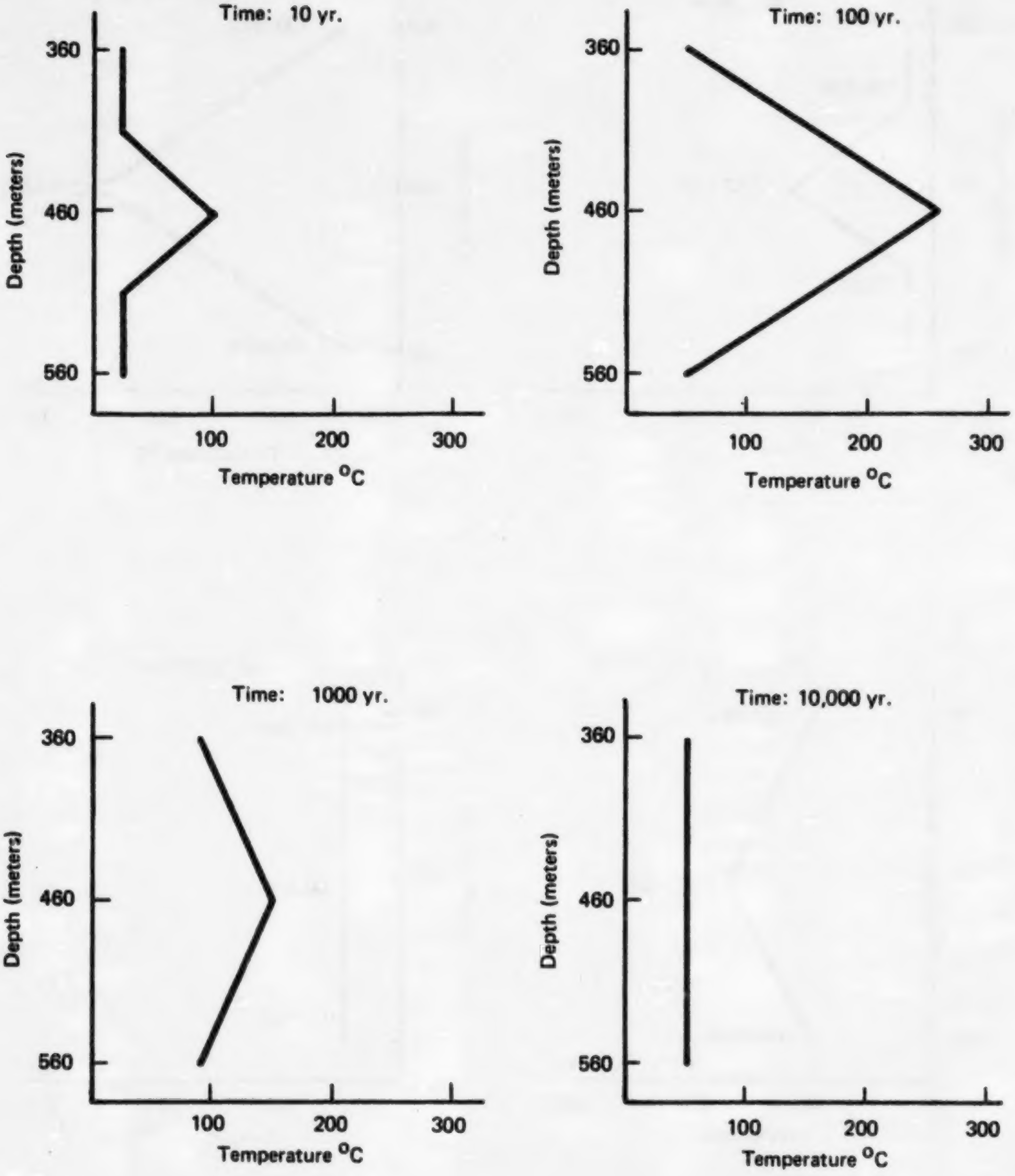

FIGURE D–VI–8 TEMPERATURE DISTRIBUTIONS FOR BASALT REPOSITORY

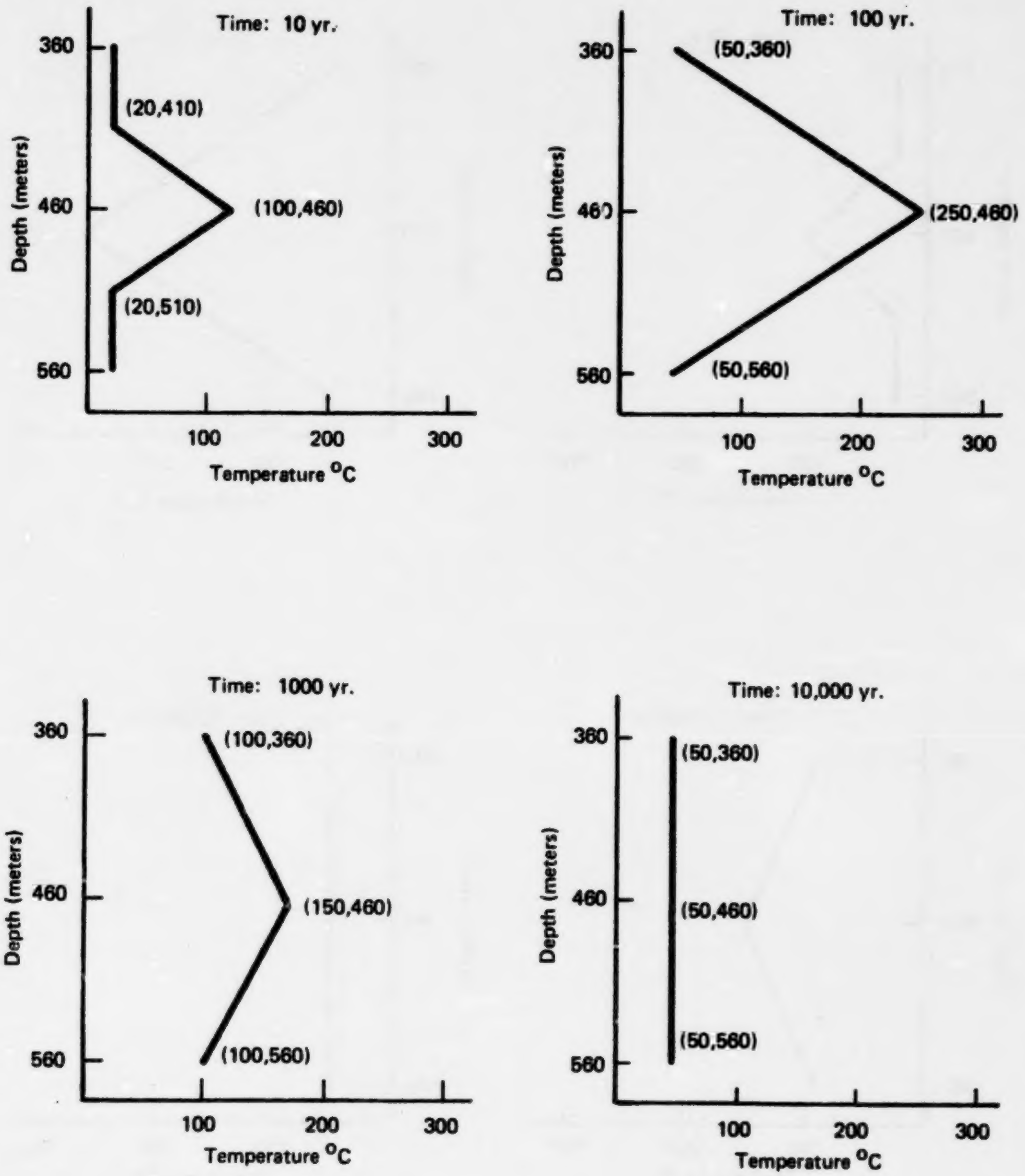

FIGURE D–VI–9 TEMPERATURE DISTRIBUTIONS FOR SHALE REPOSITORY

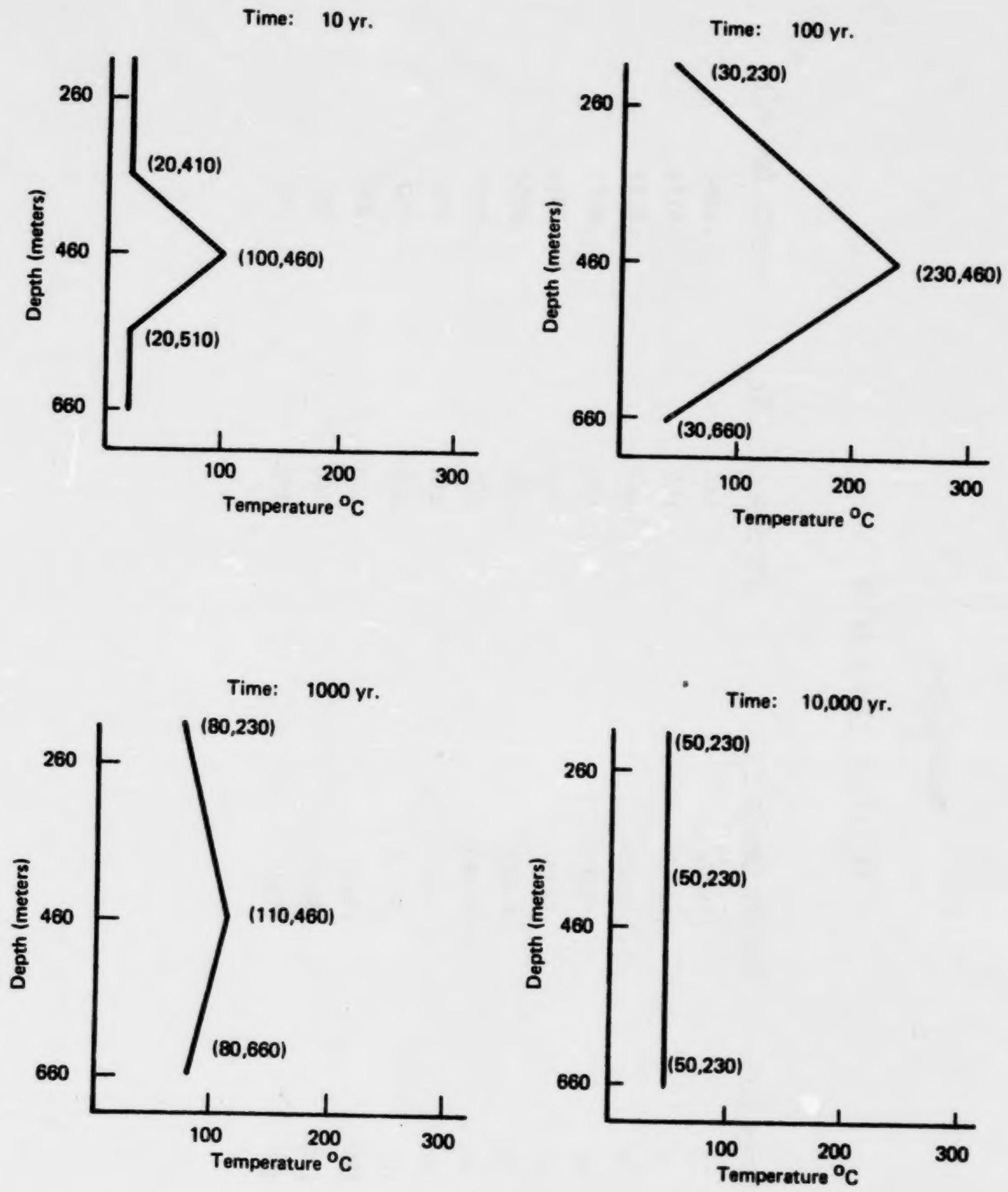

FIGURE D–VI–10 TEMPERATURE DISTRIBUTIONS IN SALT DOME REPOSITORY

TABLE D-VI-1

DENSITY OF LIQUID WATER

Temperature (°C)	Density (gm/cm^3)	Temperature (°C)	Density (gm/cm^3)
20	.99823	140	.9264
30	.99568	150	.9173
40	.99225	160	.9075
50	.98807	170	.8973
60	.98324	180	.8866
70	.97781	190	.8750
80	.97183	200	.8628
90	.96534	210	.850
100	.95838	220	.837
110	.9510	230	.823
120	.9434	240	.809
130	.9352	250	.794

The following two principles should be kept in mind:

a. The vertical velocity of the water column is proportional to the effective hydraulic gradient acting upon it.

b. The effective hydraulic gradient acting on a vertical water column (due to buoyancy) is proportional to the average density of the column.

These principles will now be applied to a repository whose vertical thermal profile has the form given in Figure D-VI-11a. The corresponding density profile is given in Figure D-VI-11b. A column of water extending down just to the repository has some average density ρ_1, as shown in Figure D-VI-11c. The slightly longer water column shown in Figure D-VI-11c has a lower average density because the addition has a density ρ_2 which is less than ρ_1. To confirm that this would increase the velocity of the column, simply note that the relatively high buoyancy force in the lower segment would tend to "push" the column above it. This effect continues to require consideration of longer columns until a point is reached where the average density of the column equals the density of the next additional increment. In calculations of this type, the maximum point will often be only roughly approximated. Examples of situations in which such longer water columns will need to be considered include the following:

- Baseline flow through repository (no breaches).
- Boreholes penetrating some distance below repository.
- Faults extending below repository.

The determination of the proper water column to consider and its average density provides the information needed to determine its mass (or, equivalently, mass per unit cross-sectional area). The numerical differences resulting from consideration of longer water columns are generally not very large.

S5: The density of a corresponding column of unheated water may be conveniently and conservatively estimated as 1 gm/cm^3. With this density, the mass of a column is easily determined.

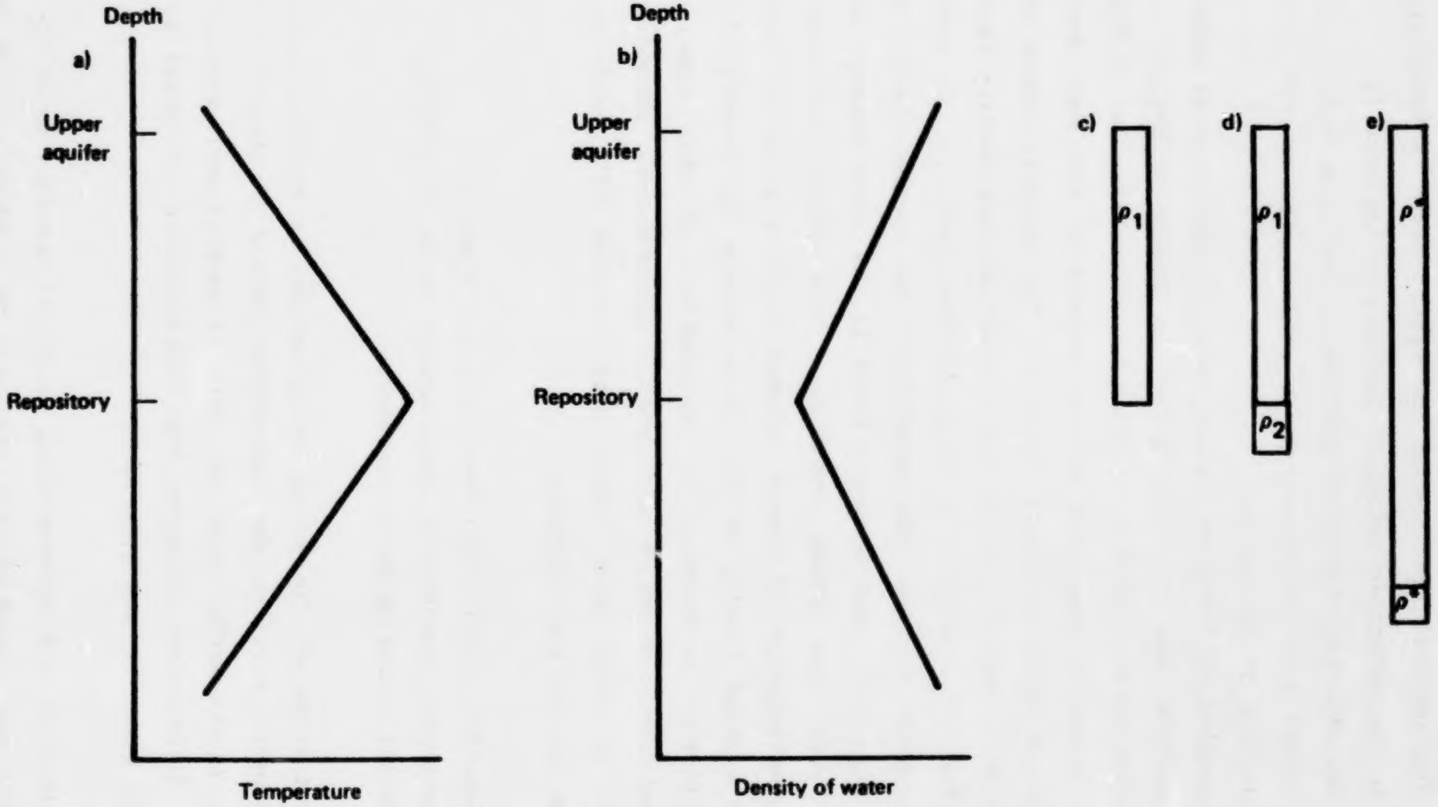

FIGURE D–VI–11 DETERMINING WATER COLUMN WHOSE VERTICAL VELOCITY IS MAXIMAL

S6: Let L represent the length of the water column under consideration and let ρ^* be its average density in gm/cm^3. Then for every square centimeter of cross-section, the gravitational force is ρ^*Lg, where g is the acceleration due to gravity. The opposing buoyant force due to a column of unheated water is $1 \cdot Lg$, and so the difference is $(1-\rho^*)Lg$.

S7: This force corresponds to a hydrostatic head of

$$\frac{(1-\rho^*)Lg}{\rho g}$$

when measured in terms of water at an arbitrary density ρ. Variations in ρ between ρ^* and 1 do not significantly affect this value, so that the computationally convenient value, $\rho = 1$ g/cm^3, will be used. Thus, the equivalent head is given by

$$(1-\rho^*)L$$

This yields a hydraulic gradient i given numerically by

$$i = 1-\rho^*.$$

Note that i is dimensionless. It is strictly equal to the quotient $(1-\rho^*)/1$, where 1 and ρ^* are both in gm/cm^3, thereby leading to the cancellation of the units.

S8: The viscosity of water is relatively insensitive to pressure in the range under consideration. Its dependence on temperature is shown in Table D-VI-2.

Because of this temperature dependence, no single viscosity value actually covers the entire water column. Nevertheless, an estimate based on average temperature can be made in order to permit the application of Darcy's law (see below).

S9: The vertical flow of the water column will be approximated by Darcy's law:

$$\dot{Q} = \frac{Ki}{100}$$

TABLE D-VI-2

VISCOSITY OF LIQUID WATER AT ATMOSPHERIC PRESSURE

Temperature (^oC)	Viscosity (poise)
20	0.0100
40	0.0065
60	0.0047
75	0.0038
100	0.0029
125	0.0022
150	0.0018

Source: American Institute of Physics Handbook, 1972.
Data compiled from other sources.

where:

$\dot{Q}$ = flow quantity (cm^3/cm^2/second)

K = permeability (hydraulic conductivity for water at viscosity 0.01, in cm/sec)

i = hydraulic gradient (dimensionless)

μ = viscosity (poise, equal to gm/cm/second)

The denominator 100μ allows for corrections due to different viscosities, although the numerical effect is at most about half an order of magnitude. Furthermore,

$$v = \frac{Ki}{100\mu n} .$$

S10: The travel time τ from the repository to the upper aquifer is given by the quotient

$$\tau = \frac{D}{v} ,$$

where D is the distance and v is the velocity. Note that D is the correct parameter here even if a longer column of water (i.e., L > D) is under consideration.

F. SAMPLE CALCULATIONS

The detailed computation of thermally induced convective flows is a matter for the consequence calculations in specific breach-of-containment mechanisms. Several examples will be worked out here.

1. Baseline Flow Through Granite Repository at 100 Years

The temperature distribution shown in Figure D-VI-7 corresponds to the density distribution shown in Figure D-VI-12. Calculations show that a water column of approximate length L = 305m has maximum vertical velocity. In particular, a running average density is recorded as the column length increases from L=0, and the increases are terminated when the density equals (approximately) the density

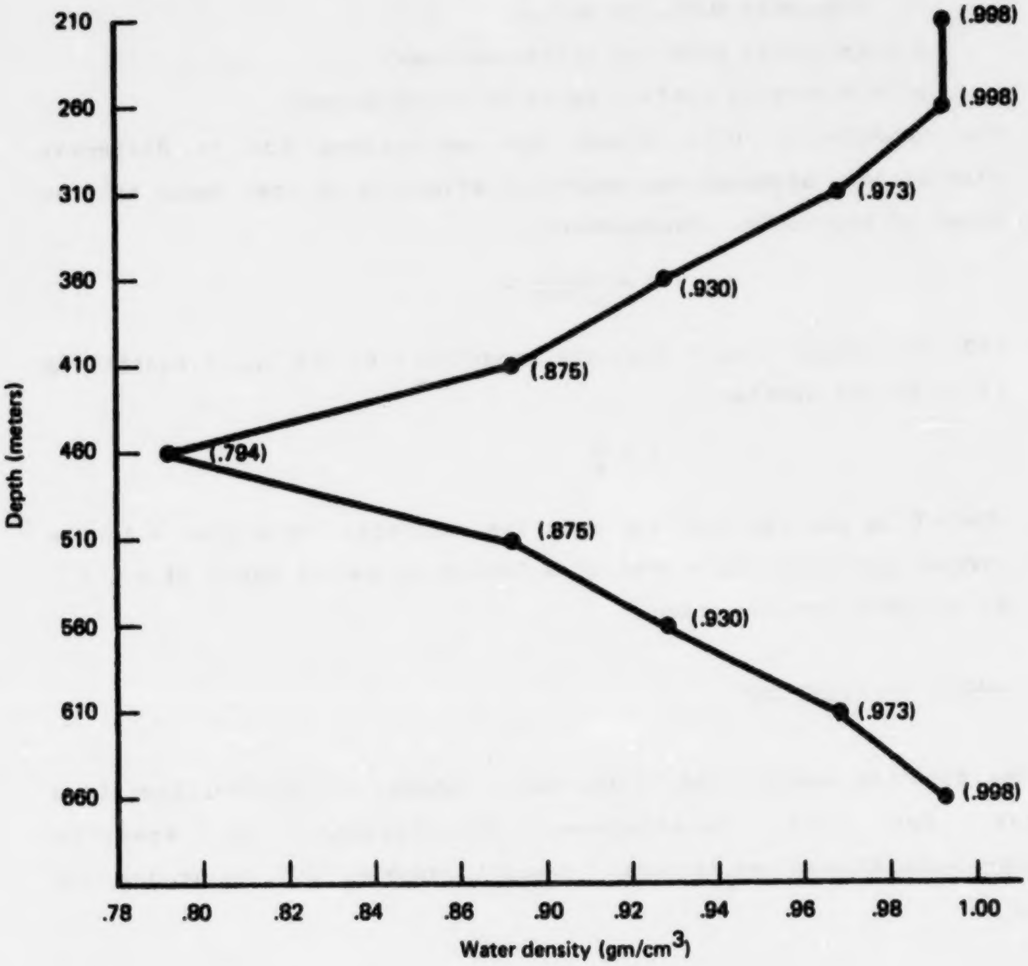

FIGURE D–VI–12 WATER DENSITY DISTRIBUTION FOR BASELINE GRANITE REPOSITORY AT 100 YEARS of the next increment. The corresponding average density value is $\rho^* = 0.899$. This yields a hydraulic gradient of

$$i = 1 - \rho^* = 0.1.$$

The other parameters will be taken as follows for this sample calculation:

$$K = 10^{-9} \text{ cm/sec}$$

$$\mu = .0022 \text{ poise} \quad (\text{taken at } 125^\circ\text{C})$$

$$n = 10^{-4}$$

$$D = 230 \text{ meters}$$

These numbers lead to a fluid velocity:

$$v = \frac{Ki}{100\mu n}$$

$$= 4.5 \times 10^{-6} \text{ cm/sec}$$

$$= 1.4 \text{ m/yr}$$

and hence a travel time:

$$\tau = \frac{D}{v} = 162 \text{ years.}$$

Note that if the permeability were 10^{-8} cm/sec, then the travel time would be about 16 years.

2. Flow Through Leaky Borehole Penetrating to a Bedded Salt Repository at 1000 Years

In this case, the length L is fixed at 100 meters, the distance from the repository to the upper aquifer. The temperature range is 100°C - 150°C, as shown in Figure D-VI-6. It is sufficient to estimate the average density to be $\rho^* = 0.94$, based on Table D-VI-1. This results in a gradient $i = 0.06$. Other parameters will be taken as follows:

$$K = 10^{-5} \text{ cm/sec}$$

$$\mu = 0.0022 \text{ poise}$$

$$\nu = 0.1$$

$$D = 100 \text{ meters}$$

These numbers lead to a fluid velocity:

$$v = 2.7 \times 10^{-5} \text{ m/sec}$$
$$= 8.5 \text{ m/yr}$$

and hence a travel time:

$$\tau = 12 \text{ years.}$$

3. General Results

Tables D-VI-3 and D-VI-4 show the effective hydraulic gradients on vertical columns of water extending between the upper aquifer and the repository or some point below it. (The difference between these two cases is usually not very great and is often blurred by the interaction between breach pathways.)

G. CALCULATION OF RELEASE TIMES

The transit times calculated earlier are useful for estimating the instantaneous transport rates at particular moments in time. However, if several hundreds or thousands of years are required for the distance from repository to aquifer to be traversed, the change in velocity over time must be accounted for. As an example of this kind of calculation, consider the case of a gradually degrading borehole seal. The question is: when do radionuclides first appear at the aquifer? For a granite repository, ignoring the effect, if any, of repository resaturation time, the permeability of the borehole is assumed (second estimate) to degrade linearly from 10^{-8} to 10^{-4} cm/sec over 10^4 years. A formula for K is thus:

$$K = 10^{-8} + \frac{10^{-4} - 10^{-8}}{10^4}\, t$$

$$\simeq 10^{-8} + 10^{-8} t$$

$$= 10^{-8}\,(1+t)\ .$$

TABLE D-VI-3

EFFECTIVE HYDRAULIC GRADIENT DUE TO BUOYANCY OF A COLUMN OF WATER BETWEEN UPPER AQUIFER AND REPOSITORY

	Time after closure			
	10 years	100 years	1000 years	10,000 years
Bedded Salt	0.02	0.12	0.10	0.03
Granite	0.01	0.10	0.06	0.01
Basalt	0.02	0.12	0.10	0.03
Shale	0.02	0.12	0.10	0.03
Dome Salt	0.02	0.12	0.07	0.03

TABLE D-VI-4

MAXIMUM EFFECTIVE HYDRAULIC GRADIENT DUE TO BUOYANCY OF A COLUMN OF WATER BETWEEN UPPER AQUIFER AND SOME POINT BELOW REPOSITORY

	10 years	100 years	1000 years	10,000 years
Bedded Salt	0.03	0.13	0.11	0.04
Granite	0.02	0.11	0.07	0.03
Basalt	0.03	0.13	0.11	0.04
Shale	0.03	0.13	0.11	0.04
Dome Salt	0.03	0.13	0.08	0.04

The average density of the water column would be approximately that at the 350 m depth (at least for all times after 100 years). From the data in Figure D-VI-7, this can be estimated as on Figure D-VI-13. The analytic approximation to the temperature curves enables straightforward computations. Now we perform a sequence of velocity calculations according to the earlier outline. The porosity is taken as 0.1. The results are summarized in Table D-VI-5; and it can be seen that for the first few hundred years (excluding about the first 50-70 years), the average velocity is approximately 1 m/yr. Thus, it requires about 200 years to cover the distance from repository to aquifer. The first releases by this mode would then be expected at about 250-300 years after emplacement.

H. RESISTANCE OF RECHARGE PATHWAY

The model which has been used in the calculations thus far was sketched as Figure D-VI-4d and is repeated as Figure D-VI-14a in this section. The true physical situation is more closely represented by Figure D-VI-14b, in which the column on the right, called the recharge pathway, is also modeled as offering some resistance to fluid flow. In this case, the total driving potential remains the same, but it is dissipated over the two columns, so that the potential acting on the release pathway (the left column) is less. It was pointed out earlier that to ignore this factor is a conservative approach. The purpose of this and the following sections is to estimate the degree of conservatism involved and to provide a more realistic model to use where appropriate.

The representations in Figures D-VI-4 and D-VI-14 are useful in determining the effective pressure differential tending to move fluid through the system, but once this has been determined (as in previous sections) it is simpler to use the model in Figure D-VI-15a with the electrical series resistance analog in Figure D-VI-15b.

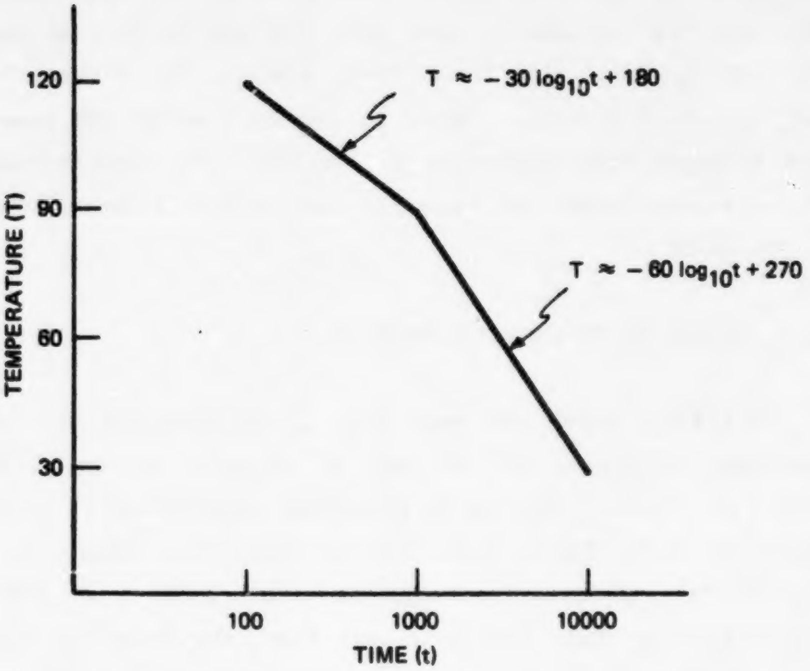

FIGURE D–VI–13 APPROXIMATE TEMPERATURE PROFILE AT 350m IN GRANITE

TABLE D-VI-5

CALCULATION OF VELOCITY FOR VARIOUS TIMES

t	T(at 350m)	ρ^*	i	μ	K(cm/sec)	v(m/yr)
100	120	.943	.057	.0023	1.0×10^{-6}	.8
200	111	.950	.050	.0026	2.0×10^{-6}	1.2
300	106	.954	.046	.0027	3.0×10^{-6}	1.6
400	102	.958	.042	.0029	4.0×10^{-6}	1.8
500	99	.959	.041	.0029	5.0×10^{-6}	2.2
1000	90	.965	.035	.0033	1.0×10^{-5}	3.3
2000	72	.977	.023	.0039	2.0×10^{-5}	3.7
3000	61	.980	.020	.0047	3.0×10^{-5}	4.0
4000	54	.986	.014	.0050	4.0×10^{-5}	3.5
5000	48	.989	.011	.0056	5.0×10^{-5}	3.1
10000	30	.996	.004	.0082	1.0×10^{-4}	1.5

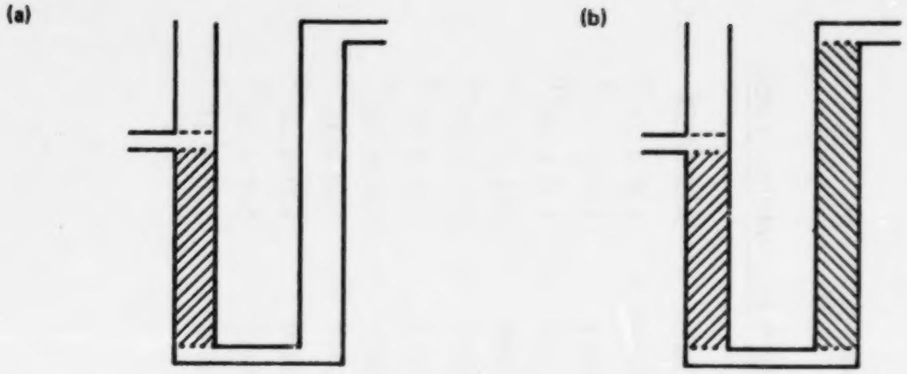

FIGURE D–VI–14 RECHARGE RESISTANCE INCORPORATED IN EARLIER BUOYANCY MODEL

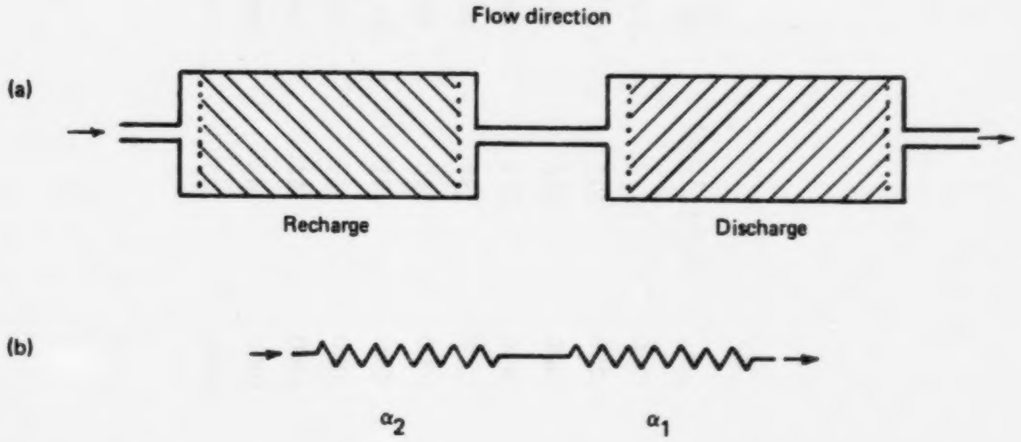

FIGURE D–VI–15 SIMPLIFIED CONCEPTUAL MODEL FOR RECHARGE RESISTANCE

(The electrical analog has been discussed at greater length in Appendix D-V.) The resistance of a pathway segment is given by

$$\alpha = \frac{L}{KA}$$

where L is the length, K is the permeability, and A is the cross-sectional area. Non-uniform pathways may be approximated by series or parallel combinations of resistances, which may then be reduced to an equivalent simple resistance. In cases where the water viscosity changes appreciably during transit (because of temperature gradients), this factor may be incorporated in the resistance term:

$$\alpha = \frac{L \cdot 100\mu}{KA}$$

where μ is the viscosity (in poises). For a potential drop (head) over a series of resistances, the drop over each one is proportional to its resistance. In particular, for a drop Δ over α_1 and α_2, the effective potential acting on the discharge path is

$$\Delta = \frac{\alpha_1}{\alpha_1 + \alpha_2} \Delta .$$

The calculations of the previous sections were based on the conservative assumption $\alpha_2 << \alpha_1$ so that $\Delta_1 \simeq \Delta$.

The following sections will discuss the application of the present model to particular breach-of-containment mechanisms. The estimation of appropriate values of A_2 and L_2 can be quite difficult because of the complicated geometry of the flow patterns. Furthermore, one must be careful in applying steady state models to systems in which parameters are changing over time.

I. RECHARGE THROUGH BULK ROCK

The approximate shape of the streamlines for the baseline flow through granite is sketched in Figure D-VI-16. The shortest recharge pathway would be from the aquifer rather close to the repository and its length could be almost as small as that of the

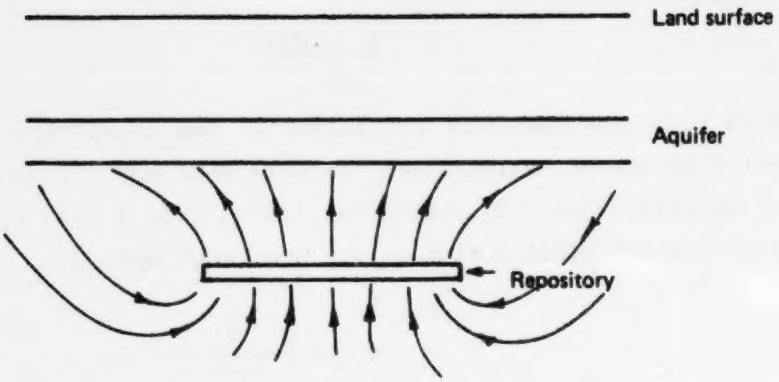

FIGURE D–VI–16 QUALITATIVE ESTIMATE OF STREAMLINES discharge path. A longer length would generally be associated with larger cross-sectional areas for the same flow, thereby tending to counteract the effect of longer length or resistance ($\alpha = L/KA$). As a consequence, one can imagine recharge paths with as little resistance as the discharge path, which would entail dividing the earlier calculated flows by a factor of 2. This difference is not significant in the order-of-magnitude calculations being carried out here; consequently, this effect has not been taken into account in determining first arrival times at the aquifer from the thermally incuded convection mechanism.

For determining long-term cumulative releases to the aquifer it is important to check whether the present calculations grossly overestimate the flow rates and, if so, what correction factors might be appropriate. In order to simplify the geometry, the model shown in Figure D-VI-17 will be used. The repository is modeled as a hemispherical surface with radius 1 km, giving an area of $2\pi(1)^2 = 6\ \text{km}^2$, or slightly less than the real repository area of $8\ \text{km}^2$. (The smaller area in the model will tend to slightly overestimate the recharge resistance.) The recharge paths are assumed to be oriented radially, so that the equipotential surfaces would be hemispherical. (This underestimates recharge near the aquifer and overestimates it deep in the rock.) Thus, the hydrostatic head, h, is a function of r alone in this model.

If water passes through the repository at the flow rate $\dot{Q}$, then in fact the same flow must pass through every concentric hemispherical surface. Since by Darcy's law, flux is proportional to pressure or head gradient, it follows that

$$\dot{Q} = K \cdot \frac{dh}{dr} \cdot 2\pi r^2$$

and that this quantity is actually independent of r. (K is the permeability; h is the head.) Viscosity is assumed to be that at low temperatures, so no correction factor is incorporated. It would be possible to incorporate lower viscosities near the repository, due to higher temperatures. In comparing the relative resistances of the recharge and discharge pathways, this factor would tend to

a) Three dimensional view

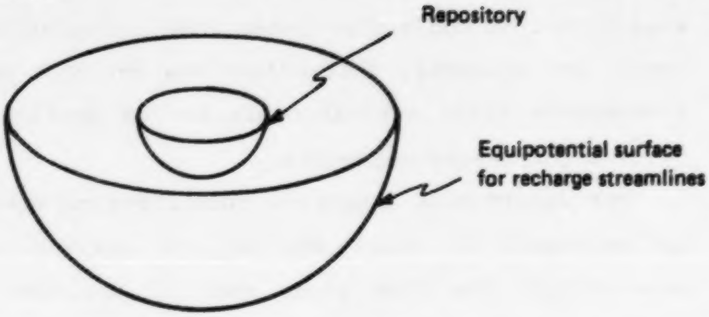

b) Two dimensional side view

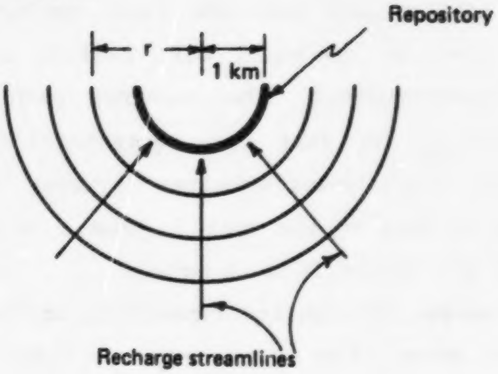

FIGURE D–VI–17 HEMISPHERICAL REPOSITORY RECHARGE MODEL increase the relative weight of the recharge pathway. Integration of the above differential equation for h, between arbitrary radii r_1 and r_2, yields

$$\Delta h = h(r_2) - h(r_1) = \frac{\dot{Q}}{2\pi K}\left(\frac{1}{r_1} - \frac{1}{r_2}\right) .$$

An equivalent resistance for the recharge path is then

$$\alpha = \frac{\Delta h}{\dot{Q}} = \frac{1}{2\pi K}\left(\frac{1}{r_1} - \frac{1}{r_2}\right) .$$

The cumulative resistance from $r_1 = 10^3$m to $r_2 = \infty$ is therefore

$$\alpha_{recharge} = \frac{1}{2\pi K}\left(\frac{1}{10^3}\right)$$

It has previously been seen that the discharge resistance is given by

$$\alpha_{discharge} = \frac{L}{KA}$$

and in the present case, L = 230m and A = 8 x 10^6 m^2. Therefore,

$$\alpha_{recharge} = 1.6 \times 10^{-4} \times K$$

$$\alpha_{discharge} = 2.9 \times 10^{-5} \times K$$

In this case the recharge resistance is larger by roughly a factor of 20.

The cumulative fraction of the total resistance between $r_1 = 1$ and an arbitrary value r_2 is given by the factor

$$1 - 1/r_2$$

for which selected values are shown in Table D-VI-6. It is clear that the preponderance of the resistance to recharge flow is close to the repository. The reason is that the effective cross-sectional area for recharge increases faster than the corresponding distance from the repository.

The implication of a recharge pathway resistance of 10 or 20 times that for discharge would be to decrease the corresponding flow rate by the same factor. Whether this factor should be incorporated depends on an additional factor, which is discussed in the next section.

J. NON-STEADY-STATE FLOW

The calculations in the previous sections have been based on the assumption of steady state flow. This assumption may underestimate actual flow in case there are transient sources of fluid closer to the discharge path. A potentially important source consists of the void spaces in the repository backfill and in the surrounding rock. Changes in temperature and hydrostatic pressure in a rock mass can cause changes in void space volume with the result that water can be stored or released. If the potential changes in total stored water are substantial, compared with the volumetric flows being calculated for certain failure elements, then the recharge resistance assumes less importance because the water may be coming out of storage instead. Figure D-VI-18 illustrates a potential storage release mechanism. The

TABLE D-VI-6

FRACTION OF TOTAL RECHARGE RESISTANCE BETWEEN $r_1 = 1$ km AND GIVEN r_2

r_2 (km)	fraction ($1 - 1/r_2$)
2	1/2
3	2/3
4	3/4
5	4/5
.	
.	
.	
n	$\frac{n-1}{n}$

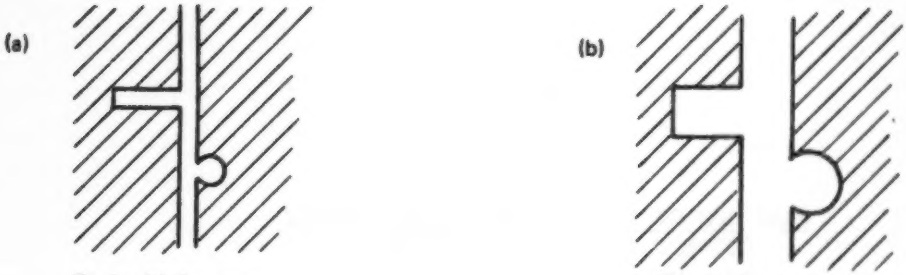

Rock with fractures and pores before repository resaturation

Expansion of openings by hydrostatic pressure during resaturation

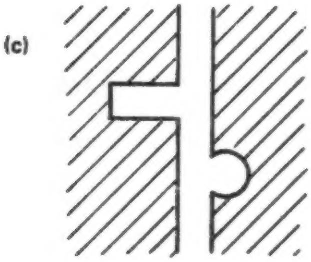

Partial contraction of openings due to decrease in hydrostatic pressure from heating of water and corresponding density change

FIGURE D–VI–18 PORE WATER RELEASE MODEL

extent of this mechanism obviously depends on the timing of resaturation compared to the peak thermal period, both of which depend on many site and repository parameters.

Since the purpose of this section is primarily to estimate whether the quantities of water available from storage could be an important factor to consider, two example calculations will be carried out, one for the water stored in the repository backfill and one for the water stored in the rock itself.

From Appendix D-II, the void space volume in the backfill is expected to be about $2 \times 10^6 m^3$. The actual volume is a function of the effective stress on the backfill, which equals the total stress minus the effect of fluid pressure. If the overburden has shifted so that the backfill has voided mechanical equilibrium, then the total stress remains essentially constant, so that changes in fluid pressure imply equal changes in effective stress, although in the opposite direction. These changes in effective stress change the volume, primarily because of grain movement. The parameter that measures this effect is the compressibility α, defined as the fractional volume change per unit change in effective stress. Representative volumes are shown in Table D-VI-5, which also shows the compressibility of water. The change in hydrostatic pressure due to changes in density of the overlying water has been discussed earlier in this report. For a granite repository with a distance of 260m from the repository to the water table, a change from $\rho = 1$ to $\rho = \rho^* = 0.95$ results in a pressure change of 17 psi at the repository depth. With a normal compressibility of 10^{-5} psi^{-1}, the corresponding volume change would be $340m^3$. This number is larger than a number of flow rates calculated in the main text, in which case recharge resistance might not be an important factor.

Similarly, the storage capacity of the bulk rock may be considered. Using a porosity value of 10^{-4}, the void space volume in the rock below the repository down to a depth of 1000m is given by

$$V = (8 \times 10^6 m^2)\ (540m) 10^{-4}$$
$$= 4 \times 10^5 m^3$$

With a compressibility of 10^{-7} psi^{-1} and a pressure change of 17 psi, the water released would equal the change in rock volume, given by

$$7.3 \times 10^3 = (8 \times 10^6 m^2)(540m)(10^{-7}\ psi^{-1})(17\ psi).$$

Note that since the rock volume is so much larger that the water volume stored in voids, the compressibility of the water itself has little importance here. At the rate calculated above, the flows through bulk rock could not be met for long using this source of water. Obviously, if the parameters were different, then possibly the compressibility could have some effect on the flow calculations.

K. CONCLUSIONS ON RECHARGE RESISTANCE

For the case of flow through granite, it appears appropriate to decrease by an order of magnitude the effective hydraulic gradients calculated by the formula $i = 1- \rho^*$, in order to account for the resistance of the recharge pathway. In basalt and shale, water is available from the lower aquifer. For large breaches, such as faults, recharge can occur through the fault itself, and no recharge resistance should be included. This appears to be a conservative approach, but not overly so. For small breaches, such as boreholes, sufficient recharge resistance can be assumed through the repository, so that significant resistance along this part of the system cannot be assumed.

REFERENCES APPENDIX D-VI

1. Dames & Moore. Technical Support for GEIS: Radioactive Waste Isolation in Geologic Formations. Vol. 21: Ground Water Movement and Nuclide Transport. For Office of Waste Isolation, Union Carbide Corporation. Y/OWI/TW-36/26. April 1978.

2. Kärnbränslesäkerket (KBS). Handling of Spent Nuclear Fuel and Final Storage of Vitrified High Level Reprocessing Waste. Stockholm, Sweden. December 12, 1978.

3. Apps, J.A., et al. An Appraisal of Underground Radioactive Waste Disposal in Argillaceous and Crystalline Rocks: Some Geochemical, Geomechanical, and Hydrogeological Questions. Lawrence Berkeley Laboratory. LBL-704. June 1978.

4. Dames & Moore. Technical Support for GEIS: Radioactive Waste Isolation in Geologic Formations. Vol. 20: Thermomechanical Stress Analysis and Development of Thermal Loading Guidelines. For Office of Waste Isolation, Union Carbide Corporation. Y/OWI/TM-36/20. April 1978.

5. Chemical Engineers Handbook. R.H. Perry and C.H. Chilton, eds. 5th Edition. McGraw-Hill Book Company, New York. 1973.

6. Freeze, R.A. and J.A. Cherry. Groundwater. Prentice-Hall, Inc., Englewood Cliffs, N.J. 1979.

APPENDIX D-VII

SALT CREEP

A. INTRODUCTION

When subjected to loads for extended time periods, many materials undergo gradual plastic deformation subsequent to the initial elastic and plastic response. This gradual deformation is known as creep and, of the geologic media under consideration, it appears significant only in the case of salt deposits. This suggests a possible advantage of salt for waste containment because certain breaches may tend to be "self-healing" through plastic creep. This appendix provides the basis for analysis of this healing process by examining the creep closure of cylindrical openings in salt. The principal mathematical method used is a standard engineering approach for the analysis of three-dimensional creep.(1) In the following analysis, this method is combined with empirical data and a stress analysis of a circular opening to produce estimates of closure times.

B. MATHEMATICAL CHARACTERIZATION OF STEADY-STATE CREEP

This analysis will be based on a steady-state uniaxial creep law due to Heard.(2) The law may be stated as follows:

$$\dot{\varepsilon} = 3 \times 10^{-6} \, e^{-11833/\theta} \, \sigma^{5.5} \tag{1}$$

where

σ = applied stress (bars)
θ = temperature (^{o}K)
$\dot{\varepsilon}$ = strain rate (sec^{-1})

After conversion of stress units to psi and evaluation at 60°C, the equation becomes

$$\dot{\varepsilon} = 1.1 \times 10^{-20} \, \sigma^{5.5} \tag{2}$$

Since this is a uniaxial law, it is necessary to develop a generalization to describe creep in response to a three-dimensional stress field. In the development, the stress field is represented by three mutually orthogonal principal stresses denoted σ_1, σ_2, σ_3 and their corresponding strains ε_1, ε_2, ε_3. The basic assumptions, based on observations of plastic flow, are that during creep there is no change of volume and that the principal shear strain rates are proportional to the principal shear stresses. Under the assumption that the strains are small compared to unity and that there is no rotation of the strain axes, these assumptions may be expressed mathematically as

$$(1+\varepsilon_1)(1+\varepsilon_2)(1+\varepsilon_3) = 1 ,$$

or

$$\dot{\varepsilon}_1 + \dot{\varepsilon}_2 + \dot{\varepsilon}_3 = 0 \qquad (2)$$

$$\frac{\dot{\varepsilon}_1 - \dot{\varepsilon}_2}{\sigma_1 - \sigma_2} = \frac{\dot{\varepsilon}_2 - \dot{\varepsilon}_3}{\sigma_2 - \sigma_3} = \frac{\dot{\varepsilon}_3 - \dot{\varepsilon}_1}{\sigma_3 - \sigma_1} = C \qquad (3)$$

where C is a constant at a given point and time in the stressed body. Together, equations (2) and (3) imply that

$$\dot{\varepsilon}_1 = \frac{2}{3} C \left[\sigma_1 - \frac{1}{2}(\sigma_2 + \sigma_3)\right]$$

$$\dot{\varepsilon}_2 = \frac{2}{3} C \left[\sigma_2 - \frac{1}{2}(\sigma_3 + \sigma_1)\right] \qquad (4)$$

$$\dot{\varepsilon}_3 = \frac{2}{3} C \left[\sigma_3 - \frac{1}{2}(\sigma_2 + \sigma_1)\right]$$

In order to fully characterize the three-dimensional creep, it remains to determine the constant C based on the uniaxial creep law of Equation 1.

There are a number of approaches to this, but a standard technique (supported by experiment) is to assume that in steady-state three-dimensional creep,

$$\dot{\varepsilon}^* = f(\sigma^*)$$

where $\dot{\varepsilon}^*$, σ^* are, respectively, the octahedral strain rate and octahedral stress as defined by:

$$\dot{\varepsilon}^* = \frac{\sqrt{2}}{3} [(\dot{\varepsilon}_1 - \dot{\varepsilon}_2)^2 + (\dot{\varepsilon}_2 - \dot{\varepsilon}_3)^2 + (\dot{\varepsilon}_3 - \dot{\varepsilon}_1)^2]^{\frac{1}{2}}$$

$$\sigma^* = \frac{\sqrt{2}}{3} [(\sigma_1 - \sigma_2)^2 + (\sigma_2 - \sigma_3)^2 + (\sigma_3 - \sigma_1)^2]^{\frac{1}{2}}$$

Combining this with Equation 4 and the uniaxial law, Equation 1, it follows that:

$$\begin{aligned}
\dot{\varepsilon}_1 &= 1.1 \times 10^{-20}(\sigma^*)^{4.5}[\sigma_1 - \tfrac{1}{2}(\sigma_2 + \sigma_3)] \\
\dot{\varepsilon}_2 &= 1.1 \times 10^{-20}(\sigma^*)^{4.5}[\sigma_2 - \tfrac{1}{2}(\sigma_1 + \sigma_3)] \qquad (5) \\
\dot{\varepsilon}_3 &= 1.1 \times 10^{-20}(\sigma^*)^{4.5}[\sigma_3 - \tfrac{1}{2}(\sigma_1 + \sigma_2)]
\end{aligned}$$

This provides the required description of three-dimensional creep in response to a general stress field.

C. APPLICATION TO CLOSURE OF A LONG CYLINDRICAL OPENING

In order to model the creep closure of a borehole or tunnel shaft, the above result can be interpreted for the case of a long circular cylindrical opening. The stresses result from the ambient lithostatic pressure. It will be assumed that the creep is steady state, the medium is isotropic, and the cylinder is very long in relation to its radial dimension. From the literature (e.g. (3)), it can be demonstrated that, based on these assumptions and if the pressure in the borehole is much smaller than lithostatic pressure, the following principal stresses are present at the boundary.

$$\begin{aligned} \sigma_z &= p \\ \sigma_\theta &= 2p \\ \sigma_r &= 0 \end{aligned} \qquad (6)$$

where p is the lithostatic pressure and the principal stress directions are taken along the cylindrical coordinate axis.

It follows that the octahedral stress, σ^* is given by

$$\begin{aligned} \sigma^* &= \frac{\sqrt{2}}{3} [(\sigma_r - \sigma_\theta)^2 + (\sigma_r - \sigma_z)^2 + (\sigma_\theta - \sigma_z)^2]^{\frac{1}{2}} \qquad (7) \\ &= 1.2p \end{aligned}$$

Application of Equation 5 implies that the radial strain rate is given by

$$\begin{aligned} \dot{\varepsilon}_r &= 1.1 \times 10^{-20} (\sigma^*)^{4.5} [\sigma_r - \frac{1}{2} (\sigma_\theta + \sigma_z)] \\ &= -2.5 \times 10^{-20} \cdot \frac{3p^{5.5}}{2} = -1.1 \times 10^{-2} \text{ yr}^{-1} \end{aligned} \qquad (8)$$

Thus, the rate of decrease in the radius is given by

$$\frac{dr}{dt} = r\dot{\varepsilon}_r = -1.1 \times 10^{-2} \, r \text{ yr}^{-1} \qquad (9)$$

which implies that

$$r(t) = r_0 \, e^{-1.1 \times 10^{-2} t} \qquad (10)$$

D. SUMMARY AND CONCLUSIONS

In performing the foregoing analysis, a number of simplifying assumptions were made. Some of the most important are:

- The creep closure is characterized as a steady-state process.
- The surrounding salt is completely homogeneous.
- The creep behavior is described as

$$\dot{\varepsilon}^* = 1.1 \times 10^{-20} (\sigma^*)^{5.5} \text{ yr}^{-1}$$

where

$\dot{\varepsilon}^*$ = octahedral strain rate
σ^* = octahedral stress

- The creep process occurs without net change of volume.
- The principal shear strain rates are proportional to the principal shear stresses.

The first two assumptions are made to permit an analytical estimate of closure rates for a generic repository. To eliminate these assumptions would require detailed finite element analysis, which is not feasible in the absence of site-specific information. Such an analysis is not, however, expected to alter the order of magnitude of the results. The third assumption is based on the most recent empirical impure data obtained for the WIPP project and is felt to represent the best available information on salt creep under expected conditions in the vicinity of a repository. The final assumptions are standard in the analysis of plastic creep and are based on extensive observations of creep processes.

The result of the analysis is that the opening will close according to the following relation:

$$r(t) = r_o e^{-1.1 \times 10^{-2} t}$$

where

r_o = initial radius
t = time since opening was created
$r(t)$ = radius at time t .

The breach-of-containment mechanisms discussed in this report involve holes in the range of 10 cm to 5 m in radius. Table D-VII-1 summarizes the resulting closure of holes in this size range.

From the governing equation it is clear that both radius and cross-sectional area, considered as functions of time, are concave up, so that between any two points they are bounded by the linear function connecting those points. For simplicity, therefore, cross-sectional area can be modeled as a linear function of time, equal to 0 at a time when the opening may be regarded as essentially closed. Since for long tunnels or holes the volume can also be modeled in this fashion. For non-circular openings, closure can be considerably faster than for circular ones and it is, in general, conservative to use the closure rates for the latter. For backfilled openings, the fractional rate of change of the pore space will be taken to be the same as for the open holes. To cover all these cases, two very simple rules have been adopted, therefore. For first estimate calculations, the void space of an open or backfilled opening in salt is assumed to decrease linearly to approximately zero in 200 years. This number is consistent with the above calculations. For second estimate calculations, the void space is assumed to decrease to approximately zero in 1000 years. Slower creep could result from the nature of the overburden and interbeds, as well as from impurities in the salt itself.

TABLE D-VII-1

ESTIMATED CLOSURE RATES OF CYLINDRICAL OPENINGS IN SALT

		Radius (m)	
Percent/closure	Times (yrs)	0.1 m initial	5 m initial
50	60	5×10^{-2}	2.5
90	210	1×10^{-2}	0.5
99	420	1×10^{-3}	0.05

REFERENCES

1. Finnie, I., and W.R. Heller. Creep of Engineering Materials. McGraw-Hill Book Company, Inc., New York, 1959.

2. Sandia Laboratories (Dawson, P.R.). Constructive Models Applied in the Analysis of Creep of Rock Salt. SAND 79-0137. Jan., 1978.

3. Timoshenko, S., and J.N. Goodier. Theory of Elasticity. McGraw-Hill Book Company, Inc., New York, 1951.

APPENDIX D-VIII

CANISTER CAPABILITIES FOR LONG-TERM ISOLATION

A. INTRODUCTION

The systems under consideration for nuclear waste isolation offer many barriers for waste containment, including the waste form itself, the canister and overpack materials, the vault sleeve and backfill materials, and the geologic formation. The geologic environments currently being investigated are salt and hardrock formations, as well as sediments on the ocean floor. The waste may be directly disposed as spent fuel rods or may be altered to a different form. This appendix will consider the protection that may be expected from the canister and overpack layers.

B. CANISTER SYSTEM DEVELOPMENT

There are four steps in the development of a canister system:

1. performance criteria development and environmental specifications;
2. materials development;
3. canister design; and
4. system demonstration.

These steps may be worked on concurrently but they must be completed in sequence.

The development of performance criteria will set lifetime goals for the canister. It must be determined whether the canister should remain intact for (a) retrievability purposes, about 25 years, (b) the high radio/thermal activity period, 500-1000 years, or (c) the radionuclide lifetimes, up to 10^5-10^6 years. The controlling failure mechanisms and rates for a given material will depend upon many environmental parameters, which in turn will vary with the geology and the waste form. Estimates for several parameters are given in Table D-VIII-1. These estimates have not been designated as design criteria but have been useful guides for experimentation.

TABLE D-VIII-1

ISOLATION ENVIRONMENTS*

Geologic Formation and Waste Type	Maximum Temperature (°C)	Pressure	Chemistry
Bedded Salt			
Transuranic-Low Level Waste	30	14.5 MPa	Dry (1/2%) 95% NaCl
Spent Unreprocessed Fuel	70-100	17.9 MPa	Dry (1/2%) 98% NaCl
High-level Waste	250	17.9 MPa	Dry (1/2% H_2O), 98% NaCl with potential localized intrusion of NaCl-KCl-$MgCl_2$ brine (due to thermally induced brine migration)
Sub-seabed Sediments			
High-level Wastes	200	55 MPa	Seawater-saturated sediments (40% solids)
Shale, Hardrock, Tuff			
High-level Waste	250-300	Atmospheric	Air + steam for $\gtrsim$ 100 years, then possibly inundated groundwater

*Does not take radiolysis into account

Source: Braithwaite, J.W., and N.J. Magnani. Corrosion Considerations for Nuclear Waste Management. In: Scientific Basis for Nuclear Waste Management, G.J. McCarthy, ed., Plenum Press, N.Y., 1979.

Once the design goals and service conditions are set, input from a materials development program is necessary. Laboratory experiments can generate general corrosion rates, but it is also important to quantify the susceptibility of materials to localized corrosion that will result in accelerated corrosion rates. Localized corrosion mechanisms include pitting, crevice corrosion, and stress-corrosion cracking. The following sections will summarize the materials development work in the United States and Sweden.

When the materials are sufficiently characterized, an integration of the information should result in a canister design that can meet the lifetime goals in the specified environment. It is not clear whether a single barrier or a multi-barrier system will be preferred. A multi-barrier system must be designed carefully, so that the presence or failure of one barrier will not inadvertently hasten the failure of another. This effect could occur by galvanic corrosion if two metals are in contact or when the corrosion product of one barrier could be especially aggressive to another barrier.

C. U.S. MATERIALS DEVELOPMENT PROGRAMS

The materials development program in the United States is in an early stage. Many materials are being evaluated but no specific systems have yet been singled out. The broadest-based U.S. study has been at Sandia Laboratories where a number of metals have been evaluated as potential high-level waste canister materials.(1,2) Laboratory investigations there have measured coupon weight losses for periods of 2-8 weeks in autoclaves. The solutions modeled brine from salt formations and seawater from sub-seabed sediments. Temperature, dissolved oxygen, and moisture content were also varied. Sandia has also been active in bench-scale heated salt block experiments as well as full-size heated field tests. As a result, Sandia has selected eight metals for further study. The criteria for selection included corrosion resistance as well as metal cost and availability. The eight metals are: 1018 mild steel; Corten A steel,(a); lead; 90-10 cupronickel; SS-Ebrite 26-1,(b); Monel 400,(c); Inconel 600,(c); and Ticode 12.(d)

Table D-VIII-2 summarizes the corrosion rates of these materials in a brine and a seawater solution.

It appears possible to design an overpack material to last thousands of years if general corrosion is known to be the only corrosion mechanism at work. This conclusion is similar to that presented in the Task B Report. Autoclave experiments provide general corrosion rates but are not very helpful in providing accelerated rates resulting from local corrosion mechanisms.

Work under way at Battelle's Pacific Northwest Laboratories (PNL) will complement the results from Sandia and continue the broad-based approach.(3) Autoclave experiments will provide further data on corrosion rates utilizing both groundwater solutions and brine. PNL will investigate ceramic and polymeric materials as well as metals.

The materials development program at Savannah River Laboratory has been limited to studying canisters for vitrification (through either continuous or in-can melting).(4) The canister lifetime goals have not been in the range of thousands of years but rather are intended for interim storage and shipping purposes. Overpack materials are not being studied.

Trademarks: (a) U.S. Steel Corporation, (b) Allegheny Ludlum Industries, (c) Huntington Alloys, and (d) TIMET.

TABLE D-VIII-2

CORROSION RATE IN BRINE AND SEAWATER OF THE EIGHT CANDIDATE MATERIALS

	Brine (mm/yr)	Seawater (mm/yr)
1018 Mild Steel	1.7	0.4
Corten A Steel	0.9	0.2
Lead	0.5	0.3
90-10 Cupronickel	0.14	0.07
SS-Ebrite 26-1	0.016	0.005
Monel 400	0.03	0.1
Inconel 600	0.009	0.005
Ticode 12	0.0006	0.005

Source: Braithwaite, J.W., and M.A. Molecke, High Level Waste Canister Corrosion Studies Pertinent to Geologic Isolation. NRC Conference on High Level Radioactive Solid Waste Forms, Denver, December 19-21, 1978.

D. SWEDISH PROGRAM

The Swedish Corrosion Institute and its research group seem to be somewhat ahead of the United States in regard to the four steps of canister development. Granite rock has been specified as the geologic environment. Three specific alternatives for the disposal of spent fuel in hardrock formations have been recommended:(5)

1. reprocessed waste in a 6 mm-thick titanium canister with a 100-mm thick lead lining,
2. spent unreprocessed fuel in a 200-mm thick pure copper canister; and
3. spent unreprocessed fuel in 100-mm thick aluminum oxide canister produced by hot isostatic pressing.

The feasibility of manufacturing aluminum oxide canisters by means of hot isostatic pressing (HIPing) has been demonstrated.(4) HIPing is a process that produces very dense ceramic bodies without excessive grain growth but is normally applied to much smaller samples. An aluminum oxide lid can be sealed onto the main body, also by means of HIPing. The flat surfaces that form the seal must first be polished to a flatness of ± 25 μm.

Aluminum oxide is in its highest oxidation state and is therefore very stable in groundwater. It will, however, be hydrated on surfaces in contact with water, which may result in flaking. This reaction is very slow and aluminum oxide should easily resist the action of groundwater for a million years. Being a ceramic, it is very susceptible to slow crack growth, which could lead to delayed failure. In order for this to occur, a surface defect and tensile stresses, both of sufficient magnitude, must be present. The stresses may be due to residual stresses from fabrication or applied stresses from rock movement. Care must be taken during fabrication of these canisters to minimize defects and residual stresses. Nondestructive evaluation techniques may be used to verify the maximum defect size before final disposal.

A copper canister was also designed for the isolation of unreprocessed spent fuel assemblies.(6,7) It is to be made from very pure oxygen-free high conductivity (OFHC) copper. The fuel rods are to be stripped from the metal components of the assembly to maximize space usage. After the rods are placed in the copper container, the spaces in between will be filled with lead. Three copper lids are then electron beam welded to seal the can.

Copper is a relatively noble metal and free oxygen and sulfide are the only constituents of groundwater that can potentially cause corrosion. Considering all of the sources of free oxygen and sulfide in the repository, a weight loss estimated at 60 kg will occur after a million years. This loss corresponds to an average corrosion depth of 0.5 mm or a maximum depth of 2.4 mm if the top of the canister is attacked more heavily. Copper is not highly susceptible to pitting but it can occur in some cases. Using an empirical model, the maximum attack depth after one million years is predicted to be 60 mm or 30% of the wall thickness.

In Sweden, the storage container for vitrified reprocessed waste has been designated to be a lead-lined titanium canister.(8) The waste is to be cast into or melted in a stainless steel cylinder. These stainless steel cans will be placed in the prefabricated lead-titanium canister and any extra space filled with molten lead. The container will be sealed by a welded-on titanium lid. Both the lead and the titanium are to be very pure.

Titanium develops a passivating layer of TiO_2, which forms spontaneously and protects against corrosion. Assuming a constant corrosion rate, the 6-mm thick casing should last beyond thousands of years. Pitting, crevice corrosion, and stress-corrosion cracking do not appear to be problems. The initial prediction of lifetime was thousands of years,(8) but a recent report has downgraded the lifetime of the titanium shell.(9) This revision was based on a slight risk of delayed failure from the presence of hydrogen, causing penetration of the titanium in a rather short time. Hydrogen can diffuse through the titanium and become concentrated at defects. This action results in embrittlement, and possibly delayed fracture, at tensile stresses much lower than those normally involved. Small amounts of hydrogen will be present in the fabricated titanium and hydrogen may also evolve as a corrosion product. It is very difficult, however, to predict the extent to which this evolved hydrogen will be absorbed. Although this type of delayed failure has never been found in unalloyed titanium, it is not completely understood, and thus, the risk of its occurring cannot be eliminated completely. Therefore, no lifetime limit has been predicted for the titanium casing.

Pure lead is also very corrosion-resistant. Because of the titanium casing, any attack on the lead would be localized, with the rate dependent upon the amount of available oxygen. Estimates of this quantity lead to a predicted lifetime of thousands of years for the 100 mm-thick lead lining. According to Swedish estimates, the total lifetime of the lead-lined titanium canister in groundwater is given as thousands of years, although it probably will be tens of thousands of years.

E. SUMMARY

The canister development program in the United States is not at the stage where it is possible to make an estimate of canister lifetime. Specifications for the service conditions must be set and considerable materials development work is still needed. When this is all integrated into a canister design, a lifetime evaluation will be possible. However, from results to date of the U.S. program and taking into account the Swedish work on specific canister systems, it seems highly likely that it is possible to design a viable canister that will last thousands and possibly tens of thousands of years.

REFERENCES - APPENDIX VIII

1. Braithwaite, J.W., and N.J. Magnani. Corrosion Considerations for Nuclear Waste Management. In: Scientific Basis for Nuclear Waste Management, G.J. McCarthy, ed. Plenum Publishing Corporation, New York. 1979.
2. Braithwaite, J.W., and M.A. Molecke. High Level Waste Canister Corrosion Studies Pertinent to Geologic Isolation. Presented at Conference on High Level Radioactive Solid Waste Forms, sponsored by the Nuclear Regulatory Commission, Denver, Colorado, December 19-21, 1978.
3. Personal communication, Max Kreiter, Pacific Northwest Laboratories.
4. Savannah River Laboratory (Rankin, W.N.) Compatibility Testing of Vitrified Waste Forms. Report DP-MS-77-115 (rev. 2/15/78).
5. Mattsson, E. Corrosion Resistance of Canisters for Final Disposal of Spent Nuclear Fuel. In: Scientific Basis for Nuclear Waste Management, G.J. McCarthy, ed. Plenum Publishing Corporation, New York. 1979.
6. Kärnbränslesäkerhet (KBS). Handling and Final Storage of Unreprocessed Spent Nuclear Fuel. Stockholm, Sweden. 1978.
7. Ibid. Copper as Canister Material for Unreprocessed Nuclear Waste Evaluation with Respect to Corrosion. Technical Report 90, Stockholm, Sweden. 1978.
8. Ibid. Handling of Spent Nuclear Fuel and Final Storage of Vitrified High Level Reprocessing Waste. Stockholm, Sweden. 1978.
9. Ibid. Corrosion Resistance of Titanium Canisters Lined with Lead for Final Disposal of Reprocessed and Vitrified Waste from Nuclear Reactors. Technical Report 107, (in Swedish), Stockholm, Sweden. 1978.

APPENDIX D-IX

THERMAL STRESS CRACKING IN SALT

A. INTRODUCTION

The purpose of this appendix is to present a set of rock mechanics calculations undertaken to assess the possibility that fracture pathways would develop from the repository to the upper aquifer, especially in the case of a repository in salt. Two types of stress have been addressed: thermal stresses and stresses around mined openings in rock, with emphasis on the former.

The existence of a repository and the heat released by it alter both the state of stress and the mechanical properties of the host formation. While stress concentrations around underground openings have been studied extensively, thermal stresses complicate the problem; for much of the time, these thermal stresses are dominant. Should the total applied stresses exceed the strength of formations surrounding the repository, fractures may breach the geologic barrier.

B. BASIS FOR ESTIMATION

Analysis of stresses about manmade underground works has been undertaken with varying degrees of sophistication for about thirty years.(1,2,3) In-situ stress measurements generally confirm the predictions of analytical models within the normal limits of accuracy of geomechanics.

With few exceptions, analyses of stresses and strength in geomechanics are deterministic. Material properties are specified as constant over large regions; it is then possible to analyze and compare them with strengths. Results are expressed as the ratio of available resisting strength to driving load in specified models of failure; the ratio is commonly called the "Factor of Safety" (FS). Because no sources of uncertainty are included in these analyses, quantitative estimates of probabilities of failure are not possible. Through long experience, rules of practice for acceptable Factors of Safety have emerged. The extrapolation of "acceptable" FS to unique cases is difficult, however.

The most important mode of failure considered in estimating the risk of high-level waste (HLW) escaping the repository is the formation of continuous channels connecting repository and aquifer. Traditional stress analyses predict zones of failure, rather than fractures. Generally, the stress field is compared with rock strength and for these regions in which strength is exceeded by stress, the rock is said to be "failed" or "plastic". A typical result is shown in Figure D-IX-1.$^{(4)}$ The conclusion of this type of analysis is that zones of failure develop adjacent to the repository, but beyond about one opening diameter from the repository (expected) stresses do not exceed (expected) strengths. The expected FS against failures that extend beyond the failed zone is typically much greater than 1.0.

Stress analysis can be made with varying levels of sophistication. Assumptions can be made about alternative deformation behavior (e.g., elasto-plastic, strain-hardening, strain-softening, etc.), about the influence of jointing, and the like. Yet, the predictive results are qualitatively the same: in some regions adjacent to the opening, stresses exceed strengths; in regions away from the opening, stresses do not exceed strengths. The shapes of failed zones are sensitive to geometric details (i.e., sharp corners concentrate stresses locally). For the purpose of estimating risks such conclusions are inadequate, since they do not follow the development of the fracturing all the way to the aquifer.

At present, there are no modeling techniques for rock fracturing that incorporate uncertainty. Thus, an approach to this problem was developed specifically for the present analysis. This approach treats rock properties as random variables, and calculates the reliability of host formations against failure in particular modes, under deterministically predicted stress fields. The approach and its underlying assumptions are presented below.

The purpose of this analysis cannot be to calculate precise probabilities for a breach of the geologic barrier through overstressing, because such calculations are not possible in the present state of geomechanics. Rather, the purpose is to establish whether the

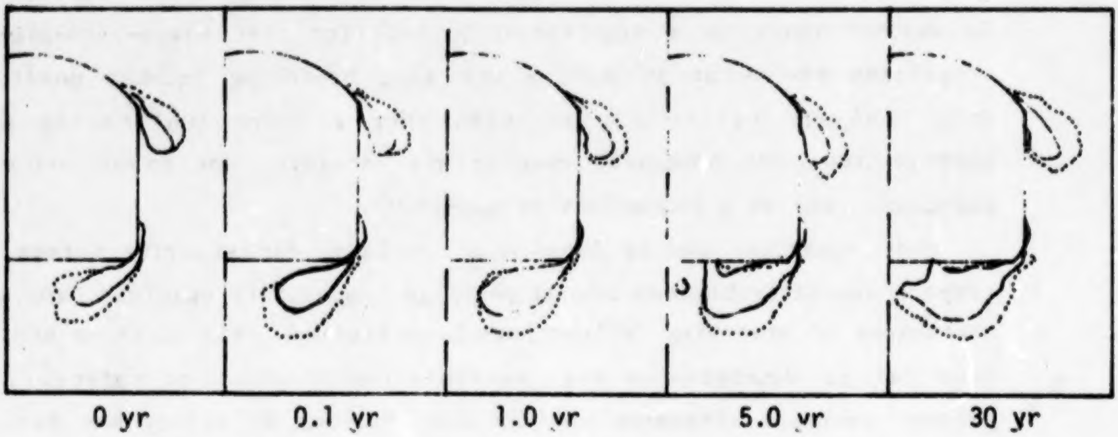

Note: Dotted areas indicate regions within the rock for which applied stresses exceeded strength.

Source: Mathab, M.A., J.L. Ratigan, and D.R. McCreath. Stability of a Radioactive Waste Repository in the Canadian Shield. 18th U.S. Symposium on Rock Mechanics, 1977.

FIGURE D–IX–1 RESULTS OF STRESS ANALYSIS STUDIES PERFORMED FOR WASTE STORAGE IN FORMATIONS OF THE CANADIAN SHIELD

inherent uncertainties in rock properties within a bedded salt formation chosen for its uniformity lead to important uncertainties on breaching. A limiting equilibrium model is constructed which, while typical of geotechnical models, is only one of many that could have been used. Reasonable estimates of material property uncertainty and spatial variability are propagated through the model. Average salt properties are sufficient to protect the repository against breaching; the question is whether there is a significant probability that worse-than-average properties may occur in such a way that breaching becomes possible. This analysis yields a prediction that is more qualitative than quantitative; the numerical results are accurate, not to an order of magnitude, but to a few orders of magnitude.

Many numerical models have been developed for studying stress and temperature distributions around potential repository openings, and many mechanisms of breaching failure have been studied. All of these studies have led to consistently high deterministic factors of safety. The present analysis estimates whether such factors of safety may lead to significant probabilities of the development of release pathways.

C. FAILURE THEORY FOR ROCK

Rock, including salt, is a frictional material the strength of which depends on two properties: one independent of ambient stresses, generally called the "cohesion"; and one dependent on ambient stresses, generally called the "friction angle". Rocks display greater strength under confinement than when unconfined, and this increase in strength is dependent on the confining stress.

The Mohr failure criterion for rock is shown in Figure D-IX-2, plotted with normal stress as abscissa and shear stress as ordinate. Following this criterion, failure occurs when the shear stress on a plane, τ, exceeds some monotonic function of the normal stress on the plane, σ,

$$\tau = g(\sigma) \qquad (1)$$

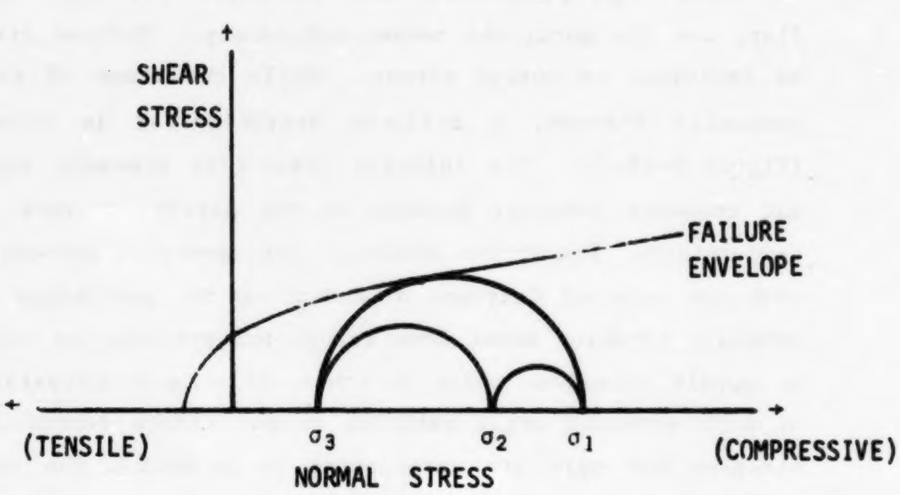

Note: Semi circles represent loci of stresses for planes of varying orientation with major principal stress σ_1, minor principal stress σ_3, and intermediate principal stress σ_2.

FIGURE D-IX-2 MOHR FAILURE CRITERION FOR ROCK

Equation 1 is sometimes approximated by the linear relationship

$$\tau = C + \sigma \tan \phi .$$

where C is the "cohesion", and ϕ, the "friction angle". Equation 2 is commonly called the Naviser-Coulomb criterion. The Mohr failure criterion (Equation 1) has been empirically verified, and is widely used.

Under high pressures, Mohr envelopes for rocks typically become flat, and the materials behave cohesively. Failure strengths cease to be dependent on normal stress. While the slope of the Mohr envelope gradually changes, a bilinear approximation is often used instead (Figure D-IX-3). The inferred transition pressure between frictional and cohesive behavior depends on the particular rock and the ambient temperature. Transition pressures decrease with increasing temperature, with the rate of decrease dependent on the particular rock. In salt, strength behavior above some transition pressure is usually assumed to be purely cohesive, while in other rocks (e.g., crystallines) strength at high stresses still exhibits slight stress dependence. Transition stresses for salt are anticipated to be within the range of stresses predicted for repositories at 460 meters.

Intact rock is not perfectly elastic, but displays ductility (i.e. nonlinearity in stress vs. strain) at high shear stresses (Figure D-IX-4). Post-failure behavior can range from strain-hardening to strain-softening, with some materials like salt displaying more ideal plasticity.

Deformation properties of rock are not important in comparing stresses with strength, but they are important in predicting stresses in the first place. According to elasticity theory, elements of rock continue to withstand and transmit stresses in a linear way up to and (theoretically) beyond what are known to be their failure limits. In reality, however, rock is not perfectly elastic, and incremental stresses are redistributed around failed elements, replacing sharp stress concentration with broader bands of lower stress.

Much work has been performed over the past ten years in numerical analysis of subsurface stresses using assumptions of various

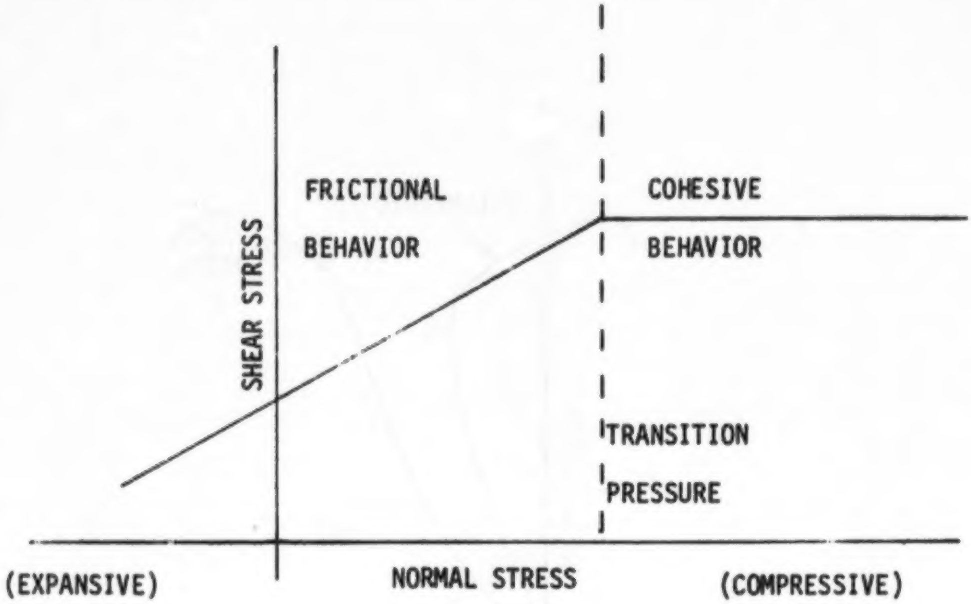

FIGURE D-IX-3 BILINEAR APPROXIMATION TO CURVED MOHR ENVELOPE

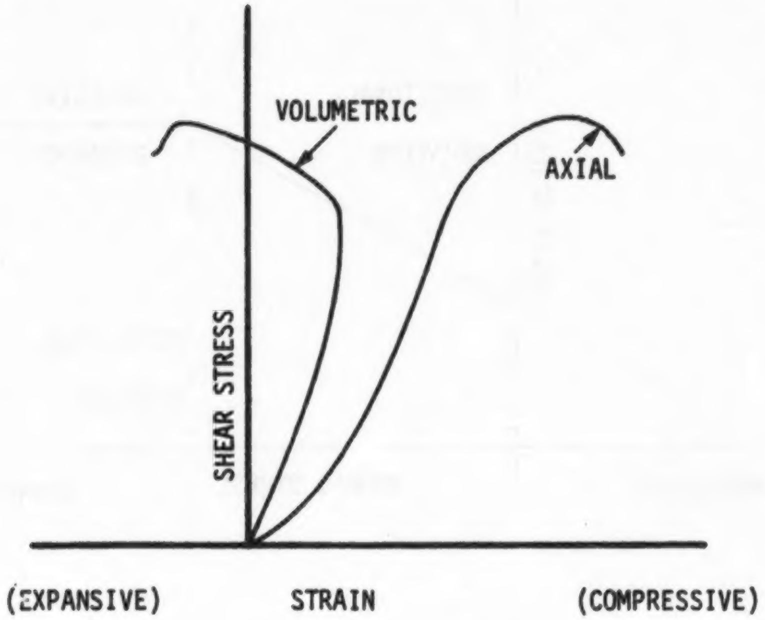

FIGURE D-IX-4 TYPICAL DEFORMATION BEHAVIOR FOR BRITTLE ROCKS complexities (e.g. elastoplastic analysis, plastic analysis, etc.). Changes of these assumptions lead to changes in predictions of stress distributions and failure zones. Of course, as pointed out before, changes in failure zones predicted by a totally deterministic analysis have little practical importance in an overall safety analysis program. It is useful, however, to emphasize the point that assumed relationships of deformation affect stress predictions.

The cost and effort involved in performing stress analysis incorporating complicated deformation properties must be balanced against the increase in information actually derived. With few exceptions, inelastic stress calculations must be made numerically, typically using finite element or finite difference techniques. Besides estimating bulk and shear moduli for the rock, one must estimate various transition stresses and moduli in each zone of the stress-strain relationship.

All of these properties can be reasonably estimated for a particular site, although the accuracy of the estimates depends on the extent of the exploration and testing program. In performing non-site-specific studies, however, such estimates are difficult; this difficulty extends to estimating an appropriate modulus for the elastic case. Therefore, one must ask whether more sophisticated deformation relations are useful in the present application. In any case, uncertainty in estimating moduli probably leads to more uncertainty in stress predictions than do the differences among different deformation models.

Rock masses differ from intact rock in that the former are cut by pervasive and nonpervasive fractures and inhomogeneities that affect mechanical behavior. Most important of these features are joints, i.e., one or more sets of subparallel fractures separating the rock mass into blocks. Joint systems are geologic in origin and exist prior to repository construction, with their character and extent determined by lithology and geologic history.

Joints affect the behavior of rock masses by lowering deformation moduli and by introducing planes of weakness. The degree to which either of these effects occurs depends on the density of joints, their sizes, and their physical properties (i.e. shear and normal stiffness, and frictional resistance). All of these properties are site-specific.

Common practice in analyzing the behavior of jointed rock masses is to use continuum models, but to modify deformation moduli and strength parameters by reduction factors. Sometimes anisotropy is also introduced. Discontinuum models for jointed rock require information specific to the rock mass and opening geometry.(5,6)

Salt is a low-viscosity material that can flow under stress and in which fractures heal quickly. Therefore, salt formations are thought to be sparsely jointed, if at all. Variations introduced by assuming salt to be intact are probably within the error band of present analysis, which among other uncertainties includes those from site-to-site variability.

D. EMPIRICAL DATA ON SALT STRENGTH

1. Rock Salt Properties

The literature was searched for empirical data on the mechanical and thermal properties of in situ salt, in order to estimate values for the following parameters:

1. thermal conductivity and heat capacity,
2. Young's (deformation) Modulus and Poisson's Ratio, and
3. strength parameters (cohesion and friction angle).

Such an estimate was difficult because of the lack of comprehensive published information on the subject, and because these properties vary with temperature and the strain rates. Some simple assumptions were therefore made in the study. Where necessary, the available published data were extrapolated to the conditions of the model repository, which were taken to be: temperatures from 0 to 300°C; strain rates from 10^{-4} to 10^{-12} min-1.

2. Thermal Properties

Thermal conductivity has been measured in several studies dealing with waste repositories.(7,8,9,10) Findings from the literature are summarized in Figure D-IX-5. Reported values of

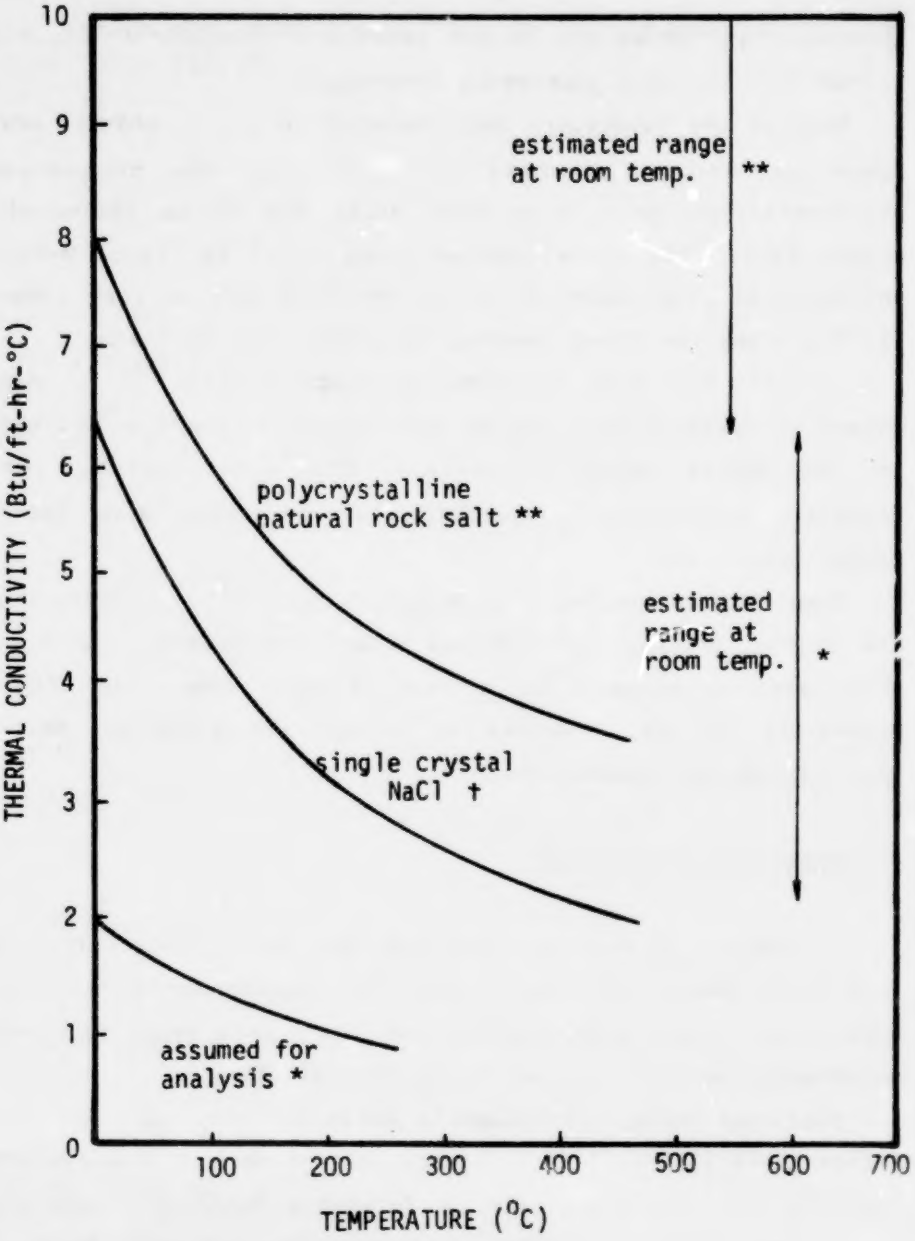

Sources: *Arthur D. Little, Inc. Task B Report.

**Westinghouse Astronuclear Laboratory, A Study of Borehole Plugging in Bedded Salt Domes by Earth Melting Technology. WANL-TME-2870, 1975.

† Kaufman, D.W. (ed.) Sodium Chloride: The Production and Properties of Salt and Brine. Reinhold Publishing Co., N.Y., 1960.

FIGURE D-IX-5 THERMAL CONDUCTIVITY OF ROCK SALT thermal conductivity are in the range 1-10 Btu/(ft-hr-^{o}C), and the values decrease with increasing temperature.(11,12)

Many of the laboratory data reported in the literature are from tests on single crystals of salt, so the properties of polycrystalline salt (i.e. rock salt) had to be estimated from sparse data. The curve labeled "rock salt" in Figure D-IX-5 was extrapolated from tests on polycrystalline salt at room temperatue (24^{o}C), using the trend observed in single crystal tests.

Specific heat data are shown in Figure D-IX-6.(12,13) Reported values of specific heat are in the range 8-11 Btu/(gm-^{o}C), which is in the upper range of values for other rocks, and are temperature-dependent. Specific heat increases with increasing temperature.

Density data are shown in Figure D-IX-7.(12,13) While the data are sparse, a range of 1.95-2.2 seems appropriate. As expected, this range is somewhat below that of most rocks. As with other properties of salt, density is temperature-dependent, decreasing with increasing temperatures.

3. Mechanical Properties

Estimation of elastic properties for salt, Young's Modulus and Poisson's Ratio, is complicated by temperature-dependence and viscosity. Creep from viscosity at low strain rates decreases the deformation moduli reported in the test results.

Published values of Poisson's Ratio for rock salt are shown in Figure D-IX-8.(11,14,15) Within the range of temperatures of interest for the repository, a Poisson's Ratio of about 0.22 is appropriate. It should be noted that the Poisson's Ratio enters stress calculations through the term $(1-\nu^{2})^{-1}$ (where ν is the Poisson's Ratio) which means that stress predictions are not sensitive to minor uncertainties in the ratio.

Published data on Young's Modulus for rock salt are shown in Figure D-IX-9.(11,14,16) Temperature trends in both dynamic and static testing are similar, the modulus decreasing slightly with increasing temperature for the range 0-300^{o}C. The disparity between

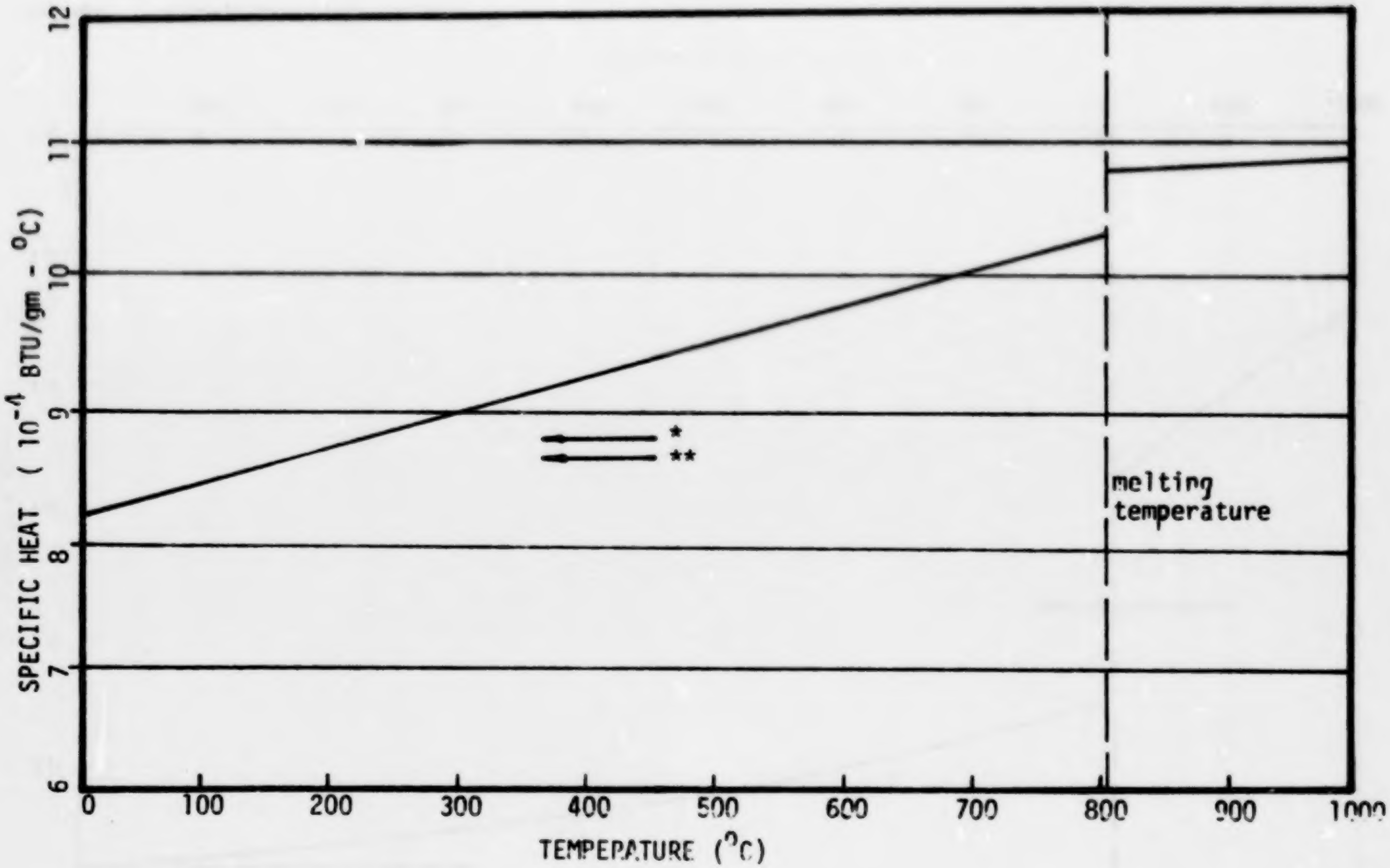

Sources: *Arthur D. Little, Task B Report.
**Gera, F. Review of Salt Tectonics in Reaction to the Disposal of Radioactive Waste in Salt Formations. Geological Society of America. 83, 1972.
†Kaufman, D.W. (ed.). Sodium Chloride: The Production and Properties of Salt and Brine. Reinhold Publishing Co., N.Y., 1960.

FIGURE D-IX-6 SPECIFIC HEAT OF ROCK SALT VS TEMPERATURE

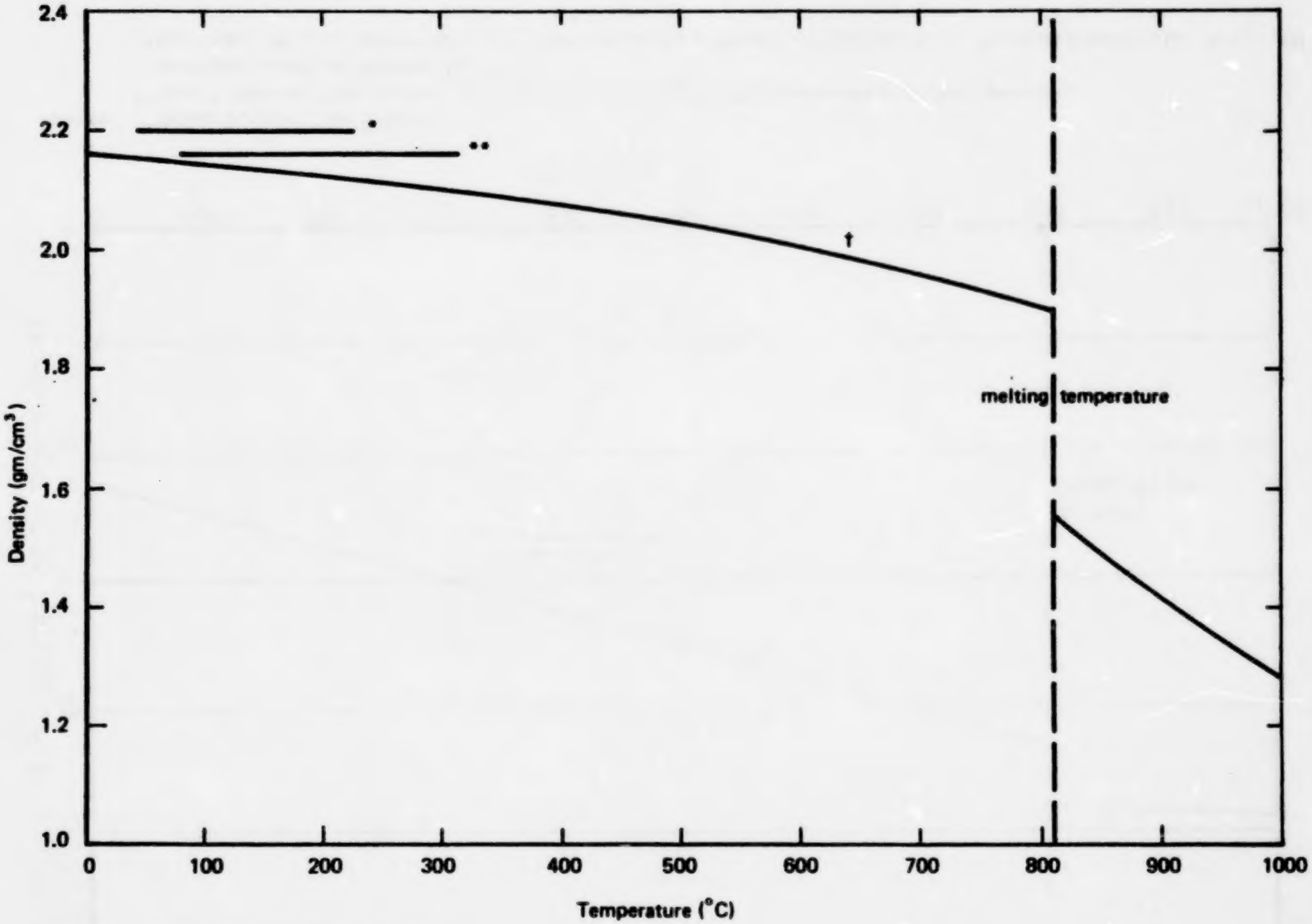

Sources: *Arthur D. Little, Task B Report.

**Gera, F. Review of Salt Tectonics in Reaction to the Disposal of Radioactive Waste in Salt Formations. Geological Society of America. 83, 1972.

†Kaufman, D.W. (ed.), Sodium Chloride: The Production and Properties of Salt and Brine. Reinhold Publishing Co., N.Y., 1960.

FIGURE D-IX-7 DENSITY OF ROCK SALT VS. TEMPERATURE

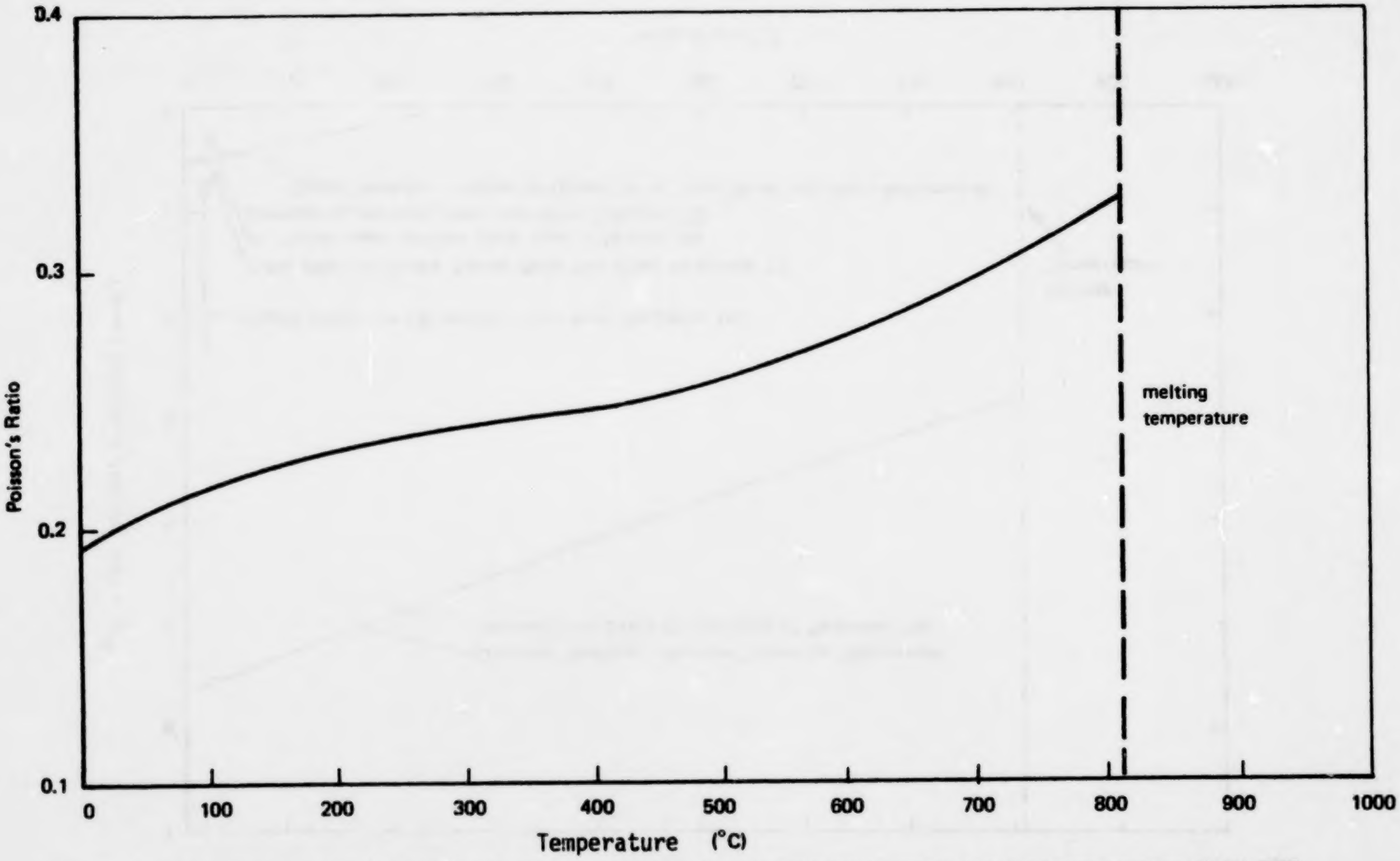

Sources: Westinghouse Astronuclear Laboratory, A Study of Borehole Plugging in Bedded Salt Domes by Earth Melting Technology. WANL-TME-2870, 1975.

Hunter, L., and S. Siegel. The Variation with Temperature of the Principal Elastic Moduli of NaCl Near the Melting Point. Physical Review, 61, 1942.

Starfield, A.M., and W.C. McClain. Project Salt Vault. J. Rock Mechanics and Mineral Sciences, 10, 1973.

FIGURE D-IX-8 POISSON'S RATIO VS. TEMPERATURE

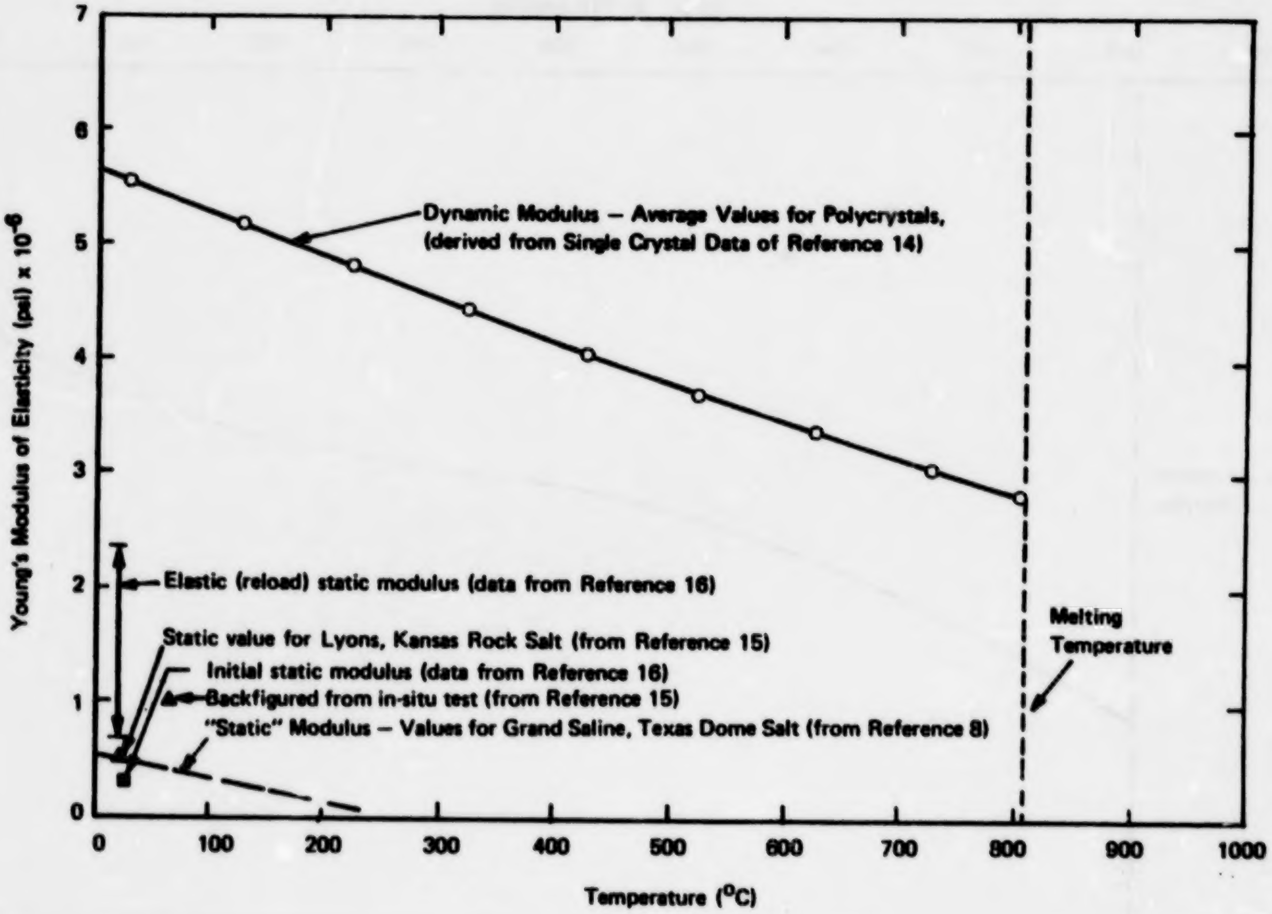

FIGURE D–IX–9 YOUNG'S MODULUS OF ELASTICITY VERSUS TEMPERATURE dynamic and static testing is much greater than the temperature effect, which suggests that strain rate and not temperature is the dominant test variable.

To determine the variation in Young's Modulus with strain rate, it was necessary to make several assumptions and to use published creep test data. It was assumed that static moduli reported in the literature (Figure D-IX-10)(15,17) were tested at a strain rate of about 10^{-2} min^{-1}. This would correspond to 10% strain in 10 minutes. It was also assumed that dynamic moduli reported in the literature correspond to strain rates of about 10^4 per minute.

In addition, values of elastic moduli have been back-calculated from published unconfined creep tests.(10) Uniaxial creep tests for rock salt, as shown in Figure D-IX-11,(17) were used to determine the strain at various compressive stresses and temperatures corresponding to strain rates of 10^{-5}, 10^{-6}, and 6×10^{-7} min^{-1}, from which values of Young's Modulus have been determined (Table D-IX-1).

Finally, the strain-rate dependence was estimated by rearranging Starfield and McClain's equation for empirically observed deformation in rock salt pillars,(15)

$$\epsilon = (0.65 \times 10^{-37}) \left(\frac{t}{60} \right)^{0.25} (T + 273)^{9.5} \sigma^{3.0} \qquad (3)$$

where

ϵ = strain

t = time in minutes

T = temperature in °C

and

σ = uniaxial stress in psi, into the form

$$E = \frac{\sigma}{\epsilon} = \left\{ \left[(1.50 \times 10^{50}) \frac{(\dot{\epsilon})^{1/3}}{\sigma^3 (t + 273)^{28/3}} \right] + 10^6 \left\{ \frac{\sigma^3 (T+273)^{38/3}}{(1.50 \times 10^{56}) (\dot{\epsilon})^{1/3}} \right\} \right\} \qquad (4)$$

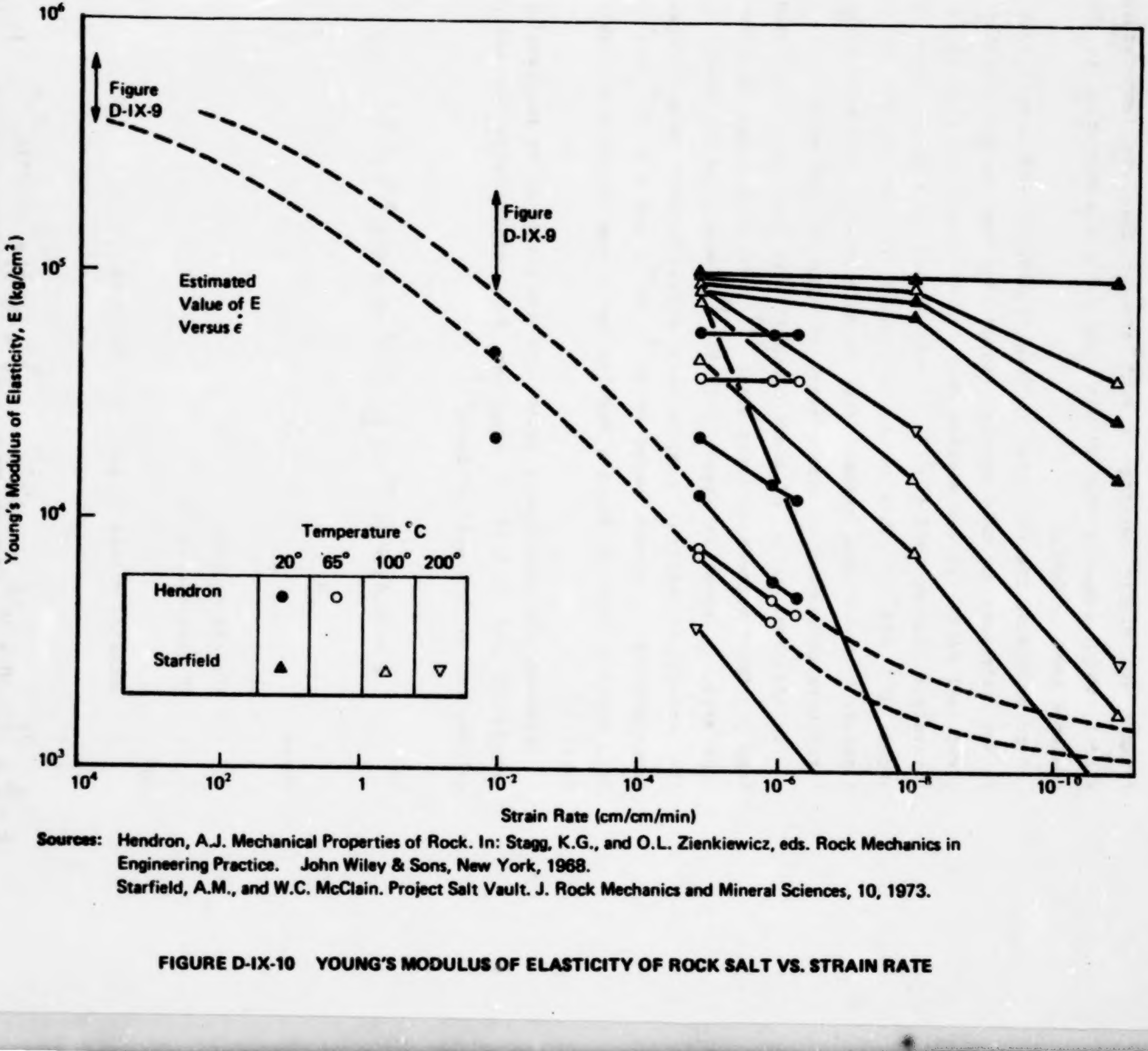

Sources: Hendron, A.J. Mechanical Properties of Rock. In: Stagg, K.G., and O.L. Zienkiewicz, eds. Rock Mechanics in Engineering Practice. John Wiley & Sons, New York, 1968.
Starfield, A.M., and W.C. McClain. Project Salt Vault. J. Rock Mechanics and Mineral Sciences, 10, 1973.

FIGURE D-IX-10 YOUNG'S MODULUS OF ELASTICITY OF ROCK SALT VS. STRAIN RATE

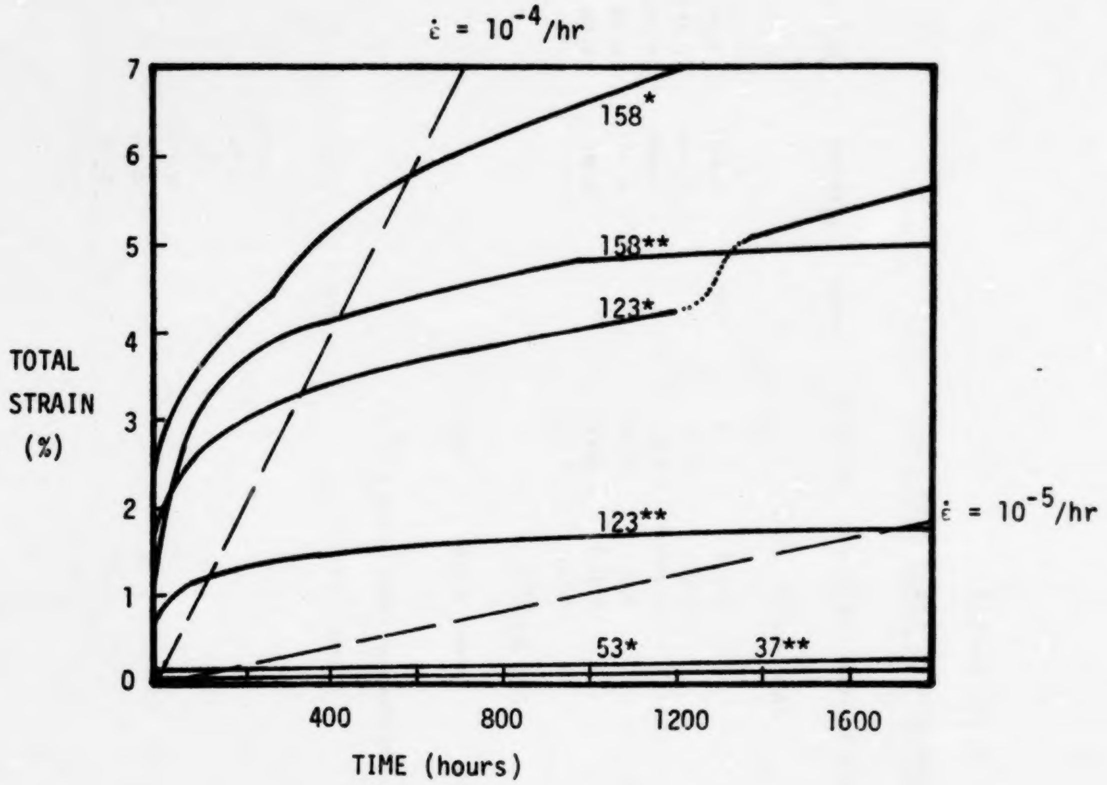

*Temp. 65°C
**Temp. 23°C

Note: Stress is indicated along curves in kg/cm².

Source: Hendron, A.J. Mechanical Properties of Rock. In: Stagg, K.G., and O.L. Zienkiewicz, eds. Rock Mechanics in Engineering Practice. John Wiley and Sons, New York, 1968.

FIGURE D-IX-11 UNIAXIAL COMPRESSION CREEP TEST FOR ROCK SALT

TABLE D-IX-1

UNIAXIAL COMPRESSIVE CREEP TEST DATA

T°C	E(10^{5}psi)	σ(psi)	ϵ(in/in)	E(10^{5}psi)	σ(psi)	ϵ(in/in)	E(10^{5}psi)	σ(psi)	ϵ(in/in)	E(10^{5}psi)
TEST DATA$^{(2)}$										
23	10^{-5}	525	0.001	5.25	1750	0.008	2.19	2250	0.020	1.13
"	10^{-6}	"	"	"	"	0.0135	1.30	"	0.0435	0.517
"	$6x10^{-7}$	"	"	"	"	0.0155	1.13	"	0.0485	0.464
65	10^{-5}	750	0.002	3.75	"	0.023	0.761	"	0.0315	0.714
	10^{-6}	"	"	"	"	0.0355	0.493	"	0.065	0.346
	$6x10^{-7}$	"	"	"	"	0.0425	0.412			
TEST DATA$^{(20)}$										
20(?)	$4x10^{-4}$	2800	0.0075	3.73	4500	0.0125	3.60			
BACK-CALCULATED FROM CREEP EQUATION$^{(19)}$										
20	10^{-5}	525	9.99		1750	9.72		2250	9.41	
"	10^{-8}	"	9.92		"	7.73		"	6.16	
"	10^{-11}	"	9.27		"	2.54		"	1.38	
100	10^{-5}	"	9.83		"	6.16		"	4.30	
"	10^{-8}	"	8.56		"	1.38		"	0.701	
"	10^{-11}	"	3.72		"	0.158		"	0.075	
200	10^{-5}	"	7.46		"	7.33		"	0.359	
"	10^{-8}	"	2.27		"	0.078		"	0.037	
"	10^{-11}	"	0.28		"	0.0079		"	0.0037	

where strain rate, $\dot{\varepsilon}$, is in min^{-1}. Values of modulus from this equation were computed for various stress levels at room temperature, for strain rates of 10^{-5}, 10^{-8}, 10^{-11} (Table D-IX-1). Although these values differ from those back-calculated from creep test data, the trends are similar.

Combining information from each of the above sources leads to a best estimate of modulus over the temperature and strain-rate ranges of interest, as shown in Figure D-IX-10. This estimate would suggest an approximately constant modulus in the range below 10^{-6} min^{-1}, which is the range of thermally applied stresses for the repository. The value of E in this range is about 3×10^4 psi.

Published values of the coefficient of linear thermal expansion were reviewed.(18) The coefficient is only slightly temperature-dependent (increasing with increasing temperature), but over the range of interest (0-300°C) the values vary only from 4.03 to 4.7×10^{-5} $^{\circ}C^{-1}$. For the purposes of this analysis, the coefficient of expansion was assumed not to vary with temperature.

Rock salt sheared at constant temperature and strain rate exhibits either brittle or ductile behavior, depending on the confining stresses. Above the brittle-ductile boundary, the Mohr envelope is flat, (i.e., a constant shear strength for all confining stresses). In the ductile range, however, the shear behavior is strain-hardening.

The brittle-ductile transition was assumed to occur, as shown in Figure D-IX-12, where the curved Mohr envelope for peak behavior crosses the residual envelope, oriented at the angle of sliding friction.(19,20,21) The angle of residual friction was derived from Figure D-IX-13 to be about 29°.(16,17,22) Reports in the literature vary from as low as 20° to as high as 40°, with most estimates lying between 25° and 35°.

A simple (c,ϕ) linear approximation to the Mohr envelope called the Mohr-Coulomb Criterion (Figure D-IX-14) was conservatively

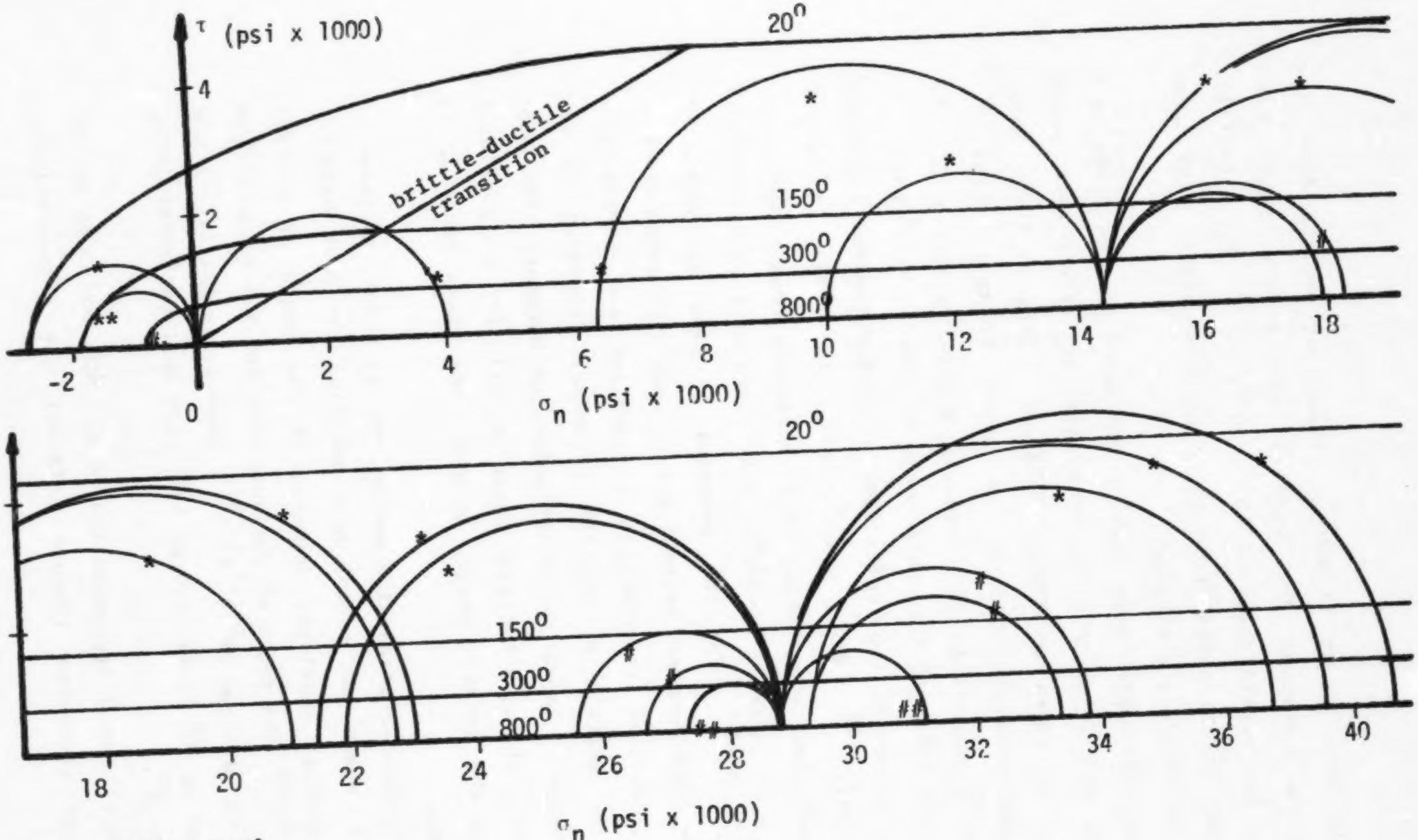

Note: TEMP°C
* 24°
#150°
**250°
##300°

Sources: Handin, J., and R.V. Hager, Jr. Experimental Deformation of Sedimentary Rocks Under Continuing Pressure: Tests at High Temperature. Bulletin, American Association Petroleum Geologists, 42: 2892–2934, 1958.

Stokes, R.J. Mechanical Properties of Polycrystalline NaCl. Proceedings British Ceramics Society, 6: 187–207, 1966.

Baidyuk, B.V. (ed.). Mechanical Properties of Rocks at High Pressure and Temperatures. Consultants Bureau Translation, New York, 1967.

FIGURE D-IX-12 SUMMARY OF PUBLISHED SHEAR STRENGTH DATA

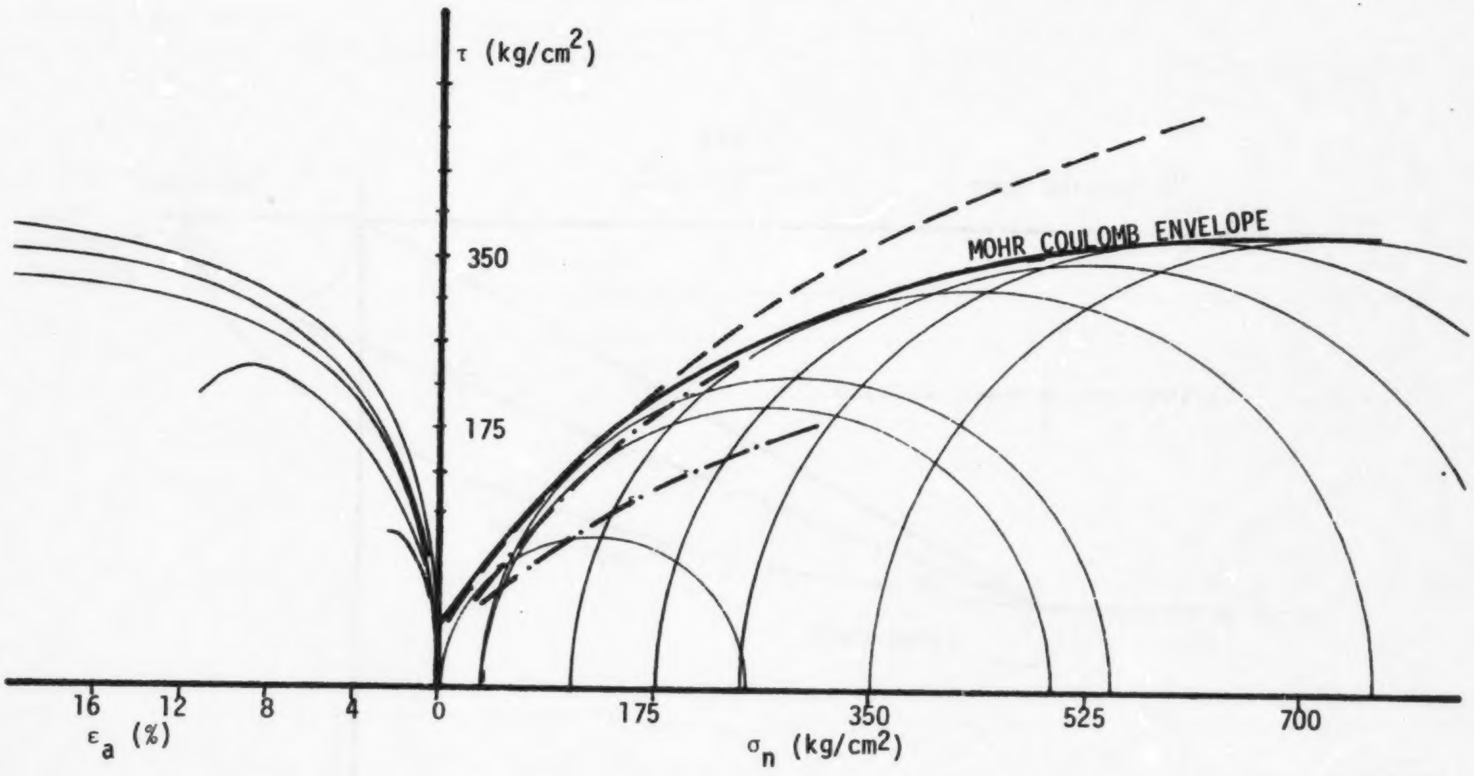

Sources: Fodor, I., and K. Tokes, Neve Forschungen Uber die Physikelischen and Mechanischen Eigenschaften des Rumanischen Steinsalzes. Theme 3, No. 78: 705-709. Proceedings 1st Congress International Society Rock Mechanics, Lisbon, 1966.

Serata, S., S. Saknrai, and T. Abachi. Theory of Aggregate Rock Behavior Based on Absolute Three-Dimensional Testing (ATT) of Rock Salt. Proc. 10th Symposium on Rock Mechanics, 1969.

Hedron, A.J. Mechanical Properties of Rock. In: Stagg, K.G., and O.L. Zienkiewicz, eds. Rock Mechanics in Engineering Practice. John Wiley and Sons, New York, 1968.

FIGURE D-IX-13 MOHR COULOMB ENVELOPE AT LOW STRESS LEVELS

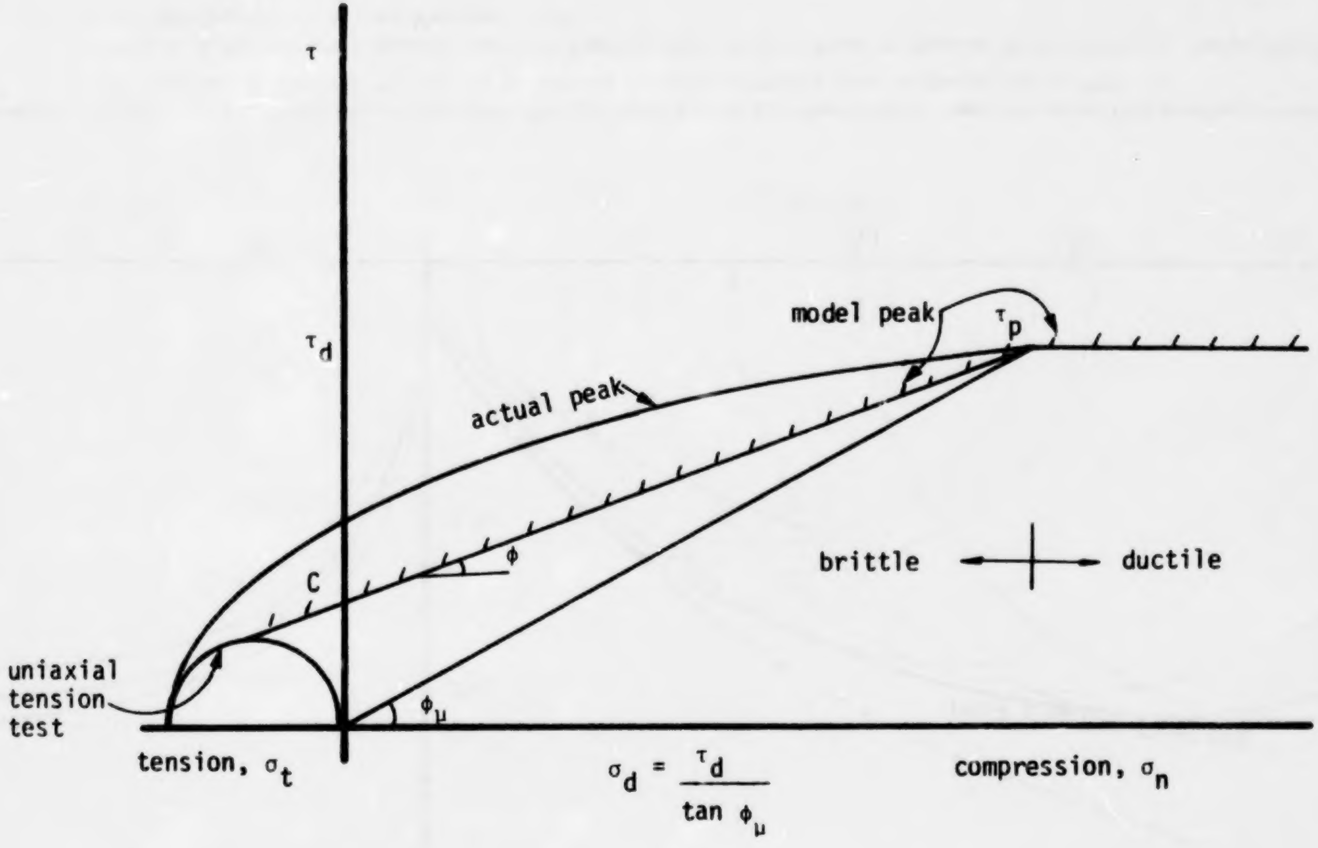

FIGURE D-IX-14 LINEAR MOHR – COULOMB ENVELOPE STRENGTH MODEL assumed to predict peak shear strength for constant temperature and strain rates. This model is expressed as

$$\tau_p = \begin{cases} c + \sigma_n \tan\phi & \sigma_n < \sigma_d = \tau_d/\tan\phi_\mu \\ \tau_d & \sigma_n > \sigma_d \end{cases} \qquad (5)$$

where

$$c = \frac{\sigma_t}{2}\left[\frac{\tau_d - \sigma_{t/2}}{\dfrac{2\tau_d}{\sigma_t \tan\phi_\mu} + 1}\right] \qquad (6)$$

$$\tan\phi = \frac{(2\tau_d - \sigma_t)\tan\phi_\mu}{(2\tau_d - \sigma_t \tan\phi_\mu)} \qquad (7)$$

τ_p = peak shear strength;

σ_t = tensile strength;

ϕ_μ = sliding fraction angle;

σ_d = ductile shear strength.

As shown in Figure D-IX-15, the peak shear strength decreases with temperature until at about 800°C the rock becomes fluid. The temperature dependence of the Mohr envelope can be approximated in terms of the decrease in both the ductile shear strength and the uniaxial tensile strength, if the brittle-ductile transition occurs, as assumed, along the temperature-independent linear residual envelope. This temperature dependence of both shear and tensile strength was derived from triaxial test data plotted in Figure D-IX-15. Temperature dependence was derived to be

$$\tau_d\ (\text{psi}) = \frac{4.9 \times 10^5}{T(^\circ\text{C}) + 74} - 540 \qquad (8)$$

$$\sigma_t\ (\text{psi}) = \frac{7.08 \times 10^6}{T(^\circ\text{C}) + 1160} - 3600 \qquad (9)$$

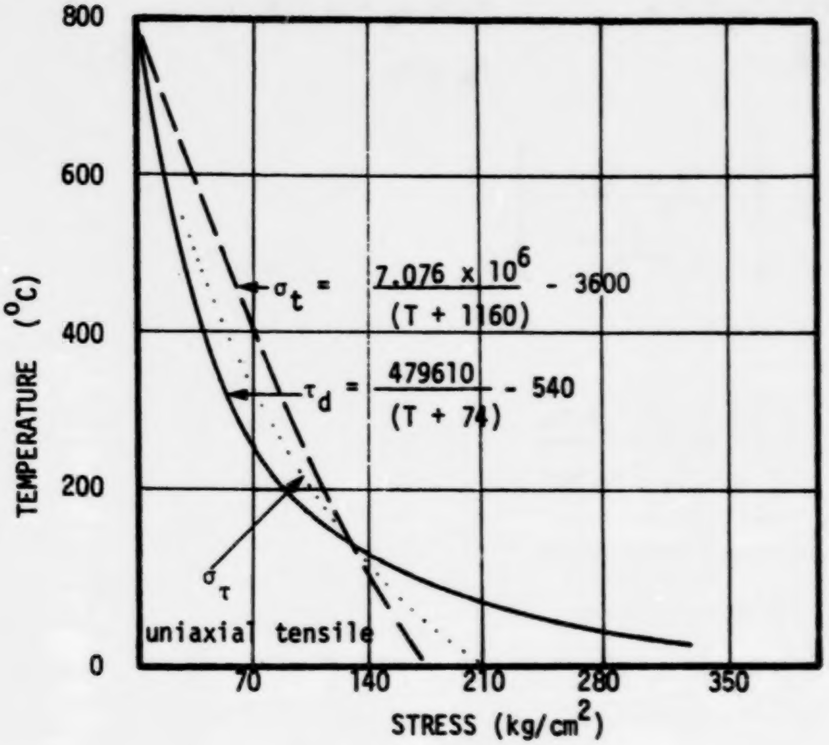

FIGURE D-IX-15 STRENGTH LIMITS OF ROCK SALT VERSUS TEMPERATURE where τ_d is the ductile shear strength and σ_t the tensile strength.

These values of shear and tensile strength were used in the strength model previously discussed, so that:

for

$$\sigma_n < \sigma_d = \left\{\frac{4.8 \times 10^5}{T(^\circ C) + 74} - 540\right\} / \tan \phi_\mu \qquad (10)$$

$$\tau_p = C(T) + \sigma_n \tan \phi_\mu \quad K(T) \qquad (11)$$

where,

$$C(T) = \frac{\left[\dfrac{7.07 \times 10^6}{T + 1160}\right] - 360 \left[\dfrac{4.79 \times 10^5}{T + 74} - 540\right] (1 + \tan \phi_\mu)}{2\left[\dfrac{4.79 \times 10^5}{T + 74} - 540\right] + \left[\dfrac{7.08 \times 10^6}{T + 1160} - 3600\right] (\tan \phi_\mu)} \qquad (12)$$

$$K(T) = \left\{\frac{2\left[\dfrac{4.79 \times 10^5}{T + 1160} - 540\right] - \left[\dfrac{7.08 \times 10^6}{T + 1160} - 3600\right]}{2\left[\dfrac{4.79 \times 10^5}{T + 74} - 540\right] + \left[\dfrac{7.08 \times 10^6}{T + 1160} - 3600\right] \tan \phi_\mu}\right\} \qquad (13)$$

where T is temperature in $^\circ C$,

σ_n is normal stress,

σ_d is the brittle-ductile transition stress, and

ϕ_μ is the residual fraction angle.

For $\sigma_n > \sigma_d$,

$$\tau_p = \tau_d = \frac{4.79 \times 10^5}{T + 74} - 540$$

The strength model is, therefore, in terms of only two exogenous variables (temperature and applied normal stress) and one material constant (the residual sliding coefficient of friction).

E. STRESS PREDICTIONS

To make predictions on the behavior of a rock mass, both the mechanical rock mass properties (strength, deformability, and permeability) and the state of stress must be estimated. These parameters and stresses are not independent.

1. In-situ Stresses

Prior to construction, a repository site will be in some state of stress depending on the rock formations and recent geologic history. For flat-lying sites in tectonically quiet regions, the principal stress directions will be very nearly vertical and horizontal. Figure D-IX-16 presents data summarizing in-situ vertical stress measurements from several sources and from sites distributed across North America.(23) The common assumption of gravity stresses for the vertical direction, about 0.23 $kg/cm^2/m$ (1 psi/ft) of depth, is slightly below the average of these measurements, but the scatter in the data is large. Among other sources of this scatter are large measurement errors from the way in-situ stresses are measured (see, e.g.,(2).

Typical densities for rock masses are in the range of 2560 kg/m^3. Salt is somewhat lower, or about 2240 kg/m^3. Thus, the assumption 0.23 $kg/cm^2/m$ (1 psi/ft) is reasonable, particularly since the analytical results are insensitive to moderate changes in vertical and horizontal stresses.

Horizontal stresses within a given profile typically vary proportionally with vertical stresses. The ratio of horizontal to vertical stress is therefore defined and assumed to be constant either for an entire profile or for individual strata or sequences of strata,

$$K = \frac{\sigma_h}{\sigma_v} \qquad (15)$$

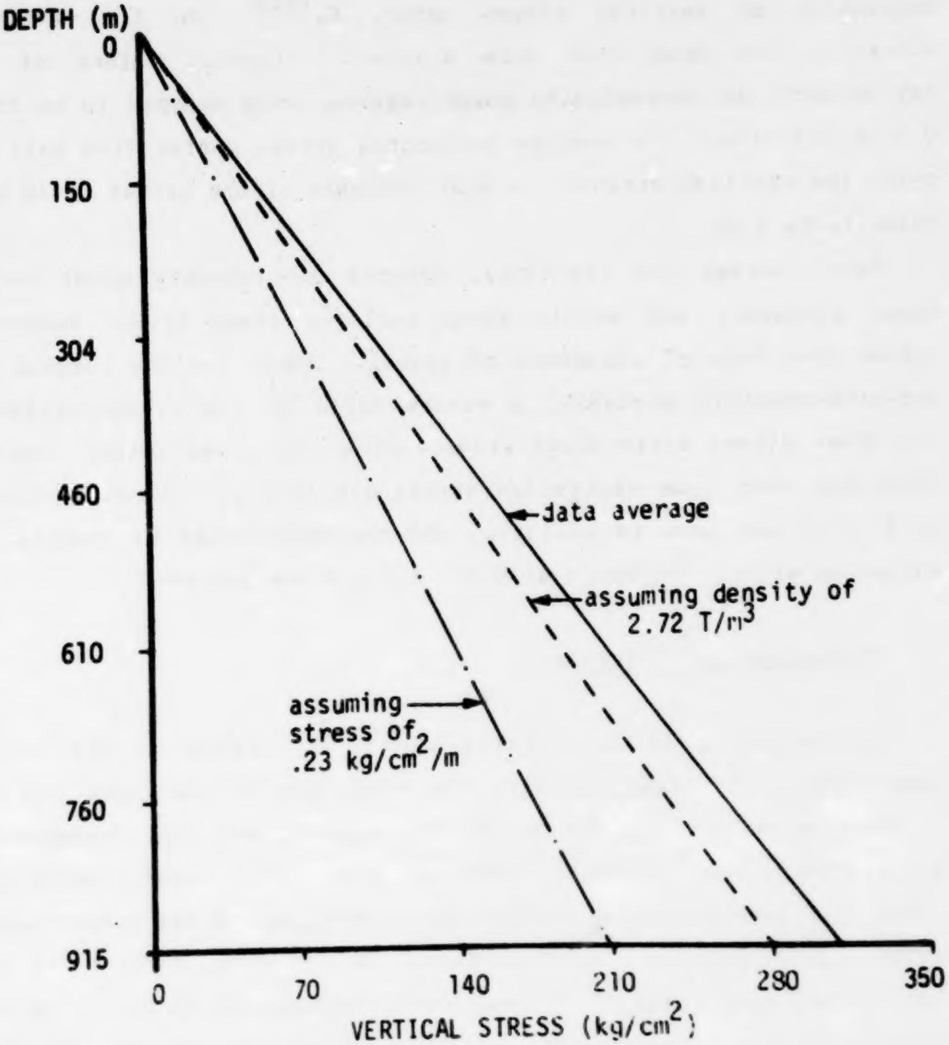

Source: Lidner, E.N., and J.A. Halpern. In-Situ Stress Analysis. 18th U.S. Symposium on Rock Mechanics, 1977.

FIGURE D-IX-16 APPROXIMATE VERTICAL STRESSES FOR SEVERAL SITES IN NORTH AMERICA

Figure D-IX-17 shows data summarizing in-situ measurements of horizontal to vertical stress ratio, K.(23) As for vertical stresses, the data show wide scatter. Typical values of K, particularly in tectonically quiet regions, were assumed to be from 0.5 to 2.0 (i.e., the average horizontal stress varies from half to twice the vertical stress). A best estimate of the stress ratio was taken to be 1.0.

Salt, having low viscosity, deforms continuously under small shear stresses, and within short geologic times (i.e., hundreds rather than tens of thousands of years). Thus, for the purpose of non-site-specific analysis, a stress ratio of 1.0 is appropriate. Any other stress ratio would produce shear stresses, induce viscous flow, and over time neutralize stress differences. A stress ratio of $K = 1.0$ was used in analysis, and the sensitivity of results to variation within the range of $0.5 \leq K \geq 2.0$ was tested.

2. Concentration of Stress

Construction of an opening within a uniform stress field concentrates the stresses, with the exact form of the concentration a function of the geometry of the opening and the deformation properties of the rock mass. Typical results for elastic media are shown in Figure D-IX-18. Analytical expressions of the concentrated stress field exist for elastic isotropic and anisotropic media and many common geometries.(24) Analytical expressions do not exist for most inelastic assumptions, although solutions can be obtained numerically.

Waste repositories will not have a single opening, like a long cylinder, but will have a series of parallel openings approximating a rectangle in the horizontal plane. Stress distributions about this series of openings will be more like those from an infinite series of holes in a medium rather than a single one (Figure D-IX-19). The present analysis considered only a single opening, however.

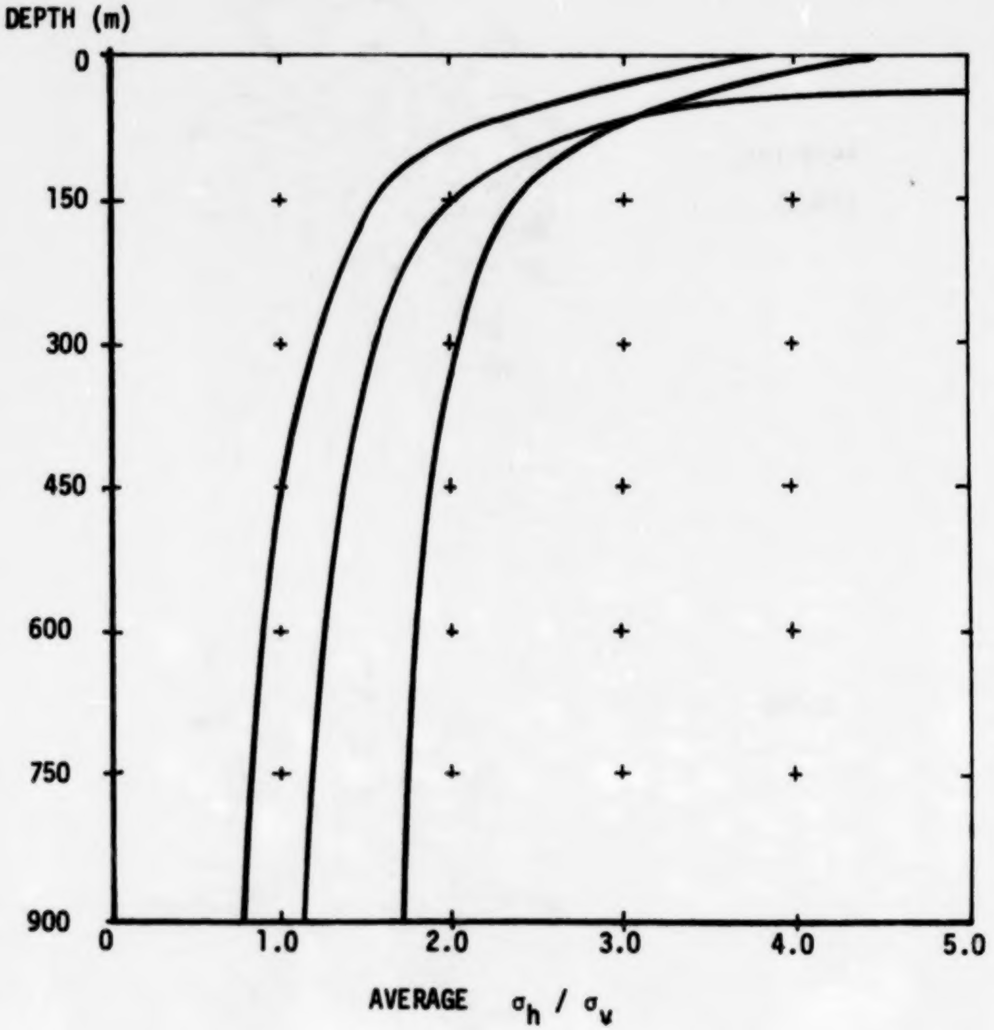

Source: Lindner, E.N., and J.A. Halpern. In-Situ Stress Analysis. 18th U.S. Symposium on Rock Mechanics, 1977.

FIGURE D-IX-17 MEASURED STRESS RATIOS FOR SEVERAL SITES IN NORTH AMERICA: HORIZONTAL STRESS ÷ VERTICAL STRESS

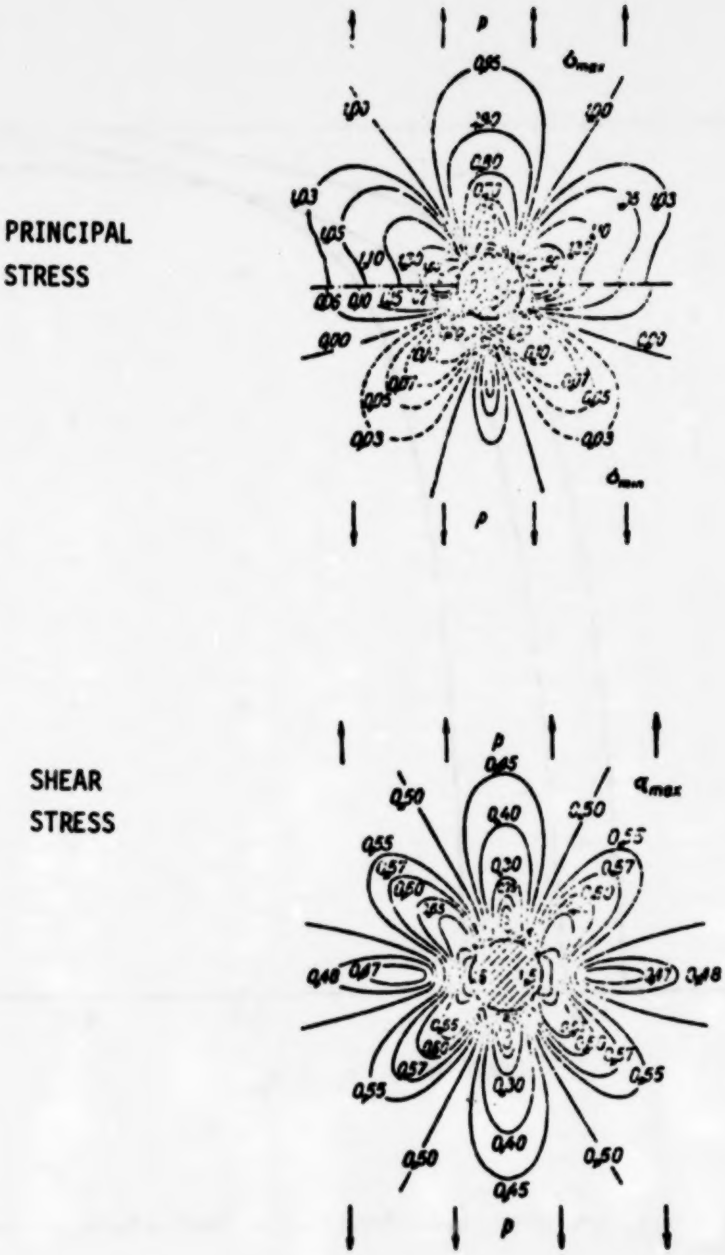

Source: Savin, G.N. Stress Distributions Around Holes. NASA Technical Translation, TTF-607.

FIGURE D-IX-18 STRESS CONCENTRATIONS ABOUT CIRCULAR OPENINGS IN HOMOGENEOUS, ELASTIC MEDIUM UNDER VERTICAL STRESS FIELD

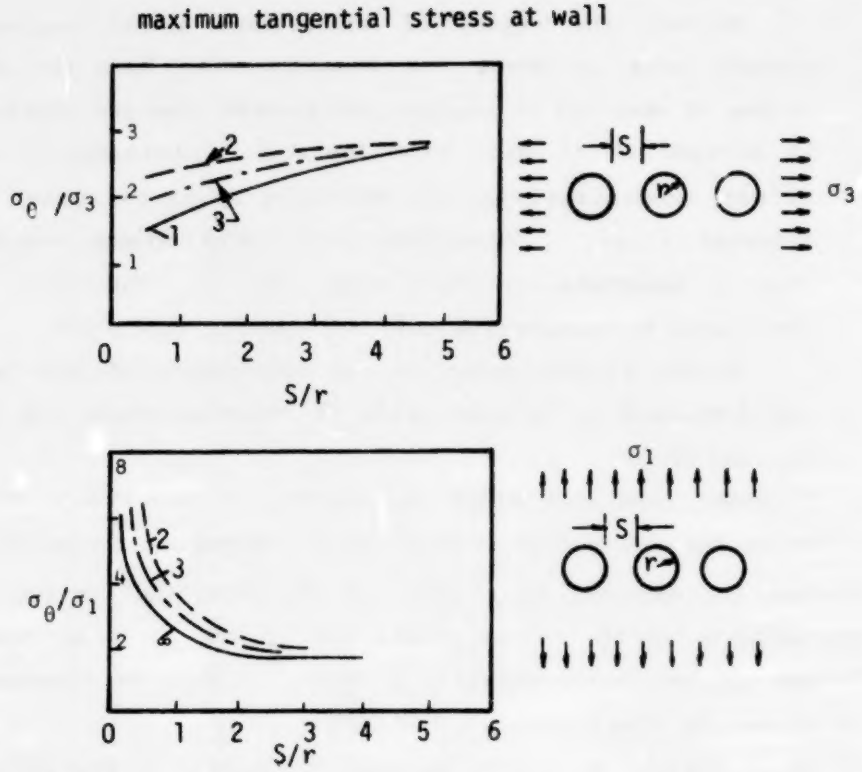

Source: Savin, G.N. Stress Distributions Around Holes. NASA Technical Translation, TTF-607.

FIGURE D-IX-19 STRESS CONCENTRATIONS ABOUT A ROW OF OPENINGS IN ELASTIC MEDIUM

The bases for choosing to consider a single opening were the following:

First, use of analytical expressions available for stresses about a single opening reduced computational effort and allowed larger parametric studies.

Second, the region of significant stress concentration extends only to about one diameter away from the opening. Series of openings at separations greater than two diameters can be modeled as if each were isolated. Increases in maximum stress concentrations for multiple openings spaced at one diameter (i.e., 2 diameters o/c), over single openings in elastic materials is less than 10%.(2) Therefore, errors introduced by considering only one opening were small.

Third, uncertainties in the conclusions of this analysis are dominated by uncertainties in material properties and the thermal field.

Stresses generated about an opening in a homogeneous medium depend on the deformation properties of the medium, in particular on whether the material is elastic or inelastic (and on the form of inelasticity in the latter case), and on the ratio of moduli and Poisson ratios if the material is anisotropic. The simplest case, of course, is elasticity.

While elastic solutions, as used in the present analysis, depend on assumptions that are not precisely correct for real rock masses, there are several arguments for their use.

First, any stress-strain relationship must be verified for real conditions. In many cases inelastic relationships are as difficult to verify as elastic ones. Given many alternative inelastic relationships, each leading to a somewhat different stress distribution, a choice must still be made among them. Errors introduced by using an elastic assumption may not be any greater than errors associated with various inelastic assumptions.

Second, appropriate moduli values are difficult to estimate even in the elastic case. Estimation is more difficult for inelastic cases, and more moduli must be estimated. Errors introduced by selecting poor parameter values may be larger than those introduced by using elastic theory.

Third, elastic solutions are analytically and computationally convenient. Therefore, larger parametric uncertainty is a primary source of predictive uncertainty in this analysis; results from parametric studies are likely to bound predictions made using other models.

Fourth, given the widespread use of elastic analyses, there is accumulated experience with these solutions, which aids in interpreting the results. This also means that results of the present analysis are more easily interpreted by those who were not directly involved in obtaining them.

For these reasons, stress distributions in the present analysis were calculated using elastic theory, and parametric studies were used to bound the range of uncertainty.

3. Thermal Stress

The major source of stress in geologic media about a repository appears to be the thermal field. Salt has a coefficient of linear thermal expansion, α, of about $40 \times 10^{-6}\ {}^{o}C^{-1}$. Rock temperatures predicted by several studies, including the present one, may reach 200-250°C at the repository wall. Because deformation of repository formations is constrained, this thermal field will induce significant stresses.

Prior to repository construction, the in-situ thermal field will be uniform, but increasing linearly with depth. For geologically stable regions (i.e., nonvolcanic), a temperature gradient of 1°C for 60-80 m is typical. Ambient temperature at 450 m (1500 ft) in bedded salt is expected to be about 30°C.

Heat generated within the repository will be a function primarily of (1) waste type and age at burial, (2) time after burial, and (3) spatial canister density.(25,26) The conditions considered were 10 years aging and 150 kW/acre for heat generation density, consistent with the Task B report. For analysis, a temperature (increase) profile similar to the Task B results were used. This profile was expressed analytically as:

$$\Delta T(^{o}C) = 222 \exp(-1.1 \times 10^{-5} r^{2}) \qquad (16)$$

where r = distance from repository.

This profile was assumed to be isotropic in the salt.

The time for peak mine temperatures differs in different analyses; fracturing probabilities are related primarily to the temperature profile and not to time (relation of shear stresses through viscous flow was neglected, which is a conservative assumption). Therefore, the results of stress analyses in the present case are not significantly affected by these time differences. For analyses, a time of 100 years to maximum mine temperature was assumed.

Stresses generated by the thermal field were calculated assuming the repository salt formations to be isotropically elastic with uniform deformation properties. Parametric analyses were performed by varying deformation moduli.

Elastic thermal stresses around the underground repository were derived by adapting a solution for the thermal stresses in a thin circular disc.(27) This solution is valid for temperature distributions symmetric about the center of the repository, and requires that the modulus of elasticity, Poisson's Ratio, and coefficient of thermal expansion be constant with temperature and location.

Expressions for radial and tangential thermal stresses are:

$$\sigma_r = \frac{E}{1-\nu^2}\left[\frac{\alpha}{r}\int_R^r T(r)\,dr\right] \qquad (17)$$

$$\sigma_\theta = \frac{E}{1-\nu^2}\left[-\frac{\alpha}{r}\int_R^r T(r)dr + \alpha T(r)\right] \qquad (18)$$

where: E = modulus of elasticity

ν = Poisson's Ratio

α = coefficient of thermal expansion

r = radial distance from center of repository

R = radius of repository

$T(r)$ = temperature increase above ambient at radius r

Rewriting equation 16 in general form as:

$$T = T_{max}\, e^{-Br^2} \qquad (19)$$

where: T_{max} = maximum temperature increase (at repository wall)

B = constant

Substituting into the equations for stresses yields,

$$\sigma_r = \frac{E}{1-\nu^2}\left(\frac{\alpha T_{max}}{r^2\, 2B}\left[e^{-BR^2} - e^{-Br^2}\right]\right)$$

$$\sigma_\theta = \frac{E}{1-\nu^2}\left(-\frac{\alpha T_{max}}{r^2\, 2B}\left[e^{-BR^2} - e^{-Br^2}\right] + \alpha T_{max}\, e^{-Br^2}\right) \qquad (20)$$

Radial thermal stresses are zero at the repository wall (r = R) and at infinity, and are compressive everywhere in between; tangential stresses are maximum at the repository wall, zero at infinity, and may be compressive or tensile in between.

It is important to note that thermal stresses are directly proportional to the modulus of elasticity of the rock salt. Errors in this modulus result in equally large errors in thermal stresses. Since there are little data on the elastic modulus of rock salt at high temperatures and low strain rates, the potential for error in estimating thermal stresses is large.

Since all stress calculations assume elastic material behavior, total stresses around the repository are obtained by superimposing the region (in-situ plus stress concentrations around the cavity) and thermal stress fields.

F. STOCHASTIC FRACTURE MODEL

1. Model Construction and Assumptions

The probability of fracturing between the repository and a overlying aquifer was analyzed by modeling rock properties as second-order homogeneous random processes,(28) and calculating the reliability of potential fracture paths against shear failure (Figure D-IX-20).

The assumption of second-order homogeneity* for rock properties implies that mean properties are constant in space or may be described by a deterministic trend, that the point variance of properties is spatially constant, and that the autocorrelation of properties (i.e., the degree to which adjacent points in the rock mass have similar properties) is a function only of the vector

---

*"Homogeneity" and "stationarity" are equivalent terms for spatially varying and temporally varying parameters, respectively. Although usage varies, "homogeneity" has been adopted in this report.

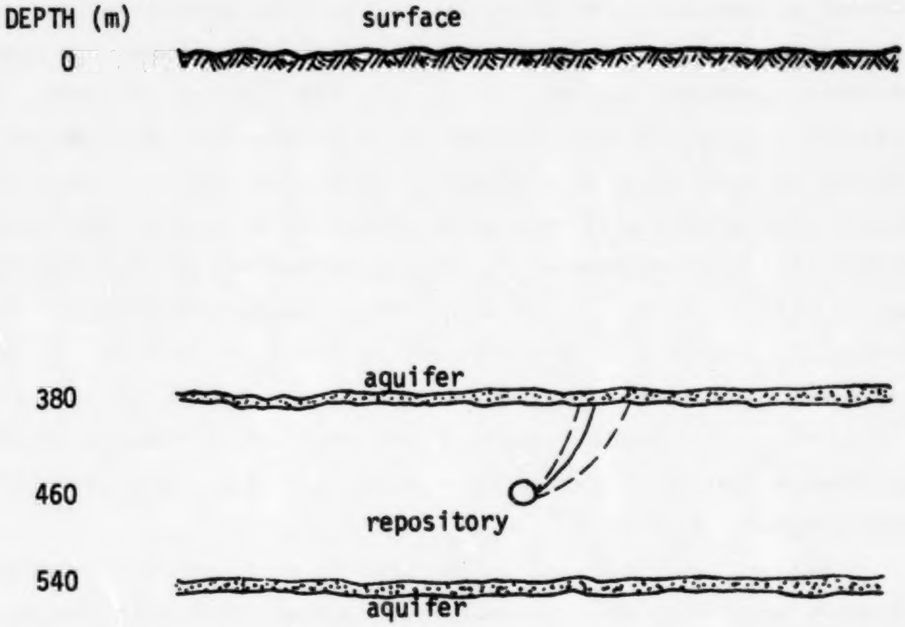

FIGURE D-IX-20 POTENTIAL FAILURE PATHS BETWEEN REPOSITORY AND AQUIFER distance separating points (Figure D-IX-21 presents these concepts). Second-order stationarity assumptions for geologic materials are generally accepted.(29)

Three sets of rock properties are important for analyzing reliability: strength parameters, deformation parameters, and thermal parameters. The first set controls the available resistance of rock to various modes of failure, while the latter two control stresses generated in the rock. In the present analysis, only strength parameters were assumed to be stochastic; deformation and thermal parameters were assumed to be deterministic. This means that analyses were performed on a stochastic strength field subject to deterministic stresses. The errors introduced by this limitation are thought to be within the scope of the desired objectives of the study. In more precise studies, and in particular for site-specific analyses, techniques for incorporating uncertainty in the stress field should be used. Because analysis of stochastic stresses involves differential rather than integral fields, their solution is more complicated.(30)

A failure mode analyzed in the present study was the development of shear zones between repository and aquifer. For this analysis, a limiting equilibrium approach was used with driving forces along potential shear paths balanced against resisting forces. Kinematic admissibility was not considered (i.e., potential shear paths were not limited to those on which continuous relative movements were possible). The requirement of kinematic admissibility, constraining the set of potential shear surfaces, would yield somewhat higher reliabilities than those from the present analysis.

Alternative modes of fracturing, in particular the development of propagating cracks by redistributing stresses at increments of crack were not considered.(31) Pre-existing anomalies in repository formations (e.g., faults) are treated in Section D-5.1. The limitation of other failure modes, other than limiting equilibrium shear failure, affected numerical results, but differences are thought to be within small multiples rather than orders of magnitude. Site-specific analyses should include both the probability of non-flaw inhomogeneities and progressive fracturing.

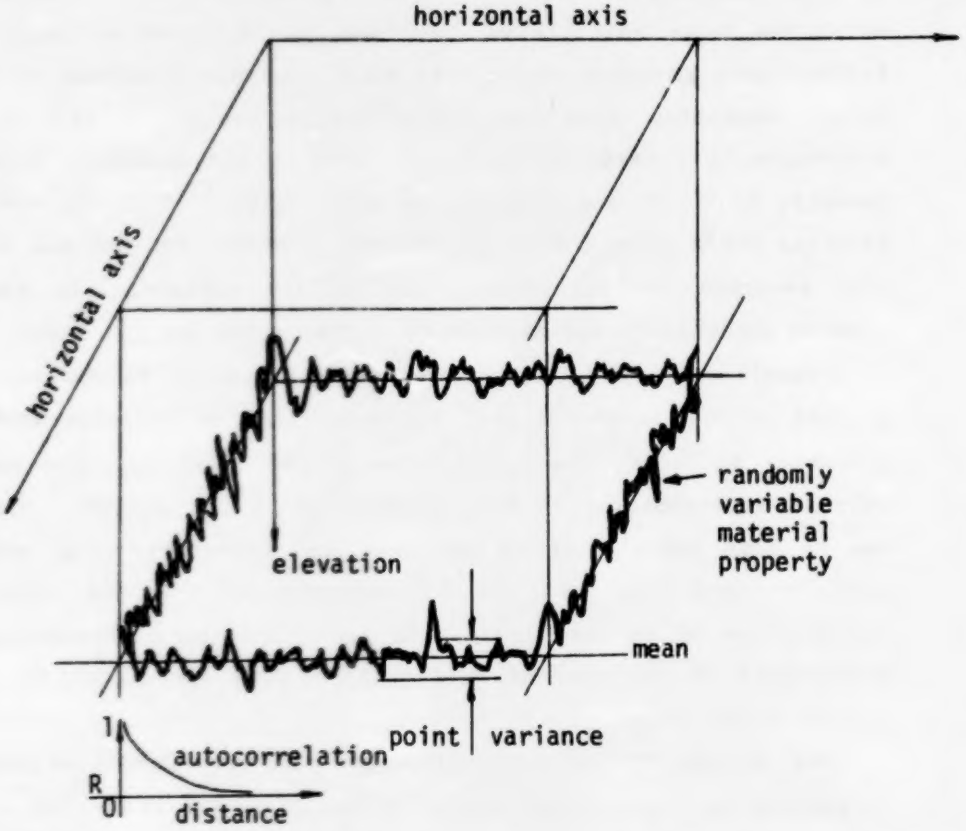

FIGURE D-IX-21 SCHEMATIC DESCRIPTION OF ROCK STRENGTH

Both of these are important in predicting stress fields and should be treated in conjunction with spatially varying deformation and thermal properties.

Figure D-IX-20 illustrates plane strain failure paths considered in this analysis. Various fracture geometries were analyzed, of which the least reliable was selected for detailed analysis. The failure path geometry used in detailed analysis consisted of a log spiral emanating from the repository at an angle $(45 - \phi/2)$, connecting to a vertical line continuing to the aquifer. This is a geometry of fracturing observed in model tests.(32,33) In analyzing failures for a given set of parameters, a search routine was adopted that searched for the minimum reliability surface. In general, minimum reliability and minimum FS surfaces are not the same.

Overall reliability against plane strain shear faiure was taken as that of the least reliable surface. With an infinite number of potential surfaces, the reliability of the least reliable path is only an approximation to the reliability of the system. However, due to high correlation of stresses and strengths along adjacent surfaces and the spatial narrownesss of low FS clusters, correlations of FS for alternative paths are high. Therefore, the reliability of the minimum surface is a good approximation to the system reliability.

The reliabiity of an individual path to shear failure was determined by integrating predicted shear stress along the surface and comparing this driving force with the integral of available resisting shear stress. (Figure D-IX-22.) The driving force was determined by decomposing the stress field at each point along the failure surface into a normal stress, s_n, and a shear stress, t, and numerically integrating over the surface,

$$DF = {}_{S}\int \tau \, ds,$$

where DF is the total driving force along path S, and ds is the differential curve length.

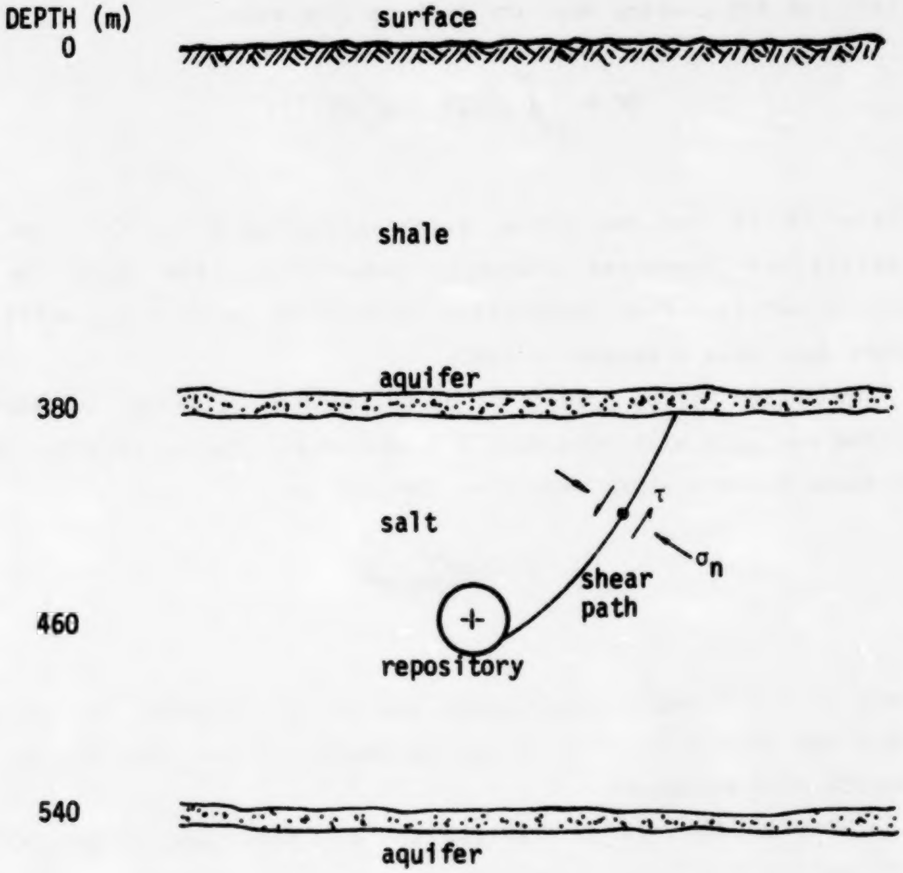

FIGURE D-IX-22 STRESS AND RESISTANCE ALONG POTENTIAL FAILURE SURFACE

The resisting force was determined by decomposing the stress field and integrating over the failure criterion,

$$\tilde{RF} = \int_S [\tilde{C}(T) + \sigma_n \tilde{\mu}(T)] ds$$

where $\tilde{RF}$ is the resisting force along path S, $\tilde{C}(T)$ is the temperature-dependent cohesion parameters, and $\tilde{\mu}(T)$ is the temperature-dependent coefficient of friction ($\mu(T) \equiv \tan \phi(T)$). A tilde indicates a random variable.

Resisting force, a function of two random variables, is itself a random variable with some mean and variance. The reliability index of shear failure along path S was defined as:

$$\beta = \frac{E[\tilde{RF}] - DF}{\sqrt{V[\tilde{RF}]}}$$

where E[ ] indicates expectation, and V[ ], variance. A reliability index was used because it is non-parametric (i.e., does not depend on distribution assumptions).

With no loss in generality, thermal reduction factors K(T) and H(T) may be introduced such that

$$C(T) = K(T)C(24^o) = K(T)c,$$

$$\mu(T) = H(T)\mu(24^o) = H(T)\mu.$$

K(T) and H(T) were assumed to be monotonically decreasing functions of temperature, evaluated on the basis of empirical evidence.

Using reduction factors, moments of the resisting force along path S can be derived as:

$$E[RF] = \int_S \{K(T)E[c] + \sigma_{ni}H(T)E[\mu]\}ds \qquad (22)$$

$$V[RF] = \int_S \int \{K_i(T)K_j(T)C_c(r) + \sigma_{ni}H_i(T)\sigma_{nj}H_j$$

$$(T)C_\mu(r)\}ds_i ds_j \qquad (23)$$

where subscripts i and j indicate arguments for the double integration, and

$C_c(r)$ ≡ autocovariance function of cohesion

$C_\mu(r)$ ≡ autocovariance function of coefficient friction

r ≡ surface distance between points i and j.

On the basis of empirical evidence, a bilinear Mohr-Coulomb failure criterion was assumed. Up to some transition stress, $\sigma_d(T_2)$, the salt was assumed to have a failure criterion specified by the parameter pair (C, μ); above the transition stress, a perfectly cohesive failure criterion specified by the parameter pair (C, $\mu = 0$). The transition stress was assumed to be monotonically decreasing with increased temperature.

Introducing a transition from frictional to purely cohesive behavior required that the potential breach path be divided into two segments, one on which $\sigma_n \geq \sigma_d(T)$ and one on which $\sigma_n \leq \sigma_d(T)$, and the resistances summed. The expected total resistance is the sum of the expected segment resistances; the variance of total resistance is the sum of the variances of segment resistances.

The variance of the purely cohesive segment of the failure path reduces to

$$V[RF, \text{cohesive segment}] = \int\int_{S'} K_i K_j C_c(r) ds_i ds_j \qquad (24)$$

where S′ indicates the cohesive segment. For constant temperature, the variance of purely cohesive surfaces can be calculated analytically for common autocovariance functions.

The analysis was expanded to three dimensions by considering cylindrical failure surfaces formed by translating the least reliability plane-strain path (Figure D-IX-23). As a first approximation, the failure surface was taken as one autocorrelation distance (r_o) wide. The question addressed in the three-dimensional analysis was how much the plane-strain reliability index is reduced by considering the potential for failure anywhere around the repository.

Considering only one opening of the repository, there is an infinite number of potential failure surfaces because the assumed r_o wide surface could be anywhere along the opening length. Let the surfaces be indexed by the location of their center points. Because adjacent surfaces overlap, their total resistances can be highly correlated.

The total shear resistance is calculated as for the plane-strain path, but now averaged over a larger two-dimensional surface. Thus, the variance in the total resistance is reduced from that of the most critical path. For a surface of width r_o this variance reduction is to 37%, and the corresponding standard deviation reduction to 61%.(28)

Assigning the total resistance of a surface to its midpoint at the repository wall, a correlated one-dimensional random process is defined. Breaching occurs if at any place along the opening, the resistance drops below the driving forces. This is equivalent to the one-dimensional random process crossing a level β standard deviation from the mean, where β is the single-surface reliability index. For large β, the probability of at least one level crossing in length L of repository opening is:

$$Pr = \frac{L \exp(-\beta^2/2)}{\pi(2\delta r_o)^{\frac{1}{2}}} \tag{25}$$

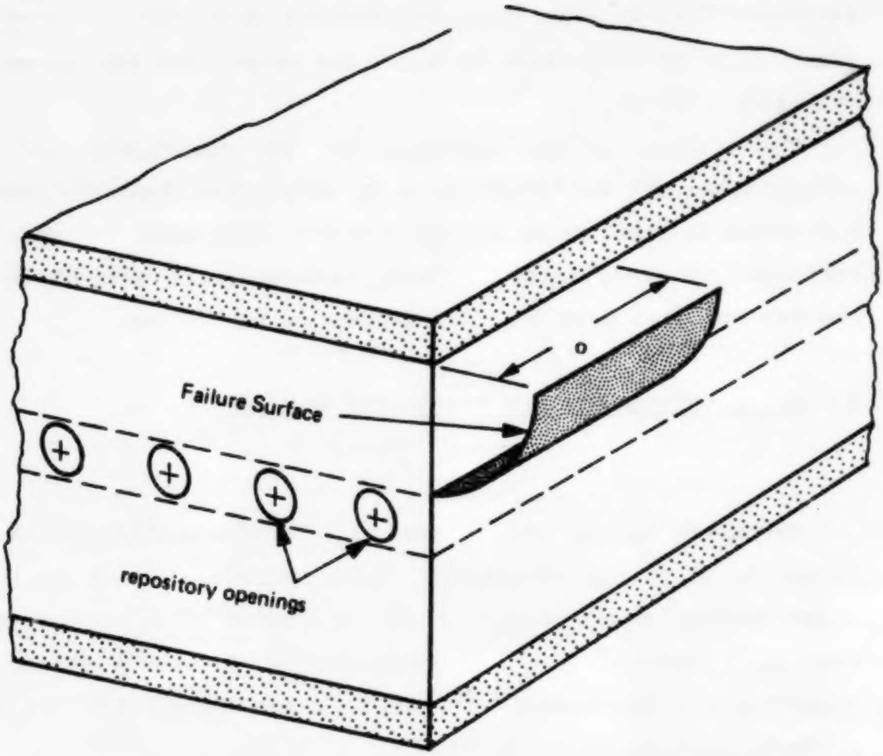

FIGURE D-IX-23 THREE-DIMENSIONAL MODEL

where δ is a length measure formed by integrating the autocorrelation function between negative and positive infinity (for exponential autocorrelation $\delta = 2r_o$).(28)

Applying Equation 25 yields the probabilities of failure at peak thermal stresses. If the peak thermal stresses occur at about 100 years, and if the cumulative probability of failure is assumed to increase linearly with time, the failure rate over the first hundred years would be two orders of magnitude lower than the values implied by Figure D-IX-24.

The results of the analysis for the reasonable and somewhat conservative 20% variation in salt properties indicate exceedingly low probabilities of breaching failure even when multiple failure surfaces are considered. These probabilities are obviously not precise and should be considered only as indicators.

2. Parametric Inputs and Results of Analysis

Parameter values chosen for sensitivity studies bounded those values found in the literature (Table D-IX-2). For a specific site these values would have to be evaluated from exploration and testing. Results were not sensitive to Poisson's Ratio, lateral stress ratio, the anisotropy ratio of autocorrelation, or the form of the autocorrelation function.

Results of plane strain analyses for coefficients of variation in material properties, are shown in Figures D-IX-24 and D-IX-25.

Trends within the results are the following:

1. Thermal stresses predominate, thus the probability of fracturing is sensitive to the thermal field. Time trends in reliability reflect time trends in rock temperatures.
2. The probability of fracturing interconnecting repository and aquifer decreases as the separation distance between repository and aquifer increases. The relationship is not linear; by decreasing the separation some proportion, the probability is increased by a greater proportion.

TABLE D-IX-2

PARAMETER VALUES USED IN ANALYZING RELIABILITY AGAINST SHEAR FAILURE BETWEEN REPOSITORY AND AQUIFER

Parameter	Low	Most Probable	High
Young's Modulus (psi)	5.0×10^3	5.0×10^4	5.0×10^5
Poisson Ratio		0.22	
Point Coefficient of Variation* (%)	5	10	40
Autocorrelation Length* (feet)	5/50	10/100	20/200
Lateral Stress Ratio	0.5	1.0	2.0

---

*Standard deviation divided by mean.

**Distance at which correlation reduces to e^{-1}.

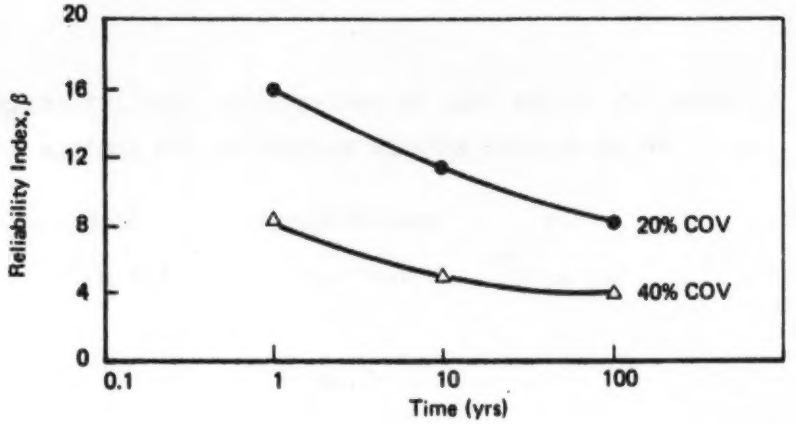

FIGURE D–IX–24 CALCULATED RELIABILITY INDEX AS A FUNCTION OF TIME

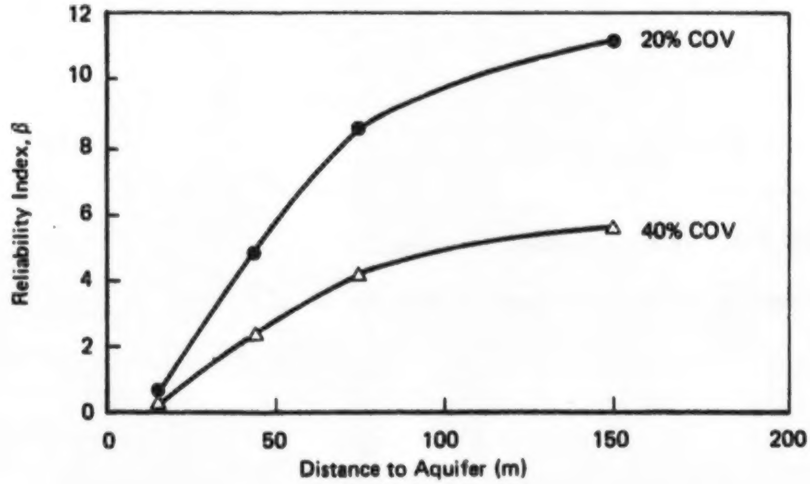

FIGURE D–IX–25 CALCULATED RELIABILITY INDEX AS A FUNCTION OF DISTANCE TO AQUIFER

3. Probabilities of fracturing are sensitive to deformation modulus and point variance of strength properties. Care must be taken in estimating these parameters for site-specific studies.

G. RECOMMENDATIONS FOR STOCHASTIC ANALYSIS IN SITE-SPECIFIC STUDIES

Stress analyses of site-specific repositories should incorporate uncertainties. In general, this is not now done. Current analyses are primarily deterministic, allowing estimates only of mean safety factors and not probabilities. The analysis performed here, owing to limitations of time and effort and in keeping with the overall objectives of the present study, serves only as a first approximation to a comprehensive stress analysis of a particular repository.

In analyzing a specific repository, the present analysis should be expanded to account for the uncertainties discussed below.

1. Stress Field Uncertainties

Uncertainties in the stress field are generated by uncertainties in deformation and thermal properties of repository formation, and by uncertainties in the regional stress field. These sources of uncertainty are coupled. Moreover, for a specific site, uncertainty will be contributed by estimation error. Despite the extensiveness of site exploration programs, uncertainties always exist in site characterization. These estimation uncertainties are increased by the conflicting objectives of placing as few new borings as possible into the geologic barrier.

The approach to modeling uncertainty in stresses would be to approximate deformation and thermal properties as second-order, homogeneous stochastic processes, and solve the differential field equation for means and variances. These solutions would most likely be numerical, as through uncertain finite element analysis. This would result in process statistics for stresses as a stochastic field (e.g., (30). Using a model of this sort, estimation error based on sampling could be quantified.

2. Crack Propagation Analysis

The present analysis has treated limiting equilibrium shear failure as the criterion of fracturing. Alternative criteria should be considered. Of particular importance would be the consideration of fracture propagation in which stress concentrations are recalculated for increments of fracture extension. The same stochastic model of strength, deformation, and thermal properties could be used to yield probabilistic predictions.

3. More Accurate Geometric Model of Repository

The present analysis has used a simplified idealization of the repository as a cylindrical opening in a uniform material. Site-specific studies should model repository geometry based on actual layouts. Although this would add analytical complexity, certain idealizations (e.g., infinite rows of identically shaped openings) are tractable.

4. Elasto-plastic Media

For specific sites, more complicated deformation models should be introduced, based on test results on site materials.

5. Jointing and Pervasive Inhomogeneities

Salt has been modeled using continuum mechanics. In materials other than salt (e.g., basalt, shales), jointing will significantly influence the mechanical behavior of the rock mass. Appropriate allowances must be made for the effects of joints, either by augmenting bulk mechanical properties or by introducing discontinuum models.(5,17,3)

6. Pore Water Pressures

Pore water pressures affect rock mass strength by reducing available frictional resistance in accordance with the effective stress concept,

$$\tau = C + (\sigma - \mu) \tan \theta,$$

where τ = the available shear resistance and

μ = the pore water pressure.

No consideration has been given to pore water pressures in this analysis. Recent work indicates that water pressure may be incorporated in stochastic analyses.(34)

H. DERIVATION OF STOCHASTIC REDUCTION FUNCTIONS

For the derivation of mean and variance of stochastic resistance for constant temperature, cohesive condition, consider an elemental volume i (Figure D-IX-26) along the potential failure path L:(a, b). The resistance to shear displacement at this point, assuming Mohr-Coulomb failure criterion, is:

$$\tau_{r,i} = c_i + \sigma_i \tan \phi_i \tag{26}$$

where

$\tau_{r,i}$ = the maximum available resisting shear stress,

c_i and ϕ_i = the cohesion and friction angle at the point, and

σ_i = the stress normal to the potential failure path at i. σ_i is assumed known, based on stress calculations; however both c_i and $\tan \phi_i$, the material properties, are assumed to be second-order homogeneous random variables.

The maximum available resisting shear force along path L is the integral of the available shear resisting stress, or

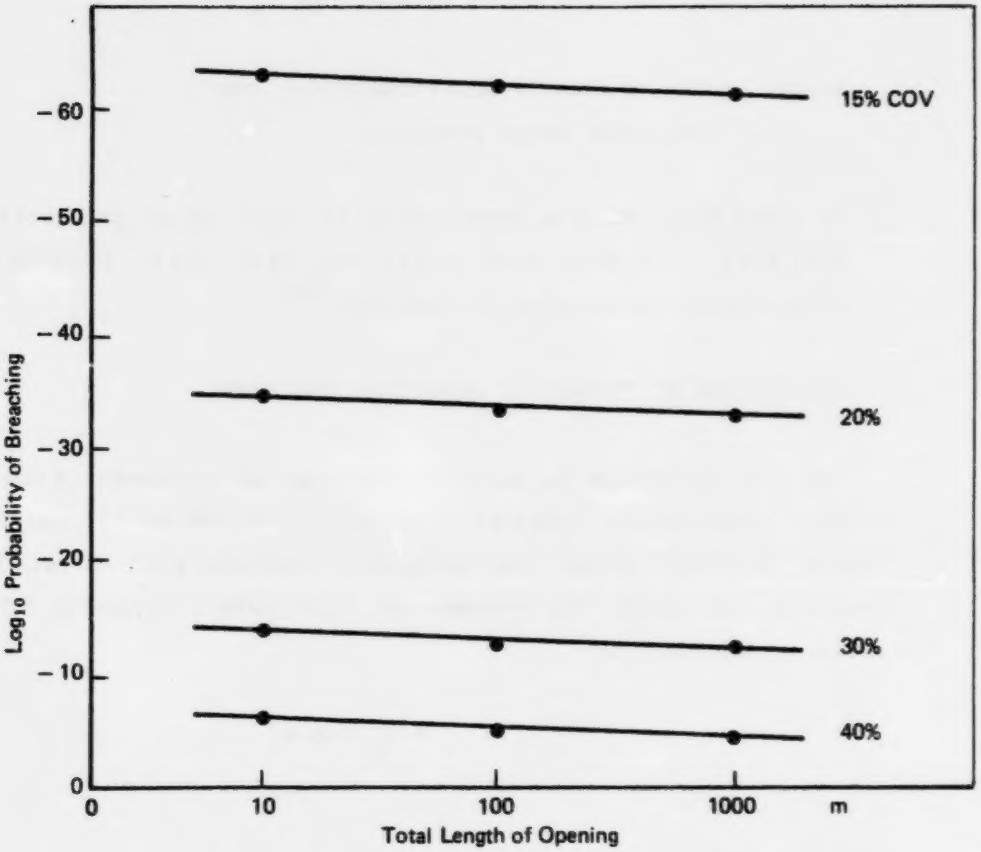

FIGURE D–IX–26 PROBABILITY OF BREACHING

$$RF(L) = \int \tau_{r,i}\, ds = \int c_i + \sigma_i \tan \phi_i \, ds \qquad (27)$$

The expectation of Equation 27 is

$$\begin{aligned} E[RF(L)] &= E[\int c_i + \sigma_i \tan \phi_i \, ds] \\ &= \int E[c_i] ds + \int \sigma_i \, E[\tan \phi_i] ds \end{aligned} \qquad (28)$$

Defining the new variable,

$$\mu_i \equiv \tan \phi_i,$$

the expected resisting shear force becomes

$$E[RF(L)] = \int E[c_i] ds + \int \sigma_i \, E[\mu_i] ds \qquad (29)$$

This value is easily calculated once σ_i is known as $E[c_i]$ and $E[\mu_i]$ are constant across space, given the assumption of statistical homogeneity. The variation of Equation 26 requires somewhat more labor to determine. By definition,

$$V[RF(L)] = E[(RF(L) - E[RF(L)])^2] \qquad (30)$$

$$= E[(RF(L))^2] - E^2[RF(L)] \tag{31}$$

$$= E[\int(c_i + \sigma_i\mu_i)ds]^2 - E^2[\int(c_i + \sigma_i\mu_i)ds]$$

$$= E[\int(c_i + \sigma_i\mu_i)ds \cdot \int(c_i + \sigma_i\mu_i)ds]$$

$$- [\int E[c_i] - \sigma_i \, E[\mu_i] \, ds]^2$$

$$= E[\int\int(c_ic_j + \sigma_i\mu_ic_j + \sigma_j\mu_jc_i + \sigma_i\sigma_j\mu_i\mu_j) \, ds_ids_j] \tag{32}$$

$$- [\int E[c_i] + \sigma_i \, E[\mu_i] \, ds]^2$$

$$= \int\int C_c(i,j) \, ds_ids_j + \int\int \sigma_i\sigma_jC_\mu(i,j) \, ds_ids_j \tag{33}$$

where

$C_c(i,j)$ = the autocovariance of the process c_i, and

$C_\mu(i,j)$ = the autocovariance of the process μ.

This equation applies for the deterministic stress field yielding σ_i known. The solution is nonparametric (i.e., does not depend on distribution assumptions) and depends only on the second-order stationary assumption (spatially constant means, variances and covariances). For purely cohesive materials Equation 33 becomes,

$$V[RF(L)] = \int\int C_c(i,j) \, ds_ids_j \tag{34}$$

which can be solved analytically for common autocovariance functions.

Under the assumption of second-order stationarity, autocovariance is a function only of the vector distance separating the points i and j. For a given failure path, two assumptions will be made. First, the process c_i and the process μ, are isotropic along any specific path with correlation length corresponding to the orientation of the line between the endpoints. In other words, while the correlation distance* may be anisotropic--larger horizontal than vertical--the correlation length is considered constant along any potential failure path. Correlation lengths will of course differ for different paths, based on the orientation of the chord joining their endpoints. Second, the path length between any two points i and j is used in calculating correlation rather than the chord length between them. This allows line integrals to be taken along the path. As long as the correlation length, r_o, is small relative to the path curvature this second assumption introduces little error.

---

*Correlation distance, r_o, is defined as the separation distance at which the correlation among points reduces to 1/e.

Following the arguments of Popoulis(35), the double integral of Equation 34 can be reduced to a single integral. The function $C_c(i,j)$, depending only on the distance $r = |i-j|L$, is constant within the shaded area of Figure D-IX-27:

$$C_c(i,j) = C_c(r) \qquad (35)$$

The area of this strip is $(L - r)dr$ when L is the total path length from a to b.

Thus Equation 34 becomes

$$V[RF(L)] = \iint\limits_L C_c(i,j)\, ds_i\, ds_j = \int_{r=0}^{L} (L - r)\, c_c(r)\, dr \qquad (36)$$

For the common autocovariance function (Figure D-IX-28)

$$C_c(r) = \sigma_c^2\, e^{-r/r_o} \qquad (37)$$

where σ^2_c is the point variance; the variance of resisting force becomes:

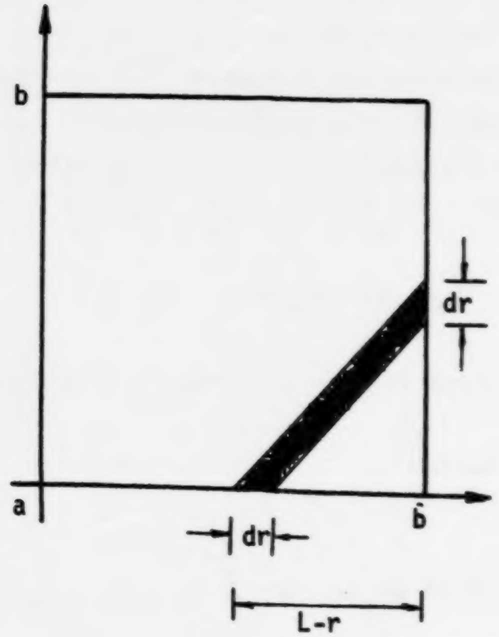

FIGURE D-IX-27 REDUCTION OF DIMENSION IN VARIANCE CALCULATIONS

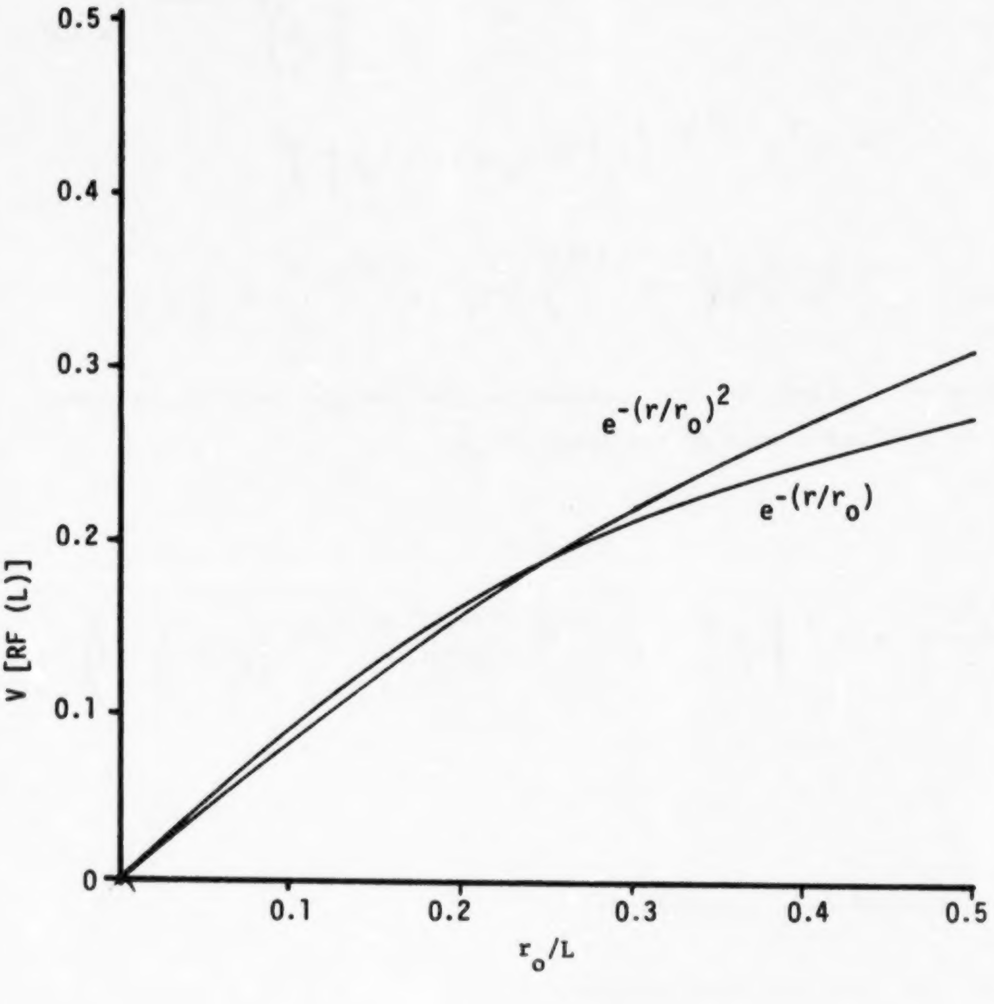

FIGURE D-IX-28 NORMALIZED VARIANCE OF AVERAGE STRESS FOR TWO AUTOCOVARIANCE FUNCTIONS

$$V[RF(L)] = \int_{r=0}^{L} (L - r)\, \sigma_c^2\, e^{-r/r_o}\, dr$$

$$= L\, \sigma_c^2\, e^{-r/r_o} (-r_o) \Big|_o^L + \frac{\sigma_c^2\, e^{-r/r_o} \left(+\frac{r}{r_o} + 1\right)}{\left(-\frac{1}{r_o}\right)^2} \Bigg|_o^L \qquad (38)$$

$$= \sigma_c^2\, e^{-r/r_o} \left\{ r_o^2 (r/r_o + 1) - r_o L \right\} \Big|_o^L$$

$$= \sigma_c^2 \{ L r_o \left(1 - e^{-L/r_o}\right) + r_o^2\, e^{-L/r_o} \left(\frac{L}{r_o} + 1\right) - 1$$

Dividing by L^2 leads to the variance in the average resisting stress, which is a function only of the ratio l/r_o,

$$V\left[\frac{F_r(L)}{L}\right] = \sigma_c^2 \{ \frac{r_o}{L} \left(1 - e^{-L/r_o}\right) + \left(\frac{r_o}{L}\right)^2 \left(e^{-L/r_o} \left(\frac{L}{r_o} + 1\right) - 1\right) \qquad (39)$$

This is graphed in Figure D-IX-29.

For the autocovariance function:

$$C_c(r) = \sigma_c^2\, e^{-(r/r_o)^2} \qquad (40)$$

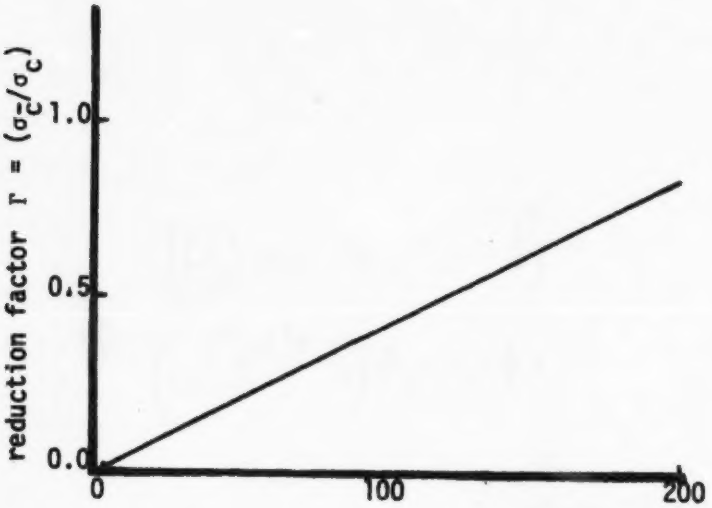

FIGURE D-IX-29 APPROXIMATE REDUCTION FACTOR AS FUNCTION OF AUTOCORRELATION DISTANCE

$$V[RF(L)] = \int_{o}^{L} (L - r)\, \sigma_c^{\,2}\, e^{-(r/r_o)^2}\, dr$$

$$= \frac{L\, \sigma_c^{\,2} \sqrt{\pi}\, r_o}{2} \operatorname{erf}\left(\frac{L}{r_o}\right) \tag{41}$$

$$- \sigma_c^{\,2} \int_{o}^{L} r e^{-\left(\frac{r}{r_o}\right)^2}$$

$$= \left[\frac{1}{2} L\, \sigma_c^{\,2}\, r_o \sqrt{\pi} \operatorname{erf}\left(\frac{L}{r_o}\right)\right] \tag{42}$$

$$+ \frac{1}{2} \sigma_c^{\,2}\, r_o^{\,2} \left(e^{-L^2/r_o^{\,2}} - 1\right)$$

Substituting the approximation

$$\operatorname{erf}(z) = 1 - (0.348t - 0.09587(+0.74785t)e^{-z^2} \tag{43}$$

$$t = [1 + 0.47047z]^{-1}$$

allows Equation 42 to be calculated numerically.

REFERENCES

1. Jaeger, J.C., and N.G.W. Cook, Fundamentals of Rock Mechanics. Methuen, London, 1969.

2. Obert, L., and W.I. Duvall, Rock Mechanics and the Design of Structures in Rock. John Wiley & Sons, New York, 1967.

3. Stagg, K.G., and O.L. Zienkiewicz (eds.), Rock Mechanics in Engineering Proctice. John Wiley & Sons, New York, 1968.

4. Mathab, M.A., J.L. Ratigan, and D.R. McCreath. Stability of a Radioactive Waste Repository in the Canadian Shield. 18th U.S. Symposium on Rock Mechanics, 1977.

5. Goodman, R.E., R.E. Heuze, and G.J. Bureau, On Modelling Techniques for the Study of Tunnels in Jointed Rock. 14th U.S. Symposium on Rock Mechanics, 1973.

6. Hoek, E., Structurally Controlled Instability in Underground Excavations. 18th U.S. Symposium on Rock Mechanics, 1977.

7. Oak Ridge National Laboratory, R.L. Bradshaw, and W.L. McClain, Project Salt Vault: A Demonstration of the Disposal of High-Activity Solidified Waste in Underground Salt Mines. ORNL 455.

8. Bradshaw, R.L., T.F. Lomenick, W.L. McClain, and F.M. Empson, Model and Underground Studies of the Influence of Stress, Temperature, and Radiation on Flow and Stability in Rock Salt Mines. Proc. 1st Congress on Rock Mechanics, Lisbon, 1966.

9. Parsons, Brinckerhoff, Quade, and Douglas, Inc., Thermal Guidelines for a Repository in Bedrock. Y/OWI/SUB-76/16504, Office of Waste Isolation, September, 1976.

10. Oak Ridge National Laboratory, R.D. Cheverton, and W.D. Turner, Thermal Analysis of the National Radiation Waste Repository: Progress through March 1972. ORNL 4789.

11. Westinghouse Astronuclear Laboratory, A Study of Borehole Plugging in Bedded Salt Domes by Earth Melting Technology. WANL-TME-2870, 1975.

12. Kaufman, D.W., (ed.), Sodium Chloride: The Production and Properties of Salt and Brine. Reinhold Publishing Co., New York, 1960.

13. Gera, F., Review of Salt Tectonics in Relation to the Disposal of Radioactive Waste in Salt Formations. Geological Society of America. 83.

14. Hunter, L., and S. Siegel, The Variation with Temperature of the Principal Elastic Moduli of NaCl Near the Melting Point. Physical Review, 61, 1942.

15. Starfield, A.M., and W.C. McClain, Project Salt Vault, J. Rock Mechanics & Mineral Sciences, 10, 1973.

16. Serata, S., S. Saknrai, and T. Abachi, Theory of Aggregate Rock Behavior Based on Absolute Three-Dimensional Testing of Rock Salt. Proc. 10th Symposium on Rock Mechanics, 1969.

17. Hendron, A.J., Mechanical Properties of Rock. In: Stagg, K.G., and O.L. Zienkiewicz (eds.), Rock Mechanics in Engineering Practice. John Wiley & Sons, New York, 1968.

18. .Department of Transportation, Office of High Speed Ground Transportation, G.B. Clark, et al., Rock Properties Related to Rapid Excavation. Final Report, PB 184756.

19. Handin, J., and R.V. Hager, Jr., Experimental Deformation of Sedimentary Rocks under Continuing Pressure: Tests at High Temperature: Bulletin, Americal Association Petroleum-Geologists. 42: 2892, 1958.

20. Stokes, R.J., Mechanical Properties of Polycrystalline NaCl. Proc. British Ceramics Society, 6: 187, 1966.

21. Baidyuk, B.V. (ed.), Mechanical Properties of Rock at High Pressure and Temperatures. Consultants Bureau Translation, New York, 1967.

22. Fodor, I., and K. Tokes, Neve Forschungen Uber die Physikelischen and Mechanishcen Eigenschaften des Rumanischaften des Rumanischen Steinsalzes. Theme 3, No. 78: 705-709. Proc. 1st Congress on Rock Mechanics, Lisbon, 1966.

23. Lindner, E.N., and J.A. Halpern. In-Situ Stress Analysis. 18th U.S. Symposium on Rock Mechanics, 1977.

24. Savin, G.N., Stress Distributions Around Holes. NASA Technical Translation, TTF-607.

25. Arthur D. Little, Inc. Technical Support of Standards for High-Level Radioactive Waste Management. Task B Report. "Effectiveness of Engineering Controls". Cambridge, Massachusetts. March-August 1977.

26. Cohen B.L., The Disposal of Radioactive Wastes from Fission Reactors, Scientific American, 236 (6), June 1977.

27. Timoshenko, S.P., and J.N. Goodier, Theory of Elasticity, McGraw-Hill Book Company, Inc., New York, 1943.

28. Vanmarke, E.H., Stochastic Modeling of Soil Profiles. J. Geot. Div. ASCE 103, 1977.

29. Agterberg, F., Autocorrelation Functions in Geology. In: Meriam, (ed.), Geostatistics, Methuen, London, 1970.

30. Beran, N.J., Statistical Continuum Theories. John Wiley & Sons, New York, 1968.

31. Cleary, M.P., Fracture Discontinuities and Structural Analysis in Resource Recovery Endeavors. AIME J. Pressure Vessel Technology (Paper 77 - Pet 3), 1977.

32. Hener, R.E., and A.J. Hendron, Geomechanical Model Study of the Behavior of Underground Openings Subjected to Static Loads. Contract Report R-69-1, U.S. Army Engineers Waterways Experiment Station, Vicksburg, Mississippi, 1969.

33. McCutcheon, A., The Behavior of Rock and Rock Masses in Relation to Military Geology. Quarterly Colorado School of Mines, 1949.

34. Gelhar, L.W., Effects of Hydraulic Conductivity Variations on Ground Water Flows. 2nd Int'l. Conference on Stochastic Hydraulics, London, 1976.

35. Papoulis, A., Probability, Random Variables, and Stochastic Processes. McGraw-Hill, New York, 1965.